NEW ZEALAND GEOTECHNICAL SOCIETY INC
www.nzgs.org

Proceedings

19th Symposium



HANGING BY A THREAD?

Lifelines, infrastructure and natural disasters

www.nzgs13.co.nz

20-23 NOVEMBER 2013

QUEENSTOWN

19th New Zealand Geotechnical Society 2013 Symposium

HANGING BY A THREAD? Lifelines, infrastructure and natural disasters

Queenstown, November 2013

ORGANISING COMMITTEE:

Tony Fairclough	Symposium Convenor	Tonkin & Taylor
Kirsti Murahidy	Sponsorship, Workshops	Tonkin & Taylor
Nick Harwood	Sponsorship, Workshops	Coffey
Paul Salter	Marketing, Website	URS
Aaron George	Field Trips	Opus
C Y Chin	Proceedings Editor	URS

PUBLISHED BY:

The Institution of Professional Engineers New Zealand
P O Box 12241, Wellington

Proceedings 19th NZGS Geotechnical Symposium. Hanging by a Thread. Ed. C Y Chin, Queenstown (2013). ISSN 0111-9532, Vol 38, Issue 1(GM) 2013

The New Zealand Geotechnical Society would like to thank the following reviewers for the arduous task of undertaking reviews of the papers presented in these Proceedings:-

TECHNICAL REVIEWERS

Gavin Alexander
Dr Brendon Bradley
Dr C Y Chin
Stephen Crawford
Prof Misko Cubrinovski
Glyn East
Tony Fairclough
Geoffrey Farquhar
Dr Peter Forrest
Nick Harwood
Dr Robert Hillier
Dr Tam Larkin
Dr Trevor Matuschka
Dr Alexei Murashev
Assoc Prof Rolando Orense
Dr Gregory Pinches
Charlie Price
Dr Bruce Riddolls
Nicola Ridgley
Paul Salter
Tim Sinclair
Dr John St George
Dr Do Van Toan
Ann Williams
Jeremy Yeats

The administrative assistance provided by Taryn Jones, Dina Sullivan and Cammeron Harris of Coffey Geotechnics (NZ) Ltd is gratefully acknowledged.

FOREWORD

It is with great pleasure that I welcome you to the 19th New Zealand Geotechnical Society Symposium which is being held in the Millennium Hotel, Queenstown on 21 and 22 November 2013.

In recent memory our planet has suffered tragic loss of life and collateral damage due to the occurrence of natural disasters. Many types of natural disasters, in particular earthquakes, are of direct relevance to the geotechnical and engineering geology community in New Zealand due to their relatively high rate of occurrence and potentially disastrous human, social and economic impact.

The recent Canterbury earthquake sequence has had an unprecedented impact on the geotechnical profession in New Zealand. It has raised the profile of our science through all levels of society, from home owners to our nation's leaders, and, has been the catalyst for a surge of invaluable observations, data and learning. It has also been a reminder to all nations as to the terrible social and economic damage which a relatively moderate but unfavourably located seismic event can inflict.

It was with the above issues in mind that the organising committee selected the subject for this Symposium:

"Hanging by a thread? Lifelines, infrastructure and natural disasters".

It is the sincere hope of the Symposium organising committee that the proceedings of this conference will

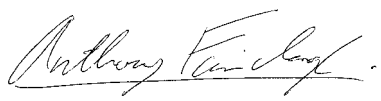
Assist future generations improve the planning, design and construction of urban areas and infrastructure,

Help reduce adverse effects of major disasters on society, and,

Expedite the short-term emergency response and long-term recovery process following future natural disasters.

At the start of day one, Professor Harry Poulos is scheduled to present a keynote address entitled "Practical approaches to seismic design of deep foundations" and at the start of day two, Dr Lelio Mejia will present his keynote address entitled "Analysis and design of embankment dams for foundation fault rupture". Both of these lectures have strong alignment and compatibility with the Symposium theme. The Symposium organising committee is extremely grateful that both of these world-renowned experts accepted the offer to speak at this Symposium and share some of their wisdom first-hand with the New Zealand geotechnical fraternity.

Finally, I wish to acknowledge the financial support which was afforded by the Symposium sponsors, and, the effort which was made by the Symposium organising committee. This event would not have occurred without each and every one of these organisations and individuals.



Tony Fairclough
Convenor
19th NZGS Symposium

NEW ZEALAND
GEOTECHNICAL
SOCIETY INC

A Collaborating Technical Group
of The Institution of Professional
Engineers New Zealand

WELCOME FROM NZGS CHAIR

As Chair of the NZ Geotechnical Society, I extend a warm welcome to participants at the 19th NZGS Symposium: Hanging by a thread? Lifelines, infrastructure and natural disasters. These events are the lifeblood of our Society. They provide our practitioners the opportunity to share research and experiences around a common theme, and I'm sure everyone will leave this event better informed and with new ideas to implement in their daily practice. Our Symposia also provide the opportunity to catch up with old friends in the profession and make new contacts. I hope you will make the most of all the opportunities that the Symposium provides.

I would like to acknowledge our Sponsors, who have played a vital part in making this event affordable. Thank you. Our exhibitors are also an essential part of an event like this, and I encourage you not just stroll past their stands but to take the time to talk to them and learn more about what they offer. They add an important dimension to our business and to this Symposium, so use this chance to find out more about them!

My sincere thanks go to the Symposium Convenor, Tony Fairclough, his organising committee, their respective home organisations and our professional conference organisers, The Conference Company, for all their efforts over the past 18 months to make this Symposium a success. They have put together an impressive programme of seminars and field trips to accompany the main sessions. The Symposium has certainly exceeded all expectations in terms of papers submitted and registrants. Well done.

All that remains is for me to welcome you to Queenstown and to the 19th NZGS Symposium. I trust you will all enjoy the Symposium and associated events.



Gavin Alexander
Chair, New Zealand Geotechnical Society

158 THE TERRACE
PO BOX 12-241, WELLINGTON
NEW ZEALAND
p +64 4 473 9444
f +64 4 474 8933
e secretary@nzgs.org
www.nzgs.org

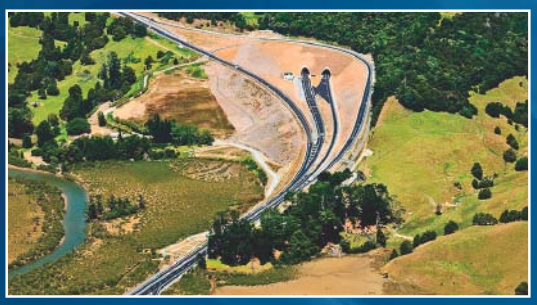


Tonkin & Taylor

Tonkin & Taylor are delighted to be a sponsor of the 2013 New Zealand Geotechnical Society Conference 'Hanging by a Thread'.









Neat Facts:

- Tonkin & Taylor have provided niche expert services in geotechnical engineering since 1959
- We employ over 130 geotechnical engineers and engineering geologists throughout New Zealand
- The experience of our current NZ staff exceeds an unparalleled 1,100 man years of geotechnical practice and experience
- We are Proudly New Zealand Owned
- We have built and operate the largest geotechnical database in the country (Since 2010 the public Canterbury Geotechnical Database alone has captured over 11,000 CPT records!)

We look forward to meeting and sharing with our professional colleagues our collective learnings from the geotechnical wonderland that is New Zealand.

For more information visit **www.tonkin.co.nz**

ENVIRONMENTAL AND ENGINEERING CONSULTANTS



Table of Contents

Day 1

KEYNOTE LECTURE		PAGE
Practical approaches to seismic design of deep foundations	Poulos, H.G.	1
SEISMIC BEHAVIOUR – 1		
Use of the dynamic cone penetrometer to assess the liquefaction susceptibility of Christchurch alluvial soils	Ashfield, D., Ashby, G., Fitch, N., Ladley, E., Power, P., & Smith, T.	29
Soil characterization using SDS data in Christchurch	Mirjafari, Y. , Orense, R.P. & Suemasa, N.	37
Liquefaction induced ground damage in the Canterbury Earthquakes: Predictions vs. reality	Bowen, H.J. & Jacka, M.E.	45
A review of colloidal silica stabilisation and microbial-induced calcite precipitation and their use to mitigate liquefaction using passive site remediation	Buhagiar, L.R.	53
SEISMIC BEHAVIOUR – 2		
Prediction of earthquake-induced liquefaction for level and gently sloped ground	Chiaro, G. & Koseki, J.	61
Liquefaction Resistance and Possible Aging Effects in Selected Pleistocene Soils of the Upper North Island	Clayton, P.J. & Johnson, J.T.	69
Nonlinear shear stress reduction factor (rd) for Christchurch Central Business District	Dismuke, J.N.	77
A practical seismic liquefaction zoning system for risk management of urban development	Halliday, G. Faulkner, P. Salt, G & Clements R.	85
The importance of accurate pore pressure response measurements when conducting CPTu as exemplified using data collected in Christchurch following the Canterbury earthquake sequence	Hébert, M.-C.	93
Use of Mononobe-Okabe equation in seismic design of retaining walls in shallow soils	Chin, C.Y. & Kayser, C.	101
Seismically induced displacement of land affecting multiple residential properties in the Port Hills, Christchurch, New Zealand, following the 2010/2011 earthquake sequence	Hunter, R.P.	109
SEISMIC BEHAVIOUR – 3		
Pore Pressure Response during High Frequency Sonic Drilling and SPT Sampling in Liquefiable Sand	Wentz, F.J. & Dickenson, S.E.	117
Evaluation of liquefaction and re-liquefaction observed in Christchurch using CPT data	Lees, J., Ballagh, R. & Orense, R.P.	125
Liquefaction potential of Rotorua soils	Pearse-Danker, E.	133
Comparison between predicted liquefaction-induced settlement and ground damage observed from the Canterbury Earthquake Sequence	Power, P.M. & Jacka M.E.	140

SEISMIC BEHAVIOUR – 4		
Sensitivity of predicted liquefaction-induced lateral spreading displacements from the 2010 Darfield and 2011 Christchurch earthquakes	Robinson, K., Cubrinovski, M., Bradley, B.A.	148
An initial assessment of the effects of seismically induced ground deformation on the occurrence of localised instability following rainfall in the Port Hills, Christchurch	Udell, H.	156
LSN – a new methodology for characterising the effects of liquefaction in terms of relative land damage severity	van Ballegooy, S., Lacrosse, V., Jacka, M. & Malan, P.	163
Reliability of lateral spreading estimates in 2010-2011 Canterbury earthquakes	Wightman, A. & Norris, N.	171
Correlations between liquefaction induced damage and former river channels in Kaiapoi	Wotherspoon, L.M., Pender, M.J. & Orense, R.P.	179
Cyclic Softening Case Study: Wendover Retirement Village, Christchurch	Heritage, R.J.	187
Design of a contiguous bored pile wall to reduce lateral spreading potential; force based and displacement based design approaches	Sutherland, S.W., Murahidy, K.M. & Palmer, S.J.	195
FUNDAMENTAL SOIL & ROCK MECHANICS – 1		
Undrained monotonic behaviour of pumice sand	Orense, R.P.	203
The undrained cyclic strength of undisturbed and reconstituted Christchurch sands	Taylor, M.L., Cubrinovski, M., Bradley, B.A. & Horikoshi, K.	211
Investigating Rock Mass Conditions and Implications for Tunnelling and Construction of the Amethyst Hydro Project, Harihari	Savage, E.S., Villeneuve, M. & Lambert, C.	219
Improvement of shrinkage and expansive soil properties using nano-copper	Taha, M.R. & Taha, O.M.	227
DESIGN – 1		
Strength reduction factors for foundations and earthquake load combinations including overstrength	Palmer, S.J.	235
A comparison of methods for measuring defect orientation from boreholes in weak rock	Roberts, R.C., O'Loughlin, B. & Elvy, J.	243
Estimation of vertical subgrade reaction coefficient from CPT investigations: applications in Christchurch	Barounis, N., Saul, G. & Lally, D.	251
Soil-foundation-structure interaction in shallow foundation spring bed modelling	Storie, L.B. & Pender, M.J.	259
Modelling of pile response in laterally spreading liquefiable ground	Wang, S. & Orense, R.P.	267
Settlement considerations for AMETI Panmure Phase 1	Ni, B. & East, G.R.W.	275
Proposed amendments to geotechnical requirements of NZTA Bridge Manual	Murashev, A.K., Kirkcaldie, D.K., Keepa, C. & Lloyd, J.N.	282
GEOLOGY/HYDROGEOLOGY		
Characterisation of active faults in the Canterbury region: a tool for risk-based minimisation of fault surface-rupture hazards to communities and infrastructure	Barrell, D.J.A., Jack, H., Gadsby, M., Strong, D.T., Van Dissen, R.J., Litchfield, N.J., Townsend, D.B. & Begg, J.G.	290
3D geological and geotechnical models of the Christchurch urban area	Begg, J.G., Jones, K.E., Rattenbury, M.S. & Ramilo, R.	298
Engineering geological characterisation of the Torlesse composite terrane in Canterbury, New Zealand	Irvine, A.G., Eggers, M.J. & Villeneuve, M.	306
Characterisation of modern and paleo-liquefaction features in eastern Christchurch, NZ following the 2010-12 Canterbury earthquake sequence	Bastin, S.H., Quigley, M., Bassett, K. & Green, R.A.	314
Development of a median groundwater table surface for Christchurch	van Ballegooy, S., Cox, S.C, Thurlow, C., & Reynolds, T.	322
The role of the ground model in design of low cost slip repairs on rural New Zealand roads	Watson, J.	330

CASE HISTORIES - 1		
Nelson-Tasman December 2011 Storm, Maitai pipeline emergency engineering response	Ellis, R.M., Fon, A.J.A., & Haydon, S.L.	338
The EQC geotechnical investigation project - Part A Project overview, evolution and SPT hammer energy calibration	Fairclough, A. & Ashfield, D.J.	346
The EQC geotechnical investigation project - Part B Lessons learnt during the CPT investigations	Fairclough, A., Ashfield, D.J., Soutar, C.M. & Wentz, F. J.	354
Lessons learnt using GIS to map geological hazards following the Christchurch Earthquake	Gerrard, L.C, Herbert J.A & Revell T.A.J	362
CASE HISTORIES – 2		
Managing ground uncertainty from investigation to design and construction	Griffin, A.K.	370
Caversham highway four laning – a case study in risk management and earthquake resistant design	Grindley J.R., Saul G., & Walsh I.	377
Earthquake Design Considerations for a Critical Water Supply Pipeline near Meckering, Western Australia	Harvey, B.M., Robins, P.N. & Kain, D.J.	385
Preservation and capping of a Mineshaft under SH25 in Thames, New Zealand	Hughes, C.G.C., Mokhtari, A. & West, B.	391
Realignment of SH35 across an active landslide on the East Cape of the North Island	Jennings, I.	399
Resilience of transportation lifelines in the greater Wellington area	Mason, D. & Brabhaharan, P.	407
Seismic response of underground utilities following the Canterbury earthquakes	McLachlan, R., Morris, J., Kathirgamanathan, P. & Callosa-Tarr, J.	415
CASE HISTORIES – 3		
Tui Mine Tailings Remediation Project – Geotechnical, Environmental and Construction Challenges	Quickfall, G.P., Croucher, B., Willson, T., Basheer, G., Jenkins, I.R. & Fellows, D.L.	423
Old Pacific Highway embankment collapse at Piles Creek – Highlighting the importance of effective maintenance and asset management of aging infrastructure	Retsos, P. & Shackell, C.	431
Land use planning for Blenheim, considering geotechnical hazards	Mason, D., Brabhaharan, P. & Hayes, G.	439
Lochnagar landslide-dam – Central Otago, New Zealand: geomechanics and timing of the event	Sweeney, C.G. Brideau, M.A., Augustinus, P.C. & Fink, D.	447
Towards the development of design curves for characterising distributed strike-slip surface fault rupture displacement: an example from the 4 September, 2010, Greendale Fault rupture, NZ	Van Dissen, R., Hornblow, S., Quigley, M., Litchfield, N., Villamor, P., Nicol, A., Barrell, D.J.A., Sasnett, P. & Newton, K.	455
Security of power transmission line tower foundations affected by natural hazards	Farquhar, G.B, Underhill, J.P.	463
A discussion of the monitoring of co-seismic land displacement observed on the Port Hills as a result of the 2010/2011 Canterbury earthquake sequence	Jackson, M. & McDowell, B.	470



Hanging by a thread?

Our multiple strands deliver strong foundations for the future.



BPC right from the start : www.brianperrycivil.co.nz

Day 2

KEYNOTE LECTURE		PAGE
Analysis and design of embankment dams for foundation fault rupture	Mejia, L.	478
INVITED LECTURE		
Management and documentation of geotechnical hazards in the Port Hills, Christchurch, following the Canterbury earthquakes	Macfarlane, D. F. & Yetton, M.D.	494
SLOPES – 1		
Terrestrial laser scanning methods to assess rockfall risk	Archibald, G.C., Massey, C.I., Lukovic, B., & Carey J.M.	513
2011 Manawatu Gorge Landslide Remediation	Avery, M.B. & Bourke, S.J.	521
Advanced numerical modelling of geogrid-reinforced rockfall protection embankments	Murashev, A., Easton, M. & Kathigamanathan, P.	529
Landslides in Sensitive Soils, Tauranga, New Zealand	Moon, V.G., Cunningham, M.J., Wyatt, J.B., Lowe, D.J., Morz, T. & Jorat, M.E.	537
SLOPES – 2		
The incidence and importance of landslide dams in inland Otago	Bryant, J.M. & Goldsmith, M.	545
Pragmatic management of slope hazards in Wellington Greywacke	Cassidy, G.A. & Mahoney, A.G.	552
Reopening Evans Pass Road, Sumner to Summit Road	Engel, J.M.	560
Millerton Cutting - Assessment and mitigation of rockfall hazards on a critical supply route	Forrest, P.D. & Molloy, J.W.H.	568
Risk Management of a complex rotational failure at Whales Back Saddle on the Inland Road, North Canterbury, New Zealand	Graafhuis, R.B. & Underhill, J.P.	576
Rockfall protection of west angelas iron ore mine using tecco mesh	Guerra, P.G. & Le, T.	584
Assessment of Post-Event Slope Stability Risk across the Central Otago Highway Network	Hodgkinson, E.J.	592
SLOPES – 3		
A rockfall risk assessment and selection of appropriate mitigation measures for The Christchurch Gondola following the 22 February 2011 Magnitude 6.3 earthquake	Howard, M.E. & McMorran, T.J.	600
3D Rockfall Modelling and Rockfall Protection – Port Hills Christchurch	Avery, M.B., Teen, A. & Salzmann, H.	608
SH2 Waioeka Gorge, Observations of failure mechanisms prior to and during a major rock slide, March 2012	Read K.J. & Jennings I.	616
Slope Assessment Procedures; a closer look	Pletz, Z.J., Codd, J. & Swatton, L.	623
SLOPES – 4		
SH35 Maraenui Hill Realignment: Use of Risk Assessment in Slope Design Optimisation and Route Security	Read K.J, Hughes C.G.C. and Cooke S.	631
Geotechnical Risk Assessment of Hilly Terrain during Post-Earthquake Response	Yates, K. Villeneuve, M. Wilson, T.	639
2011 Hawkes Bay Landslips: A Geotechnical Perspective	Soysa, S.R. & Pomfret, A.D,	647
SH6 Rocks Road, Nelson, New Zealand – Observations on Cliff Instability Risk Assessment	Stewart, D.L. & Brabhaharan P.	655
Rockfall Protection Systems – the French Approach	Villard, N. & McHugh, N.	662
Macro and micro scale assessment and quantification of sloping ground damage following the Canterbury 2010/2011 earthquake sequence	Wallace, S.	670

CONSTRUCTION – 1		
The use of polystyrene (EPS) as a lightweight embankment fill	East, G.R.W.	676
Investigation, design and construction of remediation of karstic solution feature affecting major motorway	Holliday, J.K.	683
Ground conditions and implications for construction in close proximity to a major faultline	Bradshaw, J.D. & Clayton, P.J.	691
Design and construction of a synthetic lining system for the seismic enhancement of Stuart Macaskill Lakes, Upper Hutt, New Zealand	Cherrill, H.E., Eldridge,S.F. & Torvelainen,E.P.	699
CONSTRUCTION – 2		
Mitigating geotechnical risk to embankments on mud flats – illustrated by the SH15 Waterview motorway widening	Pinches, G.M.	707
Christchurch Ocean Outfall Pumping Station Liquefaction Mitigation	Price, C.H. de G	715
Removable flood barriers: Geotechnical considerations	Sinclair, T. J. E.	723
A simplified numerical model of deep soil mixed columns used for road slip mitigation in 2D vs. 3D	Tatarniuk, C.M. & Bowman, E.T.	731
The use of vibro-replacement on the Ngaruawahia Section of the Waikato Expressway to mitigate potential seismic liquefaction	Wharmby, N., Clark, L. & Johnson, J.	739
Low mobility grout (LMG) at the Southern Cross Hospital to re-level ground bearing floor slabs and improve seismic performance	Wharmby, N., Gibb, N. & Koelling, M.	747
CASE HISTORIES – 2		
The effect of hydrothermal alteration on the mechanical and physical rock properties of lithologies from the Ngatamariki, Rotokawa and Kawerau geothermal fields, Taupo Volcanic Zone, NZ	Wyering, L.D, Villeneuve, M. & Wallis, I.	754
Estimation of site-specific and spatially distributed ground motion in the Christchurch earthquakes: Application to liquefaction evaluation and ground motion selection for post-event investigation	Bradley, B.A.	762
Use of Geographical Information Systems to Assist with Management of the EQC Canterbury Geotechnical Investigation Project	Carter, J.J. & Fairclough, A.	770
Recognition of Geotechnical Considerations in Planning Documents	Curley, B.A., Beetham, R.D. & Simms, B.S.	778
FOUNDATIONS – 1		
Geophysical testing of soft soils and embankments for road construction and risk assessment	Whiteley, R.J, Kelly, R.B & Stewart, S.B	786
Bearing capacity of foundations on slope	Balachandra, A., Yang, Z. & Orense, R.P.	794
Engineering Properties of Pumice Material and the Design of Piled Foundations	Clendon, N.K., Ho, K, & Poulos, H.	802
Designing earthquake resilience into pump station foundations	Gibson, M.F.L., Green, D.P., Holmes, S.F., & Newby, G.	810
Grouting of basalt to improve seismic resilience for bridge foundations	Hillier, R.P. & Langbein, A.C.	818
Snap-back Response of Piles in Stiff Clay	Millin, R.J.M., Wotherspoon, L.M. & Pender, M.J.	826
A Pragmatic and Non-Intrusive Procedure for Assessing the Post-Earthquake Structural Integrity of Piled Foundations	Moniz, S.R., Harwood, N. K., & Poulos, H. G.	834

POSTER SESSIONS		
Mitigation of a Landslide Impacting a Rural Road in Alameda County, California	Bruggers, D; Skinner, R. & Rudolph, W.R.	841
The impact of new springs affecting residential properties in Christchurch following the Canterbury 2010/2011 Earthquake Sequence	Lochhead, S.E.	850
Effect of specimen size on the laboratory measurements of electrical resistivity of soils	Neishabouri, M.N. & Abuel-Naga, H.M.	858
Developments in Geotechnical Site Investigations following the Canterbury Earthquake Sequence	Neeson, F.C.	866
Stress path approach to settlement analysis of soft ground	O'Sullivan, A., Soric, D. & Terzaghi, S.	874
A new multiple-step loading triaxial test method for brittle rocks	Taheri, A. & Chanda, E.	882



Aurecon provides engineering, management and specialist technical services for public and private sector clients globally.

Our skilled team work across the geotechnical spectrum of studies, ground investigations, interpretation, analysis and design, inspections and remediation.

aurecon

For more information, contact:
Jan Kupec, Technical Director, Ground Engineering
T 03 366 0821 **M** 021 350 674 **E** jan.kupec@aurecongroup.com

Leading. Vibrant. Global.
www.aurecongroup.com

Pour trust into your foundations and you can build anything



Coffey is a proud sponsor of the 19th Symposium of the New Zealand Geotechnical Society.

Coffey is a specialist ground-engineering consultancy.

We pride ourselves on:

- solving complex technical challenges
- pioneering new solutions
- delivering on-time, on-budget work
- nurturing strong relationships with our clients

coffey.com

Farquhar, G.B. & Underhill, J.P. (2013)
Security of power transmission line tower foundations affected by natural hazards
Proc. 19th NZGS Geotechnical Symposium. Ed. CY Chin, Queenstown

Security of power transmission line tower foundations affected by natural hazards

G B Farquhar
AECOM, Auckland, New Zealand
geoffrey.farquhar@aecom.com (Corresponding author)

J P Underhill
AECOM, Auckland, New Zealand
john.underhill@aecom.com

Keywords: power transmission line, transmission line tower, foundation, natural hazard, risk, stability, landslide, lahar, earthquake, erosion

ABSTRACT

The ability of New Zealand's high voltage power transmission system to withstand natural hazards is paramount. The principal natural hazards affecting the foundations of transmission line towers are slope instability and earthquakes. Secondary hazards include floods, river bank erosion and volcanic eruption. Examples are presented of foundations for steel lattice towers (steel grillage and concrete pile foundations) affected by natural hazards and methods of mitigating the risks.

New Zealand Geotechnical Society Inc. 19th Symposium, Queenstown 2013

1 FOUNDATION TYPES

New Zealand's high voltage transmission network is operated by Transpower. Towers are used to support the conductors (wires) above the ground and other obstacles to maintain safe electrical clearances. The two most common types of towers are self-supporting steel lattice towers (called pylons by the public) and monopoles (concrete, timber and steel tubular poles). This paper focuses on foundations for lattice towers.

In New Zealand broad base lattice towers have a variety of foundations (spread footings and piles) depending on ground conditions (Figure 1). Older lattice towers are generally supported on steel grillage foundations where a mesh of steel beams forms a pad footing which is connected to the end of the tower leg below ground level. The excavation for the grillage is then backfilled with excavated spoil. More recent towers have bored cast in situ concrete piles, often with belled ends to provide better uplift capacity. Less common are concrete rafts, concrete pad and chimney foundations, driven steel and timber piles, and concrete pad footings. Some concrete foundations are supplemented with ground anchors to provide uplift capacity.

2 FOUNDATION DESIGN

Lattice tower foundation loads principally comprise vertical uplift (tension) or compression forces and associated horizontal shear forces. For intermediate and angle (strain) towers with small angles of line deviation, the vertical loads may either be in tension or compression. For strain towers with large angles of deviation and terminal towers under normal climatic loadings, two legs will normally be in uplift with the other two legs in compression. Under all loading combinations, the distribution of horizontal forces between the individual footings will vary, depending on the bracing arrangement of the tower. Design of foundations for lattice tower towers with four legs is governed by uplift resistance of the foundations. It is rare for the foundations under compressive load to govern foundation design.

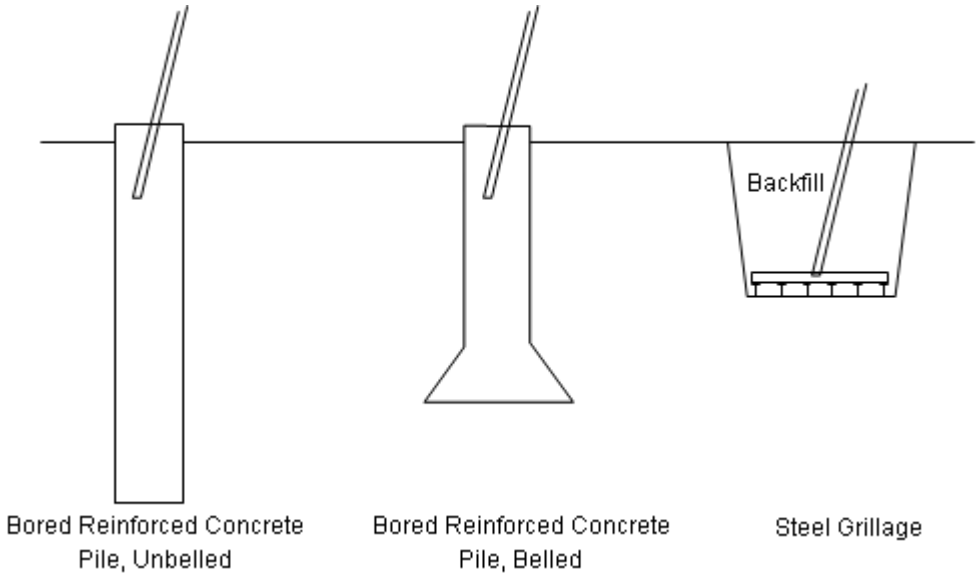


Figure 1: Types of tower foundations

3 NATURAL HAZARDS

The principal natural hazards affecting the foundations of transmission line towers in New Zealand are slope instability and earthquakes. Secondary hazards include floods, river bank erosion and volcanic eruption. These hazards affect either the whole of the foundation, i.e. all four foundations for a typical steel lattice tower, or one or more of the four foundations.

By far the most common risk is ground instability either reducing or potentially reducing the uplift capacity of foundations and presenting risk to the tower when it is subject to overturing loads. A less common risk is either the complete disruption or potential disruption of the entire foundations from instability. Other risks include the potential impact on foundations by rockfall, landslide and lahar, river bank erosion removing founding materials, strong earthquake shaking, fault rupture and liquefaction.

A large majority of towers in New Zealand were constructed between 1930 and 1970. These lines have been in operation now for between 40 and 80 years. Sites that were considered stable at the time of construction have since deteriorated. Slopes adjacent to towers continue to degrade and the risk to these towers increases with time.

The easiest way to mitigate the risk of natural hazards affecting new towers is to site them to either avoid or minimise the effects of natural hazards. More challenging is management of the risk to existing towers. Towers sited on flat or undulating land generally, but not necessarily, have a low risk of being affected by natural hazards. Due to New Zealand's rugged topography many towers are sited on ridge lines and adjacent to steep slopes. The principal means of mitigating risk are to relocate the tower, stabilise ground instability threatening foundations, and strengthen foundations against the reduction in uplift capacity caused by ground movement.

Steel grillage foundations rely on uplift resistance from the self weight of the soil mass overlying the grillage and shear resistance on the sides of the frustram of soil above the grillage. Improving uplift resistance for steel grillage foundations often comprises excavating the grillage and encasing both the grillage and tower leg with sufficient concrete to provide the necessary uplift resistance (by self weight of the foundation). Two or four legs can be tied together by concrete beams at or just below ground level. Ground anchors and piles can also be installed to provide additional uplift resistance. Retaining walls and other slope stabilisation methods can be used to prevent slope failures regressing too close to tower foundations.

New Zealand Geotechnical Society Inc. 19th Symposium, Queenstown 2013

Pile foundations (unbelled) rely on uplift resistance from pile self weight and shaft resistance. Belled piles rely on pile self weight and shear resistance on the sides of the frustram of mobilised soil above the bell. Improving uplift resistance often includes tying two or four piles together by concrete beams at or just below ground level and/or installing ground anchors.

4 EXAMPLES OF FOUNDATIONS AFFECTED BY NATURAL HAZARDS

4.1 Earthquakes

A swarm of earthquakes occurred between 15 July and 5 August 2004 centred on the north western edge of Lake Rotoehu. One hundred and forty seven earthquakes, with focal depths between 1km and 8km and Richter magnitudes up to 5.4, occurred within 5km of a Transpower line. Numerous ridge rents, most with both vertical and horizontal offset, were observed adjacent to one tower (Figure 2). The cracks, oriented parallel to the ridge, were pervasive over a 100m length approximately 6m in from the ridge edge. The 12m wide ridge was flanked by 35m to 40m high 40° slopes. Vertical displacement of around 1m of the material surrounding the grillage foundations for two tower legs occurred. The structure was assessed as being at very high risk of sudden collapse, particularly as the seismic events were continuing and heavy rainfall was forecast. The ridge is underlain by pumice breccia (medium to coarse pumiceous, gravely sand) with a 3m to 5m thick mantle of volcanic ash. The tower was relocated.

Two Transpower transmission lines cross the surface rupture of the Greendale Fault generated by the 4 September 2010 Darfield earthquake while a third line passed 2.5km east of the eastern end of the fault rupture. Towers on all three lines were affected by ground movement and liquefaction during and following the earthquake. Evidence of liquefaction was observed from sand boils on adjacent ground and ejected sand and water around the sides of piles. Effects included settlement and slight tilting of the towers, which are supported on bored piles. Dextral offset along the east-west oriented fault rupture resulted in extension of the two lines crossing it (Figure 3). Overall these effects were not adverse and the foundations performed well.



Figure 2: Ridge rents in volcanic terrain following earthquake swarm

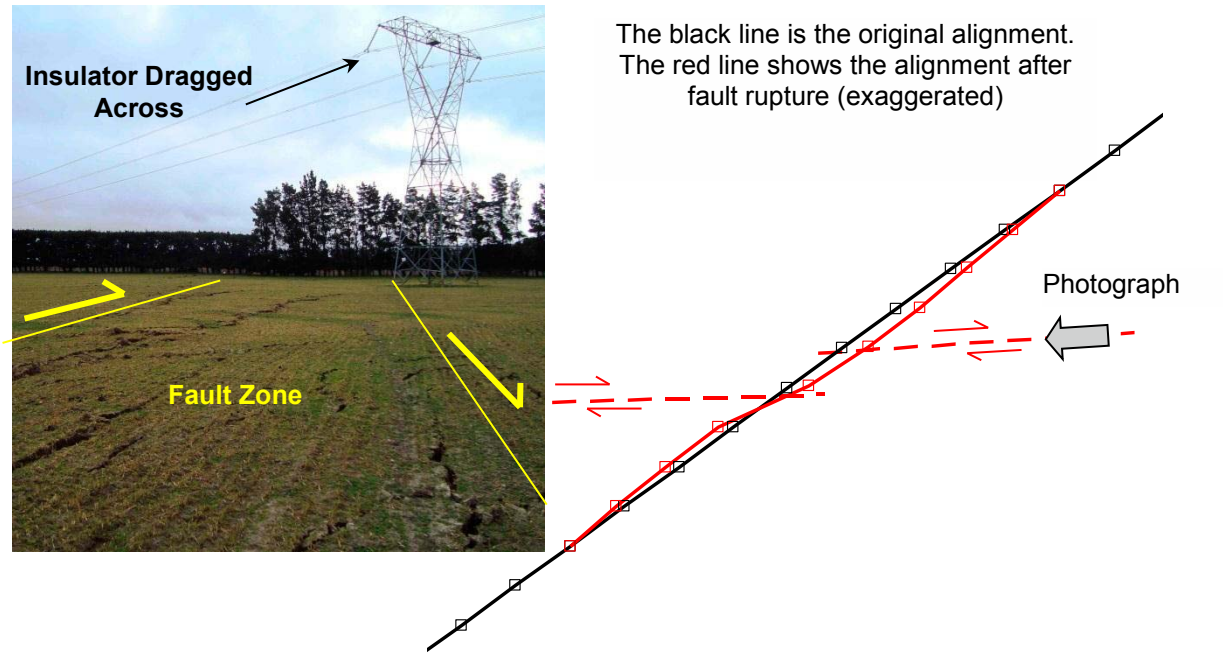


Figure 3: Surface rupture along the Greendale Fault offsetting the ROX-ISL line following the Darfield Earthquake.

A tower on the foot slopes of the Port Hills was damaged by a rock falling from the slopes above during the 22 February 2011 Christchurch earthquake (Figure 4).

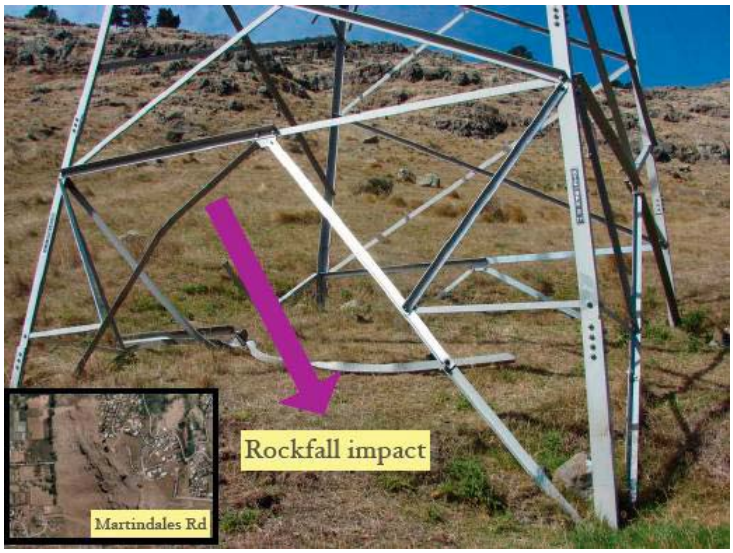


Figure 4: Transmission tower damaged by rockfall (after Eidinger & Tang, 2012)

4.2 Lahar

Over 47 lahars originating from breaches of the crater lake on Mt Ruapehu and eruptions of Mt Ruapehu have been recorded since 1861. The lahars flow down the Wangaehu River. A previous crater lake breakout on 24 December 1953 produced a lahar that caused 151 deaths in New Zealand's worst volcanic and rail disaster when the Whangaehu River bridge at Tangiwai collapsed beneath the Wellington to Auckland overnight train. In a much anticipated event on 18 March 2007, the crater rim finally breached again causing a lahar in the Wangaehu River.

Three transmission lines are sited on a river terrace, 250m away from the main channel of the river. The risk to thirteen of the towers was long recognised and modelling of the towers subjected to inundation by the expected lahar indicated that the towers could sustain impact loading from a 2.3m depth of lahar flow. Conditions assessed included lahar flow past tower legs, boulder/debris impact on individual legs and creation of a debris dam bridging across several tower legs. Mitigation options considered included encasing the legs in concrete, mounding fill around the legs, constructing bunds (chevron shaped earth mounds or chevron shaped man made barriers in front of affected towers) and constructing bunds across lahar flow path. As the debris dam condition is the most significant, the most practical method of protecting the tower legs is to deflect the main flow around the tower. Mitigation works were not constructed after evaluating the expected depth of lahar in the river channel and risk of the lahar spilling onto the river terrace. The actual lahar on 18 March 2007 stayed within the main river channel.

4.3 Large scale landslide

Seismic activity in the vicinity of Little Waihi on the southern shore of Lake Taupo in June 2009 initiated a Civil Defence emergency and evacuation of the town because of a possible landslide threat. A large number of small earthquakes were recorded, the largest being magnitude 4.4 on 26 June 2009. Historic landslide and debris flow events have resulted in death and loss of property. Two of Transpower's lines traverse the historic failure area in two spans involving 6 towers. The risk to the towers was assessed with two towers being at a moderate level of risk and two at a high level of risk of damage should landsliding occur (Figure 5). An emergency plan for temporary replacement of towers was prepared for implementation at short notice. Long term risk could be mitigated by either deviating the line around the unstable area, or relocating towers an appropriate distance back from their existing locations, or removing towers and installing conductors in a single span. A large scale landslide in another location, potentially affecting several towers, is shown in Figure 6.

New Zealand Geotechnical Society Inc. 19th Symposium, Queenstown 2013

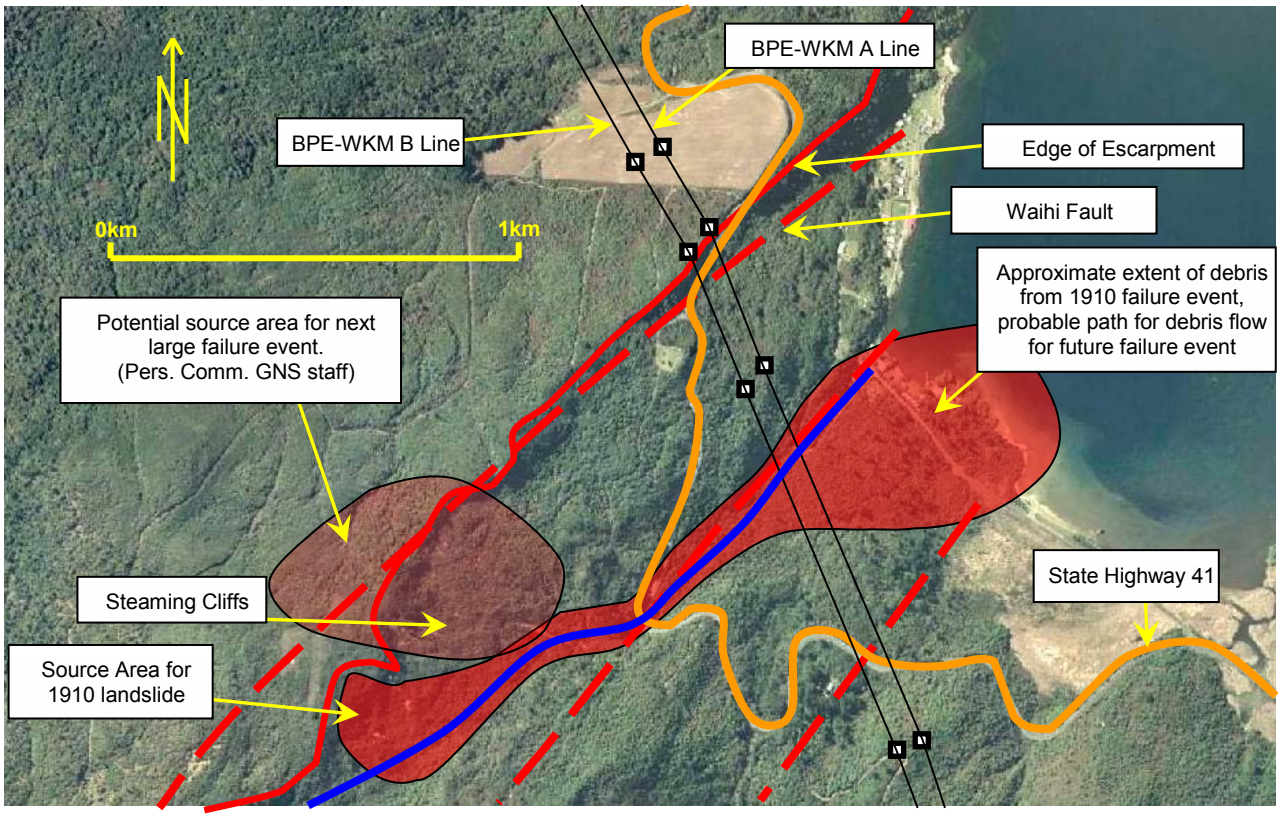


Figure 5: Potential landslide/debris flow affecting towers at Little Waihi

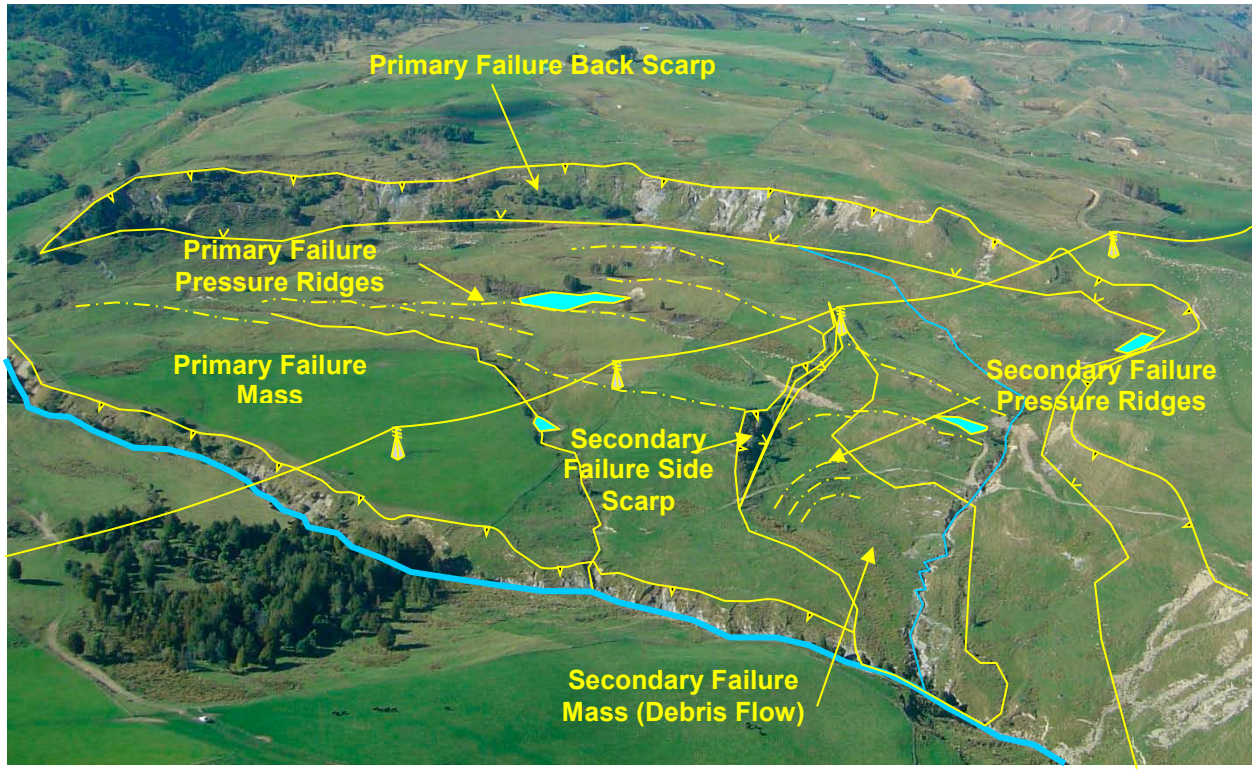


Figure 6: Large scale low angle landslide covers an area of 0.75km^2 is traversed by a 110kV line. Three towers are located on mobile ground.

4.4 Smaller scale instability

By far the most common threat to tower foundations is small scale slope instability, examples of which are shown in Figure 7. Methods of mitigating the risk to tower foundations from these small scale slope failures are discussed in section 3.



Figure 7: Small instability features threaten towers in steep country in poorly compacted fill (left) and natural ground (centre and right).

4.5 River bank erosion

Meander loop migration of the Rangitikei River has threatened Tower 130 on the Bunnythorpe – Ongarue A line since construction in 1933 (Figure 8). Regression of the 85m high near vertical cliff is largely controlled by near vertical relaxation joints spaced at 2m to 4m and parallel with the cliff. Analysis of historic photography and survey data indicates regression toward the tower at an average rate of 0.8m per year over the period between 1933 and 2002. The regression is episodic with each event involving an average of 22m of regression with an average return interval of 28 years. The risk to the tower and line was assessed to be very high. Risk mitigation involved relocating the tower at a setback from the cliff edge that provided Transpower with an acceptable level of risk. This solution required an increase in height of the tower to ensure clearance to the cliff edge. The setback distance was determined using a probabilistic approach.

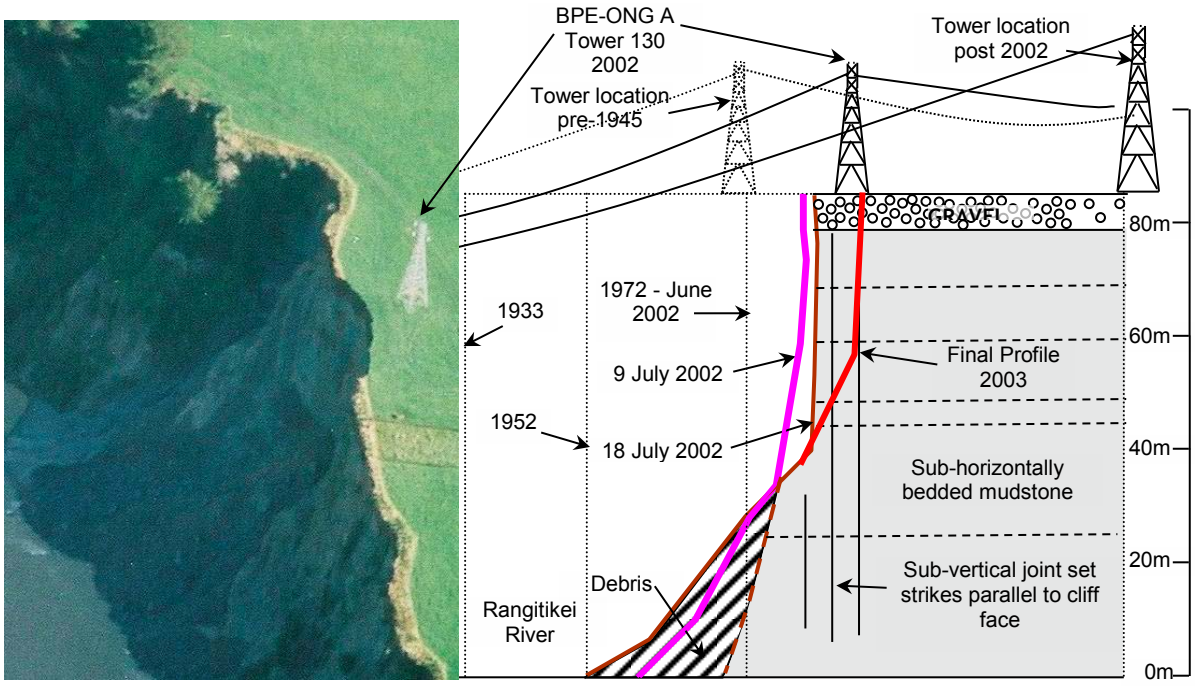


Figure 8: Tower threatened by cliff regression caused by river erosion

CONCLUSIONS

The ability of New Zealand's high voltage power transmission system to withstand natural hazards and ensure continuity of power supply is paramount. The principal natural hazards affecting the foundations of transmission line towers are slope instability and earthquakes. Secondary hazards include floods, river bank erosion and volcanic eruption. Tower foundations have been demonstrated to be resilient to the effects of natural hazards with risk assessment and appropriate mitigation measures enabling Transpower to manage the risks.

ACKNOWLEDGEMENTS

Permission from Transpower to publish this paper is acknowledged.

REFERENCES

Eidinger, J & Tang, A.K. (2012) *Christchurch, New Zealand earthquake sequence of M_W 7.1 September 04, 2010, M_W 6.3 February 22, 2011, M_W 6.0 June 13, 2011: Lifeline performance*. Technical Council on Lifeline Earthquake Engineering, Monograph No.40, ASCE

Jackson, M. & McDowell, B. (2013)
A discussion of the monitoring and measurement of co-seismic land displacement observed on the Port Hills as a result of the 2010/2011 Canterbury earthquake sequence
Proc. 19th NZGS Geotechnical Symposium. Ed. CY Chin, Queenstown

A discussion of the monitoring and measurement of co-seismic land displacement observed on the Port Hills as a result of the 2010/2011 Canterbury earthquake sequence

M Jackson
Tonkin & Taylor Ltd, Christchurch, NZ.
mjackson@tonkin.co.nz (Corresponding author)

B McDowell
Tonkin & Taylor Ltd, Christchurch, NZ.
bmcdowell@tonkin.co.nz

Keywords: Monitoring, Land, Displacement, Deformation, Co-seismic

ABSTRACT

Seismic activity during the 2010/2011 Canterbury Earthquake Sequence (CES) caused deformation to sloping ground in the Port Hills in Christchurch. Immediately after the earthquakes occurred there were concerns that some of the observed ground deformation could be representative of progressive ongoing displacement.

The authors have worked with the New Zealand Earthquake Commission (EQC) to assess and quantify the ground damage on and affecting residential land as part of the insurance response to the earthquakes. This work has included visiting affected properties, mapping land damage, and undertaking investigation and assessment, including installation of sub-surface instruments, at several key locations on the Port Hills. This work has been complemented by a collaborative arrangement for data sharing of work undertaken by Christchurch City Council (CCC) and Institute of Geological and Nuclear Sciences (GNS).

This paper briefly summarises the damage observed, and current evidence from monitoring locations and successive deformation surveys that indicates that the observed displacements are co-seismic in nature.

1 INTRODUCTION

The Canterbury Earthquake Sequence (CES) commenced in 2010 with a M7.1 event on 4th September 2010 located at Darfield, approximately 35 km west of Christchurch. Following this event there have been over 3000 aftershocks, the most severe of which was a M6.2 event on 22 February 2011 at 5 km depth, 10 km south east of Christchurch. This event resulted in loss of life and severe damage to property and land. This was followed by a M6.0 event on 13th June 2011 and a M5.9 event on 23rd December 2011.Figure 1 shows the location of the main events and some of the larger aftershocks.

The Port Hills are located to the south of the Christchurch CBD. Residential development has occurred on the lower slopes, generally extending to an elevation of 100 to 200m above sea level, predominantly over the past 60 years, stretching from Westmorland in the west to Sumner in the east.

In the Port Hills land deformation and property damage occurred mainly as a result of the February and June 2011 events. High ground accelerations in these events resulted in extensive shaking damage to buildings, cliff collapse and rock fall. Land deformation observed included cracking and bulging of loess slopes on ridge tops or within colluvial wedge deposits on the

New Zealand Geotechnical Society Inc. 19th Symposium, Queenstown 2013

lower valley slopes. Cliff regression of 10s of metres was observed and landslips exhibited tension zones up to 800 m in length with horizontal displacement in the order of 100 to 800 mm.



Figure 1: Location of Main Earthquake events and events >M5.0

The authors have worked for EQC to investigate land deformation which has occurred as a result of the CES, to assess if there has been land deformation over time since the CES, with rainfall activity and also during seismic events.

2 GEOLOGICAL SETTING

The Port Hills are underlain by the Lyttelton Volcanic Group, a non-homogeneous sequence of basaltic lava flows with intercalated scoria and pyroclastics (ash) (Brown and Weeber, 1992). The flows typically dip away from the volcanic centres of Lyttelton Harbour and (Akaroa Harbour). In the Port Hills, they typically dip to the north towards Christchurch. Figure 2 provides a summary of the main surficial stratigraphic units on the Port Hills.

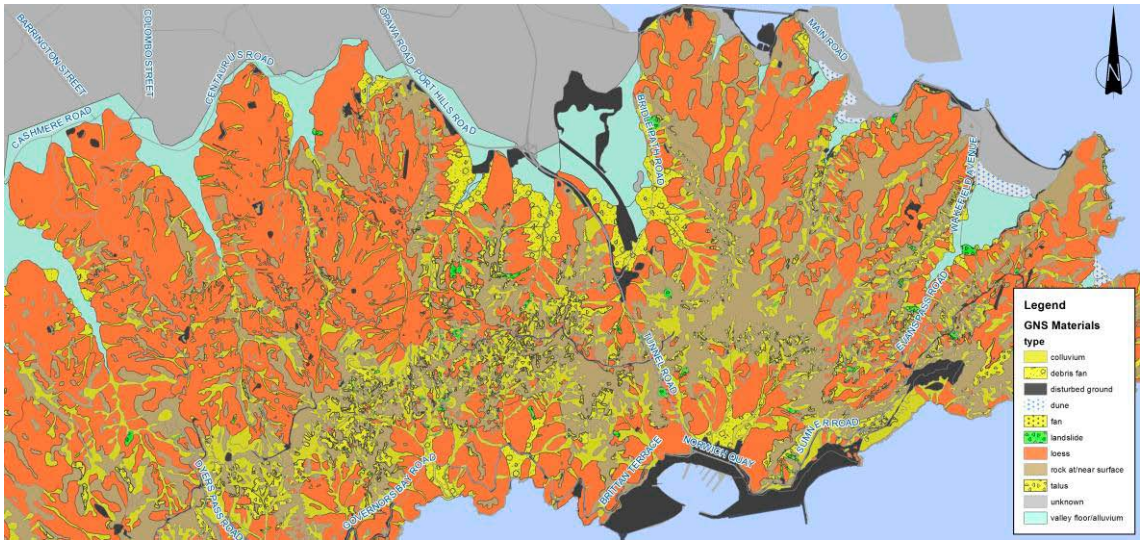


Figure 2: Extract from GNS geomorphology mapping (Townsend and Rosser 2012) showing main units on the Port Hills

On gently to moderately inclined slopes the ground surface is sub-parallel with the irregular upper surface of the lava and is typically mantled by in-situ loess (windblown glacial silt). The lower parts of the slopes typically consist of colluvium derived from redeposited loess material. In-situ and colluvial loess deposits are generally thicker on the lower and leeward slopes, and in some areas have been found to be greater than 50m in thickness.

3 LAND DEFORMATION OBSERVED

Several types of deformation have been observed in the Port Hills. This investigation focussed on large scale 'area wide' deformation as opposed to property specific deformation. The three main types of deformation are described below. The location of the deformation controls the type(s) of deformation observed. Figure 3 shows the main areas where widespread deformation has been observed and assessed by EQC.

A brief summary of the deformation observed and deformation mechanisms suggested by Tonkin & Taylor is provided below. This deformation and other mechanisms are described in more detail in the paper by Hunter (2013).

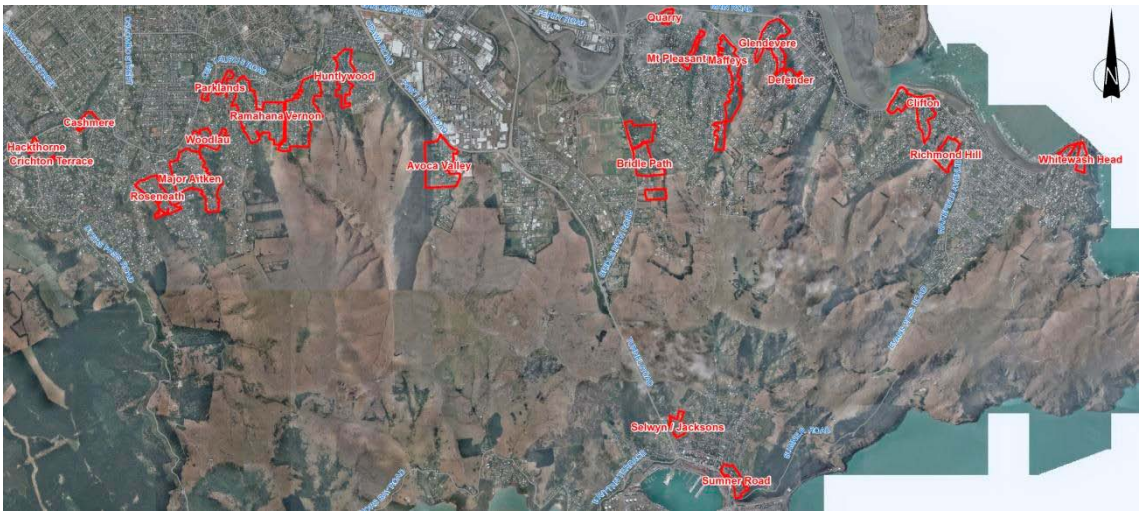


Figure 3: Main areas of land deformation identified

3.1 Deformation in Loess Slopes

Land deformation was observed as a series of tension cracks, scarps and grabens in the tension zone within in situ loess which overlies the volcanic bedrock, on ridge tops, side slopes and cliff edges. The authors suggest that deformation is confined to loess mantle and loess/rock interface, with tension cracks narrowing towards the base of the loess. Internal relative deformation may also have occurred with micro shearing visible in test pits. The Clifton area is considered to be the most developed example of deformation in loess slopes.



Figure 4: Typical examples of loess slope deformation tension cracks in the Clifton area

3.2 Colluvial Wedge Deformation

Land deformation was observed at the toe of valley side slopes as a single, or more commonly, a series of tension cracks, scarps and grabens generally within a 15-30 m width zone, but up to 100 m wide in places. Cracks are typically parallel to the contour of the lower slopes of the Port Hills valleys, generally between 10 and 25m elevation, where slope angles range between 8° and 14°. A compression zone is strongly developed at some localities and is typically 60-100 m wide where present at the edge of the valley floor with slope angles of 1° to 2°. The Vernon area is considered as the most developed example of colluvial wedge deformation.



Figure 5: Typical example of colluvial wedge deformation at Vernon with tension cracks (left) and compression cracks (right) in colluvial wedge deformation area

3.3 Cliff collapse

Land deformation was observed at current or historic sea cliffs Failure is the result of toppling and sliding on open joints and fractures in the rock mass, some forming pre-existing tension cracks behind the cliff faces. Newly formed and/or reactivated tension cracks are now visible at cliff tops.



Figure 6: Example of cliff collapse at Richmond Hill, sheared block (left) and toppled block and boulders (right)

4 INVESTIGATION & MONITORING

Ground investigation has been undertaken in many of the areas identified in Figure 3 by T&T for EQC (Tonkin & Taylor 2013), Aurecon (for CCC) and GNS (independent and for CCC). Investigation work undertaken by T&T is summarised in Table 1. This work was undertaken following the February and June 2011 events to assist the understanding of the wide spread ground deformation with respect to EQC's response to land damage claims.

Table 1: Summary of ground investigations used in assessment

	Borehole	CPT (SCPT)*	Inclinometer	Piezometer	Scala	Test Pit	TOTAL
Vernon	8	17 (4)	5	13	7	5	64
Ramahana	3	4 (3)	1	8	-	-	19
Huntlywood	-	1 (1)	-	3	-	-	5
Roseneath	-	1 (2)	-	3	-	-	6
Avoca	-	1 (2)	-	3	-	-	6
Bridle Path	-	1 (2)	-	3	-	-	6
Cashmere	-	3	-	2	-	-	5
Major Aitken	-	3	-	3	-	-	6
Clifton	17	17 (9)	3	3	17	2	65
Maffeys	7	8	2	4	-	-	21
Defender	4	3	2	3	-	-	12
Glendevere	3	2	1	3	2	7	18
Whitewash Head	-	-	-	-	5	3	8
Richmond Hill	4	2	-	3	-	4	4

*() additional tests using seismic cone

Crack separation was measured by T&T and Aurecon (Gibbons 2012) following the February and June events. Summaries of the displacement measured by various parties at Clifton and Vernon are shown in Table 2 and Table 3.

Table 2: Summary of displacement monitoring data from different sources in Clifton area

	Post Feb '11	Post Apr '11	Post June '11	Post Dec'11	Aug-Nov '12
T&T Crack displacements(March 2011)	140-350 mm		220-600 mm		
T&T Crack displacements - (Aug-Oct 2011)			320-1000 mm		
GNS GPS total stations (ongoing)*		25mm @ 127°	496 mm @285°	37 mm @ 110° 45 mm @ 116°	0 mm
Aurecon survey monitoring		15 mm	160-370 mm	0 mm	0 mm
Cadastral Boundaries (GNS)	400 mm (block) + 250 mm (loess)**		260 mm (block) + 140 mm (loess)*		
T&T Inclinometers				0 mm	0 mm

*displacement and direction of movement (bearing from north)
**Block refers to mass movement of superficial deposits; Loess refers to internal deformation within a block

Although monitoring was not undertaken prior to the February event, it was possible to estimate displacement that occurred from measuring crack widths after the event. It is evident, from visual observation (Figure 4) and measurements undertaken, that deformation occurred following the main February and June events at Clifton. It also appears that some limited displacement occurred following the April and December events, although the small amount recorded by GNS would not be large enough to show visually.

There is little evidence from monitoring or visual assessment that displacement has been progressive between large events. Ongoing movement is limited and suggests local deformation occurring over a period of weeks to months adjacent to tension cracks and scarps, including erosion and collapse in loess as a result of localised changes in drainage.

Table 3: Summary of displacement monitoring from different sources in Vernon area

	Post Feb '11	Post June '11	Post Dec '11	Aug-Nov '12
T&T crack displacements (March 2011)	350-620 mm			
T&T total crack displacements (post June 2011)		160-435 mm		
GNS GPS total stations (April '11 - Present)*		45 mm @ 290° 25-30 mm@ 225°	0 mm 0 mm	
Aurecon Survey Monitoring(2 March 11' - Dec 12')		Up to 30 mm	0 mm	0 mm
Cadastral Boundaries (Displacements are cumulative until 8/9/11)		380-600 mm		
David Smith ring fence Surveys (9-9-11 to 5-1-12)			0-10 mm	
T&T Inclinometers (May 11'- present)		45 mm	0-5 mm	0 mm

*displacement and direction of movement (bearing from north)

Monitoring data and visual inspection indicates that significant displacement occurred during the February event, which was centred directly beneath the Port Hills, and limited further displacement during the June event, which was centred on the northern edge of the Port Hills. Displacements measured after the December event, which was centred approximately 4 km north of the edge of the Port Hills, were of a magnitude which may be considered to be within the margin of error of the measurement method used, . This suggests that the proximity of the epicentre to the hills may have a significant impact on whether deformation occurs.

Monitoring between August and November 2012 post dates a rainfall event in August which resulted in a significant number of EQC landslip claims from property owners in the Port Hills (Udell, 2013). These claims show a similar spatial pattern of claims to that observed prior to the CES. Subsequent monitoring has not recorded further displacement of existing cracks following this rainfall event.

5 FUTURE MODELLING

Modelling is being undertaken by the authors for EQC at Clifton and Vernon, including the use of limit equilibrium and Newmark block methods to simulate the slope displacements that have been observed, and assess the yield conditions for deformation that could occur in the future. There are two parts to the modelling being undertaken;

- Back analysis to create and verify models with viable constraints and parameters, comparing the results of the models with records and observations of slope performance during the main events.
- Forward analysis to assess the performance of the slopes following future seismic events. This includes sensitivity analysis varying soil parameters and groundwater levels

The aim of this modelling is determine the likelihood of future deformation occurring both due to seismic events, and the potential for progressive deformation following significant rainfall.

6 CONCLUSIONS

Land deformation occurred in the Port Hills as a result of the February and June 2011 earthquake events. Evidence from monitoring results and visual inspection indicates that the deformations were co-seismic.

Evidence for ongoing deformation is limited. There is visual evidence of local deformation occurring over a period of weeks to months adjacent to scarps, including erosion and collapse in loess as a result of localised changes in drainage.

Comparing the location of the epicentre of the 22nd February and 13th June events (where deformation was observed) with those of 23rd December and other smaller aftershocks (where deformation was not observed), suggests that significant magnitude events with epicentres directly beneath the Port Hills may be required to replicate deformation observed during the CES.

Modelling is being undertaken at two of the worst affected localities within the Port Hills to assess possible failure mechanisms and determine the potential for deformation in future seismic events.

ACKNOWLEDGEMENTS

I would like to thank my colleagues Rob Hunter, Hannah Udell and Shamus Wallace for their hard work on this project which enabled this paper to be produced, and also EQC for their agreement to use the data collected on their behalf.

REFERENCES

Brown, L.J and Weeber, J.H (1992). *Geology of the Christchurch urban area*, 1:25,000 geological map 1,1 sheet + 104p. Institute of Geological and Nuclear Sciences, Lower Hutt, New Zealand

Forsyth, P. J. et al (2008) *Geology of Christchurch area*. 1:250 000 geological map 16. 1 sheet + 67 p. Institute of Geological and Nuclear Sciences, Lower Hutt, New Zealand.

GNS Science, *GPS Time Series*http://magma.geonet.org.nz/resources/gps/timeseries/

Gibbons, C (2012) *Landslide Survey Monitoring Report Ref 218782 Rev 1* 31 October 2012 for Christchurch City Council, 69p, Aurecon New Zealand

Hunter, R. (2013) *Seismically induced displacement of land affecting multiple residential properties in the Port Hills, Christchurch, New Zealand, following the 2010/2011 earthquake sequence*, Proc. 19th NZGS Geotechnical Symposium. Ed. CY Chin, Queenstown

Newmark, N.M., (1965). *Effects of earthquakes on dams and embankments.* Geotechnique 15, 139–159.

Tonkin & Taylor (2013) *Christchurch Earthquake Recovery Port Hills Area Wide Assessments Geotechnical Factual Reports* for Earthquake Commission

Townsend, D.B and Rosser, B (2012). *Canterbury Earthquakes 2010/11 Port Hills slope stability: Geomorphology mapping for rockfall risk assessment,* GNS Science Consultancy Report 2012/15 21p + maps (91P)

Udell, H L (2013) *An initial assessment of the effects of seismically induced ground deformation on the occurrence of localised instability following rainfall in the Port Hills, Christchurch,* Proc. 19th NZGS Geotechnical Symposium. Ed. CY Chin, Queenstown

Mejia, L.H. (2013)
Analysis and design of embankment dams for foundation fault rupture
Proc. 19th NZGS Geotechnical Symposium. Ed. CY Chin, Queenstown

Analysis and design of embankment dams for foundation fault rupture

L.H. Mejia
URS Corporation, Oakland, CA, USA.
lelio.mejia@urs.com (Corresponding author)

Keywords: Dam, Embankment, Earthquake, Fault Rupture, Foundation Displacement

ABSTRACT

The limited experience available regarding the performance of dams subjected to foundation fault displacements indicates that such displacements can be very detrimental to the integrity of earth and concrete dams. For example, the failure of Baldwin Hills Reservoir in California in 1963 illustrates the susceptibility of earth dams built with brittle materials and inadequate drainage to cracking, internal erosion, and piping as a result of foundation shear displacements. Because it is difficult to mitigate the risks associated with fault displacements in a dam foundation, it is widely preferred in engineering practice to avoid siting dams over active surface faults. Occasionally this cannot be avoided and several dams have been designed and built to accommodate surface fault displacements in their foundations.

In spite of the modest project experience available, insightful research into the propagation of fault rupture through soil deposits and embankment dams has been carried out in recent years and procedures for the analysis of foundation rupture effects on such dams have been recently developed. In addition, significant progress has been made by the engineering profession on the understanding of potential failure modes initiated by embankment deformations and in developing mitigation concepts applicable to the design of embankment dams to withstand fault displacements. This paper presents an overview of: a) the factors that affect embankment dam performance under foundation fault displacement, b) an approach to the analysis of embankment dams subject to foundation faulting, and c) key considerations in the design of dams for fault rupture. Selected case histories are presented to illustrate the key analysis and design considerations.

New Zealand Geotechnical Society Inc. 19th Symposium, Queenstown 2013

1 INTRODUCTION

Numerous observations of dam performance during earthquakes have been accumulated by the engineering profession over the past 50 years and constitute a valuable experience database on the performance of dams subjected to earthquake shaking. Beginning with the seminal work of Newmark (1965) and Seed (1966), significant progress has been made over the same period in developing procedures to evaluate the effects of earthquake shaking on dams. In contrast, limited experience is available regarding the performance of dams under foundation fault rupture. Comparatively few studies on the evaluation of dams for the effects of fault rupture have been reported in the literature.

Nonetheless, insightful research into the response of embankment dams to foundation faulting and the propagation of fault rupture through soil has been carried out in the past few decades (e.g. Bray, 1990, Lazarte, 1996). Although procedures for the analysis of foundation rupture effects on dams have not yet been well established, significant progress has been made in developing approaches to evaluate the response of embankment dams under foundation faulting (e.g. Mejia and Dawson, 2009). In addition, much progress has been made on the understanding of potential failure modes and in developing mitigation concepts applicable to the design of embankment dams subject to fault rupture.

This paper presents an overview of experience related to fault rupture of dams and of the factors to be considered in the evaluation of embankment dams for foundation faulting, and describes an approach to analyze the effects of such loading on embankment dam stability. It also presents an overview of the key considerations involved in the design of embankment dams for fault

displacement and illustrates the issues associated with analysis and design of such dams for fault rupture through selected case histories.

The behaviour of concrete dams under fault rupture is expected to be markedly different than that of earth dams. Because of their brittle nature, concrete dams are generally considered to be significantly less tolerant of foundation displacement than earth dams. Further discussion of the design of concrete dams for foundation displacement is beyond the scope of this paper.

2 EXPERIENCE WITH FAULT RUPTURE OF DAMS

In view of the fact that many dam foundations are traversed by faults, it seems remarkable that few dams have been affected by earthquake fault rupture. In fact, until the rupture of Shing-Kang Dam during the M 7.6 1999 Chi Chi earthquake in Taiwan, no failure of a dam as a result of earthquake fault displacement had been previously reported. A few cases of previous fault rupture beneath or near dams are described by Sherard et al. (1974). Those cases and post-earthquake observations (e.g. Bonilla, 1970; Bray et al., 1994a) have served to illustrate the mechanisms of fault rupture at the ground surface and through dam embankments.

Selected experience relevant to the design of dams to withstand foundation fault rupture is listed in Table 1. That experience serves to illustrate the state of practice in the design of dams for foundation displacement, and the types of issues encountered in defining design criteria, evaluating expected dam performance, and developing design details to mitigate the effects of foundation rupture.

Table 1. Experience related to dam design for foundation fault rupture

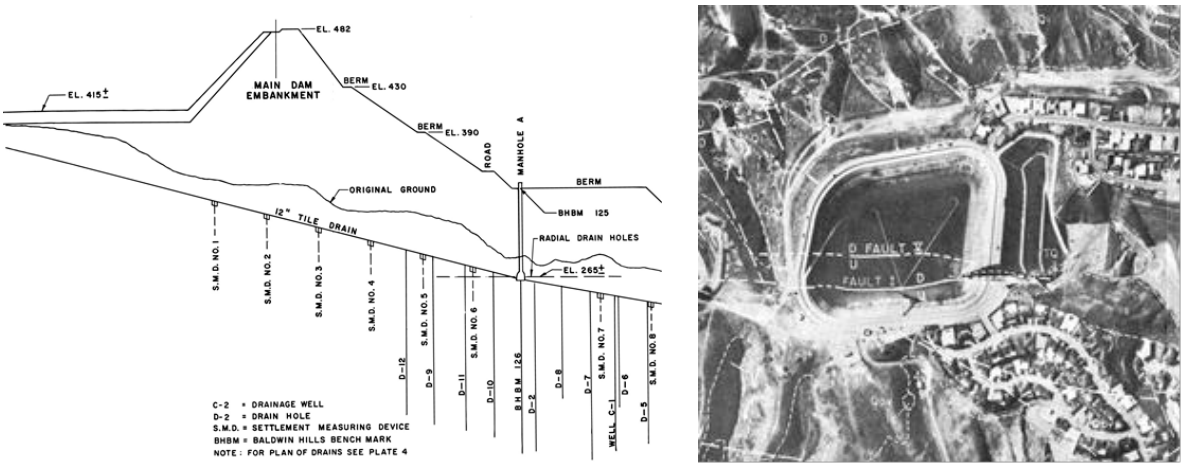
Dam Name	Location	Year Built	Reference
Aviemore	New Zealand	1960's	Mejia et al. (2006)
Baldwin Hills	California	1951	Sherard et al. (1974)
Borinquen	Panama	In progress	Mejia et al. (2011)
Cedar Springs	California	1971	Sherard et al. (1974)
Clyde	New Zealand	1990's	Hatton et al. (1991)
Coyote	California	1936	Sherard et al. (1974)
Eastside Reservoir	California	1990's	Allen & Cluff (2000)
Los Angeles	California	1977	Leps (1989)
Matahina	New Zealand	1960's	Mejia et al. (1999)
Morris	California	1935	Sherard et al. (1974)
Neelum-Jhelum	Pakistan	In progress	Dickson et al. (2013)
Seven Oaks	California	1990's	Allen & Cluff (2000)
Tarbela	Pakistan	1970's	Allen & Cluff (2000)

The limited experience available regarding the performance of dams subjected to foundation fault displacements indicates that such displacements can be very detrimental to the integrity of earth dams. For example, the failure of Baldwin Hills Reservoir in California illustrates the susceptibility of dams built with brittle soil materials and inadequate drainage to cracking, internal erosion, and piping as a result of foundation shear displacements.

The Baldwin Hills Reservoir was retained by a 47-m-high embankment dam with a 1.5-to-3-m-thick upstream impervious earth lining, underlain by a 0.1-m-thick cemented pea gravel drain. Figure 1(a) shows the embankment section including the impervious liner. Site excavation revealed the presence of minor vertical bedrock faults across the reservoir floor and the embankment foundation as shown in Figure 1(b). In December 1963, the dam breached as a result of piping failure.

The post-failure investigations indicated that an approximate 0.15-m offset (apparently associated with subsidence induced by regional oil extraction) across one of the bedrock faults cracked the impervious liner and ruptured the pea-gravel under-drain allowing internal erosion of the liner soil. Internal erosion progressed to piping and breaching of the dam within 4 hours of the initial observations of piping. Although not earthquake related, this dam failure illustrates

the vulnerability of inadequately designed embankment dams to foundation fault displacement, however small.



(a) Embankment maximum section (b) Reservoir site faults

Figure 1. Embankment section and foundation faults at Baldwin Hills Dam

3 PREVIOUS RESEARCH

Whereas research on the performance, analysis, and design of dams subject to earthquake shaking has been extensive over the past four decades, comparatively limited research has been carried out for dams subject to foundation fault displacement. Notable work has included comprehensive reviews of the state of practice on dam design for fault rupture such as those by Sherard et al. (1974), Leps (1989), and Allen and Cluff (2000). Those studies also addressed the key aspects of geologic investigations necessary to assess fault rupture hazard.

Insightful research has been performed on the mechanics and the analysis of dam rupture by foundation shear displacement. Bray (1990) reviewed earthquake observations, undertook laboratory experiments of fault rupture, performed numerical analyses using finite element techniques, and showed that the extent of fault rupture propagation through soil depends on the soil stiffness, which can be related to the shear strain at 95% of the soil's strength (referred to as the failure strain). Lazarte (1996) extended Bray's review of case histories and the experimental and analytical work and showed that strain localization is a key element of numerical modelling of fault rupture propagation through soil. Anastosopoulos et al. (2007) showed that proper modelling of dilation and strain softening are required to replicate observed behaviour in centrifuge tests in sands. Mejia and Dawson (2009) presented a methodology for the analysis of dam response to foundation fault rupture that incorporates those research findings and other essential elements of the safety evaluation of dams.

4 EFFECTS OF FOUNDATION FAULT RUPTURE

Besides strong earthquake shaking, coseismic offset of an embankment dam foundation by fault rupture will result in shearing and distortion of the embankment. Previous research (e.g. Bray, 1994b; Lazarte, 1996) indicates that the degree of shearing and the extent to which the rupture propagates upwards within the embankment will depend on the magnitude and style of the fault displacements and on the stiffness of the embankment materials. As the rupture propagates, it will offset the embankment inducing shear and tensile strains with consequent cracking and leakage or increased seepage. Additional effects may include loss of freeboard and reservoir seiche induced by the tectonic fault displacements.

Propagation of the rupture within a zoned dam will result in partial or possibly full offset of the impervious core, filters, and other zones that make up the embankment. The associated

New Zealand Geotechnical Society Inc. 19th Symposium, Queenstown 2013

deformations can result in cracking of the core and other zones and consequent leakage or increased seepage. If filters are lacking, if they sustain cracks, or if they are fully offset, leaks or increased seepage may lead to internal erosion and piping through the embankment. If not adequately drained, leaks or increased seepage may also result in high pore water pressures in the embankment that could lead to slope instability. Major leakage can also result in embankment instability through erosion and/or ravelling of the downstream slope.

Depending on the nature of the dam foundation, fault rupture may be associated with a tendency for dilation of the foundation materials and the creation of new cracks or fissures other than pre-existing features associated with previous fault rupture events. Dilation of pre-existing features and/or formation of new cracks and fissures will lead to increased seepage or leakage through the foundation. Such flows can result in internal erosion and piping of the foundation materials and of the overlying embankment, if not properly protected by filters or crack-stopper zones. Lacking adequate drainage, increased foundation seepage could also lead to excess pore water pressures and structural instability.

5 KEY FACTORS AFFECTING EMBANKMENT PERFORMANCE

The extent to which the above fault rupture effects develop in an embankment dam or its foundation will depend on several factors as summarized in Table 2.

New Zealand Geotechnical Society Inc. 19th Symposium, Queenstown 2013

Table 2. Key Factors Affecting Embankment Performance

Potential Effect of Fault Rupture	Key Factors Affecting Embankment Performance
Shear offset of embankment zones	• Amplitude and style of foundation rupture • Extent of rupture propagation within embankment
Cracking of core, impervious zones, or other cohesive embankment zones	• Amount and style of shear offset in cohesive zones • Plasticity and ductility of core or cohesive materials • Magnitude of tensile stresses and strains induced by shear deformations
Cracking or fissuring of foundation	• Amount of shear offset in foundation • Activity of past repeat displacement on dam site faults • Stiffness and ductility of foundation materials • Overburden stress from embankment loads
Leakage and/or increased seepage	• Extent, width, depth, and location of cracks • Presence and post-rupture continuity of filter and crack-stopper zones
Continued erosion and piping	• Presence and post-rupture continuity of filters, and of zones unable to support piping cavities • Erodibility of embankment and foundation materials
Increased pore water pressures and slope instability	• Post-rupture continuity of drain and/or transition zones • Strength and drainage of downstream zones
Downstream slope erosion and raveling	• Erosion resistance and protection of downstream slope • Flow-through resistance of downstream embankment zones

If shearing or cracking of the core or main water barrier occurs, a key concern will be the ability of the embankment and foundation to handle leakage without development of internal erosion or piping. This will depend on two main factors: a) the erodibility of the embankment and foundation materials and their ability to support piping cavities, and b) the extent to which filter and drainage zones remain continuous and functional across the zone of shearing to prevent internal erosion and migration of materials and the development of a piping or instability failure mechanism.

Thus, the key issues to be addressed in evaluating the effects of shearing of an embankment dam by foundation fault rupture may generally be summarized as follows:

- The extent to which the rupture will propagate from the foundation upwards within the embankment.

- The amount of distortion and offset of the foundation and of the dam's core and impervious zones, which might lead to cracking and leakage.
- The location and extent of cracking, and the amount of leakage resulting from such cracking and general distortion of the embankment and foundation.
- The resistance of the embankment and foundation materials to internal erosion under the flow velocities associated with increased seepage or leakage.
- The amount of offset and distortion of the embankment zones, such as filter and drainage zones, designed to control seepage and leakage.
- The ability of filter and drainage zones to remain functional after offset and distortion and prevent internal erosion from developing into continued erosion.
- The ability of the embankment and foundation materials to support piping cavities and the potential for continued erosion to lead to piping through the dam and/or foundation.
- The capacity of pervious downstream embankment zones to pass-through leakage flowing through piping or erosion cavities, without slope or toe erosion and instability.

6 APPROACH TO EVALUATION OF DAM PERFORMANCE

A general approach to address the key issues associated with fault rupture of an embankment dam and to analyse its performance under the effects of such rupture has been proposed by Mejia and Dawson (2009). That approach consists of the following steps.

1. Perform a numerical analysis to calculate the deformations and stresses induced in the dam by the foundation displacements associated with the fault rupture.
2. Evaluate the shear offset of the embankment zones, in particular of the core and filter and drainage zones, from the calculated deformations.
3. Based on the stresses calculated from the analysis, estimate the location and extent of cracking of the core and other embankment zones.
4. Estimate potential leakage through cracks in the core and assess the erodibility of the core and other embankment materials.
5. Based on the calculated embankment deformations and stresses, evaluate the post-rupture continuity and functionality of filter and drainage zones.
6. Assess the potential for continued erosion of the embankment and foundation materials considering the post-rupture functionality of filter and drainage zones.
7. Evaluate the through-flow resistance of any pervious downstream embankment zones.
8. Assess the likelihood of piping or instability failure based on the potential for continued erosion and development of piping cavities within the embankment and foundation and on the through-flow resistance of the embankment.

7 DESIGN CRITERIA FOR FAULT DISPLACEMENT

Although most published guidelines and regulatory requirements address the selection of earthquake vibratory motions for dam analysis, few provide guidance regarding fault surface displacements. Moreover, modest experience and precedent are available in the profession regarding the selection of foundation fault displacements for safety evaluation of dams.

The characterisation of design fault displacement should be based on adequate knowledge of the regional and site geology and careful study of foundation faults. Such studies should be aimed at defining the location and orientation of the faults, their activity and record of past surface displacement, and the characteristics and nature of possible future displacement including potential for distributed or secondary deformation. A key consideration in developing design criteria is the fact that the vulnerability of dams to foundation fault displacement can be significantly higher than that to vibratory motion.

In general, new dams are required to withstand a Safety Evaluation Earthquake (SEE) without severe damage, while existing dams are typically required to withstand such event without catastrophic release of the reservoir. New dams of economic importance are also required to withstand an Operating Basis Earthquake (OBE) with minor damage only. For high hazard

New Zealand Geotechnical Society Inc. 19th Symposium, Queenstown 2013

dams, it is common to adopt the maximum credible earthquake (MCE) as the SEE (Mejia et al., 2002). The MCE is defined as the maximum earthquake on the seismic source that is capable of inducing the largest seismic demand on a dam.

For any one fault in the foundation, the parameters required to characterise fault displacement for engineering evaluation of a dam will generally include: a) the strike and dip of the fault at foundation level, b) the displacement rake, which may be characterized by the vertical-to-horizontal displacement ratio, and c) the amplitude of displacement, which is best characterized by the horizontal and vertical separations across the fault. The displacement amplitude defines the intensity of the load while other parameters define its orientation and style. As for other loads, it is important that characterization of fault displacement adequately reflect uncertainty in the amplitude of the load and in its orientation.

Available guidance generally calls for fault surface displacement for the MCE to be defined consistently with vibratory ground motions (e.g. Mejia et al., 2002; Mejia et al., 2005). Thus, for high hazard dams, such guidance defines the MCE fault displacement amplitude at the mean-plus-one-standard-deviation level except that the displacement need not exceed the value associated with an annual probability of about 1/10,000. For medium and low hazard dams, the design foundation displacement is defined between the 50th- and the 84th-percentile levels, except that it need not have an annual probability smaller than about 1/2,500. No fault surface displacement is typically associated with the OBE.

8 DESIGN FOR FAULT RUPTURE

8.1 Design Principles

In general, the basic principles used for the design of embankment dams to withstand normal and unusual loads, including earthquake shaking, will apply to their design for foundation fault displacement. The well-accepted principles of design redundancy and of using multiple lines of defence against potential failure modes are particularly applicable to the design of dams for fault rupture. Embankment dam design to withstand such loading will generally require multiple lines of defence to: a) control leakage or increased leakage, b) minimize potential internal erosion, and c) maintain structural stability.

8.2 Leakage or Increased Seepage

Control of leakage or seepage through the embankment or foundation is generally a high priority in design, as leakage or seepage can lead to dam failure by piping or slope instability. One line of defence is to use embankment impervious materials that are plastic and can tolerate shear deformations without cracking. Another common design feature is to provide so-called 'crack-stopper' zones of broadly-graded materials upstream of locations of potential cracking in the embankment or foundation. The design concept behind such zones is that leakage flows will erode the materials into any open cracks and that material accumulation will progressively seal the cracks and staunch the leakage. However, it is difficult to assure the reliability of 'crack-stopper' zones in any given situation and thus, they are commonly viewed as a supplementary line of defence.

If significant fault displacements are possible, it is generally appropriate to: a) assume that the dam impervious materials will crack, and b) provide filter zones of cohesionless soils downstream of the impervious zones. Assuming that filter zones remain continuous across crack locations, they will limit flow velocities and prevent continued erosion of the embankment materials from enlarging the cracks or seepage paths and from leading to increased flows and piping. Furthermore, as impervious material erosion occurs it will likely blind properly designed filters at the crack locations and tend to staunch the leakage. Depending on the nature of the dam foundation, it will also be appropriate to assume that cracking will occur in the foundation and to provide filter zones to prevent erosion of foundation materials.

Assuring continuity of filters across crack locations will require the use of cohesionless materials that are unable to support open cracks. In addition, filter zones must be amply

dimensioned so that they will not be fully offset by the fault rupture and will have adequate post-rupture continuity, particularly if they also serve a drainage function. Considering the importance of maintaining filter continuity, recent practice has been to provide filter zones with a thickness at least 1.5 times greater than the expected filter shear offset corresponding to the design fault displacements and that satisfies other design and construction requirements (e.g. Wieland et al., 2008; Mejia et al., 2011). Similar dimensioning criteria have also been used for other zones where post-rupture continuity is desired, such as the embankment impervious core and drain zones downstream of the filter.

8.3 Resistance to Internal Erosion

Prudent dam design typically calls for multiple lines of defence to minimize the potential for internal erosion in embankment dams and their foundations. Impervious materials with a low susceptibility to erosion are usually considered as a desirable line of defence in dam design. Thus, dispersive soils are generally avoided in the impervious zones of dams. Often, materials of medium or high plasticity and significant ductility and resistance to cracking also have a low to moderate susceptibility to erosion. On the contrary, materials of low plasticity tend to be erodible.

The most reliable line of defence against internal erosion is a properly designed filter zone (Sherard, 1967; ICOLD, 1994). To be effective, such zone must have an adequate thickness as discussed above, and consist of durable cohesionless soils with a proper gradation to fulfil two key functions: material retention and drainage. Depending on the characteristics of the materials to be retained and of the materials downstream of the filter, two or more adjacent filter zones of compatible gradations may be required to achieve both functions in a dam. Modern guidance for the design of filter zones has been summarized in publications by USBR (1994) and ICOLD (1994). Foster and Fell (2001) have presented procedures for assessing the performance of filters that do not comply with such modern design criteria.

Where cracking of a dam and its impervious core might occur as a result of static or seismic deformation, the ability of filter materials to deform without sustaining open cracks or cavities is a critical characteristic of such materials. Because cracking of filter zones might compromise their function, special care must be exercised to build such zones of cohesionless materials that are unable to support open cracks and that prevent the development of piping cavities.

8.4 Structural Stability

Additional lines of defence to assure structural stability include: a) amply dimensioned chimney and blanket drainage zones designed to discharge possible leakage flows that might otherwise raise pore-water pressures and cause instability, b) a large downstream zone of strong, pervious materials, and c) reinforcement of the downstream slope and toe to provide a large through-flow resistance. The latter may be considered a last line of defence to control large flows through the embankment from progressively eroding the downstream slope and causing instability.

8.5 Potential Cracking of Fine Filters

Even if a filter sand is properly graded and shaped, it will typically exhibit apparent cohesion in a moist state and will be able to sustain cracks or cavities over substantial periods under moderate overburden stress. An example of a moist-and-clean sand's ability to stand vertically in a 1.5-m-deep trench is illustrated in Figure 2(a). Upon saturation, however, the sand will lose its apparent cohesion and collapse immediately; closing open cracks or cavities (Figure 2(b)).

In a moist state, apparent cohesion in a sand results from the inter-granular stresses induced by capillary forces. In a saturated state, such forces do not exist and the sand does not exhibit apparent cohesion, thus collapsing before cavities or cracks can develop. In the case of saturation by a seepage front advancing through previously unsaturated material, capillary action ceases as saturation occurs and the material loses apparent cohesion and becomes unable to support cavities or cracks.

New Zealand Geotechnical Society Inc. 19th Symposium, Queenstown 2013



(a) Trench walls (1.5 m deep) stand vertically under capillary action

(b) Trench walls collapse upon flooding with clean water

Figure 2. Behavior of moist, clean filter sand in trench collapse tests

Thus, a properly graded and shaped filter material below the phreatic surface in a dam will exhibit cohesionless behavior and not support cracks or cavities. However, filter sands above the water table are likely to support cracks and cavities to depths of at least a few meters, as schematically shown in Figure 3, which might inhibit their filter function (Mejia, 2013).

Such condition is of concern where a fine filter is unsaturated at an elevation below the reservoir level, and sudden cracking of the embankment provides a path for leakage to reach the unsaturated filter (Figure 3). If cracked, water flow will likely saturate the filter materials causing them to collapse and close the cracks. The extent to which this mechanism is successful in closing cracks before significant erosion occurs is likely to depend on: a) the crack size and depth, b) the flow velocity, and c) the downstream presence of transition or drain materials that prevent erosion of the filter, before the cracks are closed.

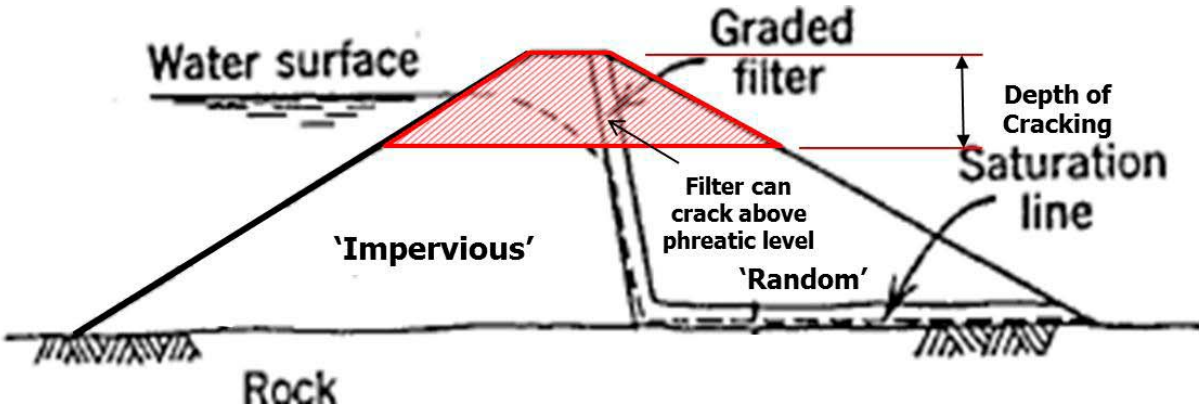


Figure 3. Potential for cracking of unsaturated fine filter below reservoir level

If embankment deformations result in small cracks, it is likely that a properly designed fine filter material would collapse before significant internal erosion takes place. However, in the presence of large cracks or cavities and absent a downstream filter-compatible transition or drain zone, progressive collapse of the filter material may not staunch flows before significant

erosion occurs. Thus, in a situation where large cracks or cavities may develop suddenly in a dam, as in the case of rupture by fault displacement or seismic deformation, zones of filter-compatible transition or drain materials are necessary immediately downstream of a fine filter to prevent erosion of the filter materials, should they crack temporarily and be situated below the reservoir level.

9 CASE HISTORIES

Two case histories are presented below to illustrate various aspects of the analysis and design of embankment dams for foundation fault rupture. They are the seismic evaluation of Aviemore Dam and the seismic retrofit of Matahina Dam. Additional details on these case histories are presented by Mejia et al. (2006) and Mejia et al. (1999), respectively.

10 AVIEMORE DAM SEISMIC EVALUATION

Aviemore Dam was built in the 1960's and consists of a 364-m-long, 56-m-high concrete gravity section, and a 430-m-long, 49-m-high earth embankment. It is classified as a high hazard structure. An aerial view of the dam is shown in Figure 4.

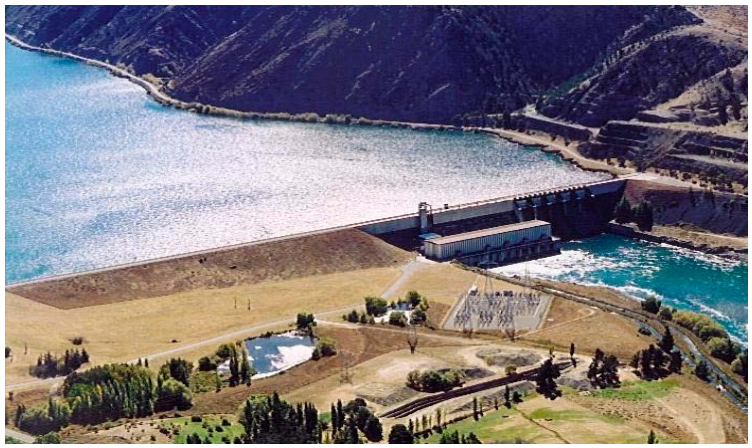


Figure 4. Aerial view of Aviemore Dam

The Waitangi fault crosses the embankment foundation about 30 m from the interface with the concrete dam, and strikes almost normal to the dam axis. The concrete dam and the embankment left (east) of the fault are founded on greywacke of Mesozoic age. Right (west) of the fault, the earth dam is founded on Tertiary claystones and sandstones and Quaternary alluvial and fan gravels.

As shown in Figure 5, the earth dam is a zoned embankment with an upstream sloping impervious core flanked by pervious shoulders. A sand filter separates the core from the downstream shoulder, and blankets the bottom of the core trench under the shoulder. The internal geometry varies along the length of the embankment because the core is flared as it approaches the concrete dam. The core consists of medium plasticity silty clay. The filter is well-graded sand and is approximately 1 m thick. Broadly graded sandy gravels with cobbles and boulders make up the shoulders.

10.1 Seismic Evaluation Criteria

During construction, the Waitangi Fault was recognized in the foundation but was not considered to be active. However, trenches excavated recently along the fault near the dam site disclosed late Quaternary single-event vertical displacements of 1 to 2 m, upwards on the earth dam side.

The SEE for analysis of the dam was defined using the criteria proposed by Mejia et al. (2002). The maximum earthquake on the Waitangi fault, a magnitude M_w 7.0 event, was adopted as the SEE. A fault vertical separation of 1.2 m and a horizontal to vertical displacement ratio (H:V) of 1:3 were adopted to define the SEE fault surface displacement at the site. Additional details of

New Zealand Geotechnical Society Inc. 19th Symposium, Queenstown 2013

the SEE characteristics and of the procedures used to develop them are presented by Mejia et al. (2005).

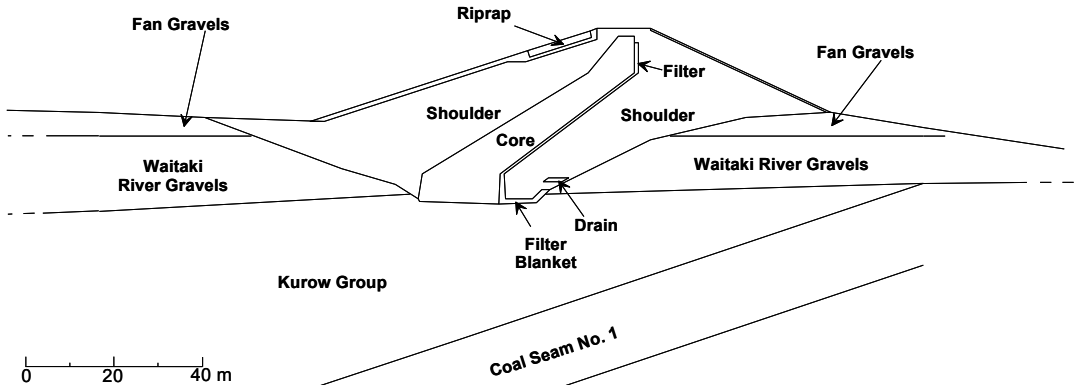


Figure 5. Representative Embankment Cross Sections

10.2 General Approach to Seismic Evaluation

The key issues addressed in the dam's seismic safety evaluation included: a) the dam's stability under strong earthquake shaking, b) its integrity under foundation fault rupture, c) the potential for dam overtopping due to reduction in reservoir storage and seiche, and d) the seismic performance of the appurtenant works. Only the analyses of the embankment dam for foundation fault rupture are described herein. Other aspects of the evaluation are discussed by Mejia et al. (2006).

Because the concrete dam is located on the fault downthrown block about 30 m away from the upthrown block, surface rupture of the Waitangi Fault is expected to shear the earth dam but not disrupt the concrete dam foundation significantly. Reverse faulting typically will not result in major disruption of the downthrown block. Furthermore, because the Mesozoic greywacke rock of the downthrown block is much stronger than the Tertiary deposits of the upthrown block, it is unlikely that significant shear deformations will extend into the downthrown block.

Shearing of the embankment by fault rupture, will occur concurrently with earthquake shaking. Although the effects of foundation rupture will be compounded with those of shaking, the embankment shearing will be driven primarily by the foundation displacement.

10.3 Analysis for Foundation Fault Rupture

The structural response of the dam to the SEE fault surface displacement was analyzed using the 3-D finite difference program FLAC^{3D} (Itasca, 2002). The finite difference mesh shown in Figure 6 was developed based on the geometry of the embankment and alluvium at the location where the fault crosses the dam foundation and the base of the model was offset at this location to simulate the fault surface displacement.

Two alternative constitutive models were used to represent the stress-strain properties of the dam and foundation materials because those properties are not known with certainty. The model parameters were obtained from laboratory testing, field shear wave velocity measurements, and published data for similar materials. Post-peak strain softening and dilation were included in both stress-strain models as those aspects of material behaviour strongly affect the localization of strains and the propagation of fault rupture (Lazarte, 1996).

10.4 Analysis Results

The 3-D finite difference mesh was used to calculate deformations and stresses throughout the embankment for various amounts of fault vertical separation (FVS). The calculated deformations and stresses were used to evaluate the nature and amount of embankment distortion and the propagation of fault rupture within the embankment, and to estimate the extent and depth of cracking.

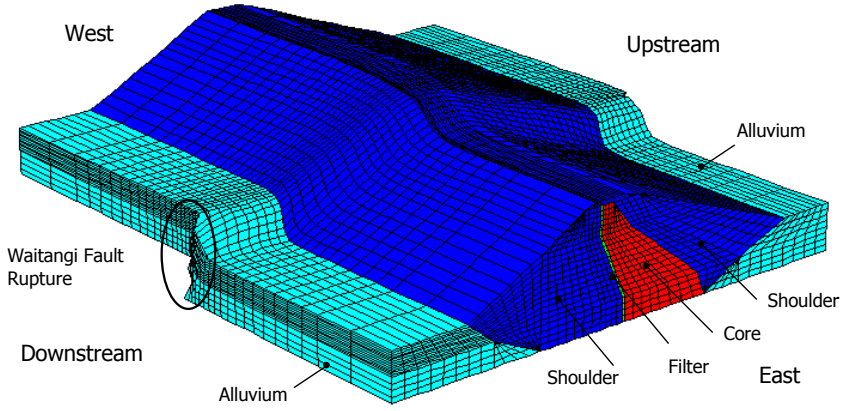


Figure 6. Three-dimensional Mesh of Dam for Analysis of Foundation Rupture

The extent of rupture propagation within the embankment was obtained from the calculated contours of stress level. This is defined as the ratio of the deviatoric stress to the strength of the material. Bray el al. (1994) found that this is a convenient parameter to track fault rupture through soil, and that the 95% stress level contour is a good indicator of the length of the rupture zone. This is because a stress level of 95% marks approximately the development of shear failure in many soils.

For example, Figure 7 shows the stress level on a longitudinal section of the embankment cut 10 m downstream of the crest centreline, for 0.5 m of FVS. The model predicts propagation of the rupture to about one-half the height of the embankment. The calculated stresses and displacements indicate that the zone of embankment deformation will likely be several tens of meters long, extending from west of the vertical projection of the foundation fault offset (see Figure 7) to near the concrete dam. The chimney filter is not expected to be fully offset anywhere along its height during the SEE. However, full offset is expected to occur across the filter blanket extending downstream over the foundation because the blanket is about 0.9 m thick.

The extent and depth of cracking were assessed based on the calculated changes in the state of stress within the embankment due to fault rupture. The results indicate that embankment deformations will likely result in cracking of the core at the crest in an approximately 30-m-long zone extending west of the rupture. Little if any cracking is expected east of the rupture. The cracking at the crest is likely to be primarily transverse to the dam axis, although some longitudinal cracking is also expected, and to extend to a depth of about 5 m. No cracking of the core is expected below a depth of about 10 m.

10.5 Effects on Embankment Stability

Cracking caused by fault rupture will be compounded with the effects of earthquake shaking. Tectonic foundation deformations could also increase the severity of cracking, possibly extending the zone of cracking and increasing the width of cracks. Cracking of the core west of the crest rupture will lead to leakage. The leakage will be controlled by the filter, which is expected to remain continuous across the zone of cracking. As the filter remains continuous across the zone of embankment shearing and cracking, it will prevent internal erosion of the embankment materials by leakage from progressing to a piping failure.

Foundation faulting during the SEE will result in full offset of the filter blanket that extends over the base of the core trench. The fault zone is a low permeability feature as demonstrated by low piezometric levels and seepage quantities observed downstream of the core. Because the faulted materials are weak rocks that have been sheared repeatedly in the past, they are expected to shear again without significant dilation that might lead to a marked increase in permeability. Therefore, it is unlikely that the fault displacements will lead to concentrated leaks or a marked increase in hydraulic gradients through the foundation.

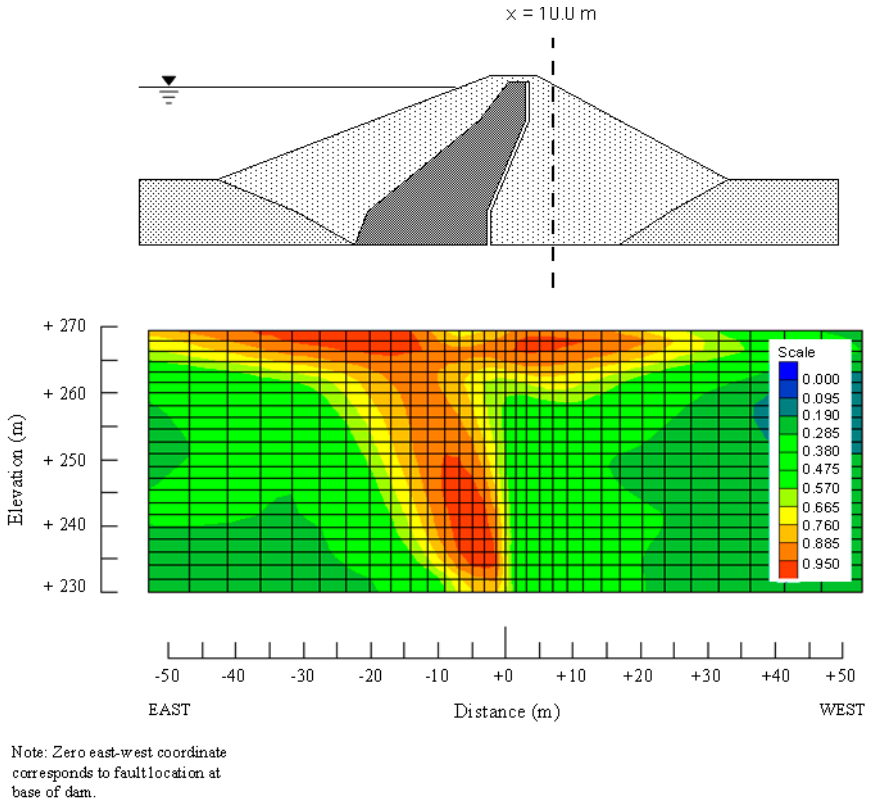


Figure 7. Contours of Stress Level 10 m Downstream of Crest Axis, Calculated for 0.5 m Fault Vertical Separation

11 MATAHINA DAM SEISMIC RETROFIT

Matahina dam is an 82-m-high, 400-m-long, zoned rockfill embankment with a sloping earth core located on the Rangitaiki River in the North Island of New Zealand. The dam is part of the Matahina Power Station. A cross-section of the dam before its seismic retrofit is shown in Figure 8. The core and inner transition zones are founded on consolidated deposits of gravelly silty sands, silts, and clays of tertiary age, in a trench excavated through the alluvium. The outer transitions and the rockfill shells are founded on alluvium (Figure 8).

The core material is sandy clayey silt to silty clay derived from weathered greywacke. It was placed dry of optimum to high densities and is stiff, brittle, and readily erodible. The inner transition consists of sandy silt sourced from unwelded ignimbrite, and was compacted to high densities with a high unconfined compressive strength. The outer transition was built with strippings of hard welded ignimbrite and grades from sandy gravel to gravelly silt. The rockfill shells consist of hard ignimbrite blocks ranging in size from 150 to 900 mm.

Since its construction in the 1960's, the dam experienced two serious piping incidents that required substantial repairs. The first occurred in 1967 during first filling when a large temporary increase in flow from the drainage blanket was observed and an erosion cavity was subsequently detected near the right abutment. The second incident occurred in connection with the 1987 Edgecumbe earthquake (M_L 6.3). The dam was repaired by reconstructing the core and transition zones and the foundation contacts at both abutments (Gillon and Newton, 1991).

11.1 Dam Seismic Evaluation

The project site is located within a zone of quaternary right-lateral strike-slip faulting known as the North Island Shear Belt. The western-most fault in this zone, the Waiohau fault, passes through the site. Although strands of the fault were exposed in the core trench during construction, they were considered to be inactive at the time. Recent studies, which included trenching across the fault near the dam, showed that the fault has generated four major

earthquakes in the last 11,800 years and that it has the potential for generating large surface fault displacements at the dam site.

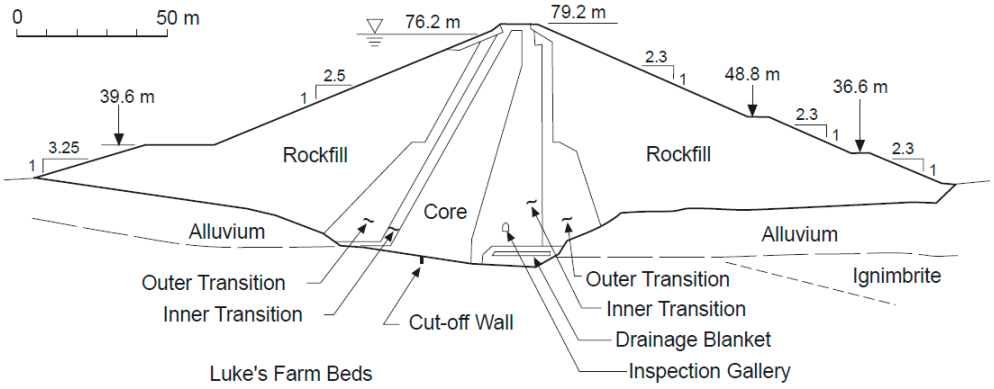


Figure 8. Dam cross-section before seismic retrofit

The SEE was defined as the maximum earthquake on the Waiohau fault, except that its vibratory motions and surface displacement needed not have an annual probability smaller than 1/10,000. Such earthquake was estimated to be a magnitude M_w 7.2 event. The fault surface displacement was characterized by 2.7 m of horizontal offset and 1.3 m of vertical offset occurring on any of the fault strands beneath the dam or distributed between them.

Field investigations subsequent to the 1967 leakage incident revealed that the core cracking was associated with differential settlements of 0.3 m near the core-abutment contact. During the 1988 repairs, numerous open cracks were encountered in the core and inner transition near both abutment contacts at depths of up to 25 m. The observations showed that small differential shear deformations were sufficient to induce cracking of the core and inner transition and initiate internal erosion of the embankment.

11.2 Dam Seismic Retrofit

Several alternatives to retrofit the dam were evaluated, including: strengthening the dam with a leakage-resistant buttress, reinforcing the downstream shell for large through-flow, in-place installation of new vertical filter and transition zones, removing and replacing the dam, flood protection with a downstream dry dam, restricting the reservoir level, and decommissioning. Strengthening the dam with a leakage-resistant buttress ranked highest in terms of performance reliability, construction feasibility, environmental impact, and cost.

The concept behind the leakage-resistant buttress is to prevent internal erosion of the core and inner transition from leading to piping of the dam and collapse of the dam crest. The design cross-section is shown in Figure 9. The buttress filter is designed to arrest migration of the core materials and to limit flows even if the core is breached. The design assumes that full reservoir head could develop on the upstream face of the filter after the SEE. The new drain is designed to limit the development of a high phreatic surface within the rockfill. The oversize rockfill zone is designed to prevent erosion at the downstream toe under through-flow in excess of 50 m^3/s.

To prevent piping through the foundation, the filter and transition zones were extended to rock in a cutoff trench through the alluvium. To provide an adequate margin against shearing of the filter, transitions, and drain, the minimum horizontal and vertical dimensions of those zones (Figure 9) were set at twice the corresponding components of fault displacement during the SEE.

Cohesionless materials that will not sustain cracks and will run into any cavities that may develop as a result of the fault displacements were specified for the filter and transition zones. The filter and transition materials were obtained by crushing hard ignimbrite rock. A field and laboratory test program was undertaken to confirm that the crushed rock materials would not sustain open cracks or cavities. In addition, special provisions were included in the

specifications to ensure that this and other desired material characteristics were obtained during construction.

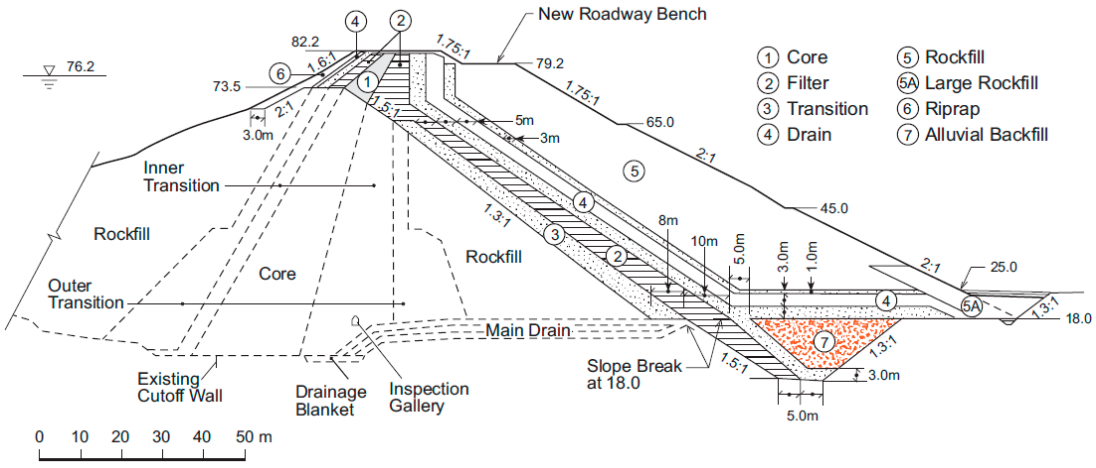


Figure 9. Cross-section of leakage-resistant buttress

New Zealand Geotechnical Society Inc. 19th Symposium, Queenstown 2013

The design concept included widening the crest of the dam and raising it by 3 m. The increased freeboard allows for seismically induced settlements, crest subsidence from possible collapse of erosion cavities, and residual freeboard to pass the 20-year flood after the SEE. The dam upgrade also included: a) strengthening the spillway and low-level-outlet gates and the spillway walls for seismic shaking, b) modifications to force open the spillway gates (if jammed), c) modifications to the gate controls and power supplies to assure emergency operability, and d) features to protect the dam from overtopping if the spillway and outlet were to be rendered inoperable.

12 SUMMARY AND CONCLUSIONS

This paper has presented an overview of experience related to fault rupture of dams and of the factors affecting embankment dam performance under foundation offset. It has also described a recently developed approach to evaluate the effects of foundation faulting on embankment dam stability, and the key considerations involved in the design of embankment dams for fault displacement. Selected case histories were presented to illustrate the issues associated with analysis and design of embankment dams for fault rupture.

In spite of the limited experience available regarding the performance of dams under fault rupture, significant progress has been made in developing an understanding of potential failure modes that may be initiated by foundation offset. Much progress has also been made in developing procedures to evaluate the response of embankment dams to foundation faulting, and in developing mitigation concepts applicable to the design of embankment dams subject to fault rupture.

13 ACKNOWLEDGEMENTS

The author wishes to acknowledge and thank the large teams of professionals from ECNZ, Meridian Energy, URS Corporation, Opus International Consultants, the New Zealand Institute of Geological and Nuclear Sciences, who contributed to the case histories presented in the paper.

14 REFERENCES

Allen, C. and Cluff, L. (2000) Active Faults in Dam Foundations: An Update, Proceedings of 12th World Conference on Earthquake Engineering, Paper No. 2490, Auckland, New Zealand.

Anastosopoulos, I., Gazetas, G., Bransby, M.F., Davies, M., El Nahas, A. (2007) Fault Rupture Propagation through Sand; Finite-Element Analysis and Validation through Centrifuge Experiments, Journal of Geotechnical and Geoenvironmental Engineering, ASCE, August.

Bonilla, M.G. (1970) Surface faulting and related effects, In *Earthquake Engineering*, E. R. L. Wiegel, Prentice Hall, New Jersey, 47-74.

Bray, J.D. (1990) The effects of tectonic movements on stresses and deformations in earth embankments, *Ph.D. Thesis*, University of California, Berkeley, California, USA.

Bray, J.D., Seed, R.B., Cluff, L.S., Seed, H.B. (1994a) Earthquake fault rupture propagation through soil, Journal of Geotechnical Engineering, ASCE, 120. No. 3, pp 543-561.

Bray, J.D., Seed, R.B., Seed, H.B. (1994b) Analysis of earthquake fault rupture propagation through cohesive soil, Journal of Geotechnical Engineering, ASCE, 120. No. 3, pp 562-580.

Dickson, P.A., Kovacich, J.R., Raptis, G. (2013) Design details to accommodate fault movement in a dam foundation, Proceedings 7th Int. Conf. on Case Histories in Geot. Eng., Chicago, May.

Foster, M. and Fell, R. (2001) Assessing Embankment Dam Filters that Do Not Satisfy Design Criteria. Journal of Geotechnical and Geoenvironmental Engineering, Vol. 127, No. 5, 398−407.

Gillon, M. and Newton, C. (1991) Abutment Repairs at the Matahina Dam, Proceedings, 17th ICOLD Congress, Vienna, Austria.

Hatton J.W., Foster P.F. and Thomson R. (1991) The influence of foundation conditions on the design of Clyde dam, Proc. 17th Congress on Large Dams, Vienna, Q.66 R.10, 5, 365-367.

International Commission on Large Dams (ICOLD). (1994) Embankment dams granular filters and drains, ICOLD Bulletin No. 95.

Itasca Consulting Group. (2002) FLAC3D, Version 2.10. Fast Lagrangian Analysis of Continua in 3 Dimensions, *User's Manual*, Minneapolis, Minnesota, USA.

Lazarte, C. A. (1996) The response of earth structures to surface fault rupture, Ph.D. Thesis, University of California, Berkeley, California, USA.

Leps, T.M. (1989) The Influence of Possible Fault Offsets on Dam Design, Water Power and Dam Construction, April.

Mejia, L. (2013) Field tests of filter material for seismic retrofit of Matahina Dam, Proceedings of ICOLD International Symposium, Seattle, Washington, USA, August.

Mejia, L., and Dawson, E. (2009) Analysis of Dam Response for Foundation Fault Rupture, Bulletin of the New Zealand Society for Earthquake Engineering, Vol. 42, No. 1, March.

Mejia, L., Forrest, M., Bischoff, J., Gillon, M., and Everitt, S. (1999) Upgrading of Matahina Dam for Foundation Fault Displacement, Proc. of Water Power '99, ASCE, Las Vegas, USA, July.

New Zealand Geotechnical Society Inc. 19th Symposium, Queenstown 2013

Mejia, L., Gillon, M., Walker, J., Newson, T. (2002) Seismic Load Evaluation Criteria for Dams of Two New Zealand Owners, *International Journal on Hydropower and Dams, Vol. 9,4, pp 138-144*.

Mejia, L., Macfarlane, D., Read, S., Walker, J. (2005) Seismic Criteria for Safety Evaluation of Aviemore Dam, *Proc. of U.S. Society on Dams Annual Conf.*, Salt Lake City, Utah, USA.

Mejia, L., Roadifer, J., Forrest, M., Abrego, A., De Puy, M. (2011) Design of the dams of the Panama Canal expansion," Proc. of U.S. Society on Dams (USSD) Annual Conf., San Diego, California, USA, April.

Mejia L., Walker, J., Gillon, M. (2006) Seismic Safety Evaluation of Dam for Foundation Faulting, *Proc. of 8th Natl. Conf. on Earthquake Engineering,* San Francisco, California, USA, April.

Newmark, N. (1965) Effects of earthquakes on dams and embankments, Geotechnique, 15, No. 2, pp. 139-160.

Seed, H.B. (1966) A method for earthquake resistant design of earth dams, Journal of Soil Mechanics and Foundations Division, ASCE, 92, No. SM1, pp. 13-41.

Sherard, J.L. (1967) Earthquake considerations in earth dam design, J. Soil Mechanics and Foundations Division, ASCE, 83:SM-4, 377-401.

Sherard, J.L., Cluff, L.S., and Allen, C.R. (1974) Potentially Active Faults in Dam Foundations, Geotechnique 24, No. 3, pp. 367-428.

U.S. Bureau of Reclamation (USBR). (1994) Design Standard No. 13, Embankment Dams, Chapter 5, Protective Filters. September.

Wieland M., Brenner R.P., Bozovic, A. (2008) Potentially active faults in the foundations of large dams Part 2: Design aspects of dams to resist fault movements, Special Session S13, Proc. 14th World Conf. on Earthquake Engineering, Beijing, China, October 12-17.

Macfarlane, D. F. & Yetton, M.D. (2013)
Management and documentation of geotechnical hazards in the Port Hills, Christchurch, following the Canterbury earthquakes
Proc. 19th NZGS Geotechnical Symposium. Ed. CY Chin, Queenstown

Management and documentation of geotechnical hazards in the Port Hills, Christchurch, following the Canterbury earthquakes

D. F. Macfarlane
URS New Zealand Ltd, Christchurch, NZ.
don.macfarlane@urs.com (Corresponding author)

M. D. Yetton
Geotech Consulting Ltd., Christchurch, NZ.
myetton@geotech.co.nz

Keywords: Port Hills, rockfall, hazards, risk

ABSTRACT

This paper outlines the scope of work undertaken by the Port Hills Geotechnical Group (PHGG) to identify, document and assist with the management of geotechnical hazards in the Port Hills area of Christchurch following the 22 February 2011 earthquake. PHGG was a group of consultants formed during the state of emergency and subsequently contracted by Christchurch City Council (CCC). The Group consisted of geotechnical engineers and engineering geologists drawn from Aurecon, Geotech Consulting, GHD, Opus and URS, with support from Canterbury University, Bell Geoconsulting, SKM, Geoscience Consulting and Meridian Energy at different times.

PHGG began as a group dedicated to documenting instability in rock slopes (cliff collapse and boulder roll scenarios) and ground cracking to identify high risk areas and dwellings that should not be occupied as well as identifying areas suitable for protective works and liaising closely with CCC and the public. Following the Civil Defence phase, the role transitioned into working closely with GNS Science and CCC to assist with the development of life-risk models and risk zones while concurrently defining and supervising work packages for interim protective works and more permanent remedial works for key Council infrastructure and parkland.

The PHGG was a very successful team of dedicated professionals that developed excellent working relationships internally and worked collaboratively with its key stakeholders (CCC and GNS). A large part of the reason for this success was that the individuals and companies involved put the job first and focussed on achieving the best possible outcome for the city and its residents.

1 INTRODUCTION

The M_w6.2 Christchurch earthquake of 22 February 2011 caused deaths and injuries, severe damage to tens of thousands of homes, and the devastation of the city's central business district (CBD). In the Port Hills suburbs, five people were killed and over 200 houses were hit and damaged by earthquake-induced rockfall.

In this paper we outline the role of the Port Hills Geotechnical Group (PHGG) and the key lessons learned from its activities during both the Civil Defence Emergency phase that ended on 30 April 2011 and the Recovery Phase that followed. PHGG was a group of geotechnical engineers and engineering geologists drawn from Aurecon, Geotech Consulting, GHD, Opus and URS that formed during the state of emergency and was subsequently contracted by Christchurch City Council. PHGG had support from GNS Science, Canterbury University, Bell Geoconsulting, SKM, Geoscience Consulting, Golder Associates and Meridian Energy at different times.

Initially, the team was dedicated to documenting failures in rock (cliff collapse and boulder roll scenarios) and areas of extreme hill ground cracking to identify high risk areas and dwellings that should not be occupied. Initial work also focussed on identifying areas suitable for protective works and liaising closely with CCC and the public. Following the Civil Defence phase, the role transitioned into working closely with GNS Science and CCC to assist with the development of life-risk models and risk zones while concurrently scoping and supervising work packages for interim protective works and more permanent remedial works on key Council infrastructure and parkland.

The earlier M_w7.1, 4 September 2010 Darfield Earthquake was a larger magnitude event but was centred 35 km west of Christchurch. The ground accelerations in the Port Hills from the Darfield earthquake broadly conformed to 450yr 'design earthquake' (i.e. horizontal PGA of between 0.3 and 0.6g, vertical PGA of 0.3g) and caused very little damage in the Port Hills.

In contrast the M_w6.2 22 February 2011 earthquake had a shallow epicentre directly under the Port Hills and generated horizontal PGAs up to 2.1g with vertical PGAs as high as 2.2g. (Massey et al, 2012a). These are some of the highest earthquake accelerations that have ever been recorded.

During the PHGG operation period there were hundreds of felt aftershocks, many of which caused further damage. The largest of these were the M_w6.2 13 June 2011 and M_w 6 23 December 2011 earthquakes. Managing risks with such high levels of ongoing seismic activity introduced significant issues and challenges.

New Zealand Geotechnical Society Inc. 19th Symposium, Queenstown 2013

2 GEOLOGICAL SETTING

The Port Hills rockfall project area is the north-facing slopes of Banks Peninsula approximately between Westmoreland in the west and Godley Head in the east, plus the slopes facing Lyttelton Harbour as far east as Purau (Figure 1). This area was significantly affected by earthquake-induced rockfalls and ground cracking on 22 February 2011 (Hancox et al., 2011) and further rockfalls were caused by aftershocks, most notably on 16 April and 13 June 2011.

The Port Hills suburbs are sited on the northern slopes of the eroded, extinct Lyttelton basalt volcano. The rocks forming the ridges, slopes and sea cliffs of the Port Hills belong to the Lyttelton Volcanics Group rocks of late Tertiary (Miocene) age, and are about 10–12 million years old (Forsyth et al., 2008). These volcanic rocks comprise layers of hard, jointed, lava flows cross-cut by numerous intruded dykes, and interbedded with breccia (scoria), agglomerate (coarse angular gravel), compact sandy ash beds and ancient buried soils. The volcanic rocks are mantled by loess soils derived from wind-blown sand and silt, typically about a 1 m thick and locally more than 5 m thick.

The north-facing Port Hills suburbs are incised by a series of valleys that drain northwards. The lava flows of the volcano extend below the gravels, marine/estuarine silts and sands that underlie the valley floors. Valley sides may be covered with talus or scree aprons from previous slope failure or rockfall intermixed with or overlain by loess colluvium.

Many natural slopes around Lyttelton Harbour and in the valleys draining northward are formed in strong, interbedded lava flows and stand at steep angles. Cliffs formed on many coastal slopes (such as those around Godley Head, Lyttelton harbour and the outer coast) extend inland into the suburbs of Sumner and Redcliffs as remnants of sea-cut cliffs that become increasingly older with distance inland. These steep (~75–85°) cliffs are typically 15 to 30 m high and locally up to ~80 m high.

3 CIVIL DEFENCE EMERGENCY PHASE

The 22 February 2011 earthquake was centred in the Heathcote Valley on the north edge of Banks Peninsula and within the Port Hills suburbs (Figure 1). A peak ground acceleration of 2.2g vertical was recorded at Heathcote School, close to the epicentre, and widespread damage



Figure 1. Areas affected by cliff collapse and boulder roll in February 2011 and June 2011 earthquakes. From Massey et al (2012), after Hancox et al (2011).

occurred within the city, particularly the CBD (where two major buildings collapsed), the eastern suburbs (liquefaction, lateral spreading, shaking damage) and the Port Hills (rockfall and shaking damage). As described by McLean and others (2012), a full emergency management structure was in place within two hours, with emergency operations command established in the Christchurch Art Gallery which had sustained only minor damage. The Minister of Civil Defence declared the situation a state of national emergency on 23 February. The state of national emergency stayed in force until 30 April 2011.

3.1 Immediate Response

PHGG began as a group of consultants, university staff and students, supported by GNS Science, who responded to the earthquake by immediately heading into areas of the Port Hills suburbs that they, as individuals or companies, knew to have the potential for stability problems that could affect dwellings or key infrastructure.

One of the first field assessments undertaken was an aerial inspection by GNS Science to identify areas affected by landsliding and to obtain a feel for the scale of geotechnical issues affecting the hill suburbs. Some of the photographs we have included in this review were taken by GNS Science on that flight on 23 February 2011.

CCC quickly recognised the benefits to be gained from having these individuals work together, and organised daily meetings with a designated Chairman (Mark Yetton) to ensure a coordinated approach and feedback of information to a central location. At that stage GNS Science were providing GIS support and collating the daily information to define hazard sources and types, and risk areas.

Within the first week the Port Hills suburbs were subdivided into nine sectors, each managed by one consultant team, to enable field inspections to be better focussed and managed effectively rather than having people operating in a random fashion as they chose. Each team managed

itself and reported back at the daily meetings, where they also shared their thoughts about the observed conditions. It quickly became apparent that different sectors had markedly different issues dominating within them, as summarised in Table 1.

Table 1: Port Hills Sectors and Sector Managers, Civil Defence Phase

Sector	Area	Team	Main Issues
1	Sumner and East	URS/SKM	Cliff collapse, boulder roll
2	Clifton Hill	Aurecon	Cliff collapse, mass movement, boulder roll
3	Redcliffs	Geotech Cons	Cliff collapse
4	Mt Pleasant	University/BGL	Retaining walls, boulder roll, cracking
5	Heathcote Valley	Opus	Boulder roll
6	Lyttelton	University/BGL	Boulder roll, retaining walls
7	Avoca/Huntsbury	GHD	Boulder roll, ground cracking
8	Inner Harbour	Aurecon	Boulder roll
9	Cashmere	University/GHD	Ground cracking, boulder roll

The daily meetings were initially also attended by GNS Science, Urban Search and Rescue (USAR) and Earthquake Commission (EQC) representatives, CCC and Environment Canterbury (Ecan) hazards analysts and GIS specialists. GNS Science handed responsibility for the data management over to CCC after about two weeks of assistance and reduced their participation to field staff. CCC provided a liaison person from about that time and this greatly improved links into the CD emergency management.

In the initial stages, USAR provided daily support to the field teams with advice on procedures for ensuring public safety. One key issue faced by the field teams was the management of Health and Safety, in particular the further instability caused by ongoing aftershocks. Initially, each team managed itself in accordance with company H&S procedures, but adapted for the aftershocks. Later, the team developed a single H&S Plan based on the individual corporate plans and requirements.

3.2 What we found

The four main types of ground damage and associated geotechnical risks observed by the field teams from PHGG and GNS Science are outlined below. Strictly speaking, all can be classified as some form of landsliding but we adopted informal terms that are more generally descriptive of the ground damage and which were more easily communicated to emergency managers and others who are not geotechnical specialists.

3.2.1 Cliff Collapse

There were four major collapses of cliffs (Redcliffs, Peacocks Gallop, Richmond Hill, Whitewash Head) as a result of the 22 February earthquake, and 40 houses were severely damaged. The collapse of cliffs created two main forms of damage and two main geotechnical risks associated with the subsequent aftershocks. These were

(i) cliff top instability with associated ground loss or ground cracking behind the cliff top, in many cases affecting houses

(ii) cliff base inundation of land and buildings (Figures 3 and 4) beneath high cliffs or fallen boulders that in some cases hit houses.



Figure 3. Cliff collapse at Redcliffs, 22 February 2011



Figure 4. Cliff collapse at Deans Head (Peacocks Gallop), 22 February 2011

3.2.2 Rockfall and Boulder Roll

Rocks were dislodged from outcrops on the slopes above lifelines and some of the residential suburbs of eastern Christchurch (eg. Sumner, Redcliffs) and the inner harbour area (Lyttelton, Rapaki, Governors Bay). Rocks fell onto roads (Figure 5) and/or rolled and bounced down hitting homes in residential areas and, in some cases, entering or passing right through dwellings (eg. Figures 6 to 8).

3.2.3 Ground Cracking and Subsidence

Extensive areas of ground cracking were initially observed in different general locations including

(i) the toe slope interface between steeper slopes and flat ground at the base of the slopes, thought at the time to be indicative of different ground responses to shaking

(ii) on loess-covered slopes as cracking roughly following the contour. Some of these areas were initially thought to be potential landslides

(iii) ridge crest cracking where strong amplification of shaking had occurred

(iv) cracking due to movement of retaining walls and/or filled areas, some of which subsided or collapsed (Figure 9).



Figure 5. Rockfall onto Sumner Road, 22 February 2011



Figure 6. Rock inside home, Morgans valley

New Zealand Geotechnical Society Inc. 19th Symposium, Queenstown 2013



Figure 7. House penetrated by rockfall, Morgans Valley, on 22 February 2011



Figure 8. House penetrated by rockfall, Rapaki, 22 February 2011

3.2.4 Mass Movement

Areas with both ground cracking and other contiguous deformation such as toe bulging were recognised as discrete mass movement features. In the short term after 22 February 2011, the main locations assessed as being affected by mass movement were Clifton Terrace (Figure 10), Egnot Heights and Vernon Terrace. Some of these areas moved more than a few hundred mm and in some cases ongoing movement appeared to be occurring.

Mass movement was also judged to be the most likely explanation for ground damage observed on Richmond Hill, and at Maffeys Road where the topography suggested possible reactivation of an old landslide.

Survey monitoring was established in each of these areas within a short period after the earthquake with regular resurveys initiated. For these area, PHGG identified houses and services that could potentially be affected by large scale or rapid movements and provided input to emergency evacuation and management plans for each area.



Figure 9. Retaining wall collapse caused by 22 Feb earthquake



Figure 10. Example of ground damage classed as mass movement, Kinsey Terrace, Clifton

3.3 Red Placards

From the first few hours after the earthquake PHGG teams responded to alerts by Civil Defence and structural engineers regarding houses or infrastructure in possible danger from falling rocks or ground movement and also checked known potentially dangerous settings in their sector. The main focus of the work in the Port Hills was to respond to life safety issues affecting lifelines, critical roads and residences.

Due to the extreme ground shaking, many houses suffered significant structural damage. As geotechnical engineers and engineering geologists, PHGG were not qualified to assess structural

damage, hence recommending red placards only on the basis of geotechnical hazards but recommending to USAR that structural assessments be carried out in some cases.

PHGG personnel would inspect the location, confirm and gather the appropriate details, apply their judgement with respect to risk and make a recommendation to USAR regarding placement of a red placard. Where houses were involved PHGG personnel liaised with the structural teams who had the designated powers to issue Red Placards requiring immediate evacuation.

PHGG consultants in each sector developed their own records of properties with dangerous geotechnical issues and were constantly updating and expanding these after further inspections as aftershocks occurred and/or new damage became apparent.

The need for red placards was reviewed at every opportunity, and these ultimately evolved after the emergency phase into S124 notices under the Building Act. When the quantified risk zones for cliff collapse and boulder roll became available following the GNS studies, there was a good correlation between quantified risk estimates and the red placards and S124 notices that had initially been issued based on judgement.

3.4 Documentation of Geotechnical Observations

3.4.1 Field Classification

Field assessment of the stability of individual rocks or rock outcrops was commenced in March 2011 after consultation with EQC and considered a number of criteria, including rock size, shape (potential to roll), evidence for recent movement, and property or lifelines at risk. In this simple classification system, unstable rocks were classified as High, Medium or Low risk on the basis of the following criteria (as shown in Table 2):

1. detached (either as loose boulders or in broken outcrop, as shown by fresh cracking above or below the individual rock or within a rock mass)?
2. ability to roll from their present position (due to their shape) ?
3. pose a direct threat to properties or lifelines?
4. currently unstable (can be wobbled or moved by hand)?

Table 2. Field stability classification for individual rocks and boulders

Criterion	Risk Classification		
	High	**Medium**	**Low**
Loose/detached	X	X	X
Able to roll	X	X	X
Threat to lifeline or property	X	X	
Currently unstable	X		

3.4.2 Data collection and management

In the immediate aftermath of the 22 February earthquake, all field teams were collecting data in any way that they could and providing it to a central location where GNS Science were collating it into a GIS database and using this to prepare preliminary hazard maps. GNS handed this role over to CCC/PHGG after about two weeks.

PHGG developed a standardised spreadsheet for use as a fieldsheet to ensure that all field teams collected the same data and recorded it in the same format. The field data could be re-entered into Excel and transferred to the database. This proved cumbersome, difficult to check and had significant potential for errors.

In recognition of the difficulties with the paper-to-GIS system, PHGG team member Aurecon proposed a real-time GIS-based data collection system that would allow the data to be entered directly in the field using an iPad for live update of the database and would also allow the data to be viewed. Over a period of time the system was refined to provide a number of layers that

could be accessed to show all available or user-selected information at any scale. This system did not become operational until mid-2011.

In terms of data collection and management, the iPad system, also duplicated on the Aurecon server where it was managed, was undoubtedly a huge step forward and was fully embraced by the PHGG consultants.

3.4.3 Field trials

To obtain a better understanding of three dimensional boulder roll patterns in Port Hills terrain PHGG personnel, accompanied by CCC and CERA representatives, undertook field trials to observe the way in which dislodged rocks behaved when rolling down slope. The trials were undertaken in remote, closed park areas on Godley Head and involved dislodging rocks loosened by the earthquakes and observing how they behaved during downslope travel.

Rocks dislodged from very steep outcrops or onto steep slopes (steeper than about 35°) gained momentum as they travelled and ran out for hundreds of metres before stopping. The majority of these rocks travelled more or less down the fall line but some gained sufficient momentum to depart from this line and travel largely independently of the topography until they slowed sufficiently to again be influenced by the terrain and turned to follow the fall line.

Based on these observations we were able to conclude that rolling boulders in Port Hills terrain could deviate by up to 30 degrees from the fall line, thus defining a cone of risk below any potential rockfall source. We also found that most rocks that gained sufficient momentum to continue to travel down slope broke up as they went thereby influencing their final travel distance.

Most of the slopes on which we conducted these trials were not vegetated but for one trial we were able to roll rocks into a gully that had been planted with flax and other native plants over a distance of about 100m. This demonstrated that vegetation was extremely effective at stopping rolling boulders.

3.5 Treatment Options

Almost immediately after the 22 February earthquake, specialised ropes-qualified contractors were brought into the Port Hills to help stabilise outcrops or detached boulders with the objective of protecting lifeline and key infrastructure. This work was extended to some slope above residential areas, partly to make bluffs safe for the field geologists to work below so that they could map and assess the slopes.

Where approved by CCC, unstable rocks were treated by

1. moving them into a stable position; or
2. breaking them into smaller pieces that could then be moved into a stable position; or
3. holding them in place (eg. with spot bolts, cables or mesh)

The work was managed as Work Packages scoped by PHGG and approved by CCC. PHGG developed interim design guidelines for mechanical fixes but there was a strong preference for stabilising or breaking rocks as these options avoided future maintenance requirements. The solution adopted at each treated site was decided in the field in consultation with the contractor who would undertake the work.

It was recognised that these solutions would not be suitable in all cases – for example for very large rocks or unstable bluffs more extensive works may be required to ensure their stability. There was no approval to undertake more major works such as anchoring, rock bolting, excavation or concreting, nor for the construction of protective works such as catch fences or other barriers.

The completed interim works were thoroughly tested by the 13 June aftershocks. Although many treated sites suffered some damage, no completed works failed in that event.

3.6 Community Liaison

One of the difficulties faced by PHGG was its role relative to that of EQC. As an insurer, operating under specific legislation, EQC was completely focussed on land and property damage whereas the priority for PHGG/CCC was the protection of life and infrastructure. While EQC did attend PHGG's daily meetings, their technical resource was initially focussed on the flat land, where much larger numbers of people were affected. During the CD Emergency phase, this left PHGG as the main point of contact for many issues that affected the Port Hills community.

3.6.1 Response to public enquiries

Throughout the CD Emergency Phase, CCC maintained a spreadsheet summarising requests for information received from Port Hills residents. Many of the requests were of a geotechnical nature and were passed to the sector teams for a response. Often this required a site visit and discussion with the owner or tenant (who may or may not have been resident at the time) with the result advised back to CCC to allow the spreadsheet to be updated and any formal response prepared.

3.6.2 Public Meetings

One of the major contributions of the PHGG team during the emergency phase was attendance at large public meetings organised by Civil Defence, large community meetings arranged by local community groups such as the Sumner Residents association and street level meetings involving smaller groups of residents. The geotechnical information shared at these meetings varied with the audience but was typically:

(i) Large public meetings – statements updating the public on the state of knowledge in their area. These were meetings managed by Civil Defence to provide information on a wide range of issues, with limited opportunity for questions and answers.

(ii) Community Meetings – usually involving several hundred people. PHGG provided: a briefing on geotechnical issues in the particular suburb, using visual aids where possible; interactive Q+A of a general nature; individual discussions in relation to individual properties or small groups of properties with common concerns.

(iii) Street meetings - briefing on geotechnical issues in the immediate area, using visual aids where possible; interactive Q+A of a general nature; individual discussions in relation to individual properties or small groups of properties with common concerns.

3.7 Key lessons from CD Emergency phase

The key lessons from the Civil Defence Emergency phase were

1. First response can be haphazard if there is no management strategy in place before such an event
2. Sectoring the affected area is extremely effective for focussing assessment teams in a systematic and more uniform way
3. Daily meetings allow the lessons and observations from each sector to be shared with others, and this better informs subsequent inspections (eg. by checking for similar issues).
4. A formal procedure on which to base the decision to recommend a red placard is essential to ensure a consistent approach and for documentation of the decisions. A simple flowchart was developed for later use.
5. Uniformity of data capture is critical to using the data effectively later. We did reasonably well but in hindsight we lost the opportunity for better quality ground cracking data and were disadvantaged by inconsistent recording of boulder sizes.

New Zealand Geotechnical Society Inc. 19th Symposium, Queenstown 2013

6. Having an electronic data collection a system in place and operational sooner would have saved much time that was spent entering data by hand, verifying data and producing paper maps for use in the field.
7. Health and safety management procedures that are appropriate for an emergency situation must be in place
8. Informal terms that are generally descriptive of the nature of ground damage, hazards and risks are more easily communicated to emergency managers and others who are not geotechnical specialists
9. Consistency and honesty with the public in meetings is ultimately repaid in good relationships and trust.

4 RECOVERY PHASE

Following the Civil Defence Emergency phase that ended on 30 April 2011, PHGG became part of the Port Hills Rockfall Recovery Project, with each of the main consultants contracted directly to CCC.

Many of our previous tasks continued with little change (for example, responding to public enquiries and attendance at public meetings and street scale meetings) the main difference being that these were now managed through normal CCC procedures and processes.

With this change at the end of the CD phase, PHGG reorganised itself to make best use of the technical abilities of its senior members. The changes included forming a leadership team, an internal 'engineering' team and transitioning the day to day sector management to the sector leaders. Regular meetings to coordinate activities, maintain awareness of what was happening in different areas and to ensure a reasonably standardised approach to tasks, documentation and reporting were continued, but the frequency was reduced and periodically reviewed.

At the same time the recognition of need for independent peer review led PHGG to recommend to CCC that they appoint an external reviewer to oversee and if necessary guide PHGG activities. Dr Fred Baynes was appointed as reviewer in June 2011 with a scope of work agreed between himself and Council.

Council subsequently appointed their own Geotechnical Advisor to liaise with PHGG, the reviewer and GNS Science, and to advise Council staff and management.

4.1 S124 notices

In July 2011, the CD Red Placards were replaced by Section 124 Notices, issued under the Building Act, that prohibited entry into or occupation of the affected dwellings. PHGG undertook a review of all 560 Red Placards on residential properties and recommended that 108 of these should not be reinstated as s124 Notices because the life-safety risk was judged to no longer remain for these dwellings. PHGG also provisionally identified 96 properties as 'retreat' properties that should be demolished and abandoned as too dangerous for safe residential occupation. All of these were within the rockfall risk areas shown on Figure 11, and were located on cliff edges or immediately under cliffs, with a small number in areas where there had been large numbers of boulders impacting homes.

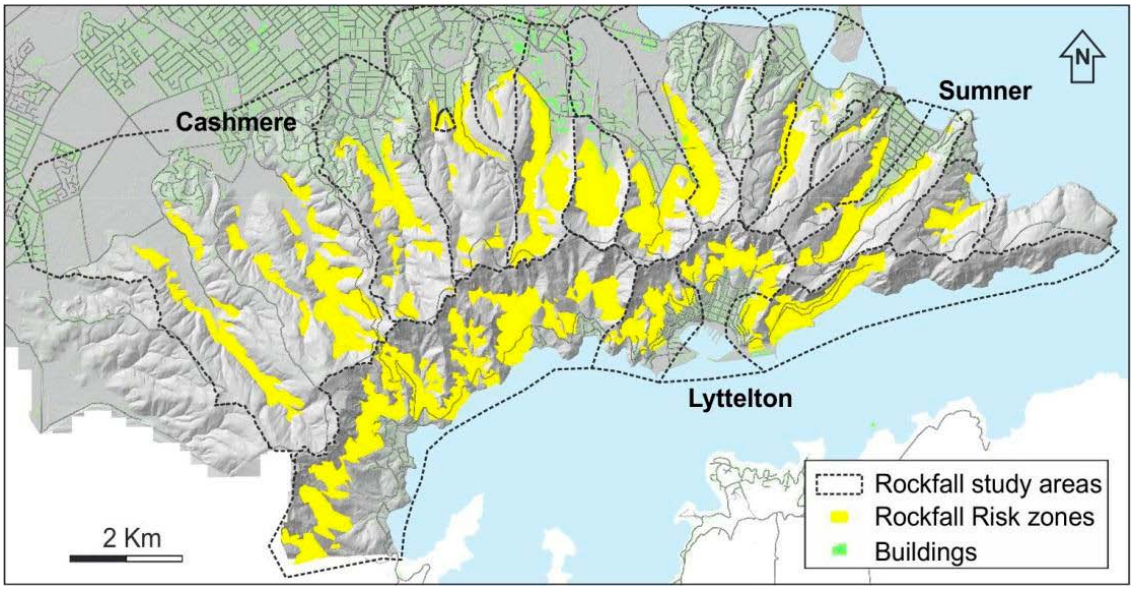


Figure 11: Rockfall risk zones. Courtesy Chris Massey, GNS Science.

4.1.1 Criteria

An s124 Notice could only be applied to a dwelling, and only where the life safety risk to occupants of the dwelling was judged to be so high that this restriction could be justified. As the majority of s124 Notices were placed well before the GNS life-safety model (released March 2012) had been developed, the s124 recommendations were based solely on individual site characteristics.

In boulder roll risk areas PHGG used field observations and judgement based on the following criteria:

1. Did rocks fall on this or an adjacent property?
2. Did rocks reach or pass the dwelling?
3. Was the dwelling hit by rocks?
4. Is the slope above the dwelling steep enough for rocks to roll down it?
5. Are there obvious sources for further rockfall?
6. Is there effective natural or man-made protection for the dwelling? This may be one or more of vegetation (e.g. shelter belts, plantations, dense scrub), another house(s), rock fences, bunds or topographic controls.

The protection was not deemed effective if it had been passed or penetrated by rockfall boulders (eg. if some rocks/boulders had passed right through a shelter belt or plantation it was not an effective barrier even if it had stopped other rocks).

For each dwelling assessed, a flow chart was completed on the basis of the joint opinion of two team members, one of whom was required to be a senior professional. Figure 12 shows the flow chart for boulder roll situations. Similar flow charts were developed for cliff top, cliff bottom, landslide and retaining wall situations.

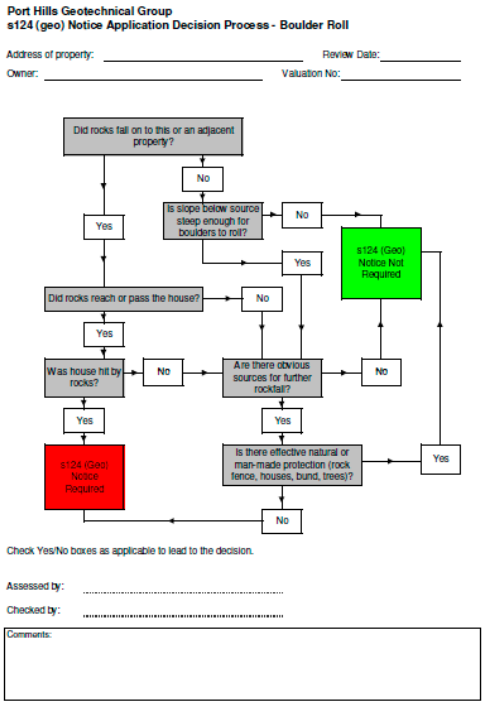


Figure 12. s124 Assessment form



Figure 13. Sample location for which s124 recommended

The breakdown of the various geotechnical issues that required the placement of an s124 notice on dwellings as of July 2011 is presented in Table 3. Risk from boulder roll was the most common reason for the s124 notices in all areas other than Sector 3, where cliff collapse is the dominant issue.

Initially, the s124 Notices expired after 60 days and had to be reassessed and replaced at that time. The Building Act was amended by an Order in Council to remove this requirement for a defined period (through until September 2013). At the time of writing, Council and the Department of Building and Housing are seeking to have this period extended.

Table 3. Main reasons for s124 Notices

Sector	Main reasons for s124 Notices (as at July 2011)					
	Boulder roll	Cliff Top	Cliff Bottom	Cracking	Access	**Total**
1	50	8	4			**62**
2	70	34	16			**120**
3	1	27	30			**58**
4	33	8	13	19	23	**96**
5	23					**23**
6	14			12	5	**31**
7	34					**34**
8	8					**8**
9	24					**24**
Totals	**257**	**77**	**63**	**31**	**28**	**456**
%	*56*	*17*	*14*	*7*	*6*	*100*

Note – 108 Red Placards were not replaced with s124 notices at this time. Most had been applied for cracking or dangerous access associated with retaining walls

4.1.2 Hazard Verification Reports

When it became apparent that some homeowners were defying the s124 notices and remaining resident in their dwellings, Council requested PHGG in late 2011 to develop a simple 'hazard verification report' that confirmed the reason for the dwelling having been assessed as hazardous, and that the dwelling was still considered to be at risk from a rockfall/boulder roll or cliff collapse event.

Council subsequently decided in December 2011 that by advising the owners who remained resident in their s124 dwelling that they were choosing to remain in a location with a heightened risk they had discharged their obligations under the Building Act. On this basis, Council would only physically enforce the notices at their discretion, based on advice from PHGG.

4.1.3 Temporary access plans (TAP's)

The Section 124 prohibited access notices only apply to buildings. In the interests of security and assessment for insurance assessment or repairs purposes, Council allows temporary access to the dwellings but people wishing to access their s124'd dwelling must complete an application form explaining the purpose, date and duration, and the proposed safety plan. Each application has been reviewed by the PHGG geotechnical lead for the sector to identify any properties with an unacceptable level of risk, to which access may be declined or restricted.

4.2 Life-risk Zoning

A very large and key part of the work undertaken to better understand and assess risks associated with natural hazards in the Port Hills has been the studies completed by GNS Science, with assistance from PHGG, to define and quantify life-safety risk zones. These studies are documented in a series of reports by GNS Science [see reference list for details] and have subsequently been used to aid Government, Council, insurers and individuals to make decisions in relation to their management of ongoing risk from those hazards.

The fallen boulder data upon which the GNS Science life-risk modelling was based was collected by GNS and PHGG. The different consultancies forming PHGG worked together with GNS Science, and agreed on the data to be gathered and on the definition of modelling parameters. The sector leaders were responsible for ensuring the integrity of the data. Without the fallen boulder data generated by the 22 February 2011 earthquake, and the subsequent further falls in various aftershocks, the reliable quantification of the risk zones would not have been possible. The fallen boulder database is now a unique and valuable asset that may have important uses in other risk studies, both in New Zealand and other countries.

4.2.1 Life-safety Risk Zones

The life safety risk zones developed by GNS Science in boulder roll areas are defined by a model developed on the basis of field data including boulder size, distribution across and down the slope, runout distances and angular relationships between source areas and runout distances. The model is based on the actual locations of boulders that fell and rolled downslope and hence includes the influence of topography, trees, fences and houses on some of the runout distances and trajectories. It was field calibrated by back tracking actual boulder paths and cross checked by rockfall modelling calibrated against slope surface materials and maximum runout distances. The modelling used the 95th percentile rock for the particular suburb and vegetation was excluded from the rockfall modelling as it cannot be considered a permanent feature of the slope. These factors combine to make the model somewhat conservative, which is normal practice for risk management.

For cliff collapse areas, the life safety risk zones were defined for both cliff top retreat and for the risk of debris inundation or flyrock at the base of cliffs.

The independent peer reviewer retained to give Council confidence that the services provided by the geotechnical consultants and GNS with respect to assessing life safety risk from rock fall and cliff collapse in the Port Hills were appropriate and reasonable.

Ground truthing

Ground truthing of the boulder roll and cliff collapse models was undertaken in early 2012 to field check the risk zones developed for the boulder roll and cliff collapse life safety risk models. Using a process agreed between GNS and PHGG, every property within the risk zones was individually assessed by pairs of experienced geo-professionals working with a standard form to ensure consistency. Individual sector leaders generally worked with a moderating geo-professional from outside the sector. The final life safety risk zones were adjusted for local topographic factors (ridges, gullies, flat areas) and source variations that could affect boulder numbers, roll paths and run out distances. Thus for each house the broad suburb scale GNS model was judged to either reasonably estimate, under-estimate or over-estimate the risk. For example, at a house within a local gully that could focus boulder roll, the risk might be assessed as greater than indicated by the GNS model.

GNS used this information to finalise the risk zones for the models and PHGG also used the field inspections to backcheck the need for s124 notices on the dwellings assessed.

4.3 Review of CERA zoning decisions

The Canterbury Earthquake Recovery Authority (CERA) is a government department formed in response to the February 2011 earthquake to help with the recovery. CERA progressively undertook zoning of the Port Hills between June 2011 and late 2012, with all dwellings ultimately being zoned Red or Green (in the interim, land was zoned white, meaning 'not yet assessed'). For properties zoned Red, the Government will make an offer to purchase the home and land; there is no Government offer for properties zoned Green. In the Port Hills, the zoning decisions were driven by life-safety risk and the Red zones were largely determined by CERA using the Year 5 risk models for boulder roll and cliff collapse risk. At the time of writing, the CERA zoning of the Port Hills is under review.

4.3.1 Pre-June 2012

The Canterbury Earthquake Recovery Authority (CERA) announced its first zoning decisions for the Port Hills on 22 June 2011, when the whole of the Port Hills and Banks Peninsula were zoned White (decision pending). By May 2012, through a series of decisions, most properties on broad gentle slopes or ridge tops had been determined to be safe for residential occupation and zoned Green.

PHGG had little involvement in these decisions, but the Green zone did include a number of properties with s124 Notices and PHGG reviewed these in May 2012, concluding that for 53 of the 77 properties reviewed there was no defensible basis for uplifting those notices.

4.3.2 After June 2012

On 29 June 2012, CERA announced the rezoning of 1107 residential properties on the Port Hills from White to Green, and that the Government's Red zone (buyout) offer would be extended to the owners of 285 severely at-risk or largely destroyed residential properties in the Port Hills. Of these properties, 191 related to cliff collapse and 94 to boulder roll. A further 158 properties that initially remained in the White zone due to mainly to boulder roll issues were subsequently rezoned Red in decisions announced in August and September 2012.

S124 notices were automatically uplifted from approximately 130 properties that were re-zoned to Green. PHGG reviewed the properties that lay close to the white/green boundary and identified twelve dwellings as 'should not have the s124 notice uplifted'. These notices were reinstated and, at CCC's request, the remainder were subsequently reviewed in August-September 2012 to confirm that the uplifts were appropriate. This review included 2D rockfall modelling that specifically considered the effects of vegetation on these slopes for the first time.

4.4 Remedial works

Physical works have been undertaken in a number of areas of the Port Hills since March 2011to remediate high risk rocks posing a hazard to houses, roads and key infrastructure, and in areas of park and conservation land. In many cases, due to the scale and complexity of the rock

outcrops these works are considered by CCC to have been interim hazard management rather than permanent remediation.

Although many treated sites suffered some damage in the 13 June aftershocks, no completed works failed in that event. However, that event loosened and dislodged many more rocks and highlighted the challenge faced in identifying and treating potential rockfall sources. As a result, work to protect homes was largely discontinued and the emphasis was placed on protection of Council assets and Parks from that time. Works at source to protect Evans Pass Road have been completed and the road reopened to all traffic (Engel 2013), and at the time of writing work is continuing on sections of the Summit Road.

4.5 Roading options studies

PHGG have carried out preliminary hazard assessments for a number of lifelines and key routes (non-NZTA) in the Port hills including Evans Pass, Summit Road (Evans Pass to Mt Pleasant Road), Port Hills Road, Dyers Pass, Lyttelton to Governors Bay (alternative to Tunnel route), Summit Road (Evans Pass to Scarborough), Mt Pleasant Road (Summit Road to Main Road) and Bridle Path Road.

Sumner Road, which runs between the Evans Pass/Summit Road intersection and Lyttelton, has been closed to all traffic since February 2011 due to debris on the road and the presence of extensive earthquake induced instability on the slopes and cliff faces above the road. In an options study reviewed by PHGG, reopening Sumner Road was compared with the upgrade of alternative routes over the Port Hills and the construction of a new road. No final decision has yet been made.

Two sections of Main Road, which links Sumner and Ferrymead, have been affected by cliff collapse. CCC commissioned engineering options reports for both the Moa Bone Cave and Peacocks Gallop areas that are currently protected by containers as an interim solution (see Figures 14 and 15).



Figure14. Containers protecting Main Road at Peacocks Gallop



Figure 15. Rockfall debris behind containers at Peacocks Gallop.

4.6 S124 reviews

Approximately 130 properties that were Green zoned as a result of the 29 June announcement were subject to automatic uplift of s124 notices. This was a policy decision and was not based on the criteria used to assess the need or otherwise for s124 notices.

PHGG's review of the automatically uplifted s124 Notices in the Green Zone was completed in October 2012 and included desktop review from which properties requiring field inspection and/or rockfall modelling for a robust decision were identified. This review provided Council with documentation of the basis for uplifting or reinstating those s124 Notices that were automatically uplifted. It was also used as a check on properties considered by PHGG to have been marginal calls for zoning decisions but have not previously had s124 Notices.

The outcomes from the review included a recommendation to reinstate 22 of the s124 Notices (including the 12 reinstated almost immediately after the 29 June announcement). For all

New Zealand Geotechnical Society Inc. 19th Symposium, Queenstown 2013

remaining properties reviewed, the uplift of the s124 notice was assessed to have been a reasonable decision.

4.7 October 2011 Rainfall Event

On 19 October 2011, the Port Hills were subject to the most significant rainfall event since the 22 February earthquake. This triggered inspections of the Port Hills areas by the sector teams to determine the effects on damaged land areas and potentially unstable rock source areas. The inspections showed widespread minor effects but no large scale changes due to the rain. Up to the time of writing the Port Hills have not been subject to the type of high intensity or prolonged heavy rainfall which can occur, particularly in the late winter period.

4.8 S124 Determinations

Property owners who disagreed with their s124 Notice were able to request a formal review (Determination) by the DBH (Department of Building and Housing, Ministry of Business, Innovation and Employment, MBIE).

At the time of writing, 12 Port Hills residents in boulder roll zones had requested a formal review of their s124 Notice by the DBH, but 3 had subsequently withdrawn.

4.9 Port Hills risk management zones (District Plan)

In late 2012, PHGG provided inputs to Christchurch City Council workshops working through a range of issues relating to future planning on the Port Hills. This work includes potential changes to the Christchurch City Plan and Banks Peninsula District Plan to strengthen the Council's existing consenting processes in the light of post-earthquake knowledge.

Changes to the District Plans relating to the management of land-use and subdivision activities in high risk areas may include zoning to prevent or control new developments and controls (resource consent requirements) for rockfall protection work (including rockfall protection structures) to keep the natural hazard risk to a level that is as low as reasonably achievable.

4.10 Rockfall protection structures

The design of rockfall protection is a complex task that requires the consideration of many different kinds of data (geological, geotechnical and topographical) from the site and source areas as well as trajectory analysis (path and bounce height) to estimate the kinetic energy that must be managed by the design.

PHGG has been involved in two levels of assessment of rockfall protection for Port Hills properties:

4.10.1 Suburb-scale rockfall protection structures (RPS)

PHGG and CERA held a combined workshop in July 2012 to discuss rockfall protection. The overall objectives of the workshop were to better define locations and dimensions for large-scale rockfall protection works suggested on the basis of preliminary 3D rockfall modelling undertaken for CERA and use this to develop cost estimates from which CERA would undertake cost-benefit analyses.

CERA subsequently concluded that area-wide (suburb-scale) protective works were not practicable for a number of reasons including uncertainty around timeliness and costs. The areas that had been considered for area-wide protective works were then zoned Red by CERA.

4.10.2 Private RPS

Following a decision by Councillor's on 6 December 2012, owners of Port Hills properties who had received a Red zone offer could apply to the Council for funding to erect a private rockfall protection structure. CCC developed, with input from PHGG, contractors, suppliers and other consultants, a *Technical Guideline* to provide design guidelines for rockfall mitigation in the Port Hills. The design objective is to reduce the life-safety risk to an acceptable level.

Approval is a two stage process. Firstly, applicants need to retain an engineer to develop a design for Council to approve, and for which building and/or resource consents may need to be issued. When the application iss received, approved consultants are retained to undertake the design review for Council. Once consented, the funding can be applied for. Funding is capped at Council's 50% share of the Red zone offer for the property.

At the time of writing, eight pre-application meetings had been held and construction was underway on one site.

4.11 Demolitions

Although no building consent is required for the demolition of houses in the Port Hills, Council has recommended that geotechnical advice is obtained prior to commencing demolitions in the Port Hills. PHGG sector leaders (using a standard form) identify any known geotechnical hazards on the basis of advice of proposed demolitions.

PHGG also created a list of properties that currently provide down-slope protection (from rockfall/boulder roll only) to other properties such that, if that property was demolished, it would be necessary to assess whether or not a new s124 would need to be placed on the property or properties currently protected by those upslope.

4.12 Lessons Learned in the Post-emergency Phase

Further lessons learned in the post-Civil Defence Emergency phase included:

1. Given our current knowledge of the future seismic hazard it is simply not possible or cost effective to identify and remediate all potential rockfall source sites over large areas, rural or park land. Protection, retreat and/or relocation of infrastructure away from these potential boulder roll sources are the only feasible solutions.
2. Further aftershocks may induce new instability in the damaged rock mass at locations that often defy prediction. In the large June 2011 aftershocks new rockfalls came from sites that had no obvious indications of damage from the previous earthquakes.
3. Potential rockfall source areas that have been built over (eg. Scarborough) did sustain shaking damage due to high PGA's but had few problems with boulder roll as roads, retaining walls and buildings constructed as part of the development prevented rockfalls or captured rocks before they gained momentum.
4. Properties that have been zoned Green or Red by CERA, primarily on the basis of application of life-risk models that necessarily 'average' the risk across a wide area, will not always align with s124 Notices placed using other site specific criteria
5. Communications to keep affected parties as fully informed as possible are crucial. Much of the angst in the community is due to the inability to provide all the information required to make individual decisions in the shortest possible time frames.

5 CONCLUSIONS

The damage caused on 22 February 2011 by a very strong earthquake located directly under the residential hill areas of Christchurch demanded an immediate emergency geotechnical response. This response came largely from locally-based engineering geologists and geotechnical engineers (working in conjunction with USAR engineers) from a range of companies and organisations, and from GNS Science.

The local consultants involved fortuitously aligned into a robust and efficient working group who became known as the Port Hills Geotechnical Group (PHGG). The PHGG was a very successful team of dedicated professionals that worked collaboratively with its key stakeholders (CCC and GNS). A large part of the reason for this success was that the individuals and companies involved focussed on achieving the best possible outcome for the city and its residents.

As soon as possible following the disaster it is essential to remove the risk to life by evacuating and/or restricting occupancy in high risk areas until lifelines and properties can be adequately assessed and/or protected.

The lessons learned during this emergency response, and the successful methods that were developed and applied to mitigate and manage the immediate risk, have potential application to other regions and towns. The organisation and preparation of appropriate management and documentation systems should not wait until a disaster that requires a geotechnical emergency response has already occurred.

Documentation in the early stages need not be complicated but systems need to be in place and be consistently applied for a sensible and defensible outcome. There was a very good correlation between high risk properties identified on the basis of site-specific factors and given Red Placards (or s124 Notices) in the immediate aftermath of the February 2011 and June 2011 aftershocks and the highest risk zones later defined in the GNS life-safety risk models.

At the time of writing (mid June 2011) many of the evacuated properties retain s124 notices and most will remain until significant mitigation (such as rock scaling or breaking, bolting, berms or rock fences) occurs to reduce the risk to acceptable levels.

It will almost certainly take longer than initially expected to recover from a major natural disaster. Consequently, consistent communications to keep affected parties as fully informed as possible are crucial during the emergency phase and must also continue through the recovery phase.

In the post emergency phase the recognition of previously unknown active faults directly under the city has led to a radical reassessment of the local seismicity model. The revised seismicity model, in conjunction with the unique dataset of the observed pattern and density of earthquake triggered rockfall, has led to the first extensive quantitative risk modelling undertaken for a New Zealand city.

The risk modelling has formed a defensible basis for long term decisions on the need for retreat from some areas of the hills and provided appropriate information that will be incorporated into future District Plan revisions.

ACKNOWLEDGEMENTS

We are proud to have been part of the very successful team of dedicated professionals drawn from Aurecon, Geotech Consulting, GHD, Opus, SKM and URS that developed into PHGG, with support in the early stages from Canterbury University, Bell Geoconsulting, Geoscience and Golder Associates, and ongoing support from Christchurch City Council. We particularly wish to acknowledge the contributions of Steve Bensberg (CCC), Chris Massey (GNS Science), Rori Green (URS) and Mark Easton (Opus).

This paper is published with the approval of Christchurch City Council.

REFERENCES

Engel, J.M. (2013). Reopening Evans Pass Road, Sumner to Summit Road. *Proc. 19th NZGS Geotechnical Symposium. Ed. CY Chin, Queenstown*

Forsyth, P.J.; Barrell, D.J.A.; Jongens, R. (compilers) (2008). Geology of the Christchurch area. Institute of Geological & Nuclear Sciences 1:250 000 geological map 16.

Hancox, G.; Perrin, N. (2011). Report on Landslide Reconnaissance Flight on 24 February 2011 following the Mw 6.3 Christchurch Earthquake of 22 February 2011. GNS Science Immediate Report.

McLean, I. et al (2012). Review of the Civil Defence Emergency Management Response to the 22 February Christchurch Earthquake. Prepared for Director of Civil Defence and Emergency Management, 29 June 2012.

Massey, C.I. et al (2012a). Canterbury Earthquakes 2010/11 Port Hills Slope Stability: Pilot study for assessing life-safety risk from rockfalls (boulder roll). *GNS Science Report CR2011/311, March 2012.*

Massey, C.I. et al (2012b). Canterbury Earthquakes 2010/11 Port Hills Slope Stability: Pilot study for assessing life-safety risk from cliff collapse. *GNS Science Report CR2012/57, March 2012.*

Massey, C.I. et al (2012). Canterbury Earthquakes 2010/11 Port Hills Slope Stability: Life-safety risk from cliff collapse in the Port Hills. *GNS Science Report CR2012/124, March 2012.*

Massey, C.I. et al (2012). Canterbury Earthquakes 2010/11 Port Hills Slope Stability: Additional assessment of the life-safety risk from rockfalls (boulder rolls). *GNS Science Report CR2012/214, September 2012.*

Massey, C.I. et al (2012). Canterbury Earthquakes 2010/11 Port Hills Slope Stability: Life-safety risk from rockfalls (boulder roll) in the Port Hills. *GNS Science Report CR2012/123, May 2012.*

Townsend, D.B.; Rosser, B. (2012). Canterbury Earthquakes 2010/2011 Port Hills Slope Stability: Geomorphology mapping for rockfall risk assessment. *GNS Science Report CR2012/15, September 2012.*

Taig, T. et al (2012). Canterbury Earthquakes 2010/11 Port Hills Slope Stability: Principles and criteria for the assessment of risk from slope instability in the Port Hills, Christchurch. *GNS Science Report CR2011/139, March 2012.*

Archibald, G.C., Massey, C.I., Lukovic, B., & Carey J.M. (2013).
Terrestrial laser scanning methods to assess rockfall risk
Proc. 19th NZGS Geotechnical Symposium. Ed. CY Chin, Queenstown

Terrestrial laser scanning methods to assess rockfall risk

G C Archibald
GNS Science, Wellington, NZ

C I Massey
GNS Science, Wellington, NZ

B Lukovic
GNS Science, Wellington, NZ

J M Carey
GNS Science, Wellington, NZ

Keywords: Terrestrial Laser Scanning, Risk Management, Christchurch, Rockfall, Hazard

ABSTRACT

The MW 6.2 Christchurch earthquake on February 22, 2011, and its aftershock sequence triggered numerous rockfalls in the Port Hills east of Christchurch. The potential for on-going rockfalls poses a serious risk to property, key infrastructure and residents. In order to manage this risk it is essential that suitable monitoring practices are adopted to monitor and measure change of the potentially unstable cliffs in the Port Hills.

This paper reviews the methodology and analysis of a series of repeat Terrestrial Laser Scans of 1.5 km of relict sea cliffs, in providing an overview of cliff evolution over a two-year aftershock sequence. The field methods proposed allow rapid collection of high quality datasets that can be repeated at either regular intervals or in response to new events. The data processing has been used to quantify rockfall volumes from specific events, which provides important input into risk and rockfall modelling, and has provided a valuable tool for assessments of future rockfall risk within the Port Hills.

The study demonstrates that TLS can be a cost-effective method to quantify change in cliffs for modelling potential future cliff behaviour. The results illustrate how TLS based approaches can be a decisive tool in determining potential hazards sites and their subsequent risk to key infrastructure.

New Zealand Geotechnical Society Inc. 19th Symposium, Queenstown 2013

1 INTRODUCTION

Terrestrial Laser Scanning (TLS) has become an accepted technology for high resolution landscape evolution studies. In many instances these studies have been carried out either in rural settings, (Schürch et al. 2011, Wheaton, J. et al. 2010, Rosser N, et al. 2007) or over small scale cliff sections (Abellán et al. 2009, Lague, 2012,). The Port Hills rockfall study was conducted in urban areas that were severely disrupted by a series of earthquakes and under real-world time and cost constraints. Such conditions require an adaptable methodology which allows for rapid collection of high quality data sets in a dynamic and hazardous environment.

The method adopted and discussed here comprises the following main steps: 1) field data capture, 2) processing of field data e.g. aligning, combining and filtering the different point clouds, 3) vegetation removal, 4) data input, post processing and analysis in ArcGIS.
The standard approach using permanent and/or temporary retro reflective targets surveyed independently of the TLS routine proved inappropriate due to the lack of safe access to place targets in the scene and constraints that limited the time spent at any one set up.

This paper presents the methodology developed for the rapid capture and processing of TLS data and reviews the relative merits of such an approach to produce cliff monitoring data to estimate potential rockfall hazard which has been used for risk assessment purposes (Massey et al., 2012).

2 DATA CAPTURE

Following the devastating Mw 6.2 February 22nd 2011 Christchurch earthquake (NZSEE, 2011) a series of TLS surveys were carried out at 3 sites in the Port Hills to monitor rockfall from relict sea cliffs. The cliffs consist mainly of volcanic rocks which include layers of hard, jointed lava flows cut by occasional dykes and interbedded with softer lava breccia, tufts and agglomerate (Massey et al. 2012).

The Cliff monitoring data set consists of up to 8 TLS survey epochs at 3 sites (Redcliffs, Shag Rock Reserve and Wakefield Avenue in Sumner) surveyed between March 2011 and December 2012. The sites comprise steep (vertical to overhanging in parts) rock slopes ranging in height from a few metres to nearly 100 metres (Figure 1). During the earthquake sequence many rocks fell from these slopes. Each site required between 3 and 5 scanner set ups. The survey period encompassed several large earthquakes (Table 1, Figure 2). A data capture routine was developed for working within areas deemed to be at risk from earthquakes. This method had to be adaptable as site access and cliff view position changed following the erection of shipping container barricades, and health and safety restrictions were modified as the project progressed.



Figure 1: Wakefield Avenue from the scanner mounted camera, June 16 2011

Table 1: Start dates of TLS survey epochs and earthquakes > Mw 5 within 10km of the study area (Ristau, 2013)

Date	Event	Date	Event
22/02/2011	Earthquake Mw 6.2	13/06/2011	Earthquake Mw 6.0
22/02/2011	Earthquake Mw 5.5	16/06/2011	Terrestrial laser scan
22/02/2011	Earthquake Mw 5.6	23/12/2011	Earthquake Mw 5.9
1/03/2011	Terrestrial laser scan	16/01/2012	Terrestrial laser scan
8/03/2011	Terrestrial laser scan	2/05/2012	Terrestrial laser scan
16/04/2011	Earthquake Mw 5.0	13/09/2012	Terrestrial laser scan
3/05/2011	Terrestrial laser scan	18/12/2012	Terrestrial laser scan
13/06/2011	Earthquake Mw 5.3		



Figure 2: Google Earth images showing the TLS study areas and the epicentre and magnitude of earthquakes > Mw 5 within 10km of the study area, during the study.

2.1 Establishing survey control in a dynamic environment

Accurate repeat monitoring surveys rely on identifying stable points, or control, from which relative measurements of the cliff can be made. The dynamic nature of the environment in Christchurch has made stable control difficult to define. Seismic events through a sustained aftershock sequence, post seismic relaxation, lateral spreading and ridge rent effects all contribute to local and broader scale deformation occurring at the study sites. Furthermore, earthquake induced landslides have been defined at the margins of the target cliffs.

The common approach to establishing control when monitoring natural surfaces with TLS uses retro reflective targets fixed on or near the target surface (Lague, 2012). This was not suitable in this instance as due to the size and unstable nature of the cliffs and on-going seismic activity it was not safe to place targets.

To overcome this, the scanner tripod positions were marked to allow the tripod to be set up in a consistent position which ensures a consistent viewing angle for each survey. Any change detected between survey epochs can, therefore, be attributed to change in the cliff topography and is not the result of variation in the scanner viewing angle. Initial scan positions were tied to local cadastral survey marks and new specifically placed steel (base) marks with GNSS observations. Over the survey period some of this control has been lost beneath rockfall runout barricades. Where scan set up positions have been lost new scan positions have been tied to existing positions with GNSS observations.

The set up positions have provided the initial control between survey epochs allowing the initial registration and alignment of scans between epochs. This approach relies on the assumption that control positions are not deforming relative to each other and the cliff. GNSS surveying has confirmed that adjacent set ups at the Redcliffs site, that are processed together, remain stable with regard to each other (Table 2). The use of the scanner set ups as initial control allows for the rapid and cost effective acquisition of TLS data at each site by a single operator in a single

day by significantly reducing the time consuming setup and surveying of temporary retro reflective targets.

Table 2: TLS positions at 03/02/2011 and 12/20/2012 relative to the nearby control point.

	Base - TLS01 (m)	TLS01 - TLS02 (m)	TLS03 - TLS04 (m)
3/02/2011	62.810	40.611	51.273
12/20/2012	62.818	40.618	51.242
difference	0.008	0.006	-0.031

2.2 Repeat survey procedure

At each set up the laser scanner was mounted directly on a level heavy duty tripod. A tribrach was not used because the scanner, weighing nearly 20kg, is less stable on a tribrach especially if the scanner head is tilted using the proprietary tiltmount. The instrument has dual axis compensators that adjust for minor dislevelment in the set up.

The scan resolution or point density was determined by user defined (stepwidth) angles in both the phi (horizontal) and theta (vertical) axes. For this study equal stepwidth angles were chosen for phi and theta in all cases. This means that point density varies with range to, and incidence angle of, the target.

During each repeat survey two scans were captured: a 360° (horizontal) panorama scan at 0.09° stepwidth angle (duration 16 minutes), and a cliff scan of between 0.016°and 0.04° [11][GA2]stepwidth angle (duration ~40 minutes), depending on the range to the target surface (Table 3). The panorama scan captures detail away from the target area to allow for the accurate alignment of scans. Where possible, additional photographs were taken with the scanner mounted Nikon D200 digital camera and14mm lens.

Table 3: Pointcloud Resolution (m) at varying stepwidth angle and range assuming a target orthogonal to the laser.

	Range (m)					
Stepwidth angle (deg)	50	100	200	300	400	500
0.016	0.014	0.028	0.056	0.084	0.112	0.140
0.024	0.021	0.042	0.084	0.126	0.168	0.209
0.030	0.026	0.052	0.105	0.157	0.209	0.262
0.040	0.035	0.070	0.140	0.209	0.279	0.349
0.090	0.079	0.157	0.314	0.471	0.628	0.785

3 PROCESSING

TLS data is recorded as ranges and horizontal and vertical angles in a scanner based coordinate system. The data can consist of many thousands or millions of points which, when visualised in a Cartesian coordinate system, is commonly known as a pointcloud. As the scanner can only measure in the line of sight of the laser, scans from different positions are required to avoid data shadows and more fully capture complex natural surfaces.

As a consequence processing is required to combine pointclouds captured from different set ups into a single coherent pointcloud. The classic method is to use retro-reflective targets placed in the scene that are common to adjacent scans. The position of scan set ups and targets is captured with GNSS or total station independently of the scanning in a geographical coordinate system (Lague, 2012). Proprietary TLS software uses least squares methods to translate and rotate (pitch, roll, yaw) adjacent scans in a geographic coordinate system to achieve a best fit based on

the TLS set up and common target positions. Experience has shown that using this method with less accurate GNSS surveying often results in an unacceptable alignment, and that Iterative Closest Point (ICP) algorithms that use overlaps in the pointclouds themselves lead to better results in this situation (Schürch et al. 2011).

3.1 Data alignment

Pointclouds from different epochs have been aligned in a common reference frame using a series of least squares (ICP) adjustments on surfaces within the pointclouds and allowing the scan position to move. Pointclouds from each scan position were accurately loaded in to the same position as the initial scan and coarsely aligned in rotation and height by eye. The panorama scan was then adjusted into alignment with the previous panorama using stable surfaces within the pointclouds and holding the initial position fixed. Horizontal translations of the second scan position onto the previous were in all cases less than 20mm.

These adjustments align the scans from each set-up with its predecessors and allow for the rapid production of initial change-maps which can determine areas of loss, or gain between scans that may indicate either rockfall erosion zones or pre-failure deformation of the rock mass.

To obtain 3D models of cliff topography from each epoch the overlapping scans from each survey were adjusted into alignment using surfaces within the high resolution cliff scans whilst holding the central scan at each site fixed. The standard deviations from this final adjustment were less than 20mm in all cases.

The surfaces used in the epoch to epoch alignment adjustments are generally manmade such as buildings, footpaths, kerbs and roads which have not been impacted by cliff fall. This approach assumes that these structures at the base of the cliffs are not moving relative to the cliffs and provide an accurate localised fixed control for the study. Whilst it is likely some deformation of these structures will have occurred during the study, the least squares algorithm was designed to discard from the adjustment any paired surfaces that were >2 standard deviations or 1 degree different. Any remaining deformation would be smoothed out between the remaining paired surfaces. For most adjustments there were 100 or more paired surfaces. The standard deviation of the alignment adjustments varied between 3 and 20mm although most were around 10mm.

The processing regime is designed to measure rockfall volumes between epochs. The alignment of scans to measure rock-fall volumes through difference calculations precludes the measurement of other deformation that may be occurring. That is, the true position of each cliff face in an external reference frame such as NZGD2000 is not reflected in the alignment of the scans over the study period. Such an alignment would not enable the estimation of rock-fall volumes due to the complex deformation occurring in the area.

3.2 Combining and filtering

The resolution (points/m^2) of raw and combined pointclouds varies from place to place. Furthermore, there is both random error noise in the laser range measurement and systematic error caused by slight misalignment of the combined scans. Examination of planar surfaces in the combined pointclouds indicates this error parameter to be < 0.05m. That is, planar surfaces when viewed edge on have a point thickness of up to 0.05m.

Once an acceptable alignment was achieved the higher resolution cliff scans from each epoch were combined together into a single pointcloud using an octree filter (Riegl, 2012) which calculates an average value for all points within a user defined voxel (cube). Applying an octree filter to the combined pointcloud is useful to average out noise, achieve a more uniform resolution and significantly reduce the file size.

3.3 Removal of vegetation

Vegetation and non-surface laser returns from dust or reflections present a major challenge for analysis of pointcloud data. Often a laborious manual process is undertaken to remove extraneous data (Schürch et al. 2011). For this study the volume of data collected made this approach unfeasible. Furthermore, a manual process is not repeatable and is open to operator bias and error. A systematic statistical approach to point classification (Brodu & Lague, 2012) was used to separate the combined point clouds into vegetation and rock classes. The rock class was further refined to include only points with statistical confidence greater than 95%. A limitation of this method is that the resulting Rock 95% pointcloud is not continuous across the entire cliff but contains data gaps where thick vegetation has obscured the rock behind. It was decided that data gaps were preferable to interpolating across holes. Automated vegetation removal algorithms are further limited by the misclassification of rock as vegetation at sharp changes of direction. In this study this effect removes points at the edges of blocky columnar basalt leaving holes in the data.

3.4 Data input, post processing and analysis in ArcGIS

The next step was to export the pointcloud data to ArcGIS for analysis and fusion with 2D geological mapping data. ArcGIS operates in 2.5D utilising rasters for analysis and calculations. Rasters of terrain data are often called Digital Elevation Models (DEMs)**.** One method to create DEMs is from xyz point data with the z value becoming the numerical value of the raster cell. This approach does not work well for near vertical cliff faces. Accordingly, a method was developed where the cliffs were divided into sections, and the corresponding pointclouds rotated and projected onto best fit vertical planes.

For each cliff section a local coordinate system (x_a, y_a, z_a) was established, where the z value of a point became the y_a value and the distance along the section became the x_a value. The remaining coordinate (z_a) represented the distance between the point and the best fit plane.

For every cliff section a series of DEMs, representing cliff surfaces were created using the PointToRaster ArcGIS Tool. The raster values were calculated as the mean value of all points within each cell. Cells containing no points were assigned NODATA. For each raster, the point-to-raster errors were calculated as the difference between input point values and the raster estimation. Surface rasters for different epochs were used to generate change-models with cell values representing the 1D difference between the two contributing rasters. A positive value indicated gain of material or deposition and a negative value indicated loss of material or erosion. Values were then colour mapped to give a visual representation of change orthogonal to the projection plane between survey epochs (Figure 2 B-D).

Rockfall volumes were calculated as the sum of the negative values multiplied by the cell area. The mean standard deviation of the point-to-raster grid calculation for each TLS epoch on a per site basis was used as a mask applied to account for inaccuracies in the contributing data (Table 4). For all TLS epochs and sites the mask ranges from ±0.07 m to ±0.09 m. That is, differences of magnitude less than mask are treated as no change and removed from the mapping and volume calculations.

When change-models are overlaid with geological mapping units it is possible to attribute individual rockfall events to specific geological strata and cliff locations (Figure 2A). Further discussion of the relationship between rockfalls, geology and slope geometry is provided in Massey et al., (2012).

Table 4: Standard deviation of point to raster calculation for Wakefield north.

Location	TLS number	TLS date	Standard deviation (m)
Wakefield North	a	1/03/2011	0.067
Wakefield North	b	8/03/2011	0.066
Wakefield North	c	3/05/2011	0.064
Wakefield North	d	16/06/2011	0.061
Wakefield North	e	16/01/2012	0.062
Wakefield North	f	2/05/2012	0.058
Wakefield North	g	13/09/2012	0.066
Wakefield North	h	18/12/2012	0.064

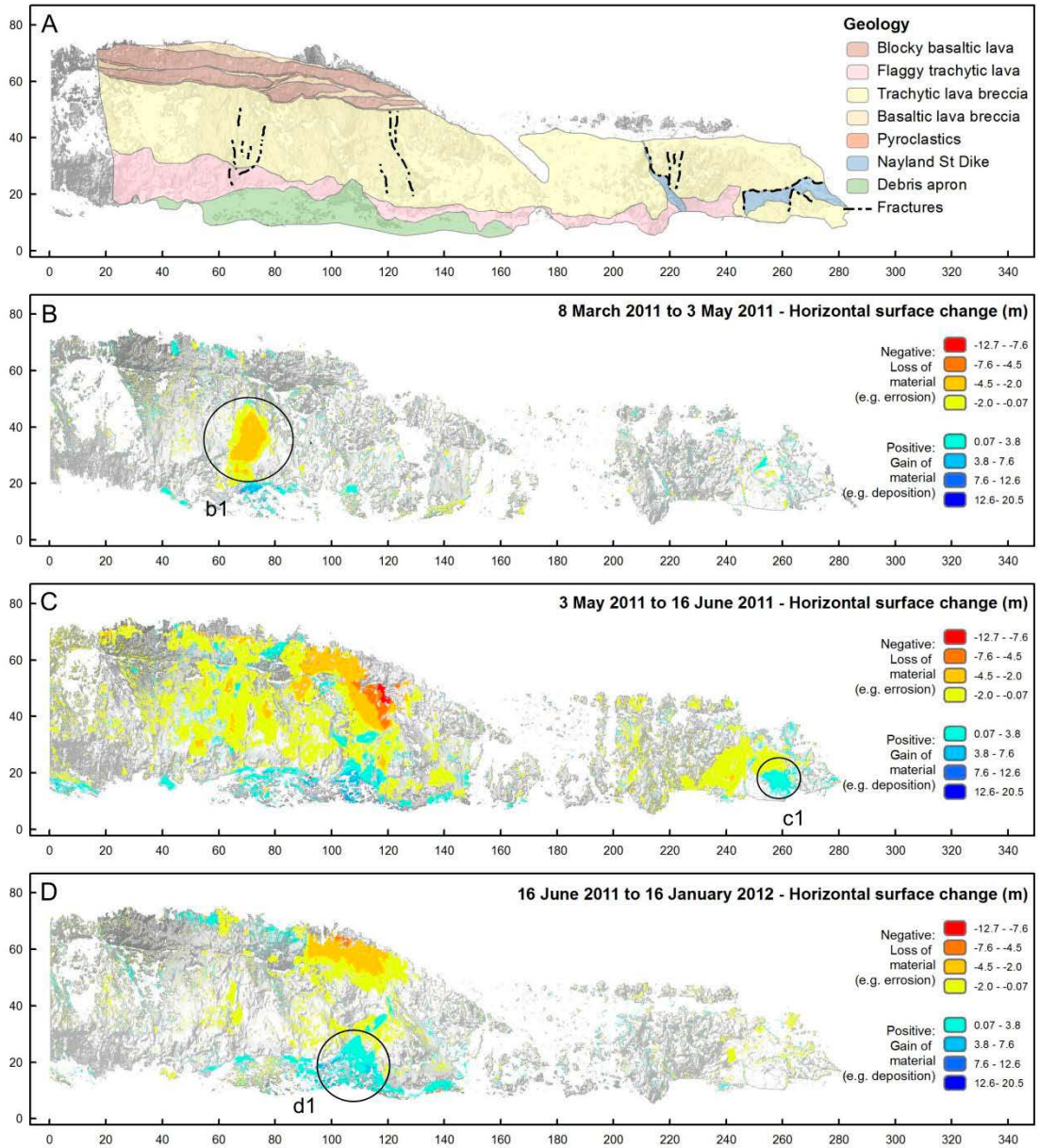


Figure 2: A series of images of TLS data from Wakefield Avenue. Image A is overlaid with the cliff geology. Images B-D are colour mapped change models from March 2011 to January 2012 showing erosion in yellow hues and deposition in blue. The grey hues represent data with no change. Highlight b1; the orange and yellow hues represent a significant rockfall event (~600m^3). Highlight c1; the blue hue shows a dyke deforming toward the viewer. Highlight d1; the blue hues represent an increase of talus on the debris apron at the base of the cliff.

4 CONCLUSIONS

A detailed review of the methods used to study cliff evolution in a challenging post disaster environment has illustrated that TLS can provide high quality data sets if suitable methodologies are adopted. By dispensing with the time consuming setup and surveying of retro- reflective targets a single TLS operator can rapidly acquire large datasets. The approach presented has shown that the use of the scanner setup positions and surrounding manmade surfaces as survey control allows for the alignment of scan data to measure rockfall volumes.

The processing regime developed has been successfully used to measure rockfall locations and volumes. Whilst the method does not represent the true position of the cliffs in an external reference frame, the alignment of the scans allows measurement of rockfall volume through difference calculations.

Both the rockfall estimates produced, and 3D terrain models created, from the TLS surveys can provide accurate cliff change data for both regional rockfall modelling and potential future rockfall risk assessments in complex dynamic environments.

REFERENCES

Abellán A, et al. (2009) Detection of millimetric deformation using a terrestrial laser scanner: experiment and application to a rockfall event. *Natural Hazards and Earth System Science.* 9: 365–372.

Brodu, N. & Lague, D. (2012) 3D Terrestrial lidar data classification of complex natural scenes using a multi-scale dimensionality criterion: applications in geomorphology. *ISPRS Journal of Photogrammetry and Remote Sensing* 68,121-134.

Lague, D., et al. Submitted (2012). A new method for high precision 3D deformation measurement of complex topography with terrestrial laser scanner: application to the Rangitikei canyon (N-Z). *ISPRS Journal of Photogrammetry and Remote Sensing.*

Massey, C.I., et al. (2012) Canterbury Earthquakes 2010/11 Port Hills Slope Stability: Pilot study for assessing life-safety risk from cliff collapse. *GNS Science Consultancy report 2012/57.*

NZSEE (2011) Special Issue: Effects of the 22 February 2011 Christchurch earthquake and its aftershocks, Bulletin of the New Zealand Society for Earthquake Engineering 44, 181-430.

Riegl (2012) RiSCAN PRO v1.7.7, Riegl Laser Measurement Systems, Austria.

Ristau, J. (2013) Personal Communication.

Rosser N, et al. (2007) Patterns of precursory rockfall prior to slope failure. *Journal of Geophysical Research* 112: F04014.

Schürch, P. et al. (2011) Detection of surface change in complex topography using terrestrial laser scanning: application to the Illgraben debris-flow channel. *Earth Surface Processes and Landforms*. 36, 1847-1859. John Wiley & Sons, Ltd.

Wheaton, J. et al. (2010) accounting for uncertainty in DEMs from repeat topographic surveys: improved sediment budgets. *Earth Surface Processes and Landforms*. 35, 136-156. John Wiley & Sons, Ltd.

Avery, M.B. & Bourke, S. (2013)
2011 Manawatu Gorge landslide remediation
Proc. 19th NZGS Geotechnical Symposium. Ed. CY Chin, Queenstown

2011 Manawatu Gorge landslide remediation

M B Avery
Geovert Ltd, Auckland, NZ
Mat.avery@geovert.com (Corresponding author)

S Bourke
Geovert Ltd, Auckland, NZ
Simon.bourke@geovert.com

Keywords: landslide, rockfall attenuator, slope stabilisation, slope barrier

ABSTRACT

The August 2011 Manawatu Gorge landslide had an initial failure of approximately 20,000 m3. The sheer volume of the failure caused the closure of State Highway 3 through the gorge and a rapid response team consisting of consulting engineering geologists and specialist contractors acted promptly to ascertain the extent, cause and short term remediation works to allow reopening of the very important transport link. In the following months several further failures continued which led to the development and design of extensive long term remedial works. A design workshop was held where scientists, engineers and specialist contractors convened to discuss options for the long term remediation of the slip. The final design included the removal of some 370,000 m3. The extents of the earthworks were determined using the DTM developed earlier in the project, based on a combination of GNS produced 3D laser scans and recently flown LiDAR. The earthworks began in December 2011 and finished (down to road level) in May 2012. Once excavation was complete the highway required an almost complete rebuild as there were a number of half and full bridge structures that were extensively damaged during the event, likely both from the sudden impact energy of material during failures and also the long term effects from thousands of tons of material loading the structures over an extended 12 month period. Stabilisation and drilling work on site included the installation of mesh drape, horizontal shallow inclined drainage holes, stabilisation of colluvium slopes using rock dowels and installation of a 500kJ Geobrugg rockfall attenuator. The stabilisation of the landslide and the rebuilding of the highway structures was completed in October 2012.

New Zealand Geotechnical Society Inc. 19th Symposium, Queenstown 2013

1 INTRODCUTION

This paper outlines the widely publicised very large landslide that affected New Zealand's Manawatu Gorge on SH3 between Ashhurst and Woodville. The first failure and subsequent road closures occurred in August 2011. The initial failure measured approximately 50m high by 100m wide. An estimated 20,000 m3 of weathered greywacke and colluvium ended up on State Highway 3 and in the river. Numerous contractors worked tirelessly under the expert guidance of the local NZTA appointed Engineer to reinstate the highway and make the route safe. Several further failures occurred in the months following the initial collapse and taking into account the finished excavated slope the final volume of material removed was in the order of 370,000 m3. The highway reopened to (controlled) two way traffic in October 2012. The initial failure occurred in August 2011 causing the complete closure of SH3 through the Manawatu Gorge, fortunately with no casualties. An initial assessment was made by NZTA's appointed engineers and it was decided that immediate temporary remedial stabilisation works were required to improve stability of the exposed slope to provide a safer working environment at road level. The work was carried out by rope access technicians and consisted of clearing of the head scarp and rock removal from the main face with mechanical scaling and blasting. During this time the roading contractors were also working on clearing the slip material from road level. This procedure was for the best part a round-the-clock operation for the first few weeks until

after the second failure in mid-September people's perspectives changed and a strategic rethink on the clearing and stabilisation was undertaken. During the excavation and clearing of the highway NZTA Engineers undertook further investigations, with the aid of rope access engineering geologists were better able to understand the processes at hand. At each new collapse event numerous rope traverses were undertaken for the purpose of geological and geomorphological mapping. Scientists from Geological & Nuclear Sciences (GNS) were commissioned in October 2011 to carry out the first of many laser scans from a helicopter drop off point on the opposite side of the gorge. These scans were invaluable and picked up minute detail of the slip surface and the surrounding area.



Figure 1 - Shortly after failure (left 2011) and near completion (right May 2012)

Over the following 3 months the slip failed twice again each time regressing further upslope. It was during these subsequent failures that MWH engaged the expertise of GNS scientists who over the following months contributed at various levels to the understanding of both the immediate and regional environment. This included a number of reports on the main feature and also on the wider gorge area.

2 SITE GEOLOGY AND GEOMORPHOLOGY

The slip itself in the early stages of the investigations proved to be driven by a larger deep seated global instability of the hillside, with initial field investigations indicating a large slip with boundaries that extend from the gully west of the slip upstream to the nearby unnamed creek. While this feature is possibly still active (moving as slow creep – likely only millimetres per year) it was not immediately affecting the recent events. Closer examination of the exposed slip surface suggested the larger scale feature has a lower slip plane day-lighting approximately 10m above road level. This was evidenced by water seeping from the face.

The mass of the main feature consists predominantly of a large melange type material including highly to completely weathered weak, sheared and crushed interbedded sandstone and mudstone (greywacke). Lesser amounts of colluvium also exist (evidenced in the upper western margin of the slip face). Amongst the weathered greywacke there exist three or four 'rafts' of more competent sandstone. These appear to be moving down slope amidst the weaker material as rafts, staying mostly intact but with weak joint planes susceptible to deformation. These rafts are often jointed very closely to widely spaced and have occasional sheared and crushed zones within them.

New Zealand Geotechnical Society Inc. 19th Symposium, Queenstown 2013

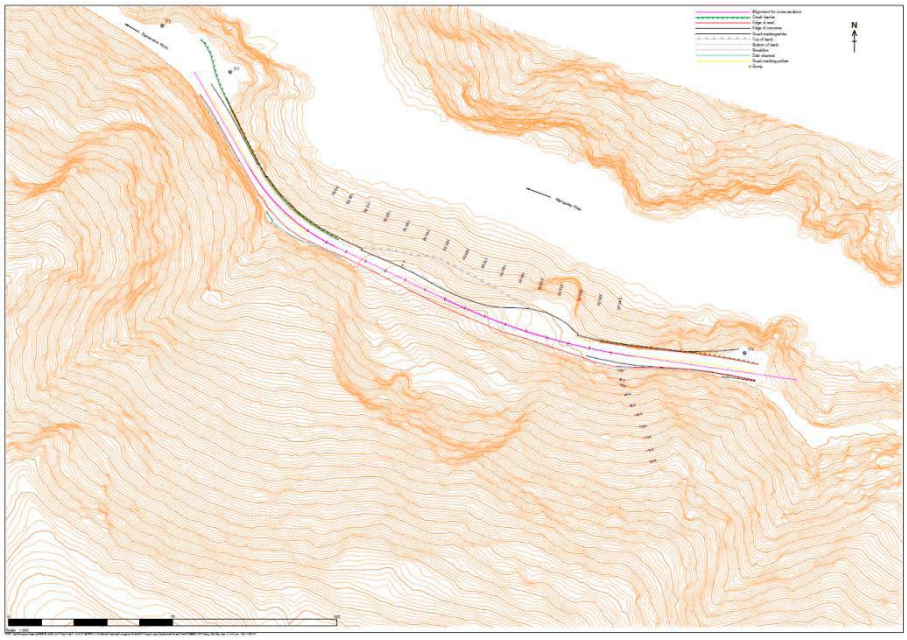


Figure 2 - Site Topographic Map August/September 2011 (Robson 2011)

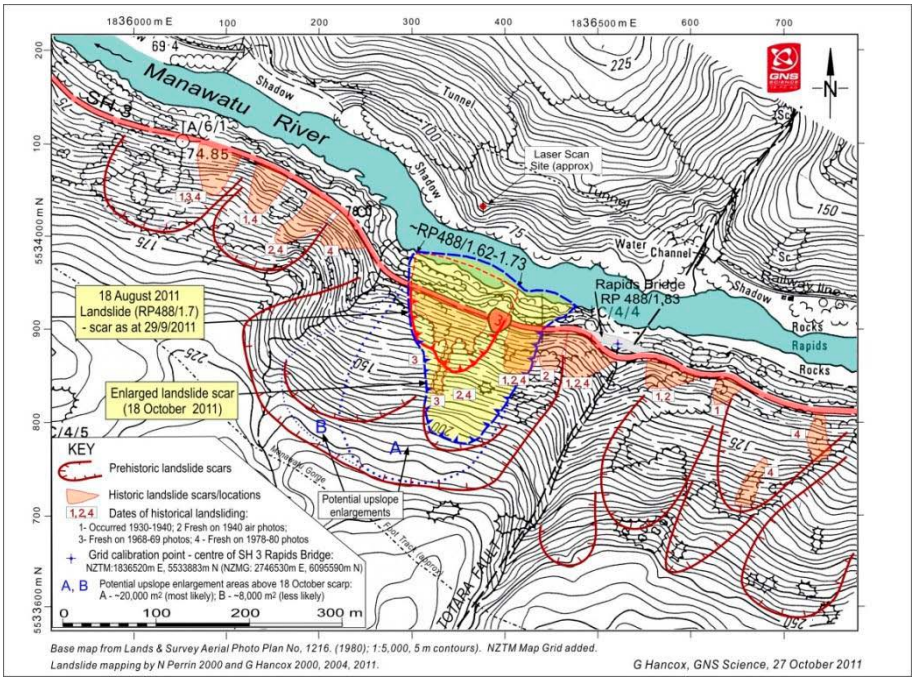


Figure 3 - Site Geomorphic Map October (Hancox 2011)

The remainder of the slip mass, approximately the downstream third, is a tightly packed, bedded colluvium and/or slope wash material, possibly resulting from multiple past landslides or mass failure events, leading to the presence of bedding, into a pre-existing gully feature. This material consists of silty sandy gravel up to gravelly boulders. The material is typically sub angular to rounded and is dry apart from a couple of seeps from approximately two thirds the way up the face at the very downstream western margin. Seeps are also intermittently present on the upstream material.

3 DESIGN CONCEPT

A design workshop was held in November whereby NZTA engineers along with Geovert and GNS scientists convened to discuss options for the long term remediation of the slip. By this

stage it was clearly evident that the full potential extent of the feature, based on historical evidence, was far larger than what was currently exposed and the site was capable of further large scale potentially rapid failures.

The basic design concept was discussed at this meeting with consensus over the following weeks that laying the slope angle back to a more stable angle by means of benching was the most suitable and cost effective option. The cost benefit analysis included consideration by NZTA of rerouting the highway permanently elsewhere. The extents of the earthworks were determined using the DTM developed earlier in the project, based on a combination of GNS produced 3D laser scans and recently flown LiDAR. The slip area was rescanned on a regular basis to help calculate the extensive volumes of material removed from the slip. The earthworks began in December 2011 and finished (down to road level) in May 2012. Approximately 370,000 m3 of material was removed from the slip. The excavation began at the top via a freshly cut track pushed in from farmland to the south and progressed down slope to road level. All excavated and cut material was pushed over the edge of the benches and removed from the base of the slope.

Once excavation was completed the highway required an almost complete rebuild as there were a number of half and full bridge structures that were extensively damaged during the event, likely both from the sudden impact energy of material during failures and also the long term effects from thousands of tons of material sitting on the structures over an extended 12 month period. Further specialist consultants including BBO and Earthtech Consulting were commissioned to investigate and design replacement structures. In addition to the earthworks a number of long term management issues were identified with the finished slope including excessive ground water egress, localised areas susceptible to surficial erosion, over steepened colluvium (not part of the earthworks program) and exposed jointed greywacke (the slope comprises interbedded, indurated greywacke sandstone and argillite, typically closely to very closely jointed) likely to release rockfall.

The installation of some form of rock retention system was identified quite early on. Once the slope was excavated to its finished surface rockfall modelling was undertaken by both MWH and Geovert Engineers to determine what remedial measures were required to improve the safety of road users (Spang, 2003). On site rockfall trials were also carried out under controlled conditions to verify the modelling results.

4 REMEDIATION AND CONSTRUCTION

Geovert were commissioned directly by NZTA under the management of NZTA engineers for all slope stabilisation and drilling work completed on site. The work included installation of a Geobrugg DELTAX mesh drape, installation of horizontal inclined drainage holes, stabilisation of the western colluvium slope and installation of a 500kJ European Technical Approval Guideline (ETAG) Approved attenuator. Geovert's contribution to the reconstruction of the highway included nearly 1000 lm of drilling including installation of anchors on the abutment of Bridge 8 (complete new build), stabilisation of the Bridge 8 Abutment D potential/slow moving wedge failure, and installation of seismic strengthening anchors for Half Bridge 7 and Half Bridge 9.

4.1 Slope work

4.1.1 Mesh drape

Carried out in May 2012 the installation of the mesh drape at the eastern margin of the slip was critical to the progress of the project. This was an NZTA engineer design utilising Geobrugg DELTAX high tensile steel wire mesh with a longitudinal strength of 55 kN/m. After initial significant delays were encountered due to weather and other construction activities on site a 6

New Zealand Geotechnical Society Inc. 19th Symposium, Queenstown 2013

day window was provided and a 24hr operation was implemented to complete the full installation inclusive of the required drilling at the perimeters.



Figure 4 - Drilling of the mesh anchors (left TTV, 11) and inclined drainage holes (right)

4.1.2 Slope drainage holes

The installation of inclined horizontal drains was intermittent during the project with more drains being drilled as the nature of the slope revealed itself during different weather patterns. The drains were typically positioned to target clay seams where water egress was greatest. In one area twelve drains were installed mid-way up the slope and when piped, to avoid surface erosion, the measured flow rate was 18,000 litres per day. At the time of writing this paper this rate has not noticeably diminished since the installation.

4.1.3 Colluvium stabilisation

The western edge of the slip consists of ancient colluvium slip material. A series of investigation holes were drilled to determine the depth to competent rock. Holes were drilled at various levels including mid slope work requiring helicopter delivery of plant several hundred meters above the road level. A design to stabilise this portion of the slope was developed based on the information gathered from these holes. The design was to retain the toe of the mass so three rows of anchors were drilled at the base of the slope to a minimum of 4.0m into rock which meant varying anchor lengths between 9 m and 12 m long. The final surface was then shotcreted prior to installation of steel waling beams secured by the anchors. Drainage holes were also installed at varying depths.

4.1.4 Attenuator installation

Very early on it was identified that there would be a residual risk of frequent low energy rockfall and debris at the site once the earthworks were completed. Geovert in conjunction with Geobrugg provided a solution to reduce this risk while at the same time allowing for simple debris clearance. A bespoke rockfall attenuator was specified with assistance from Geobrugg designed to withstand and manage impacts up to 500kJ from boulders with bounce heights up to 4.0m high (FHWA Manual, 1991). The total system length is 140 lm. Due to time and cost constraints the unique A-R posts were specified, these require no upslope support cables which reduces the amount of drilling required therefore reducing construction time. The system is located 30m above road level where bounce heights were lowest and has a 25m long TECCO G80/4 high tensile steel wire mesh tale with longitudinal load capacity of 150 kN/m. A purpose built catchment ditch was to be constructed at the base of the slope to retain material exiting the tale (attenuators typically reduce energies by 30-50% only).

Installation of the posts and cables Figure 5, and tensioning of the system was completed in two days and the mesh installation to the toe was completed in a further three days. The complete

system installation (excluding drilling) was completed in less than one week total construction time. Geobrugg engineering quality and controls along with their finite element modelling gives the client full confidence that they are protecting their asset and the road users with an engineered system.



Figure 5 - Installing the attenuator posts by helicopter

4.2 Highway Work

4.2.1 Bridge 8 drilling

The reconstruction of Bridge 8 at the eastern end of the site required the supporting of both abutments by means of ground anchors. These were primarily for seismic strengthening and designed to stop excessive movement of the abutments during an earthquake and seismic loading. The anchors were installed using a tracked anchor rig and was on critical path due to the very tight deadlines to open the road. Until this bridge was completed there was very limited access for many of the Contractors and plant through the gorge.

4.2.2 Bridge 8 Abutment D

During the excavation of the final abutment on Bridge 8 a major open wedge shaped defect was identified in the rock mass behind the abutment. There was concern that this was an active slow moving failure plane and remedial measures were designed to ensure no future movement could occur. A total of 45 m3 of concrete and grout was pumped into the void, including an initial 20 m3 of concrete pumped from the surface, a further 10 m3 of concrete pumped through injection holes. During the installation a flood washed away a portion of the working platform under the bridge and to prevent any further delays to the programme a number of anchors were drilled using a drill rig hanging from a 50t crane as can be seen in the top left photo in Figure 6.

4.2.3 Half Bridge 7 and Half Bridge 9

Two half bridges were reconstructed through the middle and western section of the site. Anchors were required on both structures and at both the anchors, drilled through soldier piles, were designed to combat any seismic induced movement. Originally the plan was to drill the holes with the tracked drill rigs from a working bench however another flood event resulted in the rig being hung beneath the structure using a 50t crane. A total of 600 lm of drilling was completed at these two sites.

New Zealand Geotechnical Society Inc. 19th Symposium, Queenstown 2013

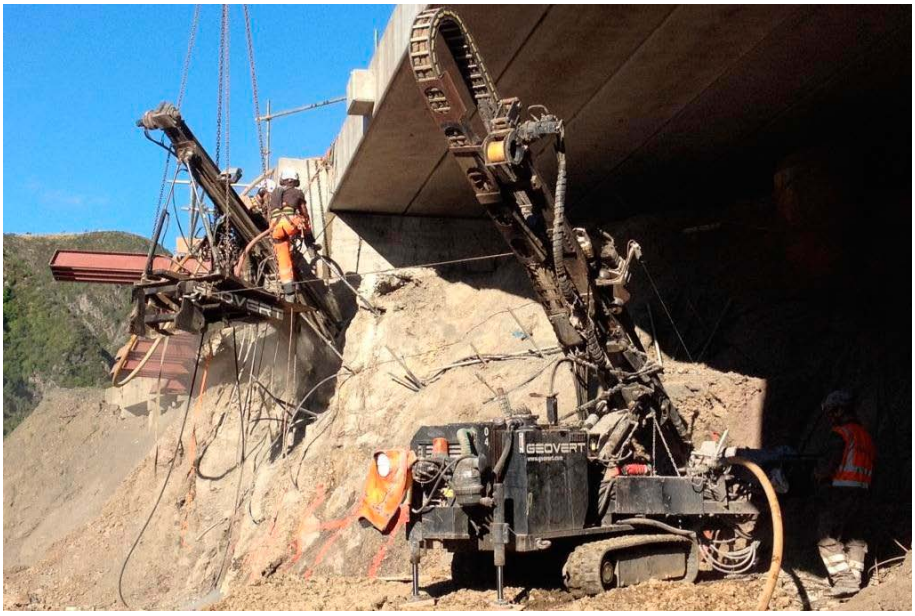


Figure 6 - Installing anchors through Bridge 8 wedge failures & Bridge 9 tie back anchors



Figure 7 - Installing the Bridge 9 tie back anchors

5 CONCLUSION

In summary the stabilisation of the Manawatu Gorge Landslide was a significant undertaking by all parties involved. While the initial slip was considered large the on-going regression and final remedial design option was far bigger than anyone initially comprehended. The project is now complete and the road is open to full two lane traffic.

Table 1 - Summary of Manawatu Gorge works completed by Geovert Ltd

Location	Equipment	Description	Number (each)	Drilling (metres)
Mesh Drape	2x Portable Rig	Drilling Mesh	62 2500m2	310
Inclined Drainage Holes	3x Portable Rig	Drilling	60	600
Bridge 7 Anchoring	1x Anchoring Rig 1x High Reach Rig	Drilling	79	525
Bridge 8 Anchoring	1x Anchoring Rig 1x High Reach Rig	Drilling	42	220
Bridge 9 Anchoring	1x Anchoring Rig	Drilling	6	75
Investigation Drilling	1x Portable Rig 1x Anchoring Rig 1x High Reach Rig	Drilling	13	240
Wedge Failure Stabilisation	1x Anchoring Rig 1x High Reach Rig	Drilling	35	420
Colluvium Stabilisation	1x Anchoring Rig 1x High Reach Rig	Drilling	123	1120
Attenuator Installation	2x Portable Rig 1x 50t crane 1x Helicopter	Drilling	36 140lm barrier	250

6 ACKNOWLEDGEMENTS

Geovert would like to acknowledge the help of the Client NZTA, the Consultants including MWH Ltd Wellington, Palmerston North and Wanganui offices and specifically Chris Robson, Mike Skelton and Murray Salter. Also BBO and Earthtech Consulting. The local Contractors including Richardson's Drilling, Morris & Bailey, HEBs Structures, Goodman's and Higgins Ltd.

7 REFERENCES

ETAG, *European Organisation of Technical Assessment*, Brussels (Belgium).

FHWA *Manual 'Rock Slopes'. November 1991.* USDOT Chapter 12 Page 19.

Hancox. G. 2011 *Email correspondence.* GNS Science

Hoek, Dr. E,. *Practical Rock Engineering* (2007)

Robson, C. (2011) *Project correspondence.* MWH Ltd Wellington

Spang, R.M. *Rockfall 6.1 Simulation Software.* Release 3.2.2003

TTV, (2000) *Private video and photos.* Tararua Television Trust, Pahiatua 4961, New Zealand, www.tararuatv.co.nz

Murashev, A., Easton, M. & Kathirgamanathan, P. (2013)
Advanced numerical modelling of geogrid-reinforced rockfall protection embankments
Proc. 19th NZGS Geotechnical Symposium. Ed. CY Chin, Queenstown

Advanced numerical modelling of geogrid-reinforced rockfall protection embankments

A. Murashev, M. Easton & P. Kathirgamanathan
Opus International Consultants Limited, New Zealand.
Alexei.Murashev@opus.co.nz

Keywords: rockfall protection, embankment, finite element modelling, geogrid

ABSTRACT

Rockfalls pose a major hazard to infrastructure, commercial buildings and residential dwellings in hilly and mountainous regions throughout New Zealand. Following the Darfield earthquake and associated aftershocks, significant rockfalls were widespread around the Port Hills south of Christchurch. In areas where rockfalls can be both substantial in size and have a greater potential for multiple design level impacts in any one single event, commonly accepted rockfall measures can be too costly to install to provide effective protection against the design event or may have an unacceptably short design life. A geogrid-reinforced rockfall protection embankment is a ductile system capable of absorbing very high kinetic energy rockfalls and withstand multiple rockfall impacts without collapse. Therefore, the use of rockfall protection embankments is becoming more common. Currently, empirical or simplified analytical methods are used to design such embankments. In order to assess behaviour of rockfall protection embankments in more detail, Opus carried out 3D numerical simulation using the finite element software ABAQUS. In the simulation process rock blocks were thrown onto a geogrid reinforced embankment at different impact angles. The effects of geogrid spacing, the presence of the steel facing mesh and impact angle have been investigated. The numerical simulation procedure can be used to develop and optimise the design of geogrid-reinforced rockfall protection embankments.

New Zealand Geotechnical Society Inc. 19th Symposium, Queenstown 2013

1 INTRODUCTION

Rockfall can occur from natural sources, such as unmodified hillsides or relict sea cliffs, and man-made features including road cuttings and mines. These rockfalls can be instigated through a wide variety of triggers (e.g. weathering, frost-jacking, seismic activity and blasting). Away from the built environment and its supporting infrastructure, rockfall poses little more than an interesting study of natural process and its risk is generally accepted as part of the natural evolution of the environment. However, the interaction of rockfall with built elements at risk (e.g. residential settlements, businesses, highway infrastructure and rail corridors) frequently causes significant threats, typically in terms of structural damage, loss of life, financial cost and service disruption. As the availability of low-risk sites suitable for development become pressured, areas at greater risk from rockfall are increasingly considered as viable options. Geogrid-reinforced rockfall protection embankments provide effective mitigation against rockfall hazard. However, currently there are no commonly accepted design methods for the rockfall protection embankments. The most advance design technique involves the use of numerical modelling. Opus utilised 3D numerical modelling to investigate the behaviour of the rockfall protection embankments under the impact of rock blocks with high kinetic energies. The design methodology for rockfall protection embankments is described in this paper.

2 RECENT ROCKFALLS IN CHRISTCHURCH

The magnitude 7.1 Darfield Earthquake of 4 September 2010 was centred approximately 40 km west of Christchurch city centre at an approximate depth of 30 km and caused significant structural and land damage. Whilst some rockfalls were recorded as a result of the earthquake, these were generally confined to localised features and areas and their resulting damaging effects were limited, primarily due to the softer ground conditions (typically encountered at the end of the winter) limiting run-out paths. The magnitude 6.3 aftershock of 22 February 2011 generated far greater levels of rockfall. In the Port Hills to the south and east of Christchurch city centre, a total land area of about 65 km^2 was affected by rockfall, stretching from Mount Pleasant in the north, Lyttelton in the south, Godley Head in the east and to Governors Bay in the west. Examples of 22 February 2011 rockfall damage are shown on Figure 1.



Figure 1: Seismically triggered) rockfall boulder resting on a block wall having passed dwelling, Morgans Valley, 22 February 2011, Christchurch (left); Impact damage to a house due to seismically triggered rockfall boulder, Morgans Valley, Christchurch (right).

Increased levels of rockfall were largely attributable to the exceptionally high Peak Ground Accelerations (PGAs) in both the horizontal and vertical planes. PGAs of 2.1g (horizontal) and 2.2g (vertical) were recorded at Heathcote Valley, the approximate epicentre of the aftershock. In addition to the high PGAs, the dry ground conditions encountered at the time of year (late summer) will have further exacerbated the impact of triggered rockfalls resulting in unusually long run-out distances, especially when compared to those of the initial Darfield earthquake. Damage and disruption caused by the rockfalls was widespread. Transportation infrastructure, businesses and residential dwellings were all affected. For residential dwellings alone over 120 individual dwelling (or ancillary building) rockfall impacts were mapped. Many thousands of individual seismically triggered fallen boulders were mapped across the region, enabling the generation of a unique and comprehensive dataset. Mapped boulder sizes were widely varied. However, the average and the 95th % percentile boulder volume values have been reported as approximately 1.0 m^3 and 3.0 m^3 respectively.

Significant numbers of seismically triggered boulders coupled with their comparatively large volumes, high coefficients of restitution of the dry ground encountered along their run-out paths and mode of travel (significant angular rotation) culminated in a multitude of high total kinetic energy boulders, even over the lower sections of the Port Hills slopes. Resulting levels of damage to the built environment caused by individual rockfall boulders were in many cases localised but considerable.

3 METHODS OF MITIGATING ROCKFALL

Physical options for mitigation of rockfall can be broadly broken down into passive and active systems, both with an element of at-source treatment (scaling). Active systems generally require retention of the unstable rockmass at source by mechanical means. Such systems often include combinations of rock bolts, high strength steel mesh, cables and concrete. With active systems, successful mitigation relies upon all potential sources being treated. Quite often this treatment needs to be carried out in hazardous construction conditions. In many cases maintenance and long-term durability issues make this option less attractive compared to passive systems. Passive systems rely upon the optimal placement of a downslope system that arrests the rockfall before impacting the element at risk. To effectively select, correctly size and place passive systems a careful blend of assessment, analysis and judgement is required. Typical examples of passive rockfall mitigation systems include dynamic and non-dynamic catch fences, attenuators, catch ditches, rock sheds and embankments (or bunds). Ultimately the selection of passive systems is governed by a number of factors that include the available construction envelope, site access, hill-slope geometrics, maintenance requirements, long-term durability and anticipated design loading (total kinetic energy and number of rockfall impacts).

For the majority of the Port Hills, the rockfall threat (based upon the observed occurrences during the 22 February 2011 aftershock) is primarily from seismic events triggering widespread releases, resulting in multiple boulders travelling down-slope with large total kinetic energies.

Passive systems in the form of Mechanically Stabilised Earth (MSE) embankments have been used in New Zealand and elsewhere to mitigate the rockfall hazard in environments similar to Port Hills. MSE embankments (including geogrid-reinforced fill embankments) are able to withstand multiple impacts of rockfalls with high total kinetic energies and can be relatively easily repaired.

MSE rockfall protection systems are cost-effective and have a considerable design life. A substantial disadvantage of this rockfall protection system is the need to have an appropriate stable site for the construction of the rockfall protection embankments.

3 ROCKFALL PROTECTION EMBANKMENTS

For sites where multiple impacts of rockfall with high kinetic energy levels are expected, MSE rockfall protection embankments present a reliable cost-effective method of mitigating rockfall hazard. Examples of such structures are shown on Figure 2.



Figure 2: Rockfall protection embankments in Europe: 12 m high rockfall protection embankment, Italian Alps (left); end section of a rockfall protection embankment near Mont Blanc Tunnel (right)

Geogrid-reinforced embankments are widely used for mitigating rockfall hazards. Methods used for the design of the geogrid-reinforced rockfall protection embankments vary from country to country.

Available design methods have been summarised by Lambert & Bourrier, (2013) and include:

- A simplified design method based on consideration of the mass of the embankment and its ability to withstand the impact;
- A simplified method based on consideration of penetration of the rock block into the embankment and assigning the minimum thickness of the embankment that will provide appropriate safety margin;
- Pseudo-static design approach that considers a load that is statically equivalent to the dynamic impact load, where the embankment's static stability is checked using commonly accepted design methods;
- Analytical design methods based on the comparison of the incident translational kinetic energy of the block with the energy dissipated within the embankment during the impact; and,
- Design methods based on numerical modelling to model the impact and assess the deformation of the embankment using either finite element method or discrete element methods.

In most of countries currently there are no recommendations or guidelines for the design of rockfall protection embankments. In Italy and Austria design standards have recently been developed and published (UNI, 2012; ONR, 2012). While simplified methods are being widely used in the current design practice, numerical modelling based on non-linear soil models and consideration of dynamic effects provides a more advanced design tool capable of detailed analysis of the stress-strain condition of the embankment, energy dissipation mechanisms and optimisation of the design of rockfall protection embankments. Currently design methods based on numerical modelling are becoming more attractive to the geotechnical designers as a large number of finite element software products are available on the market.

Numerical modelling of geogrid-reinforced rockfall protection embankments has been used for the analysis of the full scale tests data in Italy (Peila et al., 2007) and Japan (Maegawa & Van, 2011), and the numerical modelling method has been calibrated against the field test data and adopted soil models and design assumptions have been verified. In both cases (Peila et al., 2007; Maegawa & Van, 2011) the modelled behaviour of the embankments under the impact of a rock block matched the field test data reasonably well, indicating that numerical modelling provides an effective design tool that can be used in practical engineering.

4 PRINCIPLES OF NUMERICAL MODELLING OF ROCKFALL PROTECTION EMBANKEMNTS

In our analysis we modelled rockfall events using ABAQUS software. ABAQUS is a general purpose highly sophisticated finite element (FE) computer program that can be used to solve a variety of engineering and research problems. It is especially suited for nonlinear finite element analysis and is widely used in engineering and academic environments. ABAQUS enables modelling of static and dynamic problems with a high level of detail. Numerical simulation of the free fall of a rock block in ABAQUS can be carried out using two different methods:

- the rock block can be modelled at its initial drop height and ABAQUS can calculate the full motion of the block under the influence of gravity, or alternatively,

- the rock block can be modelled at a position near or very close to the soil surface with a certain mass and predefined initial impact velocity to simulate the impact.

The first option is less practical because of the large number of time increments required to complete the free fall analysis. We utilised the latter method to model the impact of the rock block on the embankment. In our analysis we used *RocFall* software to determine the striking speed, the direction of the rock block movement and the location of the impact. *RocFall* is a statistical analysis program designed to assist with assessment of slopes exposed to risk of rockfalls. Energy, velocity and "bounce height" envelopes for the entire slope are determined by *RocFall*, as well as the location of the impact. Distributions of energy, velocity and bounce-height are also calculated along the slope profile. Distributions can be graphed and comprehensive statistics are automatically calculated. Slope geometry and ground conditions that govern the coefficient of restitution should be defined to assess the direction and kinetic energy of the rock block.

Deformation of the embankment upon impact of a rock block depends on many variables. Some play a major role, while others have a minor effect. For example, the coefficient of friction between the embankment surface and the block, the Poisson's ratio of the soil, and the mechanical properties of the rock are considered to have negligible effect. On the contrary, dimensions of the rock, impacting velocity of the rock, deformation and strength properties of the soil, friction between the geogrid and the soil and the size of the embankment play a major role in its response. In our analysis we did not consider the rotational kinetic energy of the rock block as it is generally less than 10–15% of the total block energy (Chau et al., 2002). However, the rotational effects can be modelled in ABAQUS if required.

The ABAQUS modelling process involves building a model, defining material properties, introducing the finite element mesh, applying loads and boundary conditions, and running the analysis. Similar to Peila et al. (2007), our numerical algorithm was based on an explicit time integration known as "centred difference method". The simulation computation was divided into up to 40 time steps, and for each step, the instant displacement, speed and acceleration of each element of the FE mesh were evaluated. The ground was modelled using three-dimensional cubic shaped blocks with eight integration nodes.

Material properties were assigned using the ABAQUS property module. The soil embankment, the geogrids and the welded facing steel mesh were modelled as deformable materials. The rock block was modelled as rigid body. The geogrid and the facing steel mesh were modelled as elastic shell layers. The embankment material was modelled using elasto-plastic Mohr-Coulomb model. The soil, geogrid, rock block and steel mesh parameters used in the numerical simulation are given in Table 1. The size of the rock block in our analysis was chosen to approximately represent the 95th % percentile boulder volume value during the 22 February 2011 Christchurch earthquake. Also, we adopted a rock block speed representing a possible rock block speed in accordance with *RocFall* analysis for 22 February 2011 Christchurch earthquake.

Table 1: Soil, geogrid and rock block parameters

Geotechnical parameters	Soil	Geogrid	Rock Block	Steel Mesh
Unit Weight, kN/m^3	19	0.0042 (kN/m^2)	24	78.5
Young's Modulus, MPa	120	200	Rigid body	200x10^3
Poisson's Ratio	0.3	0.3	Rigid Body	0.3
Friction Angle, degrees	32	2/3 (tan ϕ) (geogrid-soil contact)	As for the soil (block – soil contact)	2/3 (tan ϕ) (geogrid-soil contact)
Cohesion, kPa	2	0 (geogrid-soil contact)	0 (block – soil contact)	0
Striking speed, m/s			28	
Size, m			1.5x1.5x1.5	

The geometry of the analysed embankment and the rock block, as well finite element mesh and a typical image of the crater created by the rock block are shown on Figure 3. The length of the analysed section of the embankment was chosen based on a number of initial numerical simulations that identified the minimum distance to the edge boundaries where the boundary conditions had minor effect on the stress-strain state at the impact location. The adopted crest width of the embankment was 1 m, and the adopted angle of the batter slopes to the horizontal was 60°. The geogrid layer spacings of 0.5 m and 1 m were analysed. Effect of the presence of the facing steel mesh was also analysed.

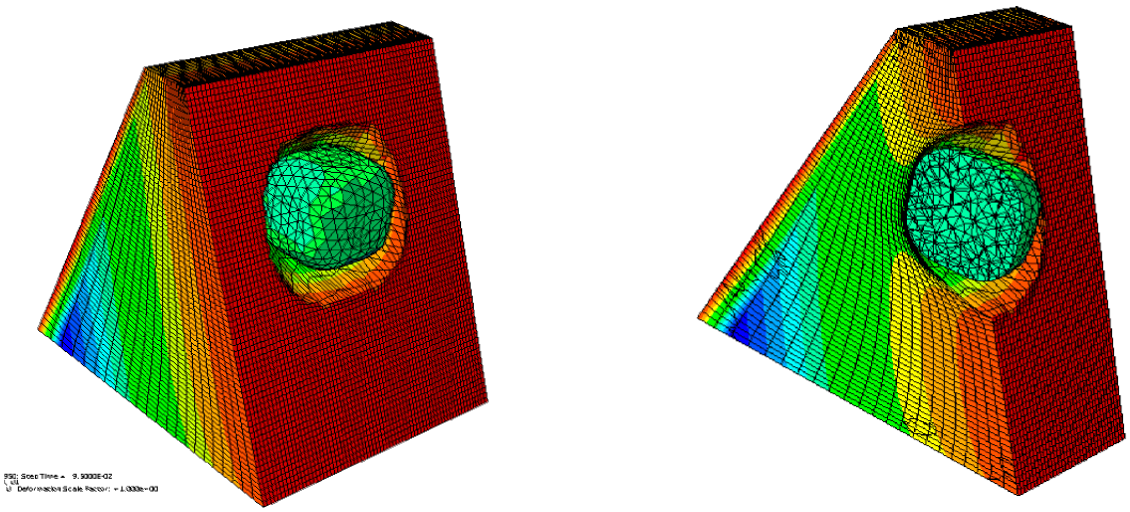


Figure 3: Analysed rockfall protection embankment (image from ABAQUS): typical impact (left); impact at the end of the embankment (right)

For the analysis of a typical impact, the rock block was thrown into the middle section of the modelled embankment (Figure 3, left). For the analysis of the effect of the impact's proximity to the end of the embankment, the rock block can be thrown at the edge of the embankment (Figure 3, right).

5 MODELLING RESULTS

Numerical simulation was carried out for striking angles of – 30°, 0° and +30° (positive angles correspond to the downward movement of the rock block). The total displacement contours within body of the embankment from ABAQUS outputs are shown in Figure 4. It can be seen that the depth of crater and the displacements depend on the striking angle of the rock block and reach their maximum values at the striking angle of 30°. This is explained by the fact that the proportion of the frictional dissipation energy is substantially higher for the striking angle of – 30°, compared to the case with the striking angles of 0° and + 30° where plastic deformation penetrates substantially deeper into the body of the embankment (Figure 4).

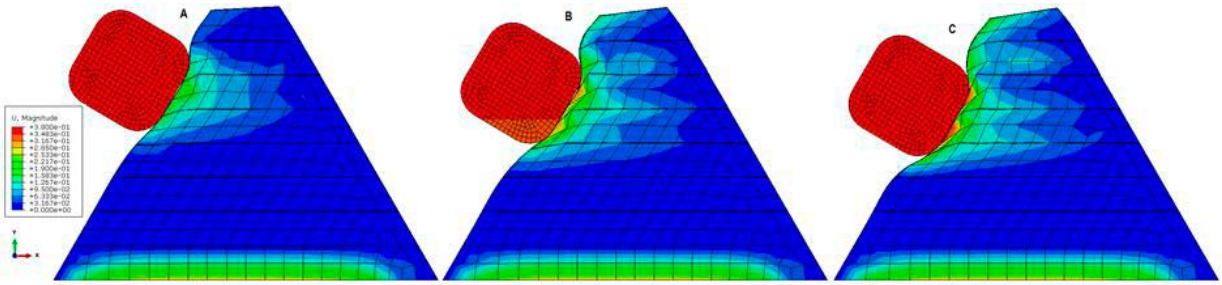


Figure 4: Total displacement for striking angles of -30° (A), 0° (B), and +30° (C)

The effect of the spacing of the geogrid layers on the behaviour of the embankment have been also investigated (Figure 5). Numerical simulations were carried out for the striking angle of +30°. The modelling data indicated that the strengthening effect of closer spaced geogrid layers can be adequately modelled by ABAQUS enabling the designer to optimise the design of the geogrid-reinforced soil embankment and to achieve cost savings on the imported fill and amount of geogrid.

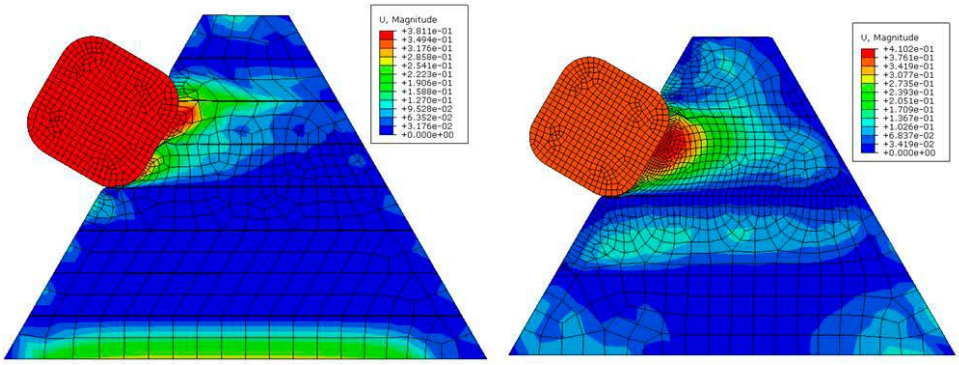


Figure 5: Total displacements from ABAQUS outputs for geogrid spacing of 0.5 m (left) and 1 m (right)

Our analysis of the embankment with and without the facing steel mesh (Figure 6) indicated that while the shapes of the crater created by the rock block for the two cases are substantially different, the effect of the presence of the steel mesh on the overall performance of the embankment is relatively minor, which agrees well with the test data published by Peila et al. (2002).

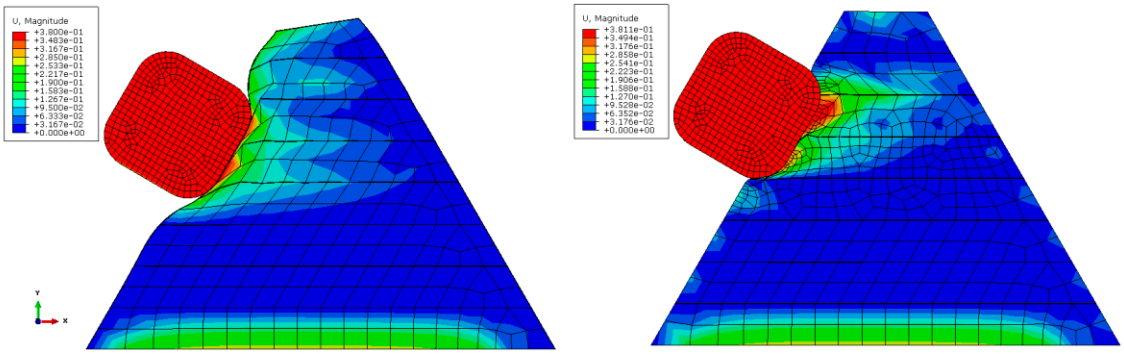


Figure 6: Total displacements from ABAQUS outputs for the embankment with the facing steel mesh (left) and without the facing steel mesh (right)

ABAQUS also enables the designer to predict the single impact energy and the number of lower energy impacts that will cause the failure of the embankment.

6 CONCLUSIONS

Rockfalls pose a major hazard to infrastructure, commercial buildings and residential dwellings in hilly and mountainous regions throughout New Zealand. The magnitude 6.3 Christchurch earthquake of 22 February 2011 generated substantial levels of rockfall and resulted in damage to infrastructure and residential dwellings. For sites where multiple impacts of rockfall with high kinetic energy levels are expected, geogrid-reinforced rockfall protection embankments

present a reliable cost-effective method of mitigating rockfall hazard. While a number of simplified design methods for rockfall protection embankments are available, advanced numerical modelling gives the designer an opportunity to analyse various load cases, to optimise the design and achieve cost savings where possible.

REFERENCES

Chau, K T , Wong, R H C , Wu, J J (2002) Coefficient of restitution and rotational motions of rockfall impacts. Rock Mechanics and Mining Science 39.

Lambert, S & Bourrier, F (2013) Design of Rockfall Protection Embankments. Engineering Geology Journal 154, 2013.

Maegawa, K & Van P T (2011) Experiments on Rockfall Protection Embankments with Geogrids and Cushions. International Journal of Geomate. Oct. 2011, Vol. 1, No. 1 (Sl. No. 1).

ONR, 2012. ÖNORM 24810: Technical protection against rockfall — Terms and definitions, effects of actions, design, monitoring and maintenance. Austrian standard institute, Vienna (draft 21 August 2012, in German).

Peila, D, Oggeri, C, Castiglia, C, Recalcati, P & Rimoldi, P (2002) Testing and modelling geogrid reinforced soil embankments subject to high energy rock impacts. Geosynthetics - 7 ICG – Delmas.

Peila, D, Oggeri, C & Castiglia, C (2007) Ground reinforced embankments for rockfall protection: design and evaluation of full scale tests. Landslides, Vol.4(3), Springer-Verlag, Sep. 2007.

UNI, 2012. UNI 11211–4 — Opere di difesa dallacaduta massi. Parte 4: Progetto definitivo ed esecutivo (in Italian).

Moon, V.G., Cunningham, M.J., Wyatt, J.B., Lowe, D.J., Mörz, T., Jorat, M.E. (2013)
Landslides in sensitive soils, Tauranga, New Zealand
Proc. 19th NZGS Geotechnical Symposium. Ed. CY Chin, Queenstown

Landslides in sensitive soils, Tauranga, New Zealand

V G Moon, M J Cunningham, J Wyatt, D J Lowe
Department of Earth and Ocean Sciences, University of Waikato, Private Bag 3105, Hamilton 3240, NZ
v.moon@waikato.ac.nz (corresponding author)

T Mörz, M E Jorat
Marum – Center for Marine and Environmental Sciences, University of Bremen, Klagenfurter Strasse, DE-28359 Bremen, Germany

Keywords: sensitive soil, Tauranga, halloysite, pore water pressure

ABSTRACT

In the Tauranga region sensitive soil failures commonly occur after heavy rainfall events, causing considerable infrastructure damage. Several notable landslides include a large failure at Bramley Drive, Omokoroa in 1979, the Ruahihi Canal collapse in 1981, and numerous landslides in May 2005; recently the Bramley Drive scarp was reactivated in 2011. These failures are associated with materials loosely classified as the Pahoia Tephras - a mixture of rhyolitic pyroclastic deposits of approximately 1 Ma.

The common link with extreme rainfall events suggests a pore water pressure control on the initiation of these failures. Recent research on the structure of the soils shows a dominance of halloysite clay minerals packed loosely in arrangements with high porosity (51 – 77 %), but with almost entirely micropores. This leads us to conclude that the permeability is very low, and the materials remain continuously wet. The formation of halloysite is encouraged by a wet environment with no episodes of drying, supporting this assumption.

A high-resolution CPT trace at Bramley Drive indicates induced pore water pressures rising steadily to a peak at approximately 25 m depth; this depth coincides with the base of the landslide scarp. We infer that elevated pore water pressures develop within this single, thick aquifer, triggering failure through reduced effective stresses. The inactive halloysite clay mineral results in low plasticity indices (13 – 44 %) and hence high liquidity indices (1.2 – 2.4) due to the saturated pore space; remoulding following failure is sudden and dramatic and results in large debris runout distances.

New Zealand Geotechnical Society Inc. 19th Symposium, Queenstown 2013

1 INTRODUCTION

In the Tauranga region sensitive soil failures commonly occur after heavy rainfall events, causing considerable infrastructure damage. A history of large landslides over the past 35 years includes:

- a large failure at Bramley Drive, Omokoroa in 1979, as a result of which 5 houses were removed (Gulliver and Houghton, 1980);
- the collapse of the Ruahihi Canal in 1981 which resulted in more than 1 million m3 of material being eroded and transported into the Wairoa River (Hatrick, 1982); and
- a series of landslides in various parts of Tauranga City and its surroundings in May 2005.

Recently, the Bramley Drive scarp, which had remained essentially stable for 30 years and had developed a good vegetation cover, was reactivated in 2011, and continued regression of the scarp face has occurred throughout 2012 (Figure 1).



Figure 1: Reactivated landslide at Bramley Drive, Omokoroa, January 2013

A striking feature of these landslides is the long run-out distance of the debris and apparent fluidity of the debris flow. This long runout is associated with, and evidence of, the sensitive nature of many materials in the Tauranga region (Keam, 2008, Wyatt, 2009, Arthurs, 2010, Cunningham, 2013). Sensitivity is recognised as a loss of strength upon remoulding, and is quantified as the ratio of undisturbed to remoulded undrained strength where both strengths are determined at the same moisture content. Values of < 2 are insensitive, 4 – 8 are considered sensitive, 8 – 16 are "extra sensitive", and > 16 are referred to as "quick clays" (New Zealand Geotechnical Society, 2005).

Sensitive behaviour is well described from glacial outwash deposits in Norway and Canada, where leaching of salt from an open, flocculated structure in low activity illite clay minerals results in a loss of cohesion of the soils, which are then prone to failure in response to a weak trigger. Characteristic failures are spreads and flows as the loose structure contains large quantities of water that is released upon remoulding. In Tauranga however, we do not have glacial clays, and the sensitivity is developed in sequences of rhyolitic pyroclastic materials, including primary pyroclastic fall deposits (tephra), pyroclastic flow deposits (ignimbrite), and a wide variety of reworked pyroclastics including slope wash, fluvial, and aoelian variants. A different origin for the development of sensitivity in these materials is thus needed. This paper considers the microstructural influences on the properties of the soils leading to sensitivity.

2 MATERIALS

The stratigraphic sequence seen in the Tauranga area is complex, but an overall stratigraphy recognizes several "packages" of material that are well exposed in the present scarp of the Bramley Drive failure at Omokoroa where the sequence is very thick (Figure 2). At the top are Pleistocene and Holocene materials representing recent eruptives, predominantly from the Taupo Volcanic Zone, and modern soil materials; the base of this unit is comprised of the Rotoehu Ash of approximately 60,000 years (Briggs *et al*., 1996). The Rotoehu Ash lies on a very distinctive paleosol formed on the Hamilton Ashes. The Hamilton Ashes are comprised of a series of tephra deposits with intercalated paleosols ranging from ~0.08 to 0.38 Ma (Lowe *et al.*, 2001). At Bramley Drive the Hamilton Ashes reach a total thickness of ~ 9 m; this thickness is variable around the region. The Hamilton Ashes lie on top of another very well developed, dark brown paleosol (Figure 2) which marks the top of the Pahoia Tephra sequence – a poorly defined sequence of primary and reworked rhyolitic volcaniclastic materials ranging in age from approximately 0.35 to 2.18 Ma (Briggs *et al*., 1996). The Pahoia Tephras are part of the Matua Subgroup which is a widespread, complex unit throughout the Bay of Plenty (Briggs *et al*., 1996). At the Bramley Drive site, the Pahoia Tephras include at least 6 units to a thickness of > 12 m. Below this is believed to be the Te Puna Ignimbrite (Briggs *et al*., 1996, Gulliver and Houghton, 1980) based on nearby exposures, which in turn is underlain by a lignite deposit at shore platform level.

New Zealand Geotechnical Society Inc. 19th Symposium, Queenstown 2013

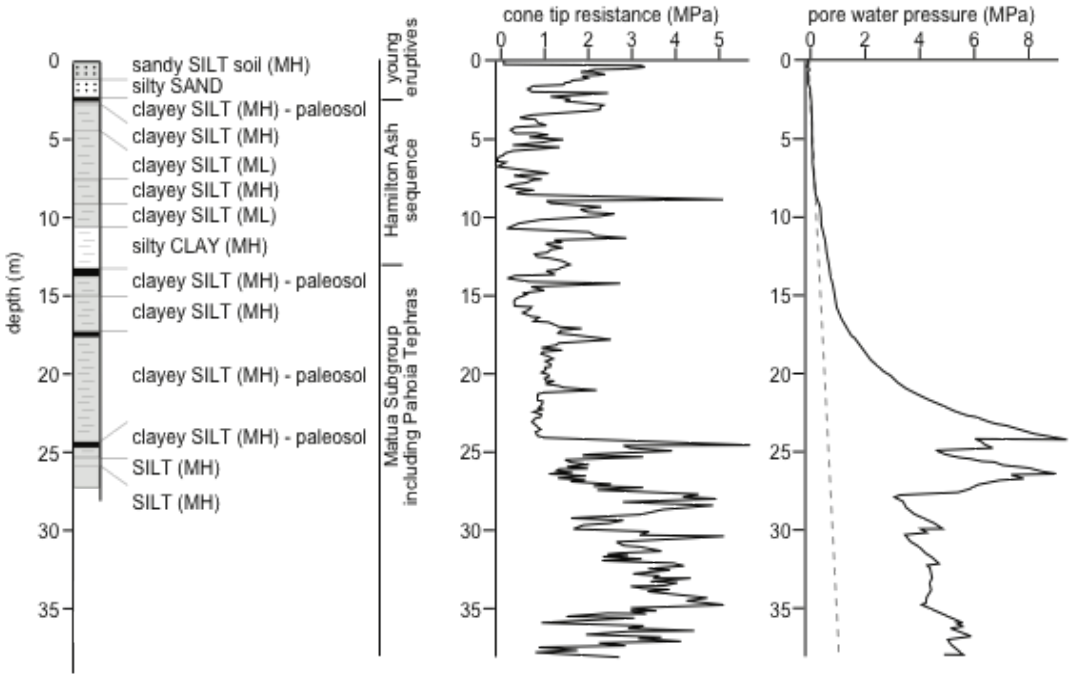


Figure 2: Profile log and cone penetrometer trace from the scarp of the Bramley Drive landslide. CPT trace measured in March 2012, profile log described in January 2013; textural descriptions are from particle size analysis, classification from Atterberg limits

It is the Pahoia Tephras that are associated with the sensitive soil failures observed in the Tauranga region. This sequence is in places very thick, but thinner in others, and it is difficult to correlate single layers across any significant distance. It is likely that many of the units are formed by local reworking of primary pyroclastic material, and hence have small lateral extents. In this paper, materials from individual units within the Pahoia Tephras at Omokoroa Peninsula (OMOK1 and OMOK2), Pahoia Peninsula (PAHO1), Te Puna (TEPU1), Otumoetai (OTUM1, OTUM2, OTUM3 and OTUM4), and Tauriko (TAUR1, TAUR2 and TAUR3) were sampled and tested. Site locations are presented in Table 1, and further details of site stratigraphy and sample locations can be found in Wyatt (2009) and Cunningham (2013).

Sampling was undertaken based on recognition of sensitive layers in the field from vane shear tests following standard methods (New Zealand Geotechnical Society, 2001). A selection of data from sensitive units is presented in Table 1. Mineralogy was determined from XRD analysis of both bulk samples and clay separates. Natural water content, dry bulk density, and Atterberg limits were determined following ISO standards (ISO/TS 17892-1:2004(E), ISO/TS 17892-2:2004(E), ISO/TS 17892-12:2004(E)), except that specimens were not allowed to dry when preparing for Atterberg limits tests; and particle density was determined using density bottles following the method outlined by Head (1992). Effective cohesion and friction angle from consolidated, undrained triaxial testing were measured following standard BS 1377-8:1990. Coefficients of consolidation (c_{vi}) and volume compressibility (m_{vi}) were determined for each applied loading in consolidation stages of the triaxial testing (BSI, 1999), and the coefficient of permeability was estimated using the method described by Head (1986).

Texturally, the samples are identified in the field as clayey silts or silty clays. This is in keeping with a pyroclastic fall (tephra) origin, but does not preclude reworking of initial tephra deposits as suggested by Arthurs (2010). Mineralogically the samples are dominated by glass or alteration products of volcanic glass (Table 1). The clay mineralogy is in all cases dominated by halloysite clay minerals, with some kaolinite also identified in OTUM3 and OTUM4 samples. Allophane was not identified in any of the samples. Sensitivity values (Table 1) show generally "sensitive" to "extra sensitive" materials (New Zealand Geotechnical Society, 2005). These values are comparable with others measured on volcanic soils in NZ, both in Tauranga (Wesley,

2007, Keam, 2008, Arthurs, 2010) and more widely (Jacquet, 1990). Dry bulk density is typically very low (Table 1), with associated high porosity and void ratio values. Natural moisture content is high, meaning that the soils are characteristically at or close to saturation in their normal field conditions (Table 1).

Atterberg limits (Table 1) are high, but are in keeping with those measured on halloysite-dominated soils in Indonesia by (Wesley, 1973), though values of the plastic and liquid limits and plasticity index all extend to lower values than the ranges given by Wesley (1973) suggesting the inclusion of some dehydrated halloysite. All samples plot below, but parallel to, the A-line in the same range as shown for halloysite soils by Wesley (1973); they are classed as high compressibility silts (MH). Likewise, effective strength parameters (c', ') are also high; they span a range for the soils measured, but averages of c' = 15 kN m^{-2} and ' = 33° are in agreement with Wesley's (1973) values.

Estimated coefficients of permeability are generally within the range of 10^{-8} to 10^{-9} m s^{-1}, in keeping with Wesley's (1977) results in the range of 10^{-7} cm s^{-1}. Wesley interprets this as a high permeability given that the soils he was considering were dominantly clay materials. In this case, however, the soils have a very large silt component, and the measured coefficients of permeability are much lower than might be anticipated.

3 MICROSTRUCTURE

Components of the microstructure include:

- glass fragments which are generally angular and show pumice vesicle wall forms indicating the fragmental pyroclastic origin (Figure 3A) - these are generally of silt to fine sand sizes;
- occasional sand-sized quartz and plagioclase crystals; and
- ubiquitous fine clay-size (< 2 m) material (Figure 3B).

Halloysite is commonly envisaged as a tubular mineral (Joussein *et al*., 2005). However, in the halloysites identified here a wide range of morphologies is seen, including tubes (Figure 3C) which range from common short, stubby forms (< 0.4 μm) to less common long tubes up to 2 μm, plates (up to 2 μm) that have coalesced into books as large as 50 μm long (Figure 3D), and spheres of approximately 0.2 – 0.7 μm (Figure 3F).

The microstructure sees few grain-to-grain interactions, with most being mediated by clays (Figure 3B). Interactions between matrix clay minerals create a flocculated structure, but not in the normal way of a card house, in this case the tubes etc interact by edge contacts alone as there are no platy surfaces (Figure 3E). Interaction of clays in this way results in a highly porous structure (porosity 62 – 77 %), but the pore space is hugely dominated by ultrapores (< 0.1 m) and micropores (< 5 μm) with dominant pore sizes being < 1 μm (Figure 3F). Whilst these micropores impart high porosity, we infer that they are poor at transmitting water, hence the low measured coefficients of permeability.

4 CONE PENETROMETER

A cone penetrometer test (CPT) was undertaken at a site immediately behind the scarp of the Bramley Drive landslide at Omokoroa in February 2012. The instrument used (GOST) is an offshore CPT instrument developed at Bremen University (MARUM – Center for Marine Environmental Sciences) in Germany. GOST incorporates a small (5 cm^2) piezocone, and thus gives high-resolution traces. The traces of tip resistance and pore water pressure are shown alongside a graphic log of the scarp face in Figure 2.

Table 1: Measured geomechanical data for sensitive materials from the Tauranga region. [1] Data for halloysite and allophane from Indonesia from Wesley (1973, 1977), [2] Allophane data from Wesley (2010)

	location (NZTM)	peak vane strength (kN m^{-2})	remoulded vane strength (kN m^{-2})	sensitivity	dry bulk density (kg m^{-3})	porosity (%)	natural moisture content (%)	void ratio	saturation (%)	PL	LL	PI	LI	c' (kN m^{-2})	phi' (°)	permeability (*10^{-9} m s^{-1})
OMOK1	5831082.0N 1868958.5E	92 ± 6	8 ± 6	11 ± 0.6	834 ± 14	66 ± 3	84 ± 4	1.9 ± 0.1	107 ± 8	46	72	27	1.44	8.0	37.0	-
OMOK2	5831082.0N 1868958.5E	74 ± 4	5 ± 0.6	15 ± 2	779 ± 14	68 ± 3	89 ± 1	2.1 ± 0.1	103 ± 8	51	74	22	1.71	16.0	28.0	-
TEPU1	5827011.0N 1872145.4E	122 ± 6	12 ± 1	11 ± 2	688 ± 6	69 ±1	109 ± 7	2.2 ± 0.1	109 ± 9	46	89	44	1.45	16.0	41.0	-
PAHO1	5831343.7N 1865826.9E	69 ± 2	6 ± 0.3	11 ± 0.5	975 ± 2	62 ± 3	68 ± 2	1.6 ± 0.1	108 ± 7	34	53	19	1.79	15.0	32.0	-
PAHO2	5831269.8N 1865368.7E	67 ± 2	8 ± 0.3	9 ± 0.4	952 ± 8	63 + 3	70 ± 2	1.7 ± 0.1	106 ± 7	36	54	18	1.91	10.0	36.0	-
TAUR1	5817385.4N 1872985.1E	58 ± 3	6 ± 3	9 ± 1	656 ± 41	74 ± 5	115 ± 1	2.9 ± 0.3	103 ± 12	57	81	24	2.39	11.8	27.3	0.5
TAUR2	5817385.4N 1872985.1E	45 ± 3	2 ± 3	20 ± 2	589 ± 13	77 ± 3	109 ± 1	3.3 ± 0.2	83 ± 8	47	73	26	2.41	-	-	-
TAUR3	5817385.4N 1872985.1E	151 ± 3	34 ± 3	5 ± 1	966 ± 10	62 ± 3	64 ± 1	1.6 ± 0.1	100 ± 8	39	52	13	1.88	24.0	31.1	6.2 ± 4.7
OTUM1	5824797.3N 1877275.8E	101 ± 6	13 ± 4	8 ± 1	656 ± 8	75 ± 3	104 ± 3	3.0 ± 0.2	91 ± 8	47	90	43	1.33	34.5	25.7	160 ± 130
OTUM2	5824797.3N 1877275.8E	125 ± 7	15 ± 3	10 ± 1	893 ± 51	66 ± 4	69 ± 4	2.0 ± 0.2	94 ± 12	32	57	25	1.46	4.7	38.5	130 ± 120
OTUM3	5824797.3N 1877275.8E	> 227	36 ± 3	> 6	920 ± 15	65 ± 3	66 ± 3	1.9 ± 0.1	93 ± 8	54	96	42	0.27	8.3	35.4	22 ± 17
OTUM4	5824797.3N 1877275.8E	72 ± 8	5 ± 3	14 ± 0.5	743 ± 9	72 ± 3	86 ± 3	2.6 ± 0.1	88 ± 8	37	73	36	1.35	13.7	28.5	130 ± 40
ranges		**45- >2272 - 36**		**5 - 20**	**656-975**	**62-77**	**64 - 109**	**1.6-3.3**	**83 - 100**	**32 - 57**	**52 - 96**	**13-44**	**0.3-2.4**	**5-35**	**27-41**	**0.5 - 160**
halloysite[1] Indonesia				not sensitive			31-51		100	55-75	70-110	20-45		14	37	1 - 13
allophane[1] Indonesia				not sensitive			68-180		100	65-150	85-190	20-50		14	37	10.8 - 27
allophane[2]				5 – 55			50 - 300	1.5 - 8	90 - 100				0 - >1	20	40	

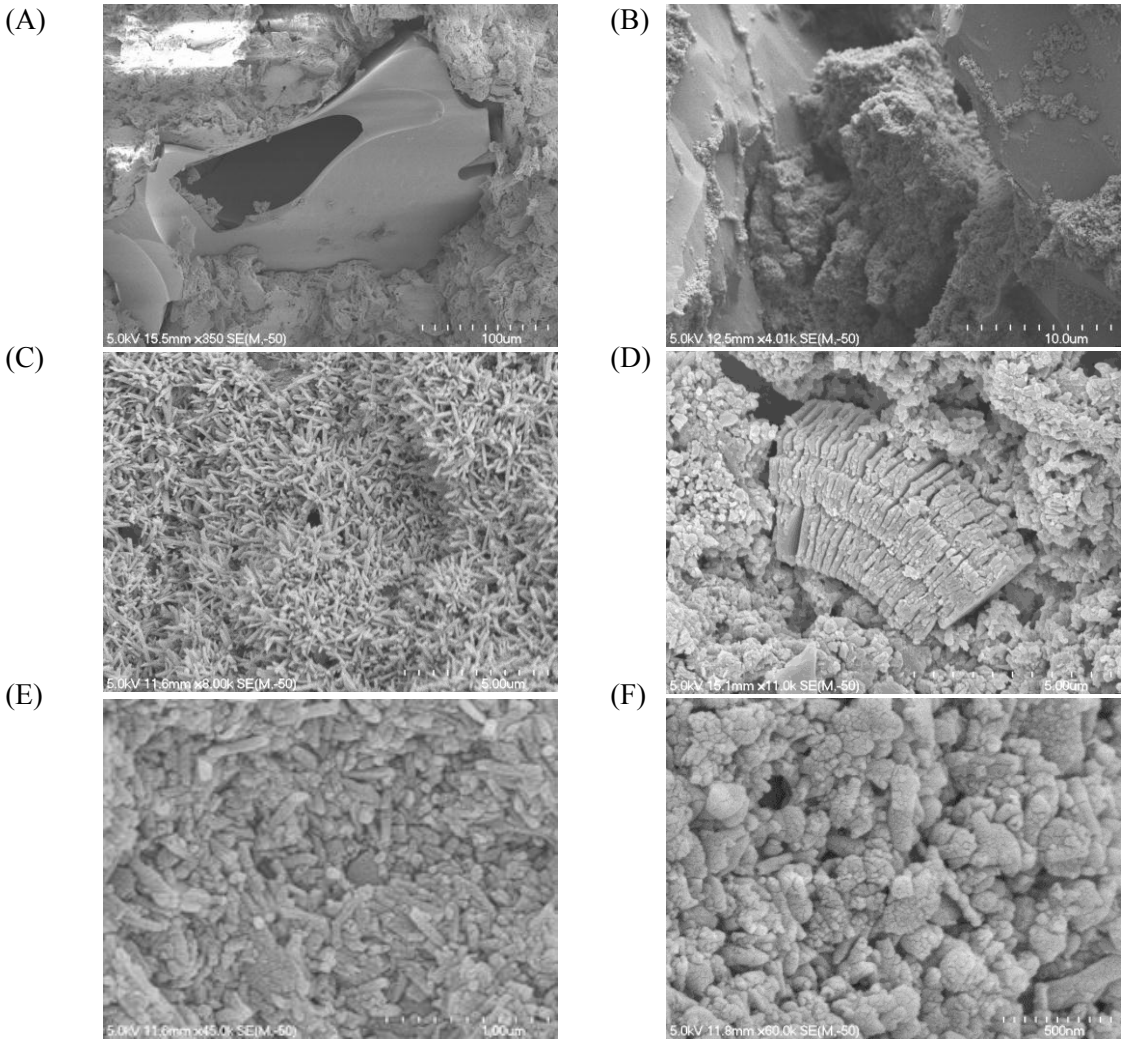


Figure 3: (A) Glass fragment from Tauriko showing vesicular pyroclastic texture. (B) Accumulated clay minerals forming bridge between two glass shards. (C) Typical tubular halloysite forms. (D) Platy halloysite joined to form books. (E) Edge to edge contacts between tubular clay minerals form an open, porous structure. (F) Spherical clay mineral grains form ultrapores. Photos H. Turner

In the CPTu profile, the tip resistance is responsive to effects of soil formation, with increased tip resistance near the present ground surface, and spikes in the measured resistance at each of the identified paleosols. Between these spikes, the tip resistance of the materials is generally low (< 1.5 MPa). However, just below the exposed sequence (about 28 m), the tip resistance increases, and generally stays high until the maximum depth of 38 m was reached; this represents the ignimbrite underlying the Pahoia Tephra sequence.

The pore water pressure shows a water table depth of approximately 1.5 m, followed by a steady rise in induced water pressures to a depth of 24 m. It then falls sharply at this point, corresponding with a spike in the tip resistance (a coarser layer) and then rises to a further peak at approximately 28 m, after which the induced pore water pressures fall in the ignimbrite, though still remain above hydrostatic. A zone from about 17 – 24 m depth shows particularly high induced pore water pressures, indicating low permeability in these materials. This location is believed to be the approximate position of the initial failure zone for the 1979 failure at Bramley Drive (Gulliver and Houghton, 1980), where it was assumed to lie near the contact of the ignimbrite and overlying materials.

From this we infer that there is essentially a single aquifer overlying the ignimbrite near the base. There seems to be little leakage through any more permeable zones, and even the paleosols, which have a well-developed soil structure that in other traces in the region allow partial water transmission (Jorat *et al*., in press), are of low permeability. The only "leak" is in the zone just below 24 m, above the top of the ignimbrite, but within the volcaniclastic sequence.

5 DISCUSSION

In summary, the results presented here show these halloysite-dominated soils to have high porosity, high Atterberg limits, but with non-plastic characteristics, and high shear strength, all in keeping with previously published data for halloysite. The materials are saturated under field conditions, and with high porosities they have liquidity indexes typically greater than one. These conditions make for highly sensitive materials with low remoulded strength.

Initial estimates of the permeability from laboratory testing suggest low permeabilities. These values are supported by the CPTu testing that indicates that the profile at Bramley Drive consists largely of a single aquifer with very high induced pore water pressures developed in poorly-drained materials. The microstructure of these materials shows a variety of morphologies of the halloysite minerals, but most importantly, the clay sizes are small, and their arrangements mean that the high porosity occurs almost entirely within very small pore spaces. Thus, the materials can hold very large amounts of water, but that water cannot move readily within the soils (low permeability).

Wesley (1973, 2010) suggests that allophane is transformed to halloysite as a later stage in the weathering sequence. However, more recent work indicates that allophane and halloysite form directly from dissolution of primary minerals via different pathways. Halloysite formation is favoured by a Si-rich environment (Joussein et al, 2005) and a wet, even "stagnant", moisture regime (Churchman et al., 2010). Allophane, conversely, forms preferentially in soils where Si is low in solution, allowing development of Al-rich allophane. This occurs with better drainage where Si is removed from the profile, and in andesitic materials where the original Si content is lower. Thus, halloysite forms preferentially in the Tauranga region where the overlying rhyolitic Hamilton Ashes provide a ready source of Si that is leached into the Pahoia Tephras; the high porosity yet low permeability of these units results in consistently high natural moisture contents with limited water transport.

The materials at the top of the profile are highly permeable, allowing rapid infiltration of surface water. Deeper layers have lower permeability, meaning that transport from the profile is low, and water tables remain high year-round, creating consistently high saturation levels. Consequently, pore water pressures can rise quickly and easily, triggering failure; the very high porosity and high liquidity indexes result in sensitive soils that generate extensive debris flows.

ACKNOWLEDGMENT

The authors acknowledge funding by Deutsche Forschungsgemeinschaft (DFG) via the Integrated Coastal Zone and Shelf Sea Research Training Group INTERCOAST and the MARUM Center for Marine Environmental Science at the University of Bremen. Access to the Bramley Drive site was provided by Western Bay of Plenty District Council. Special thanks to Mr. Wolfgang Schunn for managing instruments and operation of the CPT unit.

REFERENCES

Arthurs, J. M., 2010. The nature of sensitivity in rhyolitic pyroclastic soils from New Zealand. PhD thesis, University of Auckland, New Zealand.

Briggs, R. M.; Hall., G. J.; Harmsworth., G. R.; Hollis., A. G.; Houghton., B. F.; Hughes., G. R.; Morgan. M. D.; Whitbread-Edwards., A. R. 1996: Geology of the

Tauranga Area - Sheet U14 1:50 000. Department of Earth Sciences, University of Waikato Occasional Report 22.

Churchman, G.J., Pontifex, I.R. and McClure, S.G., 2010. Factors influencing the formation and characteristics of halloysites or kaolinites in granitic and tuffaceous saprolites in Hong Kong. Clays and Clay Minerals 58(2): 220-237.

Cunningham, M. J., 2013. Sensitive rhyolitic pyroclastic deposits in the Tauranga region: mineralogy, geomechanics and microstructure of peak and remoulded states. MSc thesis, University of Waikato, New Zealand

Gulliver, C. P. & Houghton, B. F., 1980. Omokoroa Point land stability investigation. Report prepared by Tonkin & Taylor for Tauranga County Council (N.Z.). 54p.

Hatrick, A. V., 1982. Report of Committee to Inquire into the Failure of the Ruahihi Canal. Ministry of Works and Development, New Zealand.

Head, K.H., 1992. Manual of soil laboratory testing; volume 1: Soil classification of compaction tests. Pentech Press, London.

Head, K.H., 1986. Manual of soil laboratory testing; volume 3: Effective Stress Tests. Pentech Press, London.

Jacquet, D., 1990. Sensitivity to remoulding of some volcanic ash soils in New Zealand. Engineering Geology, 28 (1–2): 1–25.

Jorat, M.E., Kreiter, S., Mörz, T., Moon, V. and de Lange, W., in press. Utilizing cone penetration tests for landslide evaluation. Proceedings, 6th International Symposium Submarine Mass Movements and Their Consequences. 2013.

Joussein, E., Petit, S., Churchman, J., Theng, B., Righi, D. and Delvaux, B., 2005. Halloysite clay minerals – A review. Clay Minerals 40(4): 383 – 426.

Keam, M. J., 2008. Engineering geology and mass movement on the Omokoroa Peninsula, Bay of Plenty, New Zealand. MSc thesis, University of Auckland, New Zealand.

Lowe, D.J., Tippett, J.M., Kamp, P.J.J., Liddell, I.J., Briggs, R.M., and Horrocks, J.L., 2001. Ages on weathered Plio-Pleistocene tephra sequences, western North Island, New Zealand. In: Juviglle. E.T. and Rainal. J·P. (Eds). Tephras: Chronology, Archaeology, CDERAD editeur, Goudet. Les Dossiers de l'Archéo-Logis 1: 45-60.

New Zealand Geotechnical Society, 2001. Guideline for hand held shear vane test. New Zealand Geotechnical Society.

New Zealand Geotechnical Society, 2005. Guidelines for the field classification and description of soil and rock for engineering purposes. New Zealand Geotechnical Society.

Wesley, L. 1973: Some basic engineering properties of halloysite and allophane clays in Java, Indonesia. Géotechnique 23 (4): 471 - 494

Wesley, L. 1977: Shear strength properties of halloysite and allophane clays in Java, Indonesia. Géotechnique 27 (2): 125 - 136.

Wesley, L. 2007. Slope behaviour in Otumoetai, Tauranga. New Zealand. Geomechanics News 74: 63–75.

Wesley, L. D., 2010. Geotechnical Engineering in Residual Soils. Chapter 9 Volcanic Soils. Hoboken, NJ, USA: Wiley. 189 – 222.

Wyatt, J. B., 2009. Sensitivity and clay mineralogy of weathered tephra-derived soil materials in the Tauranga region. MSc thesis, University of Waikato, New Zealand.

Bryant, J.M. & Goldsmith, M. (2013)
The incidence and importance of landslide dams in inland Otago
Proc. 19th NZGS Geotechnical Symposium. Ed. CY Chin, Queenstown

The incidence and importance of landslide dams in inland Otago

J M Bryant
Geoconsulting Ltd, Queenstown
jeffbryant@ihug.co.nz (Corresponding author)

M Goldsmith
Otago Regional Council, Dunedin
michael.goldsmith@orc.govt.nz

Keywords: Otago, landslide dams, economic impacts, community vulnerability

ABSTRACT

The South Island's Southern Alps and subsidiary ranges contain many steep, deeply incised valleys formed by tectonic uplift, glaciation and rapid erosion. Much of this area is also subject to high annual and storm event rainfalls plus earthquake shaking leading to landsliding as a significant factor in landscape evolution. Large, rapidly emplaced landslides can dam rivers where the geometry of the valley and the volume of displaced material favours blockage.

This study looks at the incidence of landslide dams within the Otago hinterland and the implication they have towards valley morphology, hydrology and communities. The potential for landslide dams in the rivers around the main towns of Queenstown and Wanaka is reviewed and found to be low but with potentially serious consequences. Whilst landslide dams are not expected to directly impact these towns or the distant communities, they could well disrupt the tourist activities on which the local economy depends whether or not breaching occurs.

New Zealand Geotechnical Society Inc. 19th Symposium, Queenstown 2013

1 INTRODUCTION

The upland backbone of the South Island of New Zealand is dominated by the Southern Alps and the subsidiary ranges which spread out to the southwest. A few towns and isolated settlements are scattered about the more accessible parts of this area, but in general, the bulk of the hinterland is remote, has little or no infrastructure and sees only small numbers of visitors.

This discussion focuses on the hinterland region of northwest Otago Province in which the regionally important tourist towns of Queenstown and Wanaka are located. Landslides are a common form of erosion within this region. They supply excessive amounts of sediment to the fluvial system leading to considerable channel modification through aggradation and avulsion downstream. This process is exacerbated when landslide dams are formed. The resultant lakes may be short-lived (from a few days to a few years) or may last for millennia. Some may eventually become infilled and cease to pose a threat from uncontrolled breaching.

2 GENERAL GEOLOGY

2.1 Physiography

Extensive glaciation during the Pleistocene has left many steep, deeply incised valleys with relative relief often in excess of 1000 m. Over the last 500,000 years, successive advances appear to have been of lessening thickness and extent to the south and east. The last valley glaciers are believed to have retreated between 12-15,000 years BP leaving a number of large, moraine-impounded lakes on the shores of which a number of tourist-oriented towns have developed.

A period of rapid erosion and downcutting followed retreat of the last ice advance with narrow gorges incised into valley floors and screes, fans and deltas deposited mainly by tributary streams but also by major rivers into the glacial lakes. Retreat of valley glaciers also seems to be associated with widespread landsliding and the range of ages noted appears to be related to successive advances and retreat. Landsliding continues to be an important valley morphology modifier although perhaps not to the same extent in the present day climate.

2.2 Rock type

Schist forms the basement throughout the area of interest and is almost the sole rock type forming outcrops. Both psammitic and pelitic (quartz and mica rich varieties respectively) are present with pelitic schist being more susceptible to surficial physical weathering and erosion. Foliation, the most pervasive defect, is often well developed particularly in the pelitic schist.

2.3 Landslides

Extensive landslides have developed on the flanks of most valleys, particularly those with high relief. The style of failure is generally that of a rock slide with rock avalanches and rock falls also present. However, less clear cut styles of failure ranging from thin sheets of displaced regolith to deep-seated rock mass creep or sagging (Hutchinson 1988) are also common. Depths and volumes of landslides vary tremendously and at the extreme end of the spectrum can exceed 100 m and 1 x 10^9 m^3 respectively.

Structural defects and rock mass strength together with slope relief play an important role in landslide development although underlying controls are not always similar from area to area. Foliation dip slopes are frequently associated with instability particularly where foliation shears are embedded within the rock mass. However, failures on scarp slopes and slopes with intermediate orientations are also common. The preponderance of slope failures in valleys trending in all directions leads one to suspect that the deep downcutting and progressive relaxation has lead to the development of sheeting or exfoliation joints subparallel to the valley slope (Hencher *et al* 2011).

Failures on the steepest slopes have the greatest potential for long run-outs and rapid emplacement onto the valley floor. The behaviour here is more like a rock fall or rock avalanche although large scale debris slides and flows can shift sufficient material to form a blockage. It is the long run-out/rapid emplacement type of landslides that are of most interest due to their potential to form landslide dams.

3 OCCURRENCE OF LANDSLIDE DAMS

3.1 Spatial distribution

In contrast to the widespread occurrence of bedrock landslides, the incidence of landslide dams is very patchily distributed. Previous inventories of landslide dams have been undertaken (Perrin & Hancox 1991, Korup 2004) with both studies highlighting the upland areas of the Southern Alps including Fiordland and Northwest Nelson as having a high concentration of the total New Zealand population.

Since the above studies, several new landslide dams have formed, some of which are of significance and some of which have had only a transient presence with breaching or infilling occurring within a year or two of formation. Figure 1 shows the location of significant landslide dams in the Otago hinterland.

New Zealand Geotechnical Society Inc. 19th Symposium, Queenstown 2013

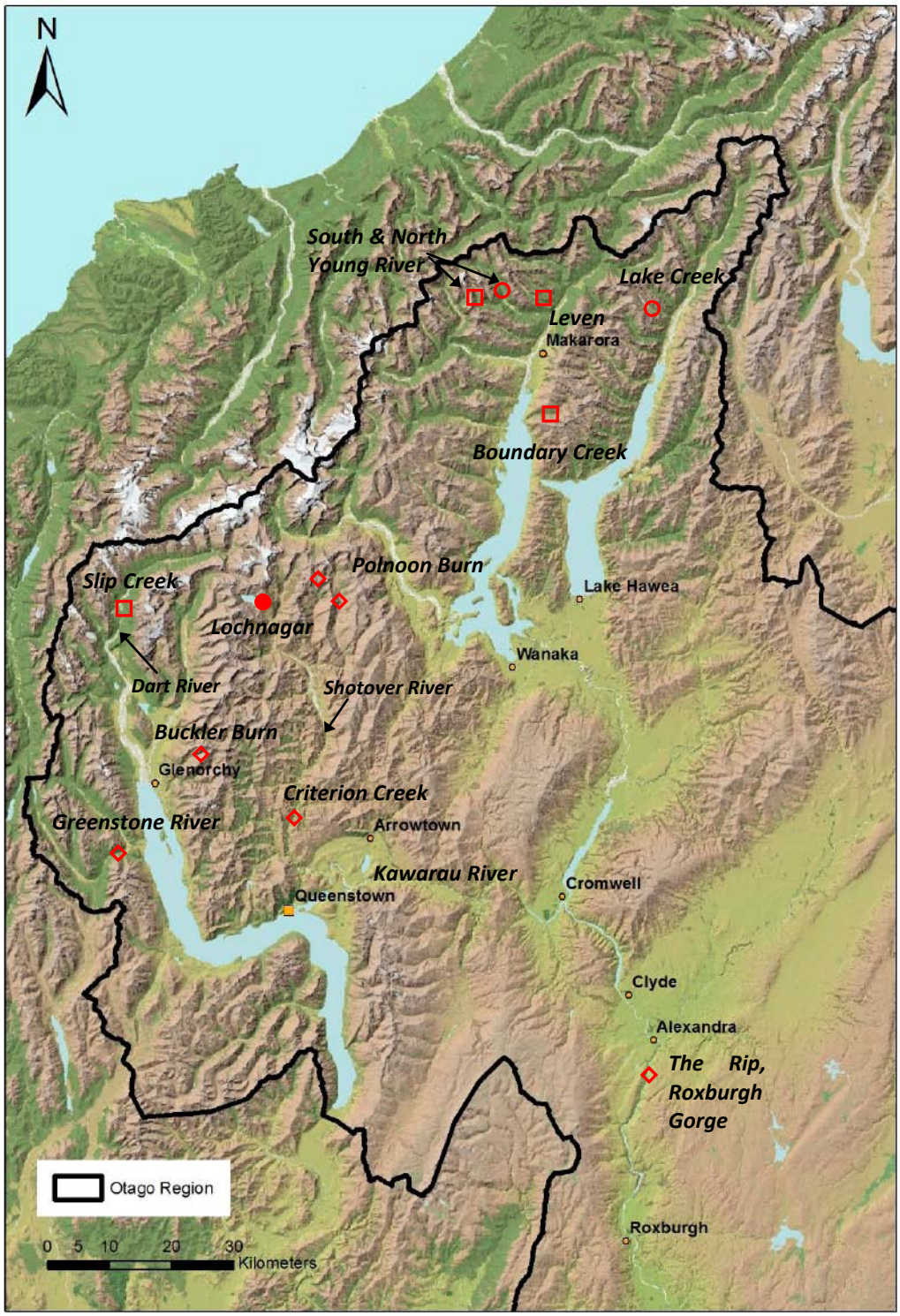


Figure 1: Map of Otago hinterland showing significant landslide dams.

○/● **Type 1A/B dams** □ **Type 2 dams** ◇ **Type 3 dams**

3.2 Dam status

As with other studies, landslide dams can be categorised depending on their current status:

- Type 1: Lake impoundment with either -
  - 1A: River flowing across a spillway channel formed on the low point of the dam crest, or
  - 1B: Lake outflow discharging as seepage through the dam.
- Type 2: Lake bed infilled with extensive river flats extending upstream of dam crest

- Type 3: Dam breached with river back to its former profile or elevated upstream above partial infill of valley.

Figures 2 & 3 show prominent examples of Type 1A (left) and Type 1B (right) dams.



Figure 2: North Young rockslide dam and lake with overflow channel (6 years old).



Figure 3: Lochnagar, upper Shotover River, passes all outflow subterraneanly (> 1000 years).

The rockslide dam in the North Young formed in 2007 and developed without any triggering factors. The cause of failure appears to be due to progressive relaxation of a mountain valley oversteepened by glaciation and post-glacial downcutting (Bryant 2010).

Type 2 dams are considered greatly under-reported mainly due to the length of time required for infilling of the lake bed and the consequent modifying effects of erosion and reafforestation of the slide scar masking their identification. There are many examples of old landslides positioned at the downstream extent of river flats, some of which may be coincidental but some are strongly indicative of very old landslide dams. The middle reaches of the Dart River display one such example with two landslides combining to block the valley just downstream of the extensive Dredge Flats. Recent reactivation has led to an overlay of debris flow deposits that temporarily dammed the river (Bryant 2013) (Figures 4 & 5).





Figures 4 & 5: Slip Stream dam, mid Dart River. Initial failure has blocked river in prehistoric times with subsequent infilling to form Dredge Flats upstream. Recent debris flows have overlain the fan surface leading to a temporary impoundment.

The final category (Type 3) is less frequent in number (Perrin & Hancox 1991, Korup 2004) which again may be due to ongoing modification hindering identification. An 18 m high landslide dam formed in the Greenstone River valley in 1999 and partially breached following overflow of the impounded river shortly after. The dam was progressively lowered in the following years such that only a remnant pond exists today (Figures 6 & 7).

New Zealand Geotechnical Society Inc. 19th Symposium, Queenstown 2013





Figures 6 &7: Landslide dam in the Greenstone River valley. Left hand view shows remains of dam on right bank and debris fan leading up to source on opposite side. On right, view is looking downstream past remnant pond to breached dam in distance.

4 REGIONAL IMPORTANCE

4.1 Threat to outdoor activities

The tourist towns of Inland Otago have a strong emphasis on 'action-adventure' types of activities. Jet boating, rafting, river surfing and kayaking are all commercial and recreational, river-based attractions with tramping, fishing and hunting predominantly recreational pursuits often undertaken near the valley floor.

Queenstown is the main base for such activities with Wanaka, Glenorchy and Makarora also of local but lesser importance. The Shotover River is a major tributary of the Kawarau Valley with a catchment area of 1088 km^2 and mean flow of 40 cumecs at Bowens Peak, some 8.5 km upstream from the Kawarau River confluence. Tourist activities on the river are estimated to have a total annual value of $37M or around $100,000/day. A blockage (Figures 8 & 9) or impending threat of blockage can result in an enforced suspension of activities with consequent economic losses.





Figures 8 & 9: Shotover River showing potential for rockslides to dam gorge with one such failure near Criterion Creek (right) causing a temporary drop in flow with full breaching after 4 years.

Major landslide dams are known in the headwaters; e.g. Lochnagar (Type 1B) and Polnoon (Type 3) and minor ones have occurred in the middle gorge section between Moonlight Creek and Long Creek. In the last twenty years, two small blockages have occurred with another rock

slide threatening but eventually not able to form a blockage. The dam near Criterion Creek formed a lake 1.5 km long and up to 3 m deep (Crampton & Bryant 1993). Flow recorded at a station 15 km downstream halved over 75 minutes but flow returned to normal within two hours after the dam overtopped. In such narrow canyons, even relatively small dams can have adverse impacts.

Other valleys, e.g. Dart and Young, have also had outdoor activities disrupted by formation of landslide dams with potential adverse economic effects to the nearest towns of Glenorchy and Makarora respectively. Foot access to the lower Young Valley and its North branch was closed for just over a year in response to concerns about breaching of the landslide dam (Palmer 2007). The closure and negative publicity impacted greatly on the local community even though the economic loss was small compared to the Shotover River example.

4.2 Threat to communities

The effects of a landslide dam on the community can be felt either directly at the point of failure, or indirectly at other locations. Direct effects may include the loss of, or damage to critical lifeline infrastructure (e.g. roads, electricity transmission networks); or the direct impact of falling debris. An example is the potential for a blockage of the Kawarau River at the confluence with Owen Creek, about 11 km downstream from the Lake Wakatipu outlet, which was investigated by Thomson (2009). Although the risk to river users and those living upstream due to inundation was deemed to be very low, potential exists for a landslide failure to damage or destroy pylons which support the only electricity transmission line into the Wakatipu Basin.

Indirect effects include changes in water levels upstream and downstream of the dam, and the effects of those changes on the environment. This includes the inundation of land which is not normally affected by flooding, both upstream (due to impoundment of water above the dam) and downstream (due to catastrophic dam failure and subsequent release of water). The effects of a sudden release of water due to dam failure on the community may include bank erosion; and damage to bridges, roads and other assets. The threat of a landslide dam failure, however remote, may also raise fears in the community about the potential downstream effects. Concerns raised by the Makarora Valley community following the formation of the Young River landslide dam in 2007 (Bryant 2010, Palmer 2007), and the processes put in place to warn of any failure of this feature are an example.

5 CONCLUSIONS

Landslide dams have a sparse distribution in the area of interest with many of them formed in prehistoric times under conditions no longer in existence today. Nevertheless, dams continue to form to this day at least one of which developed without any apparent initiating or triggering factors. Such features pose significant threats to the local communities which are highly dependent on tourist activities.

Recent experience has shown that it is not so much the size of the dam and volume of impounded lake but the location in relation to tourist activities or vulnerable communities that is the main concern.

ACKNOWLEDGEMENTS

The authors wish to thank Dr Gavin Palmer, ORC, for his review of the draft.

REFERENCES

Bryant, J. (2010) North Young Landslide Dam. *Proc. 11th IAEG conference, Auckland*

Bryant, J. (2013) Slip Stream Landslide. *Report to Otago Regional Council, Feb 2013.*

Crampton, N & Bryant, J (1993) Criterion Creek Rock Slide, Shotover River. *ECNZ (Clyde Power Project) internal report.*

Hencher, S. Lee, S.G. Carter, T.G & Richards, L (2011) Sheeting Joints: Characterisation, Shear Strength and Engineering. *Rock Mech. Rock Eng. 44 1-22*

Hutchinson, J. (1988) General report: morphological and geotechnical parameters of landslides in relation to geology and hydrogeology. *5th Int. Symp. on landslides, Lucerne p3-35*.

Korup, O. (2004) Geomorphometric characteristics of New Zealand landslide dams. *Engineering Geology 73 p13-35*.

Palmer, G. (2007) Young River Landslide Dam. *Otago Regional Council internal report 2007/584, 9 November 2007.*

Perrin, N. & Hancox, G. (1991) Landslide-dammed lakes in New Zealand – Preliminary studies on their distribution, causes and effects. *6th Int. Symposium on landslides. Christchurch p1457-1466.*

Thompson, R. (2009) Potential for Kawarau River blockage at the Owen Creek confluence. *Report to Otago Regional Council, 29 July 2009*

Pragmatic management of slope hazards in Wellington greywacke

G A Cassidy
Geoscience Consulting, Wellington, NZ. (Corresponding Author)

A G Mahoney.
Aurecon, Wellington, NZ

Keywords: Geohazards, Rockfall, Slope Stability, Risk Mitigation.

ABSTRACT

As the population of Wellington has increased over the last three decades, so too has the amount of residential, commercial and infrastructure development to cope with demand. This demand has forced engineers to consider steeper cut batters, taller retaining walls and alternative foundation systems in previously undeveloped areas – often pushing geotechnical boundaries.

Wellington's distinct steep topography is due in part to the underlying Greywacke rock. While not exclusive to Wellington, Greywacke is well known in the region and much knowledge and data has been collected over many years on its characteristics, both geological and geotechnical.

This paper explores the following four elements: 1) Characterisation of the geotechnical risk typically posed by Greywacke rock in Wellington; 2) Historic performance of cut batters above key pieces of infrastructure; 3) Typical tried and tested mitigation approaches; and 4) Pragmatic, alternative solutions.

The paper concludes by commenting on the risk appropriateness of several rockfall protection systems typically seen in the Wellington Region. A recommended decision process chart is also provided to aid geotechnical practitioners when choosing appropriate mitigation measures with their Clients.

1 INTRODUCTION

The population of the Wellington Region was last recorded in the 2006 Census as around 450,000 people (around 11% of the National population) and demonstrates a continual growth over previous decades (a 9% increase on 1996 data, for example). This upward trend is likely to continue for some time into the future. This increase of around 4,000 to 5,000 people per year in population will demand quality accommodation and improved transportation infrastructure.

Such increased demand creates challenges in the steep Wellington terrain that is typically prone to slope hazards. While the old real-estate adage "they aren't building new land" remains factually correct (reclamation projects aside), it's also a fact that developers are having to look at land they had previously discounted as unviable (or at least unattractive) for development. Such bold thinking from developers and architects alike is pushing the boundaries for many ground engineering practitioners. Taller walls, steeper cuts and alternative foundation systems.

It is the intent of this paper to discuss observations and conclusions made by the authors of local case histories and is not intended to provide comment on available numerical analytical procedures or to analyse actual stability of various rock types in Wellington.

New Zealand Geotechnical Society Inc. 19th Symposium, Queenstown 2013

2 CHARACTERISATION OF GEOTECHNICAL RISK

The bedrock geology of Wellington comprises interbedded grey to dark grey argillite and sandstone of the Rakaia Terrane, which forms part of the Torlesse Supergroup of Jurassic Age (250 million years BP). Commonly termed 'Greywacke', the rock mass is typically weak to very strong, slightly to completely weathered, and ranges from finely interbedded sandstone/argillite to essentially massive sandstone. The rock mass has been folded and sheared over several major deformation events over the last 250 million years resulting in an extremely variable group of rock properties.

Due to this often highly fractured and deformed state, Wellington Greywacke does not always perform as initially expected in some slope cuts and excavations. This inherent uncertainty around cut batter performance can result in over-conservatism in analysis and design which is explored further in this paper. The Wellington Region is full of long standing, unsupported cuts and excavations that provide useful observational information and precedence in how Greywacke can behave. The historic performance of slopes in the Wellington Region is discussed further in Section 3; however, it is fair to say that much of the rock slope risk analysis carried out in such terrain is a qualitative technique based on historic slope performance rather than a purely analytical approach. Given the pervasively jointed nature and unpredictable orientation of controlling defects of much of the Greywacke rock in Wellington traditional kinematic or modern numerical analysis is often of little value in assessing the likely slope stability. The argillite rock mass in particular can often appear more like tightly packed, angular gravel within a slope face and can be very unpredictable when excavated. Less common are the more intact exposures of blocky sandstone which perform more reliably in a rock mass defect controlled fashion.

The types of geotechnical risk present as a result of the Wellington Greywacke terrain are varied and commonly include rockfall from cut and natural slopes that descend onto roads, railways and private property. Other risks include rockfall from beneath structures, temporary stability of deep excavations and long term performance of tunnels through Greywacke sequences. Such risks are widespread among residential and commercial building owners and transportation infrastructure asset owners alike. Up until the late 1990's the principal method of slope remediation has been a reactive approach, clearing up rockfall and landslide debris after the event. However, with increased demands for public safety on transport lifelines and commuter routes, as well as a lack of available land for new private development, Clients are starting to explore proactive measures to help prevent slope risks turning into reality.

For the purposes of clarity, this paper will focus on natural and cut rock slopes above infrastructure and other elements at risk. The presence of rock fill slopes beneath roads and railways associated with cut to fill operations will not be discussed in this paper.



Figure 1: Typical small rockfall event in Wellington.

3 HISTORIC SLOPE PERFORMANCE

The principal material types encountered at a given Greywacke site in Wellington will vary according to a combination of properties which determine strength and behaviour exposed in the cut face. The dominant properties are largely controlled by the combination of rock type, structure and degree of weathering. Between these main properties, plus water (both ground and surface) the greywacke's stability for a specific slope cut angle, is generally determined.

Other than for the above comments it is not the intention of this paper to elaborate on these properties further as they have been described in detail by a number of previous authors, in many readily accessible publications such as Read, *et al* (2000). This following section is based on over 40 years of the author's personal (unpublished) experience working in and around the Wellington region.

The behaviour of greywacke slopes in the region is extremely variable, according to the nature of their mass properties and the slope angle. Much of the present day topography has been formed by regional faulting, tilting and aggressive peri-glacial erosion. The more unstable natural slopes are commonly found on the very young coastal marine cut slopes, river/stream side slopes and fault escarpments. Unfortunately, many of these geographic features form the basic arterial routes servicing the region. Aside from their inherent marginal stability, any man made excavation into these slopes usually only adds to the risk of slope failure. No substantial excavation of steep faces in greywacke should be carried out without careful consideration of the potential stability risk involved (both short and long term).

Cut slopes on the high side of public roads and highways in Wellington City and surrounding areas have been under construction for some 150 years. The number, extent and height gradually increasing with growing population and modes of transportation. Old photographs record frequent examples of localised slope failure, many presumed likely to have occurred soon after excavation. These cuts are often in the upper more highly weathered rock. These old unsupported slopes commonly were cut at a relatively uniform slope of 65 degrees (off horizontal) or steeper where less weathered material was encountered.

In the 20th century, roading has extended into even steeper terrain, existing roads widened and alignments improved to accommodate trams then buses, etc. This has resulted in higher cuts, often involving intermediate level benching once mechanical excavation processes were available for their excavation (post 1940's). Looking at these larger cuttings throughout the steeper hillside suburbs, it is noticeable that while the original cut faces of around 65 degrees were continued into the 20th Century, many have regressed to shallower batter angles due to post construction failures. Much of the older cut faces are characterised by having very irregular face profiles or have since been retained.

During the 1920/30's depression a large number of substantial retaining structures were built to stabilise unstable sections of high cut faces around the city. It is the authors opinion that if one were to carry out a detailed survey of the city's road side cut faces older than 50 years of age, it is likely that for 65 degree or steeper cuts in highly to moderately weathered greywacke in excess of 4 metres height, these will have undergone recognisable slope failure over around 50% of their face area. In the suburban setting this has had a severe impact upon service lines, pathways and adjacent private property plus frequent disruption to the roads below.

One of the more impressive early construction feats in the region involving some very steep, deep cuttings in the full range of the weathered greywacke is found on the Ngaio Gorge section of the Wellington to Johnsonville railway. This line constructed in the 1870's includes a number of successful steep (i.e. >65 degree) cuts because of the favourably oriented defects in the fresh to moderately weathered sandstone/siltstone. To date, the stability of these more impressive cuttings has been relatively good, based on the geotechnical performance observed by the authors. At other locations on this section of track in slightly more weathered rock, both

manmade cuts and failures from high up on the natural face above have been an on-going source of local rock fall onto the track below. This is largely due to due to the open fractured, fissile sandstone and argillite units present and lower rock mass strength. Substantial mitigation measures, including anchored rockfall netting, have only recently been installed to help control the risk at these sites.

A good example of the combination of both natural slope instability and manmade excavation causing stability problems to main roads is found on the Taita Gorge Road and on the Marine Drive to Eastbourne, Lower Hutt. For many years, these roads have been subject to active rockfalls due to the combination of fissile siltstone and argillites, densely fractured sandstone, sparse vegetation cover and in some instances, rapid concentrated storm water runoff from large catchments above. Again, substantial mitigation measures have been put in place (generally at road level) to overcome the worst risks of these sites.

The Johnsonville to Porirua motorway built in the early 1950's has many cut slopes that appear to have remained remarkably stable to date. Other than for a few locations, the batters have been originally cut back at about 45 degrees and expose highly to completely weathered greywacke plus natural soils above. Presumably setbacks of the higher level road boundary plus more moderate sloping terrain above has helped facilitate the initial use of less steep 45 degree slope profiles, compared with the 65 degree slopes typically constructed in earlier years.

Ngauranga Gorge (State Highway 1) provides a good example of a major arterial route, originally traversing an extremely steep sided natural stream eroded valley. This route has been upgraded/modified many times over the last century and encounters a variety of generally less weathered predominately sandstone and minor argillite (moderately weathered grading down to fresh rock). The rock materials exposed display a wide variety of predominant bedding and jointing planar control features with minor faulting and crush zones also encountered. This major road has a variety of side slopes, cut at different times, according to localised road formation modifications, ranging from stepped faces cut at approximately 75 degrees into fresh rock mass tens of metres in height. The current cut slopes (Figure 2) are approximately 45 degree slopes (or flatter) which are regularly benched and cut into folded rock, exposing dominant jointing within the closely spaced, hard sandstone beds with orthogonal jointing that often dominates the rock slope stability.

Due to good engineering of these large cut faces, the slopes have remained generally stable under static conditions over the past 30 years. Minor fretting and unravelling of the more weathered rock mass has been contained by recently constructed rockfall barriers at road level.



Figure 2: A view down SH1, Ngauranga Gorge looking north (right) and close-up of rock slope (left).

A final example of greywacke structure and weathering grade determining slope stability is in the very large reclamation borrow area located at the base of Ngauranga Gorge, currently occupied by the Jarden Mile Industrial Park, fronting onto the Old Hutt Road. This area was developed by very extensive excavation works with cutting in a series of stepped benches down the western and southern margin over a maximum depth of 80 metres. The original cutting was sloped to an overall grade of approximately 40 degrees over the more weathered upper slope and 45 degrees over the lower two fifths height, plus a series of 2m wide benches. Early years saw many localised failures on these steeper bottom faces, generally in the form of planar controlled rockfalls (joint and shear structures) often resulting in characteristic wedge failures. The higher up the face the more the original individually cut benches have been naturally regraded by erosion and small fretting and spalling of rock over time. Now with the very extensive regenerating native bush cover on these slopes, other than for the lower level, the hillside appears to present a more uniform natural surface. From a technical performance perspective this cutting has proven to be a success so far over its fifty year (approx.) life.

4 MITIGATION APPROACHES

Learning from past construction works completed in the range of ground conditions typically encountered in the Wellington greywacke terrain, the potential for encountering stability problems is high. The cost of remediating unstable ground ranges greatly and there is rarely a single approach where one solution fits all. The use of any particular system will depend to a large extent upon cost effectiveness and restrictions imposed by geometric constraints (ie, height, slope steepness, legal boundaries, etc) of the location and environmental effects.

Typically, methods of controlling rock fall hazards in greywacke (as with other rock types) can be categorised as either preventative or containment. Prevention measures typically include slope re-grading and in-situ retaining. Containment measures typically include methods to control the descent of debris, located away from the source of the unstable material, either on or at the base of the slope.

4.1 Historical tried & tested methods

Common remediation practices used to lower the risk of rockfall in the last century have included:

- Excavated catch ditches and simple earth bunds;
- Simple timber walls/fences to catch falling debris;
- Light weight catch fences using steel waratahs and steel wire mesh;
- Driven railway iron walls, with either timber lagging or steel wire mesh;
- Hand rendered concrete facings or simple cast in-situ concrete walls.

Many of the above remediation techniques used in Wellington have performed adequately for a period of time, accepting the fact that corrosion protection technology has progressed considerably in the past two decades. Where space permits, excavated ditches with or without earth bunds have been proven to be very effective in containing small to medium rockfalls and debris flows. A number of driven railway iron walls using steel mesh have also proved successful in certain applications, including sites adjacent to railway and highway corridors where space is often limited. Over time, such old protection systems have been replaced with similar systems where they have worked well but using more modern components.

In other cases, the old systems installed have been inappropriate for the level of risk and have been overwhelmed in one or more rockfall/landslide event. A number of sites in Wellington with old hand rendered concrete and cast in-situ concrete, typical of the 1950/60's, show evidence of surface cracking and overturning failures. Mid-slope catch fences constructed from steel waratahs and wire mesh have often been forgotten about and neglected if located high up

New Zealand Geotechnical Society Inc. 19th Symposium, Queenstown 2013

on steep slopes, resulting in the systems becoming over-loaded, often resulting in failure. These poorly performing systems are generally replaced with alternative modern solutions.

4.2 Pragmatic & modern alternatives

Traditional concepts of reducing the risk associated with rockfalls onto houses or roads below are being challenged – instead of a wall at the bottom of a hill why not hold the rocks in place or slow down their descent? In extreme cases there is an argument to do nothing and simply monitor the rock face remotely and provide warning if a significant event does occur. The following sections explore these alternatives in more detail and while they are not exclusive to Greywacke rock slopes, they have shown to be appropriate measures in the Wellington region.

Spot bolting, scaling and netting. This is the true definition of treating the problem at source. Using skilled abseil technicians, the process of scaling or removing loose rocks and material can be a very effective way of reducing the risk of imminent rockfall. By removing this loose material the effects of natural erosion is accelerated by an order of magnitude. Scaling will not prevent further rocks becoming loose in the future and so, unless routinely undertaken, scaling is not a long term solution. For more persistent or aggressive rockfall problems, the subject rock blocks may be spot bolted to secure them in place. Such anchors will extend some way behind the likely rear plane of the target block and anchor heads may be tied together with high strength steel ropes if required.

Where the rock mass is more fractured, rockfall netting may be installed. The mesh is held in place by a series of rock anchors where the anchor spacing is designed to prevent unacceptable bulging effects close to road or track level. Designers should consider the maintenance requirements associated with rockfall netting, which can often require annual inspections and removal of debris. Complete component replacement may be required as soon as fifteen to twenty years in more aggressive marine applications.

Rockfall attenuation systems and mid-slope deflection structures. Where the source area of potentially unstable rocks is large, the costs associated with significant quantities of rock anchors and/or netting can be prohibitively high. An alternative to rockfall netting is to use an attenuator system that is positioned in a mid-slope location with an open-mouth netting system that effectively 'swallows' falling rocks/debris and reduces both speed and energy of this falling material. Fallen material is collected in a small ditch or behind a bund at the bottom of the slope. This type of system reduces the amount of netting required, significantly reduces the number of rock anchors installed and is easier to maintain than conventional rockfall netting as the debris is located at the base of the slope.

Mid-slope deflection barriers can be designed to either catch falling rocks and debris at a mid-slope location or alternatively, they can deflect the falling material to fall to a different location that carries a lesser risk, ie, the rocks would avoid a house at the base of a slope and land in a garden. The technology surrounding the rockfall barrier industry has advanced greatly in the past decade to the point where such systems can be designed to stop energies of up to 8,000kJ. Maintenance requirements as above also apply.



Figure 3: An example of a mid-slope attenuator system.

Shotcrete and anchor walls. While the technique of spraying a concrete facing on a slope with drilled anchor support is not a new technique for slope stabilisation, the technology and technical understanding has advanced considerably over the last decade. The application of fibre reinforced concrete has meant that in limited access sites, the shotcrete doesn't require preparation of steel reinforcement prior to spraying, reducing construction time. Other advances in corrosion protection and chemical additives in concrete have led to a more reliable, long lasting solution where outward deflection in the slope face is not allowable (i.e. roadside sites).

Open space and remote monitoring. This option represents the polar opposite to treating the problem at its source. At some sites it may be permissible to allow rocks and debris to fall down a slope. Such sites are usually relatively open and computer analysis would be undertaken to confirm that falling rocks will not reach the element at risk. In other cases, the element at risk may be physically relocated outside of the high risk zone (i.e. a house).

In some remote locations where rockfall events pose a significant hazard to road and rail, yet budgets do not allow for full in-situ remediation or route realignment, it may be practical to install remote monitoring systems to maintain coverage of the high risk area and initiate an alarm should a major event occur. While the likelihood of a given event remains unchanged, the consequence is managed in that people and vehicles are not allowed to enter a high risk area due to monitoring equipment triggering a visible or physical alarm.

5 CONCLUSIONS

As the population of the Wellington Region increases, so too does the geotechnical risk associated with developing the remaining available land. Historic cut slope performance offers ground engineering practitioners ample opportunity for hind-sight. Included in this opportunity are the many examples of retaining measures around the city, some which have performed well and others that have not.

It is important that consultants consider the wider context of rockfall risk and mitigation approach. While large retaining walls and shotcrete can offer robust solutions for certain sites, there are often alternative solutions that are worthy of consideration. For the reduction of risk from rockfall events where ample space is available, it is hard to beat a catch ditch and earth bund, or indeed re-grading the slope to a flatter, safer batter angle.

Rockfall remediation technology is quickly and positively advancing in response to demand. Budget conscious Clients are demanding cost effective solutions and the market is responding accordingly – attenuator and mid-slope deflection barriers are good examples of this. The technology surrounding early warning systems is also improving, providing text message and email alerts plus real time, solar powered cameras streaming images of your road or railway at risk direct to your laptop.

Finally, the following flow chart (Figure 4 overleaf) has been prepared by the authors and is intended to provide a logical decision making thought process for ground engineering practitioners to use while they discuss rockfall hazards and risk with their Clients. This flow chart will be applicable to most rockfall hazards and is not restricted to Wellington.

REFERENCES

Begg, J. G & Mazengarb (1996) "Geology of the Wellington area, scale 1:50,000" Institute of Geological and Nuclear Sciences geological map 22.

Begg, J. G & Johnston (2000) "Geology of the Wellington area, scale 1:250,000" Institute of Geological and Nuclear Sciences geological map 10.

Reid, A. L, Richards, L & Perrin, N. D (2000) "Assessment of New Zealand Greywacke rock masses with the Hoek-Brown failure criterion.

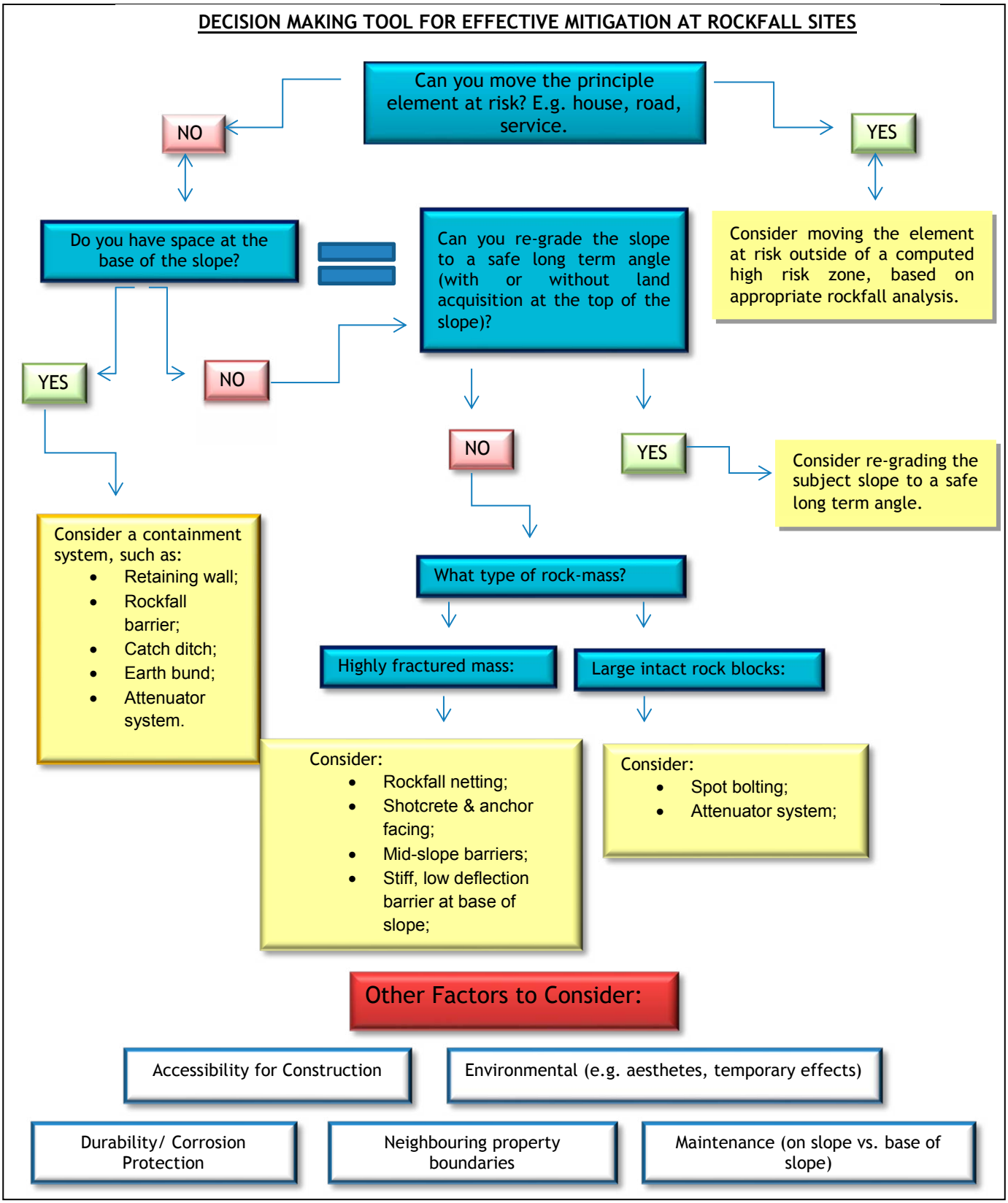


Figure 4: Decision Making Tool for Effective Mitigation at Rockfall Sites

Reopening Evans Pass Road, Sumner to Summit Road

J M Engel
Engineering Geologist, Sinclair Knight Merz, NZ
mengel@globalskm.com

Keywords: earthquake, Evans Pass, rockfall, mapping, remediation

ABSTRACT

Following the 22 February 2011 earthquake in Christchurch significant rockfall, cliff collapse and landslides occurred around the Port Hills. Rocks from a series of bluff systems and individual outcrops above Evans Pass Road fell from these sources ending up on or impacting the road. Evans Pass Road is the only route out of Sumner if Main Road, below the 60 to 70 m high cliffs at Peacocks Gallop, is damaged or impacted by events such as rockfall and cliff collapse.

This report focuses on the processes undertaken to reopen Evans Pass Road to the public. The main stages of reopening the road were rockfall and source rock mapping, determining risk assessment criteria and assigning risk ratings, determining remedial options, undertaking the remediation, and reviewing and reassessing completed works. Remediation methods employed above Evans Pass Road included scaling, rock rolling, low and high energy blasting, and mechanical restraint; the reasons for using these methods at specific locations are discussed.

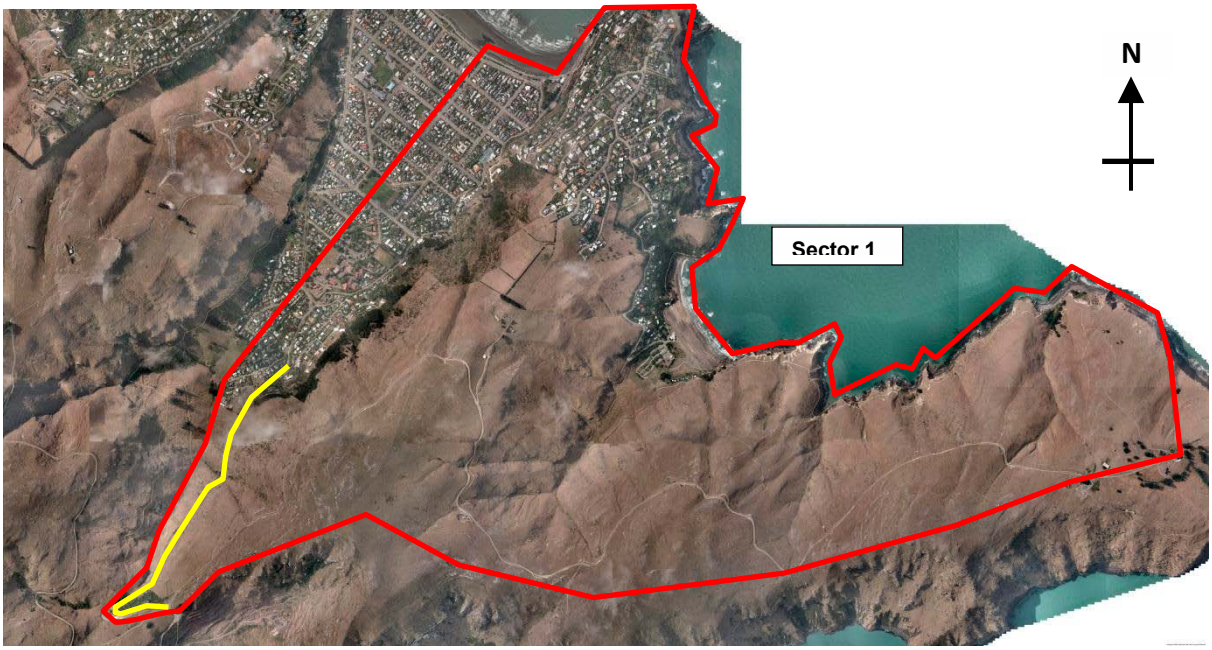
New Zealand Geotechnical Society Inc. 19th Symposium, Queenstown 2013

1 INTRODUCTION

The 22 February 2011 M6.3 earthquake caused significant damage to the Christchurch area with damage and collapse of buildings in the city centre and significant land damage especially in the eastern suburbs. In the Port Hills there was significant rockfall, cliff collapse and landslides. The 13 June 2011 M6.4 aftershock had peak ground accelerations (PGAs) exceeding 2g (Geonet) which created considerable rockfall and cliff collapse especially around the Sumner and Godley Head area.

Christchurch City Council (CCC) formed the Port Hills Geotech Group (PHGG) after the 22 February 2011 earthquake to under mapping, risk analysis and mitigation of the hazards around the Port Hills. The PHGG was made up of engineering geologists and geotechnical engineers from multiple consultancies contracted to CCC. The Port Hills were split into nine sectors and the consultants were assigned sectors. In this paper I will focus on Sector 1 which encompassed the eastern half of Sumner through to Godley Head as shown in Figure 1.

United Research Services (URS) and Sinclair Knight Merz (SKM) teamed together to map and assess the rockfall hazards in Sector 1. Initially the critical areas to map were the slopes above Heberden Avenue, La Mar Lane and Awaroa Lane where houses were potentially at risk of rockfall from the on-going aftershocks. After the immediate life and limb issues were dealt with, the focus of the project shifted to securing critical lifelines.



New Zealand Geotechnical Society Inc. 19th Symposium, Queenstown 2013

Figure 1 – Sector 1 encompassed the eastern half of Sumner through to Godley Head as shown outlined in red. Evans Pass Road is shown in yellow.

2 EVANS PASS ROAD

Evans Pass Road provides a critical lifeline link to Christchurch city centre for the residents of Sumner, Scarborough and Taylors Mistake. The main access into Sumner is via Main Road which passes alongside the Heathcote and Avon Estuary below a 60m cliff at Peacocks Gallop. Significant cliff collapse occurred at Peacocks Gallop undermining some of the houses on Kinsey Terrace with tension cracking up to 80m back from the new cliff edge. Some of the fallen rock material, in particular at the western and eastern ends where the road is immediately below the cliff, came to rest on Main Road.

If Main Road is inundated by rockfall or impassable due to damage, the only route out of Sumner, Scarborough and Taylors Mistake is via Evans Pass Road to Summit Road. Given the importance of the route, focus was put into securing access in case of further aftershocks. Evans Pass Road is a critical link to Christchurch as future works to remediate the damage at Peacocks Gallop may require an alternate access route for certain periods of the works. Evans Pass Road also has significant recreational value providing access to a number of tracks in the Godley Head area.

I will focus on the process undertaken to assess, remediate and reopen Evans Pass Road, in particular the rockfall and cliff collapse risks.

3 MAPPING ROCKFALL AND SOURCE ROCK

The first stage of reopening Evans Pass Road was to map the rock outcrops and boulders on the slopes above Evans Pass Road and identify which sites could potentially affect the road. A team of approximately ten engineering geologists and geotechnical engineers mapped the rockfall and unstable bluffs on the slopes above Evans Pass Road. A list of five key indicators were developed to assist mapping unstable boulders and to allow consistency between the teams mapping the sites:

- Are there signs of recent movement? (Fresh faces, tension cracks, moss on the underside of the boulders)
- What size is the boulder? (Generally boulders less than 100mm diameter would be stopped by vegetation and were therefore not considered as a threat)
- Does the boulder wobble?
- What shape is the boulder? Is it conducive to rolling or is its shape likely to limit rolling?
- What structures are at risk down slope of the boulder?

The site mapping involved identifying the stability of insitu boulders and bluffs with signs of recent movement (i.e. tension cracking) and recently fallen boulders. A site could contain a single boulder, multiple boulders close together or it could be a bluff.

Every site identified had certain information recorded – Site ID, Size, GPS coordinates, Shape, Wobbles, Tension Crack, Boulder Support and Structures at Risk. The sites were reported in the council's GIS database, initially by recording it in the field on paper and then entering the data into the system in the office until a mobile GIS system was setup using ArcGIS run on an iPad.

To determine what structures could be at risk from a boulder falling, it was considered a boulder could roll anywhere within a 60 degree cone below its start point, i.e. if a line was drawn from the boulder or site straight down the slope (the fall line), the boulder could fall within an envelope 30 degrees either side of the fall line.

Each site was assessed and assigned a risk rating using the criteria outlined in Table 1 below. The sites were assessed as High, Medium or Low. If a site was currently unstable and/or was a threat to a lifeline or property it was automatically assigned a Medium or High risk rating meaning it would require further assessment or some form of remediation.

Table 1 - Risk Rating Assessment Criteria

Criterion	Risk Classification		
	High	**Medium**	**Low**
Loose/detached	X	X	X
Able to roll	X	X	X
Currently Unstable	X	X	
Threat to lifeline and/or property	X	X	

(This table was taken from the PHGG Mobile GIS guidance document)

The mapping of the slopes above Evans Pass Road had been completed and remediation had started in some areas before the 13 June 2011 M6.4 aftershock. Following the June aftershock a full reassessment of the slopes above Evans Pass Road was undertaken. The very high PGAs during the June shake destabilised a lot more rock. During the remapping process it was noted that the June shake had confirmed the suitability of the mechanical restraints and rock relocation which had already been completed in the area (post February / pre-June quake) with no new instability recorded for remediated material.

4 REMEDIATION OPTIONS

The types of remediation used above Evans Pass Road can be split into two groups, deconstruction or removal of the hazard and mechanical restraint. CCC's preferred method of

remediation above Evans Pass Road was removing the hazards and reducing, or in a lot of cases, eliminating the need for on-going maintenance inspections and costs.

Rockfall modelling was undertaken to help assess which sites could affect Evans Pass Road and areas where remediation could be limited to larger unstable features. All modelling was supported by in the field ground truthing to confirm or supplement the modelling results.

4.1 Deconstruction or Removal of Rockfall Hazards

Two different methods were used above Evans Pass Road. In Area A the unstable sites were carefully deconstructed and the material relocated to more secure locations such as natural or dug out benches. In Area B the hazards were removed or reduced by rolling or scaling the hazards and allowing them to come to rest in more secure locations such as gentler slopes or in the valley below Evans Pass Road.

Deconstruction or removal of the rockfall hazards was achieved by scaling using pry bars and hand tools, rolling boulders using airbags and crow bars, blasting with high and low energy explosives and controlled lowering and relocation using hand winches and belay lowering systems.

4.2 Mechanical Restraint

Mechanical restraint was used in places where the size of the boulders, the quality of the rock or risk to down slope properties meant that removing or relocating the boulders could not be feasibly done. Above Evans Pass Road mechanical restraint was only used in Area A, it wasn't used in Area B due to the absence of sensitive structures below the area. The feasibility of deconstructing or relocating boulders considered not only cost but the time it would take to achieve; in some cases deconstruction or relocation would have considerably delayed reopening the road.

Mechanical restraint options included combinations of cables, mesh and bolts or anchors. These were used in various combinations depending on the rock outcrops and the potential anchor options available. All mechanically restrained sites in Area A apart from one site (U317) are considered to be temporary structures installed to allow the reopening Evans Pass Road in a timely manner.

U317 is a 30 m^3 boulder above a steep gully which had become destabilised following the 13 June 2011 aftershock. A site specific permanent mechanical restraint was designed and installed for this site due to the difficulties of deconstructing the site at a later date.

CCC and the PHGG produced a design philosophy which would allow the contractors to quickly determine onsite what level of restraint was required for the outcrops based on the size of the boulder. The design philosophy made the following assumptions:

- The weight of basalt is 2.7 T/m3
- The cables, anchors and/or mesh were supporting the full static weight of the boulder (i.e. there is no support from surrounding rockmass or soil)
- The ultimate strength of the components were halved to give a design load for each component

- The weakest component would govern the number of cables, anchors or meshing required.

The above design philosophy introduced a high level of conservatism but reduced the need for site specific investigations and designs which would have taken considerably longer to achieve and would have notably increased the cost. The June aftershock was a full scale test of the mechanical restraints, none of which failed.

5 REMEDIATING UNSTABLE SITES

Contractors worked with the consultants to develop remediation options for the identified sites. The work above Evans Pass Road was undertaken with Abseil Access. Options for each site were considered in terms of what was achievable and which remediation option could be used. Some complex sites such as Car Crash Corner (discussed later) required extensive discussion between the contractor and the consultant to determine the most feasible remediation option.

The area above Evans Pass Road was split into Work Area A and B (as shown in Figure 2). The sites without houses below the unstable material were rolled and, when necessary, blasted to reduce size; this was done at the upper end of Evans Pass Road in Work Area B. While the boulders did cause some damage to the road surface, repairs were required due to the earthquake generated rockfall and it was determined that it would cost more to carefully relocate the boulders or mechanically restrain them than it would to repair the road.

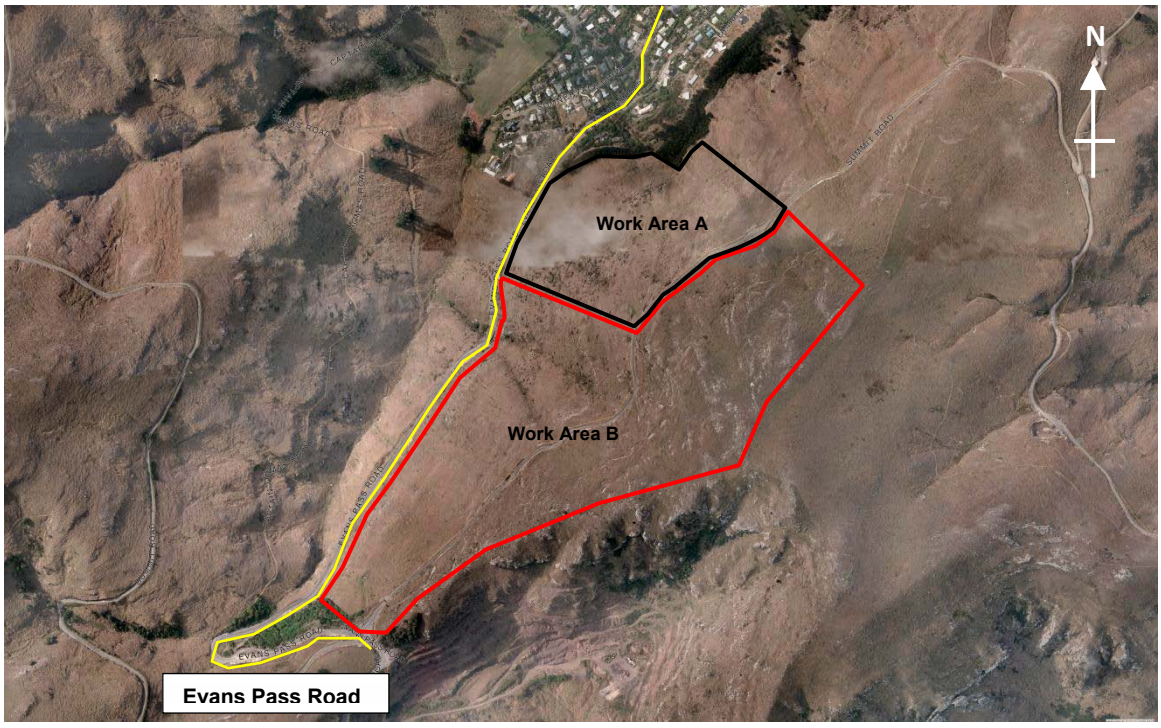


Figure 2 - Work Area A and B are shown in black and red respectively above Evans Pass Road.

Rolling the boulders down slope allowed valuable information to be gained about how boulders would behave on the specific slopes we were working on. This information allowed a check of our risk assessments and what sites we determined could impact Evans Pass Road. It was noted that some tabular boulders, when rolled on their thin edge, came to rest outside the 60 degree

envelope we assumed the boulders would fall within. This was information was used to reassess some sites in Work Area A.

At the lower end of Evans Pass Road (Work Area A) boulders could not be freely rolled as the potential risk that they could run out to the houses on Upper Sumnervale Drive was considered too high. In this area boulders were relocated using controlled deconstruction and lowering techniques such as using multiple hand winches or belay systems to shift the boulders to more secure locations such as dug out or natural benches (Figure 3). Another method used include installing mesh around the loose or unstable boulders and using low energy explosives, expanding grout or hydraulic breakers to deconstruct the material which could then be relocated using hand winches or by hand if small enough (Figure 4).



Figure 3 - The unstable boulder was lowered using hand winches onto a dug out bench below. Figure 4 - This boulder was wrapped in mesh and held in with cables while it was deconstructed using expanding grout and low energy explosives.

5.1 Car Crash Corner Bluff

One of the more significant sites that were remediated above Evans Pass Road was a 25 m high, 25 m long bluff locally known as Car Crash Corner (Figure 5). Numerous inspections of the bluff were undertaken due to is overhanging profile and position relative to the road.

During some light scaling work in March 2012 it was noted that a 60mm tension crack in the rockmass at the top of the bluff had opened up. It was determined that the tension crack was a result of the 23 December 2011 M6.0 aftershock. Multiple inspections undertaken in early December 2011 had not identified the tension crack and the only aftershock considered large enough to cause this damage between December 2011 and when it was noticed in March 2012 was the 23 December 2011 event.

Abseil inspections were undertaken to try and determine how far the tension crack continued and how much material was affected. From this information, an options report was put together outlining four remediation options for the bluff:

1. Deconstruct the rockmass in front of the tension crack using low energy explosives, pry bars and airbags
2. Drill and blast to re-profile the bluff
3. Mechanical restraint
4. Monitor the bluff for further movement.

A monitoring or observational approach was ruled out as it was thought if the bluff failed it was likely to be a catastrophic failure which would inundate the road with little to no warning. Mechanical restraint was not preferred as the total mass to be supported was difficult to ascertain, any bolts would have to continue deep into the rockmass to be sure of being in good rock and it would require contractors working in front of the unstable mass.

A rough costing exercise was undertaken for the deconstruction option and the drill and blast option. The cost estimates suggested that both methods would be of similar cost. The main concern with the deconstruct option was if the tension crack was found to extend deep into the rockmass, the bluff may require blasting similar to the drill and blast option.

CCC agreed that going for the drill and blast option and re-profiling the face would achieve the required result and provide some longer term stability of the bluff reducing on-going maintenance and inspection requirements.



Figure 5 - The bluff at Car Crash Corner was significantly overhanging Evans Pass Road prior to remediation. Figure 6 - The bluff was re-profiled with the overhang removed and the face reclined back at approximately 60 to 70 degrees

A three stage blast was undertaken to re-profile the face which allowed inspection after each blast to determine how far to take the bluff back. A fourth blast was used to remove some large material still hung up on the face. Scaling using airbags, air lances and pry bars removed the small material from the face to leave a clean face as shown in Figure 6. In total, approximately 2400 m^3 (or 6500 T) of rock was removed from the bluff.

6 WORKING ARRANGEMENT BETWEEN CONSULTANTS AND CONTRACTORS

The consultants and contractors worked closely throughout the project with regular site visits to review progress and discuss any issues found on site. Two of the most common issues were more unstable material was found as sites were deconstructed, and new sites were identified as the contractors moved around the area.

These issues were not unexpected. Often the volume of unstable material was difficult to quantify until the contractors started to deconstruct the sites. Due to the large work area and the on-going aftershocks, there was never a guarantee that all of the potentially unstable sites had been inspected during the initial mapping process. Through regular contact between the consultants and contractors, any new sites or increased unstable material was generally quickly included into the work packages to allow consistent and quick remediation. The contractors

were aware of the mapping criteria we had been using so they were able to easily apply this to any new sites located. This meant reviews of the new sites by the supervising consultant were able to be undertaken quickly and efficiently.

The clear lines of communication and regular site visits meant that the work packages were progressed smoothly without any major surprises or issues. Whenever issues were developing, they were addressed early to allow works to seamlessly proceed. Having the consultant onsite with the contractors regularly, especially in the initial stages meant that both parties could discuss what was achievable and what the finished result at each site should look like.

7 REVIEW AND SIGN OFF OF COMPLETED WORKS

As the sites were being completed, they were being reviewed and signed off by the consultant. This process meant that any extra work or tidy up that might be required was instructed before the contractors had demobilised from the area or site which minimised delays and cost overruns.

All of the site work undertaken was peer reviewed by another consultant within the Port Hills Geotech Group; typically by one of the Sector Leaders. The Peer Reviewer reviewed the physical work that had been completed, compared this to the planned work scope, and assessed the work area holistically to make sure the level of remediation was suitable for the intended use of the area below. The peer reviews were an important part of the process and ensured that a consistent approach was being employed across the Port Hills in respect to risk assessment and remediation.

8 CONCLUSION

Evans Pass Road provides and critical lifeline to Sumner, Scarborough and Taylors Mistake. The 22 February 2011 M6.3 aftershock, 13 June 2011 M6.4 aftershock and 23 December 2011 M6.0 aftershock caused considerable damage to rock outcrops, bluffs and cliffs around the Port Hills.

The Port Hills Geotech Group was formed under the direction of Christchurch City Council to assist with the mapping, risk analysis, management and mitigation of the hazards. Wherever possible, unstable sites were deconstructed or the hazards were relocated to more secure locations. In areas where deconstruction or relocation was deemed not feasible, mechanical restraints consisting of cables, mesh and bolts were installed to stabilise the unstable material. One of the big factors which helped the success of this project was the regular communication between all parties involved and regular site visits with the consultants and contractors.

ACKNOWLEDGEMENTS

This project was undertaken for CCC as part of a post-quake emergency response operation. The open and frank discussions throughout the project between CCC, PHGG, URS and the author allowed a robust process to be developed quickly and resulted in a smooth reopening process for Evans Pass Road. The author would like to thank all those involved in the project.

REFERENCES

Geonet (2011) *Jun 13 2011 - Large earthquakes strike south-east of Christchurch: Peak Ground Accelerations for the magnitude 6.3 earthquake.* http://info.geonet.org.nz/display/home/2011/06/13/Jun+13+2011+-+Large+earthquakes+strike+south-east+of+Christchurch

Port Hills Geotech Group (2011) *Port Hills Geotech Group Mobile GIS.*

Millerton Cutting - Assessment and mitigation of rockfall hazards on a critical supply route

P D Forrest
Aurecon Group Limited, Auckland, NZ (formerly of GHD Ltd)
peter.forrest@aurecongroup.com (Corresponding author)

J W H Molloy
Terra MDC Limited, Dunedin NZ (formerly of GHD Ltd)
james.molloy@terramdc.co.nz

Keywords: Rockfall, hazard, risk, route security, mitigation, drainage, blast damage, catch ditches, rock bolts, drapery netting

ABSTRACT

The Millerton Cutting was constructed in 2006 to provide improved access and route security to the Stockton Mine for Solid Energy NZ and Millerton residents. The new road alignment cut through weak and variable sandstones of the Brunner Coal Measures, dipping at approximately 35° to the north, with batters formed up to 25 m in height at an elevation of circa 800 m above sea level. Imposed environmental constraints compromised the geometric alignment, resulting in reduced sight distance, and varying speed environments for mine and residential traffic and inadequate rockfall catch ditches.

By May 2007, rock fall and degradation of the slope, expedited by up to 8 m per annum rainfall, resulted in rockfall debris impacting the carriageway, posing a significant risk to traffic from direct impact and collisions due to avoidance.

Engineering geological mapping proved three pervasive joint sets, stress release and preferential weathering of softer bedding planes were promoting wedge and block failure. A semi quantitative risk assessment following the procedure by Bunce et al (1997) indicated a level of intolerable risk to road users. Remedial works needed to consider the environmental constraints whilst maintaining the constant and uninhibited access in and out of the mine.

Scoping of remediation measures identified significant accessibility issues to undertake comprehensive re-profiling comprising trimming and heavy scaling of the rock faces along with spot bolting. Fulltime site supervision provided for continual monitoring and control of the scoped remedial measures, resulting in specific mitigation works being applied to the rock faces. A section was also identified for rock fall netting protection, with profiled netting directing debris into the drainage ditches which were pre-formed during the original road construction.

New Zealand Geotechnical Society Inc. 19th Symposium, Queenstown 2013

1 INTRODUCTION

1.1 Background

The Millerton Cutting is situated on the main access route from Granity to Stockton Mine, approximately 30 km north of Westport on the West Coast of New Zealand's South Island. The site comprises a rock cutting approximately 525 m long, trending approximately NW/SE and up to 35 m depth. The cutting was excavated during construction of the realignment of Millerton Road, which was required to alleviate the rockfall hazard and security issues associated with the former route. The new road is the only access to the Stockton coal mine on the Stockton Plateau, with approximately 90 % of the vehicle movements along the route related to mine haulage and mine staff. The site location and position of the new road are shown in Figure 1.

1.2 Construction History

The cutting was constructed in 2005/06 and officially opened in 2007. The excavation of the cutting was undertaken by drilling and blasting and removal of spoils by bulk excavation.
The southern batter (downhill carriageway) was first excavated as a single 20 m to 30 m face but due to stability concerns this was subsequently re-engineered to two sub-parallel cut faces separated by a 6 m wide bench. Both the upper and lower faces were generally steeply inclined at approximately 60 to 80 degrees, ranging in height from 6 m to 12 m. The northern batter (uphill carriageway) comprised a single approximately 20 m to 25 m high sub-vertical (80 degrees) cut face. The general gradient of the road was designed to 11 %.



Figure 1: Site Location and Position of New Road



Figure 2: Aerial view of the cutting circa June 2008

The horizontal geometric alignment was slightly compromised in order to protect Buller District Council (BDC) road designation, Department of Conservation (DoC) land, and a particular flora present on the north western section of the site. This resulted in relatively poor sight distance for vehicles travelling uphill due to the tight curvature of the alignment, the steep cut of the rock face and its proximity to the road shoulder.

The table drainage on the outside of both carriageways was also compromised in some areas, with their dimensions generally less than recommended design chart allocations (Ritchie, 1963), resulting in narrow ditches that have failed to contain fully any fallen debris. Figure 2 shows an annotated aerial photograph of the cutting looking east.

1.3 Post Construction Conditions

From its construction, the cutting showed continued signs of distress and local failure, manifested by frequent rock fall leaving debris across the table drain and both carriageways. Both batters had a blocky appearance (Figure 3) with overhanging and precarious blocks common along the cut. Talus had been caught on small rock ledges across the length of both faces. The cut slopes were proximal to the road verge separated by catch ditches of varying width, but generally less than 1 m wide on the uphill carriageway, which proved inadequate in preventing fallen debris from reaching the road (Figure 4).

Debris observed in the road drainage ditches predominantly comprised cobble to boulder sized (60 mm – 500 mm diameter) angular sandstone rock fragments, although larger blocks > 1 m^3 were also reported. Some soil mass from the crest of the cutting slope was also observed throughout the talus. Solid Energy staff reported a strong correlation between rockfall and rainfall events, after which there was increased debris reaching the carriageways. The area has an average rainfall of up to 8 m per annum[1] (Figure 5). Due to the drainage paths above the cutting, surface water would often flow across the cut faces, removing debris and further loosening the rock face (Figure 6).



Figure 3: Typical blocky appearance of the cut faces, with loose debris and talus.



Figure 4: Debris in the southern catch ditch.



Figure 5: Large rocks reaching the road is not uncommon during rain events, proving to be a hazard to oncoming traffic.



Figure 6: Waterfalls after heavy rainfall from run off in the above catchment.

There was a risk that rock or debris could strike vehicles or rocks on the carriageway could cause evasive driver action on a road that already presented challenges to safe passage through its geometric alignment, poor visibility due to frequent inclement weather conditions and various speed environments depending on the vehicle and direction of travel.

2 GEOLOGICAL INVESTIGATIONS

2.1 Scope

Solid Energy NZ commissioned an engineering geological mapping exercise and geotechnical assessment leading to a quantitative risk assessment of rockfall. Quantification of the perceived risk to the road users was required so that appropriate mitigation measures could be established, cost benefit analyses of those measures carried out and treatment of the hazards implemented accordingly. As the only route up to and out of the Stockton Mine, the route security and safety of Solid Energy's personnel was paramount to the organisation.

2.2 Site Geology

The site is mapped as being predominantly within the Brunner Coal Measures, with the western portion within or nearby the Kaiata Formation. The Brunner Coal Measures are described as non-marine quartz sandstone, conglomerate, carbonaceous shale and coal seams. Kaiata Formation marine sediments conformably overlie these deposits. The Kaiata Formation is described as massive carbonaceous mudstone with minor muddy sandstone.

Locally, bedding dips at approximately 15 to 20 degrees to the north. The exposed cut faces show multiple joint sets with some weak anticlinal folding, the axis of which is quite variable on the upper face above the southern bench. The Granity fault is located at the western (downhill) terminus of the cutting. A number of small offset faults can also be seen within the cutting, often present in discrete pairs.

Geological mapping was undertaken along the southern batter in order to classify the rock mass and compile structural data for stereographic projection analysis, primarily to confirm the likely failure modes of the cut faces. An overview of the findings is presented in Table 1. Dip and dip azimuth of noted major defects and bedding planes were recorded and plotted in lower hemisphere equal area stereographic projections using the "Stereo32" software package. These were analysed in accordance with the methods outlined by the Transport and Road Research Laboratory to determine qualitative risk of planar, wedge and toppling failure, the results of which are summarised in Table 2.

Table 1: Geological Description and Structure

Chainage	Rock Mass Material	Qualifying Descriptions
0 m to 169 m	Medium grained, weak to very weak sandstone	Cross-bedded, occasional concretionary nodules up to 1 m diameter. Onion skin weathering. Possible blast fractures.
169 m to 226 m	Medium to coarse grained, very weak to weak sandstone	Thickly bedded 0.1 m to 2 m larger block size. Concretionary nodules.
226 m to 420 m	Medium to coarse grained, very weak to weak sandstone	Occasional shear zones. Lower beds composed of softer cross-bedded material.
420 m to 525 m	Medium to coarse grained, very weak to weak sandstone	Dominated by sub-parallel joint faces and large blocks.

Table 2: Failure Type and Occurrence

Failure Type	Northern Batter (uphill carriageway)	Southern Batter (downhill carriageway
Planar	Unlikely (none within dataset)	Unlikely (one within dataset)
Wedge	Many in dataset	Many in dataset
Toppling	Some in dataset	Some in dataset

2.3 Preliminary Quantitative Risk Assessment

A semi-quantitative approach was adopted for the preliminary risk assessment based on the methods detailed in the Australian Geomechanics Society (AGS) Guidelines (2007) and on best industry practice. The risk assessment adopted AGS criteria based on the classification of the cutting as a 'New Constructed Slope'.

The data was limited in terms of rock fall quantity, frequency and distribution, with further assumptions being made for traffic data, based on anecdotal and informal information from Solid Energy together with a short questionnaire answered by their staff and road users. An analysis using best estimate data was carried out in order to estimate the risk from direct impact only. The parameters used in the estimation of risk are summarised in Table 3.

Table 3: General Parameters Assumed in Best Estimate Case

Frequency of Rock Fall Uphill	Frequency of Rock Fall Downhill	Speed km/h U/H and D/H[1] km/h	Length of Section Affected (m)	Total Daily Traffic
52	26	36 and 66	300	102
Specific Vehicle Parameters used for Individual Vehicle Method				
Vehicle	**Length**	**Daily Average (Return Trips)**	**Vulnerability $V_{(R)}$[2]**	**Speed km/h U/H and D/H[1]**
Car/Light Vehicle Mine Related	4.7	67	0.5	50 and 80
Car/Light Vehicle Non Mine Related	4.7	25	0.5	50 and 80
Fuel Tanker	20	3	0.3	30 and 60
Truck and Trailer	17	7	0.3	30 and 60

1. U/H = Uphill, D/H = Downhill
2. $V_{(R)} = 0$ equates to no loss of life, $V_{(R)} = 1$ equates to a fatality. Larger vehicles are less vulnerable than lighter passenger vehicles.

Estimates of the risk of any vehicle being hit by rockfall in any one year were calculated using both an average vehicle (total traffic) probability and also the individual probabilities for the range of vehicle types identified from traffic data. The individual probabilities were summed and compared against the averaged vehicle approach as a check (Table 4). Values of risk obtained using the above parameters for probability of fatality of an individual in the total exposed population (i.e. total traffic) from direct impact in any one year are presented below:

Average traffic method = 1.66×10^{-2}

Summed vehicle type method = 1.06×10^{-2}

This would indicate in this case the total averaged traffic method slightly overestimates the risk in comparison to the summed vehicle type method.

Table 4: Summary of Direct Impact Risks for various Vehicle Types

Vehicle Type	Return Trips per Annum	P(DI) * (Return Trip)	P(D)* per Annum
Cars/Light Vehicles Mine related	24455	2.64×10^{-7}	6.45×10^{-3}
Cars/Light Vehicles Non mine related	9125	2.64×10^{-7}	2.41×10^{-3}
Fuel Tanker	1095	4.76×10^{-7}	5.21×10^{-4}
Truck and Trailer	2555	4.60×10^{-7}	1.17×10^{-3}
Totals	**37230**		**1.06×10^{-2}**

** P(DI) probability of fatality to individual exposed to a hazard during a return trip and P(D) probability of fatality in population exposed to a hazard per year.*

Using the AGS risk level for individual loss of life for the element at most risk, a tolerable level for New Constructed Slopes is given as $1x10^{-5}$ (approximately 1 in 100,000 that a driver will be fatally injured by rock fall). Based on data supplied by Solid Energy the individual at most risk was likely to be the Ngakawau Operations Supervisor who travelled through the cutting 1032 times per annum (516 return journeys or average of 3 times per day), in a car or light utility vehicle.

Based on these assumptions the individual at most risk was exposed to a risk of approximately 1.36×10^{-4} from a direct impact event (i.e. return period of 7352 years). This probability would only have increased if risks from colliding with previously fallen material and failed avoidance actions were also included in the calculations.

Even based solely on direct impact, the risk was considered unacceptable for individuals, and also very high (i.e. on the marginal upper limit of acceptable) for a total fatality risk to road users. The actual risk is probably much higher due to the other scenarios that have not been quantified which include vehicles hitting rocks, rockfall avoidance accidents and economic disruption. It is these latter points which have been given further credible emphasis in the risk analysis of the road's safety record, as both the operation and economics of the Stockton Mine requires an uninterrupted route up to and out of the mine.

The return period indicated by the current direct impact approximates to between 60 - 94 years (range is due to the two methods of analysis used). This risk is only part of the total risks involved i.e. excluding collision with previously fallen material and may potentially double once such scenarios are accounted for. With these values of risk identified, Solid Energy proceeded to commission rockfall mitigation works.

3 STAKEHOLDER CONSULTATION

The cutting is on a newly designated road reserve, which is operated and maintained by Buller District Council (BDC), albeit mainly for the servicing of the Stockton Mine. As such, any upgrade or remedial works would have to be in line with BDC requirements and also undertaken in accordance with their procurement and construction strategy.

The original optimal alignment of the road cutting had been constrained to satisfy concerns about protection of significant flora on the north western boundary. For the same reason, any rock fall mitigation works that would be undertaken would need to ensure the protected species was not compromised.

Consultation with the stakeholders was also necessary, both to validate reported rockfall and to agree a baseline of acceptable mitigation measures based on a cost-benefit assessment to determine the most cost effective means of addressing the issues. In other words, the road maintainer and users needed to be confident that the mitigation would provide them with an affordable solution to secure a safe route to work and homes.

4 MITIGATION WORKS

The road, as the only access route into the Stockton Mine, could not be closed for extended periods of time; as such a 'least disruption' solution for the mitigation works was required. Other constraints on the physical mitigation works were to minimise the volumes of excavated spoil, complete restoration of spoil tips generated during the original cutting excavation and to prioritise the northern cutting face as this was where most rock-falls had been observed in the past. A funding arrangement was put in place for the BDC Roads department to undertake the project with Solid Energy as a direct linked stakeholder.

A limited enquiry was put to local and specialist contractors to determine availability of resources, with the intention of completing a heavy scaling and spot bolting operation. Access to the top of the cutting was to be reformed with environmental constraints permitting a 5 to 6 m wide track to be formed on the crest of the cutting. From the contractor enquiry responses and specific details derived from a site visit a full scope of works was detailed and scheduled, including for a one-way traffic management system, local protection of the road surface and full reinstatement of the road and drainage following the mitigation works. Due to the relatively remote location of the site, it was agreed with BDC to have full time geotechnical supervision on site so the works could be altered to suit local conditions and arrange for spot bolting and local treatment of specific anomalies with minimal disruption to the works' progress.

Mitigation works comprising rope access scaling and heavy scaling using a road header mounted on a tracked excavator were initially undertaken, with one-way traffic management established and operated by radio control. The access to the crest was formed, cutting a 5 m wide track along the crest and cleaning out old drainage channels, with new channelling formed to promote surface water flow away from the crest. The early scaling works revealed several sections of the rock which were more friable and blast damaged than initially thought. One area was targeted for bulk fill dentition using shotcrete (Figure 7) as the rock was considerably undermined for a substantial section of the cutting face with evidence of ongoing compressive crushing of remaining pillars of bedrock. A further section was noted to be quite fissile during mapping and rockfall drapery netting was designed for this section of the face using rock netting resources from the Stockton mine.

The slopes along the cutting were generally re-profiled by 0.5 m to 1.2 m (Figure 8) using the excavator mounted road header to reduce the overhanging sections and this proved good value in improving the perceived sight distances (feedback from the Stockton Mine manager and operatives).



Figure 7: Shotcrete dentition works to infill over blasted rock face, noting columns of overstressed rock to left of operatives.



Figure 8: Traffic management in place with scaling and drilling works ongoing at crest.

Following the scaling, a full geological mapping and topographical survey was undertaken recording the exposed rock joints and facilitating a re-analysis of defects for determining spot bolting locations and orientation of the bolts. In parallel, the netting was being designed and a specification defined for the installation of the rockfall drapery netting, which was issued for construction. However, due to budget constraints, the netting was not installed. Rock bolt design was based upon assumptions of rock strength and joint frictional characteristic plus details provided from the Stockton Mine's geotechnical engineers for geological parameters and rock characteristic design values. This was corroborated by a number of pull out tests being completed on sacrificial bolts installed at the crest, with results proving the design was within an acceptable tolerance of the design Factor of Safety.

The spoils from the works were relocated to a previous tipping site 300 m down the Millerton Road, which allowed improved landscaping. As the excavated spoil was quite soil rich from the crest track excavation works, this proved to be beneficial to establishing areas for future planting and rehabilitation. The potential damage to the road and the drainage ditch at road shoulder was limited due to the contractor establishing fills at locations where heavy scaling was undertaken, providing a cushioning effect to scaled-off rock and debris. The road traffic was locally constrained from passing through the cutting during the works to avoid rockfall generated by either over tipping from the crest works or during rock access scaling.

5 CONCLUSIONS

Quantification of risk from rockfall to road users requires significant data collection, both geological and transportation based, which is not always available or may be prohibitively time consuming to collect. Whilst rockfall can be quite obvious, there are several other factors (such as transport vulnerability, geometric aspects and visibility due to prevailing weather conditions) that can significantly influence the level of perceived risk and decision making in terms of mitigation. The semi-quantitative risk assessment completed for Millerton also demonstrated the difficulty in assessing levels of risk to acceptable and tolerable levels within the New Zealand environment, which justifies having to refer to the AGS tolerable levels for correlation for a new slope construction.

Providing full time supervision on a technically and logistically challenging site provided benefits to keeping the continuity of site works and Contractor planning seamless. The scope of works had sufficient detail and scope to permit significant changes within budget, thereby permitting a focussed solution to be selected based upon actual ground conditions encountered and the logistical constraints imposed.

AKNOWLEDGEMENTS

Solid Energy NZ, Stockton Alliance, Buller District Council, GHD Limited, Shelley Nankeville – site engineer and the contractors Geotech Ltd and West Reef Ltd, John Seward (member of the original GHD team)

REFERENCES

C. M. Bunce, D. M. Cruden, N. R. Morgenstern (1997): Assessment of the Hazard of Rock fall on a Highway. *Canadian Geotechnical Journal* -, vol. 34, no. 3, pp. 344-356

Guidelines for Landslide Susceptibility, Hazard and Risk Zoning for Land-use Planning (2007) *Extract for the Australian Geomechanics Society Journal*, Vol. 42 No 1

E I. Stewart, F. J. Baynes and I. K. Lee (2002). The RTA Guide to Slope Risk Analysis Ver. 3.1, *Australian Geomechanics Society*

G. D. Matheson (2002) *Laboratory Report 1039* Transport and Road Research Laboratory,

Ritchie, A. M. (1963) Evaluation of Rockfall and Its Control. *Highway Research Record*, No. 17, pp. 13-28.

Graafhuis, R.B. & Underhill, J.P. (2013)
Risk Management of a complex rotational failure at Whales Back Saddle on the Inland Road, North Canterbury, New Zealand
Proc. 19th NZGS Geotechnical Symposium. Ed. CY Chin, Queenstown

Risk management of a complex rotational failure at Whales Back Saddle on the Inland Road, North Canterbury, New Zealand

R B Graafhuis,
AECOM NZ Ltd,
rhys.graafhuis@aecom.com (Corresponding author)

J P Underhill
AECOM NZ Ltd
john.underhill@aecom.com

Keywords: risk management, rotational slump, probability of failure, antecedent precipitation

ABSTRACT

During the last 55 years a landslide has affected and periodically closed the Inland Road near Kaikoura, New Zealand. During winter the landslide undergoes continuous creep which is driven mainly by increased porewater pressures resulting in reduced strength along discrete clay gouge zones and partially by increased weight of the failure mass where localised areas become saturated with water.

Groundwater levels that will trigger accelerated movement are correlated with precipitation records, inclinometer and survey marker monuments. From these observations the probability of failure has been determined for various return period precipitation events based on cumulative precipitation period of 5 to 30 days. Long term movement can be predicted and if required alarm levels set as part of a risk management strategy. A management strategy has been developed based on evaluation of remedial options, associated residual risks and the cost for each option. As expensive stabilisation measures are not warranted, a monitor and repair strategy is an acceptable method of managing the landslide risks.

1 INTRODUCTION

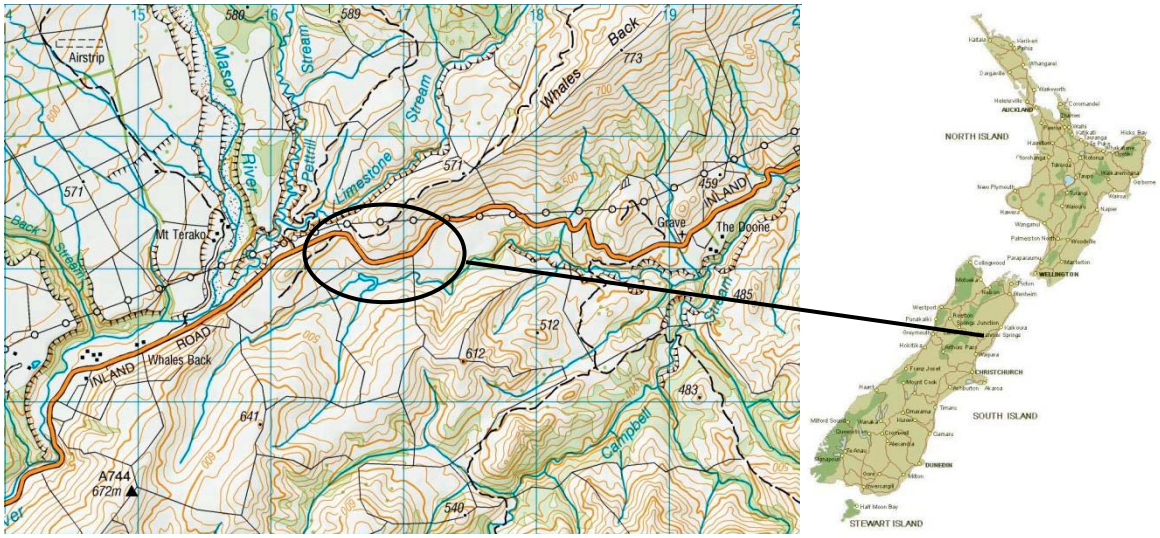


Figure 1: Site location

The Inland Road is the designated over dimensioned route between Kaikoura and Christchurch (Figure 1). Ground movement at the Whales Back Saddle has affected this route since 1955. Following prolonged snow and rainfall in July and August 2008 the route was closed by movement of the failure.

New Zealand Geotechnical Society Inc. 19th Symposium, Queenstown 2013

AECOM undertook geotechnical investigations to assess the failure and movement mechanisms between August 2008 and July 2010. The investigations comprised engineering geological mapping, machine drilling, groundwater measurement, inclinometer monitoring for 12 months, ground survey monitoring for 23 months, and analysis of daily precipitation data dating back to 1955. During the investigation the failure underwent continuous slow creep with two sudden movements in 2008 and 2010.

Remedial works where recommended following the 2008 movement. These were undertaken during 2010 and involved lowering, levelling, and resealing the road, and reforming the cut slope above road level.

1.1 Description of 2008 Movement

The 2008 movement involved the reactivation of an historic rotational slump type failure. The failure is anecdotally reported to have first moved 30 to 50 years ago and at that time involved a 10m to 20m vertical and horizontal movement of approximately 350,000m3 of material that offset the road by several metres and dammed the stream in the valley below. The 2008 movement was approximately half a metre and resulted in distress to the road pavement including vertical offset, and compressional and extensional cracking. Some of the features of the 2008 movement are illustrated in Figure 2, Figure 3, Figure 4 and Figure 5.



Figure 2: Soil slumping onto road



Figure 3: Drop out on road



Figure 4: Displacement of road at southern flank of failure



Figure 5: Failure from opposite side of valley

2 SURFACE DATA

2.1 Description of failure

An engineering geomorphic map prepared from field mapping showing key geomorphic features is presented in Figure 6.

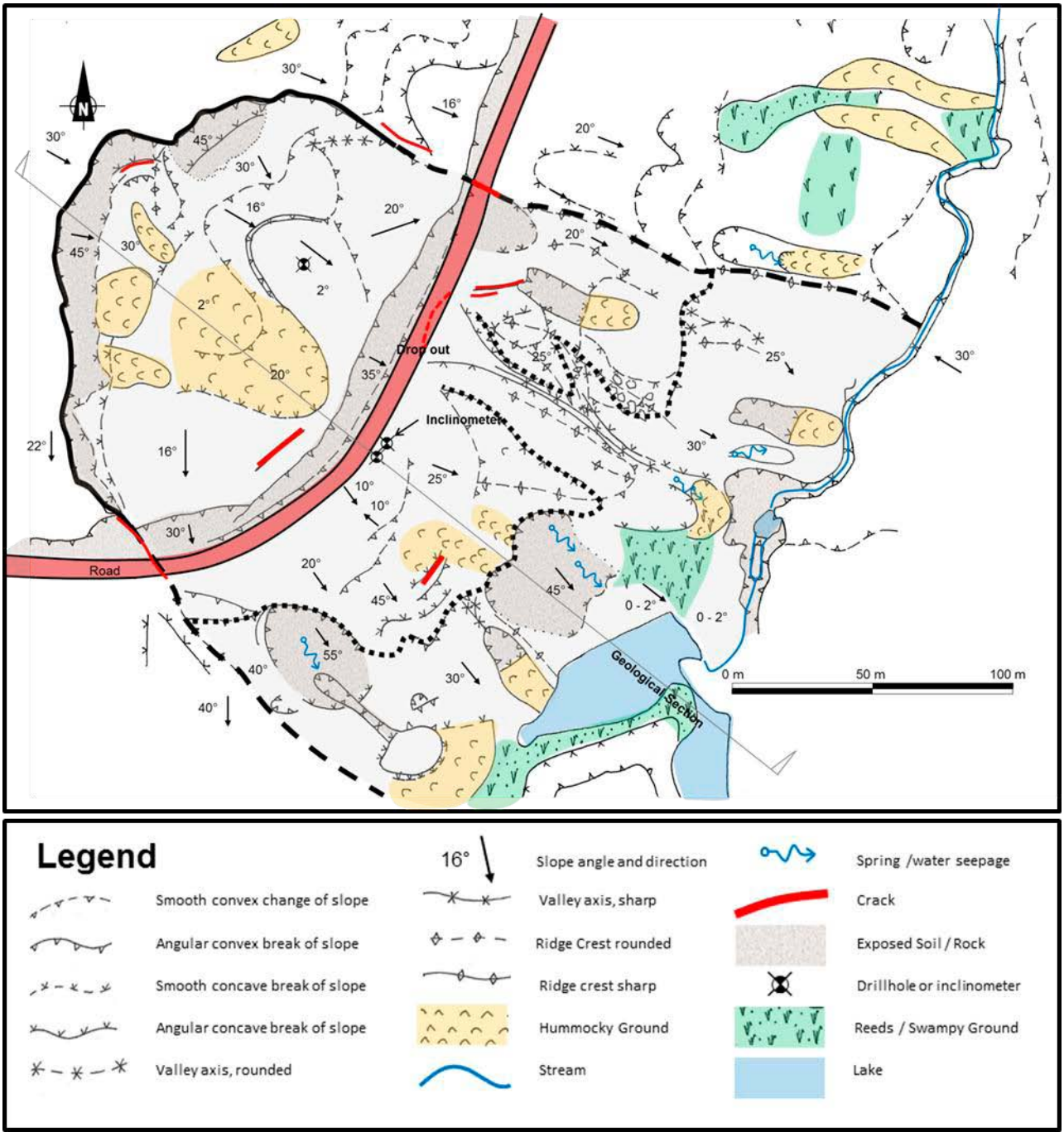


Figure 6: Geomorphic Map

The Whales Back slip is located on a south facing hill side is approximately 200m wide, 300m long and divided horizontally by approximately 250 m of road. A steep 10 m to 15 m high curved back scarp defines at the back of the slip. Soil is exposed across much of the scarp with localised slumps forming hummocky ground in front of the scarp. Lack of vegetation on many of these small slumps indicates relatively recent movement. A secondary back scarp has resulted in a high bench in the centre of the slip with deep tension cracks between the main back

scarp and bench. Deep tension cracks occur on the slip parallel to the eastern end of the back scarp.

During construction of the remedial works in March 2009, a soft gouge zone comprising a brown clayey paelosol was exposed that correlated well with the interpreted eastern edge of the slip, and numerous voids were exposed in other construction excavations.

Below the road the ground steepens towards the stream with many small fresh slumps, scarps, benches, and terracettes with tension cracks running parallel to the road. During the field mapping period (March and April 2009) springs and swampy areas were more numerous with larger flows at higher elevations on the western side of the failure than on the eastern side.

2.2 Survey Monitoring

A survey monitoring network was established across the slip area and surrounding ground in August 2008. The network comprised 30 monuments, steel pegs driven into the ground, and levelling marks installed in the road pavement. The movement of these monuments was measured at regular intervals.

New Zealand Geotechnical Society Inc. 19th Symposium, Queenstown 2013

3 SUBSURFACE DATA

3.1 Drilling

Three rotary machine holes were drilled into the failure mass. One was above the road and two were at road level. All drillholes encountered landslide failure debris over almost their entire length. In-situ breccia (volcanic tuff) was encountered at 39m and 48m depth beneath the road. Numerous crush and gouge zones were encountered throughout the failure debris. In general encountered failure debris was heterogeneous. Ground conditions are shown on the geological section (Figure 7). Drilling investigations and field mapping confirmed the complex nature of the failure.

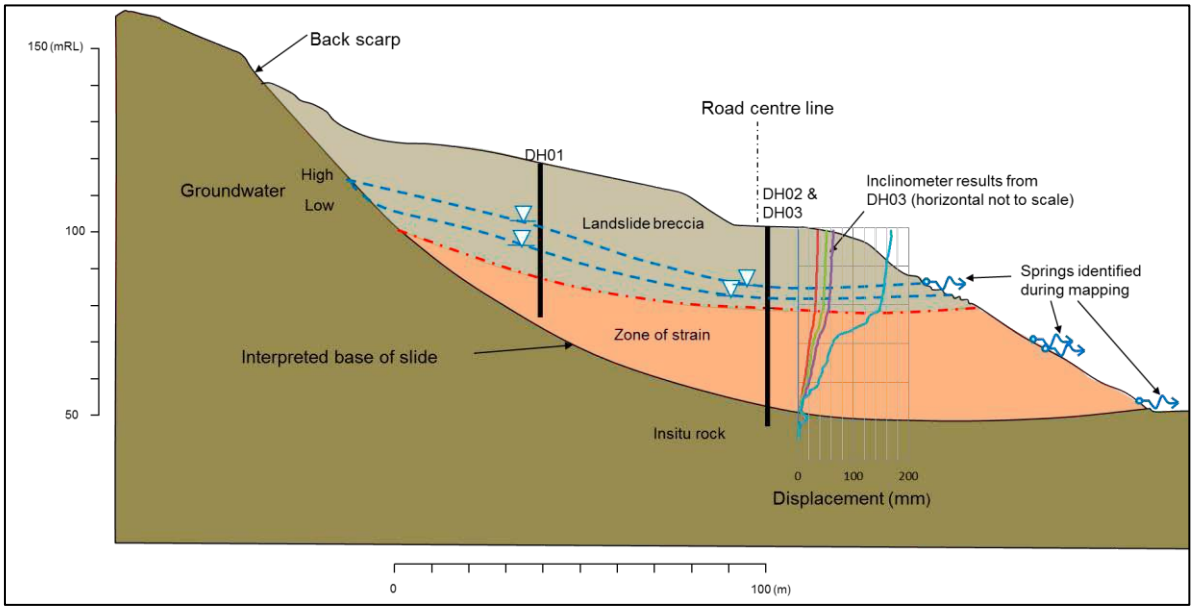


Figure 7: Geological Section

3.2 Inclinometer Data

An inclinometer was installed in DH03 from road level to a depth of 55.0m. A baseline reading was undertaken on 27 April 2009 and subsequent readings were undertaken on 27 July 2009, 18 November 2009, 17 March 2010 and 5 July 2010.

The measurements of the inclinometer coincided with survey network monitoring. The inclinometer results indicate that strain in the failure mass is taken up over its lower half and is not confined to a single narrow zone or surface. Inclinometer deflections are shown on the geological section in Figure 7.

Inclinometer results indicate a total of 145 mm of displacement from the beginning of monitoring. The majority of this (145 mm) occurs between 21.5 m to 44.5 m depth. With zones of strain coinciding with crush and gouge zones logged in DH02. Due to the shape and complex internal structure of the failure, the zones of strain most likely vary laterally across the failure.

The deflections measured in the inclinometer indicate that approximately 47 mm of displacement occurred between 27 April 2009 and 17 March 2010 at an average velocity of 0.15 mm/day. A further 100 mm of displacement was recorded between 17 March 2010 and 5 July 2010 at a velocity of 0.91 mm/day. However this movement is assumed to have happened at a much higher rate over a short period in late May 2010 and may have been as much as 20 mm/day.

3.3 Results of Ground Monitoring

Ground movement monitoring was initiated immediately following the large movement of August 2008. It is assumed that movement quickly decreased after the initial movement. Movement then increased to peak at 13.2 mm /day around 28 August 2008 then decreased again settling to a slow creep by February 2009. From February 2009 until July 2010 the slip moved at a slow creep of around 0.1 mm / day. By July 2010 the slip appeared to have accelerated to an average movement over the four month period of 0.8mm a day, however this movement is assumed to have happened at a much higher rate over a much shorter period in late May 2010.

Monitoring results indicate that slip movement is confined to a zone extending between the main scarp and the base of the steep slopes approximately 30 m from the stream at the bottom of the valley.

4 PROBABILISTIC ANALYSIS

4.1 Historical Failure Movement

Historical slip movements before 2008 were identified from entries in the Highgate Station farm diary. Two more recent events have been measured on 31 July 2008 and 18 June 2010. A total of six events have been recorded between 1955 and June 2010. The farm diary from Highgate Station indicates Whales Back Saddle slip moved on 14 May 1959, 14 July 1963, 4 September 1974, and 23 December 1993. However, it is possible that other large movements of this slip occurred were not noted. The Highgate Station diary also indicates slips or wash outs at locations other than the Whales Back Saddle slip on 6 May 1959, 16 July 1963, and 26 August 1979. The owner commented that the slip is constantly creeping.

4.2 Failure Trigger Mechanisms

The three principal trigger mechanisms assessed were:
(1) seismic events
(2) failure mass geometry and

New Zealand Geotechnical Society Inc. 19th Symposium, Queenstown 2013

(3) antecedent precipitation (preceding precipitation).
Seismic events and failure mass geometry showed no correlation with historical failure movements and are not considered principal trigger mechanisms. Assessment of historical records indicates the principal trigger mechanism is preceding precipitation. The intensity of this precipitation directly affects the probability of failure movement. Antecedent precipitation prior to failure movement is the most likely trigger of rapid movement.

4.3 Antecedent Precipitation

Antecedent precipitation is simply the precipitation (both rainfall and snow) over a specified timeframe leading up to a specified event, in this case movement of the failure. Antecedent precipitation in the days preceding movement will infiltrate the surface resulting in groundwater rising and saturation of the failure mass. Increasing porewater pressure on less permeable failure surfaces will result in a reduced factor of safety and accelerated movement of the failure mass.

4.4 Correlation of Failure movement and Antecedent Precipitation

Documented failure movements at Whales Back Saddle have been correlated with daily precipitation data. An analysis of precipitation data indicates a correlation exists between antecedent precipitation and accelerated movement. Antecedent precipitation was calculated for periods of 2 days, 5 days and in 5 days increments up to 55 days. For example Figure 8 shows that the 25 days antecedent precipitation exceeds the 1 in 5 year event on 11 occasions from 1955 to 2010; the failure mass moved on six of these eleven occasions; resulting in a probability of movement of p = 0.54% for 25 days antecedent precipitation exceeding a 1 in 5 year event.

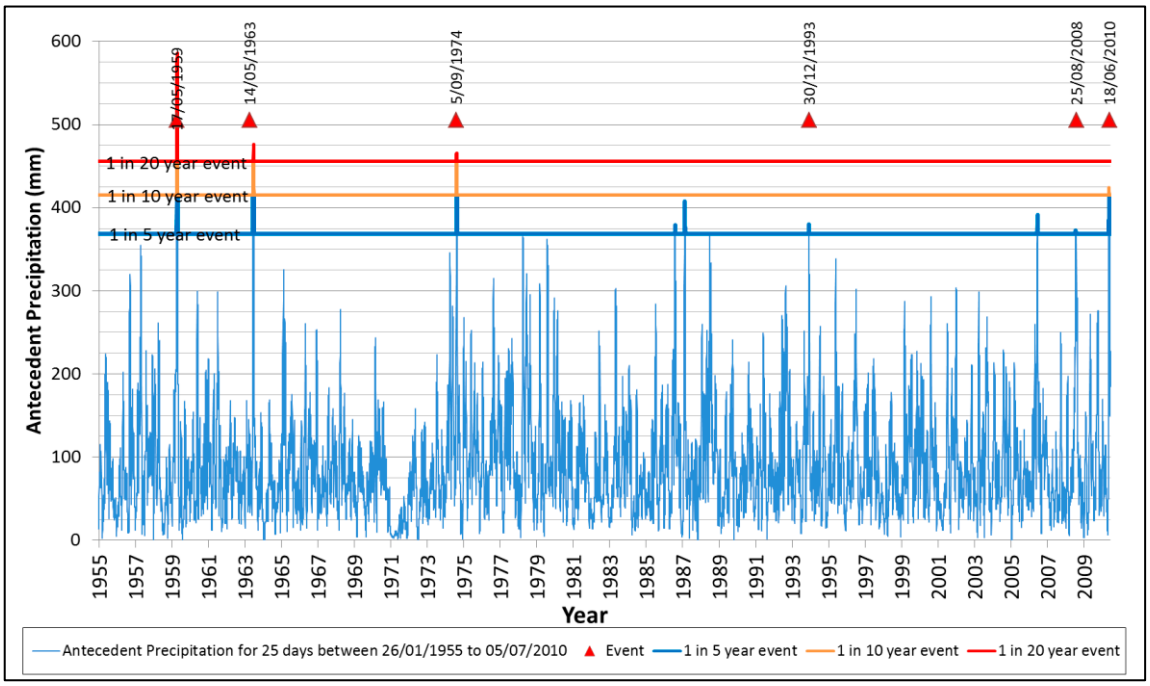


Figure 8: Antecedent Precipitation for 25 days from 1955 to 2010

Annual Exceedance Probabilities (AEP) of 1 in 5, 1 in 10 and 1 in 20 year events was calculated and is plotted on Figure 9.

The probability of failure movement for each period was calculated by assessing the number of precipitation events that exceed the 1 in 5 year, 1 in 10 year and 1 in 20 year event for the range of cumulative periods up to 55 days; and by assessing the number of sudden movement events

associated with these precipitation events. The probability of future movement is shown by the appropriate regression lines on Figure 9.

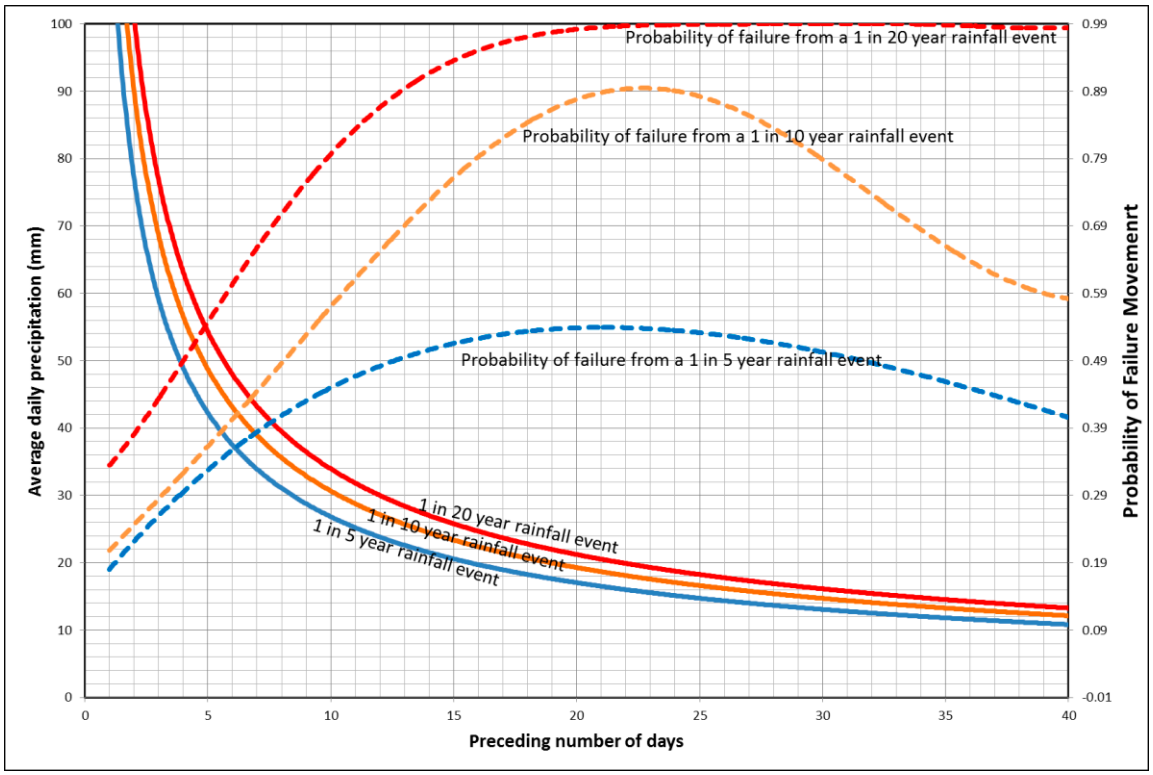


Figure 9: Annual exceedance probability of antecedent precipitation triggering failure movement

4.5 July 2010 event

Late May 2010 was particularly wet, with 5 days antecedent precipitation exceeding the 1 in 20 year event, as a result additional monitoring was undertaken. Antecedent precipitation for 5 days is shown on Figure 10. Monitoring comprised measurement of the inclinometer and piezometers on 18 June 2010 and the survey monitoring network on 5 July 2010.

Monitoring results show that 100 mm of measured displacement was recorded between 17 March 2010 and 5 July 2010 at a velocity of 0.91 mm/day. However this movement is assumed to have happened at a much higher rate over short period in late May 2010 and may have been as much as 20 mm/day, as is shown by the green dashed line on Figure 10.

The prediction of the July 2010 event using Figure 9 confirms that this plot can be used as a predictive tool to quantify the precipitation intensity required to induce movement.

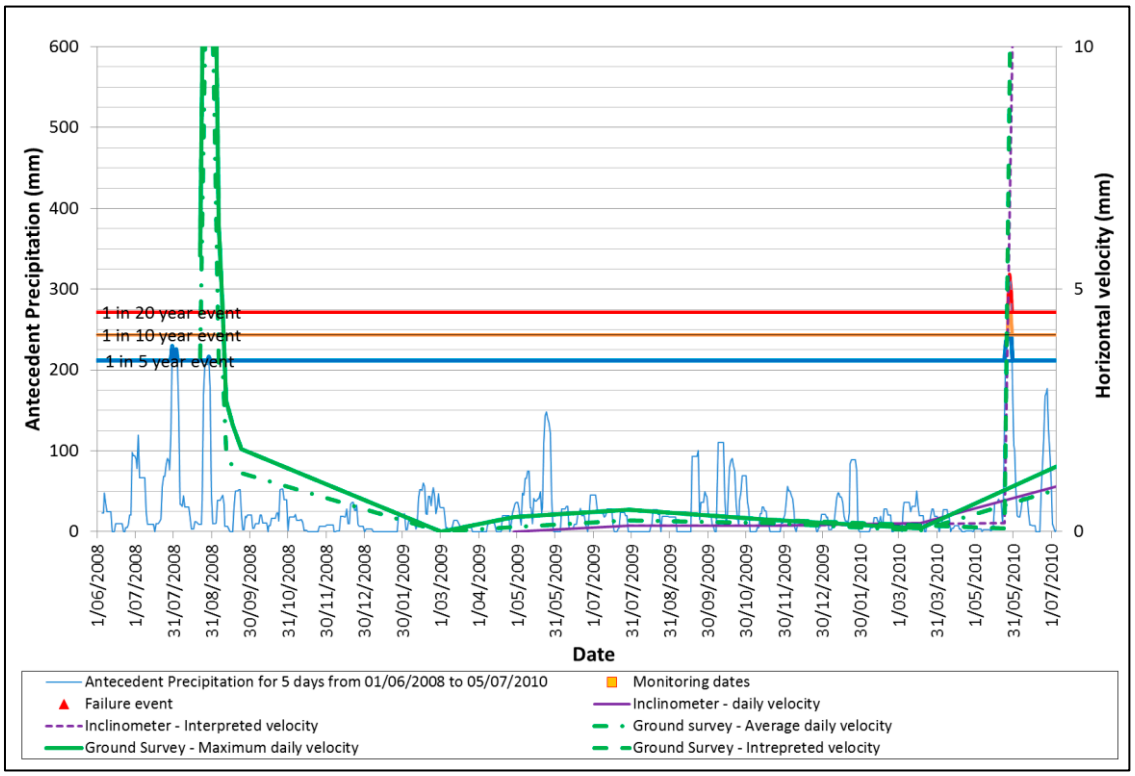


Figure 10: Antecedent precipitation for 5 days and monitored movement from 2008 to 2010

5 CONCLUSIONS

The likelihood of further movement for this rotational failure can be estimated from the cumulative precipitation over a preceding period of 5 to 30 days.

Probabilistic analysis of this type enables the likelihood of failure to be quantified without the need for expensive ground investigations. This method of estimating failure movement could be adapted to other failures where increased pore water pressure is considered the primary trigger of movement. This method could form the basis for effectively managing and setting budgets for remediating infrastructure that is exposed to these types of failures.

6 ACKNOWLEDGEMENTS

We would like to acknowledge David Edge from Hurunui District Council for allowing publication of this paper; and Jane and Hugh Northcote from Highgate Station for supplying rainfall and slip movement observations dating back to 1955.

Rockfall protection of West Angelas iron ore mine using H.T.W.M.

P Guerra
Geovert Pty Ltd, Sydney, Australia
Paulo.guerra@geovert.com

T Le
Geovert Pty Ltd, Sydney, Australia
tin.le@geovert.com

Keywords: rockfall, slope stabilisation, soil nailing, landslip, high tensile mesh, *Tecco*

ABSTRACT

This paper presents a rock fall protection technique employed at the West Angelas iron ore mine located in the Pilbara region of Western Australia. The technique involves the installation of rock bolts and fully dimensioned high tensile wire mesh (HTWM) covering an area of approximately 6000 m2 of the overhang 150m above the pit floor. In order to evaluate the surface stability of the slope and to propose adequate design, an analysis was undertaken using surficial slope stabilisation calculation techniques to define nail geometry, type and diameter and appropriate mesh cover. The final design approach and construction methodology are also discussed and presented in this paper. The design of the rock fall mesh system has been proved to be satisfied as it successfully stopped a 1.5 m3 detached boulder falling off the crest in February 2012. Due to the simple installation procedure, the high tensile mesh system had allowed the project to be completed in shorter duration with minimal disruptions from technical related issues.

New Zealand Geotechnical Society Inc. 19th Symposium, Queenstown 2013

1 INTRODUCTION

The West Angelas open pit mine and ore processing plant is located 110 km west of Newman in the East Pilbara region of WA. After a major slip failure along the North wall of the centre pit north (CEPN) (figure 1), a significant amount of material was left overhanging at the top of the slope producing significant risk of rockfall. Mining of the area directly below the area of overhang was the critical long term operations target for the client. Blasting has subsequently been conducted to reduce the size of the overhang; however it was not completely removed and suffered further damages during the blasting operations. As a consequence further treatment was required to secure the crest area where the hazards were more prevalent. Once the hazard was identified with a surficial instability of a 0.75 m layer thickness overhanging the slope, a solution was developed with nails and high tensile mesh installed using light weight drilling rigs, cranes and rope access personnel to solve the surficial stability problem.

An active slope stabilisation retains material in its place with force preventing material such as unstable rocks and soil masses from sliding or falling. Therefore no maintenance is required as occurs with other passive systems such as drapes, bunds or rockfall barriers. The design, layout and nailing of the HTWM slope stability system considers fast and easy installation, taking into account that many installations are constructed in difficult, steep and remote terrain. Lightweight parts, a minimum of nails and quick mesh installation are important construction aspects. The wire mesh, nails and the bespoke spike plates are the major components of the system. Loads arising from sliding rocks and soil masses are transmitted to spike plate and nails. Diamond shaped wire meshes, made out of high tensile steel wires have proven to be very effective in their containment capacity.

The principal function of the nailing and the spike plates is to retain the mesh. Special diamond-shaped system spike plates matching the HTWM serve to fix the mesh to soil or rock nails. By tightly pre-tensioning the spike plates on the nail head into the ground to be stabilised, the mesh is uniformly tensioned to the face transferring force into the surface and tightening the spaces

between the nails. Rock bolts transmit the forces into the substrate. The appropriate nail pattern is determined by applying the RUVOLUM dimensioning software, considering both geotechnical as well as material aspects.

2 AVAILABLE DATA

The Hamersley Iron Province is characterised by a 2500 million years old late Archaean and early Proterozoic rock formation known as "Hamersley Group", predominantly composed of Banded Iron Formation (BIF) which is formed by alternate layers of Iron-rich and Silica-rich layers. The Marra Mamba Iron Formation hosts the principal ore body. The slip occurred by planar sliding on a shale bed dipping into the pit at an angle of approximately 40 degrees. No significant geo-hydrological influence has been identified.

The dimensions of the slip failure are shown in figure 1. The exposed rock was identified as shale band. Due to the conditions of the post failure back scarp, rock fall events could be trigged by an increase in ground accelerations (from blasting's, earthquakes, heavy machines, drilling, etc.) boulders may start to move and finally fall down the slope. The geotechnical parameters considered to represent the area in analysis, and used in the design are:

- Inclination of slope $\alpha = 400$
- Slab thickness (overhang thickness) t = 0.75m
- Ground friction angle $\phi' = 320$
- Cohesion c' = 0 kPa Bulk weight density of the rock was assumed to be 30kN/m^3

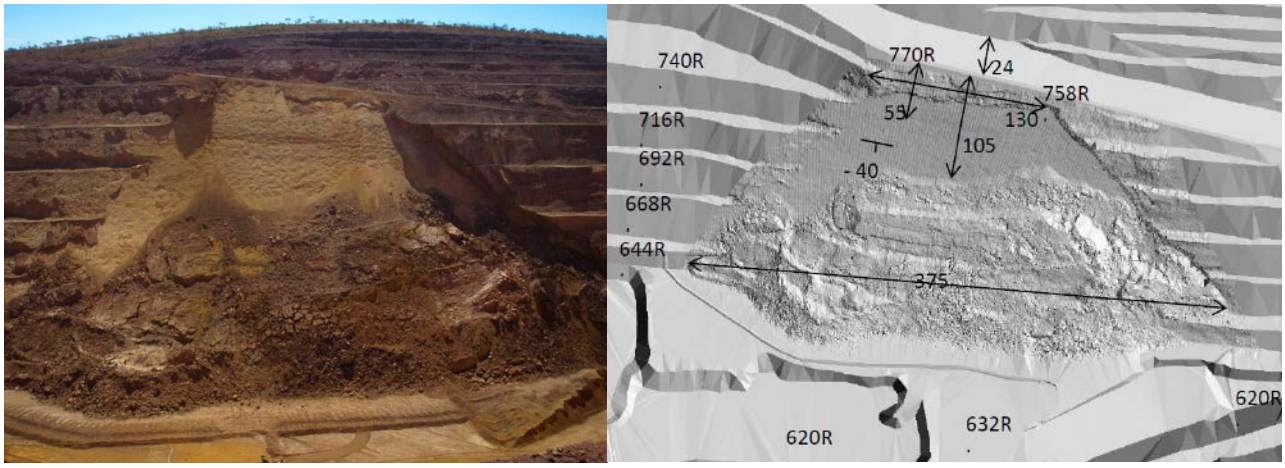


Figure 1: Major slip failure with dimensions, West Angelas (Joass et al, 2013)

3 ROCK FALL STABILISATION DESIGN

3.1 Design Constraints Consideration

A selected recovery option was required for the bulk of the slip to be mined out, to allow the high grade ore directly below the slip area be accessed (Joass et al, 2013). Due to the drill and blast operation to remove or reduce the overhanging risk, work was focused on securing the crest area suffering damage during blasting operations. The rockfall risk at the top of the plane failure, at RL740 to RL770, roughly 4000m2, as shown in Fig.1, presented a significant safety challenge for ongoing mining activities, as well as construction methodology of rockfall protection. With these difficulties, mitigation options were limited to those which should be completed using top-down installation techniques. This eliminates the option of barrier construction directly at the middle batter of the high wall without prior stabilisation to make it safe for construction crews. The suggested option actively stabilises the overhang with high tensile wire mesh, which reduced drilling and ultimately decreased construction time and costs. The slope stabilisation system designed and installed is a flexible facing to stabilise and prevent these surficial blocks from falling from the slope, even with continued seismic loading from the mining operations.

3.2 Design Analysis and Calculation

Rio Tinto geotechnical engineers provided geotechnical design recommendations and risk management plans for the ore recovery. As such it was not required to assess global slope stability in this design for the rockfall mitigation system. Only superficial instability down to a depth of 0.75 m was considered in the analysis and solution. In order to evaluate the surface stability of the slope and to propose adequate measures, an analysis based on the software Ruvolum (Geobrugg, 2010) for superficial slope stabilisation design, developed by Geobrugg, has been carried out on a characteristic cross-section. The results of the analysis provide information such as nail spacing, type/ diameter and appropriate mesh cover. See input parameters on table 1.

Table 1: Design Input

Description	Symbol	Value	Unit
Slope Inclination	α=	40	degrees
Nail distance Horizontal	a=	3	m
Nail distance in line of slope	b=	3	m
Layer thickness	t=	0.75	m
Radius of pressure cone, top	ζ=	0.15	m
Inclination of pressure cone to horizontal	δ=	45	degrees
Friction Angle ground (characteristic value)	ϕ=	32	degrees
Cohesion ground (characteristic value)	ck=	0	kPa
Volume weight ground (characteristic value)	γ_k=	30	kN/m3
Slope - Parallel Force	Z_d=	15	kN
Pre tensioning force of the system	V=	30	kN
Nail inclination to horizontal	ψ=	20	degrees
Partial safety correction value for friction angle	γ_ϕ	1	
Partial safety correction value for cohesion	γ_c	1	
Partial safety correction value for volume weight	γ_γ	1	
Model uncertainty correction value	γ_{mod}	1.5	
Elements of the System - as specified by the manufacturers			
Applied mesh type	TECCO G65/3mm		
Applied spike plate	TECCO system spike plate		
Bearing resistance of mesh to selective, slope-parallel tensile stress	Z_R (kN)	30	
Bearing resistance of mesh to pressure stress in nail direction	D_R(kN)	180	
Bearing resistance of the mesh against shearing-off in nail direction	P_R(kN)	90	
Applied nail type	GEWI	25mm	
Taking into account rusting away	Yes		
resistance of nail to tensile stress	T_{Rred}(kN)	173	
Nail to shear strenght	S_{Rred}(kN)	100	
Cross-section area of the applied nail with rusting away	A_{red} (mm2)	346	

3.2.1 Investigation of Superficial slope-parallel instabilities

The investigation of superficial slope-parallel instabilities addresses the cover “layers” sliding off the stable rock. In this case, the nailing system is the stabilizing agent against the slide hence

New Zealand Geotechnical Society Inc. 19th Symposium, Queenstown 2013

the rock capacity of the nails against the sliding effect is required to be investigated. Figure 2 demonstrates the relevant forces acting on the nailing system.

G: Dead load of the cubic body

T and N: direction of the sliding surface

S: Shear stress acting on the nail

t: thickness of the layer

b: nail distance in line of the slope

V: Pre-tensioning force of the system

α: slope inclination

ψ: nail inclination to the horizontal

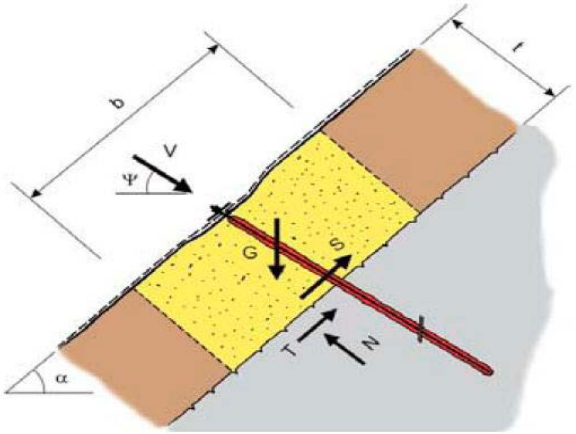


Figure 2: Forces acting on the cubic body (Geobrugg, 2010)

In Eurocode 7 the following three proofs of bearing safety must be addressed for superficial slope parallel instabilities: (1) proof against a superficial layer sliding off, (2) proof of the mesh against puncturing and (3) proof of the resistance of the nail to combined stress

New Zealand Geotechnical Society Inc. 19th Symposium, Queenstown 2013

3.2.2 Proof against superficial layer sliding off a parallel to the slope

This is to prove that the cubic body of width a, length b and thickness t does not shear along the sliding surface which is inclined by the angle α in respect to the horizontal plane. According to Geobrugg, 2010:

The governing condition is $S_d \leq \frac{S_R}{\gamma_{SR}}$

S_d: is the shear stress under consideration for the geotechnical parameters and the external, stabilizing force V_{d1}, whereby the following applies: $V_{d1} = V * \gamma_{d1}$(γ_{d1}= 0.8 is generally taken).

S_R: nail resistance to shear stress.

γ_{SR}: resistance correction value based on Eurocode , and is generally assumed equal to 1.5.

S_d is calculated as below.

$$S_d = \frac{1}{\gamma_{mod}}\{\gamma_{mod} * G * \sin\alpha - V_{d1} * \gamma_{mod} * \cos(\psi + \alpha) - c' * A - [G * \cos\alpha + V_{d1} * \sin(\psi + \alpha)] * \tan\phi\} \quad \text{Equa. 1}$$

$$G = \gamma_k * a * b * t = 30 * 3 * 3 * 0.75 = 202.5 \text{ kN} \quad \text{Equa. 2}$$

$$V_{d1} = V * \gamma_{d1} = 30 * 0.8 = 24 \text{ kN} \quad \text{Equa. 3}$$

Therefore, the value of $S_d = 44.9 \text{ kN} \leq \frac{S_R}{\gamma_{SR}} = \frac{100}{1.5} = 66.67$ kN (fulfilled)

3.2.3 Proof of mesh against puncturing

This proof is to verify if the mesh is able to absorb the force V applied in nail direction and transfer it into the stable subsoil. Hereby, the value of the externally applied force V is compared with the bearing resistance of the mesh to pressure stress in nail direction, whereby the resistance correction value for puncturing is taken into account

$$V_{d2} \leq D_R/\gamma_{DR}$$

V_{d2} is the dimensioning value of the external force V with which the slope stabilisation system is pre-tensioned against the nails $V_{d2} = V * \gamma_{V2}$ where γ_{V2} is generally taken as 1.5

$$\text{So, } V_{d2} = 30 * 1.5 = 45\text{kN} \leq \frac{180}{1.5} = 120 \text{ kN (fulfilled)} \quad \text{Equa. 4}$$

γ_{DR} is the resistance correction value, generally equal to 1.5.

D_R is the mesh resistance against pressure stress in nail direction.

3.2.4 Proof of the nail to combined stress

This proof is to verify the capacity of the nail under simultaneous applied tensile stress from the pre-tensioning and the shear stress from the sliding cubic body. The governing condition is as followed

$$\sqrt{\left\{\frac{V_{d2}}{T_R/\gamma_{VR}}\right\}^2+\left\{\frac{S_d}{S_R/\gamma_{SR}}\right\}^2}=\sqrt{\left\{\frac{45}{173/1.5}\right\}^2+\left\{\frac{44.9}{100/1.5}\right\}^2}=0.778\leq 1 \text{ (fulfilled)} \quad \text{Equa. 5}$$

3.2.5 Investigation of local instabilities between the individual nails

The second investigation focuses on the local bodies liable to break out between the individual nails. This investigation is in order to ensure that all local bodies liable to break out will be retained within the mesh and maximum occurring forces are absorbed and transferred to the stable rock. In a triangular nail pattern, above each nail is a field of width a and length 2xb which must be secured against local instabilities. As every single nail is pre-tensioned to a certain load (30kN in this case), this will cause the spike plate (please see figure 3) to press firmly into the ground. And as part of the investigation, the pressure cone region is not considered as part of the local body liable to slide off. The pressure cone is characterised by the radius of the pressure cone (usually 0.5*width of spike plate = 0.5 * 0.3 = 0.15m) and the inclination angle δ (45^0). Hence, the local body's cross section area is trapezoidal as seen in figure 3. For simplification, the trapezoidal cross section can be transformed to rectangular with equivalent area of the width.

$$a_{red}=\left(a-\frac{t}{tan\delta}-2*\zeta\right)=1.95m \quad \text{Equa. 6}$$

ζ: radius of the top of the pressure cone

(normally ζ is considered = 0.5xD_{plate})

ξ: radius of the base of the pressure cone

δ: inclined angle of the pressure cone = 45^0

DPlate: diameter of the base plate

η: is the distance of cone base of nails

V: pre tensioning force of the system

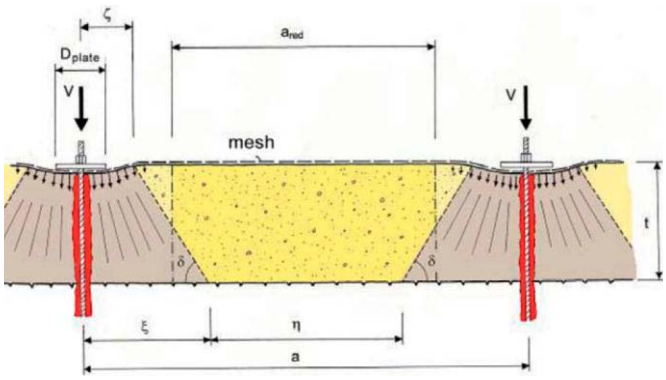


Figure 3: Cross section of the local body liable to slide off with the nail pressure cone (Geobrugg, 2010)

Depending on the slip failure angle β, there are 2 fault mechanisms of single-body sliding- Mechanism A and double-body sliding – Mechanism B as illustrated in figure 6 below.

Fault Mechanism A:

$$P[kN]=\frac{G[\gamma_{mod}*\sin\beta-\cos\beta*\tan\phi']-Z*[\gamma_{mod}*\cos(\alpha-\beta)-\sin(\alpha-\beta)*\tan\phi']-c'A}{\gamma_{mod}*\cos(\beta+\psi)+\sin(\beta+\psi)*\tan\phi'} \quad \text{Equa. 7}$$

Where $\gamma_{mod}=1.5$, A = L*a_{red} and G is the dead weight of the body liable to break out and is calculated in terms of β as in equation 8.

$$G=\gamma_k*a_{red}*\frac{4b^2*\sin(\psi+\alpha)*\sin(\alpha-\beta)}{2*\sin(\beta+\psi)} \quad \text{Equa. 8}$$

Fault Mechanism B: Fault mechanism B is characterised by two bodies liable to break out: the upper trapezoidal body presses over the contact force X onto the lower wedge-shaped body II. The width of the two bodies is a_{red}. The force X is calculated as below

$$X[kN] = \frac{1}{\gamma_{mod}} * \{G_I * (\gamma_{mod} * \sin\alpha - \cos\alpha * \tan\phi') - c' * A_I\} \quad \text{Equa. 9}$$

$$P(kN) = \frac{G_{II}[\gamma_{mod} * \sin\beta - \cos\beta * \tan\phi'] + (X - Z) * [\gamma_{mod} * \cos(\alpha - \beta) - \sin(\alpha - \beta) * \tan\phi'] - c' A_{II}}{\gamma_{mod} * \cos(\beta + \psi) + \sin(\beta + \psi) * \tan\phi'} \quad \text{Equa. 10}$$

$$\text{Where } G_I = \gamma_k * a_{red} * t * \frac{1}{2} * \left[4b - t * \left(\frac{1}{\tan(\alpha - \beta)} + \frac{\sin(\psi + \beta)}{\sin(\alpha - \beta) + * \sin(\psi + \alpha)}\right)\right] \quad \text{Equa. 11}$$

$$G_{II} = \gamma_k * a_{red} * \frac{t^2}{2\tan(\alpha - \beta)} \quad \text{Equa. 12}$$

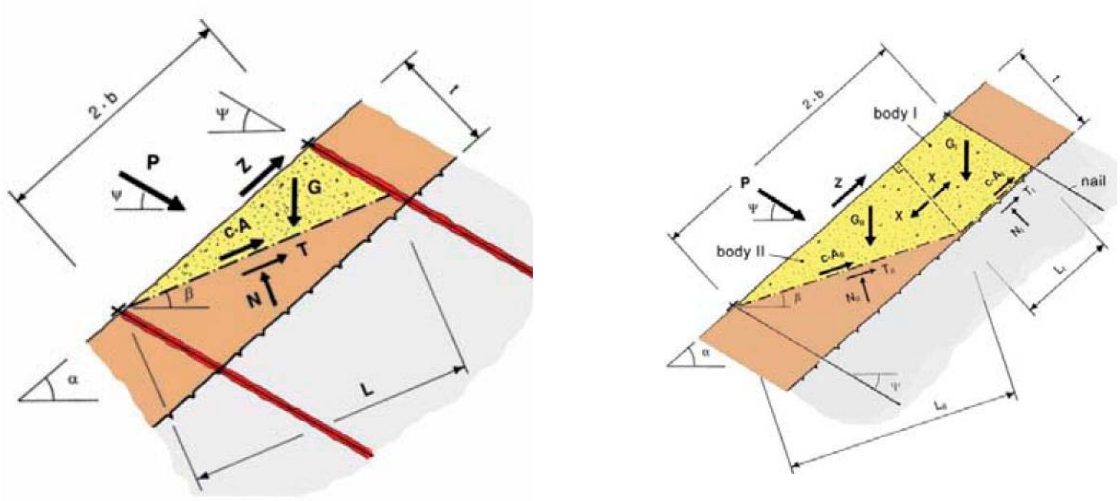


Figure 4: Fault mechanisms A and B (Geobrugg, 2010)

- P: Max stress on the mesh for shearing-off nail direction
- c.A: is the surface area of the sliding body and the cohesion of the ground. This measures the shear resistance
- Z: Slope parallel Force
- As can be observed, the value for β is ranging from -200 to 400 in relation to the horizontal. The range of β in which each mechanism occurs is as below
- Mechanism A: $33.35^0 \leq \beta \leq 40^0$,
- Mechanism B: $-20^0 \leq \beta \leq 33.35^0$
- By equilibrium the force P is determined in the two fault mechanism as follow (Geobrugg, 2010)

3.2.6 Proof of the mesh against shearing off at the upslope edge of the Spike plate

If the investigated body liable to break out threatens to slide off, it presses outwards in the area of lower nail with this maximum force P. The force P is determined using the maximum value between fault mechanism A and fault mechanism B. The mesh must be sufficiently strong to withstand this shear stress and to carry the force P away over the spike plate onto the nail. This means to verify the condition below is true.

$$P_d \leq \frac{P_R}{\gamma_{PR}} \quad \text{Equa. 13}$$

P_d is dimensioning value of the maximum shear stress on the mesh at the upslope edge of the spike plate on the lower nail

P_R is bearing resistance of the mesh against shearing off in nail direction, and to be determined by means of test developed specifically for the purpose. $P_R = 90$ kN

γ_{PR} is resistance correction value and is generally taken as 1.5

By utilizing the set of equations provided in the above section, the value of maximum force P in each fault mechanism is calculated and the greater value between fault mechanism A and fault mechanism B is the value for P_d

For Mechanism A, $P_{max} = 8.83$ kN at $\beta = 33.35^0$ Equa. 14

For Mechanism B, $P_{max} = 32.0167$ kN at $\beta = 22.1878^0$ Equa. 15

Therefore $P_d = 32.0167 \text{ kN} \leq \frac{P_R}{\gamma_{PR}} = \frac{90}{1.5} = 60\text{kN}$ (Fulfilled) Equa. 16

3.2.7 Proof of the mesh to selective transmission of the slope parallel force Z onto the upper nail

The slope parallel force Z must be transmitted selectively from the mesh over the spike plate onto the upper nail. Proof of bearing safety concerning the selective transmission of the force Z from the mesh onto the upper nail is established as below

$$Z_d \leq Z_R/\gamma_{ZR} \quad \text{Equa. 17}$$

Z_d is the dimensioning value of the stress in slope-parallel direction

Z_R is bearing resistance of the mesh against selective, slope-parallel tensile stress, $Z_R = 30$ kN

Z_{PR} is resistance correction value and is generally taken as 1.5

So, $Z_d = 15\text{kN} \leq \frac{30}{1.5} = 20$ (fulfilled)

3.3 Proposed design and Solution

According to the calculation provided in the above section, all the proofs are fulfilled. The distance between single nails can be optimized to a maximum distance of 3.0 x 3.0 m with 3.5m deep HDG 25 mm bar. The top row of nails was 5.5 m with 3.0 x 3.0 m spacing to stabilise the slope from blasting. At the slope head it was proposed to use additional shorter spaced nails with a length 3.5m, spacing 2.80m to stabilise the slope crest. The TECCO mesh was fixed to a wire rope at the crest of the slope. TECCO mesh G65 has a longitudinal Strength of 150 kN/m and a lateral Strength of 60 kN/m. The mesh has a uniform strength i.e. no weak point at the seam of the panels. In case of a broken wire, the spiral does not unravel.

4 PROJECT DELIVERY

A total of 498 anchor locations were drilled. In addition, 4 locations were drilled in order to install the wire rope anchors. As part of the design, locations were drilled to a minimum depth of 3.5m utilising light weight drill rigs (Figure 9), specially developed for this type of work. A 64mm bit was used as the permissible bond stress. Following drilling, a 4m x 25mm Ø galvanised thread bar was installed and prepared for grouting with mesh and cable tensioned to finish the installation. Testing for 5% of the anchors was completed. Due to continual mining operations occurring in proximity, several boulders have released from the overhang (figure 10) and have been retained by the installed protection system. The largest bolder, circled on the left in figure 9 above is approximately 3.5m long x 0.75m thick x 1.5m wide and weighs approximately 12 tons. The TECCO system carried out its function successfully by stopping the boulder and detaining it within the mesh without damaging any part of the system.

So checking the slope-parallel force:

- Slope inclination = 400
- Specific weight of Rock = 30 kN/m3
- Layer thickness = 0.75 m
- For every m2 of the mesh, the slope parallel force (Zd) is:
  $Z_d = 30 * 0.75 * \sin(40^0) = 14.6$ kN Equa. 18

New Zealand Geotechnical Society Inc. 19th Symposium, Queenstown 2013

The input for Z_d in the analysis is 15 kN and in the calculation output we get a safety factor of 1.5, so we can say that the system is designed to sustain the forces on analysis. The mesh shearing capacity is proven to be sufficient in the local instabilities between nails. The nail shearing capacity is proven to be sufficient.



Figure 5: Drilling (left) and mobilised boulders under installed mesh (right)

5 CONCLUSIONS

The HTWM System installed at the West Angelas iron ore mine for rock fall protection purposes has been physically proven as successful. The design of the system was carried out using the concept of superficial stability to assess the safety factors of the system. The ease in installation of the system allowed the construction process to be carried out without significant technical issues which minimises any possible delays and ultimately makes it a cost and time saving solution. The success of high tensile mesh system proposes an evolutionary rock fall mitigation option to the mining industry. The system was not intended to eliminate completely the rock fall hazards as the failure rock blocks are not to be emptied; the system however sufficiently reduces the risk to an acceptable level for the temporary mining operations to be successfully completed underneath.

6 ACKNOWLEDGEMENT

Geovert would like to acknowledge Rio Tinto for allowing the use of project information and data included in this paper and thank Geobrugg for continued technical support and the quality information on the TECCO system presented in this paper.

7 REFERENCES

[1] Geobrugg, (2010), *TECCO Slope Stabilisation System Summary of Published Technical Papers 1998-2009 – Dimensioning and application of the flexible slope stabilisation system TECCO made from high-tensile wire mesh in combination with nailing and anchoring in soil and rock*

[2] G.G. Joass, R. Dixon, T. Sikma, S. Wessels, J. Lapwood and P. de Graaf, (2013) Risk *Management and remediation of the North Wall slip, West Angelas mine, Western Australia. Slope Stability proceedings*, International Symposium on Slope Stability, Brisbane 2013.

Assessment of post-event slope stability risk on the Central Otago State Highway network

E J Hodgkinson
Opus International Consultants Ltd, Queenstown, NZ

Keywords: rockfall, landslide, risk assessment, hazard, highway, Central Otago, risk communication, network, lifeline, future event, risk rating, risk

ABSTRACT

Three key questions often asked after a rockfall or landslide event on a roading corridor are "will it happen again, how severe will it be and when will it occur?". As with most geotechnical hazards, there is usually no simple definitive answer to these questions and the complex answer is difficult to express in a way that communicates clearly to those without geotechnical knowledge and training. On the Central Otago State Highway Network, this problem is solved by classifying each new slope stability event or established hazard by a risk rating system that has been developed from several internationally recognised standards and adapted to local conditions. The client, or owner of the at-risk asset, is able to use this rating to assess the new hazard relative to other existing hazards and prioritise funding and remediation accordingly. The rating system takes into account geological and highway characteristics, hazard history, anticipated future events and their effects on the road user.

This paper describes in detail the rockfall and landslide risk rating systems and illustrates their use through a case study of the Dave's Bluff Slip. The Dave's Bluff Slip is a site on State Highway 6 between Makarora and Hawea where two large events occurred in September 2012, with the volume of failed material totalling approximately 10, 000m^3. After 2.5 months of extensive slip clearing, the complex geological hazards at the site were assessed and risk ratings developed to illustrate the technical data in a meaningful way to the client.

1 INTRODUCTION

Rockfall and landslide events are a common hazard for motorists on New Zealand roads with the potential for wide reaching adverse social and economic effects. Our isolated islands are frequently buffeted by extreme weather conditions, which, when combined with less than desirable tectonically disturbed ground conditions, results in a high potential for catastrophic events. The winter season for many New Zealand Geotechnical Engineers and Engineering Geologists usually involves at least several incident response slope stabilisation projects.

When multiple rockfall and landslide hazards exist in a highway network, communication of the relative risk posed by each hazard site to the client needs to be quick, clear and meaningful. The presentation of an array of complex geotechnical terms and explanation is unnecessary and often frustrating unless the client has a geotechnical background. A succinct translation of the geotechnical assessment into a form that is meaningful to the client enables efficient allocation of funds to remediate the highest risk hazards and ultimately producing the safest environment for the road user.

Effective communication is achieved in the Central Otago Highway Network through the formation for each hazard site of a 'rockfall hazard rating' (RHR) or 'landslide hazard rating' (LHR). This risk rating system has been developed from internationally recognised systems and standards and modified for local conditions. These ratings enable all hazard sites in the network to be comparatively ranked and remediation funding prioritised across the entire network.

New Zealand Geotechnical Society Inc. 19th Symposium, Queenstown 2013

2 DEFINITIONS OF RISK AND HAZARD

The terms 'hazard' and 'risk' are often used incorrectly and therefore they are important to clearly define in the context of this paper.

1) A 'hazard' is the source of potential damage, harm or adverse effect on someone or something. A hazard does not exist unless there are people or objects affected.
2) 'Risk' is a measure of the chance or likelihood that a person or object will be harmed or experience an adverse effect if exposed to a hazard; and the magnitude of the likely harm or consequence that will be experienced.

3 THE CENTRAL OTAGO STATE HIGHWAY NETWORK

The Central Otago State Highway Network in New Zealand is subject to a wide variety of significant slope hazards that require proactive and ongoing preventative maintenance. Approximately 40% of the 537km of highway passes through mountainous terrain formed by highly weathered and metamorphosed Haast Schist. Slope hazards commonly experienced along the highway include rockfall (minor and major), landslides and debris flows. The Network includes several high profile extreme hazard sites such as Nevis Bluff (east of Queenstown, SH6 RP 956/13.0) and Pipson Creek (Makarora Valley, SH6 RP 828 / 3.6).

New Zealand Geotechnical Society Inc. 19th Symposium, Queenstown 2013

In 2003, a 'Slope Check Inspection Programme' was produced by Opus International Consultants Ltd (Opus) for Transit New Zealand (now the New Zealand Transport Agency, NZTA) to facilitate management of the large number of slope hazards. This system started the development of the RHR and LHR criteria used today and the formation of a site inventory. It is the primary management tool for hundreds of hazard sites. This programme efficiently transfers detailed geotechnical evaluation of the slope hazards into a risk rating system that is able to be used by NZTA, Opus and the highway maintenance contractor to schedule preventative slope remediation works.

2 RISK RATING SYSTEMS

Each existing or potential slope hazard on the Central Otago Highway Network is classified through 'Risk Rating' criteria. Separate criteria are used for rockfall and landslides.

2.1 Rockfall Hazard Rating (RHR)

The RHR system used in the Central Otago Highway Network is based on the Oregon State Highway Division's Rockfall Hazard Rating (RHR) System in the United States (Pierson et al, 1990). This system is internationally recognised as a way of effectively ranking hazardous rockfall sites. It allocates points depending on:

1. Physical road features (likelihood)
2. Geological characteristics (likelihood)
3. Site history (likelihood)
4. Site location (likelihood)
5. Predicted event characteristics (consequence)
6. Detour length (consequence)

The RHR system used in Central Otago has been modified to suit local conditions and includes 11 assessment categories. It gives a final RHR Score that typically varies between 100 and 500 (less than 100, the hazard is usually deemed not severe enough to add the site to the inspection regime). After ranking of all sites and prioritisation for remediation work, Table 1 presents the approximate remedial implications in Central Otago according to the RHR score.

Table 1: RHR Remedial Implications: Central Otago

RHR	Risk Level	Remedial Implications
0 - 250	Low Risk	Site is likely to only need on-going 6 monthly monitoring for hazard development and possibly some minor remediation work.
250 – 400	Moderate Risk	Site is likely to require minor remediation work within the next 12 to 24 months, which would be programmed as part of the annual routine general site scaling works, or general network maintenance.
400 - 500	High Risk	Remediation work is likely needed within the next 6 to 12 months. The hazard could be reduced through using annual routine general scaling works funding, however it may also need an application for specific funding.
> 500	Very High Risk	Site likely to be a serious hazard to the highway and remedial work is likely to be needed within 6 months. Is likely to require more extensive remediation work and therefore a specific application for funding is necessary.

2.2 Landslide Hazard Rating (LHR)

The Landslide Hazard Rating (LHR) system for Central Otago was developed based on the Guidelines for Landslide Risk Management developed by the Australian Geomechanics Society (Australian Geomechanics Society, 2000). It divides landslides into five risk levels, from 'Very Low Risk' to 'Very High Risk'.

The system uses 11 assessment categories that analyse the:

1. Physical road features (likelihood)
2. Geological characteristics (likelihood)
3. Site history (likelihood)
4. Site location (likelihood)
5. Predicted event characteristics (consequence)
6. Detour length (consequence)

Points are totalled to give 'likelihood' and 'consequence' scores, which are then applied to a 'Risk Matrix Table' to give an overall risk level for the landslide. Table 2 details the approximate remedial implications for each LHR.

Table 2: LHR Remedial Implications: Central Otago

LHR	Remedial Implications
Very Low	12 monthly walkover inspection. Landslide does not require remediation and rare (>5 year recurrence) repairs to highway necessary.
Low	6 monthly walkover inspection. Landslide does not require remediation and infrequent repairs (3-5 years recurrence) to highway necessary.
Moderate	6 monthly walkover inspection. May require installation of monitoring pins. Repairs needed to highway every 2-3 years.
High	Detailed investigation to be programmed within 12 months and remediation likely necessary. Repairs needed to highway every 1-2 years.
Very High	Immediate commencement of extensive detailed investigation and research, planning and implementation of remediation necessary to reduce risk to an acceptable level. Highway repairs required several times per year.

4 CASE STUDY: SH6 DAVE'S BLUFF SLIPS, LAKE WANAKA, SEPTEMBER 2012

Overnight on Wednesday 5 September 2012, approximately 6000m^3 of material failed as a planar schist rockslide following rainfall, blocking both lanes of SH6 on the shores of Lake Wanaka. The highway was able to be re-opened to one way traffic later in the same day; however a significant volume (~500 m^3) of shattered unstable rock and unsupported colluvium was left in the top head scarp of the failure. Abseil assisted scaling, helicopter sluicing and drill and blast commenced in order to stabilise the head scarp, under the direction of an Opus Geotechnical Engineer.

Ten days later, on 15 September 2012, a second rockslide occurred overnight at the same site, releasing around 3000m^3 of material. The total height of the slip had now doubled to around 100 m. Failed material compounded on previous slip material and exposed new rockfall hazards. See Figure 1.



Figure 1: Dave's Slip – Photograph taken 15 September 2012.

Incident response at this slip site continued until the end of November 2012, when it was deemed safe to open the highway to 2 way traffic. A 3.0m high temporary rockfall protection bund was left as rockfall protection at the base of the Bluff. The client, NZTA, now needed to understand the magnitude of the current level of risk to the road user so it could decide on the appropriate remedial action.

There are considered to be three key possible geological failure mechanisms that present a hazard to the road user at the site. These are presented in Table 3.

Table 3: SH6 Dave's Slip – Geological Hazards

HAZARD	DESCRIPTION
1. Erosional Margin Failure 	**Description:** Release of on average 300mm (maximum 500mm) diameter blocks from the upper colluvium margins of the slip. Failure likely to occur over time or after heavy rainfall events through erosion of the silt matrix surrounding the blocks, causing eventual release. Release may occur as individual blocks or as a mass section of the colluvium matrix. Due to the approximately 50° slip back face angle , close proximity of the highway to the base of the slope, the clean nature of the slope (i.e. no vegetation) and minimal natural barriers such as horizontal benches, it is considered highly likely blocks will reach the highway. Rockfall analysis using the Rocscience Rocfall programme has been carried out and suggests this also.
2. Massive Planar Failure 	**Description:** The slip back face is predominantly formed by one joint set (Joint Set 1) adversely oriented towards the highway at 46/295 NW (dip/dip direction). This joint set is intersected at approximately 3-8m intervals horizontally by another joint set oriented at 60/020 NE (dip/dip direction). This has formed sloping 'steps' in the back face and resulted in a series of undercut slabs (no toe support) progressing up the face. It is considered that the initial slip at Dave's Bluff on 5 September 2012 and subsequent slip on 16 September 2012 was caused by the planar failure of one or more of similar underlying slabs after a period of heavy rainfall. Groundwater originates at the top north (Makarora) end of the slip and flows down the back face. It is likely a tributary to the small creek approximately 20m to the south of the slip. Since the September 2012 failures, this groundwater has constantly flowed down the rock face at an estimated rate of 0.5l/min. This rate would of course increase slightly after rainfall events. The groundwater can be seen to pass under several of the slabs on the face. This indicates that the adversely oriented Joint Set 1 is already open on parts of the face behind the slabs. The extent of this opening has not been measured but is estimated to be in the order of around 40mm. It is considered that this hazard will develop over time and show some signs of impending failure such as an increase in join openness and loss of rock from around the joints.
3. Topple Failure from Upper Bluff 	**Description:** Slab topple failure from the ~30m high upper bluff is a hazard. Recent evidence of this occurring can be seen 50m to the Wanaka side of the slip, where a massive (~900m^3) failure occurred in October 2010. Fortunately the existing vegetation on the slope below stopped around 90% of the material from reaching the highway however most of the vegetation was completely destroyed and an approximately 50m long and 25m wide debris fan was formed. This fan has periodically (every 6 months on average) released around ~300-500mm diameter blocks to the highway below. As the vegetation at the Dave's Bluff Slips site has been completely removed, there is now nothing to halt large topple failure from reaching the highway. All material is considered likely to deposit into the roadway. While the upper bluff has not been assessed using abseil techniques, no unstable material can be noted when observing from the slip headscarp and a failure is not considered to be imminent.

The 3.0m high temporary rockfall protection bund was modelled in the software Rocscience Rocfall and found to stop around 80% of the rockfall from the on-going erosional rockfall hazard (Hazard 1). However the stability of the un-engineered rock debris bund after impact from a massive planar or topple failure is uncertain and therefore cannot be relied on as a protection mechanism from geological Hazards 2 and 3.

To describe the above risk to NZTA, RHR values were calculated by Opus for the two main geological hazards (Hazards 1 and 2). These are presented in Table 4 and the full RHR analysis sheets attached to this paper in the Appendices as Figures A1 and A2.

Table 4: RHR values for SH6 Dave's Bluff Slip (2012)

Geological Hazard	RHR
Erosional Hazard *without temporary rockfall protection bund*	487
Massive Planar Failure	571

The effect of a variety of remedial measures on the risk to the road user was also investigated. Table 5 presents the results.

Table 5: RHR values after remediation for SH6 Dave's Bluff Slip (2012)

Geological Hazard	Remedial Option	RHR
Erosional Hazard	Temporary 3.0m high rockfall protection bund	415
	Road realigned away from Bluff by 20m	433
	Road realigned by 20m and 5.0m high terramesh bund installed	385
	Current alignment with rockfall attenuator system & rock bolts	343
Massive Planar Failure	Temporary 3.0m high rockfall protection bund	517
	Road realigned away from Bluff by 20m	571
	Road realigned by 20m and 5.0m high terramesh bund installed	499
	Current alignment with rockfall attenuator system & rock bolts	337

These values are then presented to NZTA and compared relatively against other sites in the Central Otago Highway Network and throughout New Zealand. A decision can then be more easily made about the necessary monitoring and remedial work at the site. The effects of different remediation options could also be clearly communicated to the client.

5 CONCLUSION

Communication of technical information in a quick and meaningful way is something that challenges professionals from many occupations. The use of the Risk Hazard Rating and Landslide Hazard Rating Systems translates the technical assessment of a geotechnical hazards into a number that has value for the client. This paper has outlined the modified system used frequently and successfully in the Central Otago Highway Network and provided a recent case study to illustrate its use.

6 ACKNOWLEDGEMENTS

The NZ Transport Agency, especially John Jarvis, Area Manager Central Otago. Opus International Consultants Ltd, especially Rob Bond, Reece Gibson and Robin Whiting.

REFERENCES

Australian Geomechanics Society (2000). *Landslide Risk Management Concepts and Guidelines – Australian Geomechanics Society : Sub-committee on landslide risk management.* 'Australian Geomechanics' Pg 49-92, Vol 35 No. 1, March 2000

Pierson, L.A., Davis, S.A. and Van Vickle, R. (1990*) Rockfall Hazard Rating System Implementation Manual.* Federal Highway Administration (FHWA) Report FHWAOR-EG-90-01. FHWA, US Department of Transportation

APPENDICES

Preliminary Risk Assessment Fieldsheet - Rockfalls					
Site ID: Dave's Bluff Slip (Erosional failure - no remediation)					
SH: 6		**Area: Lake Wanaka, 1km south of Boundary Creek**		**Length: 110m**	
RP: 847/1.1				**Date: 15/11/12**	
Assessed by: Emily Hodgkinson					
AADT (including year observed and location): 631 (Lake Wanaka Camp Creek Bridge)					
Category		**Rating Criteria and Score**			
		Points 3	**Points 9**	**Points 27**	**Points 81**
1. Slope Height		<10m	10-20m	20-30m	>30m
2. Ditch effectiveness		Good catchment: all or nearly all of falling rocks are retained in the catch ditch	Moderate catchment: falling blocks occasionally reach the roadway	Limited catchment: falling rocks frequently reach the roadway	No catchment: no ditch or ditch totally ineffective
3. Average vehicle risk (speed limit used)		≤25%	50%	75%	100%
4. % of decision sight distance		Adequate sight distance, >90% of low design value	Moderate sight distance, 60-90% of low design value	Limited sight distance, 40-60% of low design value	Very limited sight distance, < 40% of low design value
5. Roadway width including paved shoulders		13.4 m	11.0 m	8.5 m	6.1 m
6. Calculated Road Width Pts		43			
Geological Character	**CASE 1: for slopes where discontinuities are the dominant structural feature**				
	Case 1 **7. Structural condition**	Discontinuous joints, favourable orientation	Discontinuous joints, random orientation	Discontinuous joints, adverse orientation	Continuous joints (joint persistency >3m), adverse orientation
	Case 1 **8. Rock Friction**	Rough, irregular	Undulating	Planar	Clay infilling, slickensided or low friction mineral coating
	CASE 2: for slopes where differential erosion or oversteepened slopes is the dominant condition that controls rockfall.				
	Case 2 **7. Structural Condition**	Few differential erosion features	Occasional erosion features	Many erosion features	Major erosion features
	Case 2 **8. Difference in Erosion Rates**	Small difference; erosion features develop over many years	Moderate difference; erosion features develop over a few years	Many erosion features; erosion features develop annually	Major erosion features; erosion features develop rapidly
9. Block size		300 mm	600 mm	900 mm	1500 mm
10. Quantity of rockfall/event		1 m^3	1.5 m^3	2.5 m^3	3.0 m^3 or greater
11. Climate and presence of water on slope (adjusted for Southland conditions)		Low to moderate precipitation e.g. <450mm/year; no freezing, no water on slope	Moderate precipitation 450mm-2m/yr or few freeze thaw cycles (<1 week) or intermittent water on slope (seasonal or in response to rainfall)	High precipitation >2m/yr or many freeze-thaw cycles (>1 week) or continual water on slope	High precipitation >2m/year and many freeze-thaw cycles (>3 weeks) or continual water on slope
12. Rockfall history		Few falls; rockfall only occurs a few times a year or less	Occasional falls; rockfall can be expected several times a year	Many falls; frequent rockfalls during a certain season, e.g. winter freeze-thaw	Constant rockfalls; rockfalls occur frequently throughout the year
				Total =	**487**

Figure A1: Rockfall Hazard Rating Example – Dave's Bluff Slip Erosional Failure.

Preliminary Risk Assessment Fieldsheet - Rockfalls				
Site ID: Dave's Bluff Slip (Massive planar failure - no remedia				
SH: 6	**Area: Lake Wanaka, 1km south of Boundary Creek**		**Length: 110m**	
RP: 847/1.1			**Date: 15/11/12**	
Assessed by: Emily Hodgkinson				
AADT (including year observed and location): 631 (Lake Wanaka Camp Creek Bridge)				
Category	**Rating Criteria and Score**			
	Points 3	**Points 9**	**Points 27**	**Points 81**
1. Slope Height	<10m	10-20m	20-30m	>30
2. Ditch effectiveness	Good catchment: all or nearly all of falling rocks are retained in the catch ditch	Moderate catchment: falling blocks occasionally reach the roadway	Limited catchment: falling rocks frequently reach the roadway	No catchmen or ditch totall
3. Average vehicle risk (speed limit used)	≤25%	50%	75%	100
4. % of decision sight distance	Adequate sight distance, >90% of low design value	Moderate sight distance, 60-90% of low design value	Limited sight distance, 40-60% of low design value	Very limited s distance, < 4 design value
5. Roadway width including paved shoulders	13.4 m	11.0 m	8.5 m	6.1
6. Calculated Road Width Pts	43			
Geological Character / **Case 1**	**CASE 1: for slopes where discontinuities are the dominant structural feature**			
7. Structural condition	Discontinuous joints, favourable orientation	Discontinuous joints, random orientation	Discontinuous joints, adverse orientation	Continuous j persistency > adverse orier
8. Rock Friction	Rough, irregular	Undulating	Planar	Clay infilling, slickensided friction miner
Case 2	**CASE 2: for slopes where differential erosion or oversteepened slopes is the dominant co that controls rockfall.**			
7. Structural Condition	Few differential erosion features	Occasional erosion features	Many erosion features	Major erosior
8. Difference in Erosion Rates	Small difference; erosion features develop over many years	Moderate difference; erosion features develop over a few years	Many erosion features; erosion features develop annually	Major erosior erosion featu develop rapic
9. Block size	300 mm	600 mm	900 mm	1500 mm
10. Quantity of rockfall/event	1 m^3	1.5 m^3	2.5 m^3	3.0 m^3 or gre
11. Climate and presence of water on slope (adjusted for Southland conditions)	Low to moderate precipitation e.g. <450mm/year; no freezing, no water on slope	Moderate precipitation 450mm-2m/yr or few freeze thaw cycles (<1 week) or intermittent water on slope (seasonal or in response to rainfall)	High precipitation >2m/yr or many freeze-thaw cycles (>1 week) or continual water on slope	High precipita >2m/year and freeze-thaw c weeks) or co water on slop
12. Rockfall history	Few falls; rockfall only occurs a few times a year or less	Occasional falls; rockfall can be expected several times a year	Many falls; frequent rockfalls during a certain season, e.g. winter freeze-thaw	Constant roc rockfalls occu frequently thr the year
			Total =	**571**

Figure A2: Rockfall Hazard Rating Example – Dave's Bluff Slip Massive Planar

Howard, M.E. & McMorran, T.J. (2013)
A rockfall risk assessment and selection of appropriate mitigation measures for the Christchurch gondola following the 22 February 2011 Magnitude 6.3 earthquake
Proc. 19th NZGS Geotechnical Symposium. Ed. CY Chin, Queenstown

A rockfall risk assessment and selection of appropriate mitigation measures for the Christchurch gondola following the 22 February 2011 Magnitude 6.3 earthquake

M E Howard
Golder Associates (NZ) Ltd, Christchurch, NZ

T J McMorran
Golder Associates (NZ) Ltd, Christchurch, NZ

Keywords: rockfall, risk assessment, bund, catch fence, attenuator

ABSTRACT

The Christchurch Gondola is a major tourist attraction that takes visitors from the Heathcote Valley to the top of Mount Cavendish on the Port Hills. Extensive rockfall occurred in the Gondola catchment during the 22 February 2011 Magnitude 6.3 earthquake. Although impact damage from rockfall was minimal, the facility was closed due to the obvious hazard to visitors from future rockfall. A risk assessment was conducted that evaluated the probability of loss of life to visitors and compares them with established guidelines. Scaling of rocks enabled the identification of five source zones and typical rock trajectories, which contributed to the risk of different elements of the Gondola, such as the towers supporting the Gondola cable, or the Base Station and car park area. The risk of loss of life was assessed as being approximately within acceptable criteria, however additional risk reduction was achieved by protecting the Base Station and one of the Gondola towers. Computer rockfall simulation was used to design a 40 m long, 2.4 m high, reinforced soil bund for the Base Station and visitor car park. At Tower 6, a 40 m long attenuator catch fence was constructed. Installation of the rockfall mitigation measures resulted in the re-opening of the Gondola in March 2013, just over two years after its closure.

1 INTRODUCTION

The Christchurch Gondola is an iconic tourist attraction that takes visitors on an almost 1 km journey to the top of Mount Cavendish on Christchurch's Port Hills (see Figure 1). The epicentre of the 22 February, 2011 Magnitude 6.3 earthquake was located approximately 3 km west of the Gondola and produced strong shaking in the area. A peak acceleration of 1.46 g was recorded at nearby Heathcote Valley Primary School. The resulting rockfall across the Port Hills resulted in substantial damage to houses, roads and other infrastructure, and caused several fatalities.

Hundreds of boulders fell in the catchment that contains the Gondola. Damage to Gondola infrastructure from rock impact was negligible, although several boulders came to rest only metres from the Base Station, and it was presumed that numerous boulders had passed close to the towers. As a result, the Gondola was issued with a closure notice from the Christchurch City Council (CCC), and the operation was suspended. Additional earthquakes on 13 June, 2011 caused further rockfall.

New Zealand Geotechnical Society Inc. 19th Symposium, Queenstown 2013

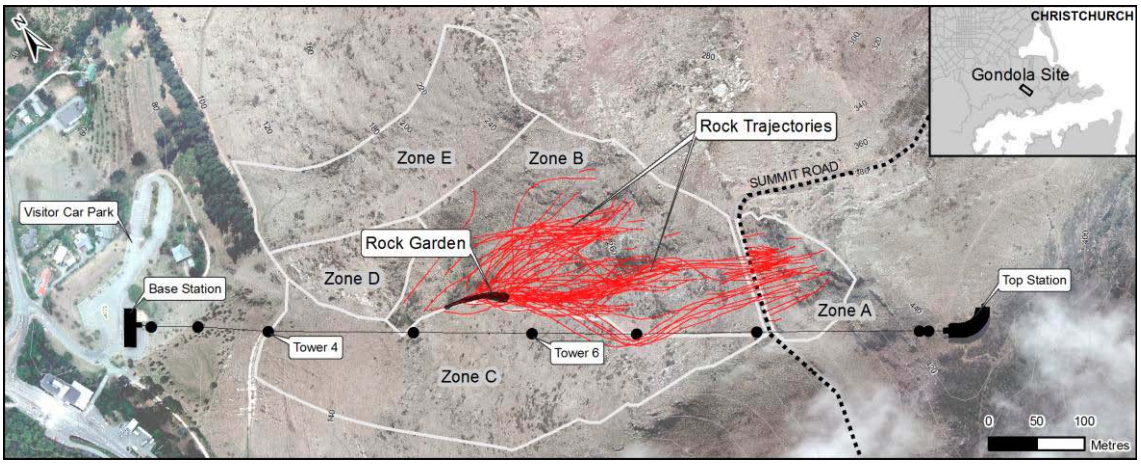


Figure 1: Plan of rock zones and trajectories of the Gondola catchment

The owner of the Gondola had been initially advised that the risk of future rockfall was so high as to make the venture untenable. Assessment by the owner was further complicated as it was not initially clear who was responsible for the source of fallen rocks and who was liable for addressing the rockfall risk, such that the facility could reopen. Gondola visitors journey over land variously owned by the Gondola, the CCC, the Department of Conservation and a public road (Summit Road).

Assessment of earthquake-related rockfall elsewhere on the Port Hills has taken place by the CCC, GNS Science and the Canterbury Earthquake Rebuild Authority (CERA). Prior to the 2011 earthquakes, the scale and significance of rockfall on the Port Hills had not been fully appreciated. As a result, the approach to assessing and mitigating rockfall hazard was an evolving process, which made defining a strategy for achieving the goal of reopening the Gondola difficult. In 2011, the CCC had commissioned an assessment to provide order-of-magnitude costs for mitigating the rockfall hazard. This proposed a number of potential protective systems such as temporary shipping containers, protective pads for the towers, slope scaling, an earth bund, catch fences and tree planting. The cost of these works was in the order of $3M.

Golder was engaged by the Gondola owner to provide geotechnical guidance and interpretation in a technically challenging and politically uncertain task. The Golder scope included a full risk assessment, design of rockfall mitigation measures and construction supervision of a rockfall bund and attenuator catch fence.

2 INITIAL WORK

To achieve the client's objective of reopening the Gondola, a rockfall assessment was required to specify appropriate mitigation measures (if required) to meet a yet-to-be-defined criterion that would satisfy the CCC. A year had passed since the damaging February 2011 earthquake and CCC, GNS Science and CERA had adopted a risk approach to rockfall hazard. It had become accepted that a certain acceptably low risk to life from rockfall could be tolerated.

To define an acceptable risk range for visitors to the Gondola, the CCC commissioned an assessment by risk specialist T. Taig (GNS, 2012). The report considered the upper threshold of tolerable risk to the lives of those travelling on the Gondola by comparison with: other modes of transport; other risks facing visitors to New Zealand; risks with travelling on aerial ropeways generally. A suggested fatal accident frequency per one way trip of between 1 per 15,000 years to 1 per 1,500 years and 1-10 fatalities per billion trips was suggested. The aim of the Golder study was to use data from the area to estimate if the Gondola was within this range, and if not, select appropriate rockfall mitigation measures.

3 GEOTECHNICAL APPROACH

With uncertainty of who would ultimately be responsible for rockfall remediation, a staged approach was proposed to the client. The first stage was to commence scaling (removal) of loose rock from the slopes above Summit Road in the Gondola catchment area. We reasoned that this would be required for the Gondola to reopen, and therefore would not be wasted effort. In addition, mapping of the lower slopes was previously not undertaken due to the hazard from rockfall. Scaling of rock to a level to allow short term access by field staff enabled inspection of slopes that could previously only be viewed remotely. As progress rates became better defined, scaling continued down slope, below the Summit Road.

Rocks were loosened by rope access crews using hand tools and occasionally, small scale blasting. Access could not safely be gained to install temporary protection to Gondola infrastructure, and the risk of rock impact damage during scaling was accepted by the client. The topography of the Gondola catchment meant that rocks could be rolled downhill for hundreds of metres, unlike residential areas of the Port Hills, where care had to be taken not to cause further damage to houses and roads.

It was soon realised that boulder trajectories represented a potentially important source of rockfall data. These trajectories were video recorded where possible for later analysis. It is estimated that scaling caused an order of magnitude more rockfall than following the total of the 2011 earthquake triggered rockfall, as estimated from rock accumulation on Summit Road (see Figure 2).



Figure 2: Rock accumulation on Summit Road following scaling

4 ROCKFALL ANALYSIS

The videoed trajectories of over one hundred boulders were viewed and plotted onto a plan of the Gondola valley showing boulder start and finish locations, bounce locations and where rocks fragmented (Figure 1). This was done to identify which areas of the slope were a hazard to the different Gondola infrastructure elements. What became evident was that the imposing rock slopes above Summit Road were not necessarily the source of all boulders that had travelled close to Gondola infrastructure, which was the intuitive conclusion when first viewing the hundreds of earthquake-related boulders across the site. No rocks scaled from this area travelled further than Tower 4, which is about 300 m uphill of the Base Station. Most rocks lost momentum in the valley near Tower 4 and Tower 5, informally referred to as the Rock Garden. In this location the valley was slightly less steep, with a collection of many hundreds of boulders that were the result of scaling, earthquakes or of pre-earthquake rockfall.

New Zealand Geotechnical Society Inc. 19th Symposium, Queenstown 2013

Five rockfall source zones (Zone A to E) were defined based on slope geometry (steepness), amount of exposed rock/vegetation cover and potential hazard to Gondola infrastructure (see Figure 1). Two dimensional rockfall analysis using RocFall software by RocScience was undertaken to assess the trajectory of rocks from each zone and compared to field observations. This was useful in linking earthquake-triggered boulders to a particular slope where no scaling was necessary. The following conclusions were made at this stage of the project:

- Most rock from Zone A was retained on the slope or on Summit Road
- The Summit Road vehicle safety barrier was effective as a rockfall barrier for rocks that did not bounce over it
- Most rocks from Zone B fell towards the Rock Garden and Tower 4 and were not likely to impact Tower 5 and Tower 6.
- Rocks falling from Zone D appeared to travel less than 50 m from the toe of the slope and were unlikely to reach Gondola infrastructure.

Despite the number of boulders released during rockfall (from scaling and earthquake triggering) there was negligible impact on exposed towers and the Base Station (although some did pass close to Tower 6). It was recognised that the ground hardness during summer may have greater elasticity than in autumn, when the scaling took place.

5 BOULDER SIZE ESTIMATION

The observation of fallen rocks from scaling and earthquakes was useful in estimating the boulder size that could be expected for future earthquake events. The anticipated boulder size is important as this, together with the boulder velocity, determines the boulder's kinetic energy. A 95th percentile boulder size of 1 m^3 was conservatively estimated, which was considerably smaller than the 3 m^3 estimated by the CCC for equivalent slopes on the Port Hills. This is probably because the CCC sample was collected near the slope base near houses, which underrepresented the smaller size boulders.

6 RISK ANALYSIS

The approach to the rockfall risk assessment used the methodology described in AGS (2007). In broad terms, the risk can be divided into the risk to physical structures (buildings and infrastructure) and to people, described as the loss of life risk. This study addresses only the loss of life risk, which is defined as:

$$\mathbf{R}_{(LoL)} = \mathbf{P}_{(H)} \times \mathbf{P}_{(S:H)} \times \mathbf{P}_{(T:S)} \times \mathbf{V}_{(D:T)}$$

Where:

$\mathbf{R}_{(LoL)}$ is the risk (annual probability of loss of life (death) of an individual).
$\mathbf{P}_{(H)}$ is the annual probability of the event (i.e., rockfall) occurring.
$\mathbf{P}_{(S:H)}$ is the probability of spatial impact of the rockfall impacting a building (location) taking into account the travel distance and travel direction given the event.
$\mathbf{P}_{(T:S)}$ is the temporal spatial probability (e.g., of the building or location being occupied by the individual) given the spatial impact and allowing for the possibility of evacuation given there is warning of the landslide occurrence.
$\mathbf{V}_{(D:T)}$ is the vulnerability of the individual (probability of loss of life of the individual given the impact).

It is usual that the application of the methodology of the AGS (2007) risk assessment process is tailored to account for specific project geotechnical requirements. The characteristics that are specific to the Gondola that differ from risk studies conducted for the rest of the Port Hills includes the following:

- The Gondola is a single entity that covers a large area, passing from near the rock source to near the limit of rock run out – a distance of almost 1 km.
- The risk is predominantly in numerous, isolated zones i.e., individual towers and the Base Station and car park.
- The rockfall sources are numerous and each may influence the risk of different components of the facility.
- The occupants of the Gondola use the facility for a relatively short time and have a well-defined exposure time.

The Golder study aimed to identify the vulnerable parts of the infrastructure and to quantify the risk from each relevant rockfall zone. In Table 1 each element of infrastructure that is vulnerable to rockfall impact is listed, with the rockfall zones that provide the source material. The loss of life risk has been calculated for each zone to identify the most exposed element of the Gondola. The sum of these risks gives the total lives risk for the Gondola, which is compared with the recommended risk levels by GNS (2012). Infrastructure that is not listed in Table 1 is considered to be exposed to negligible rockfall risk.

To determine the best use of mitigation measures, the risk parameters were re-evaluated with the inclusion of, for example, a rockfall bund to protect the Base Station. This approach highlighted the areas in the system that were high risk and where mitigation measures would be most effective.

Non-seismic levels of rockfall were assessed as being a negligible contributor to the total risk, especially when extensive scaling removed much of the unstable source rock that could be expected to be triggered by rainfall or freeze-thaw processes.

Table 1: Infrastructure at risk from rockfall and source zones contributing to risk

Infrastructure	Rockfall Zone
Base Station / car park	B & C
Tower 4	B & C
Tower 5	A, B & C
Tower 6	A & C

6.1 Annual Probability of Rockfall ($P_{(H)}$)

The approach for calculating the annual probability of rockfall for the Port Hill has been modelled by GNS (2011). In this, $P_{(H)}$ is defined as the annual frequency of a given number of rockfalls being triggered over a given period of time. To estimate this, the annual frequency of four seismic peak ground acceleration (pga) bands was calculated for: pga 0.1 g to 0.4 g; 0.4 g to 1.0 g; 1.0 g to 2.0 g, and; 2.0 g to 5.0g. The 0.1 g to 0.4 g range of pga is not expected to result in rockfall and was ignored. Each pga band had an estimated frequency of occurrence and each occurrence had an estimated number of boulders, or 'rock process rate' for the Port Hills suburbs.

For the Gondola, each Zone (A to E) was assigned its own rock process rate as part of the Golder study. Aerial photographs taken after the earthquakes of 22 February and 13 June 2011 allowed a reasonably accurate boulder count of earthquake triggered rocks on Summit Road. These were used to back calculate the rock process rate for Zone A. This rate was extended to other zones on a pro rata basis by comparing the slope size, topography and exposed rock. Seismic shaking of 2.0 to 5.0 g has not been recently experienced, so back calculation was not possible for this range. The GNS (2011) used an order of magnitude difference between the 1.0 g to 2.0 g and 2.0 g to 5.0g bands, and this was used for the Gondola. As a conservative approach, no reduction factor was applied due to the extensive scaling that had taken place.

New Zealand Geotechnical Society Inc. 19th Symposium, Queenstown 2013

6.2 Probability of Rock Impact ($P_{(S:H)}$)

The "probability of impact" is the likelihood that a boulder from a particular zone will strike the Gondola infrastructure. This study focusses on the impact on Towers 4, 5, 6 and the Base Station and visitor car park, which was calculated from each zone. The direct impact of a boulder bouncing and striking a cabin was considered to be negligible. This was calculated by assuming a width of 20 m where rocks of this trajectory would pass, with the impact zone being 2.6 m wide (0.6 m wide tower plus twice the design boulder dimension of 1 m). The resultant $P_{(S:H)}$ was calculated to be 0.13.

6.3 Temporal Probability of Rock Impact ($P_{(T:S)}$)

The temporal probability number used for the Gondola towers was calculated as the number of people per cabin at any time, multiplied by the number of cabins that would be affected by a tower collapse. Annual visitor numbers of 130,000 (pre earthquake), the number of cabins, the time taken for a trip, the operation hours and the distance between cabins was used to estimate the average number of people exposed to rock impact on each of the susceptible items of Gondola infrastructure.

6.4 Vulnerability of the Individual ($V_{(D:T)}$)

The vulnerability of the individual for the Gondola is the probability that a rock impact on a tower or in the Base Station or car park area would result in a fatality. Judging the likelihood of a fatality due to tower failure is subjective, particularly as gondola travel is a very safe activity and the number of reported accidents worldwide is very low. The GNS (2012) study concludes that the most likely scenario for a tower strike is that no cars would fall and no fatalities or serious injuries or fatalities would result.

The probability that rock impact on the tower would cause failure resulting in a fatality was estimated by geotechnical engineers to be:

- 10% for towers supporting the weight of the gondola cable and cabins (i.e., Towers 5 & 6), where cabins would fall to the ground after failure.
- 20% for Tower 4, which holds the gondola cable down and whose failure could result in cabins rapidly accelerating upwards.

For the Base Station and visitor car park, the probability of a fatality from a rock entering the area is considered to be 10%. Boulders reaching this area are inferred to have relatively low energy and may be halted by vehicles or the Base Station structure.

6.5 Total Estimated Loss of Life Risk

To consider the sensitivity of the risk criteria above, T. Taig was engaged by Golder to apply some sensitivity to the model and to peer review the Golder assumptions. He estimated a range to the input values that previously were necessarily conservative. An example is the probability of rock impact on the tower resulting in death. Visitor concentration in the Base Station and car park was also varied to account for times that were quiet and busy. At this time, lower predicted seismic probability information became available from GNS Science (unpublished). These substantially reduced the rockfall process rate, which contributed to an approximate halving of the overall loss of life risk.

Judgement was used to assess how risk would change with lower visitor numbers as the Gondola recovered as a business. It was estimated that in the first year of reopening there would be half of the 130,000 pre-earthquake annual visitor numbers, recovering linearly to that number in approximately 8 years. Greater visitor number increases the risk due to the increased

exposure. During the same period, the seismic risk is predicted to decrease, lowering the loss of life risk. Visitor numbers of 130,000 and the seismic risk for 2016 were used to balance these two opposing components of the risk model.

The assessment provided a range of risk of 260 to 77,000 years per fatal accidents and 0.03 to 20 fatalities per billion trips for single trip journeys (see Figure 3). These ranges are large, reflecting the uncertainties in the risk paramaters. The range crosses those recommended by T. Taig (see Section 2), but the midpoint is either within the range (years between fatalities) or below it (risk per billion trips).

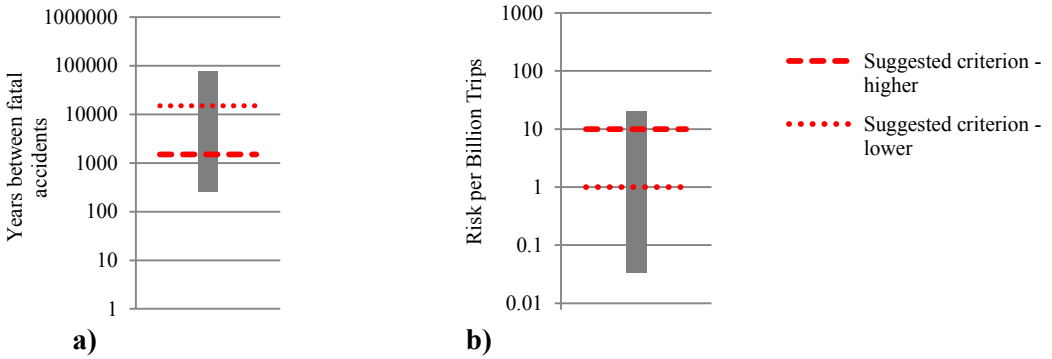


Figure 3: Comparison of the recommended range for the Gondola loss of life risk with the estimated risk for single trip journeys. a) is time between fatal accidents (260 to 77,000 years). b) is fatality risk per billion trips (0.03 to 20 trips)

7 SELECTION OF MITIGATION MEASURES

By using the risk assessment, reopening the Gondola with no additional mitigation could be justified. However, from a public perception viewpoint, mitigation measures could be expected. There is an acute awareness of rockfall hazard in the community following the earthquakes of 2010/2011 and the closure of the Gondola due to rockfall has been well publicised. In addition, future earthquakes may result in an increase of the predicted seismic hazard, which could cause a repeat of the prolonged closure of the facility.

When higher seismic hazard data suggested mitigation would be required to lower the total risk to life, the elements exposed to the greatest risk were the Base Station and car park, Tower 6 and Tower 4. The client opted to proceed with construction of Golder specified 40 m long, 2.4 m high Maccaferri Green Terramesh (GTM) bund for the Base Station and car park. A 40 m long, 4 m high Maccaferri attenuator was chosen to protect Tower 6. The attenuator comprises the skeleton of a 2000 kJ rock fence, with the addition of a 10 m long drape that allowed greater energy absorption and a much increased capacity for multiple boulders. The bund and attenuator were specified by estimating boulder energy and bounce heights for the 1 m^3 design boulder using RocFall simulations and observed trajectories of scaled rocks.

The bund and attenuator were constructed over a period of four weeks, commencing in late March 2013. The Gondola was officially reopened in April 2013 by Prime Minister John Key.

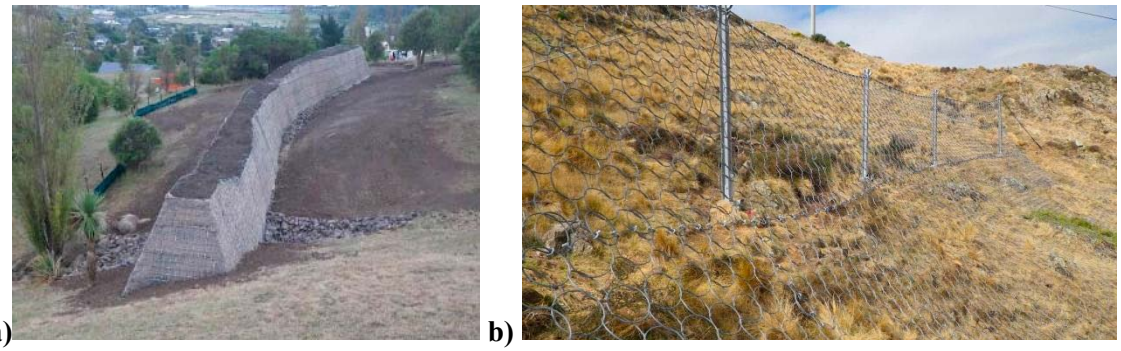


Figure 4: Gondola rockfall mitigation measures, a) GTM bund, and b) attenuator fence

8 CONCLUSIONS

A loss of life risk assessment was conducted at the Christchurch Gondola to estimate the current level of risk compared with an acceptable range. The assessment method considers the probability of the event occurring, the probability of a rock impacting Gondola infrastructure, the probability of people being present and the vulnerability of the individual. Input parameters were obtained by analysing boulder trajectories during scaling, fallen boulder locations, computer rockfall modelling, annual visitor numbers, duration of trip and the likelihood of a fatality arising from a rock impact on Gondola infrastructure. The assessment provided a range of risk of 260 to 77,000 years per fatal accidents and 0.03 to 20 fatalities per billion trips for single trip journeys, the midpoint of which was within or below the recommended range.

Although it could be argued that no rockfall mitigation was required, the public awareness of rockfall and the possibility of future increase in seismic probability resulted in the selection of a 40 m long rockfall bund to protect the Base Station and visitor car park and a 40 m long attenuator fence for Tower 6.

The bund and attenuator were constructed in February/March 2013 and the Gondola was officially reopened in April 2013, over two years after the 22 February 2011 earthquake forced its closure.

9 REFERENCES

AGS (2007) *Practice Note Guidelines for Landslide Risk Management 2007, "AGS (2007c)"*. Australian Geomechanics Society. Vol 42, No 1, March 2007.

GNS (2011) Canterbury Earthquakes 2010/11 Port Hills Slope Stability: Pilot Study for assessing life-safety risk from rockfalls (boulder rolls). GNS Science Consultancy Report 2011/311 Final.

GNS (2012) Canterbury Earthquakes 2010/11 Port Hills Slope Stability: Fatality Risk Criteria for the Christchurch Gondola. By T. Taig. GNS Science Consultancy Report 2012/102, April 2012.

3D rockfall modelling and rockfall protection – Canterbury Port Hills Christchurch, New Zealand

M B Avery
Geovert Ltd, New Zealand
mat.avery@geovert.com

A Teen
Geovert Global Pte Ltd, Singapore
anthony.teen@geovert.com

H Salzmann
Freefall ZT GmbH, Austria
hannes@free-fall.at

Keywords: Modelling, earthquake, rockfall, barriers, 3D, bounce heights, impact energies, bunds.

New Zealand Geotechnical Society Inc. 19th Symposium, Queenstown 2013

ABSTRACT

After the February 2011 Christchurch earthquakes Geovert were commissioned by the Canterbury Earthquake Recovery Authority (CERA) to provide the desperately needed answers to the widespread rockfall hazard. Including how best to protect people and assets, how much will it cost and how long will it take. To provide this information Geovert proposed the use of a newly developed state of the art 3D rockfall modelling program which was capable of modelling the vast area affected by rockfall in the Christchurch Port Hills. The modelling focused on possible remedial options and their costs, and associated construction programmes, to provide supplementary information to the current Christchurch City Council (CCC) commissioned Geological and Nuclear Sciences (GNS) reports. The outcomes of the modelling were to assist CERA in making critical decisions relating to areas where rockfall hazard exists and where protective works may effectively reduce the this hazard. The 3D modelling was carried out by a sub-consultant using HyStone, a specialist rockfall modelling programme from the University of Milan, Italy. Typical results indicated energies were in the order of 1000kJ to 2000kJ with relatively low bounce heights (less than 3-4m high). Treatment of this level of energy is relatively straight forward with proprietary products readily available. While the extent of the rockfall issue surrounding the Christchurch earthquakes is very widespread, the requirements for rockfall protection are by no means exceptional on a global level.

1 INTRODUCTION

This paper outlines detailed 3D rockfall modelling of multiple areas within the Canterbury Port Hills near Christchurch, New Zealand, and presents 3D modelling results and rockfall prevention and protection options provided to the Canterbury Earthquake Recovery Authority (CERA). The paper looks at a number of remedial options to treat the rockfall hazard and provides supplementary information to the concurrently run Christchurch City Council (CCC) commissioned Geological and Nuclear Sciences (GNS) reporting.

The aim of the modelling and hazard remediation was to provide possible outcomes to assist CERA in making critical decisions relating to areas where rockfall hazard exists and where protective works may effectively reduce the this hazard. The study was very high level with the intention that the data may have been used to identify properties assessed as having a very low or low hazard from rock fall. The results from the study were provided to enable prioritisation

of work and budget forecasting. The 3D modelling was carried out in Italy by a sub-consultant to Geovert forming one part of the bigger picture in this exercise.
Note that this study outlines the results of a high level preliminary analysis looking at technical aspects only with the purpose of informing policy development. No political matters were considered in this study including land access from an owners perspective nor maintenance and long term ownership issues. The information provided was intended for the purpose of government use only and it was not to be used for detailed design or assessment purposes. This study also does not specifically consider the issue of boulder flux (i.e. multiple earthquake generated boulders) that did occur in some places in the Port Hills.

2 SITE GEOLOGY AND GEOMORPHOLOGY

The geology of the Christchurch Port Hills is relatively simple with pre historic basaltic volcanic activity providing the bulk of the material. This basalt is then overlain by a layer of Loess of varying thickness. At a detailed level the volcanic product forms lava flows, scoria and ash layers, and rubbly airfall deposits which have then formed large cliffs, some sea cut, deep erosion controlled gullies, low angle debris fans and over steepened slopes. This provides a multitude of sources but the main seed areas are present day cliff features or rubbly material that has fallen from them and is now resting on steep slopes below. As well as the large cliffs the basalt in places forms at or near surface low angle (slope parallel) exposures that occur for 5 to 10m down slope. The Loess slopes (by far the predominant surface cover material) are typically firm and provide little in the way of pacifying rockfall when dry.

3 3D ROCKFALL MODELLING

3.1 3D modelling using HyStone

HyStone is a rockfall modelling software utilising numerical code to analyse rock falls, the related hazard and the associated risk. The software is the result of collaboration between FEAT (Finite Element Application Technology, NL) and the University of Milano (Bicocca, Dipartimento di Scienze Geologiche e Geotecnologie). The main features of the code are;

- use of Digital Elevation Model (DEM) to describe topography with no restriction on resolution,
- definition of rock fall sources as point, polygons or lines,
- modelling parameters (topography, sources, energy restitution and rolling friction coefficients) are spatially distributed,
- kinematic (lumped mass) and hybrid (mixed kinematic-dynamic) algorithms to simulate free fall, impact and rolling motions, with different damping relationship available to simulate energy loss at impact or by rolling,
- stochastic modelling to include the variability parameters,
- elasto-visco-plastic model to simulate impact on soft ground,
- simulation of passive countermeasures with specific geometry and energy absorption capability,
- raster and vectors output, including rock fall frequency, minimum, mean and maximum values of velocity, fly height and energy, as well as information about the type of motion, the location of impacts, etc., and,
- simulation of the occurrence of fragmentation of main blocks into small flying rocks.

Similar to a more traditional 2D analysis the 3D modelling takes into account a number of site specific parameters including source area size and height, slope angle, surface material properties (soil, rock etc.), surface roughness and conditions of the run out zones (Spang, 2003).

3.2 Input parameters

For modelling purposes the Port Hills were treated as 'green field' and as such did not includeany trees or vegetation on the slopes or runout zones (other than minor tussock), neither were any houses, buildings, roads or structures included anywhere in the model.

The data for the modelling was predominantly supplied by the Client including,

- LiDAR data to build the DEM,
- Catalogue of mapped boulder locations and boulder parameters as a result of the February and June earthquakes,
- Rockfall source area shape files for source area locations,
- Typical block characteristics including rock type and properties including size and shape,
- Geological and geomorphological maps of the majority of the considered area,

Some surface characteristic information was provided by GNS to assist with model calibration. Additionally high resolution aerial photographs were used to assist in source area location and identification. The input parameters for the rock properties, including starting velocity and rotational velocity, are outlined in Table 1 below. For all modelling a specific weight of 2.70t/m3 was used.

Table 1 - Restitution coefficients inputs used

Class	Normal Restitution Dn (%)	Tangential Restitution Dt (%)	Rolling Friction Coeff Rw (tan)
alluvial deposit, bare	25	73	0.38
alluvial deposit, grass covered	25	73	0.38
colluvial deposit, bare	27	84	0.33
colluvial deposit, grass covered	27	84	0.33
loess deposit, bare	27	84	0.31
loess deposit, grass covered	27	84	0.31
outcropping rock, bare	35	85	0.30
outcropping rock, grass covered	35	85	0.30
subcropping rock, bare	30	85	0.31
subcropping rock, grass covered	30	85	0.31
debris deposit, bare	30	75	0.40
debris deposit, grass covered	30	75	0.40
dune, bare	20	50	0.40
Road	35	80	0.30
building	10	20	1.00
Stoch distribution (all classes)	Normal distribution	Normal distribution	Normal distribution
Minimum value (all classes)	10	20	0.30
Maximum value (all classes)	50	95	1.00
CoV (all classes)	20	20	20

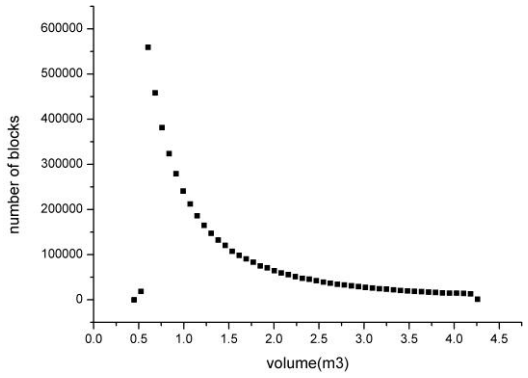
3.3 Field observations

In addition to the computer modelling, and in order to aid calibration of the model, a number of full scale boulder rolling exercises were carried out on the Port Hills. These tests, which were digitally recorded by video camera, proved invaluable as the boulders showed unique behaviour with particularly variable bounce heights and a wide variable in the number of blocks that either stayed intact or fell apart mid slope.

4 MODELLING OUTPUTS

The results of the modelling were very consistent with the real life data collected by the Port Hills Geotech Group (PHGG) in regards to bounce heights and runnouts. While this to a certain extent is to be expected the most useful output from the modelling was the energy levels of the boulders. As no real time figures were gathered during the earthquake events the determination of actual energy levels was critical to the development of remedial options. The following images show a number of the sector outputs with bounce heights, energies and runnouts presented graphically. For the modelling an exponential boulder size distribution was used with a minimum boulder size of 0.30 m³ and a maximum boulder size of 4.25 m³. This distribution curve is represented below in Table 2.

Table 2 - Boulder size distribution used for modelling



The modelling also shows the extent of gullying that has occurred across the Port Hills; that is the amount of boulders which come from multiple or wide source areas and flow into narrow gully features – this is a unique feature of the 3D modelling. The gullying has a positive effect on remedial option design as the highest concentrations of boulders occur in much localised areas. Mitigation structures can be located in these areas meaning smaller (shorter) structures, while outside these areas lower levels of treatment, in some cases none, are required.

Table 3 - Summary of all Sectors – showing maximum bounce heights and energies

Sector	Energy		Bounce Heights	
	Minimum	Maximum	Minimum	Maximum
Sector 1	1000	5000	3	8
Sector 2	500	ACTIVE*	3	7
Sector 3N	500	1000	3	7
Sector 3S	500	ACTIVE*	3	6
Sector 4	1000	5000	3	8
Sector 5	500	8000	3	8
Sector 6	500	8000	3	8
Sector 7	100	ACTIVE*	3	7
Sector 8N	500	8000	3	7
Sector 8S	1000	5000	4	6
Sector 9	500	3000	3	5

*ACTIVE implies energies greater than 8000kJ

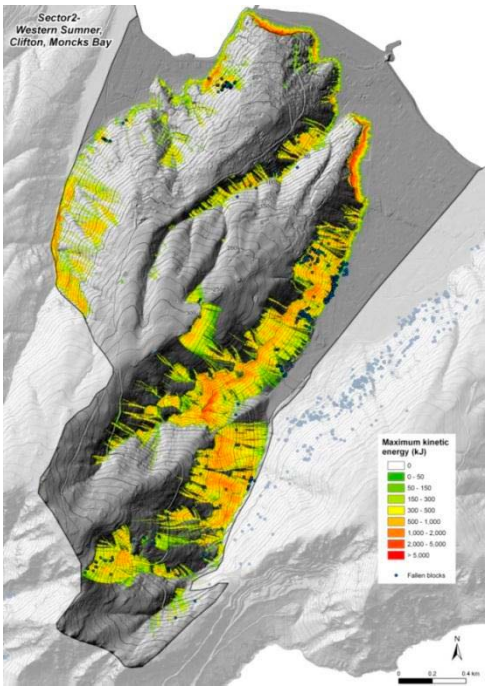


Figure 1 - Sector 2 energy (kJ)

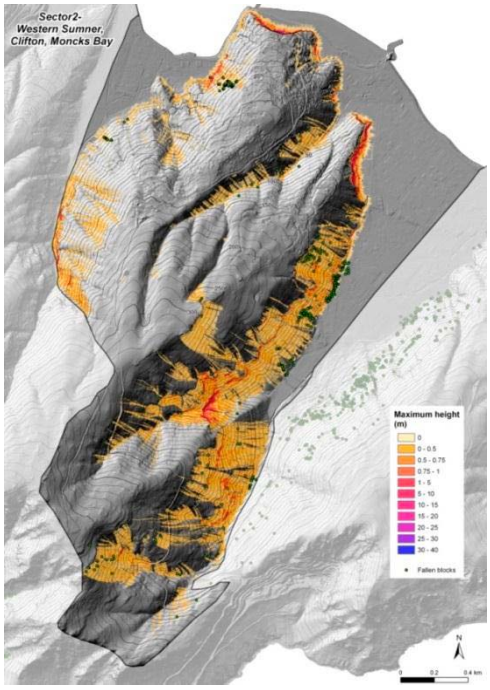


Figure 2 - Sector 2 bounce heights

5 ROCKFALL MITIGATION AND PROTECTION OPTIONS

Various options exist for treating rockfall and the decision to use one method over another is controlled by a number of factors, including access, budget, time and physical constraints. The main treatment options are as follows:

1. Remove the human aspect (house, road etc.) that is being impacted,
2. Remove the hazard source area,
3. Treat the hazard source area,
4. Provide protection from falling rocks/boulders. This can be achieved by,
    a. Mass earth rockfall bunds,
    b. Flexible rockfall barriers,
    c. Natural protection including trees (limited ability)

5.1 Do nothing

This option is always available however for the purpose of this study it was not deemed appropriate to include.

5.2 Treat the source area

The most comprehensive form of rockfall prevention, or risk elimination, is to permanently treat the source area by actively removing, stabilizing or retaining the rocks in situ. The down side to this is that it is typically a more expensive option for a number of reasons, namely it often involves very difficult access which requires specialist plant and materials, and as is often the case and especially so in the Port Hills area the size of the source areas can be very extensive.

For much of the Port Hills the 3D Modelling has shown that, taking into account the above factors including the very large source areas and relatively low rockfall energies and bounce heights, passive measures are likely to be significantly more economical than active source area treatment.

5.3 Rockfall arrest by construction of earth bunds

Earth bunds can be used as feasible options to control rockfall. Typically they are also able to contain larger volumes of rock than rockfall barriers. Earth bunds are most suited where there is ample flat (or low angle) land available for construction, along with ease of access. They generally consist of a steeper front face (upslope) with a gentler downslope face. To achieve a steep upslope face requires the use of reinforced earth. This is also essential in earthquake prone environments to ensure the structure does not collapse during a ground shaking event. The greatest benefit of an earth bund is the ability to arrest multiple boulders (given suitable design) however it is important to note that they will require substantial and time consuming repair post event. As with all systems there are pros and cons with earth bunds. Some of these are highlighted here:

Pros	Cons
Relatively inexpensive to construct	Susceptible to erosion/collapse from large impacts
Easily constructed as general earthworks	Large area of flat or gently sloping land required
Greenable final surface	Creates large unusable area around bund
Arresting large number of boulders	Max height and width limited by available land
Ability to sustain multiple impacts before requiring maintenance	Construction only suitable for slopes less than 22 degrees
Low maintenance / long design life	Tracks for maintenance and cleaning of debris

5.4 Rockfall Arrest by Installation of Tested Certified Rockfall Barriers

Rockfall barriers are steel structures consisting of posts (generally with upslope support wires), wire mesh panelling, end support ropes and brake elements. They come in a multitude of different energy capacities with ETAG (European Technical Approval Guideline) approved systems available up to 8000kJ. ETAG approval is provided by EOTA (European Organisation for Technical Assessment) is a European authority that sets and monitors standards for design, construction and performance. Barriers are flexible structures that absorb energy by dissipating it throughout the system. Key to effective barrier design is the ability to replace individual elements post impact, i.e. post replacement, brake element replacement etc. This allows for rapid re-deployment of the system giving the owner complete confidence.

Pros	Cons
Ease of installation	Requires specialist installers
Construct on flat or steep slope terrain	Lead time on materials ex. Europe
Minimal maintenance requirements	Maintenance after maximum design impacts
Small footprint	Requires room for deflection
Variety of impact ratings	Uncertified system installation - uncontrolled
Tested and certified systems available	Cannot be used to arrest rocks which result in energy transfer greater than 8000 kJ.

Basic assumptions for the rockfall barriers are as follows,

1. Locations shown in report indicative only with final locations confirmed on each site
2. Minimum acceptance criteria - all barriers to be tested and certified to ETAG 27 (minimum Category A) and CE marked, or more stringent Swiss Guideline (BAFU)
3. Barriers specified using maximum energy level
4. All barriers are minimum 3.0m high, varying lengths, varying impact ratings,
5. Barrier materials to be corrosion protected to allow minimum 30 year design life.

5.5 Active source treatment

Active treatment is varied but typically includes scaling, blasting, rock bolting and mesh application, and in some cases earthworks. Depending on the complexity of the source area any number or combination of these activities can be employed at a given site. Modern mesh products include the use of high tensile steel wire which gives 3-4 times improved performance over mild steel wire mesh products.

6 DESIGN ASSUMPTIONS AND CONSTRAINTS

Because of the 'greenfield' approach requested by the Client there were only two constraints affecting the result of the modelling, these were topography and bund/barrier capacity.
The effects of topography affected the proposed final solution in that terrain over approximately 20-22deg was deemed too steep to construct bunds on. While slopes steeper than this can be modified to suit the construction of bunds with few difficulties the cost of this operation, and the extent of land required to construct an effective structure proved cost prohibitive.

The second constraint was the capacity of available barriers. ETAG approved systems, at the time of writing, are restricted to 8000kJ. For impacts greater than this active source area treatment, or 'do nothing', were the only other suitable options.

7 PROPOSED REMEDIAL SOLUTIONS

In the majority of cases it was deemed that barriers were the most suitable solution. This was for two reasons mainly one being cost to construct and the other based on terrain controls. While bunds can be less expensive to construct this normally relies on a shallow slope angle. To place bunds on low sloping terrain means energies and bounce heights are starting to get so low that protection hardly becomes necessary. A small number of areas required active source treatment due to the very high energies experienced further down the slope.

The table below outlines the extent of remedial measures and the different types as proposed following the 3D rockfall modelling study.

Table 4 - Port Hills rockfall protection summary

Sector (#)	Proposed length of barriers (m)	Proposed length of bunds (m)
1	2628	
2	1821	
3	1445	300
4	1364	
5	5277	
6	5025	
7	3634	
8S	3668	
8N	1219	
9	1416	
Total	27497	300

8 QUALITY ASSURANCE

The model, once up and running, provided detailed information on bounce heights, energies and run outs of thousands of boulders. The data was cross checked with 2D modelling through Rockfall 7.1. In addition to the 3D and 2D rockfall modelling a number of field trials were executed by Geovert and Freefall Geotechnical Engineering to better understand the unique dynamics of the Port Hills rockfall issue. This data was used in the final remedial option assessment. Once the accuracy of the data was established and assessed the suitability of the terrain for rockfall remediation options. Note that this study does not look at maintenance or long term ownership issues.

9 CONCLUSIONS

The inputs, while being extensive in volume, are the direct outputs of a very large earthquake event that was not only unexpected but produced far higher vertical and horizontal acceleration than anyone anticipated. As authors of this report we attempted at every point in the study to ensure the outputs of the study matched as close as possible the real outputs of the earthquake as measured in the field. To achieve this numerous discussions, meetings and workshops were held with stake holders, scientists, engineers and geologists from local and international organisations. As a result of these communications it became apparent that the results of the 3D modelling tied very well with the evidence from the field in 95% of the study area.

New Zealand Geotechnical Society Inc. 19th Symposium, Queenstown 2013

The individual Sector results outline the type, location and extent of protection measures required to reduce the hazards associated with rockfall in the Port Hills. While a number of options were considered as part of the study it was immediately evident given that the most appropriate solution to the hazard was the installation of rockfall barriers. Treatment of the source area is often a suitable solution, and is not ruled out for individual cases, however given the extent of the source areas identified in the Port Hills this solution on a whole was not considered viable, nor was in general the construction of mass earth bunds. These options may become more suitable at detailed design stage when site specific investigations are completed, however at this high level they score low on suitability.

10 ACKNOWLEDGEMENTS

Geovert wish to acknowledge the support of the Canterbury Earthquake Recovery Authority (CERA) namely Mr John Scott (Project Manager Port Hills) and Jan Kupec (Ground Engineering Advisor) and their ongoing support during the investigation. We would also like to thank the Port Hills Geotech Group for providing data, discussion and support throughout the project. Lastly we would like to thank the Christchurch City Council (CCC) and GNS for their support and communication during the modelling with multiple meetings and discussions around the outputs of the modelling.

REFERENCES

Crosta, G.B. and Agliardi, F. (2003) "A methodology for physically based rockfall hazard assessment", Natural Hazards and Earth System Sciences (2003) 3, 407-422.

EOTA (2008) ‘ETAG 27 Guideline for European Technical Approval of Falling Rock Protection Kits’ Edition 2008

FHWA (1991) Manual ‘Rock Slopes’. November 1991. USDOT Chapter 12 Page 19.

Hoek, E.(2007) ‘Practical Rock Engineering (2007 ed.)’ (online version)

Spang, R.M. (2003) Rockfall 6.1 Simulation Software. Release 3.2.2003

SH2 Waioeka Gorge, Observations on failure mechanisms prior to and during a major rock slide, March 2012

K J Read
Geotechnical Work Group Manager, Opus International Consultants, Hamilton, NZ.

I Jennings
Engineering Geologist, Opus International Consultants, Napier, NZ.

Keywords: Rock fall, discontinuities, observation

ABSTRACT

A 30m high rock cutting in weathered and highly fractured greywacke on State Highway 2 at Sandy's bluff, approximately 30km south of Opotiki in the Waioeka Gorge has a long history of occasional rockfalls and slope instability.

In early 2012, after a period of heavy rainfall a series of rock falls occurred over a period of a few days. This required temporary closure of the road to clear the debris. On the afternoon of Saturday 3 March a major rock slide occurred during clearing operations. Approximately 100,000m^3 of rock and soil came down in a period of less than 2 minutes. The resultant slip debris blocked the road and temporarily dammed the adjacent Opatu stream.

Site staff had been withdrawn to the limits of the slip before the major rock fall and none were injured. The highway was subsequently closed for a period of 4 weeks while a temporary road was constructed across the slip debris.

In this paper we present the geological and engineering background to the site, and the geotechnical models historically used in assessing the risk associated with the cut prior to the slip. We also present observations made on site during the slip of 3rd March, the failure mode, the gradual acceleration of movement and the processes leading to the major failure.

Possible lessons that we may draw from these observations to aid the safety of those involved in the immediate response phase of slip clearance, assessment and survey of rock slips are discussed.

New Zealand Geotechnical Society Inc. 19th Symposium, Queenstown 2013

1 SITE LOCATION AND GEOLOGICAL SETTING

The rock cutting at Sandy's Bluff is located on State Highway 2, approximately 30km south of Opotiki where the highway passes through the Waioeka Gorge, Figure 1.
At this point the road runs parallel to the river, and has been formed by a combination of cut and fill. Above the road, cuts are as steep as 60° and up to 10m high. Below the road rockfill batters extend down to the river some 4 to 5m below.

The published geological map of the area shows the site to lie within the deformed 'Whakatane Melange'. The melange is a mixed zone of rocks formed from steeply dipping deformed, sheared and folded greywacke. Folding and weathering has made it very difficult to identify original bedding features in the rock mass exposed.

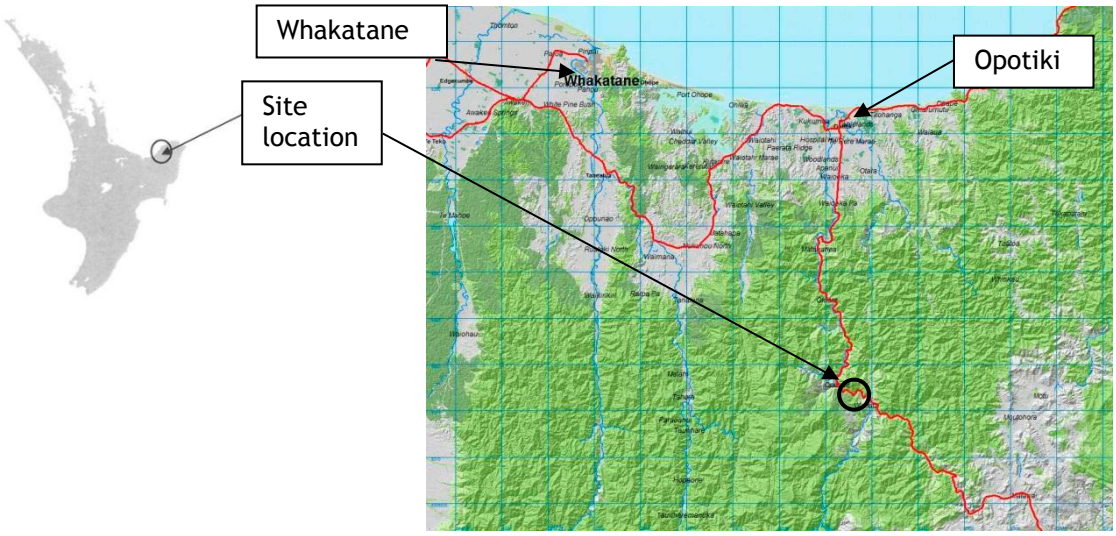


Figure 1: Site location

The map also shows a series of approximately north-south trending faults passing close to the site.

The rock at the site is typical of the local Greywacke comprising weak fine grained sandstone and siltstone with many randomly orientated small fractures and a number of larger continuous fractures. Overall stability of the hillside is controlled by a relatively few large fractures with the smaller randomly orientated fractures governing local stability of small blocks and localised sections of rock faces.

At Sandy's bluff, surveys and engineering geological mapping carried out shortly before the major slip identified 3 sets of intersecting large scale discontinuities dipping out of the rock face at gradients and directions that posed a high risk of major block movement.

For a rock mass to slide on such discontinuities the weight and loading of the rock on those discontinuities must be such that it overcomes the friction forces resisting that movement, those discontinuities must be dipping out of the hillside at a steep enough angle, and they must be sufficiently continuous within the rock mass to allow large blocks to be released.

There is a large degree of randomness within the discontinuity orientations (and condition) in the rock at Sandy's Bluff, but there are 4 components that are persistent and we consider to be the main structural controls to the site. These are:

- A fault that cuts through the site at a high angle, with a strike at a low angle to the road line.
- A joint set (J1) that dips out of the face at about 45°
- A series of joints (J2) that are sub vertical and strike perpendicular to the face
- The respective orientations of the road and joint set (J1)
- The steepness of the cutting with respect to joint set (J1) such that this joint set sloped out of the rock face.

The most likely failure was expected to be a near planar failure on joint set J1.

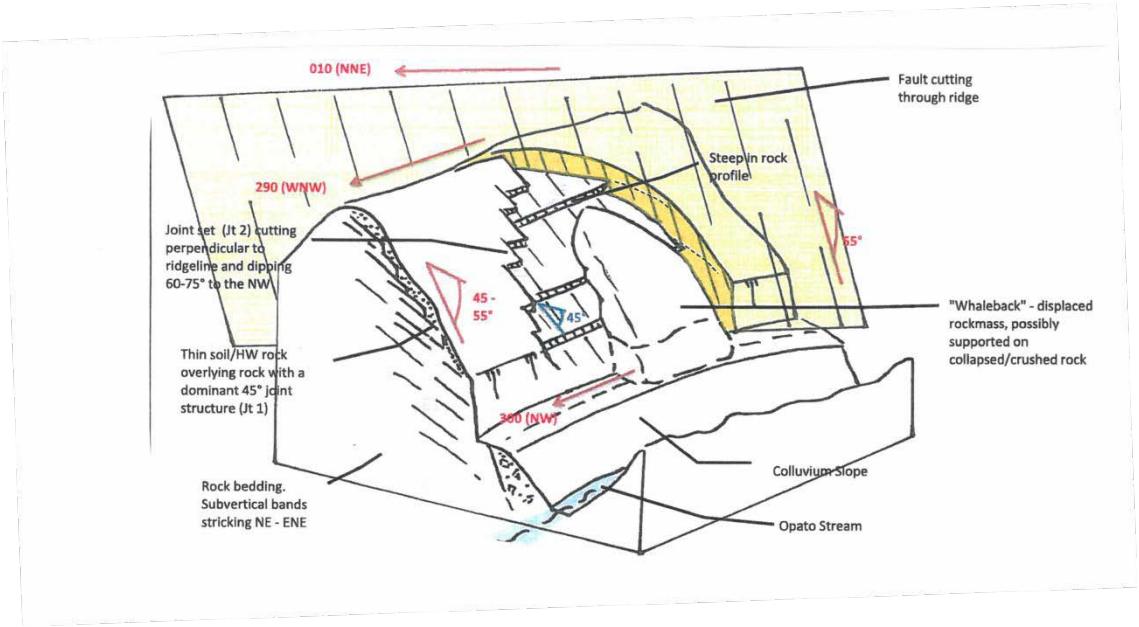


Figure 2: Schematic section of Sandy's Bluff showing principal geotechnical features

It is likely that the geological history of these rocks, through folding and localised faulting has reduced the frictional resistance on some discontinuities and may have induced pre-existing shears in places. Further the steep hillsides and erosion of the gorge may have generated localised historic slips and initiated gradual creep of the hillsides in places. This can be seen in the bent tree trunks seen on the hillsides above the site.

In addition the cutting is believed to have been formed by drill and blast techniques in the 1960's which in themselves may have contributed to opening the natural discontinuities and fractures left in the blasted rock mass after clearing. In addition this work effectively over-steepened the toe of the hill slope. Stress relief over the intervening decades is expected to have occurred resulting in further opening and loosening of the near surface materials.

2 THE DEVELOPMENT AND TIME LINE OF THE MAJOR SLIP

Along the 50km length of the highway within the gorge there is a long history of rock fall and slope movement. The topography and geology combine to cause a constant threat of block falls and occasional mass movement event. The frequency of block falls is such that he highway is swept twice a day of gravel to cobble sized rock fragments that have come down from the numerous cuttings and natural exposures on the route.

The cutting at Sandy's Bluff was no exception to this behaviour, and was to some extent typical of many on this section of SH2. A major slip had occurred approximately 100m north at Sandy's Bridge in 2000 and the cutting at Sandy's bluff is part of the regular rock face inspection and risk rating program for the SH2.

In late February 2012 following significant rainfall, over a period of about a week a gradual increase in block falls and a comparatively minor slip of at least 100m^3 of material occurred at Sandy's Bluff. This generated a 30m high 60° face with a large section of hillside above where topsoil and vegetation had also slipped off, Figure 3. The scale of this movement follows a pattern that has been occurring on average once every 2 to 3 years.

The road was closed to allow clearance of slip debris with works planned to continue over the weekend of 3rd and 4th of March 2012.



Figure 3: Initial slip clearing operations on 3rd March, prior to major slip.

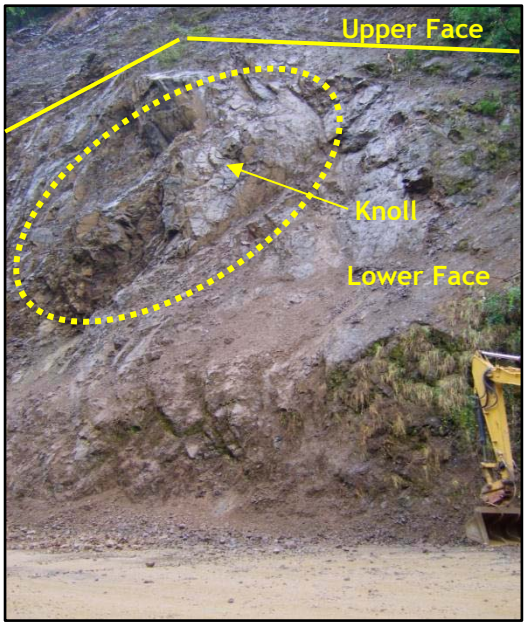


Figure 4: The knoll causing concern prior to the major slip

As clearance works progressed on the 3rd of March the operation gradually revealed a prominent knoll of rock at the eastern end of the cutting which the contractor's spotters considered potentially unstable, Figure 4. At that point an engineering geologist was called in to advise on the stability of that block.

We observed that the frequency of block falls was increasing and these were originating well above the extent of the original cut surface.

In the following narrative the times given are approximate and are based on the photograph and video timing from the day, and the authors recollections.

By 3.30pm 'showers' of gravel sized rock fragments were occurring at irregular intervals, but with increasing frequency and duration from levels above the original cut height. This was concentrated around and above the knoll, and at that point personnel and plant were withdrawn from below that location.

By 3.45pm after considering the continued block fall showers originating from above the crest line of the lower face and uncertainty over what the residual rock face would do if the knoll "failed" all personnel and plant were withdrawn to the outer edges of the slip face.

Between 3.45 and 4.20pm significant and increasing block fall showers occurred from high on the face.

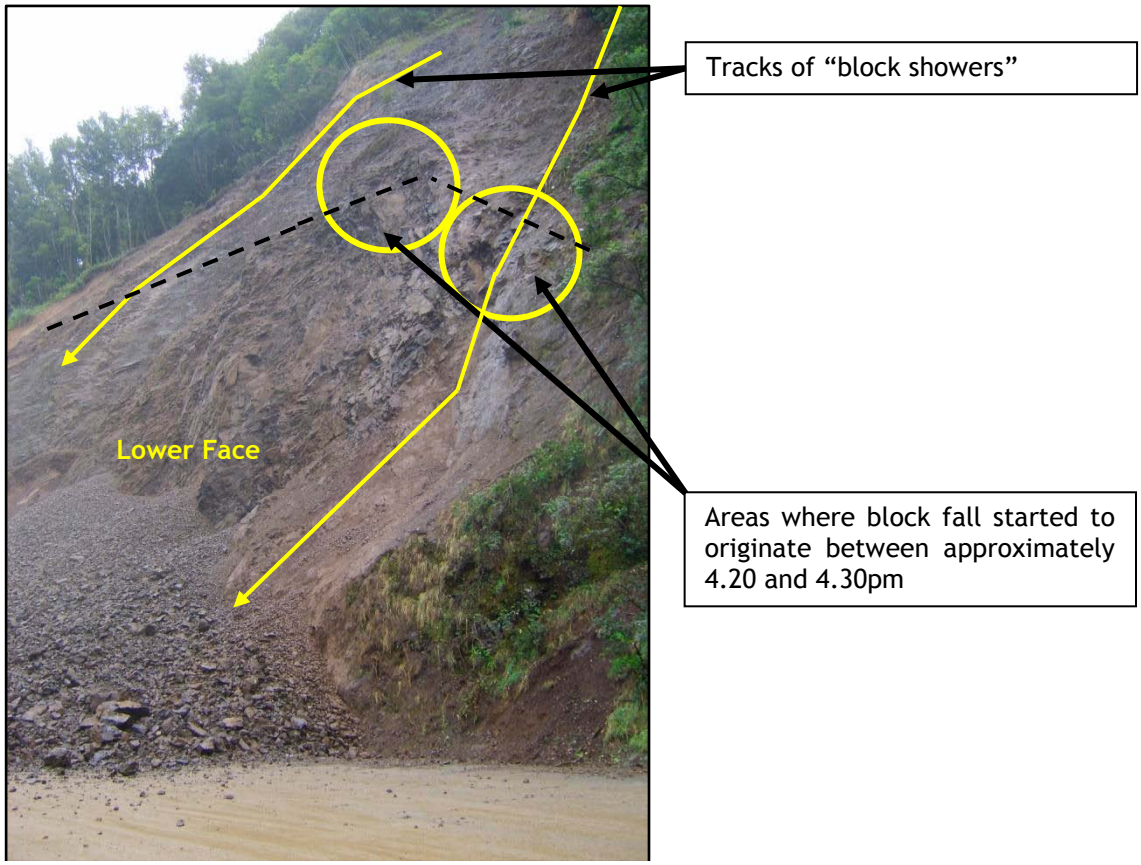


Figure 4: Locations and tracks of block falls and 'showers', at approximately 4pm, prior to the major slip.

Over a ten minute period from 4.20pm to 4.30pm there was a significant change in the style of block falls. As well as near continuous block showers from high on the slip face, block spalling from the lower face of the knoll and the area just above occurred. Tension cracks were observed opening close to the crest of the knoll and large sections of the knoll were displaced out of the rock face. As these sections moved they would very quickly, almost instantaneously, disintegrate into coarse gravel sized fragments that then flowed down the face.

For the next twenty minutes there was a cyclic pattern of a few minutes quiescence, followed by block showers from above, then spalling of rocks from near the crest of the lower face, then another period of quiescence.

Then at 4.53pm the lower face "collapsed". Initially the materials just above the knoll spalled off as before but within seconds rock from below also started spalling off with some speed and the whole rock mass stated moving. As it did so it broke up into gravel components and effectively became a major granular flow slide.

Debris buried the road to a depth of over 8m, crossed and temporarily blocked the adjacent river and moved at an estimated velocity of 10m/s. (Figures 5 and 6)

An estimated 100,000m^3 of material fell in a period of approximately 2 minutes.

New Zealand Geotechnical Society Inc. 19th Symposium, Queenstown 2013



Figure 5: The immediate aftermath of the major slip, looking west.



Figure 6: The temporary dam formed by major slip debris.

3 DISCUSSION ON FAILURE MODE

The failure observed was governed by the joint set dipping out of the face at 45° and the general close fracturing of the rock mass.

The progression from a steady and increasing frequency and volume of block showers from high on the face, through intermittent lower face failure and block showers from high on the slope to very rapid mass failure of the lower face suggests to us a sequence of failure possibly comprising:

- creep of the upper sections of the rock mass on the key joints sets, releasing loosened and over-steepened fragments from high on the slope
- increasing stress on initially 'locked' sections of rock mass lower on the slope and deeper in the initial rock mass, prior to the initial slip
- overstressing of the lower rock mass resulting in rapid failure once movement of locked mass was initiated

4 LESSONS FOR OBSERVERS AND SITE CLEARANCE PERSONNEL

Slope failures of rock and soil are frequently progressive and can occur over long and protracted lengths of time. Arguably this example may have started weeks or even years before the main event and is perhaps an extreme example of an accelerating movement.

A key thing we want to bring out from this is that watchers and observers during site clearance should not only be looking for individual blocks of rock that may fail, but must observe trends and changes in the overall environment of the slip.

We also consider that observers and spotters need to be regularly changed at relatively short intervals, say every 15 minutes. This is to prevent 'boiled frog syndrome' where by changes are so gradual that the spotter does not realise the extent of them over a long time period. ("Boiled frog syndrome" alluding to how a frog in a pan of cold water subsequently heated to boiling does not leap out as it is unaware of what is happening until too late). Good briefing between observers at handover times would be essential.

In this instance personnel withdrew to the limits of the slip but plant was still hit by debris. Consideration should be given to keeping all but essential plant well back from the margins of a slip during clearance and those clearing debris have clear and planned escape routes. Trucks awaiting loading should be positioned well away from the works area and only brought forwards when necessary.

ACKNOWLEDGEMENT

The authors would like to thank the New Zealand Transport Agency for their permission to prepare and submit this paper.

Pletz, Z.J., Codd, J. & Swatton, L. (2013)
Slope Assessment Procedures; a closer look
Proc. 19th NZGS Geotechnical Symposium. Ed. CY Chin, Queenstown

Slope Assessment Procedures; a closer look.

Z J Pletz
Ground Engineering, Aurecon New Zealand Ltd., Christchurch.
Zoe.Pletz@aurecongroup.com

J Codd
Ground Engineering, Aurecon New Zealand Ltd., Christchurch.
James.Codd@aurecongroup.com

L Swatton
Ground Engineering, Aurecon New Zealand Ltd., Christchurch.
Luci.Sawtton@aurecongroup.com

Keywords: Slope, geotechnical, risk, hazard, likelihood, consequence, risk register, geohazard, rockfall, landslide, earthquake, assessment, lifelines New Zealand, Canterbury, Christchurch, Port Hills, Banks Peninsula.

New Zealand Geotechnical Society Inc. 19th Symposium, Queenstown 2013

ABSTRACT

Effective geohazard risk assessment for lifelines can decrease risk to life and reduce maintenance and/or repair costs associated with asset damage due to slope failure. There are many tools and methods used to assess geotechnical risk to lifeline roads, in particular, some of which are based on the application of geotechnical risk registers.

Following the recent Canterbury earthquake sequence, many roads in the Port Hills and on the Banks Peninsula have been affected by slope instability issues, such as rockfall and landslides. Various slope risk assessment methods have been adopted by different local authorities and government organisations in New Zealand. However, there are no universal guidelines or standards outlining which methods are most appropriate for the country's roads. The requirement for a slope risk assessment tool has been identified for use on the hills around Christchurch and so a review of New Zealand and international slope risk assessment methods has been undertaken to determine appropriate methods for use in the area.

Several assessment tools have been reviewed and trialled on highways sites in the Port Hills, including methods used in New Zealand, Australia and the United Kingdom. It was found that each method has been designed for specific aims and project goals. With no definitive method proving completely applicable to the Port Hills, the review concluded that aspects of each method have merit. The review has identified the requirement for the development of a new slope risk assessment tool, specific to the needs of the Port Hills and Banks Peninsula.

1 INTRODUCTION

Slope failures are a common occurrence in New Zealand and roads are sometimes blocked for days or even weeks while debris is cleared and repairs and mitigation works undertaken. The correct identification of geohazards such as landslides, rockfall, embankment failures and other mass movements are important in the prediction, monitoring and management of lifeline routes.

Many slope risk assessment methods allow the analysis of geohazards by using a series of risk registers, generally based on the concept of risk being a function of likelihood and consequence. Some methods use this derived risk value to proactively categorise and prioritise sites that require further attention. Some slope hazard assessments use a score based system to determine a hazard rating, which is used to prioritise sites.

Slope assessment tools are often created for a particular authority or project and so may take into account specific goals such as budgets, available resources and asset types. Many methods currently used in New Zealand have been adopted or modified from international systems, such as the Oregon Department of Transportation's *Rockfall Hazard Rating* system (Pierson, 1990), the Australian Geomechanics Society's *Landslide Risk Management Concepts & Guidelines* (2000) and the Institute of Civil Engineers' *Managing Geotechnical Risk* (Clayton, 2001).

Following the recent Canterbury earthquake sequence, land damage and slope instability have become more prevalent in the Port Hills and Banks Peninsula. With some lifeline roads currently closed or partially blocked with many at risk from rockfall and landslides (i.e. closure of part of the Summit Road), the requirement for an effective slope stability tool for assessing and rating geohazards is recognised. The objectives of this paper are to:

- Provide an overview of selected New Zealand and international geotechnical slope risk assessment and hazard rating methods;
- Trial the selected methods at three unique road sites in the Port Hills;
- Briefly review each method to determine their application in the Port Hills.

2 SLOPE RISK ASSESSMENT & HAZARD RATING METHODS OVERVIEW

Several slope risk assessment and hazard rating methods were selected for the review, based on those commonly used in New Zealand and the authors' experiences. Some others were reviewed but not included in the site trials due to similarities with those included. Slope methods trialled have been summarised in the following sections.

2.1 Transit New Zealand National Rockfall Hazard Rating System

The RHR system is currently used for NZTA, as part of the Slope Check inspection programme, on the state highway network in Central Otago (Opus & NZTA, 2003). The system was modified from part of the Oregon Department of Transportation system (it does not include a screening assessment), which was developed for the assessment of hazardous rockfall sites on their highway network. The Oregon RHR system has been adapted for use by many departments of transportation throughout the United States and Canada (Pierson et al, 1990).

The Transit New Zealand RHR is a score based system that assigns a value to site features. The sum of these values is used to assign a score to the site, to allow prioritisation for further assessment or remediation. Site features include slope height, ditch effectiveness, traffic volumes, speed limits, decision sight distance, geological character, climate and history. The system is purely a hazard assessment method and does not attempt to assess risk. It does not consider likelihood or consequence.

2.2 New Zealand Transport Agency Landslide Hazard Rating System

Like the RHR, the NZTA LHR is also used on the Central Otago highway network as part of the Slope Check inspection programme and comprises a score based system used to rank or prioritise landslide hazards that require further assessment or mitigation(Opus & NZTA, 2003). In addition to the scoring system, the LHR incorporates some aspects of Australian Geomechanics Society (2000) to assign likelihood and consequence and ultimately assess risk using risk registers and a matrix.

2.3 KiwiRail Slope Hazard Rating System

Used by KiwiRail for slope assessments on the national railway network, the Slope Hazard Rating System is a score based system, defined as a ranking system (KiwiRail, 2011), which is

used to prioritise sites. The KiwiRail system was developed to assist with hazard management and preventative maintenance along the network and incorporates some aspects of the UK Network Rail examination of earthworks process (Justice, 2011).

The system uses the sum of factors contributing to the likelihood of a failure occurring, multiplied by the sum of factors contributing to the consequence if a failure occurs, to determine a risk level. The system is primarily points based, so that high scoring sites generally have a higher associated risk and slopes that have a lower score will have a lower risk.

2.4 Wellington City Council Qualitative Risk Assessment Framework

Adopted by Wellington City Council and several other local authorities in New Zealand to assess risk along lifeline routes, the QRAF is a simplified likelihood by consequence risk rating system. Derived values are then assessed in a risk matrix to determine risk level and implications for risk management.

Modified from the Australian Geomechanics Society (2000) *Guidelines for Landslide Risk Management*; the QRAF system was developed as a quick and easily repeatable method for assessing risk to lifeline routes. The method has been used by consultants on behalf of the local authorities in Wellington, Nelson and Christchurch.

2.5 New South Wales Roads and Maritime Services Slope Risk Analysis

This procedure was developed by RMS following disruption to roads resulting from extensive flooding and landslide damage and forms part of their Road Slope Management System database. It is based on the Australian Geomechanics Society (2000, 2007) *Guidelines for Landslide Risk Management* and the Australian Standard for *Risk Management* (AS/NZS 4360 2004). Before carrying out a RMS Slope Risk Analysis for the NSW RMS, certification via a training course must be obtained. This provides a consistency in approach between assessors, which in turn provides a consistency in results for the database.

Several stages form the RMS Slope Risk Analysis method; including a site description, hazard identification, slope risk analysis and supplementary ratings for event magnitude, scale and velocity of failure and Slope Attribute Score (SAS). The slope risk analysis results in an Assessed Risk Level (ARL), which ranges from ARL1 (very high) and ARL5 (very low).

2.6 Highways Agency Risk Assessment of Geotechnical Features (HD41/03)

Developed by the Highways Agency (2003) of England and Wales but also used by Transport Scotland and Northern Ireland's Roads Service, Highways Document (HD) 41/03 is used to assess all earthworks on the United Kingdom's motorways and arterial routes. The results of the assessment contribute to a comprehensive geographical information system known as the Highways Agency Geotechnical Data Management System (HAGDMS), accessible to the authority and their consultants.

The assessment determines the level of risk on all geotechnical features based on the results of a principal inspection, which is undertaken and re-assessed at regular intervals. The method uses a combination of class, location index and timeframe tables to determine a risk level and to determine appropriate remedial actions.

3 SLOPE ASSESSEMENT TOOL IN THE PORT HILLS

Several Port Hills sites were suggested by the local authority for inclusion in the review, to trial each of the above slope assessment methods. From these sites, three were selected to represent a range of geohazards on different types of road. The sites included areas affected by boulder roll,

cliff collapse, landslide, embankment and retaining wall failures. A desktop study of each site was conducted prior to the field assessment, to gather information required for each, such as traffic volumes and speed limits. Three independent assessors were engaged for each assessment at each site.

4 OVERVIEW OF SITE LOCATIONS AND GEOHAZARDS

Selected sites are identified in Figure 1, with a brief summary of each below:

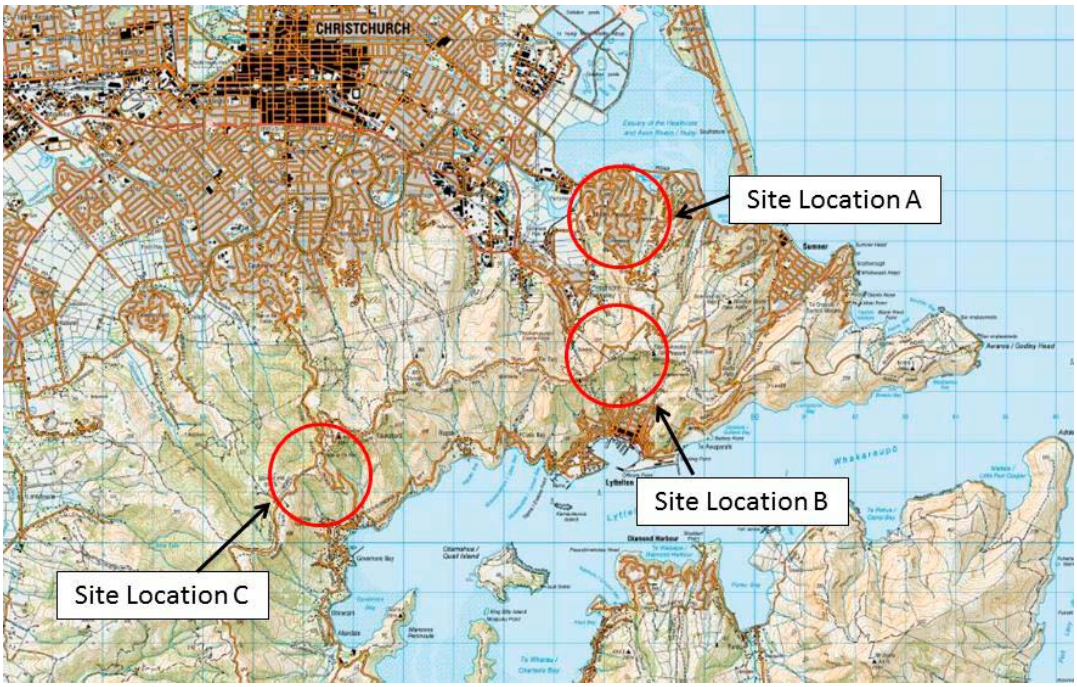


Figure 1. Site locations A, B and C in the Port Hills (LINZ, accessed 2012).

Site A consisted of a 20 m section of a low traffic volume residential road, bounded on one side by a loess cutting. The soil slope height was approximately 5 m with an average slope angle of 40 to 45°. The slope face was vegetated with dense grass, scattered shrubs and small trees. A cloudy seepage was observed at the toe of the slope, discharging into and partially blocking the road drainage system. The primary geohazard affecting the road at the site was an existing shallow loess slip (Figure 2).



Figure 2. Site A, including the shallow loess failure.

Site B comprised a 50 m road section (figure 3) currently closed due to extensive rockfall from bluff failure. From road level, the natural slope height was about 30 to 40 m with an average

slope angle of 70° to 80°. The slope face consisted of exposed volcanic rock with limited grass coverage. No visible signs of seepage were observed. Geohazards included further rockfall from bluffs further up the slope, as indicated by previous events. Many blocks were observed to have fallen onto and beyond the road. Unstable or loosened blocks were also observed on the slopes above the road. Partial embankment failure was noted on the downslope edge with large tension cracks and extensive vertical displacement on the road pavement.



Figure 3. Site B; rockfall on road (left), embankment failure (right).

Site C consisted of a 100 m road section on a moderately trafficked lifeline route (figure 4). The cut slope was approximately 5 to 8 m high at about 80°. The cut slope exposed loess, loess derived soils and volcanic rock. The overall natural slope height was approximately 100 to 115 m with an average slope angle of about 35°. The cut slope was bare to moderately grassed. Vegetation on the natural slope consisted of dense grasses, moderate shrub coverage and scattered small trees. No visible signs of seepage were observed. Geohazards included; the failure of small rock blocks and shallow loess on the cut slope; potential bluff failure leading to boulder roll on the slopes above the road and; embankment failure indicated by tension cracks in the road pavement.



Figure 4. Site C; slope features (left), tensions cracks in embankment (right).

5 REVIEW OF SLOPE ASSESSMENT METHODS

Each slope assessment method produced varying results. Dependent on the aims and layout of each method, outcomes varied. The following criterion was used for comparators to determine the application of each method in the Port Hills:

- Are the factors for assessing slopes applicable for roads in the Port Hills and are they appropriate for hazards that may be triggered by a seismic event?;
- Can the method be used to assess multiple geotechnical hazards (e.g. rockfall, landslide, embankment failure etc.)?;
- Is the method repeatable at multiple locations in the Port Hills?

New Zealand Geotechnical Society Inc. 19th Symposium, Queenstown 2013

5.1 Transit New Zealand National Rockfall Hazard Rating (RHR) System

As the Transit New Zealand National RHR system is not designed to assess landslide hazards, it was only used at Sites B and C, where rockfall hazards were present. The results of the Transit NZ National RHR system were relatively consistent between assessors and sites. Designated points for criteria were fairly spread and range from 3, 9, 27 and 81. This suggests a substantial variation in tallied points between assessors could occur based on the subjective categorisation of criteria. For example, for structural condition, the evidence of 'many erosion features' in comparison to 'major erosion features' has a difference of 54 points. Points are not narrowly grouped into risk levels like other systems and instead a higher tally of points infers a higher risk and a lower tally of points infers a lower risk. The use of quantitative parameters, such as the quantity of rockfall/event, block size, decreases subjective interpretation and should minimise variation in results between different assessors.

The Transit NZ RHR system proved useful for rockfall hazard rating, however as the name suggests, this system can only be used for geohazards associated with rockfall.

5.2 NZTA Landslide Hazard Rating (LHR) System

As indicated in the name of the NZTA LHR, the system is only applicable to sites affected by landslides and is not appropriate for assessment of other geohazards. For this reason this slope assessment tool was not trialled at Site B, which was not affected by any significant landslide hazards. The results of the trials undertaken by each assessor did vary but were similar enough to consider consistent.

The NZTA LHR system proved a useful landslide hazard rating tool. The descriptors defined in the assessment were easy to follow with site characteristics expressed through a series of questions for likelihood and consequence.

It should be noted that for Site C both the RHR and LHR methods had to be applied to assess the different geohazards at the site. The requirement to use two different methods on one site was considered problematic when ultimately trying to prioritise different hazards.

5.3 KiwiRail Slope Hazard Rating System

The KiwiRail method produced relatively consistent results across all sites. However, this system was developed for the railway network and this is reflected in the characterisation of the consequence. The charts and tables in this system were compiled for railway specification and are based on terminology that is inappropriate for use on roads e.g. the site distance factor, which incorporates line of sight and stopping distance for different types of train.

Although a useful systematic hazard rating system for multiple geotechnical hazards, the KiwiRail method was somewhat limited in this study with its application of a railway hazard assessment tool for road assets. To carry out assessments on the highway network consequence parameters would need to be modified to suit traffic.

5.4 Wellington City Council QRAF

The Wellington City Council QRAF produced consistent to inconsistent results at different sites. Based on a two category approach, subjective interpretation of likelihood and consequence parameters varied producing a range of risk levels amongst assessors. As this is a qualitative approach, the limited number of factors in the characterisation of risk infers greater room for subjective interpretation. The QRAF only assesses consequence for life/injury, unlike some

other systems which also include asset/property damage. However, at each site location, the QRAF is a simple method with the potential to cover large sections of road in a short timeframe.

The QRAF system proved useful for slope assessment in the Port Hills, however the variation in results inferred more categories for risk calculation is required to reduce subjectivity.

5.5 NSW RMS Slope Risk Analysis (Version 4.0)

The NSW RMS Slope Risk Analysis produced more detailed notes in comparison to the other methods. The system incorporates the probability of hazard detachment and travel to determine likelihood and similarly incorporates temporal probability and vulnerability (including categorisation of traffic volume and block size) to determine consequence. This comprehensive process reduced the subjective interpretation of risk levels, defined as the ARL.

The RMS method proved useful in covering multiple geotechnical hazards including embankment, cut and natural slope failures as encountered at each site. Although the ARL risk assessment process can be fairly quick to complete, conclusion of the full assessment requires the completion of several pages of documents, some of which do not contribute to the actual risk assessment (e.g. slope attribute scores, event magnitude, hazard classification).

In summary, the NSW RMS Slope Risk Analysis proved a comprehensive and useful tool for slope assessment. However, the system is relatively complicated and time consuming, when compared with other methods. In addition, the RMS recommends that an assessor undertakes a week long training course before assessing slopes with this system. Due to the training course being undertaken in Australia and the process of assessment taking a long time it may not be appropriate in New Zealand as an initial assessment tool. Overall, the system is comprehensive and the ARL process always gives consistent results.

5.6 Highways Agency Risk Assessment of Geotechnical Features (HD41/03)

The Highways Agency HD41/03 method produced results that were repeatable between assessors but inconsistent with other systems. As the system is designed for UK motorways and arterial routes with high volumes of traffic, it assumes a low level of acceptable or tolerable risk. This means that where a geohazard is likely to affect part of the highway infrastructure, the assessment results in high risk, indicating the urgent requirement for remediation. For site conditions in the Port Hills, this method did not adequately differentiate risk between the different sites and all were flagged as requiring urgent attention. However, the principal inspection forms were comprehensive without being time consuming.

Although the UK Highways Agency HD41/03 can assess multiple geotechnical hazards and is a repeatable method, the factors for assessing risk levels are not considered appropriate for roads in the Port Hills, due to the significantly lower volumes of traffic and a different cultural acceptance of risk.

6 CONCLUSIONS

A review of New Zealand and international slope hazard assessment methods has concluded each system is designed for specific aims and project goals. An understanding of these aims allows their relevancy to each application to be determined. Upon application of various slope assessment methods to roads in the Port Hills, the following is summarised:

- The Transit New Zealand National RHR and NZTA LHR systems are designed for specific geohazards. The LHR determines a risk level whilst the RHR is purely a point based system. The requirement to use two different systems may prove problematic when comparing and assessing multiple geohazards at one site;

- The KiwiRail system has been designed for railway assets. Descriptors and consequence values are defined for railways and would need to be modified for use on highway infrastructure;
- The Wellington QRAF method is quick and allows long sections of road to be covered in a short timeframe. The number of parameters for risk level calculation allows for subjective interpretation and variation in results.
- The NSW RMS method achieved consistent results at each site and has the ability to assess multiple geohazards using detailed likelihood and consequence parameters. The lengthy process, cost and training requirements may be restrictive in New Zealand, however with some modifications a similar process may be appropriate.
- The Highways Agency HD41/03 method was developed for road with high volumes of traffic and typically resulted in high levels of risk at the assessed sites. This system is therefore not suited to the Port Hills or New Zealand, where traffic volumes are significantly less. The layout of the forms in the system allowed for repeatable and clear results.

Based on the results of this study, for assessments in the Port Hills and potentially other regions, the development of a two-stage slope risk assessment approach is recommended, comprising an initial phase and a detailed phase. The initial phase could provide an overview of the main geotechnical hazards relatively quickly and that could be repeatable. This would allow higher risk sites to be easily identified and targeted for a second phase analysis, which could provide a more detailed inspection of site specific geohazards.

It is likely that the assessments at both stages would incorporate some aspects of each of the Wellington QRAF and the HD41/03 at the initial phase. The detailed phase may incorporate aspects of the NSW RMS Slope Risk Analysis for determining and categorising risk.

REFERENCES

Australian Geomechanics Society. (2000) Landslide Risk Management Concepts and Guidelines. *Australian Geomechanics*, **35**(1), pp 49-92.

Clayton, C.R.I (2001) *Managing geotechnical risk; improving productivity in UK building and construction*. Thomas Telford, London.

Highways Agency. (2003) HD 41/03, Maintenance of Highways Geotechnical Assets. *Design Manual for Roads and Bridges.* Volume 4.

KiwiRail. (2011) *Development of Slope Hazard Risk Ranking System*. Wellington, New Zealand.

Justice, R. (2011) *Development of a Slope Risk Rating System for New Zealand Rail*. ANZ 2012 Conference Proceedings. Wellington, New Zealand.

Land Information New Zealand. LINZ. (2012) *Topo50 Maps* [online], Available at http://www.topomap.co.nz/ [accessed 02/12/2012].

Opus International Consultants Ltd. & New Zealand Transport Agency (2003) *Slope Check Inspection Programme*. New Zealand.

Pierson, L.A. (2012) Rockfall Hazard Rating Systems. *Rockfall: Characterisation and Control*. Chapter 3. pp 56-71.

Roads & Maritime Services (2011) *Guide to Slope Risk Analysis*. New South Wales, Australia.

Standards Australia (1999) Australian Standard AS/NZ 4360. *Risk management*., Sydney.

Wellington Council (2000) *Qualitative Risk Assessment Framework*. Wellington.

Read K.J, Hughes C.G.C. and Cooke S. (2013)
SH35 Maraenui Hill Realignment,
Use of Risk Assessment in Slope Optimisation and Route Security
Proc. 19th NZGS Geotechnical Symposium. Ed. CY Chin, Queenstown

SH35 Maraenui Hill Realignment: Use of Risk Assessment in Slope Design Optimisation and Route Security

K J Read
Geotechnical Work Group Manager, Opus International Consultants, Hamilton, NZ

C G C Hughes
Geotechnical Engineer, Opus International Consultants, Hamilton, NZ

S Cooke
Engineering Geologist, Opus International Consultants, Hamilton, NZ

Keywords: rock slope stability, risk assessment

ABSTRACT

In August 2010 a major slip permanently closed a 500m stretch of SH35 at Maraenui Hill, approximately 30km east of Opotiki. SH35 is a regional distributor highway that is a life-line route for communities around the East Cape.

Realignment of the highway to 50km/h design standards involved upgrading a temporary 1.2km detour by easing curves and forming a number of cuttings of up to 50m height. The highway at this location passes through steep rugged terrain formed from deeply weathered, highly altered and tectonised greywacke known to be prone to slips and rockfalls. The material present in the cuttings ranges from highly weathered greywacke where stability is controlled by rock fracture orientation, to a residual soil with relict rock fabric where a combination of soil and rock failure modes may be present. In consequence reliance was placed on observation of discontinuity data and weathering condition with the cutting design reviewed as site works progressed.

In this paper we discuss how sections of the new route have been individually assessed for likely failure modes and how the realignment was assessed for long term risk in the context of route security for SH35 as a whole.

We also discuss two significant post construction events, a slip and a washout, and their possible relation to nearly co-incident seismic events in proximity to the site. In each case, surface water drainage, rock weathering and fracture orientation combined to create specific localised areas of risk which appear to have been exacerbated by the seismic events.

INTRODUCTION

The new alignment generally follows the route of a former forestry track around the south side of the bluff across steeply dipping and gullied hill slopes. The cut slopes above the new highway alignment, which is generally founded on stable in-situ ground, consist of benched cuttings with batters at generally 60°, 4m to 7m high with 2m to 4m wide benches. During construction the finished shape of the cut batters did have to change in some locations due to access and construction difficulties. Cutting flatter above road slope gradients (to about 45°) would have improved stability even more but at significant extra cost. At a very early stage in the design process a systematic assessment of risks associated with changing the route alignment and slope cut angles was carried out in accordance with the NZTA Risk Management Process Manual (Transit 2004), and is described by Read *et al.* 2012.

New Zealand Geotechnical Society Inc. 19th Symposium, Queenstown 2013

The design for the above road cut slopes was based on restricted site investigations (due to access difficulties and the urgency of the situation) and observation of exposed slopes in the vicinity of the forestry track and adjoining ephemeral gullies. The objective of the overall project design was to develop an affordable route alternative around the failing bluff that was not out of character with SH35 as a whole.

The rock mass at the Maraenui site is a complex sequence of folded, weathered and altered greywacke. The original bedding of the bedrock has been lost through the weathering, folding and alteration of the material to form a highly variable and closely fractured rock and soil mass. A significant fault was identified during construction at Ch400 between Cuts 3 and 4.

The cuttings for the new highway alignment have been formed in a material that changes rapidly both laterally and vertically from a stiff silt soil at one extreme to a weak closely fractured rock at the other. In general the more soil-like parts of the rock mass are near the original ground surface, with the rock becoming more dominant with depth below the original ground surface, However, this is not always the case, as softer bands of soil-like materials also occur through the rock mass.

SLOPE STABILITY ASSESSMENT

To assist in consideration of the longer term stability of the now excavated above-road cut faces rock discontinuity data has been collected during construction from Cuts 3 to 9 inclusive and assessed for the three most common modes of rock slope failure - toppling, planar and wedge block failure. For the purposes of this paper we have taken the second largest of the cuttings, Cut 4, approximately 70m height as the lead example, Figure 1.



Figure 1: Cuts 2, 3 and 4 looking east.

We have used conventional stereonet analyses to identify the potential for future failures to occur.

New Zealand Geotechnical Society Inc. 19th Symposium, Queenstown 2013

Figures 2 to 4 below illustrate the distribution of the discontinuities for Cut 4.

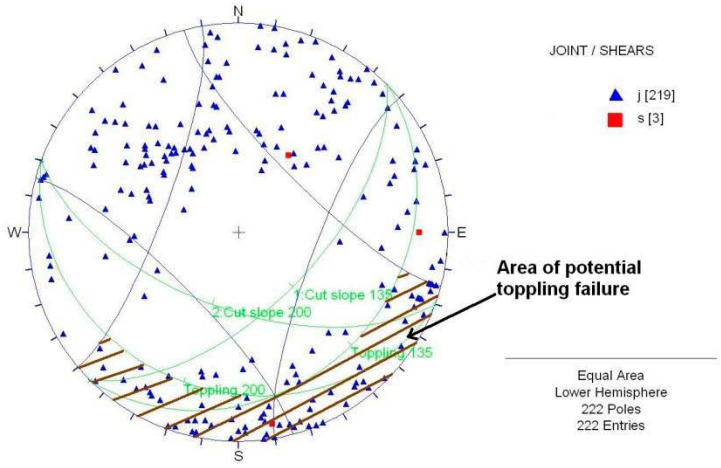


Figure 2: Cut 4 – Potential Toppling Failure Stereographic Assessment

New Zealand Geotechnical Society Inc. 19th Symposium, Queenstown 2013

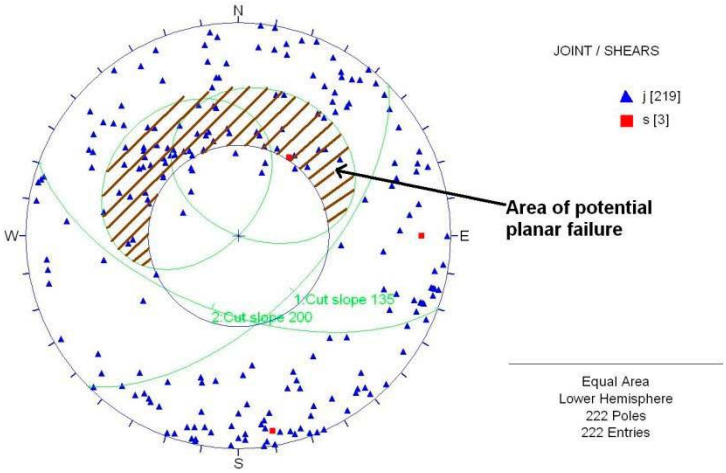


Figure 3: Cut 4 - Potential Planar Failure Stereographic Assessment

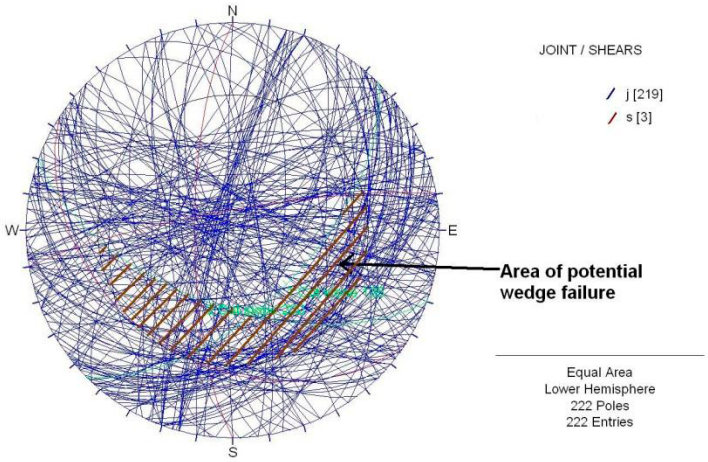


Figure 4: Cut 4 - Potential Wedge Failure Stereographic Assessment

The stereonet analyses demonstrate that little advantage would be gained from flattening the slope angles to reduce the potential for generating failure blocks due to the nature of the discontinuity orientations.

In general terms there is a near random series of discontinuities throughout the rock mass across the site with the vast majority of the fractures being short and discontinuous. Persistent discontinuities are rarer but do occur, as are zones of consistent joint or fracture sets, and apparent "shear zones".

As a result there is a persistent threat of small scale planar and wedge block failure and 'fretting' of the rock face in all the cuttings. This can be readily seen in the cut faces today.

Locally where the more persistent discontinuities are present there is an increased threat of larger volume block failures occurring at specific locations.

POST CONSTRUCTION OBSERVATIONS

Stress relief since formation of the cutting has, and will continue to generate flaking and slaking of the exposed face materials which then forms coarse gravel scree at the toe of each bench face.

Blocks from the fretting type failures have been and in the short to medium term are expected to be largely retained on the slope benches and verge side.

To date a significant wedge failure has only occurred at CH190 on Cut 2. The cut was completed in May 2011 and in June and July 2012 slips occurred affecting the lower 3 benches, Figure 5. At 7.30pm on Friday 10 August a 4.69M earthquake occurred approximately 12km north of the site, at 44.4km depth and was felt strongly by site staff living locally.

On Saturday 11 August a further slip comprising predominantly planer movement of near surface soil and rock, and vegetation cover occurred immediately west of the previous slip and regressed up another two benches, Figure 5.



Figure 5: Cut 2 Showing Wedge Failure

Smaller wedge type failures are now present and active in Cuts 2, 4, 5 and 8.

A small washout / slip occurred at CH900 (Cut 9) after heavy rain in October 2011 in completely weathered to highly weathered greywacke. We believe that this resulted from surface water flow along the benches in a south to north direction passing from grey, highly

New Zealand Geotechnical Society Inc. 19th Symposium, Queenstown 2013

weathered closely fractured sandy greywacke onto yellow brown completely weathered and very closely fractured silty greywacke, and partly washing out material and the sharp interface between these two materials, Figure 6.

This washout/slip appeared to have reached a steady equilibrium with no further movement/regression observed despite several periods of wet weather prior to the 18 September 2012 event. The day before the event between 130 and 150mm of rain fell in the Opotiki area. From inspection of the partially cleared scar on the hill side we believe that a debris flow/washout type of slip has occurred with surface water scouring out a channel in the middle to lower parts of the face and undermining the upper soil like parts. Prior to clearing the debris site staff reported that it appeared to have originated between benches 3 and 4 above the road. Photos taken on 8 August 2012 show this area being scoured by surface run-off, Figure 7.



Figure 6: CH900 on 8 August 2012.

There is a sharp boundary on the south side of the scar formed by the contact between the two rock types described above, and the material that has been removed is the completely weathered silty greywacke.

It is unclear if a 4.28M seismic event, 38.6km deep and close to the site on 4th September 2012 (some 2 weeks prior to the event) played any role in generating this washout. However it is possible that the shaking 'loosened up' material on the interface between the two rock types where erosion had created space for it to move into. Subsequent rainfall and surface water flow on the 18th may have then exploited this creating the washout and subsequent loss of materials. Both these events caused disruption to road users.



Figure 7: Ch900 on 18 September 2012

RISK ASSESSMENT

We determined that there is a threat of small to medium sized rock block failing from the cut batters across the whole of the re-alignment route. This is due to the small scale random fracturing of the bedrock as a whole. The majority of these are on faces above road level and debris is retained on the benches.

There are some isolated locations where major discontinuities (more than 2m long) are present. At these locations it is probable that in association with the many less continuous fractures we may get localised zones of failure blocks.

For the purposes of our risk assessment we considered two types of rockfall event,

1: Events that could reach road level

2: Events we believe will not reach road level.

Our assessment was carried out in accordance with the NZTA Risk Management Process Manual (Transit 2004) and the results for events that could reach road level on Cut 4 are presented on Table 1. This process also included assessment of possible mitigation measures.

CONCLUSIONS

The perceived threats to the road users cover all categories from “low” to “high” risk with likelihoods of “rare” to “quite common”. Potential consequences also range from “minor” through to “substantial”.

Table 1: Risk Assessment for Cut 4.

		Qualitative Risk Analysis			Risk Evaluation		Risk Score	Risk Priority	Threat Rank	Risk Reduction Measures & Mitigation
	Threat or Opportunity	How likely is the event?	Consequence Rating	What are the consequences of event?	Likelihood Rating	Consequence Rating				
Wedge failure on Bench 1	**Threat**	Quite Common	Medium	Passing vehicle could be struck by falling debris or damaged by running over rock debris.	3	40	120	Very High Threat	2	Monitor for movements, install BH drains if seepages and movement observed
Soil Failure on slope above Bench 1 (Short term)	**Threat**	Unlikely	Minor	Passing vehicle could be struck by falling debris or damaged by running over rock debris.	3	10	30	Moderate Threat	4	Much may be retained on Bench 1 - keep bench clear of debris, encourage revegetation of soil on slope
Soil Failure on slope above Bench 1 (Long term)	**Threat**	Rare	Minor	Passing vehicle could be struck by falling debris or damaged by running over rock debris.	1	10	10	Low Threat	8	Much may be retained on Bench 1 - keep bench clear of debris, encourage revegetation of soil on slope
Large block fall or large slip	**Threat**	Unusual	Substantial	Passing vehicle could be struck by falling debris or damaged by running over rock debris.	2	70	140	Very High Threat	1	Monitor for movements, install BH drains if seepages and movement observed

Our assessment of the potential hazard using the NZTA Risk Management Process Manual indicated that for both cases acceptance and management of the hazard is an acceptable way forwards for this new section of highway. It also allowed objective comparison of the new route section to existing sections of the road.

The new slopes will continue to change as the outer material layers weather and undergo stress relief. This is no different to the now vegetated cut slopes on either side of the new alignment.

The two significant events that have occurred to date that have reached road level occurred at CH190 and CH900. We consider these to be due to localised unfavourable combinations of rock weathering, fracture orientation, surface water flow and to have possibly been exacerbated by seismic events.

In order to maintain a similar level of overall risk on this section of SH35 as is already experienced elsewhere on the route, we recommended the following works:

- In specific locations where the potential for larger wedge type failures is present, NZTA should consider the risk and determine if monitoring is appropriate.

- In areas where groundwater seepage is observed in the cut faces targeted bored drains into the slope should be used assist to relieve groundwater pressures in areas where the joint sets are also unfavourable.

- At road level, the widest possible unsealed shoulder between the edge of the road and the bottom of the cut benches should be maintained clear of debris as a first line of defence should colluvium reach road level. In specific areas where the width of the road shoulder is constrained, rock fall barriers should be considered in line with the NZTA Rock Fall Hazard Rating assessment procedures.

ACKNOWLEDGEMENTS

The authors would like to thank the New Zealand Transport Agency for their permission to prepare this paper.

REFERENCES

Read K J, D'Ath N and McNaughton M, 2012, "Use of 'Lean Construction' and Risk Management techniques in the design and construction management of the realignment of part of State Highway 35 at Maraenui Bluff." Proceedings of ANZ 2012, 11th Australia - New Zealand Conference on Geomechanics, Melbourne

Transit New Zealand "Risk Management Process Manual, Manual Number AC/MAN/1" September 2004.

Yates, K. Villeneuve, M. Wilson, T (2013)
Geotechnical risk assessment of hilly terrain during post-earthquake response
Proc. 19th NZGS Geotechnical Symposium. Ed. CY Chin, Queenstown

Geotechnical risk assessment of hilly terrain during post-earthquake response

K Yates
Department of Geology, University of Canterbury, NZ
Katherine.yates@pg.canterbury.ac.nz (Corresponding author)

M Villeneuve
Department of Geology, University of Canterbury, NZ
Marlene.villeneuve@canterbury.ac.nz

T Wilson
Department of Geology, University of Canterbury, NZ
Thomas.wilson@canterbury.ac.nz

Keywords: Canterbury Earthquakes, risk assessment, geotechnical, guidelines, landslides

New Zealand Geotechnical Society Inc. 19th Symposium, Queenstown 2013

ABSTRACT

The 2010-2012 Canterbury Earthquake sequence has highlighted and identified the value of standardised, practical and co-ordinated guidelines for geotechnical risk assessment for inhabited areas in the aftermath of a natural disaster. The lack of guidelines and provisions to manage the assessment of geotechnical hazards hindered co-ordinated, timely and transparent management of geotechnical risk in the hilly suburbs of Christchurch.

The earthquake sequence triggered rockfall, landslide and cliff collapse events throughout the Port Hills. This damaged thousands of houses and critical infrastructure, and created a life risk issue for people inhabiting the area. Given the high seismic hazard in New Zealand and the location of significant active faults near populated centres, it is beneficial to learn from the response undertaken following the Christchurch Earthquake sequence to inform geotechnical risk assessment guidelines for future events.

This paper examines our proposal for research into how the geotechnical risk assessment approach evolved throughout the earthquake sequence and in the apparent post-sequence period. This research will aim to establish the evolution of information needed as the response progressed, and identification of lessons learnt. The basis for geotechnical risk assessment guidelines has been derived from the analysis of experiences from key municipal, management and operational stakeholders who were involved in the geotechnical risk assessment during the Canterbury earthquake sequence.

1 INTRODUCTION

The Christchurch Earthquake sequence that initiated on the 4th September 2010 has been a learning curve for most geotechnical professionals involved in the post earthquake response. Over the past 70 years, New Zealand has had limited exposure to widespread earthquake induced slope failure in largely urbanised and populated areas such as the Port Hills, Christchurch. Because of this, the majority of the response and risk assessment methodologies were developed reactively after the 22nd February 2011 earthquake. Geotechnical Engineers and Engineering Geologists were deployed to areas of Christchurch to assess the landscape response and subsequent damage to slopes from the earthquake sequence. This assessment of the landscape led Geotechnical Engineers and Engineering Geologists to then examine the risk to life safety of residents exposed to slope failures induced by the earthquake sequence. The lack of guidelines for assessing this risk hindered a co-ordinated and timely response. Because of this it became clear that it would be beneficial to New Zealand to have a framework which outlines how to respond to earthquake induced slope failures.

New Zealand has a high level of earthquake risk due to a number of highly active faults that feature throughout the country. This partnered with growing urbanisation in areas of steep terrain can present a life risk issue from earthquake induced slope failures. Since 1840 there have been at least 22 recorded earthquakes in various locations through New Zealand that have resulted in widespread earthquake induced landsliding (Hancox et al 2002). Examples include the 1929 Murchison earthquake and the 1968 Inangahua earthquake which resulted in some loss of life from extensive landsliding induced by ground shaking. However, most of the 22 earthquakes have occurred in sparsely populated areas, minimising loss of life and damage to infrastructure. Because of this, the experiences, management strategies and lessons learnt by those responding to slope failures induced by the Canterbury earthquake sequence offer a rare, valuable and perishable opportunity for documentation of this information in order to prepare for future earthquake events. Ideally, the systematic investigation and documentation of these lessons will provide a foundation for New Zealand to develop a planned response in the form of guidelines for future earthquake events.

This paper outlines a methodology proposed for developing guidelines for geotechnical risk assessment in the aftermath of an earthquake. The development of these guidelines is primarily focussed on the response and management systems that originated and were refined during the Christchurch earthquake sequence. Details of the Christchurch earthquake sequence and the response to the earthquake sequence will be presented as a case study to support the development of such guidelines. The use of terminology in this paper is consistent with ISSMGE Glossary of Risk Assessment Terms (listed on TC304 web page: http://140.112.12.21/issmge/2004Glossary_Draft1.pdf) where "risk" is described as the measure of the probability and severity of an adverse effect to life, health, property or environment.

New Zealand Geotechnical Society Inc. 19th Symposium, Queenstown 2013

2 METHODOLOGY FOR THE DEVELOPMENT OF GUIDELINES FOR GEOTECHNICAL RISK ASSESSMENT

As part of the proposed research methodology, guidelines for post earthquake geotechnical risk assessment will be developed through examination of a combination of response techniques from an international and a local level that addresses the geotechnical issues particular to New Zealand. The proposed research has been divided into two phases, currently the first phase of the research has been completed and the second research phase is due to commence. The first phase of the research aimed to examine the response systems performed by other countries during international earthquakes which have induced slope failure. During the second phase, geotechnical experts who responded to the Christchurch earthquake sequence will be interviewed in an effort to record the local level response methods and lessons learnt from the Christchurch earthquake sequence. Information gathered during these two phases of research will be used to make recommendations for guidelines for geotechnical risk assessment.

2.1 Phase One -Review of international case-studies

At an international level, methods of geotechnical response used during the 1994 Northridge earthquake, the 1999 Chi-Chi earthquake and the 2008 Wenchuan earthquake have been identified to show an outline of practised response methodologies. Review of published literature was used to identify relevant information from these international events. The individual aspects of response identified provide suggestions for typical components of geotechnical response. The majority of these methods are comparable to the geotechnical response to the Christchurch earthquake and are therefore applicable to the New Zealand context.

2.2 Phase Two - Analysis of the geotechnical response on the Port Hills during and following the Canterbury earthquake sequence

At a local level, review of the response to earthquake-induced slope failure in the Port Hills during the Christchurch earthquake sequence has been helpful for understanding how geotechnical response developed in New Zealand. This information has been obtained through a series of interviews with key municipal, management and geotechnical experts who participated in the response to earthquake induced slope failure initiated by the Christchurch earthquake

sequence. This approach has been taken because little information regarding the mechanisms of response has been recorded since the earthquake sequence commenced. It would be useful to collaborate experiences and lessons learnt from these individuals who responded in order to prepare for future events.

As part of the proposed research, participants involved in the interview process will be divided into three groups: strategic level response, tactical level response and case study participants (Figure 1). Tactical level response refers to the geotechnical engineers or engineering geologists who were involved in observing and assessing slope failures and making decisions about the associated risk on site. Strategic level response refers to the management operatives who were involved in making large scale decisions and took part in organising and managing the overarching approach to geotechnical risk assessment. In some cases individual participants can be categorised in to both or neither of these roles, and in this circumstance the question set was tailored to their specific role.

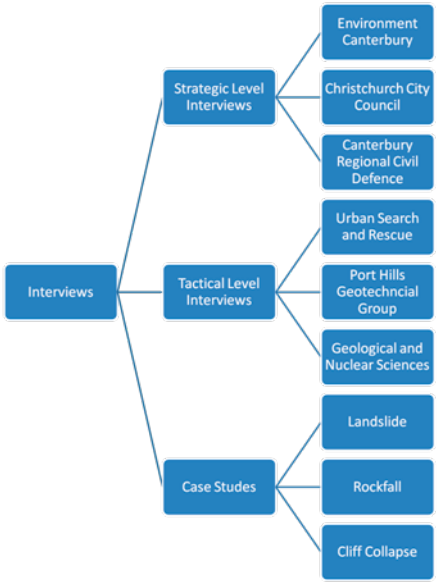


Figure 1 - Framework for interviews

Up to four case study sites will be examined to gain an understanding of the requirements of geotechnical response for site specific failure mechanisms. This will be achieved by interviewing the tactical level geotechnical experts who responded to each of the sites. The question set will focus on the failure mechanisms and geotechnical response efforts for each of the sites. Methods of practically assessing the geotechnical risk in post earthquake environment will be identified from interviewing participants from the tactical response group and the case study level group. This will form the basis of 'on the ground' response methodologies in the guidelines for geotechnical risk assessment.

Interviews with strategic level participants will seek to shed light on the management of geotechnical response which developed after the 22nd February 2011 earthquake. This is important for identifying what information is required for finalisation of higher level decisions such as zones of evacuation. These interviews will also focus on the reporting system that developed within management level organisations during the response to earthquake induced slope failure. Interviews will be semi-structured and will be guided by a question set. Additional questions may be added throughout the interview to follow up and explore key statements and themes conveyed by the participants. Participants will be asked questions that aim to walk them thought the disaster sequence from the 4th September 2010 to December 2011. Depending on their level of involvement this timeframe may be shortened.

A representative timeline of key events during this period will be presented to each of the participants to act as a visual aid to prompt memories and experiences during that time. Key events include government level decisions such as states of emergency and introduction of

legislation regarding the Christchurch earthquake sequence. Large rainfall and snowfall events have also been included because these had the potential to affect the geotechnical response. Participants will also be presented with a topographic map of the Port Hills as a spatial aid to discern where in the area they were active during the response.

These tactical, strategic and case study level interviews will highlight which approaches hindered and which aided a timely and coordinated response in the initial days to weeks after the 22nd February 2011 earthquake. These will be combined with successful response approaches used in international examples to generate guidelines for geotechnical risk assessment in a post-earthquake environment.

3 INTERNATIONAL CASE STUDIES FOR GUIDELINE DEVELOPMENT AND RESEARCH

Analysis of international case studies such as the 1994 Northridge earthquake, the 1999 Chi-Chi earthquake and the 2008 Wenchuan earthquake has been useful for identifying components and organisational aspects of response used internationally. For example, during the 1999 Chi-Chi earthquake the seismic hazard was managed by a collaboration of several government level organisations and the mobilisation of engineers and scientists who undertook ground reconnaissance. Technical support and information and data management was divided between two national science organisations with the National Science Council acting as the over-arching organisation responsible for the management of seismic hazard (Loh & Tsay 2001). This organised approach to disaster response enabled a systematic post earthquake reconnaissance of earthquake induced hazards.

After the 1994 Northridge earthquake in California as part of the response plan government level organisations collected and analysed reconnaissance information commencing hours after the earthquake (USGS 1996). Using this information, probabilistic seismic landslide hazard maps and spatial mapping of earthquake induced landslides enabled a growth of knowledge regarding the susceptibility of slopes in the area to failure (Jibson et al 2000, Parise & Jibson 2000). This research has enabled geotechnical experts in California to learn from the event by the identification of higher risk areas that are likely to fail again from further seismic events. This could aid post-disaster decisions such as the deployment of geotechnical experts because areas that are likely to have failed can be easily located.

4 THE CHRISTCHURCH EARTHQUAKE SEQUENCE AS A CASE STUDY FOR GUIDELINE DEVELOPMENT AND RESEARCH

The initial earthquake in the Christchurch earthquake sequence (M_W 7.1) took place at 4:35am on the 4th September 2010. The earthquake initiated from rupture on the previously unknown Greendale fault, southwest of the city (Berryman 2012). Although there was no loss of life and widespread damage in the Central Business District (CBD), the earthquake caused only minor rockfall in the Port Hills. Less than 6 months after the first earthquake a smaller earthquake (M_W 6.2) ruptured at 12:51pm on the 22nd February 2011. The earthquake was located on the Christchurch fault directly southeast of the city and caused the loss of 185 lives, damage to infrastructure, life lines and residential areas (Berryman 2012).

Extensive earthquake induced slope failure was initiated in the Port Hills by the 22nd February earthquake. These features were widespread in the hilly suburbs and were responsible for the loss of five lives. Earthquake induced landslides became an umbrella term for four categories of slope failure: rockfall, cliff collapse, landslides and retaining wall failure. From accelerometers located near the Port Hills measured peak ground accelerations (PGA) in the vertical direction reached up to 2.21g, while PGA in the horizontal direction reached 1.41g at Heathcote Valley Primary School (Wood et al 2011). Scientists have attributed the strong ground shaking felt in the Port Hills area to these high PGA values. This is likely to have been the cause for the extent of geotechnical failure in the Port Hills (Massey et al 2012b). Following the 22nd February earthquakes several large aftershocks triggered further slope failure in the Port Hills. These included earthquakes on the 13th June 2011 (M_w 6.0) and 23rd December 2011 (M_w 5.9). The

New Zealand Geotechnical Society Inc. 19th Symposium, Queenstown 2013

worst of these was the 13th June 2011 earthquake which initiated similar maximum horizontal peak ground accelerations to that of the 22nd February 2011 earthquake (Berryman 2012). Further slope failure from these earthquakes required many sites to be re-evaluated by geotechnical experts.

4.1 Response to earthquake induced slope failures in the Port Hills

Understanding the geotechnical response to the Christchurch Earthquake sequence is important for the development of guidelines for New Zealand as it presents a recent example of geotechnical risk management. At the current stage in the research, the response to earthquake induced slope failures in the Port Hills can be divided up into four components: Organisation and mobilisation, slope failure assessment and evacuation, monitoring, and mitigation. The response to the 22nd February 2011 earthquake in particular is likely to form the majority of the information for guidelines for geotechnical risk assessment primarily because it was the most significant event in the sequence for the development of the response. The geotechnical response to life safety risk was significant after the 22nd February 2011 earthquake because it was the first earthquake in the sequence to cause extensive slope failure in urban areas.

4.1.1 Organisation and Mobilisation

The majority of the response after the 4th September 2010 earthquake was organised by local council. This included minor rockfall induced by the earthquake that was cleaned up by local contractors. Because earthquake induced slope failure was minor there was no need for an extensive organised geotechnical response.

New Zealand Geotechnical Society Inc. 19th Symposium, Queenstown 2013

Hours after the 22nd February 2011 earthquake geotechnical experts responded to the situation often by their own self-mobilisation or mobilisation by their employer, rather than as a coordinated response initiated by a pre-formed national response framework. Days after the 22nd February 2011 earthquake geotechnical experts responding to the earthquake began meeting together. This aided the development of organised deployment of geotechnical experts in the Port Hills. Because this was still in the developmental stages days after the earthquake some sites were still assessed several times by multiple geotechnical response teams. Within days after the 22nd February 2011 earthquake, as more geotechnical experts became involved the Port Hills Geotechnical Group formed. The Port Hills area was divided up into several sectors which were then assigned to various geotechnical engineering companies or research institutes within the group.

4.1.2 Slope failure Assessment and Evacuation

Evacuation of properties commenced hours after the 22nd February 2011 earthquake and continued months to year after the event. As geotechnical experts assessed the slope failures mandatory evacuation was enforced for properties that could be exposed to inundation by further boulder release or cliff collapse, or could be damaged from further ground deformation from tensile cracking or compression features (Dellow et al 2011). Often the basis of the evacuation decisions was formed from information collected by geotechnical experts assessing the evidence for slope failures that had or could affect a property; however, the final decisions to enforce evacuations were made by the Urban Search and Rescue (USAR) contingent. Days to weeks after the 22nd February earthquake empirical data from field mapping became available. This enhanced the assessment of risk for particular areas where data had been collected (Dellow et al 2011).

4.1.3 Slope Monitoring

Within days of the 22nd February 2011 earthquake, evaluation of slope failures induced by the earthquake consisted mainly of visual observations of the features of each failure mechanism. Visual inspections of cracks for both landslide and cliff collapse failures were important to understand the mechanics of movement. Measurements of crack widths were taken regularly to monitor rates of movement. Rockfall that had been located in residential areas was often traced back to the source area. The rock mass of the source area was examined visually to identify loose material that could be released by subsequent aftershocks.

Monitoring systems were installed on landslides that were identified immediately after the earthquake. Days after the 22nd February 2011 earthquake these monitoring systems mainly consisted of string lines and pins installed across cracks at the head-scarp of the landslide. As equipment became available continuous global positioning systems (cGPS) and strong motion instruments were installed. Many of these devices are still in use in order to gather further information regarding slope movements. Approximately two weeks after the 22nd February 2011 earthquake terrestrial light detecting and ranging (LIDAR) data was used to analyse cliff faces and identify areas of loose material (Massey et al 2012). This was used to calculate the volume of mass released from a cliff face during aftershocks and establish the movement patterns of the slope failures (Dellow et al 2011). Generally slope movements were either initiated from aftershock activity, or were creeping continuously. The nature of the landslide movements could also be observed by the deformation of buildings which straddled tension cracks or compression features (Dellow et al 2011).

4.1.4 Mitigation

Days after the 22nd February 2011 earthquake evacuation was the most common form of mitigation against rockfall and cliff collapse until other measures could be achieved. Mitigation of the effects of cliff collapse included the installation of barriers such as ballasted containers along the base of the cliff to limit the extent at which the material could travel. Loose material was removed from slopes to mitigate the risk of inundation via further cliff collapse or rockfall.

New Zealand Geotechnical Society Inc. 19th Symposium, Queenstown 2013

5 DEVELOPMENT OF GUIDELINES FOR GEOTECHNICAL RISK ASSESSMENT

Developing guidelines for geotechnical risk assessment enables New Zealand to move forward and prepare for future earthquake events. Because New Zealand is such a seismically active country with a history of earthquake induced slope failure it is likely that a similar large-scale earthquake event could occur in a highly populated area with similar resulting geotechnical hazards. Capturing lessons learnt from the Christchurch earthquake sequence will assist in identification of response to earthquake induced slope failures and in developing a methodology for effective response. This will ensure that geotechnical experts involved in future response will have the tools necessary to undertake geotechnical risk assessment.

The development of guidelines will standardise the approach taken to risk assessment and ensure that all tactical and strategic level personnel have a consistent response to the situation. This will ensure that assessments of geotechnical hazards completed during the response phase will be uniform and comparable. Having a framework in place will enable a coordinated response by which the geotechnical hazard can be assessed more efficiently and life risk issues can be addressed promptly. Achieving coordination between response teams will eliminate or reduce communication frustrations and ensure timely analysis and processing of data. This should also minimise the amount of 'lost time' in effort to coordinate the response and enable a more timely mitigation of slope failures.

Guidelines for post disaster geotechnical risk assessment will be developed as a series of recommendations aimed at advising the geotechnical community and government level organisations. These recommendations will aim to illustrate methods for the management and practice of assessment of geotechnical risk in a post disaster context. Recommendations will be developed from processes and information needs that were reflected upon during the interview process. Examples of historical earthquake events will be used to guide and support these recommendations.

Guidelines will be initially divided into management or organisational recommendations and tactical level recommendations. Management level recommendations will refer to key operational aspects of geotechnical risk assessment such as critical path communication between organisations involved. Within this division of the guidelines it would also be helpful to develop a schematic framework of the responsibilities, interaction and requirements of and between each organisation active during the post-disaster response period. This would include

government and municipal organisations, geotechnical organisations and research institutes. It would be useful within this framework to outline the information needs for each organisation to participate in the response.

Tactical level recommendations will refer to key aspects of geotechnical risk assessment that provide the fundamental analysis of risk associated with earthquake induced slope failure. Key aspects of tactical level recommendations should include logistical requirements for reconnaissance work, data documentation and analysis, methods for assessing earthquake induced slope failures, and spatial distribution of geotechnical experts. The focus of this tactical division of the guidelines will be to emphasise practical methods for assessing geotechnical risk "on the ground" and then progress to recommendations for centralisation of data and information collected during reconnaissance work.

Logistical requirements during reconnaissance should include a framework for reporting observations and analysis. In addition to this it would be prudent to suggest the use of a pro forma to be used as a method for ensuring consistency of assessing earthquake induced slope failures. Centralisation of data immediately after the earthquake will enable processing of information to commence soon after it is recorded. It would also be useful for providing organisations involved in the response with information collated from ground reconnaissance.

New Zealand Geotechnical Society Inc. 19th Symposium, Queenstown 2013

Tactical recommendations could also encompass suggestions for data analysis. This initially will be derived mainly from examples of data analysis from international earthquake events such as the 1999 Chi-Chi, Taiwan earthquake, and the 1994 Northridge earthquake in California. After both of these earthquakes data such as ground motion information and landslide location information was displayed spatially in order to present a visual representation of the distribution of these two data sets. Similar spatial analysis was also undertaken during the Christchurch earthquake sequence.

It will also be an important part of the guideline development to suggest relevant skill criteria and training requirements for geotechnical experts who are involved in the post disaster geotechnical risk assessment process. This is important because for the risk to be assessed adequately the assessor must exhibit competence in the geotechnical field. It is likely that this recommendation of skill criteria will be one of the founding components of the guidelines.

It is also likely that recommendations for pre-earthquake components of geotechnical risk assessment will be included in the guidelines. This is likely to include suggestions for slope stability analysis and identification of slopes with potential risk of failure triggered by earthquakes. This information regarding the stability of slopes would be useful particularly for hilly areas that are urbanised or populated. Prior knowledge of slope stability would enable geotechnical experts to assess slopes with a background knowledge regarding the risk of failure. It is possible that this information would also be useful for distinguishing which areas post-earthquake will have experienced the most slope failure and which areas are required to be examined first by geotechnical experts.

6 CONCLUSIONS

The Christchurch earthquake sequence has highlighted the need for guidelines for risk assessment of seismically induced slope failures. As part of ongoing research, guidelines will be developed from documentation of experiences and events that took place in the aftermath of the Christchurch earthquake sequence. This information will be captured from a series of tactical, strategic and case study level interviews with geotechnical experts who were involved in the response.

Because New Zealand is a seismically active country and has a history of earthquake induced slope failures, it is important that as a country we learn from the Christchurch earthquake sequence so that preparation can be made for future inevitable events.

7 ACKNOWLEDGMENTS

We would like to acknowledge the involvement of those who took the time to contribute to this study. We are also grateful for the support that Environment Canterbury and Opus International Consultants have provided for this project.

8 REFERENCES

Berryman K. (2012). Geoscience as a component of response and recovery from the Canterbury earthquake sequence of 2010-2011. *New Zealand Journal of Geology and Geophysics. Vol. 55 (3): 313-319.*

Dellow G, Yetton M, Massey C, Archibald G, Barrell D J A, Bell D, Bruce Z, Campbell A, Davies T, De Pascale G, Easton M, Forsyth P J, Gibbons C, Glassey P, Grant H, Green R, Hancox G, Jongens R, Kingsbury P, Kupec J, Macfarlane D, McDowell B, McKelvey B, McCahon I, McPherson I, Molloy J, Muirson J, O'Halloran M, Perrin N, Price C, Read S, Traylen N, Van Dissen R, Villeneuve M, Walsh I. (2011). Landslides caused by the 22 February 2011 Christchurch Earthquake and Management of Landslide Risk in the Immediate Aftermath. *Bulletin of The New Zealand Society for Earthquake Engineering, Vol.44 (4): 227-238.*

Hancox G T, Perrin N D, Dellow G D. (2002). Recent studies of historical earthquake-induced landsliding, ground damage, and MM intensity in New Zealand. *Bulletin of the New Zealand Society for Earthquake Engineering, Vol. 35 (2): 59-95*

Jibson R W. Harp E L. Michael J A. 2000. A method for producing digital probabilistic seismic landslide hazard maps. *Engineering Geology, Vol 58: 271-289.*

Loh C-H, MEERI, Tsay C-Y. 2001. Responses of the Earthquake Engineering Research Community to the Chi-Chi (Taiwan) Earthquake. *Earthquake Spectra, Vol 17, (4): 635-656*

Massey C I, McSaveney M J, Yetton M D, Heron D, Lukovic B, Bruce Z R V. (2012). Canterbury Earthquakes 2010/11 Port Hills Slope Stability: Pilot Study for assessing life safety risk from cliff collapse, GNS Science Consultancy Report 2012/57.

Massey C I, McSaveney M J, Heron D, Lukovic B. (2012b). Canterbury Earthquakes 2010/11 Port Hills Slope Stability: Pilot Study for assessing life safety risk from rockfalls (boulder rolls), GNS Science Consultancy Report 2012/311.

Parise M, Jibson R. 2000. A seismic landslide susceptibility rating of geologic units based on analysis of characteristics of landslides triggered by the 17 January, 1994 Northridge, California earthquake. *Engineering Geology, Vol 58: 251-270.*

Geological Survey (U.S.G.S). 1996. USGS Response to an Urban Earthquake: Northridge '94. U.S. Dept. Of the Interior, U.S. Geological Survey. Open-File Report 96-263

Wood C M, Cox B R, Wotherspoon L M, Green R A. 2011. Dynamic Site Characterisation of Christchurch Strong Motion Stations. *Bulletin of the New Zealand Society for Earthquake Engineering, Vol 44, (4): 195-204*

Soysa, S.R. & Pomfret, A.D. (2013)
2011 Hawkes Bay landslips: A geotechnical perspective
Proc. 19th NZGS Geotechnical Symposium. Ed. CY Chin, Queenstown

2011 Hawkes Bay landslips: A geotechnical perspective

S R Soysa
Tonkin & Taylor Ltd, Auckland, NZ
ssoysa@tonkin.co.nz

A D Pomfret
Tonkin & Taylor Ltd, Auckland, NZ
apomfret@tonkin.co.nz

Keywords: Landslides, extreme groundwater, earthquake

ABSTRACT

New Zealand Geotechnical Society Inc. 19th Symposium, Queenstown 2013

Across Easter Weekend 2011, heavy rainfall affected coastal Hawkes Bay from Mahia in the north to Blackhead Beach in the south with some significant rainfall totals being recorded. This period of heavy rainfall was followed by a magnitude 4.5 earthquake centred off the Central Hawkes Bay Coast at 10:30am on Tuesday 27th April. This combination of saturated ground (caused by the rainfall) and minor earthquake triggered significant landslips in the Central Hawkes Bay hill country. In addition, widespread flooding and debris flows inundated rural communities with Pourerere Beach and Waimarama being the worst affected. Also numerous landslips occurred in the densely populated Napier Hill area due to stormwater run-off.

This combination of extreme rainfall and the earthquake represents the unlikely geotechnical scenario, where elevated groundwater is combined with an earthquake. This extreme case was especially evident in the rural communities of Pourerere Beach and Blackhead Beach where many properties are located at the base of steep slopes which historically have been unstable during extreme rainfall. This event triggered 388 Earthquake Commission (EQC) claims with significant costs at a time when EQC was dealing with the Christchurch Earthquakes. The Authors were requested to assess these claims on behalf of the EQC and present possible remedial solutions.

1 INTRODUCTION

This paper sets out the damage experienced from a severe weather event that impacted the Hawkes Bay region in 2011. The Authors firm responded to this event on behalf of the Earthquake Commission (EQC) in the subsequent weeks following the event.

Heavy rain affected coastal Hawkes Bay from Easter Sunday through to early Tuesday morning. Areas affected were from Mahia in the north to Blackhead Beach in the south of the region. The scale of this event was striking with huge swathes of farmland affected by shallow landslips in addition to the damage to residential land and property. At the start of this process, a significant lack of stormwater control in steeply sloping built up areas such as Napier Hill was observed. In addition to this, numerous properties were observed to have been sited at the base of steep slopes where signs of historical shallow landslips (probably caused by heavy rainfall) existed.

Official rainfall totals over this 72 hour period were as follows (from North to South).

Table 1: Rainfall Totals

Town/Community	Rainfall
Mahia	300 mm
Napier	211 mm
Hastings	60 mm
Ocean Beach	424 mm
Waimarama	322 mm
Kairakau	303 mm
Pourerere Beach	378 mm
Blackhead Beach	301 mm

To emphasise how the weather event only affected coastal Hawkes Bay, Hastings is 20 km inland from Ocean Beach and only received 15% of the coastal rainfall. Reports exist of some coastal hill country stations recording up to 800 mm of rain in the 72 hour period. In addition at 10.00am on the Tuesday morning, a small (Mag. 4.5) earthquake occurred at a depth of 20 km off Blackhead Beach in Central Hawkes Bay. A combination of saturated slopes and a small earthquake created many landslips and tension cracks on the slopes near in Central Hawkes Bay.

2 EQC Event

The EQC set up a field office in Hastings to deal with 388 claims from the event. Prior to the Christchurch earthquakes, the Napier hill area accounted for the highest number of landslip claims for the EQC on a yearly basis. Fortunately, the Central Hawkes Bay damage was centred on a largely rural community so claim numbers were not excessive in this area. The spread of landslip claims from region were as follows:

Table 2: EQC Claims

Town/Community	No. of Claims
Mahia	2
Napier	120
Ocean Beach	8
Waimarama	40
Pourerere Beach	57
Blackhead Beach	20

It can be seen that even though rainfall totals in Napier were lower than the coastal communities to the south, a significant number of landslip claims were generated due to the higher housing density and lack of stormwater control (to be discussed later). Further south whole communities were affected by landslips but the claim numbers were low due to the lower population.

The majority of the landslips inspected by T&T were debris flows. These shallow landslips formed due to the fully saturated upper soils sliding on the rock interface. This was particularly evident in Central Hawkes Bay. In addition, T&T observed numerous hillsides where tension cracks formed following the small earthquake near Blackhead Beach. The local farming community noted that these tension cracks appeared directly after the earthquake and further landslips occurred even though the rainfall had eased.

New Zealand Geotechnical Society Inc. 19th Symposium, Queenstown 2013

These tension cracks were of concern, especially for properties that were located directly below them as the imminent risks to the properties would likely have been realised with further rainfall.

The damage observed by T&T personnel during the event was as follows:

- Flooding
- Bridge damage
- Erosion of river banks
- High percentage of damage to farmland
- Major inundation of roads and houses.

3 CASE STUDIES

3.1 Case Study 1 - Napier Hill Landslips

New Zealand Geotechnical Society Inc. 19th Symposium, Queenstown 2013

Bluff Hill (to the north-east) and Hospital Hill (to the west) are collectively known as Napier Hill and comprise approximately 2000 residential dwellings as well as numerous commercial buildings. Napier hill is an uplifted massif located at the northern extent of the City of Napier, formed from calcareous, cross-bedded sandstone and limestone of the Scinde Island Formation (GNS 2011). This distinct cross bedding is likely to have developed due to strong tidal effects of the Ruataniwha Straight (GNS 2011), and along with the vertical jointing, is a common medium for seismically induced instability in the form of large scale block failures as was witnessed in the 1931 Napier earthquake. During periods of heavy rainfall however, failure of the steep slopes of Napier Hill are typically in the form of translation landslips and debris flows. There is evidence of historical instability in these slopes of translational and deep-seated (block) failure from both, seismic and extreme rainfall events.

The Napier Hill area received approximately 210mm of rainfall over a 72 hour period and this is likely to have saturated the upper residual soils of the Scinde Island Formation.

Following this intense rainfall, significant damage was caused to properties and lifelines on and directly below Napier hill by the land evacuation and inundation that occurred as a result of the landslips. Approximately 100 EQC landslip claims (EQC) were lodged and these landslips were typically of a translational/debris flow nature, with the most prominent of these being the Guys Hill and Karaka Road Landslips. The main contributing factor to the numerous landslips within Napier Hill were the elevated ground water levels caused by the heavy rainfall and poorly controlled stormwater runoff from dwellings and roads.

3.1.1 Guys Hill Road Landslip

A large translational landslip occurred at the top of a slope approximately 30m high and 55° steep at 22 Guys Hill Road. As shown in Figures 1 and 2 below, this caused substantial evacuation of land from the property, causing inundation and damage to the properties below at 19 Chaucer Road. Due to the precariously positioned nature of the dwellings above and below the landslip, these properties were immediately evacuated following the event. The property at 22 Guys Hill Road was ultimately removed because the required solution to ensure a safe and stable building platform (and minimising imminent risk) was deemed to be too expensive and difficult.



Figure 1: 22 Guys Hill Road Landslip



Figure 2: 22 Guys Hill Road Landslip

3.1.2 Karaka Road Landslip

Another large translational landslip occurred at the top of the slopes supporting 22A and B Karaka Road and 24A Seapoint Road above Breakwater Road at the northern end of Napier Hill. As shown in Figures 3 and 4 below, this caused significant retreat of the cliff face supporting these residential dwellings. At the height of the storm, 7 properties were evacuated by civil defence. Inundation of Breakwater Road by this landslip resulting in this major road being temporarily unpassable until the debris was cleared and traffic management was required numerous weeks after this event. As this landslip headscarp traversed three separate properties, the solution ultimately comprised a large 50m long, 15m deep reinforced concrete retaining wall with ground anchors.



Figure 3: Karaka Road slopes prior to failure



Figure 4: Karaka Road landslip

The existing stormwater capacity on Napier is fully allocated and the majority of the older properties on Napier Hill discharge stormwater run-off directly into the ground whilst any new dwellings on Napier Hill discharge stormwater to the kerb. Due to this, a high percentage of the EQC claims on Napier Hill can be attributed to poor stormwater management.

3.2 Case Study 2 – Waimarama

Waimarama is a small coastal community at the south-eastern area of the Hawkes Bay. The developments in this town primarily consist of residential dwellings and a few commercial buildings. The town is formed on Holocene beach and estuarine sediments consisting of unconsolidated sand, gravel, silt and mud deposits. The hills to the north, overlooking the township are tectonically uplifted sea cliffs comprising poorly to moderately cemented sands and silts. There is evidence of historical deep seated and translational landslips in these hills from seismic events.

The Waimarama area received approximately 322mm of rainfall over a 72 hour period, which was the highest officially measured rainfall during the event in the Hawkes Bay. In addition to this, the Kaikopu Stream overflowed its banks due to a coinciding high tidal level blocking the mouth of the watercourse, preventing the ability of the excess water to flow out to sea.

New Zealand Geotechnical Society Inc. 19th Symposium, Queenstown 2013

Following this intense rainfall and flooding event, significant damage was caused to properties and lifelines at Waimarama by the deep seated landslips and debris flows originating from the hills above as well as the widespread flooding. Approximately 30 residents were evacuated immediately and the main road into Waimarama was unpassable and closed due to flooding and debris. In addition to this, the bridge into the township was damaged and shortages of drinking water occurred due to damage to local reservoirs. In the weeks and months following this event, 40 landslip and flooding claims were lodged with the Earthquake commission. Figure 5 below shows the extent of the damage to the northern section of the township one week removed from the event.



Figure 5: Shallow debris flow behind Waitangi Road Properties



Figure 6: Severe debris inundation of fields and roads in Waimarama

The authors company were involved in constructing a protective bund around the property at 145 Waitangi Road, to reduce the imminent risk of damage to property and life from a future event of this nature. This 3m high bund was constructed using compacted locally sourced material and tested for 98% of maximum dry density. We understand that a group of residents further along Waitangi Road have combined their EQC payouts to construct a protective bund to safeguard their properties from debris inundations.

An on-going risk currently exists of large amounts of failed material on the slopes above the township. This will require significant stabilisation measures as well and it would be prudent for an early warning system to be installed to protect the lives, properties and lifelines below.

3.2 Case Study 3 – Pourerere Beach

Pourerere Beach is a small coastal settlement comprising less than 100 residential dwellings at the southern extents of Hawkes Bay. At the southern end of Pourerere Beach lies a small cluster of approximately 33 residential dwellings. The developments in this area primarily consist of residential beachfront dwellings and a public camping ground. The settlement is situated at the base of a steep hillside running parallel to the coastline. These are late to Middle Miocene deposits and comprise calcareous mudstones and interbedded fine grained sandstones (GNS 2011).

The Pourerere Beach area received approximately 308mm of rainfall over a 72 hour period and this is likely to have saturated the soils of the hills that overlook this section of the settlement. In addition to this, Pourerere Beach is located approximately 5 km to the north of the epicentre of the 4.0 magnitude earthquake, which occurred within close proximity to the town at nearby Blackhead Beach.

Following this intense rainfall and small seismic event, significant damage was caused to properties and lifelines directly in this area of Pourerere Beach by the land inundation that occurred as a result of the landslips. Approximately 57 EQC landslip claims were lodged and these landslips were a combination of deep seated and translational failures. We consider the rare event of elevated ground water conditions being combined with a seismic event to be the cause of the large-scale slope failures with significant debris inundation of dwellings.



Figure 7: Landslips above Pourerere Beach settlement



Figure 8: Large tension crack in hills above Pourerere Beach

Following the landslips, the hillside above the dwellings was assessed to be unstable, with large tension cracks appearing behind the existing landslip headscarps. The authors company led regional study of this area led to the conclusions that 27 of the 33 residential dwellings and 50% of the camp ground site in this area of Pourerere Beach were considered to be at imminent risk and at "total loss" in accordance with EQC provisions. This was due to these dwellings being located directly below (and within the inundation paths) the unstable sections of the slope (as illustrated in Figure 9) that are expected to fail in the short term. As the dwellings were located

at close proximity to the base of the slope, a debris barrier could not be considered due to the failed land being owned by others, EQC cannot remediate land not owned by the claimant.

For the properties that were not deemed at total loss, an early warning system was implemented by the CHBDC and operated by the local fire service to help safeguard lives during periods where the slopes are deemed to be unstable. The local residents have been notified of this warning system, including evacuation procedures following activation of the siren.

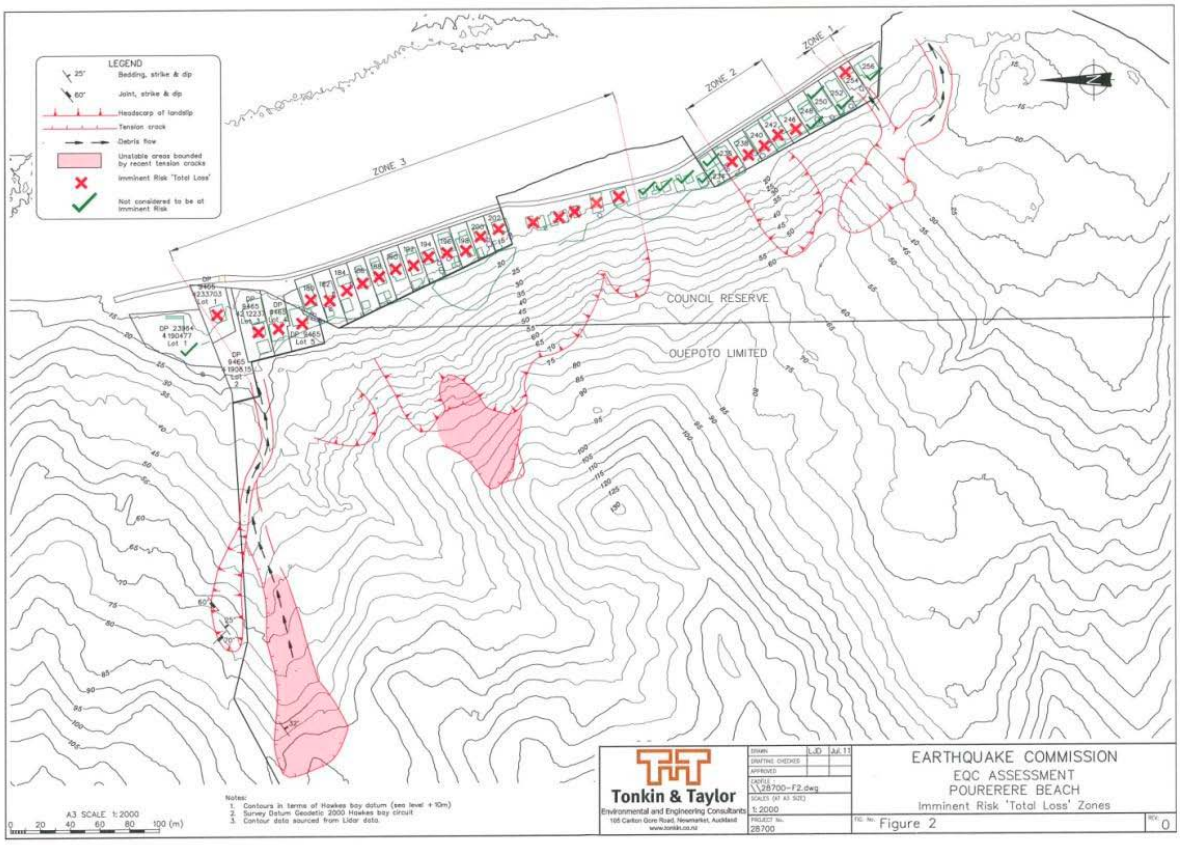


Figure 9: The Properties at Pourerere Beach that were classed at imminent risk – Total Loss for the EQC

4 CONCLUSIONS

Based on the observations from this extreme weather event the following point's conclusions can be made:

- Council's must be proactive in relation to the new stormwater connections and provide suitable disposal areas to prevent further stormwater runoff into the underlying residual soils of the Scinde Island Formation at Napier Hill.
- Prior to the Christchurch earthquakes, the Napier Hill area had the highest average landslip claims year on year for the EQC.
- This event showed that with saturated near surface ground conditions, a relatively minor earthquake can cause severe damage to land and property.
- Rural Councils often allowed properties to be sited at the base of historically unstable slopes without any conditions attached – this is slowly being changed.
- Severe rainfall events can impact on lifelines to rural communities. It is therefore important that strong collaborative efforts be made between local councils and rural communities in ensuring procedures are in place to deal with these events.
- In situations where communities are at future risk from unstable ground, the implementation of early warning systems and evacuations procedures such as the scheme utilised at Pourerere Beach would be an effective means of managing the risk to lives.

ACKNOWLEDGEMENTS

The Author acknowledges the help and contribution of the Earthquake Commission, Central Hawkes Bay District Council and Napier City Council for their input and permission to publish this paper.

REFERENCES

Lee, J.M.; Bland, K.J.; Townsend, D.B.; Kamp, P.J.J (2011): Geology of the Hawke's Bay area. Institute of Geological & Nuclear Sciences ;:250 000 geological map 9. 1 sheet + 93 p. Lower Hutt, New Zealand. GNS Science.

Stewart, D.L. & Brabhaharan, P. (2013)
SH6 Rocks Road, Nelson, New Zealand – Observations on Cliff Instability Risk Assessment
Proc. 19th NZGS Geotechnical Symposium. Ed. CY Chin, Queenstown

SH6 Rocks Road, Nelson – Observations on Cliff Instability Risk Assessment

D. L. Stewart
Aurecon NZ, Wellington, NZ (formerly Opus International Consultants, Wellington).
david.stewart@aurecongroup.com

P. Brabhaharan
Opus International Consultants, Wellington, NZ.
brabha@opus.co.nz

Keywords: Rocks Road, Nelson, cliff slope instability, road risk mitigation.

ABSTRACT

The Rocks Road section of State Highway 6 in the city of Nelson is vulnerable to slope failures from a 400 m long former sea cliff which rises 40 m high above the road. Rocks Road is a key arterial highway carrying over 20,000 vehicles and about 1000 bicycles per day. The cliff is comprised of steeply dipping Tertiary age sandstone and mudstone rocks. The mudstones are subject to ongoing slaking and slabbing failures, with failures in sandstone less frequent and more typically defect controlled. Rock falls and slips have been hazards for road users ever since the road opened in 1899. This paper outlines the history and modes of slope failures on the cliff and the engineering geological investigations, risk assessment, and risk mitigation actions that have been used to manage the risk to road users. The paper focuses particularly on risk assessment and risk mitigation that occurred following failures in 2005, 2008 and December 2011. A risk management strategy was developed for the whole cliff in 2008, which included a risk assessment. The heavy rain events of December 2011 allowed a review of the 2008 risk assessment, and observations are presented.

New Zealand Geotechnical Society Inc. 19th Symposium, Queenstown 2013

1 INTRODUCTION

The cliff above Rocks Road (State Highway 6) between Nelson and Tahunanui has a long history of instability affecting the road (Photograph 1). The cliff is subject to frequent rock falls and soil slips, which result in debris encroaching onto the road carriageway. Opus International Consultants are responsible for the management of the road network in this area for the NZ Transport Agency.
This paper outlines the history of instability, its impact on the highway network, and the risk assessment process carried out.



Photograph 1: Rocks Road Cliff

A major slip that blocked the highway in 1990 resulted in the assessment of mitigation options for the cliff, with remedial measures being implemented in this part of the cliff in 1994. Following failures in 2008 (Photograph 2), a strategy was developed by Opus to manage the risks to road users from failures from the cliff. In December 2011, two severe rainfall events resulted in closure of the highway for a number of days to allow clean-up and inspections, as well as risk assessment and implementation of remedial and safety measures. Other stakeholders include residents who live above the cliff and Nelson City Council, who are considering reconfiguring the corridor to improve pedestrian and cycleway facilities along this scenic waterfront route.

2 SITE DESCRIPTION

Rocks Road is a two lane (50 km/hour) highway with in excess of 20,000 vehicles per day and over 1000 cycles per day using dedicated cycle lanes. A pedestrian walkway is located on the sea side of the road (Photograph 2). The cliff is 20 to 40 m high with slopes of 40° to 80° or steeper. For purposes of risk management, the cliff has been divided into eight sectors as shown on Figure 1.



Figure 1: Vertical and oblique photo images of Rocks Road cliff, and Cliff Sectors (A to H)

3 ENGINEERING GEOLOGY AND SLOPE FAILURE MODES

The cliff is comprised of Tertiary age sandstone and weak mudstone beds, with bedding dipping steeply into the cliff (at about 65°). Joints in the rock strongly influence the stability of the cliff. The most dominant joint set dips out of the face at 40° to 55°. This joint set is considered to control the overall ultimate stable slope angles along the cliff (angle varies in different parts of the cliff).

Observations of failures from the cliff over a period of time have allowed characterisation of the main modes and distribution of failures.

Failure modes observed:

- Slaking and slabbing of mudstones
- Planar failures (joint controlled)
- Small rock falls

- Larger rock falls/ rock slides
- Soil slumps

The highest risk sites occur where the weaker mudstone slopes have eroded back to flatter angles undermining the overlying more resistant sandstone layers. Collapse of the resulting overhangs (eg Photographs 2 and 3) has resulted in large failures which have closed Rocks Road. Other failure modes including soil slumps and isolated rock falls also pose risks to road users, in particular southbound cyclists. In the last few decades the slope instability has predominantly been concentrated in the section between No 28 and No 36 The Cliffs (Sectors E and F); however a significant rock fall event in July 2008 occurred from below No 14 / 16 The Cliffs (Sector C) indicating the potential for high consequence events elsewhere along the cliff.

4 SLOPE FAILURE EVENTS

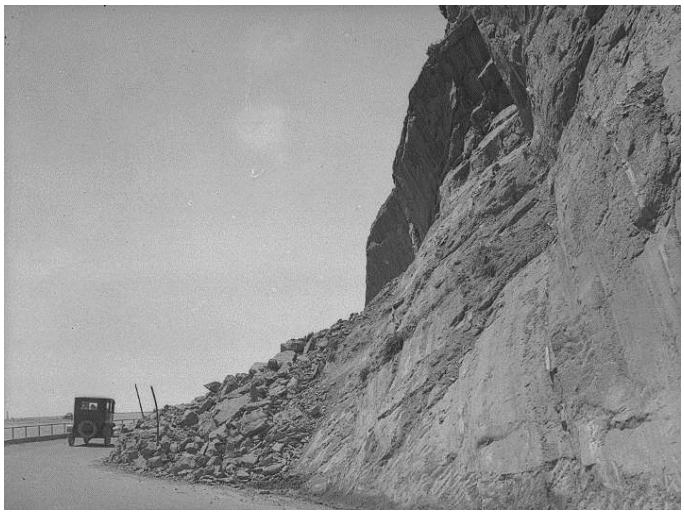
4.1 Late 19th and Early 20th Century

A week after the road opened in 1899, loose rocks were removed from the cliff face after a car was struck by falling rocks (Anderson, 2002). Photograph 3 shows the site of a rockslide event early in the 20th century.

New Zealand Geotechnical Society Inc. 19th Symposium, Queenstown 2013



Photograph 2: July 2008 rock slide debris (Sector C) with pedestrian walkway to left (Nelson Mail Photo)



Photograph 3: Early 20th century rock slide debris with overhangs formed along bedding (Sector G?/H?)

4.2 1990 Failures

Rock falls hit cars in two events in early 1990 and a large (500 m^3) slip in Sector F closed the road for 2 days in August 1990. As a result of these failures, an assessment of risk mitigation options for the cliff was considered, and a number of reports were prepared in the early 1990's. In 1994 in Sector F a programme of significant slope works involved installation of grouted steel dowels, draped mesh, and a slope crest palisade wall (Palmer and Denton, 1998).

4.3 2000's Failures

Two planar rock block failures occurred from the lower cliff within 10 m of each other in Sector E in 2005. Engineering geological mapping following these events suggested that the blocks had failed on the same 50° outward dipping joint plane, and that failure of the intervening (larger) intact block was a possibility. The associated risk to the road was assessed

as high, and rock bolting of this block was carried out in 2008 as a pre-emptive risk mitigation measure.

On 11 July 2008, a 70 m^3 rock slide occurred from an overhang at mid cliff height in Sector C following heavy rain, approximately 100 m south of the Basin Reserve, in an area not normally prone to rock fall / slips. Debris covered the full road width (Photograph 2). Engineering geological inspections (with the aid of a crane and abseiling) of the source area and adjacent cliff identified open partings along bedding on either side of the failed area, suggesting further similar failures were likely. Anchoring of these areas was recommended, and was carried out in 2009.
In addition to the rock failures, soil slips were common after heavy rainfall with debris encroaching onto the south-bound lanes.

5 RISK ASSESSMENT

Following the 2008 rock slide event, risk assessment of the whole cliff was carried out, based on an engineering geological characterisation of the cliff and observations of past failures. The risk assessment involved assessment of the likelihood and consequence of failure events on road users. The cliff was subdivided into 8 sectors (Figure 1) based on factors affecting the risk, such as: slope angle and height, precedent failure events, shoulder width and the presence of stabilisation measures. Key modes of failure within each sector were identified and each mode then assessed for likelihood of occurrence and consequence to road 'users' if they did occur. The resultant risk for each mode of failure was determined and the highest risk determined and assigned as the risk for that sector.

The highest risk sites were determined to be the slopes immediately adjacent to the July 2008 rock fall site in Section C where longitudinal cracks suggested incipient failure, and Section E (below 28 the Cliffs), with the next highest risk being identified at Section H (below No 36 The Cliffs) - Table 1.

The strategy for managing the cliff was to:

- Target the higher risk sites (those which have highest likelihood of having high consequence events) and implement risk mitigation at those sites
- Manage the risk at other 'lower' risk sites though inspections and monitoring and implement mitigation measures locally where an increased risk is identified from the inspection / monitoring programme.

6 RISK MITIGATION

The 2008 risk assessment identified the risks along the cliff, and recommended specific stabilisation actions in the short term for the higher risk sites. The highest risk site, in Sector C, was subsequently stabilised with anchors and shotcrete in 2009 – reducing the risk in this area to 'moderate'.
The next highest risk sites identified were in Sector E (high risk) and Sector G (moderate to high risk).

Risk mitigation has been carried out reactively and/or proactively. When failures occur 'without warning', debris clean-up and inspection to determine the remaining risk is carried out. If the risk is deemed acceptable the road is reopened. However, where there is uncertainty over the risk, or if the risk is determined to be significant, risk mitigation measures are implemented.

Risk mitigation measures at Rocks Road have included:

- Routine and post-slip event scaling of loose material / inspections by abseiling
- Geotechnical inspections – crane, abseil, helicopter

New Zealand Geotechnical Society Inc. 19th Symposium, Queenstown 2013

- Monitoring of cliff crest using survey targets in Sector E
- Installation of temporary debris barriers (water filled plastic barriers, weighted shipping containers in Sector B in December 2011)
- Slope cutback (large scale - sector H, 1960's, moderate scale - sector E, 1990)
- Anchoring of vulnerable blocks using: grouted steel dowels and draped mesh (Sector F - 1994), grouted rock bolts, and reinforced shotcrete (Sector E - 2008, Sector C – 2009, Sector B - 2012)

It is envisaged that future risk management strategies along the cliff will be a combination of a number of these methods. Other options include permanent catch barriers and relocation of traffic lanes further away from the cliff. In the 2008 assessment, further assessment of mitigation options was proposed to determine the most appropriate methods for the various sections of the cliff.

7 DECEMBER 2011 EVENTS

The Nelson city area was subject to approximately 300 mm of rain from 13-15 December 2011. This resulted in significant damage around the region with a State of Emergency called for a period of at least 1 week. Landslides and flooding resulted in damage to roads, buildings, properties and utilities. Significant slippage occurred from the Rocks Road cliff which resulted in closing the road, one of the two main routes out of the city to the south and west. Below the Rocks Road cliff, the road was affected by rock slides (Photograph 4), slippage of soil overlying bedrock and flooding (Photograph 5). After initial clean-up of debris, a crane and abseil based engineering geological inspection was made of the whole cliff to identify any further imminent failures. During this process obvious loose material was removed by abseil contractors. Open partings along bedding were identified behind new overhangs formed above the main rock fall site (Photograph 4) indicating the potential for further significant rock fall. A further 150 mm of rain fell on 27 December 2011 with rock fall onto the road from Sector E, resulting in road closure for a further 24 hours.

New Zealand Geotechnical Society Inc. 19th Symposium, Queenstown 2013



Photograph 4: December 2011 rock fall site from overhanging section (s) at northern end of cliff (Sector B). Rock fall boulders on road edge (b).



Photograph 5: Failure of soil mantle overlying rock (Sector G) and consequent flooding (Dec 2011), with slips also evident in Sector H at right. Draped mesh of Sector F at left. Fairfax Photo.

8 LESSONS LEARNT

The December 2011 heavy rainfall events provided an opportunity to review of the 2008 risk assessments for the cliff (Table 1). During the December 2011 events significant failures occurred, particularly in Sector B (Moderate risk in 2008 assessment) and Sector G (Moderate to High risk in the 2008 risk assessment).

Table 1: 2008 Cliff risk assessment and observations of slope failures in December 2011

Sector	2008 Risk Assessment[1]	December 2011	Comment
A	Very Low	Road not affected. Small rock falls into bushes away from road (<15 m^3).	
B	Moderate	Large rock fall/slide from overhang, debris covers cycle lane and into southbound lane.	Influence of overhangs needs more attention.
C	Moderate [2]	No significant failures	
D	Moderate	Numerous soil slumps onto road with associated flooding.	Very heavy rain saturated all soil with most soil peeling off rock.
E	High	No failures in 13 December event. But rock fall failure in 27 December rain event resulting in re-closure of Highway for 24 hours	2008 'High' risk validated by late December rockfall.
F	Low	Numerous soil slumps under draped mesh (1994) – affected south-bound cycle lane.	Damage to mesh from soil slumping under mesh.
G	Moderate to high	Moderate sized soil failure onto south bound lane, with flooding over full road width.	Consistent with 2008 Assessment.
H	Low to moderate	Significant soil slump failures onto road edge.	As for Sector D extent of failures not anticipated by 2008 assessment.

1. Relative risk only
2. Sector C risk reduced from 'high' in 2009 after anchoring measures implemented

The extent of failures in the extreme December 2011 rainfall event, on 'low – moderate' risk sites was not anticipated by the 2008 Cliff assessment, but the consequences of these failures were low. Over-saturation of the soils resulted in pervasive slumping of soils in Sectors D and H, and uncontrolled overland stormwater flow resulting in debris floods and flooding (Photograph 5). The 2008 assigned risk in these areas was lower, in part because the impact of soil failures does not typically have the same threat to life safety as rock fall.

The 'moderate' risk assigned in 2008 to Sector B in part reflected the perceived ability of the lower slope, being shrub-covered and low to moderate-angled, to 'catch' much of the debris from small to moderate size events. The fact that the debris which fell in December 2011 only had a minor encroachment onto the road (as compared with 2008 rock fall – Photograph 2), was not inconsistent with this assigned risk.

However, the December 2011 Sector B rock fall has highlighted that the risk of significant collapse of overhangs is not just confined to Sector C (where the 2008 rock fall occurred), and that attention should be given to mitigating the risk of overhang collapse elsewhere in both

these sectors, and elsewhere on the cliff eg Sector D. Evidence from historic photographs (Photograph 3) backs this up.

9 CONCLUSIONS

Ongoing slope failures on Rocks Road cliff have resulted in development of a risk management strategy for cliff stability along this section of the state highway. Recent risk mitigation along the cliff has involved abseil scaling inspections, anchoring of vulnerable sections of cliff and closure of the road following the December 2011 storm event. Experience from this location indicates the importance of careful geotechnical inspections, documentation of the location and modes of failures, and risk assessment to allow optimal targeting of risk mitigation measures.

Risk assessment has involved assessment of the likelihood and consequence of events on road users. As part of this, the cliff has been characterised into 8 Sectors based on factors affecting risk such as slope angle and height, precedent events, shoulder width and the presence of stabilisation measures.

Two severe rain events in December 2011 allowed assessment of the validity of the 2008 risk assessment. In general the 2008 risk assessment was confirmed, with significant failure events occurring in the highest risk areas. However, the potential for infrequent (but high consequence) events eg. overhang collapse, has highlighted the importance of targeting these failure mechanisms in future risk management of the cliff. Although the moderate risk assessed was consistent with the lower likelihood, action should be considered from a resilience and safety perspective. Access to good documentation of previous failure events, as well as the ability to identify the key failure mechanisms in different parts of the cliff, will continue to assist future cliff risk management.

10 ACKNOWLEDGEMENTS

The authors acknowledge permission for publication of the paper from the New Zealand Transport Agency for whom Opus carried out the work. The contribution of various other geotechnical professionals – Janet Duxfield, Selvem Raman, Jayne Flack, Tiffany Krall and Doug Mason - in the assessment and implementation of the remedial works is acknowledged.

REFERENCES

Anderson, G (2002). "A History of Rocks Road Seawall". A contribution to the Journal of the Nelson Historical Society.

Palmer, S and Denton, P (1998). "Cliff Face Stabilisation Works, Rocks Road, Nelson". Roading Geotechnics '98. NZ Geotechnical Society Symposium. Auckland. P253-258

Opus International Consultants Limited (2008). "SH6 – Rocks Road, Cliff Management Strategy Report". December 2008 Draft. Report GER 2008/33.

Rockfall protection systems - the French approach

N Villard
G.T.S. (NGE), Grenoble, FRANCE
nvillard@gts.fr (corresponding author)

N McHugh
Avalon Industrial Services Ltd, Hamilton, NZ
neil.mchugh@avalonltd.co.nz

Keywords: rockfall, slope hazard mitigation, catch fence, dynamic barrier,

ABSTRACT

In the French Alps the latest generation of high performance rockfall protection systems have been developed by G.T.S. taking a relatively lightweight approach, developed from decades of experience of working with more traditional catch fence systems. The new barriers have minimal anchoring requirements and are effective in difficult ground conditions. They are designed to be as simple and rapid as possible to install in any location, including high on the slope, by rope access workers. Barriers can now cost effectively be installed near the rockfall source, where energies are lower and where shorter fences can effectively mitigate the hazard. System components have been kept as simple as possible to ensure maximum lifetime, minimise maintenance and to facilitate repairs in the field at low cost when necessary.

New Zealand Geotechnical Society Inc. 19th Symposium, Queenstown 2013

1 INTRODUCTION

Rock instabilities pose a significant risk to infrastructure and development in mountainous areas. Risks are being increased in the European Alps by global climate change at the same time as research is increasing knowledge of instabilities and their propagation. Over recent years, significant developments have been made in assessment and mitigation methods, especially in the range of options available for rockfall fences. Catch fence solutions, first engineered in the 1950s, are well established and can replace or complement *'active'* solutions. Other *'passive'* protections structures such as galleries or embankments can be expensive and usually require large space and heavy foundations whereas places to install them can be rare (Boutillier, 2011).

It is important to design optimised structures. Rockfall fences need to offer efficient installation and maintenance, which often means minimising steel weight and anchoring. In locations where other solutions are not feasible, the latest generation rockfall fences come into their own, especially on difficult access sites, with steep irregular slopes and difficult soil and rock conditions.

Recently the new European ETAG 027 guideline (EOTA, 2008) has defined some minimum requirements, including full scale tests. Optimising mitigation strategies using dynamic barriers means using these standards and going further (Stelzer, 2011), through a pragmatic field approach, as historically followed in the French Alps, and more and more used as a best practice reference worldwide.

2 BACKGROUND

2.1 Historical developments

The management of natural hazards in French territories takes place in a wide range of environments, from high mountains to tropical islands, with a high density of 60 million citizens exposed not only to landslides, rockfall, avalanches or debris flow but also volcanoes, earthquakes, tsunami, and flooding. This diversity through centuries experience and some major

disasters, led to a balanced management strategy always bringing in pioneering measures and new developments.

Created in 1860, the official government department in charge of restoration and reforestation in mountain territories (Figure 1) is the oldest service in geohazard mitigation (RTM, 2010). Following World War II, the increasing density of infrastructure lead to the development of conventional protection with at source active and passive measures (bolting, nettings, and concrete abutments) or occasionally massive passive structures. Early rockfall fences were first derived from static snow barriers against avalanches, then in the 1950s, stockpiles of anti-submarine ring nets used for protecting ports during the war were diverted from their initial purpose onto rock slopes.

In the 1970s, methods to mitigate rockfall were revolutionized, initially in France, when mountains guides and cavers improved and adapted alpine rope access methods for professional geotechnical contracting use (the Petzl family were one of the early developers and became well known later for manufacturing climbing gear). Finally, regarding rockfall protection, one of very first Guidelines for barriers was adopted in the French Alps (NF, 1996).

New Zealand Geotechnical Society Inc. 19th Symposium, Queenstown 2013



Figure 1: geohazard mitigation in Dauphiné, 1890 (courtesy ONF RTM 38)

Nowadays about 19 % of municipalities are exposed to landslide risks (PPR, 1999), mainly rock slopes instabilities. Furthermore, some very low risk acceptance infrastructures such as nuclear plants, TGV high speed train or urban metropolis in the Alps (Table 1) have resulted in optimised and efficient policies in land planning, well known to be the most conservative in Europe (Abbruzzese, 2011).

Table 1: indicative events in Grenoble valley, 500 000 citizens (INTERREG, 2005)

Size of rock slides:	100 m^3	10 000 m^3	100 000 m^3
Return period:	1 year	20 years	80 years

2.2 The search for efficiency

This extensive experience has led to balanced practices, with both quantitative and qualitative methods, sometimes deterministic but always preferring empirical expertise and observational data from the field. Experience has led to modeling tools being used moderately and most often as a decision support (liability considerations and the facility to obtain meaningless figures had sometimes lead to bad decisions when using modeling alone). As far as possible, relatively light structures are installed upslope on hillsides, near the source. Over and above the use of rope access, adapting the solution to the field is a guiding principle, rather than the opposite, which is seen sometimes with curative and oversized solutions. Best practice geomechanical engineering now permits us to better control the propagation of falling rocks, dealing with changing nature rather than working against it.

Some related innovations illustrate this philosophy, which also takes into account cultural and liability aspects. For example; warning systems using electrical wire rope fences have been widely installed since 1970 on sections of the French rail network exposed to rockfall, a total of 2,300 km (Pollet, 2011). Other structures have been developed such as composite embankments and energy absorbing rock shelters (Figure 2) incorporating buckling steel dissipaters (Tonello, 2001). Recently, the protective effect of forest against rockfall has also been integrated in new and efficient risk management practices (Berger, 2012), sometimes offering efficient eco-structural measures.



Figure 2: innovative rock shed with buckling fuses (Tonello, 2001)

2.3 The case of rockfall barriers

In this environment some contractors developed early dynamic fences long before ETAG standards were proposed with a "field approach" different to industrial solutions. The primary objective was to offer cost effective well engineered options to meet their own and their client's needs. As mentioned, the emergence of rope access in the French Alps coincided with the pioneering of guidelines for rock fall mitigation. The need to install these solutions in steep, narrow and remote locations lead to a relatively lightweight approach with minimal anchoring requirements. The efficient use of helicopters for lifting materials required design loads to be optimized under 800 kg. Moreover, fences have been designed not only for ultimate extreme events, but also very much with maintenance in mind and therefore taking into account the small and very common impacts over a reasonable 20 – 25 years lifetime. Some original and unique concepts have been developed such as nets on the upslope side of the fence and posts without anchors or foundations (Trad, 2011). 25 years ago the calculation of the performance of such fences was already in the early stages and some contractors conducted pioneering full scale tests in addition to theoretical guidelines (NF, 1996). .

3 FENCE DESIGN AND DEVELOPMENT

Stopping boulders effectively requires fences to dissipate the energy of the rock with a suitable safety factor. A fence's flexibility provides advantages over most rigid barriers through reduced costs, more versatile placement options, and simple design process using well tested systems. Some fences offer interesting alternative solutions (Trad, 2011) in being able to be installed far upslope, above the facility and near the rockfall source area.
Fence structures are constituted of the following components:

- Nets to intercept the rock
- Post to offer height of interception and to stretch out the nets
- Energy dissipation devices
- Cables and accessories
- Anchors and foundations (often these are underestimated with heavier fences)

New Zealand Geotechnical Society Inc. 19th Symposium, Queenstown 2013

3.1 Components

3.1.1 Nets

Historically, anti-submarine ring nets were widely adapted to rockfall protection throughout Europe. When stocks became depleted, similar ring nets were reproduced by industrial manufacturers when it would probably have been more useful to look at improving on the existing solutions. Some products were indeed too rigid and static, others would severely contract when being installed on a cliff (Badger, 2009) so that it was very difficult for crews to pull and shackle adjacent panels and to have 100 % of the paid nets surface effective on the slope.

As an installer of these primitive systems, in response, the contractor G.T.S. decided to develop and manufacture new nets, especially designed for rockfall protection and using a patented concept of versatile woven wire rope connected with autostable clips (Figure 3). These nets are designed to accommodate nonlinear deformation and to ensure additional high energy dissipation through cable friction and plastic deformation of the clips. The asymmetric geometry of the mesh distributes impact forces over a large area and reduces the stress on upper structures and anchors. Numerical DEM and FEM models have been developed with good agreement to multi-scales tests (Trad, 2011).

The new net concept remains flexible yet does not have the contraction problems, it is resistant (up to 900 kN/m), light (10 kg/m2), easy to install below a helicopter and repairable in-situ with clip replacements. It has been used worldwide since 2005, including for example on one of the largest operation in rockfall mitigation under severe coastal conditions, with about 250,000 m^2 on Reunion Island, Indian Ocean (Figure 4).

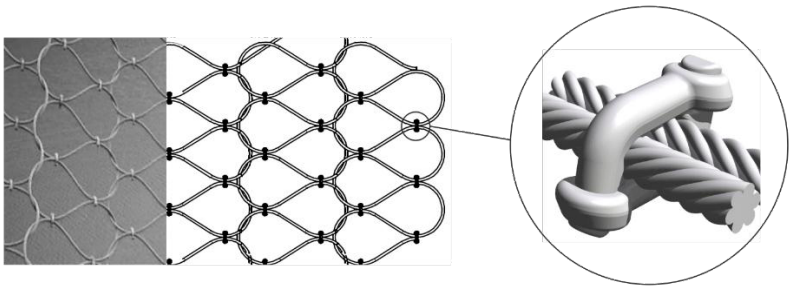


Figure 3: G.T.S. clip and anisotropic nets (here 350 mm diameter loops, 16 mm cable)



Figure 4: 250,000 m^2 of anisotropic nets on Reunion Island (Indian Ocean)

3.1.2 Dissipation devices

To absorb high energy during impact, dissipation devices have to develop permanent deformation. The latest concept developed uses the buckling of an aluminum profile containing two loops of a reeving wire rope (Figure 5). This innovation permits us to control force, deformation and elongation under energies up to 400 kJ (Trad, 2011).

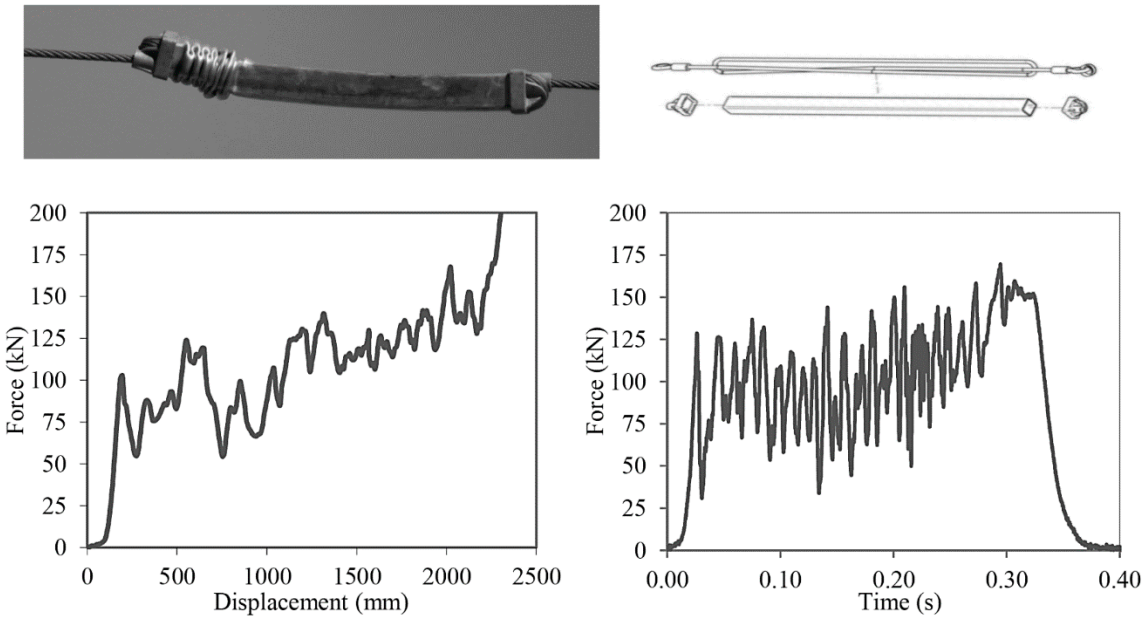


Figure 5: buckling mode dissipation devices with some static and dynamic tests

3.2 Implementation of high energy fences

Since the 1990s, these high energy rockfall fences (3000 kJ and 5000 kJ) have conformed to the principles below, which provide high performing and cost-efficient technologies (Figure 6). These fences now also have the new ETAG 027 and CE certification.

- The structure should distribute energy as widely as possible. The use of orthotropic nets optimizes loads on anchors and maximizes post to post distances (currently 12 m).
- Maintenance on rockfall fences has proven to be mainly due to small and common events. Posts can be protected by installing nets on the upslope side (sack geometry). This also simplifies and reduces costs of crossing creeks and irregular field topography. Furthermore, components are designed to be individually replaceable and repairable, avoiding the need to removing large parts of the fence after rockfall events. Dissipation devices are implemented on each post and net panels are supported by only one top rope.
- Supply of fences being a relatively minor part of the installed cost, these fence designs are optimized for rapid installation; they do not use any anchors or concrete footings for the posts, having ground ropes linked to a single upslope and downslope anchor.

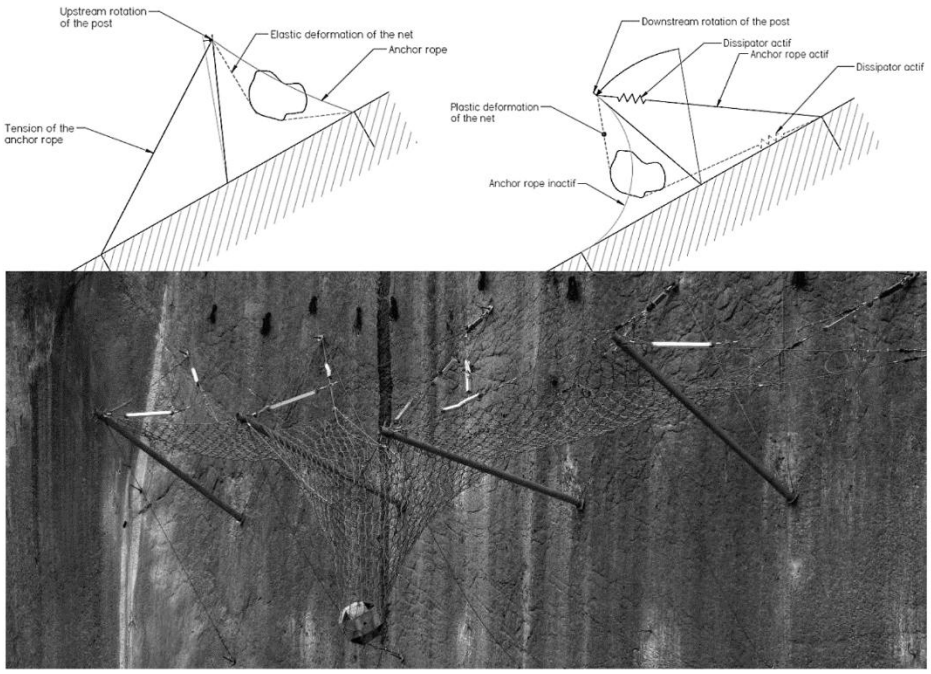


Figure 6: implementation and kinetic of a 3000 kJ barrier test to ETAG 027

3.3 Design process and lifetime

3.3.1 Risk assessment

Common nomenclature for rockfall fences uses a design impact load called *'service energy level'* (SEL) and an ultimate level called *'maximum energy level'* (MEL). Our experience is that these must be applied very carefully and only after taking into consideration the site's specific requirements. ETAG 027 is a very recent guideline which ensures a minimum quality with full scale tests but still needs additional experience and guidance to be used effectively. The first design step is to choose whether to design using a MEL or SEL approach, usually this is dependent on frequency of rockfall events (Peila, 2011).

An indicative classification (category A, B, or C) has been given in the ETAG, solely based on residual height for MEL level approach designs, but this is often wrongly used as it doesn't define a global performance indicator for the fence.
For instance; *'category A'* gives a residual height of 50 %, versus 30 % - 50 % for *'category B'*. With high frequency rockfall events, 50 % is not enough and this sole criteria of residual height is inadequate. Moreover, *'category A'* fences have sometimes shown lower performance to *'category B'* due to length effects and important surface reduction on lateral modules. This is why this category is only one of the necessary pieces of information to take into account. Other parameters to be considered include safety of installation, anchoring requirements and ease of future replacement of components. The use of lower specified energy levels such as *'Functional Energy Level'* (FEL) may then be relevant to analyze the lifetime (Richards, 2012). Finally, installing *'category B'* fences may be more cost-effective than installing *'category A',* which have often proved oversized. ETAG 027 requirements combined with these field considerations has confirmed the success of the strategy developed early in the 1990s on the now certified G.T.S. fences.

3.3.2 Installation and maintenance

Fence construction costs are commonly 2 to 3 times the cost of materials, sometimes 4 to 5 times in difficult locations. Moreover, post foundations and anchors account for the major portion of installation (Duffy et al, 2012) almost always when helicopters or rope access is required.

Originally developed to offer alternative scenarios to heavy structures or at source treatments, lightweight fences are now the only option for rockfall mitigation in some cases. Advantages are simplicity, rapidity and safety to install for crews in any location and with almost any ground quality. Since recent new guidelines, installation feedback from contractors highlights very differential ratios (from 1 to 3) for the overall same solution from different manufacturers, such as: weight of fence and steel, quantity of anchors or concrete foundation, duration of installation, number of modules to dismantle to maintain components, and of course global cost. That's the reason why attempting to separate tenders for supply and installation can be impossible.



Figure 9: installation and maintenance of high energy ETAG 027 fences.

CONCLUSION

The best practices of the French approach to rockfall barriers have been developed following extensive experience on the field. Relatively lightweight but high energy fences are sometimes the last remaining option, offering optimized barriers which are able to be installed everywhere, including near the rockfall source, at minimal expense.

Improvements now under research and development include the appropriate use of ETAG 027 guidelines within the design process and scientific framework such as non-linearity modeling between components (Volkweins, 2004) or inertial limitations (Hambleton,et al 2012).

REFERENCES

ABBRUZZESE, J.M. et al. (2011) Influence of hazard zoning guidelines and methodologies on land use planning, in *Interdisciplinary Rockfall Workshop proceedings*, Innsbruck, AT.

BADGER, T.C. et al. (2009) Use of ring nets for slope protection for rockfall, in *Experimental Feature Study* WSDOT Washington, US.

BERGER, F. et al. (2012) Integrating forests in the analysis and management of rockfall risks, in *Landslides and Engineered Slopes proceedings,* Banff, CA.

BOUTILLIER, B. et al. (2011) Designing a high energy rockfall kit, in *Applied mechanics and materials* Vol 82 pp 692-697 Trans Tech Publications, Switzerland

DUFFY, J.D. et al. (2012) Flexible rockfall fences, in *Rockfall: characterization and control, by A.K. Turner and R. L. Schuster* pp. 526-553 Transportation Research Board, Washington, US.

EOTA (2008) ETAG 027 Guideline for European Technical Approval of Falling Rock Protection Kits. *EOTA*, Brussels, BE.

HAMBLETON, J.P. et al. (2012) Perforation of rockfall protection barriers by normal block impact, in *46th US Rock Mechanics Geomechanics Symposium* Chicago, US.

INTERREG (2005) II Prévention des mouvements de versants et des instabilités de falaises *Programme Interreg II C Falaises*, France – Italy.

NF (1996) Equipements de protection contre les éboulements rocheux, écrans de filets *Norme française NF P 95-308 AFNOR* Paris, FR.

PEILA, D. et al. (2011) Design of rockfall net fences and the new ETAG 027 European guideline, Technical note in *Nat. Hazards Earth Syst. Sci., 9,* pp 1291–1298 EGU, Vienna, AT.

POLLET, N. (2011) Gestion du risque rocheux sur le réseau ferré, in *Géologues 169*, Paris, FR.

PPR (1999) Plan de prévention des risques naturels, mouvements de terrain, guide méthodologique *La documentation française*, Paris, FR.

RICHARDS, L. (2012) Rockfall design strategy, *Project memo CERA CCC,* Christchurch NZ.

RTM (2010) 150 ans de lutte contre les risques naturels, in *Restauration des terrains de montagne* ONF, Ministère de l'alimentation, de l'agriculture et de la pêche, France.

STELZER, G. et al. (2011) ETAG 027, And now what? in *Interdisciplinary Rockfall Workshop proceedings*, Innsbruck, AT.

TONELLO, J. (2001), Couverture pare-blocs structurellement dissipante, in *Label IVOR 01.1. Mission Génie Civil*, Ministère de l'Equipement, France.

TRAD, A. et al (2011) Multi-scale analysis on an innovative flexible rockfall barrier, in *Rockfall engineering, by S. Lambert & F. Nicot* pp 303-342 ISTE - Wiley, London, UK.

VOLKWEIN, A. (2004) Numerische simulation von fexiblen steinschlagschutzsystemen, *Ph D Thesis, ETH,* Zurich, CH.

Wallace, S. (2013)
Macro and micro scale assessment and quantification of sloping ground damage following the Canterbury 2010/2011 earthquake sequence
Proc. 19th NZGS Geotechnical Symposium. Ed. CY Chin, Queenstown

Macro and micro scale assessment and quantification of sloping ground damage following the Canterbury 2010/2011 earthquake sequence

S Wallace
Tonkin & Taylor Limited, Christchurch, NZ
Swallace@tonkin.co.nz

Keywords: Earthquake, Land, Deformation, Mapping

ABSTRACT

Earthquakes in September 2010, and February and June 2011 caused significant damage to land in the hill suburbs (Port Hills) in the city of Christchurch, New Zealand. Ground damage observed included; failure of retaining structures; failure of unsupported cuts and fills; displacement of natural slopes, and collapse of cliffs, as well as rock fall.

Identification and quantification of the ground damage in the Port Hills at a macro scale began soon after the M6.3 earthquake on 13 June 2011. Assessment of the micro scale damage on an intensive property by property basis was undertaken over a 12 month period.

This paper provides an overview of the macro scale ground damage mapping and micro scale land damage assessments undertaken in the Port Hills, on behalf of the Earthquake Commission.

1 INTRODUCTION

The city of Christchurch, in Canterbury, New Zealand, and the surrounding area, was subject to significant close proximity seismic activity, for more than a 12 month period following the M7.1 'Darfield' earthquake which struck on 4 September 2010. Subsequent significant earthquakes included the M6.2 earthquake on 22 February 2011, M5.9 and M6.3 earthquakes on 13 June 2011 and, a M5.9 earthquake on 23 December 2011. These earthquakes are collectively known as the Canterbury Earthquake Sequence (CES).

Christchurch is located on the coastal margin of an alluvial plain, north of Banks Peninsula. The seismic shaking caused by the CES resulted in extensive damage to land; generally comprising liquefaction and lateral spreading of flat land, and; significant deformation of sloping land, particularly in suburbs on the Port Hills, which comprise the northern slopes of Banks Peninsula,

In New Zealand the Earthquake Commission (EQC) is the primary insurer of residential land and property that suffers damage that is the direct result of a natural disaster. Immediately after each significant earthquake of the CES, macro scale mapping of the observed ground damage was undertaken by geotechnical professionals, working on behalf of the EQC.

Significant damage to residential land in the Port Hills was not realised in the initial 4 September 2010 earthquake, however subsequent events, particularly the 22 February and 13 June 2011 earthquakes resulted in widespread damage to land on residential properties in the Port Hills.

This paper outlines the processes used to characterise and capture the observed land damage in the Port Hills suburbs, at a variety of scales, and provides some commentary on the observations made, and lessons learned.

The physical processes and mechanisms that result in the different types of ground damage that were observed are discussed in other papers in these proceedings (Hunter 2013, Jackson & McDowell 2013, and Udell 2013).

New Zealand Geotechnical Society Inc. 19th Symposium, Queenstown 2013

2 GEOLOGY AND GEOMORPHOLOGY

Most of Christchurch City is constructed on relatively flat to gently sloping former alluvial outwash plains and swamp/back-beach/beach deposits (Brown & Weeber, 1992 and Forsyth et al. 2008). The Port Hills comprise the northern slopes of the Banks Peninsula Volcanic complex, which penetrates through the sediments, to rise above the Plains, and form Banks Peninsula.

The Port Hills are covered by a variable thickness of loess (windblown silt) which generally increases in thickness downslope. Colluvium, derived from loess, is generally encountered on the flanks of slopes, thickening downslope, forming wedge shaped fans with gentle to moderate slopes that interfinger and overlap. The colluvium and loess overlies the basaltic bedrock of the Lyttelton Volcanic group, a non-homogenous unit of basalt lava dominated by flow deposits that radiate outwards and slope gently downwards from the former volcanic vent, located within the present day Lyttelton Harbour, interbedded with scoria and pyroclastics (ash).

The ground surface is generally sub-parallel to the irregular upper surface of the underlying bedrock. Slopes range from gentle to steep, generally being steepest nearer to the ridge crests. Bedrock outcrops are located sporadically throughout the hill suburbs, in particular near the crest of spurs and ridges, and close to the present day coast, where relic sea cliffs, up to 80 m high, are located.

New Zealand Geotechnical Society Inc. 19th Symposium, Queenstown 2013

Groundwater is not typically encountered within the soils/bedrock that form the slopes of the Port Hills, although variations in moisture levels are commonly associated with changes in geological conditions. In the alluvial materials at the base of the sloping ground, groundwater is generally encountered with 2 to 3 m of the ground surface.

3 ASSESSMENT OF LAND DAMAGE

3.1 Background

As the only insurer of residential land in New Zealand, the EQC, acting in response to the Earthquake Commission Act 1993, requires that every residential property that has suffered significant ground (land) damage as a result of a natural disaster be subject to a site specific land damage assessment, as part of the insurance claim settlement process.

Observations made by Engineers and Geologists from the author's firm immediately after the 4 September 2010 earthquake indicated that land damage had predominantly been confined to flat land. This land damage was principally related to the effects of liquefaction and lateral spreading.

The epicentre of the 22 February 2011 earthquake was directly beneath the Port Hills, less than 6 km southeast of the Christchurch CBD. The felt shaking intensities/ground accelerations experienced by many residents in the urban environment exceeded those felt in September 2010, despite the lower magnitude earthquake. Significant damage to land, infrastructure and buildings in the hill suburbs, previously only slightly affected, was observed following this earthquake, and again following the two closely spaced earthquakes of 13 June 2011.

The types of land damage observed in the Port Hills suburbs as a result of the February and June 2011 earthquakes could generally be categorised into one of the following:

- Rock fall and cliff collapse;
- Large scale land movement;
- Small scale land movement and retaining wall failure.

A more detailed quantification of the land damage is provided in the following sections of this paper and in other papers in these proceedings (Hunter 2013, Jackson & McDowell 2013, and Udell 2013).

Mapping and assessment of sloping land was based on the success of similar rapid assessment of

damage to flat land; a process that began soon after the 4 September 2010 earthquake, which was repeated and refined following each subsequent significant earthquake of the CES. This mapping generally followed a pattern, decreasing the scale, and increasing the detail captured, starting at a macro-scale, and moving to local and then micro-scale assessment. The processes followed in the Port Hills are detailed below.

The land damage mapping and classification described in this paper was primarily undertaken to assist the EQC in understanding the nature of the event, in order to prepare the appropriate insurance response.

3.2 Macro Scale land damage assessment

Following the 4 September 2010 earthquake, regional scale (macro) mapping of the observable damage to flat land was undertaken initially by aerial survey from a helicopter, and, following this, rapid vehicular road level reconnaissance. This regional scale approach to land damage mapping was possible as the effects of liquefaction of the subsurface (ejected sand/silt and water) were easily distinguished from the air and when driving around the city. As only minor land damage was recorded in the Port Hills suburbs as a result of the 4 September 2010 earthquake, regional scale mapping of these areas was not undertaken.

The 22 February 2011 earthquake caused widespread damage to residential land and dwellings in the Port Hills. However, regional (macro) scale mapping of the land damage was not completed in the Port Hills suburbs, as the site specific damage (cracks in the ground, damaged retaining walls and fallen boulders) was significantly more difficult to accurately assess from an aerial perspective. Additionally, rapid assessment of land damage from vehicles on roads was difficult because the slope of the land and urban development prevented the damage from being readily observed.

3.3 Local scale land damage assessment

Following the two earthquakes of 13 June 2011, which caused further significant damage to land in the Port Hills, local scale, at a level between macro and micro scale, land damage mapping of residential properties in the Port Hills was undertaken.

This process comprised a walkover road level observational assessment of land damage, recording details on large scale (typically 1:3000) plans. Geotechnical professionals rapidly assessed the type of damage on each residential property by walking street to street throughout the hill suburbs. The land damage on each property was noted on the large scale plans, using a common legend to represent the seven different categories on sloping land (see Table 1). The plans completed in the field were returned to the office at the end of each day and the information captured was digitised and able to be used to inform decision makers about the worst affected areas soon after being captured.

As there was often more than one mechanism causing land damage on the hill properties, the process that had been used on the flat land, where a property was designated as having only one land damage 'category' was altered, such that additional information, in particular information about retaining wall damage, could be captured easily. This required that damage to retaining walls be noted by colour coding a border around the property on the plans, while the type of damage to the land was denoted by coloured hatching

New Zealand Geotechnical Society Inc. 19th Symposium, Queenstown 2013

Table 1: Local scale land damage assessment categories

Land Damage Category	Mapped Colour	Description
Rockfall		Large scale 'collapse' of bedrock cliffs resulting in inundation of properties (land/structures/assets) at the base of the cliff.
Minor land movement		Cracking and deformation of land resulting in lateral and vertical displacement. Future displacement unlikely. Individual cracks less than 50mm wide, or less than 100mm cumulative crack widths over a typical 30 m section.
Major to severe land movement		Cracking and deformation of land with downslope component and/or cracking may result in future downslope lateral or vertical displacement. Individual cracks greater than 50mm wide, or more than 100mm cumulative crack widths over a typical 30m section.
Inundation		Inundation from failed slopes (retained or unretained)
Minor retaining walls		Retaining walls less than 1.5 m high damaged
Major retaining walls		Retaining walls more than 1.5 m high, or less than 1.5 m high and supporting the dwelling or accessway damaged
None[1]		No apparent observed land damage or signs of land cracking visible at the surface.

1 – Although no ground damage was noted, building damage is still possible

Figure 1 below is an example of the results of the local scale mapping. Figure 2 shows the detail that was captured on a property by property basis for one area of the Port Hills.

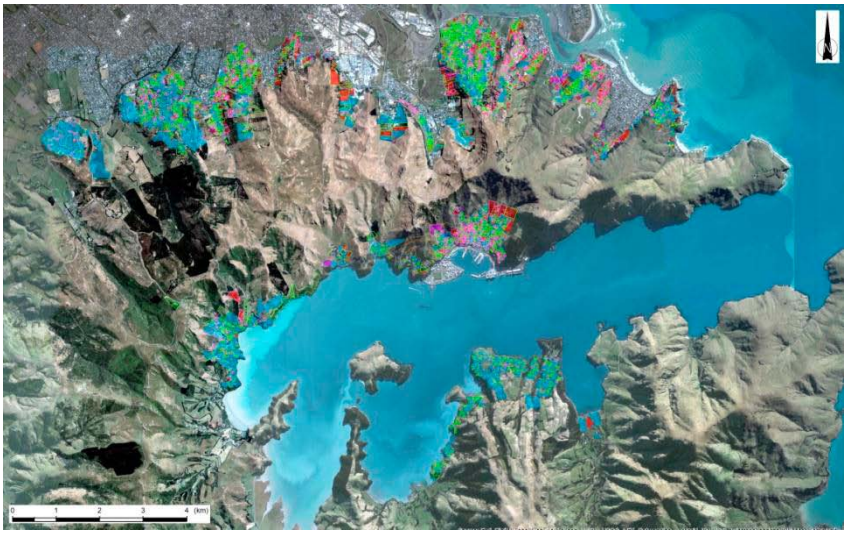


Figure 1: Local scale mapping undertaken as a foot based road level assessment identified the severity of the ground damage observed on the Port Hills following the 13 June 2011 earthquakes



Figure 2: Detail view of local scale mapping obtained after 13 June 2011 earthquake

3.4 Micro scale land damage assessment

A property specific inspection and assessment of each residential property that suffered damage as a result of the earthquakes was completed for the purposes of EQC insurance claim settlement. These site by site assessments are considered to be the ultimate, or micro scale, assessment of land damage.

Micro scale assessments of land damage on properties on the Port Hills began soon after the 22 February 2011 earthquake, before the overall macro and local scale mapping for the Port Hills had been completed. Assessments were initially undertaken on an 'as requested' basis. However it soon became apparent that some areas were more significantly damaged than others, and in some of the more significantly damaged areas, similar damage, and damage that appeared to represent a mechanism that extended across a number of properties, could be traced across neighbouring properties.

Approximate boundaries were drawn around these properties to define the areas. These areas were termed 'Area wide assessment areas' (AWAA's) and properties within these areas were subject to a more detailed assessment, which in some cases included sub-surface investigations and installation of monitoring equipment.

On completion of the local scale mapping after the 13 June 2011 earthquake 22 AWAA's were identified across the Port Hills. These areas ranged in size from less than 10 to more than 300 residential properties. The observations made and results of the ongoing micro scale AWAA work are discussed in more detail in other papers in these proceedings (Hunter 2013).

Micro scale assessment of land damage on more than 5000 properties on the Port Hills has been completed to date. The information collected continues to be used by EQC to assist in claim settlement. The information held by EQC relating to specific damage on individual properties is privileged and as such, plans showing the damage at this 'micro' scale have not been reproduced publicly.

New Zealand Geotechnical Society Inc. 19th Symposium, Queenstown 2013

4 CONCLUSIONS

Land damage observation and characterisation at a variety of scales has proven to be a useful tool in planning and responding to the aftermath of multiple earthquakes in the Christchurch region.

The information obtained has been, and continues to be used in the ongoing recovery of the region. This emphasises the need for high quality management of data, including collection by experienced personnel, using proven systems to ensure continuity and reliability of data collected from widespread areas and as a result of multiple events.

The information collected also provides insight into the likely effects of any future events in the hill suburbs of Christchurch, and could be used to allow appropriate planning for these events, both locally and in other areas where residential development has occurred on sloping land that may be affected by seismic events.

ACKNOWLEDGEMENT

I wish to thank the Earthquake Commission and Tonkin & Taylor Ltd for supporting the preparation of this paper, in particular to Tim Sinclair for his comments and review.

I would also like to acknowledge to the professional people working together in cross consultancy and inter-agency networks in a common response and commitment to provide information to and to help the recovery of the Canterbury region in the aftermath of the Canterbury Earthquake Sequence. These people, in particular the staff of agencies that are not always thanked appropriately for the work that they do in difficult circumstances, are also acknowledged.

REFERENCES

Brown L.J. & Weeber J.H. (1992) Geology of the Christchurch Urban Area. Scale 1:25,000. Institute of Geological & Nuclear Sciences geological Map 1.

Forsyth, P.J.; Barrell, D.J.A.; Jongens, R. (compilers) (2008) Geology of the Christchurch area. Institute of Geological and Nuclear Sciences 1:250 000 geological map 16. 1 sheet + 67 p. Lower Hutt, New Zealand. GNS Science.

Hunter, R.P. (2013) Seismically induced displacement of land affecting multiple residential properties in the Port Hills, Christchurch, New Zealand, following the 2010/2011 earthquake sequence *Proc. 19th NZGS Geotechnical Symposium. Ed. CY Chin, Queenstown.*

Jackson, M. & McDowell, B (2013) Monitoring and Measurement – Is the land displacement observed in the Port Hills as a result of the 2010/2011 Canterbury Earthquake sequence co-seismic? *Proc. 19th NZGS Geotechnical Symposium. Ed. CY Chin, Queenstown.*

Udell, H. L. (2013) An initial assessment of the effects of seismically induced ground deformation on the occurrence of localised instability following rainfall in the Port Hills, Christchurch *Proc. 19th NZGS Geotechnical Symposium. Ed. CY Chin, Queenstown.*

The use of polystyrene (EPS) as lightweight embankment fill

G R W East
Opus International Consultants Ltd, Auckland, New Zealand
Glyn.East@opus.co.nz

Keywords: Polystyrenes, EPS, Lightweight Fill, Embankment, soft ground

ABSTRACT

Polystyrene products have been used successfully for the construction of lightweight fill embankments in Europe principally Scandinavia, USA and Japan for 20 – 30 years. It has been used in New Zealand for similar roading applications for over 20 years and has become more prevalent in recent years.

Relevant properties for engineering structures are discussed and design parameters outlined. Construction and design issues are discussed and a case study in New Zealand is presented. The case study is associated with the Esmonde Road Motorway Interchange project where the construction of a 250m length, 3m to 6m height polystyrene (ESP) embankment with bridge approaches was undertaken over a veneer of harbour reclamation fill overlying up to 10m of soft compressible marine mud adjacent live traffic lanes and bridges.

1 INTRODUCTION

EPS products have been used successfully for the construction of lightweight fill embankments in Europe principally Scandinavia, USA and Japan for 20 – 30 years. It has been used in New Zealand for similar roading applications for over 20 years.

First highway use in NZ was in Northland at SH10 Kahoe Bridge abutment in the mid 1980's after the approach fill collapsed into the river during construction. Recent applications have included embankments over compressible soils and/or sensitive services, slip repairs and bridge abutment backfill to enable approaches and bridge construction to be undertaken simultaneously.

Its use could be considered innovative but it is becoming mainstream. With a cost of approximately \$100 to \$170 /m^3, depending on the protection, EPS embankments can have a considerable overall lower comparative construction costs in sites where settlement would affect existing infrastructure or a surface loading would affect global stability. Wick drains and preloading are not suitable for such sites and other alternative ground improvement methods are not as effective, especially when time delay is considered. It is certainly has a significant lower cost than an equivalent length bridge structure which is a typical comparison.

2 TYPICAL ENGINEERING GRADE POLYSTYRENE

EPS (Expanded Polystyrene) is an intact flexible material manufactured in block format (common size 6m x 1.2m x 0.8m) with strength and modulus properties similar to that of a firm/stiff soil.

The blocks are 1.5% the weight of earth fill (nominally 20 – 30 kg/m^3 for engineering grade versus 1,800 kg/m^3 for earth fill). A least two New Zealand suppliers can satisfy the testing standards and specifications. At this stage there is no formal specification for this civil engineering application of EPS but NCHRP Report 529 2004 (Ref 4) outlines a recommended standard. ASTM C 578 is the standard specification for the general construction of the EPS material.

This significant difference in density between EPS and soil fill means that settlement and stability issues under an embankment become almost negligible.

3 SIGNIFICANT ISSUES FOR ROADING EMBANKMENTS AND OTHER CIVIL ENGINEERING APPLICATIONS

A number of mechanical, chemical and durability properties are required of the EPS polystyrene that can be certified by suitable suppliers but the significant issues from a roading embankment point of view are:

Buoyancy: Typically EPS (Geofoam) fill will not be placed below the design high flood level although floatation uplift can be compensation for by surcharge fill or the pavement.

Protection of the blocks from a petroleum spill: A petroleum resistant liner or geo-membrane should be placed between the Geofoam EPS and the pavement and/or an overlay of a thin (<200mm) concrete slab can be utilised. Currently in NZ specific petroleum containment liner products such as Nylex product Aeon Elvaloy or Coolguard FTL40E are being utilised (0.5mm) but High Density Polyethylene (HDPE) (1-3mm) is still used. A concrete slab is not considered essential. Other projects have omitted the slab and placed the pavement directly on the polystyrene utilising the design CBR as outlined in Table 1.

Flammability: EPS is currently manufactured in New Zealand with flame retarder the material to be self-extinguishing.

4 ENGINEERING PROPERTIES

4.1 Design values of engineering properties

Nominal Density (kg/m^3)	Elastic Limit Stress (1% Strain) (kPa)	Young's Modulus (MPa) Rebound & Recompression Inelastic Compression)	Poisson's Ratio	Coefficient of Lateral Earth Pressure (at rest), K_0	CBR (%)
15	40	4	0.09	0.1	(See Note 1)
24	75	7.5	0.14	0.16	3
28	100	10	0.16	0.19	4

Note 1: The use of EPS with density ≤ 15 kg/m3 directly beneath paved areas is not recommended

Table 1: Design Values of Engineering Properties

4.2 Other properties

Durable: EPS is not biodegradable, does not dissolve or deteriorate in ground and has no nutritive content for organisms. It will become brittle if exposed over a period of years to UV.

Environmental Effects: EPS is not inherently hazardous. It has no long term out-gassing of potentially toxic gases and does not interaction with the ground or groundwater. If burnt the major combustion products are carbon dioxide and water.

Water Absorption: The void spaces of EPS are essentially sealed against any significant water intrusion.

Creep: Generally creep is not considered to be significant if the material loaded less the elastic limit stress (Table 1).

5 DESIGN ISSUES

5.1 Seismic stability

The stability of polystyrene embankment under seismic accelerations does not appear to be a significant issue. A Japanese study (Ref 5) of 10 sites with earthquake intensities ranging from V to VII showed little inertia damage although surrounding structures were seriously damaged.

A NCHRP study (Ref 3) reviewed three modes of failure (i) translational sliding of the upper pavement and polystyrene concrete cap (ii) translational sliding between the blocks and (iii) translational sliding along the foundation soils interface. The analytical study indicated that for a range of acceleration of 0.05g to 0.2g the interface angle of friction would need to be less than 15° before the stability safety factor reduced to below 1.2. At a typical angle of friction of 30° for EPS/EPS, concrete/EPS and EPS/foundation soil interfaces the safety factor was in excess of 2 for 0.2g design acceleration**.**

Assessment may be required for larger earthquake events but means are available to increase all the interface friction values. Spiking and bonding have been utilised.

5.2 Loads on bridge abutments

Utilising polystyrene the horizontal forces on an abutment from gravity loads or seismic loads are largely generated by the upper pavement and slab, if present, as the polystyrene introduced negligible mass and has a low active earth pressure coefficient. Restraint of seismic loads in a "locked in" bridge abutment can be designed as a spring type system utilising the elasticity of the polystyrene rather than a passive failure wedge. This is where the polystyrene blocks become a structural component

5.3 Load bearing

The load bearing capacity of polystyrene requires selection of an appropriate grade such that the elastic limit stress is not exceeded. Table 1 indicates a range of elastic limit stresses for different polystyrene densities, 40kPa for 15kg/m^3 to 100kPa for 28kg/m$^{3.}$ Respectively equivalent to some 2 and 5m of earth fill.

6 CASE STUDY ESMONDE INTERCHANGE – NORTHERN BUSWAY

Esmonde Interchange, just north of the Harbour Bridge on Auckland's Northern Motorway, was upgraded to provide access for Buses and High Occupancy Vehicle to the new Northern Busway, a new cross-motorway arterial linkage and additional approach ramps to the motorway (Figure 1). This project is part of the wider transport strategy that Transit New Zealand (now NZTA), in conjunction with North Shore City, has implemented to improve the road network and enhance use of public transport in Northern Auckland. Opus International Consultants Ltd

New Zealand Geotechnical Society Inc. 19th Symposium, Queenstown 2013

was the principal consultant. Planning for the upgraded interchange commenced in 1997. Construction was commenced in 2003 and was completed in late 2006.

The interchange lies in a complex coastal/estuarine area and contains varied and challenging topography, geology and ecology. The original 1960's motorway through the Esmonde Interchange area was constructed as part of reclamation of the Waitemata Harbour foreshore. A motorway bridge crosses a tidal stream Hillcrest Creek that meanders through the interchange. The underlying material is fine grained marine mud overlying Puketoka alluvial soils over Waitemata Group (East Coast Bays Formation) residual soils and weak sandstone, bound to the west by volcanic tuff from a nearby explosion crater and to the east by remnant peninsular of Waitemata Group "bedrock". Any small preconsolidation of the marine mud was taken up by the previous construction making the material truly normally consolidated and very compressible.



Figure 1: Esmonde Interchange South Facing

6.1 Embankment challenges

The construction required the Esmonde Road to be widened from 2 lanes to 5 lanes with a 3m to 6m embankment, an abutting motorway southbound off ramp, three new bridges over Hillcrest Creek and the construction of a Busway "tunnel" overbridge within the embankment. The adverse geotechnical conditions required specific mitigation design.

The presence of relatively thick (4-10m), very soft, compressible, fine-grained marine mud under up to 6m of embankment fill created construction instability and significant long term post-construction consolidation settlement (300-800mm) issues. The off ramp had few constraints and was constructed using relatively convention wick drains, reinforcement geotextile and a 1 year progressive preload to improving the strength and accelerate the adverse consolidation settlement, but the Esmonde Road embankment widening had an issue largely because of adjacent live traffic lane. Settlement with conventional earth fill, even with wick drains, would result in large differential settlements within the existing Esmonde Road adjacent traffic lanes and services and the existing Hillcrest Bridge abutment and approaches. The

highway trafficability would be compromised the and abutment and settlement slab damaged. The approaches to the required new structures over Hillcrest Creek, the busway tunnel overbridge, an adjoining bus station Link Bridge and a northern link road bridge would also suffer high settlements.

To determine the best mitigation measures, a number of alternative systems were reviewed. These included a viaduct bridge over the 250m length, or stone columns, insitu soil mix piles, conventional piles, all with capping geogrids. The viaduct bridge and has a high cost and the column and pile alternatives have high risks associated with design and performance in the marine muds. All have a higher or comparable cost when compared with an EPS polystyrene lightweight fill construction**.**

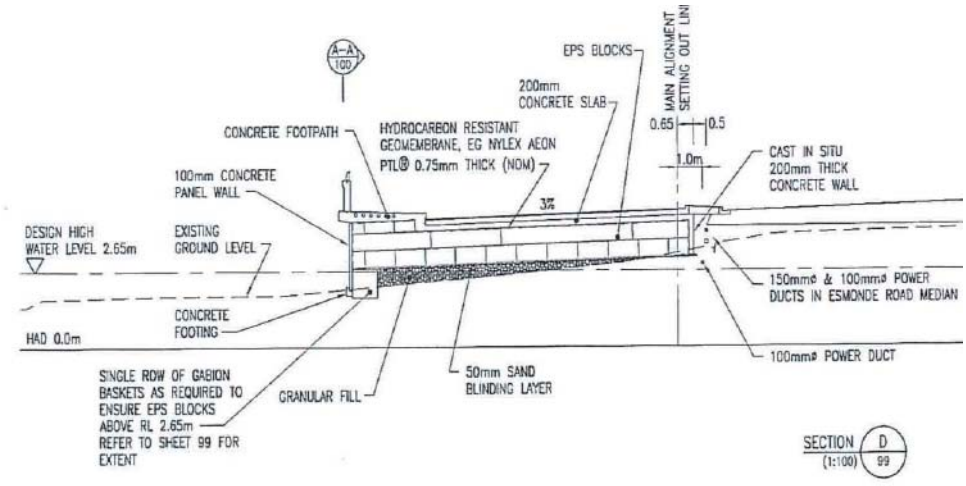
The design approach adopted was to use medium density (24 kg/m^3) grade EPS polystyrene blocks, carefully placed, trimmed and dogged together, wrapped in hydro-carbon resistant membrane and capped and surrounded by reinforced concrete. The new embankment and was successfully constructed using this method.

6.2 Construction and design details

The following construction and design details where incorporated (Figures 2 and 3)

Figure 2: Typical Esmonde Polystyrene Embankment Details

1 The polystyrene blocks were placed over a thin layer of sand/gravel to maintain freeboard above a water level that incorporate sea level rise and wrapped to the ground by Aeon Elvaloy hydro-carbon resistant membrane.
2 A 200mm 20MPa reinforced concrete slab was placed over the membrane and polystyrene.
3 The Esmonde Road embankment required TL4 concrete barriers and these where incorporated into concrete slab.

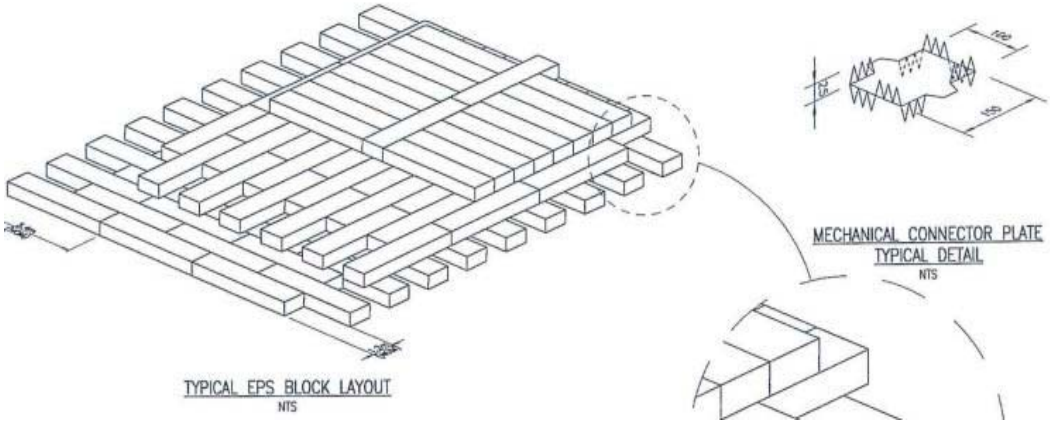


4 The embankment required vertical sides which were lined with concrete panels draped from under the concrete barriers. Urban design was incorporated into the panels.
5 The seismic performance of the polystyrene was assessed with the concrete slab and barrier to be adequate.

New Zealand Geotechnical Society Inc. 19th Symposium, Queenstown 2013

Figure 3: Typical Polystyrene Construction Detail

6 The polystyrene fill vertical bridge abutment seismic lateral load requirements utilised the elasticity of the polystyrene rather that the traditional passive resistance of an earth



embankment. Settlement slabs where incorporated into the abutments largely to enhance seismic performance.

New Zealand Geotechnical Society Inc. 19th Symposium, Queenstown 2013

7 The north link road bridge utilised a traditional lateral batters of stepped polystyrene cover with a veneer of soil.



Figure 3: Busway Overpass Construction and Completion

6.3 Performance

The embankment is performing adequately. Some small order settlement was generated in local areas near the Hillcrest Creek where the underlying sand/gravel was thicker than anticipated during design. The polystyrene bridge abutments have not settled unlike those of the existing bridges. The original unbound pavement with a SMA seal proved to be inadequate because the overall poor underlying drainage of the system. This pavement was replaced by structural asphaltic concrete.

A comparison can be made with the eastern abutment of the Hillcrest Bridge where the low lying topography precluded the use of polystyrene (Figure 4). Here severe differential settlement is ongoing with minor additional earth fill that requires major shape correction**.**

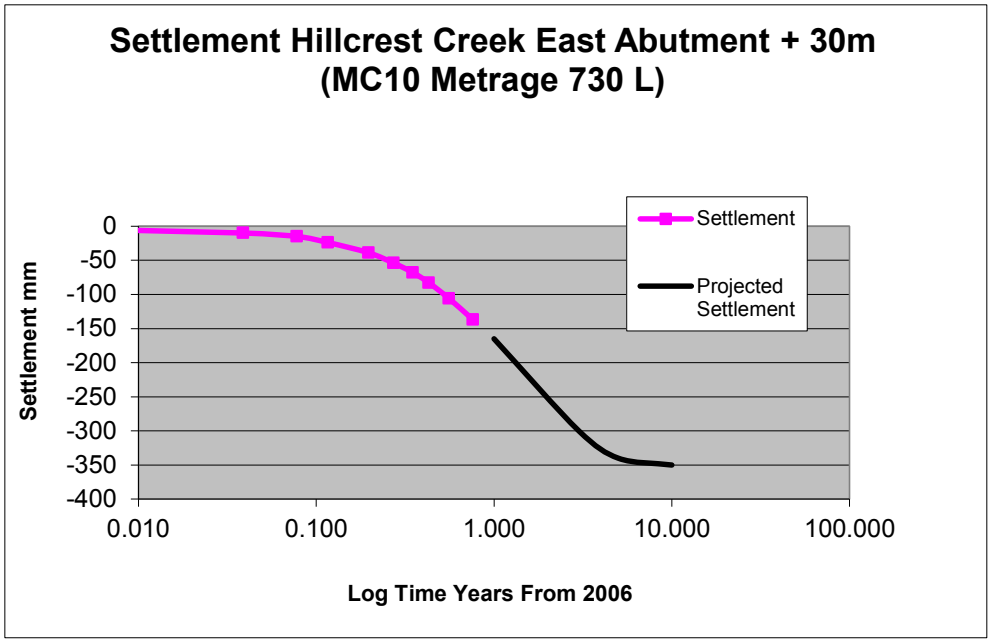


Figure 4: Settlement without EPS under 2 m of granular fill

7 CONCLUSION

The use of ESP polystyrene in civil engineering has become more prevalent in recent years. The engineering properties are now understood and manufacturers are producing products to specification at a reasonable cost. Utilising the material can enable projects with difficult ground conditions and adjoining or underlying sensitive infrastructure to go forward with the minimum cost and delay.

REFERENCES

Horvath, J.S. 2001. Geomaterials Research Project – Concepts for Cellular Geosynthetics Standards with an Example for EPS-Block Geofoam as Lightweight Fill for Roads, Research Report No. CGT-2001-4. Manhattan College School of Engineering, Center for Geotechnology, New York. 76p.

Horvath, J.S. 1995. Geofoam Geosynthetic. Manhattan College School of Engineering, Center for Geotechnology, New York. 217p.

Geofoam Applications in Design and Construction of Highway Embankment. Transport Research Board NCHRP Document 65 (Project 24-11) July 2004

Guidelines and Recommended Standard for Geofoam Applications in Highway Embankments. NCHRP Report 529 2004

Report of Results of Assessment of Damage to EPS Embankments Caused by Earthquakes. Hikara Hotta et al. EPS Tokyo ’96 Japan, October 1996

Holliday, J.K. (2013)
Investigation, design and construction of remediation of karstic solution feature affecting major motorway
Proc. 19th NZGS Geotechnical Symposium. Ed. CY Chin, Queenstown

Investigation, design and construction of remediation of karstic solution feature affecting major motorway

J K Holliday
Associate, Aurecon Australia Pty Ltd, Sydney, NSW, Australia.
jonathan.holliday@aurecongroup.com

Keywords: subsidence, geotechnical investigations, solution features, chalk, compaction grouting

ABSTRACT

This paper describes the investigation, design and construction of remediation to stabilise a karstic solution feature that caused a major subsidence affecting the M2 Motorway in Kent, United Kingdom (UK) in 1995.

The subsidence appeared as a small void within the motorway central reserve. Further subsidence occurred that resulted in a void approximately 3 m^3 that undermined the eastbound fast lane of the M2 motorway. The thick concrete road construction enabled the road slab to temporarily span the void.

It was apparent from investigations that the subsidence was the result of a pre-existing solution feature that had been reactivated by a leaking drainage pipe and exacerbated by discharge of storm water. Local knowledge of solution features enabled specialist geophysical and geotechnical investigations to be rapidly deployed in response to this emergency event. The investigations enabled characterisation of the nature and extent of the solution feature and differentiated the weak and disturbed infill from the more competent surrounding geology.

Aspects of the design and construction of the remediation, including the diversion of the highway drainage together with compaction grouting to stabilise the solution feature infill and minimise the risk of future reactivation, are presented.

New Zealand Geotechnical Society Inc. 19th Symposium, Queenstown 2013

1 INTRODUCTION

Several cases of subsidence affecting the M2 Motorway, Kent, UK, have occurred over recent years and leaking drains have often been cited as the main cause of collapse.

On 16 June 1994 a subsidence occurred within the central reserve of the M2 Motorway between Junctions 5-6 (marker posts [MP] 75/9-76/0). The subsidence consisted of a collapse creating a void which extended toward fast lanes of the coast and London bound carriageways. In 1994-95 the M2 Motorway was managed by Kent County Council's (KCC's) Motorway and Trunk Roads Unit (MTRU) acting as agent to the Department of Transport (now UK Highways Agency). KCC Geotechnical Group (KCCGG) undertook an assessment of the subsidence.

An initial investigation of this subsidence concluded that the subsidence was probably caused by a broken drainage pipe at the base of a filter drain located within the motorway central reserve. A temporary repair using road planings to support the carriageway was implemented and a plan to carry out permanent repairs to the broken drainage pipe was scheduled for future works.

In addition to the temporary repairs, a desk study was carried out to assess other factors such as the occurrence of artificial and natural cavities in the chalk that may have contributed to the subsidence.

The geology of the site consists of superficial Head Brickearth and Clay with Flints overlying solid geology of Thanet Beds overlying Upper Chalk. In this area, Head Brickearth is a structureless, silty material; Clay with Flints consists of flint nodules in a stiff clay matrix; the Thanet Beds consist of mainly fine sand with green coated scattered flints at the base. Importantly, the interface between the Thanet Beds and underlying chalk is unconformable and variable and often marked by solution features. Chalk in this area is weak, jointed and highly variable in bedding thickness and hardness and belongs to the Seaford Head Member (Mortimore, 1986).

The site is at an elevation of 73 m above Ordnance datum (AOD) and ground slopes are very gentle. Groundwater was recorded to be at between 33 m to 43 m AOD and movement of water will therefore be dominated by a vertical flow component.

Considerable reference was made during the preliminary investigations to a previous study on solution features in the chalk of Kent (Holliday, 1992). This study discusses investigation strategies and design approaches for remediation works to solution features in the chalk. Natural solution features are broadly defined as conical, funnel shaped, hemispherical or irregular closed depressions, or shaft-like holes forming closed depressions as a result of differential solution weathering. They vary in size and shape and typically range from 1 m to 100 m in diameter and up to 45 m in depth.

New Zealand Geotechnical Society Inc. 19th Symposium, Queenstown 2013

Solution features are usually filled with material derived from overlying deposits. The stability of a solution feature is amongst other things dependant on the nature of the infilling. Ground subsidence may occur within unstable solution features in chalk either as (i) a *collapse sinkhole* which appears as a hole in the ground and is often associated with granular infill, or (ii) a *subsidence sinkhole* which is a gradual and slow form of subsidence often associated with cohesive materials and resulting in an enclosed depression of various dimensions.

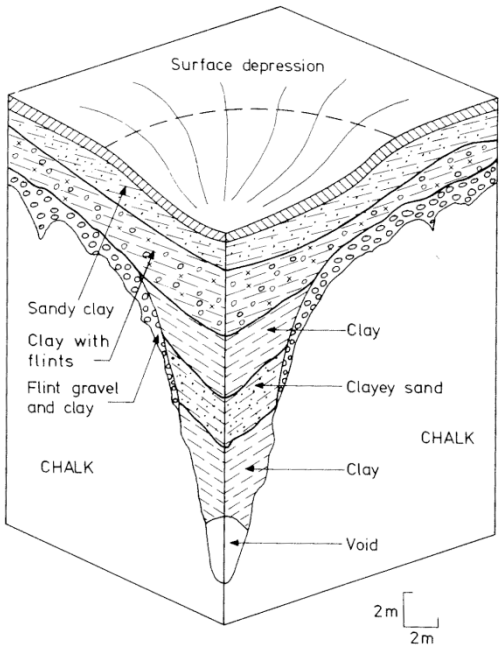


Figure 1: Section through a sinkhole in chalk (after Clayton, Simons and Matthews, 1982).

A collapse sinkhole is often associated with granular infill. Granular infilling may typically be loose and contain weakly bridged cavities and hence it is generally weaker and more compressible than the host chalk bedrock.

Numerous cases of subsidence within the chalk have been reported (e.g., Holliday, 1992; Francescon and Twine, 1993). The three main processes affecting subsidence within chalk solution features are:

1) The action of **solution** of the Chalk bedrock produces widening of fissures with the creation of voids;
2) **Soil piping** is a form of erosion which requires flow of water as an erosive seepage force which tends to remove soil particles in the direction of downward flow toward widened fissures within the Chalk bedrock;
3) Sinkhole collapse occurs by the collapse of an arch or dome which spans an air-filled void, a process commonly referred to as **soil arching**.

On 8 December 1994, a further collapse occurred within the temporary reinstated section of backfill and the area of previous collapses. This collapse followed a period of prolonged and very heavy rain and it was evident that an excessive amount of water had discharged into the area of collapse.

Preliminary desk study findings and limited intrusive investigations suggested the subsidence was consistent with the leaking drain triggering collapse due to piping erosion of fine grained granular soils into either: i) an artificial cavity such as denehole (i.e., a manmade vertical shaft in chalk), chalkwell, or tunnel, or ii) a natural cavity such as an infilled solution feature occurring within the chalk bedrock.

A detailed ground investigation was immediately mobilised to identify the scale of the problem; to determine whether or not any trafficked areas were at risk of serious subsidence such as sudden collapse; and to provide the basis for design of remedial works.

2 INVESTIGATION

A ground investigation was scoped and supervised by KCCGG in December 1994. The investigation comprised 2 No. light cable percussion boreholes with sampling and in-situ testing to depths of up to 20 m; 25 No. dynamic cone penetration testing (DCPT) probes to depths of up to 12 m; logging of exposures within excavation trenches and a geophysical survey using gravimetric and impulse radar techniques. A limited programme of laboratory testing was undertaken to classify the soils encountered.

The boreholes encountered: Head Brickearth - a firm fine sandy SILT to a depth of up 3 m; Thanet Beds - a firm slightly glauconitic clayey fine sandy SILT to a depth of up to 5.4 m, the Thanet Beds overlay a sequence of highly weathered chalk, black coated flints and fine sandy silts extending to a depth of up to 9.7 m. The mixture of chalk and matrix was highly variable and interpreted as Metastable Infill to a solution feature. Intact, structured chalk (Upper Chalk) was encountered below depths of 9.2 m to 9.7 m. The chalk at this level generally consisted of extremely closely spaced bedding and extremely to very closely spaced sub-vertical and open fissures. The intact chalk was typically weak to very weak of low to medium density.

DCPT was carried out using the SRS15 or *heavy* DPH type penetrometer. The test is similar to the Standard Penetration Test (SPT), but uses a 50 kg hammer and drop of 0.5 m, with a 15 cm² cone, in accordance with BS1377:Part 9:1990. In general, DCPT blow counts can be comparable with the SPT. Based on simplified theoretical comparison and local experience, DCPT resistance (N_{100}) has been shown to correlate with the SPT resistance (N) i.e., SPT N ~ 2.N_{100} (e.g., Muromachi and Kobayashi, 1974). In general, 2 types of DCPT profiles emerged and were classified as follows:

Normal - Profiles (N_{100} generally >4) indicate stable Head Brickearth and Thanet Beds supporting the carriageway and these in turn overlie chalk at a depth generally between 4.6 m to 6.5 m.

Metastable - Profiles (N_{100} generally ≤ 2) occur within the zone of the active solution feature. The probe locations have been used to delineate the extent and area of influence affected by subsidence.

The investigation did not encounter any voids but confirmed a wide variation of depth to chalk bedrock of between 4.6 m to 10.8 m. The average depth to chalk for profiles not affected by the subsidence was 5.2 m. The predicted depths to chalk and spatial distribution of data points confirmed a roughly oval shaped depression formed within the general chalk bedrock level. The extent of the depression and the nature of the subsidence were consistent with a ***collapse sinkhole***.

The sinkhole had a maximum depth of 9.3 m to 10.4 m and was centred in the area of DCPT holes (e.g., DP9, 10, and 11 of Figure 2). It was approximately 9.5 m by 6.5 m in plan at the general chalk level of 5.2 m and reduced in plan with increasing depth below 5.2 m. The sides of the sinkhole were predicted to be relatively steep (approximately 60°). The sinkhole was infilled by very loose and soft materials in a metastable condition.

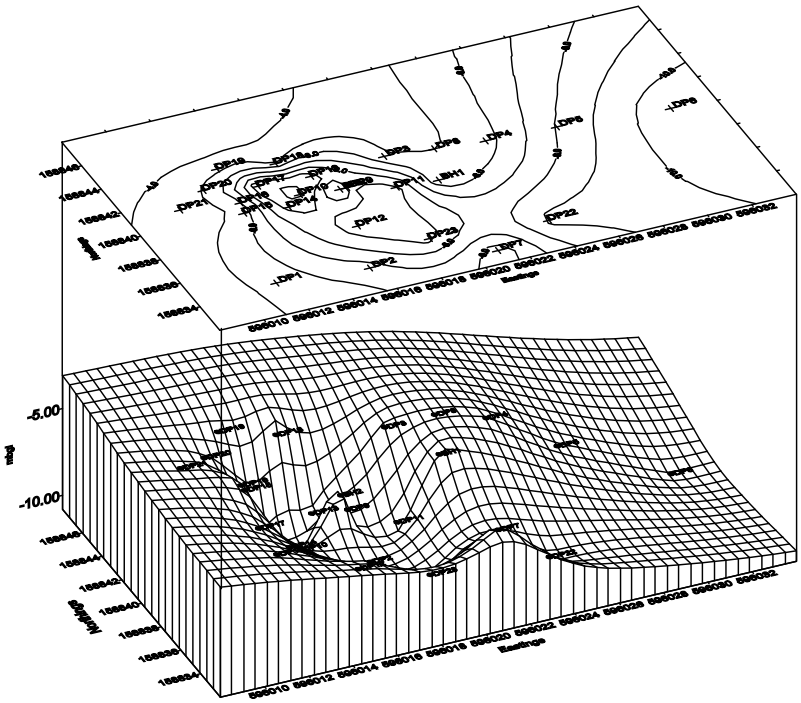


Figure 2: Surface of the chalk detected in geotechnical investigation

3 DESIGN

The geotechnical interpretative report prepared by KCCGG indicated that the main causes of subsidence resulted from the re-activation of the solution feature due to periodic but concentrated and uncontrolled discharge of water from the leaking drainage pipe. It was suggested that water had flushed and eroded previous solutionally widened and infilled fissures and that soil piping had removed infill materials toward a solutionally modified zone within the chalk and created voids which had progressively migrated upwards. Large surface water flows collected by the drainage system and vibrations from heavy traffic have probably been the main triggers to the sudden collapses.

The area of instability is referred to as a "zone of influence" which is similar to the theoretical "angle of draw" for a typical subsidence trough. The centre of subsidence is taken as the level of bedrock with the angle of draw related to the predicted steep sides of the sinkhole approximating an active failure condition. The projected "area of influence" at the surface

represents the predicted maximum extent of ground surface affected by subsidence requiring treatment. The design of the remedial works was developed around the following main requirements:

Table 1: The main design objectives and works requirements

Design Objectives	Remedial Works Requirements
Control of water to minimise further discharges into the area of collapse	The pipe affecting the site should be diverted from the area of subsidence. Surface water run-off from the London bound carriageway should be positively drained. An effective, impermeable hard 'cover' was recommended for the central reserve between MP 75/8.5 to 76/0. A filter drain was recommended within the area affected by subsidence to intercept seepages through the pavement layers.
Treatment of solution feature to provide appropriate and cost effective repair	A combination of compaction grouting and excavation and replacement locally within the central reserve was recommended as the most appropriate technique for treating the solution feature. This option would cause a minimum of disruption to traffic.
Carriageway remedial works to areas likely to have suffered distress due to subsidence	Transverse cracks and joints within the carriageway were recommended to be treated and sealed to minimise entry of surface water run-off into the underlying sub-base layers.

Compaction grouting involves the injection of a low slump mortar paste at pressures many times greater than overburden pressure to displace and compact the surrounding ground. The purpose of using grout with low slump is to prevent hydrofracture so that the grout remains local to the injection source forming either an expanding grout bulb or columns, depending on the geometry of the grout source. The bulbs have been quoted to be 0.5 m – 1 m diameter in pseudo-spherical or cylindrical form depending on whether the injection pipe has been held still or withdrawn during injection. The surrounding ground is tightened with an intensity which falls off radially. Ultimately the upward force exerted by the grout on the overlying ground will exceed the combined effects of gravity and soil shear strength resulting in heave of the ground surface.

In this case the agreed preferred option for treating the feature was by compaction grouting. A summary of the main design and construction considerations for the works is as follows:

a) Drilling would be by cased auger drilling. Holes would be terminated 1 m into sound chalk;
b) Compaction grouting would entail injection of low slump grout through casing which is withdrawn in stages as the grout is injected;
c) Surface movement accurate to levels of up to 2 mm would be monitored using a rotary laser system siting on audibly and visibly alarmed targets;
d) Termination (i.e. stopping injection of any stage) would be according to the following criteria:-
   - Maximum stall pressure or pre-set pressure of 10 Bar (0 - 5m) or 20 Bar (5 m+) exceeded; or
   - Maximum volume of 10 m³ exceeded; or
   - Surface movements of +2 mm detected.

4 CONSTRUCTION

Site work commenced on 6 March 1995. A grid was set out with holes at 2 m centres, covering an area 22 m × 10 m. The locations were numbered in *Column/Row* format, commencing in the southwest corner at 0/0 and proceeding northeast to 22/10. The grid layout is shown in Figure 2 that includes additional locations which were added later. In relation to the existing road, Row

2 was situated approximately along the southern edge of the central reserve and Row 10 was in the middle of lane 2 of the eastbound carriageway.

Two track mounted diesel-hydraulic drilling rigs were employed throughout the contract. Casing, 114 mm in diameter, was driven to a 'firm stratum' and the material within augered out. Auger drilling was continued to approximately 1 m into hard chalk. Due to the confined area of working the grout was pre-mixed and delivered in 'Ready-Mix' wagons. Bentonite and water were added at the time of discharging into the pump to control pumpability. On average 26 kg of bentonite was added to 3 m^3 of grout. The grout was sampled from the chute of the wagon for slump and strength tests.

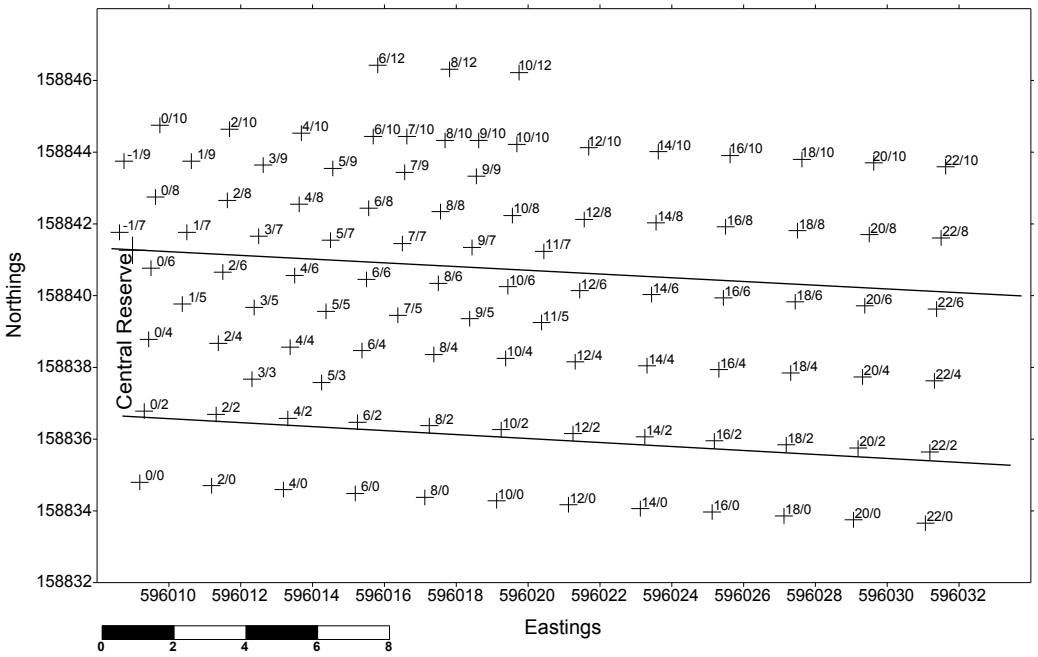


Figure 3: Grout hole location plan (dimensions in metres)

Drilling commenced at Hole No.**10/6** as this was close to the original location where the subsidence occurred. The hole was drilled to 23 m to detect the quality of the underlying chalk. This hole took a significant amount of grout (5.2 m^3).

During the works there was evidence of voids being present within the area of interest that included: no return on the augers during drilling; large volumes of grout injected (up to the 10 m^3 limit); visual evidence (detected by shining a torch down the drill holes); and grout encountered during drilling. However, the interpretation of data was not straight forward, and the existence of one of the above factors was not evidence alone of a void.

Grouting of each hole was carried out until any of the termination criteria stated above were met. Initially the stall pressure was set at 20 bar and when this was reached the casing was withdrawn, generally in 2 m stages and grouting recommenced. Pressures were monitored on two gauges mounted within the hose close to the pump and the injection hole. The volume of grout injected was estimated from the number of strokes performed by the pump.

Hole No.4/8 was the first hole to have 10 m^3 of grout injected into it and drill records indicate that no return of material and hence possibly a void occurred between 8 - 10.5 m. Hole No.4/4 did not show signs of a void during drilling but when grouted, took 6 m^3 between 6 m and 7 m, which brought it up to the limit of 10 m^3.

At an early stage it was agreed to lower the stall pressure from 20 bar to 10 bar to prevent the grouting operations possibly fracturing sideways into adjacent features and some intermediary locations along columns -1, 1, 3, 5, 7, 9 and 11 were added to the scope of work.

DCPT testing was undertaken between grout holes on 25 and 26 March 1995 to assess ground improvement. Many of the additional intermediate holes encountered grout during the drilling but the actual grout take was generally very low. The contractor specified improvement to an equivalent minimum SPT N = 10 and an average N = 15. By applying the approximate correlation (i.e., SPT 'N' = 2 × DPN_{100}) the equivalent improvement criteria was for a minimum DCPT $N_{100} \cong 5$ and an average $N_{100} \cong 7$ - 8. DCPT results along rows 3 and 5 showed values generally below 7 m down to a depth of 8 – 10 m. Below this the results become more widely spread however, nearly all the probes showed zones of 1m or more where the blows were 3 or less. Results of probes close to the locations of previous probes carried out in the site investigation showed little significant improvement in the relative density of the ground.

The depth where grout was detected during drilling appeared to coincide with the interface between the superficial deposit and the chalk. It was considered possible that the grout flowed preferentially along this interface. This phenomenon was also encountered in the Castle Mall project reported by Francescon & Twine, (1993).

A total of 98 No. injection points within an area of 276 m^2 were installed and 1200 m of drilling was carried out of which 573 m were cased. A total of 100m^3 of grout and 885 kg of bentonite were injected to an average depth of 12.2 m which equates to approximately 3 % of the total volume treated. Total cost of the compaction grouting works was approximately £98,000.

5 CONCLUSIONS

It is concluded that treatment of the solution feature by compaction grouting has provided an appropriate and cost effective repair that should successfully prevent the reoccurrence of future subsidence. The control of water to minimise further discharges into the area of collapse is expected to significantly reduce the risk of further washout of material.

The drilling records confirmed the profile of the solution feature predicted in the geotechnical investigation although a more precise profile could be deduced due to the greater amount of information. Although the actual voids encountered during the grouting work were not previously detected, it is probable that they developed during the winter period since the investigation was carried out as it was apparent that the feature had become increasingly active.

The geophysical surveys did not predict the amount of subsurface voiding or ground disturbance. This was most probably due to the inherent lack of sensitivity of the gravimetric survey to locate small voids. The impulse radar survey was significantly affected by interference.

Compaction grouting of the solution feature was considered to be the most appropriate treatment method. The works were carried out relatively quickly, with minimum disruption within a confined working space, while maintaining dual two way traffic utilising the hard shoulders. Densification of the infill has been local to the injection points. However, the area has been significantly strengthened by the installation of a large number of grout columns.

DCPT testing did not show the ground improvement that was originally specified. This may be due to the properties of the infill which appeared to show only a very localised zone of compaction around the injection point. Test locations were also restricted due to significant coring required through the thick reinforced concrete pavement construction. In addition, the DCPT may not be sufficiently sensitive or wholly suited to detecting this ground improvement.

The contractor considered that there was a risk that the injection of the grout at pressure may have been causing some fracturing of the ground adjacent to voids. It was also apparent that the grout flowed preferentially along the interface between the superficial deposit and the chalk. Both these effects would be expected to reduce the effectiveness of the densification of the

surrounding soils from the grout injection. To reduce the risk of fracturing the maximum grouting pressure was reduced from 20 bar to 10 bar. This is also likely to have reduced the effectiveness of the treatment, resulting in a more localised zone of influence.

Several issues raised during this project have been described by Francescon & Twine, (1993). They consider continuous monitoring and logging of the injection pressure and pump rate to be essential both to permit technical reviewing of the works as it progresses and to provide records for quality control. The type of pump used is also considered important. The pump should not produce pressure surcharges or peaks which could affect the risk of hydrofracture.

ACKNOWLEDGEMENTS

The author would like to gratefully acknowledge the cooperation and assistance throughout the project of the following:

Kent County Council Motorway and Trunk Road Unit, the UK Highways Agency South East Construction Unit; Keller Colcrete; and colleagues of the Kent County Council Geotechnical Group and in particular Steve Huntley, Ian Payne and Keith Pearce who had significant input to the construction phase of the remediation works.

REFERENCES

Clayton, C.R.I., Simons, N.E. and Matthews, M.C. (1982) *Site Investigation: A Handbook for Engineers.* Granada.

Francescon, M. and Twine, D. (1993) Treatment of solution features in Upper Chalk by compaction grouting. Proc. Conf. on Grouting in the Ground. ICE, London, 1993.

Holliday, J.K. (1992) The Genesis, Occurrence and Engineering Significance of Solution Features in the Chalk of Kent. Unpublished MSc. Dissertation. University of Surrey. September, 1992.

Mortimore, R.N. 1986. Stratigraphy of the Upper Cretaceous White Chalk of Sussex. Proc. Geol. Assoc., 97 (2), 97-139, 1986.

Muromachi, T. and Kobayashi, S. (1974). Comparative study of static and dynamic penetration testing in Japan. Proc. 2nd European Symposium on Penetration Testing. Amsterdam. Vol. 1. p. 297 – 302.

Bradshaw, J.D. & Clayton, P.J. (2013)
Ground conditions and implications for construction in close proximity to a major faultline
Proc. 19th NZGS Geotechnical Symposium. Ed. CY Chin, Queenstown

Ground conditions and implications for construction in close proximity to a major faultline

J D Bradshaw
Beca Ltd, Wellington, NZ.
jennifer.bradshaw@beca.com (Corresponding author)

P J Clayton
Beca Ltd, Auckland, NZ
philip.clayton@beca.com

Keywords: Faulting, Shearing, Soil Nails.

ABSTRACT

Engineering works in close proximity to major fault lines offer challenges beyond those related to the direct effects of rupture. Ground conditions can differ considerably from those typically experienced in the same geologic unit elsewhere.

The engineering properties of the Rakaia terrane greywacke as found in the Wellington region (Wellington Greywacke) are relatively well understood with published test results and established rules of thumb for bearing capacity, batter slope angles and anchor skin friction.

Two engineering projects, the Karori Tunnel seismic strengthening and the Karori Wildlife Sanctuary (Zealandia) were recently completed in close proximity to the Wellington Fault. These projects both encountered similarly poor conditions within the in-situ greywacke with highly fractured rock, clay gouge and elevated groundwater. These projects both involved the construction of soil nail walls, high strength anchors and shallow foundations. The engineering challenges are described with particular reference to the geology and hydrology encountered, and implications for engineering design and construction.

New Zealand Geotechnical Society Inc. 19th Symposium, Queenstown 2013

1 INTRODUCTION

Two engineering projects, the Karori Tunnel seismic strengthening and the Karori Wildlife Sanctuary (Zealandia) visitors centre building were recently completed in close proximity to the Wellington Fault (Figure 1).

Zealandia is a predator-fenced wildlife sanctuary within a NE-SW aligned valley at the south end of Waiapu Road, Karori. In 2007 Beca was commissioned by Karori Wildlife Sanctuary Trust to provide structural and geotechnical design for a new three storey visitor centre partly overlying the eastern flank of the Lower Karori dam, and partly benched into the toe of a steeply sloping gully. The building is founded partly on piles extending through dam fill into underlying rock. Soil nails were installed to retain the cut behind the building, with nails/ anchors also positioned at floor levels and connected to the structure to resist structural seismic loads, tying the building and slope together.

Karori Tunnel forms a key road link between the suburb of Karori and Wellington's CBD. The c.1900 brick-lined Tunnel is approximately 400 m NW of Zealandia, running W-E from Chaytor Street to Glenmore Street through a narrow ridge beneath Raroa Road. Due to instability during construction, the eastern portal is partially cut-and-cover. In 2011 Beca was commissioned by Wellington City Council (WCC) to provide structural and geotechnical design for seismic strengthening of the Tunnel as part of a programme to improve the earthquake

resilience of transport routes and infrastructure. The project included buttress replacement, the addition of new capping beams and portal walls to the existing mass concrete structure, and anchoring of the portals through the fill behind into in situ rock. The scope was extended to include retaining works (a soil nailed wall with shotcrete facing) for a slope immediately south of the eastern approach - which was also identified as a seismic risk (Perrin, 2004).

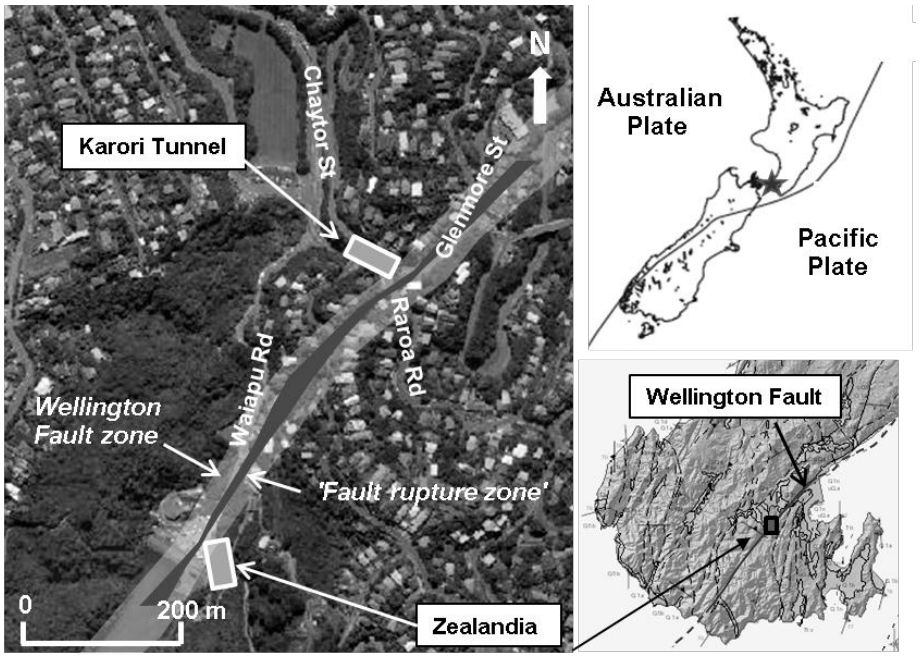


Figure 1: Project locations in relation to Wellington Fault (photograph from Greater Wellington Regional Council GIS maps; approximate fault zone/ rupture zone location after Wellington City Council District Plan maps; geological map, Begg and Johnston, 2000)

2 GEOLOGICAL SETTING

2.1 Wellington Greywacke

The study area, encompassing both the Zealandia and Karori Tunnel projects, is located within the western hills of Wellington, at the eastern edge of the suburb of Karori. The published geology (Begg and Mazengarb, 1996; Begg and Johnston, 2000) indicates the area is underlain by Rakaia Terrane (Torlesse Complex) greywacke rock, of Late Triassic to early Jurassic age.

Wellington greywacke mainly consists of fine grained sandstone beds (in the order of metres thick) with variable amounts of interbedded mudstone (argillite). The rock is extensively faulted, steeply tilted and folded (Begg and Mazengarb, 1996). Wellington greywacke is considered to have non-persistent, very closely to closely spaced joints, with orientations variable at least over short distances (bedding defects and shear zones being the exception).

2.2 Seismicity of the Wellington Region

The NE-SW orientated strike-slip fault system which dominates the Wellington Region (and beyond), the North Island Fault System, developed with the convergent plate boundary that divides New Zealand (refer Figure 1). The oblique subduction of the Pacific plate beneath the Australian plate produces a component of strike-slip strain, taken up by the faults parallel to the plate boundary, some of which, such as the Wellington Fault, are believed to extend the full

depth to the subduction interface (Begg, J. et al., 2008). The major faults have a history of repeated rupture along well defined fault traces.

2.3 Wellington fault

The Wellington Fault is a steeply dipping to subvertical, dextral strike-slip fault, generally upthrown on its western side however the greater part of its movement is horizontal (Begg and Mazengarb, 1996). In the project area the greywacke/ argillite bedding and the Wellington Fault orientation are sub-parallel, striking approximately NE-SW (Perrin, 2004).

The published geology shows the position of the Wellington Fault varying from 'approximate' in the base of the valley at Zealandia, to 'accurate' on Glenmore Street, east of Karori Tunnel (Begg and Mazengarb, 1996), passing within 5 to 20 m of the eastern portal (Perrin, 2004). This part of Glenmore Street is believed to follow an old fault-aligned stream gully (Perrin, 2004).

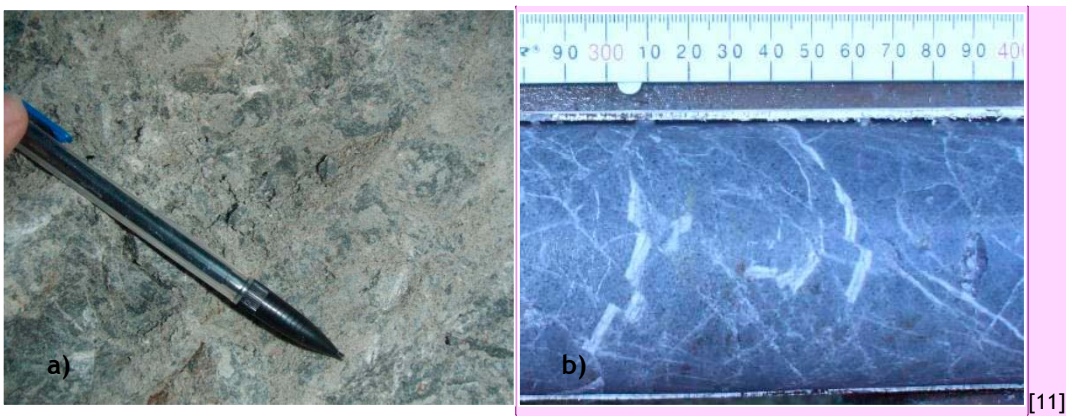
The Wellington City Council District Plan Map, sheet 11 (Wellington City Council, 2000-2011) defines a 50 m wide 'fault zone' for the Wellington Fault in this part of Karori, with a central 'fault rupture hazard zone' of 10 -15 m shown on the 'Hazard (fault line) area: Wellington Fault Map 5'. The piled foundations for Zealandia are partly within the buffer area of the rupture zone (20m wide strip bordering the mapped rupture zone).

2.4 Fault zone geology

The presence of a major fault has a significant impact on the geology it passes through; fault movements crush and shear the rock, altering its fabric. The effect is greatest at the central fault plane where the rock may be crushed into fine fragments, 'fault breccia', crushed further into rock flour, sometimes forming a clayey 'fault pug'. A mixed zone of breccia and pug form the 'fault gouge', which for the Wellington Fault may be around 2 m wide (Stevens, 1974).

Beyond the fault gouge there typically exists a brecciated zone, in the order of 50 m wide. Within the brecciated zone the rock can be so heavily sheared and crushed that its fabric is destroyed; effectively reduced to sand to fine gravel sized fragments (Figure 2). This typically light grey/ whitish grey rock is soft, often weakly cemented by coatings of secondary minerals such as zeolites (Opus, 2011).

Beyond the brecciated zone the rock is progressively less disturbed. The full width of fault affected rock is known as the 'fault zone', the Wellington Fault zone is up to 0.75 km wide (Stevens, 1974).



[11]

Figure 2: Fault zone greywacke: a) crushed rock within excavation at Karori; b borehole sample of heavily fractured rock at Zealandia (coarse ruler divisions 1 cm apart)

Fault zones can also disrupt groundwater flows; fault pug forms low permeability zones (sometimes groundwater is held under pressure in fault zones (Hoek, 1999)), and the highly fractured rock forms high permeability zones.

Due to the erodibility of fault zone geology, stream valleys often follow faults. The topography of Wellington with its numerous lineaments is believed to reflect the underling fault pattern, the main fault strikes (NE/SW to N/S) can be recognised in the topography, along with cross-cutting features which could represent tensional splinter faults (Stevens, 1974).

3 GROUND CONDITIONS

The ground conditions encountered at the Zealandia and Karori Tunnel sites reflects their close proximity to the Wellington Fault. The nature of the fault zone rock for these projects is described from observations in both the geotechnical investigation and construction phases.

3.1 Zealandia

Ground investigations included outcrop logging, test pitting and borehole drilling (six no., including one in the slope screened as a piezometer for long term monitoring); and the logging of benches cut in the valley side as the soil nail wall and building construction progressed. The rock encountered was extremely weak to moderately strong, slightly weathered, highly fractured/crushed greywacke with extremely closely spaced steeply inclined defect sets. Apparently intact rock fragments were grey, mineralized white, and friable; readily broken down with finger pressure into fine gravel sized fragments and further into sand and silt. Numerous steeply inclined thin to moderately thick sheared and crushed zones and fissile and slickensided argillite bands were also found (Beca, 2007; 2008).

Stereonet plotting of defect measurements (~300 no.) indicated a dominant NE-SW striking defect set, matching the bedding orientation (Perrin, 2004) and the Wellington Fault strike. The next most abundant defect set was roughly perpendicular to this, striking SE-NW (Figure 3). Similar lineament orientations are seen in aerial photographs of this area, possibly reflecting an underlying pattern of tensional splinter faults, as noted by Stevens (1974).

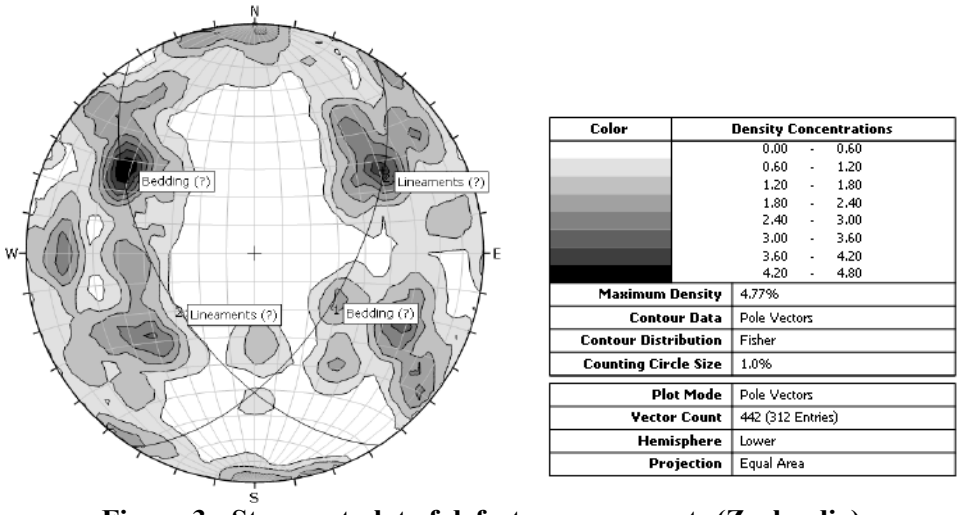


Figure 3: Stereonet plot of defect measurements (Zealandia)

Groundwater seepage was noted near the slope toe prior to construction, and the water table was recorded mid-slope in the rock behind the visitor centre. During construction, significant seepage was encountered in the cut batters, but flows were variable; some soil nail holes

intercepted defects holding groundwater under pressure, and adjacent holes (<3 m offset) were dry.

3.2 Karori Tunnel

Geotechnical investigations included concrete cores within the tunnel, hand augers (by others) and borehole drilling. No piezometers were installed at this site. Investigations and construction works indicated fill and colluvium over the south slope of the eastern approach (infilled valley), underlain by in situ greywacke rock. The in situ rock on both sides of the tunnel and across the south slope of the eastern approach (in total some 90 m width) resembled that found at Zealandia. The rock was brecciated, with extremely closely spaced steeply inclined defects, grey, mineralized white, and friable - readily broken down with finger pressure into fine gravel sized fragments and further into sand and silt (Beca, 2011).

During the investigation phase, little groundwater seepage was observed, mainly from south facing cut slopes around the portals, and a perched water table within the colluvium of the south slope. During construction, groundwater was encountered under pressure when drilling the soil nail holes in the south slope, especially the lower rows.

4 DESIGN CONSIDERATIONS

The engineering properties of typical Wellington greywacke are relatively well understood, with published laboratory test values, such as those presented by Pender (1980) – typical published friction angle (phi') values for highly weathered greywacke are in the order of 27 to 35°, and effective cohesion (c') in the order of 36 to 58 kPa. Moderately weathered rock (and better) is modelled with increasing c' reflecting the high intact strength, albeit dependant on the failure mode modelled – defect controlled failures will be influenced by weaker joint infills.

Both project sites were noted to lack a typical greywacke weathering profile, instead moving quickly into slightly weathered rock near surface; possibly due to uplift on this, the western side of the Fault, and/ or due to the erodibility of the fault zone rock, preventing a deep weathering profile from developing.

While largely unweathered, the rock is noted to be significantly weaker than might ordinarily be anticipated and the typical properties for a slightly weathered state were considered inappropriate. A literature search was carried out, however there appears to be limited published data on fault zone rock, so a generally 'first principles' (rather than precedent based) approach was taken to derive engineering properties for design (both for Zealandia and Karori Tunnel), as described below.

4.1 Mohr-Coulomb parameters

Read et al. (2000) present laboratory testing for similar unweathered, poor quality greywacke rock masses with extremely closely spaced joints, crushed zones and gouges - from Aviemore (South Island, also Rakaia Terrane). The resultant Mohr-Coulomb parameters were phi' 48° and c' 0 kPa.

Back analyses were undertaken for both the Zealandia and Karori Tunnel projects, based on existing slopes nearby which were known to have failed historically, or the geomorphology of which had shown evidence of possible historical instability. [12]The Hoek-Brown failure criterion was also used with software Roclab v 1.0 (Rocscience, 2007) to refine the Mohr-Coulomb parameters. A key input to the criterion is the rock mass rating using the Geological Strength Index (GSI), which characterises the rock mass based on its engineering geological description. For these fault zone sites the rockmass was assigned GSI categories of 'poor'

discontinuity surface condition and 'disintegrated' structure, resulting in a GSI in the range of 15 to 25. Sensitivity checks were undertaken for the values of this and other inputs to the Hoek-Brown criterion[1].

The final properties adopted were phi' 40°, and a range in c', to reflect varying site conditions:

- A particularly weak sheared gully zone at Zealandia (10 kPa).
- More dilated fault zone rock within 10 m depth below ground (15 kPa).
- Fault zone rock at depths greater than 10 m below ground (50 kPa).

4.2 Bond strength

The bond strengths for the soil nails and anchors for both projects were estimated using material values presented in the FHWA Geotechnical Engineering Circular No. 7, Soil Nail Walls (Lazarte et al, 2003) which indicated ultimate bond strength values of 200 – 300 kPa for weathered sandstone, and 100 – 180 kPa for cohesionless sand/ gravel. These were refined using sacrificial pre-production testing of two bonds strengths, as detailed in Table 1:

Table 1: Soil nail bond strengths

Bond Strength	Rock mass	Applicable locations
200 kPa geotechnical ultimate (failure)	Most heavily crushed and sheared greywacke	Gully zone at Zealandia, and south slope adjacent to Karori Tunnel (where Wellington Fault is mapped)
400 kPa geotechnical ultimate (failure)	More competent (but still extremely closely jointed) rock	Assessed from site investigation data to occur beyond ~10 m depth at Zealandia, and within Karori Tunnel, west of the Wellington Fault

Pre-production testing of the nails at both Zealandia and Karori confirmed the adopted strengths, with the design bond strengths being achieved. The pre-production testing of the anchors for the Karori Tunnel portals started to yield at approximately 300 kPa – which was less than the design geotechnical ultimate of 400 kPa for that area. The portal anchor design was duly altered to compensate for the reduced bond strength.

5 CONSTRUCTABILITY

Construction of the Zealandia (Z) and Karori Tunnel (KT) projects illustrated the unique challenges of working within ground affected by a nearby active fault, in terms of the engineering geological and hydrogeological conditions encountered. Some of the related issues which arose during construction are briefly summarised in Table 2 below.

Table 2: Constructability considerations[13]

Issue	Underlying Cause	Consequence/Mitigation
Loss of grout to the ground (Z)	Highly fractured, dilated rock mass with localised high permeability zones	Production nail failure due to complete grout loss from bond zone/Use of low W/C ratio grout[14] (maximum 0.4), careful monitoring and 'top up' grouting
Down-hole hammer becoming blocked/ jammed (KT)	Fines generated by drilling, mixed with water forming 'pug', blocking the hole	Slower progress with drilling

[1]Uniaxial compressive strength, a material constant mi, a disturbance factor and Young's Modulus.

New Zealand Geotechnical Society Inc. 19th Symposium, Queenstown 2013

Issue	Underlying Cause	Consequence/Mitigation
Groundwater flows higher than expected (Z, KT)	Drilling intercepting pressurised groundwater within joints in the fault zone	Seepage/Installation of additional drainage measures including some inclined bored drains added to the soil nail wall design
Inability to grout the soil nail due to groundwater flow (KT)	Groundwater flowing under pressure in excess of hydrostatic head of grout	Loss of grout from the soil nail, potentially impacting on capacity and durability/Additional drainage measures required
Trench wall and soil nail batter instability (Z)	Unfavourably orientated steep dipping weak argillite zones	Over-break in spillway excavation/ Provision of additional stabilisation

For both these projects, groundwater flows from anchor/ soil nail holes were encountered and resulted in additional work to install additional drains or additional soil nails. Drainage measures had been addressed in the design; though these had largely been passive (weep holes) or inclined drains to be drilled form the toe of the slope on completion of nail installation. During construction it became clear that more active drainage (inclined bored drains) were necessary and the early installation of these could assist construction.

Based on our experience in these projects such drains could best be installed as far ahead of soil nail construction as possible. A solution may be to drill longer drains in the lower batter area, which are subsequently partially excavated.

6 CONCLUSIONS

The Wellington region is dissected by a number of active faults, bound by zones comprising highly fractured/ crushed, and sheared greywacke rock, tens to hundreds of metres wide. The rock encountered in fault zones is noted to be significantly weaker than is typically encountered elsewhere.

Two projects were undertaken in close proximity to the Wellington Fault, with ground investigations and construction works encountering highly fractured rock, fragments of which could be readily broken down further into sand and silt sized particles under finger pressure. Both projects required specific consideration of these aspects in design due to the nature of the fault zone rock and hydrogeology.

In design for these projects a weaker rock mass strength than might otherwise be expected for their weathering grade was adequately assessed using conventional soil and rock mechanics techniques and confirmed by back analysis/ load testing.

Groundwater flows were known to be variable within fault zones, with both high and low permeability zones attributable to the presence of faulted rock. Conventional site investigation methods were found to be generally unsuitable for identification of localised high groundwater flows encountered during construction. This is not surprising. Based on our experience on these projects, where additional active drainage is needed, it is best installed early rather than on completion of excavation as is common.

While the challenges associated with working within fault affected ground were not necessarily unforeseen, some aspects such as groundwater behaviour or localised low strength zones are likely to remain difficult to identify based on conventional geotechnical investigation. As a result some elements required to be recognised and responded to during the course of construction. The ongoing involvement of the designer through construction is essential when working in these conditions.

7 ACKNOWLEDGEMENTS

The authors wish to thank Karori Sanctuary Trust and Wellington City Council for permission to publish this paper.

REFERENCES

Beca (2007) *Karori Wildlife Sanctuary New Visitor Centre – Geotechnical Factual Report*. Prepared for Karori Wildlife Sanctuary Trust.

Beca (2008) *Karori Wildlife Sanctuary New Visitor Centre – Additional Geotechnical Investigation, Factual Report*. Prepared for Karori Wildlife Sanctuary Trust.

Beca (2011) *Karori Tunnel Refurbishment – Soil Nail Wall - Factual Geotechnical Report*. Prepared for Wellington City Council.

Begg, J.G., Mazengarb C. (1996) Geology of the Wellington area, scale 1:50 000. *Institute of Geological & Nuclear Sciences geological map 22. 1 sheet + 128 p.* Lower Hutt, New Zealand: Institute of Geological & Nuclear Sciences Ltd.

Begg, J.G. & Johnston, M.R. (compilers) (2000) Geology of the Wellington area. *Institute of Geological & Nuclear Sciences 1:250,000 geological map 10*. Lower Hutt, Institute of Geological & Nuclear Sciences Ltd.

Begg, J., Langridge, R., Van Dissen, R., & Little, T. (2008) Field Trip 1. Wellington Fault: Neotectonics and Earthquake Geology of the Wellington-Hutt Valley Segment. *Geosciences '08' Field Trip Guides, Wellington Fault*.

Lazarte, C., Elias, V., Espinoza, D, and Sabatini, P.J. (2003) *Geotechnical Engineering Circular No. 7 – Soil Nail Walls*. Publication No.FHWA-IF-03-017.

Opus (2011) *Transmission Gully Project, Assessment of Environmental Effects. Technical Report No. 3, Geotechnical Engineering Report*. Prepared by P. Brabhaharan for New Zealand Transport Agency and Porirua City Council, July 2011.

Pender, M.J. (1980) Friction and Cohesion Parameters for Highly and Completely Weathered Wellington Greywacke. *3rd Australia-New Zealand conference on Geomechanics: Wellington, May 12-16, 1980. Wellington, N.Z.: Institution of Professional Engineers New Zealand, 1980: 1-171-1-175. Proceedings of Technical Groups; Vol. 6, no. 1, part 1.*

Perrin, N.D. (2004) *Karori Tunnel - Geological Aspects.*

Read, S. A., Richards, L., & Perrin, N. D. (2000) Assessment of New Zealand greywacke rock masses with the Hoek-Brown failure criterion. *GeoEng2000, Melbourne*.

Stevens, G.R. (1974) *Rugged Landscape - the Geology of Central New Zealand*. A.H. & A.W. Reed Ltd., Wellington, Sydney & London.

Wellington City Council (2000-2011) *Plans, Policies and Bylaws – District Plan, Volume 3: Maps*. Map 11, 1:10,000 (2000, updated 2011): Karori, Wrights Hill, Highbury, Kelburn, Aro Valley, Map 54, 1:10,000 (2004): Hazard (Fault Line) Area: Wellington Fault – Map 5 (retrieved 2/5/2013 from http://wellington.govt.nz/your-council/plans-policies-and-bylaws/district-plan/volume-3_-maps).

Cherrill, H.E. & Eldridge, S. & Torvelainen, E. (2013)
Design and construction of a synthetic lining system for the seismic enhancement of Stuart Macaskill Lakes, Upper Hutt, New Zealand
Proc. 19th NZGS Geotechnical Symposium. Ed. CY Chin, Queenstown

Design and construction of a synthetic lining system for seismic enhancement of Stuart Macaskill Lakes, Upper Hutt, New Zealand

H E Cherrill
Tonkin & Taylor Ltd, Wellington, NZ
HCherrill@tonkin.co.nz (Corresponding author)

S Eldridge
Tonkin & Taylor Ltd, Auckland, NZ
SEldridge@tonkin.co.nz

E Torvelainen
Tonkin & Taylor Ltd, Wellington, NZ
ETorvelainen@tonkin.co.nz

Keywords: Water Reservoir, Seismic Design, Geomembrane, Wellington Fault

New Zealand Geotechnical Society Inc. 19th Symposium, Queenstown 2013

ABSTRACT

The Stuart Macaskill Lakes are High Potential Impact Category earth embankment dams, forming two raw water storage lakes, supplying Wellington, Porirua, Upper Hutt and Lower Hutt Cities, New Zealand. A Tonkin & Taylor (T&T) feasibility study in 2008, looking at increasing the storage capacity of the lakes, found that seismic design requirements have increased significantly since the construction of the lakes. This paper focuses on the design and construction of a synthetic lining system for the seismic enhancement of the lakes.

Construction of the lakes, owned by Greater Wellington Regional Council (GWRC), began in 1982 and they were commissioned in 1985. The lakes are constructed on terrace gravel deposits adjacent to the Hutt River and are located within approximately 20 to 50 metres of the Wellington Fault Deformation Zone. A Maximum Design Earthquake Peak Ground Acceleration of 1.08g illustrates the high seismic hazard.

When complete, the new lining system, made of linear low density polyethylene (LLDPE), will cover an area of approximately 14.5ha. Sliding of cover materials over the LLDPE liner and spanning of cracks were primary considerations in the design of the liner. LLDPE was specifically selected over other lining materials for its strength, ductility and frictional properties.

Of particular interest is the laboratory testing undertaken for the design of the liner and the performance of the bentonite seal at the base of the lining, a key design consideration. Laboratory testing included large shear box and tilting table testing. It is recommended that this type of testing should be used more in New Zealand.

1 THE EMBANKMENTS

The Stuart Macaskill Lakes ("The Lakes") were designed by Tonkin & Taylor Ltd (T&T) on behalf of Wellington Regional Council (now GWRC) during the early 1980's and were commissioned in 1985. The Lakes are constructed on terrace gravel deposits between the Hutt River and the rising ground of Kaitoke Hill as shown on Figure 1. The two lakes are at different levels, separated by a terrace scarp approximately 12 m high. The lakes are formed with a combination of embankments, up to 16 m high, and sidling fill against the Kaitoke Hill. Upstream side slopes are 1 vertical (V) to 3 horizontal (H) (18.4degrees), flattening to 1V to

6H (9.5degrees) towards the base. Downstream side slopes are 1V to 2H (26.6degrees). Refer to Figure 2 for typical embankment section.

The upstream surface of the embankments is covered by a composite earthen liner system generally constructed from processed site won materials. The soil liner is overlain by a protective layer of sandy rounded gravel overlain, in turn, by riprap armour.

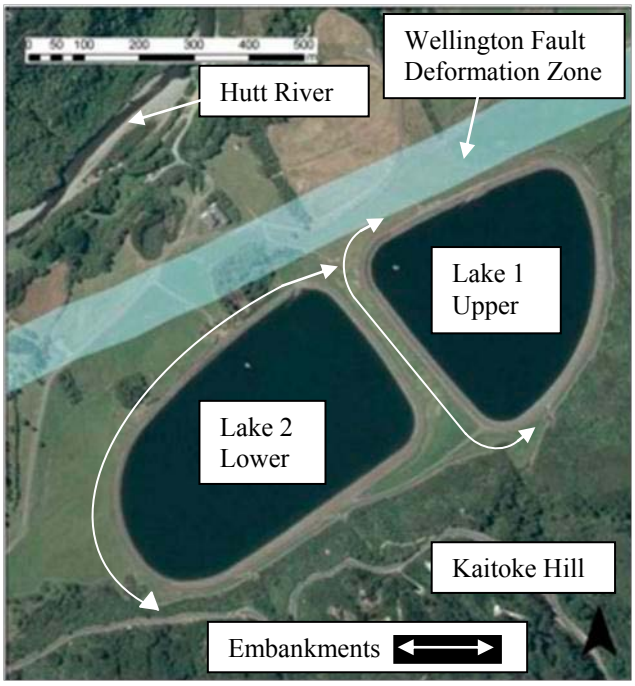


Figure 1: Plan showing The Lakes and the Wellington Fault (McVerry et al. 2008)

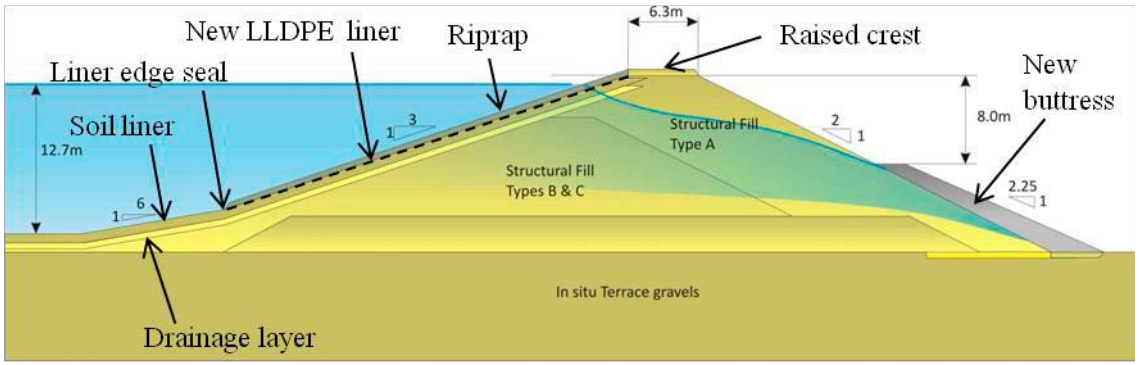


Figure 2: Typical embankment section with position of seismic improvements shown

2 EMBANKMENT SEISMIC RISK

In 2008 Greater Wellington Regional Council (GWRC) commissioned T&T to investigate the feasibility of increasing the lakes storage volume (originally 3280 ML). A key outcome of the feasibility study by T&T was the recommendation that seismic enhancement works should be undertaken to mitigate the expected cracking of the existing soil liner in a Maximum Design Earthquake (MDE).

New Zealand Geotechnical Society Inc. 19th Symposium, Queenstown 2013

Figure 1 shows the expected extent of deformation associated with a Wellington Fault rupture zone (McVerry et al. 2008). Whilst the zone passes very close to the north eastern embankment of Lake 1, it does not directly impinge on the embankment.

A site specific seismic hazard assessment (McVerry et al. 2008) recommended the MDE be derived deterministically from a Wellington-Hutt Valley fault strike-slip rupture event (moment magnitude 7.6). This gave a design Peak Ground Acceleration (PGA) of 1.08g, which was an increase of approximately 54% on the original 1980's design PGA of 0.7g. Assessment of the embankment seismic response indicated design crest accelerations of 1.9g.

Assessment of the consequences, under a MDE, for the embankment indicated:

- The calculated factor of safety for the global stability of the embankments is sufficient;
- The potential settlement of the embankments in response to the MDE is up to 400 mm and the crest is likely to suffer from significant differential settlement along its length;
- There is likely to be significant damage to the lining system of the lakes and;
- Internal erosion and concentrated leaks through the embankments resulting from a damaged lining system is more likely than other mechanisms to compromise impoundment.

The seismic enhancement works include:

- Provision of a geomembrane lining over the existing soil liner on the internal faces of the embankments to span any cracks and reduce the likelihood of leaks post an earthquake; and
- Construction of rock buttresses to control flow through the embankment should the geomembrane fail.

Additional works including raising the embankment crest level, are also being undertaken to facilitate a 1.3m increase in water depth, increasing the lakes storage volume to 3730ML. The liner and crest raising works were designed by T&T and peer reviewed by Damwatch Services Ltd.

This paper focuses on the liner design and construction to improve the seismic security of The Lakes.

3 GEOMEMBRANE ENHANCED LINER

The enhanced lining system to the embankment faces is shown in Figure 3. Construction of the new lining system requires the existing riprap and gravel protection layers to be removed without damaging the soil liner beneath. The new LLDPE liner is then installed over the soil liner and the cover materials replaced over the LLDPE liner.

The primary design requirements for the geomembrane liner are that it should be able to span potential cracks in the existing soil liner and maintain its stability and integrity in the event of the design earthquake. LLDPE was selected because of its combination of good strength and high elongation properties. The selection was further refined to a 1.5mm thick LLDPE product with spray on texturing on both sides for frictional resistance. Spray on texturing does not reduce the tensile strength and elongation properties of the sheet material, unlike other texturing types. Approximately 145,000 m^2 of LLDPE geomembrane was supplied and placed.

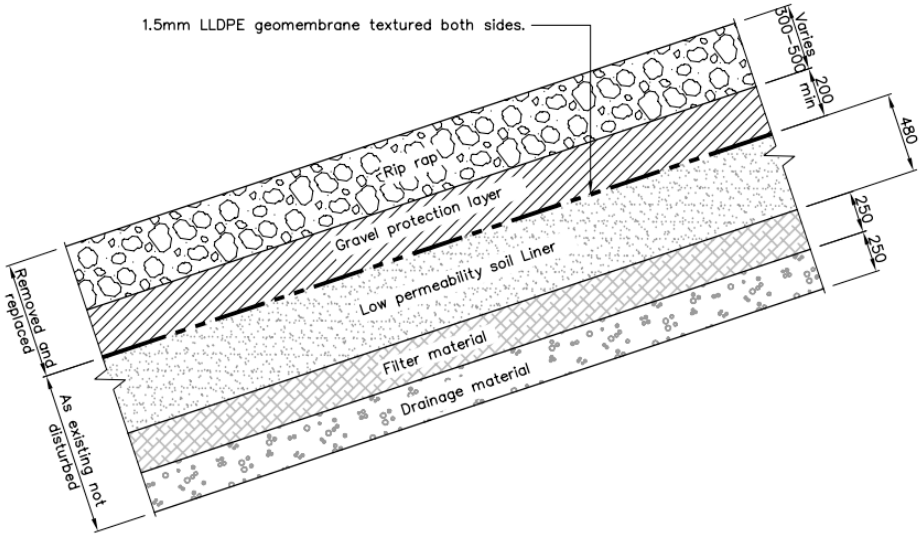


Figure 3: Typical lake liner detail with new LLDPE geomembrane

4 GEOMEMBRANE LINER DESIGN – SLIDING

The purpose of the liner is to minimise seepage through the embankment post earthquake, if the soil liner was to crack. Rupture through tearing or punching of the liner needs to be minimised when the embankment undergoes seismic deformation.

In the event of the MDE the gravel protection layer and riprap is estimated to move down the lined slopes of the reservoirs in the order of several meters. The most likely mechanism for damage to the LLDPE liner is dragging and scouring from the sliding material. The design approach adopted was therefore to ensure that the cover materials will slide over the liner without dragging it down the slope.

Assessing potential sliding, the critical surfaces identified were the interfaces between the liner and the soil, above and below. Sliding on these interfaces can be considered to be a function of:

1. The interface shear strength made up of friction and 'adhesion'
2. The normal effective stress on the interface

These are related by the following expression:

$$\tau = \sigma_n \tan \delta + a \quad (1)$$

Where τ = shear stress, δ = interface friction angle, a = 'adhesion' and σ_n = normal effective stress at the interface.

The friction and adhesion on the interfaces depends on the liner surface and the material it is placed against. The normal effective stress force is a function of the effective weight of the soil cover layers and the pore water pressure.

If the geomembrane liner is effective as a seal over the soil liner, conditions beneath the geomembrane will be dry and the effective normal stress on the underside interface of the geomembrane will be greater than that on the top interface, by an amount equal to the pressure of water overlying the liner. This would give the underside interface considerably greater strength compared to the topside interface, as the topside interface only has the buoyant weight

of the soil acting on it. If this condition were to be achieved it would promote sliding of the cover layers over the liner.

However, the liner only extends to the toe of the embankment slopes. Therefore there is a submerged edge to the liner. If this edge is not fully sealed to the existing soil liner then hydraulic continuity may be maintained on both sides of the geomembrane. In this case, the effective stress on both sides of the liner will be equal.

In order to try to promote 'dry' conditions under the geomembrane, bentonite edge seals have been incorporated along the lower edge of the geomembrane. However, the design conservatively assumes that dry conditions will not be achieved and that effective stresses will be equal above and below the geomembrane. It is therefore necessary to demonstrate that the underside interface of the geomembrane has higher friction than the topside during an MDE.

Texturing, with a greater roughness on the underside than on the top side, was specified to help promote a higher interface friction on the underside of the liner. This was achieved through the use of a spray on texture, with specified different asperity heights of the texture on the two sides of the LLDPE sheet.

A minimum factor of safety of 1.3 against sliding, in the static condition, was also to be achieved and therefore the design required minimum frictional characteristics whilst achieving the required difference between the underside and top interfaces.

The likely difference in shear strength between the two interfaces of the liner was small, controlled by project specific characteristics such as the spray on texturing and properties of the soils above and below. For this reason, reference to literature values was not appropriate. To confirm the required interface shear strengths were achieved, a series of large shear box tests were undertaken. This is discussed further in Section 6.

5 GEOMEMBRANE LINER DESIGN – CRACK SPANNING

One of the primary objectives of the geomembrane liner system is to prevent or limit leakage through cracks that are likely to be formed in the existing soil lining system in a major earthquake.

To assess the width of crack that could be spanned by the LLDPE geomembrane, the methodology developed by Giroud, Bonaparte, Beech and Gross (1990) was used. This method considers the stress and strain in the geomembrane with deformed shape to resist the imposed fluid pressure and cover materials. The calculations indicated that the LLDPE geomembrane could span, unsupported, significantly greater crack width than the anticipated maximum design crack based on deformation analysis of the embankments, which was assessed as 50 mm.

6 LABORATORY TESTING

Large shear box testing was carried out, by Geotechnics Limited, to confirm the shear strength on the liner interfaces.

The normal stress range that the liner will experience in The Lakes is approximately 7 to 14 kN/m². The lowest normal stress practical, with the apparatus used, was 10kN/m². The testing was carried out at normal stresses of 10, 30 and 50 kN/m².

An initial series of tests was carried out during the design stage using samples of liner obtained from the manufacturer. Subsequently similar material to that tested was specified. On receipt of material supplied for use in the works, inspection showed that the spray on texturing technique

produced a variable pattern of texturing with some sheets having a rougher surface than others. A second series of tests was therefore undertaken, repeating the earlier tests but with liner samples reflecting the range of texture pattern of the supplied material. In total eight shear box tests were carried out.

Testing of the top and bottom liner interfaces was carried out under wet and dry conditions. The tests were continued to displacements of 40 to 65mm to establish residual shear strengths.

The results of the testing are given in Table 1 for the primary design case of the submerged liner, assuming a wet interface between the LLDPE geomembrane and underlying soil liner.

Table 1: Shear box testing results

Interface	Moisture Condition	Results			
		Measured Strength	Friction Angle (degrees)	Apparent Adhesion (kPa)	Design Consideration
Top – Gravel to LLDPE	Wet	Peak	27	4	Upper Bound
Bottom – LLDPE to Soil Liner		Peak	33	10	Lower Bound
		Residual	29	5	Lower Bound

Some variation in the frictional properties of the different liner texturing was found in the testing. The test results in Table 1 represent the upper bound value of disturbing shear force on the topside of the liner and lower bound resisting shear strength of the underside interfaces for the material used in the works. These results represent the worst case combination of liner texture variation. Use of a wet underside interface in the testing also represents the worst case condition in the field resulting from ineffective liner edge seals.

The laboratory testing indicates that the shear strength of the topside interface is always less than the underside interface. This is true even when considering the residual strength on the underside interface although, with no movement of the liner over the subgrade, the shear strength should not reduce to residual strength values. These results confirm that the liner will remain in place while the overburden material slides over it.

To further confirm the sliding mechanism an inclined plane test, otherwise known as a tilting table test, was undertaken. A tilting table apparatus, as shown in Figure 4, was constructed following the guidance contained in ISO12957-2. This apparatus was used to construct the full liner sequence of soil liner, LLDPE geomembrane and protection gravel layer. Weights were added to provide a representative normal stress. The table was tilted until the box containing the protection gravel slid downward. The following results were obtained:

- The gravel slid downslope at a tilt angle of 41degrees to the horizontal. The shear strength calculated from this result is in good agreement with the shear strength parameters obtained from the shear box testing; and
- The gravel slid over the LLDPE geomembrane without dragging the LLDPE.

This test confirms that the gravel protection layer and riprap will slide over the geomembrane before the geomembrane is dragged over the soil liner, in accordance with the design intent.

Examination of test samples from both the tilting table test and the shear box tests indicated no significant damage to the LLDPE liner.

New Zealand Geotechnical Society Inc. 19th Symposium, Queenstown 2013



Figure 4: Tilting table test apparatus

7 CONSTRUCTION AND PERFORMANCE OF BENTONITE EDGE SEALS

Works to Lake 2 were completed and the lake refilled in 2012. Works to Lake 1 are currently underway. Figure 5 shows the construction works. Inspection and quality assurance procedures are in place for each stage of construction. This includes inspection of the LLDPE liner material as it is deployed to confirm that the texturing on each side conforms to acceptable pattern and roughness as determined by the testing programme.



Figure 5: LLDPE liner placement sequence

Completion of Lake 2 has provided the opportunity to review some of the design assumptions. In particular, as noted previously, the liner does not extend across the base of the lakes and a seal was constructed along the submerged edge of the liner to try to promote dry conditions under the liner. Piezometers installed under the liner indicate that dry conditions have not been achieved, the pizeometer pressures recorded being equal to the depth of overlying water.

It was always recognised that an effective edge seal would be difficult to achieve and the data now available confirms the importance of the conservative design assumption made that the edge seal would not be effective. The reason a seal has not been achieved is unclear, however it is likely that a very small void exists between the LLDPE liner and the gravelly soil liner that allows water pressures to be transmitted beneath the liner from any leakage points.

8 CONCLUSIONS

This project has demonstrated the value of large shear box and tilting table testing. Verification of the acceptability of the design, for this project, would not have been possible without this testing that provided confidence to the designer, owner, peer reviewers and regulatory authority.

The authors understand that this is the first project in New Zealand to use the large shear box test since the 1980's. The authors recommend that shear box testing and tilting table testing is considered whenever the shear strengths on liner interfaces is critical to the design.

Monitoring of piezometers has shown that there is transmission of water beneath the LLDPE liner. The project has also demonstrated the importance of clearly identifying design criteria and assumptions and procedures for following these through to construction to confirm that the design intent is achieved.

9 ACKNOWLEDGEMENTS

The authors would like to thank John Duggan and Alastair McCarthy of Greater Wellington Regional Council for their support in writing this paper.

REFERENCES

Giroud J P, Bonaparte R, Beech J F, Gross B A (1990) "Design of soil layer geosynthetics overlying voids" Geotextiles and Geomembranes 9 (1990) pp11-50.

ISO 12957-2, Geosynthetics – Determination of friction characteristics. Part 2, inclined plane test. ISO 2005.

McVerry, G.H, Van Dissen, R., Litchfield, N, Begg, J.G (2008) "Earthquake spectra and displacements for Stuart Macaskill Lakes, Te Marua". GNS Science Consultancy Report 2008/312.

Pinches,G.M. (2013)
Mitigating geotechnical risk to embankments on mud flats – illustrated by the SH15 Waterview Motorway widening
Proc. 19th NZGS Geotechnical Symposium. Ed. CY Chin, Queenstown

Mitigating geotechnical risk to embankments on mud flats – illustrated by the SH16 Waterview Motorway widening

G M Pinches
Aurecon, Auckland, NZ.
gregory.pinches@aurecongroup.com (Corresponding author)

Keywords: embankments, sea level rise, soft soil, settlement, ground improvement

ABSTRACT

Infrastructure constructed in the coastal environment is exposed to several natural hazards. Where such infrastructure runs on embankment to cross intertidal mudflats it may be exposed to flood risk from storm surge, tsunami or sea level rise.

A typical response to mitigate the flood risk is to raise the level of the embankment but this commonly exposes it to further geotechnical risk from the presence of soft soils supporting the embankment, which are susceptible to both settlement and instability.

For new embankments aligned on soft soil, this paper discusses the benefits and limitations of a range of approaches to overcome the geotechnical risks, such as dredging, staged construction and various ground improvement techniques. Where existing lifelines have to remain open during construction however, the options are more constrained.

This paper presents the initial philosophy for the proposed widening of the Causeway section of the SH16 Northwestern Motorway, demonstrates the geotechnical risks and provides a case study in the assessment of the approaches to mitigate those risks.

Widening requires new fill supported by normally consolidated fine soils to abut an existing embankment supported by partially consolidated soil, potentially leading to instability or large differential settlement. The solution proposed for the consented design was to improve the natural ground by in-situ stabilisation but the level of the motorway also had to be raised. This is a balance between the amount of fill to be placed, the resultant settlement and the operational life; it requires placement of compensatory fill to offset additional settlement.

New Zealand Geotechnical Society Inc. 19th Symposium, Queenstown 2013

1 INTRODUCTION

1.1 Coastal lifelines and their potential impact from natural disasters

Where roads and railways connect coastal communities or are aligned across bays, estuaries or the foreshore, perhaps to bypass mountainous terrain or urban areas in the interior, they need to be constructed in the coastal environment. Not only is coastal infrastructure exposed to the same seismic hazards as inland infrastructure (from proximity to faulting) or landsliding (where it is aligned along slopes), it has the potential for exposure to additional hazards in the marine environment. Lifelines carried along an embankment are exposed to erosion and inundation by storm surge, wave overtopping or tsunami (Fig 1). The risk from these hazards is increasing as a result of climate change and associated sea level rise.

1.2 Coastal mudflats – their nature and properties

It is widely published that world sea levels have risen by about 100m since the end of the last glaciation (c. 10 - 12,000 years ago). Former valleys and basins have been blanketed in littoral and marine deposits which, in low energy environments, are predominantly composed of silts

and clays. In estuaries and bays these soils often emerge at the surface and may appear as extensive mudflats. Whether permanently underwater or intermittently subaerially exposed, these young deposits are typically very soft and normally to lightly consolidated. Similar materials are reported worldwide, such as the Bothkennar Clay, Grangemouth, Scotland (Hight et al, 1992) or the Hang Hau Formation at Chek Lap Kok, Hong Kong (Plant et al, 1998).

In Auckland intertidal mudflats are a characteristic of both harbours (Manukau and Waitemata). Recent investigations in the inner Waitemata Harbour for the Waterview Causeway project (Aurecon 2012) indicate very low shear strength: typical Su of 5 kPa increasing at 1.7 kPa/metre depth, Mohr-Coulomb parameters of φ' 25° c' 0 kPa; these values are similar to marine mud tested offshore. The low strength is associated with high compressibility and low density; eg Cc (compression index) 0.97, Cα 0.031 (creep index), ɣ14.8 kN/m^3 (Aurecon 2011).



Figure 1: Inundation by storm surge at Spring tide; SH16 Causeway, January 2011

2 EMBANKMENTS ON MUD FLATS

2.1 The Issues

Embankments built on top of the soft soils of coastal mudflats are at risk of collapse during construction due to bearing capacity failure and side slopes are at risk of slip failure through the underlying low shear strength soil. Even if an embankment is successfully constructed on top of a layer of this material, it is prone to suffer severe settlement effects due to its high compressibility; lifelines carried by the embankment are at risk of suffering unacceptable distortions. Being low-lying, such embankments are exposed to inundation, wave action or erosion as water bodies lap at their toes and they thus require additional protection measures.

2.2 Mitigation Options

For formation of a new embankment to be aligned over mud flats in their virgin (normally consolidated) condition, a range of mitigation options are available, a selection of which are presented in Table 1. The table identifies distinct approaches which differ in how the poor characteristics of soft soils are mitigated. In reality some ground improvement techniques work in more than one way to improve the soil, for example the soil may be stiffened and drained at the same time. Although described independently, some techniques are typically used in combination with others eg wick drains can be used to enhance the efficacy of preloading. Furthermore options can be refined by addition of other elements, such as:

- Drainage Blanket – placed between fill and wick drains to remove groundwater
- Geogrids – to reinforce a fill embankment to steepen side slopes
- Geogrids and aggregate – to form a working platform
- Geotextile – placed on the surface of the mudflats as a separation layer.

New Zealand Geotechnical Society Inc. 19th Symposium, Queenstown 2013

Table 1: Constructing Embankments over Normally Consolidated Soft Soils – Selected Mitigation options

Mitigation Option (How it works)	Techniques	Commentary	Shortcomings
Removal Soft ground is removed and replaced with a stiffer soil	Dredging (marine)	Mud[a] can be removed by grab or pumped from seabed from floating barge.	Expensive to deploy. Unsuited to tidal zone. Soft pockets may remain.
	Excavation (undercut)	Long reach excavator can be deployed.	Instability of sides, difficult below GWL[c].
	Jet grout, vibroreplacement	Columns of soil are excavated.	Plant needs to deploy onto mud[1] surface.
Lightweight Fill Imposed load is lowered to reduce the stresses causing instability, reduce consolidation and reduce consequent settlement	Pumice, scoria or other naturally lightweight soil	Density 13-14 instead of 18-19 kN/m^3 may adequately increase Factor of Safety.	Reduction in stress may be insufficient to satisfy settlement criteria
	Polystyrene	Extremely light: settlement & instability minimised. Well suited to transition zones with hard structures.	Susceptible to chemical solution, rodent burrowing and flotation – requires protective cladding. Expensive; unavailable in volume.
Advanced Consolidation Pore water is drained out of the soft soil, the void ratio is reduced and the shear strength increased. Best coupled with instrumentation to monitor ground improvement.	Preloading	Embankment raised in advance.	Risk of instability. Requires long time.
	Staged Construction	Each lift consolidates before next is placed.	Takes a long time.
	Surcharge	Consolidation advanced by temporary load.	Risk of instability. Double handling of fill.
	Vertical Drainage (wick or band drains, stone columns)	Installation substantially shortens drainage paths: rapid consolidation.	Requires fill placement for consolidation to commence. Heavy plant needs WP[b].
	Vacuum consolidation	Pore water removed under vacuum.	Specialist equipment – expensive.
Soil Densification Soil is compacted	Dynamic compaction (DC)	Dropping weight compresses soil below.	Best suited for granular, heavy plant requires working platform
	Vibrodisplacement	Vibroflot displaces soil laterally.	Plant needs to deploy onto mud[a] surface.
Soil Displacement Soft soil moved out of the way	End tipping, Lightweight tamping, explosives.	Fill falls through mud[a], possibly assisted by additional tamping.	Little control – soft mud[a] may mix in to form uneven material. Treatment depth varies. Mudwaves may form in front.
	Dynamic compaction (DC)	Dropping weight forms crater, then infilled.	
Soil Mixing Soil is mixed with an additive that chemically reacts with free water and forms strengthening bonds.	In-situ stabilisation	Cement or lime mixed in by rotators.	Mixture inconsistency. Max. depth 6m.
	Ex-situ stabilisation	Mud[a] dug out, mixed and put back.	Excavation stability. Treatment depth.
	Deep soil mixing (DSM)	Rotating tools mix additive evenly in deep columns; can form large panels.	Uncommon plant, heavy (needs working platform) and expensive to use.
Soil Reinforcement Stiffer elements installed	DSM columns Stone columns	DSM as above. Stone columns installed by vibrodisplacement or vibroreplacement.	DSM as above. Complex modelling of rigid elements in soft matrix.
Embankment Foundation Stresses taken to stiffer underlying layer by load spreading or transfer.	Raft Foundation	May be rigid (reinforced concrete) or flexible (eg geogrids with aggregate)	Settlement little reduced.
	Piles	Driving, drilling/cast-in-place, jet grouting.	Expensive, slow and heavy plant needs WP[b].

Notes: a.) mud = fine grained sediment, typically normally consolidated, soft, and of marine or littoral origin. b.) WP = working platform. c.) GWL = groundwater level

3 THE CAUSEWAY SECTION OF THE SH16 NORTH-WESTERN MOTORWAY

3.1 The widening project

The development of Auckland's western suburbs has led to an increased road useage on the North-western Motorway with heavy congestion in peak periods. The NZ Transport Agency (NZTA) has been studying options for increasing traffic capacity for many years but have now decided to widen the motorway. The need has increased further by the strategic incorporation of the motorway into the Western Ring Route Road of National Significance. With further traffic programmed to come onto the motorway when the SH20 Waterview Connection tunnel opens, NZTA has recently engaged an Alliance to complete the design and construct a widened motorway. This paper reflects the situation prior to that tendering.

3.2 The Causeway

Between Waterview Interchange and Rosebank Interchange, the existing motorway comprises 3 west-bound and 3 east-bound (city-bound) traffic lanes plus shoulders and a dedicated cycleway / walkway aligned on a section of embankment known as the Causeway. Initial construction commenced in 1952 over mud flats formed of very soft normally consolidated marine silt and clay ("mud"); the embankment was widened in 1959. Ground investigations (Thomas et al 2010) show that this soft soil is typically 10-12m, reaching a maximum thickness of 14m. The mud flats are further underlain by assorted soils up to about 40m thick before the Miocene East Coast Bays Formation is encountered. Although the Geological Survey (Edbrooke 2001) assign all these soils to the Tauranga Group, engineering geologists discriminate between the Holocene normally consolidated uppermost intertidal to marine mud, which will be responsible for most of the settlement and stability issues, and the older Plio-Pleistocene materials. The latter still include some moderately compressible layers which will need to be accounted for in the design.

Confirming the characteristics of the mud, Newland and Allely (1952) reported that the original embankment failed in places and they reported settlements of about 0.5m occurring in 12 months after construction. Consultation of historic records, back analysis (Aurecon 2011) and anecdote indicates that about 1.2-1.5m of settlement has occurred since original opening. Drilling through the embankment shows the base of the fill can be about 3m below the equivalent mudflat level, indicating a fill accumulation due to construction phase settlement, the incorporation of any original working platform as well as building up to offset settlement.

Although primary settlement of the marine mud below the Causeway embankment may now be complete, secondary creep is potentially still ongoing and, if the embankment is raised, primary consolidation will recommence. Furthermore the low shear strength of the marine mud means that, as the embankment is raised, there is a risk of slope instability of its shoulders.

3.3 Embankment Level

The elevation of the existing motorway is too low (+2.1m RL at the northern crest) to safeguard this lifeline from occasional inundation by storm surge. The Intergovernmental Panel on Climate Change (IPCC, 2007) indicate that global warming will lead to a greater frequency and intensity of storms so that storm surge and increased wave heights will lead to more frequent inundations of the motorway. Furthermore sea level rise (SLR) is predicted to raise static sea levels so that during the 100 year design life, without mitigation, the motorway would be more subject to flood events. Initially the design level (DL) at the shoulder crest was set relative to the Mean High Water Spring (MHWS) tide by:

DL = MHWS Tide + 1 in 100 year Storm surge + Wave max + SLR (100) + Settlement

For initial calculations, the post-construction settlement component was set at 500mm. Hence, whereas the design level at 100 years at the seaward crest might be +3.1mRL to withstand SLR, storms and wave action, this was set at +3.6m RL, to allow for ongoing settlement.

New Zealand Geotechnical Society Inc. 19th Symposium, Queenstown 2013

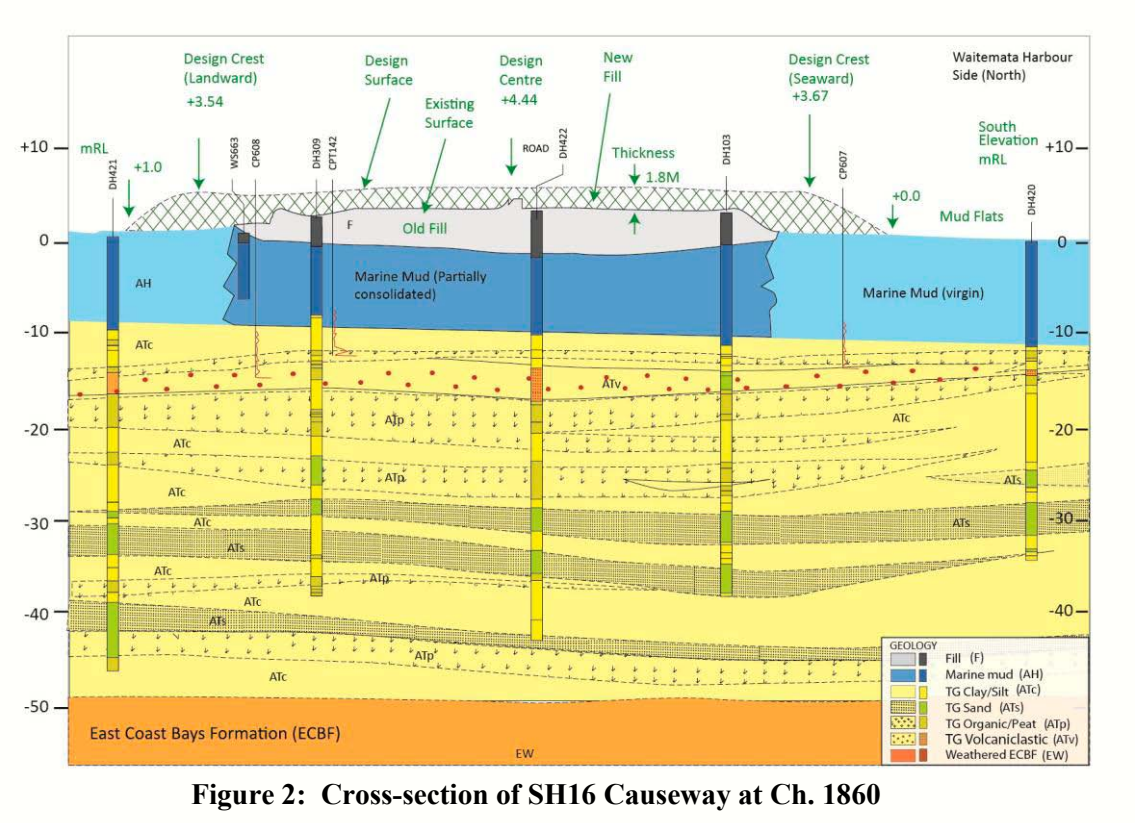


Figure 2: Cross-section of SH16 Causeway at Ch. 1860

3.4 Constraints and Considerations

The SH16 project is primarily constrained by the fact that it is widening of an existing section of infrastructure which must remain open during the works; the main constraints are:

- Ground improvement can be undertaken under the new shoulders but it generally cannot be applied to ground below the existing traffic lanes.
- The duration of the project is short; additional lane capacity west-bound must be in place by the time that the Waterview Connection tunnel is open.
- The lower factors of safety that may typically be acceptable for the construction phase of a project do not apply since the public are actively using the existing embankment.
- The adjacent ground on either side of the embankment is tidal; Plant can only access the shoulder areas from the motorway itself.
- The site lies in an environmentally sensitive zone. As well as lying in the Coastal Marine Area, below the high tide mark is a designated marine reserve subject to more onerous environmental consents.

Some of the options that could be considered for a new embankment cannot be applied. For example the original construction of the motorway (Newland and Allely, 1952) employed end-tipping and was accompanied by some embankment failures. Dry land operations can only take place intermittently at low tide or have to occur within a cofferdam, until such time as a working platform can be built above high tide. Fully marine operations from floating barges and the like are not feasible when the ground dries twice daily.

3.5 Uncertainty in Sea Level Rise predictions

Since the IPCC (2007) publication, satellite observations have shown sea levels at the upper level of the IPCC predictions, greater uncertainty is evident and many recent projections exceed those of the IPCC (RSNZ 2010). Following the MfE (2008) guidelines, the Consented design adopts a Medium scenario SLR of 0.8m by the year 2100 but the project was evaluated to accommodate a 1.1m SLR in the High scenario. To account for the 100 year motorway design life from project completion in 2017 SLR was extrapolated to 1.05m (Medium) and 1.40m.

3.6 Preliminary Design

3.6.1 Road Design Philosophy

The consented design for the project was based on widening occurring on both sides of the causeway. The philosophy for this design was controlled by traffic management and based on a three stage approach. In the first stage traffic would be diverted to the south side of the embankment to open up the northern shoulder for widening works. Then traffic would be moved onto the new northern shoulder to free the south side for widening works there. In the third stage traffic would be parted to north and south to allow the centre of the embankment to be raised to the final level. Initial analysis assumed earthworks durations of 2 years each under the northern and southern shoulders, then filling in the central zone over a single earthworks season. This scenario would allow 3 years of consolidation under the northern shoulder but only 1 year under the southern shoulder before project completion.

3.6.2 Settlement

Following the design philosophy above, Table 2 presents calculated settlements over a 100 year design life due to fill placement. The analysis uses simple one-dimensional consolidation theory and assumes no ground improvement or other mitigation. To offset construction phase settlement, additional ("compensatory") fill needs to be placed to achieve the notional +3.6mRL project handover level. As shown however, the post-construction continuation of primary consolidation plus secondary compression (creep) exceeds the notional allowance of 500mm. So the crest elevation at 100 years is well below the level to prevent overtopping. Every additional fill increment further increases the settlement, requiring yet more compensatory fill. Without other mitigation, at least an additional metre of fill needs to be placed to achieve the design life level. Not only will this extra fill add to costs, a range of other unwelcome effects will be manifested. These include additional embankment width, out of tolerance distortions relative to the centre line, compromising of the drainage and a potential increase in instability.

Table 2:Settlement and the application of compensatory fill; Northern crest, Ch 1800

Case	Built Level mRL	Primary Consolidation		Creep mm	Elevation 100 years
		During works	Operation		
Design Level with 0.5m operational tolerance	3.6	340 mm	730 mm	150	2.38mRL
Compensatory Fill 400mm to achieve 3.6m level	4.0	377 mm	811 mm	150	2.66mRL
Compensatory Fill 820mm shortfall at 100 years	4.42	417 mm	896 mm	150	2.96mRL
Extra fill required placing a further 180mm	4.6	434 mm	932 mm	150	3.08mRL

Besides consolidation and creep, the ground below the embankment will experience immediate (elastic) settlement. This will be evident as an additional volume of fill material needing to be placed; eg an additional 235mm thickness to offset deflection caused by 3.6m of fill.

With a design crossfall of 3% for lateral drainage and traffic requirements, the centre of the embankment has to be raised to +4.4mRL for a crest height of +3.6 mRL. As the mud here has consolidated under the weight of the existing embankment for 60 years, the post-construction settlement is assessed at 380mm, yielding a centre-to-edge differential settlement of 500mm. This 1.7% differential in cross-fall exceeds the 1% tolerance. Once compensatory filling is accounted for, this unacceptable differential settlement will be even worse. Should the parameter values or layer thicknesses vary from the design values used in calculations, there may be further distortion of the pavement and potential compromising of the road drainage.

3.6.3 Geotechnical considerations and the need for ground improvement

If the weight of new embankment shoulders comes onto the normally consolidated soil too quickly, excess pore pressures will cause slope instability or bearing capacity failure. Consolidation of these soft deposits would also cause the road surface to fail to meet the design criteria. When an embankment is raised slowly enough, the foundation soil can improve by consolidation to have a greater shear strength and lower compressibility. With fill heights of 3.6 to 4.6m over this soft soil however, the approach will be too slow for the 5 year programme originally planned. Hence, ground improvement measures from Table 1 were considered, the primary strategy being to overcome instability. A solution for instability will partially address the settlement, which can then be further overcome by other less radical ground improvements.

3.6.4 Prospective Mitigation Options

Of the various approaches reviewed in Table 1, it was considered during the preliminary design that a form of soil mixing would yield a sufficient improvement to permit the shoulders of the embankment to be raised without triggering slope instability or a bearing capacity failure. Initially insitu stabilisation was favoured to mix soil with cement to form a raft of stabilised soil ("mudcrete") up to 5m thick. With sufficient cement and even mixing, the mud could be replaced by a soil-cement mixture with a uniaxial compressive strength of up to 1 MPa.

Although a mudcrete raft offers a significant improvement in settlement characteristics, the issue still persists. Even though post construction settlements can be kept to within the notional 500mm allowance, so that the design levels against inundation can be met, this can only be achieved if some additional "compensatory fill" is placed.

At the Specimen (Reference) Design stage, the crest design level was increased to +4.2m RL to extend the design life to 2120 and allow for the higher SLR predictions. Additional ground investigation had become available and, with the benefit of PLAXIS finite element analysis, a shallow raft alone could not resist all failure modes. Hence the ground improvement panels below the embankment shoulders were to be vertically stiffened with rigid inclusions formed by deep soil mixing (DSM). A mudcrete raft was still required however to form a working platform for the DSM plant and to force the potential slip circles deeper into the marine mud.

3.6.5 Differential Settlement

Even though DSM can stabilise the embankment shoulders, the stiffening of the soil will be in contrast to the centre of the embankment. As soil mixing cannot be done under the centre, primary consolidation and secondary compression will recommence as soon as the embankment here is raised. Despite application of preloading and surcharge at the shoulders, there is the potential for out-of-tolerance differential settlements relative to the centre, leading ultimately to the need for shape correction to maintain cross falls and longitudinal profiles.

3.7 Discussion

The inherent assumption with the Reference design approach is that the embankment has to be built now to accommodate changes that will not happen for many decades and may occur more slowly than estimated; the complete cost of construction is met today to address a need many years away. Alternatively the embankment could be raised to a lower level that meets sea level rise needs in the shorter term; by so doing the amount of fill to be placed immediately and the consequent settlement impacts are reduced. Ultimately the embankment would have to be raised again but the costs for doing so would be met in the future and the timing could be refined according to how the embankment actually performs.

Should the embankment be built to a lower interim design level, it is important that the full ultimate design width is maintained. As the embankment consolidates and sea level rises, its effective width (above high tide level) is reduced. If the embankment is subsequently raised and the angle of the revetment is maintained, the available width at the top is reduced further.

4 CONCLUSIONS

- The paper has shown that aligning a Lifeline over coastal mud flats exposes the infrastructure to a number of natural hazards.
- The benefits and limitations of a range of mitigation approaches have been presented.
- Illustrating with a current project shows how complex may be some of the considerations required in order to make the project a success.
- When critical infrastructure is aligned through the coastal environment, asset owners and their designers are recommended to consider some of the approaches identified in Table 3 in order to minimise the threat from natural hazards.

Table 3: Recommended considerations when planning a coastal lifeline over mudflats

Issue	Consideration
Alignment	Must the lifeline track at low elevation across settlement-susceptible soils?
Programme	How much time is available to undertake the measures? With more time, less intrusive lower cost solutions may be applied.
Design Life	Must the typical 100 year design life apply? Can an interim level be accepted?
Tolerances	Can the most rigid design requirements be relaxed over this section?
Cost	Has the whole-of-life cost been considered to take into account aspects such as future reprofiling as a result of differential settlement?
Environmental Uncertainty	Does the design have to accommodate the worst case climate change extrapolations? Can an adaptable solution accommodate the uncertainty?
Geotechnical Uncertainty	How well is the soil characterised? How well might the proposed ground improvement techniques work? Could a trial embankment be beneficial?

ACKNOWLEDGEMENTS

This paper is produced with the permission of New Zealand Transport Agency. I also wish to thank Joseph Owusu, Raymond Lo and Doru Bobei for your considerable contributions, partly captured herein, and for the stimulating dialogue over the years with numerous other colleagues.

REFERENCES

Aurecon (2011) SH16 Earthworks Specimen Design Report.210155-007-04. 12 Dec 2011.

Aurecon (2012) SH16 Causeway Stage 4 – Geotechnical Interpretative Report. 210155-005-05, 7 Mar 2012.

Edbrooke, S.W. (2001) Geology of the Auckland Area. *Institute of Geological and Nuclear Sciences Ltd., Lower Hutt, NZ,* ISBN 0-478-09714-X.

Hight, D.W., Bond, A.J. and Legge, J.D. (1992) Characterisation of the Bothkennar Clay: an overview. Géotechnique, Vol. 42, No. 2, p303-347.

IPCC (2007) Climate Change 2007. The Fourth Assessment Report of the Intergovernmental Panel on Climate Change (AR4).

MfE (2008) Coastal Hazards and Climate Change. A Guidance Manual for Local Government in New Zealand. *Ministry for the Environment*. ME892.

Newland, P.L.& Allely, B.H. (1952) Further Evidence of Increase of Shear Strength with Depth Provided by Vane Tests on a Recent Deposit of Soft Clay. *Proceedings of the1st Australia-New Zealand Conference on Soil Mechanics and Foundation Engineering,* p123-134.

Plant, G.W., Covil, C.S. & Hughes, R.A. (1998) Site preparation for the new Hong Kong International Airport. *Thomas Telford*. 576pp.

RSNZ (2010) Sea Level Rise. Emerging Issues. *The Royal Society of New Zealand*.

Thomas, B.I., Costello, D.A. & Pinches, G.M. (2010) Auckland Waterview Causeway: Geo-Model of a Sinking Motorway. *Proceedings of the 11thConference of the IAEG, Geologically Active*. Auckland, NZ.

Price, C.H. de G (2013)
Christchurch ocean outfall pumping station liquefaction mitigation
Proc. 19th NZGS Geotechnical Symposium. Ed. CY Chin, Queenstown

Christchurch ocean outfall pumping station liquefaction mitigation

C H de G Price
Chief Geotechnical Engineer, Asia Pacific Design, MWH Global, Christchurch,
formerly Principal, URS New Zealand Ltd, Christchurch.
Charlie.H.Price@MWHGlobal.com

Keywords: pump station, liquefaction mitigation, deep soil mixing, soil replacement

ABSTRACT

This paper describes the liquefaction mitigation works carried out for the Christchurch Ocean Outfall Pump Station (OOPS), which is located adjacent to the Avon estuary in Eastern Christchurch, and forms part of the water-retaining structure of the ponds.

The outfall pumping station was completed in 2008, and the pipeline in 2010, just prior to the commencement of the Canterbury earthquake sequence in 2010. The site lies 7km north of the epicentre of the devastating 22nd Feb 2011 M6.3 event, during which horizontal and vertical PGAs of 0.6g and 2.0g, respectively, were recorded at a station about 3.5km west of the OOPS site. Liquefaction occurred in the surrounding estuary immediately adjacent to the pump station during at least three of the seismic events; cracking and slumping of the oxidation pond embankments occurred in the Sept 2010 and Feb 2011 events. The pumping station survived each of the seismic events with no known damage.

Pre-tender design was based on the use of deep soil mixing (DSM) to liquefiable foundation soil within discrete cells formed of rows of overlapping DSM columns. Following contract award, the successful tenderer offered to carry out total soil replacement as an alternative to the DSM design. This offer was accepted and the potentially liquefiable foundation soil was excavated and replaced to a depth of 7.2m. The paper describes the foundation conditions, the factors governing the foundation treatment method selection, the alternative DSM and soil replacement designs, and their implementation.

New Zealand Geotechnical Society Inc. 19th Symposium, Queenstown 2013

1 INTRODUCTION

Christchurch City Council constructed a new waste water outfall between 2007 and 2010 in order to discontinue the discharge of treated water into the Avon and Heathcote River Estuary, and to move the outfall point offshore (Figure 1). Further details of the scheme are given by Moore, Fleming and Jones (2008).

The scheme included a 5km long 1800mm diameter pipeline, constructed partly by microtunnelling (onshore) and partly by dig and lay (offshore). The pipeline conveys 6 m3/sec of treated water, at maximum flow, from oxidation ponds located adjacent to the Avon-Heathcote estuary to diffusers 3km offshore. Details of the tunnelling are provided by Moore, Fleming and Jones (2008) and by Price (2010). Flow in the pipeline is by gravity under normal operating conditions, but the pump station located on the periphery of the 230 Ha oxidation ponds is designed to provide the higher velocities periodically needed for cleansing of the pipeline. The oxidation ponds were commissioned in 1960.

This paper discusses the design and construction of mitigation carried out to prevent damage to the ocean outfall pump station (OOPS) from liquefaction of the foundation soil in the event of an earthquake. The civils work for the pump station was designed inhouse by the City Council, with specialist input from URS for foundation design. The pump station was constructed by EDI Downer. The overall project value was in the region of NZ$85M, and the pump station NZ$...M.



Figure 1. Christchurch Ocean Outfall, showing the pump station and pipeline alignment

2 GEOLOGY AND GEOTECHNICAL INVESTIGATIONS

The project site is located in eastern Christchurch, with the pump station situated immediately adjacent to the Avon River estuary and within 1.5 km of the coast (Figure 1). The surface geology in the area consists of alluvial deposits laid down during recent times in a marginal marine setting as estuary or lagoon deposits. The deposits are mainly silts, sands and gravels, accompanied by some peats and other remnants of swamps and overbank flood deposits. A depth of some 500m of such alluvial deposits overlie bedrock in this region, which consists of basalt, sedimentary and Greywacke rock.

2.1 Geotechnical Investigations

The initial investigations for the pump station were carried out in 2005 and included eight CPTs and continuous sampling using the 'dual push tube' method at two locations. The proposed location for the pump station at this early stage was outside the pond area, beneath the existing embankments and between the pond and the estuary, and investigations were therefore limited to this area. However the pump station footprint was subsequently shifted 'upstream' into the pond area, and investigation of this part of the site was carried out at commencement of construction. This later investigation included CPTs and sampled cable tool percussion boreholes with SPTs.

The 'dual push tube' technique normally recovers continuous soil samples, but recovery was poor at this site and sampling was not successful below the upper 2.8m of natural ground, or 3.8m into embankments. Soil characteristics for design purposes were therefore based on the CPTs during pre-tender design, and these were confirmed by further CPTs and soil sampling in cable tool percussion boreholes sunk after contract award at the commencement of construction.

2.2 Ground Conditions

The investigations identified two main soil units, the upper deposits (unit 1) consisting of 4m to 8m of loose uniform fine to medium sand with some silt, inter-bedded with soft or firm silt layers, overlying lower deposits of cleaner uniform fine to medium sand (unit 2). The existing embankment fill material was confirmed in the investigations as very dense clean sand, with a

New Zealand Geotechnical Society Inc. 19th Symposium, Queenstown 2013

high relative density. Some difficulty was encountered by the CPTs in penetrating the existing embankments.

The two key geotechnical design issues identified in the early investigations were the variability of the thickness of the upper soil unit (unit 1), and the relatively low density of the upper 4m of the unit 2 deposits. The Unit 1 deposits were generally around 4m deep within and 'downstream' of the pump station footprint, but CPTs to each side of the pump station were anomalous and encountered the base of unit 1 at around twice that depth, 8m below ground level. When the pump station footprint was subsequently moved 'upstream' into the pond area this difference in the unit 1 thickness became more significant, as the deeper unit 1 deposits were thought to represent an infilled channel running through the new pump station location. However, since this area was covered by a pond the anomaly could not be investigated easily at this stage, and further CPTs and boreholes were carried out to investigate this more closely at the commencement of construction.

Typical gradings of the unit 1 and 2 deposits are given in Figure 2, which shows that the gradings of the sand parts of the two units are generally indistinguishable from each other, being uniform fine and medium sand with some silt, with a coefficient of uniformity of around 2.5. However, in addition to the sand, unit 1 also contains silt in layers and as gradation zones. Testing of the old 1960s embankment fill following the removal of those parts overlying the proposed pump station, showed that they had similar grading to the unit 1 and 2 sand, but with a lower coefficient of uniformity of 1.5 and almost no fines. The existing embankment grading is shown in Figure 2.

New Zealand Geotechnical Society Inc. 19th Symposium, Queenstown 2013

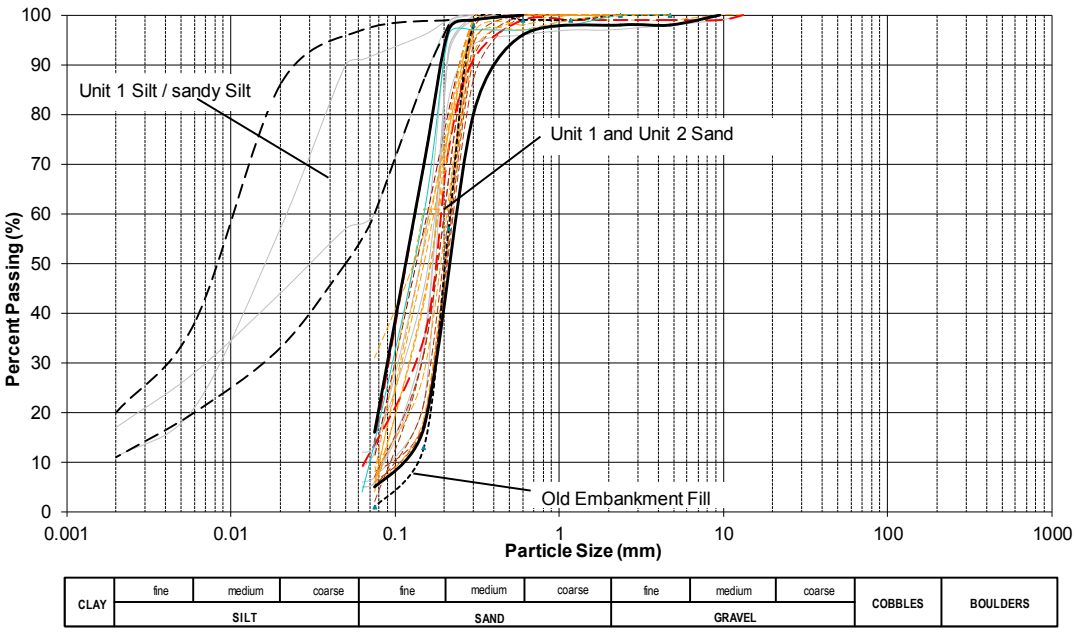


Figure 2. Particle Size Distribution Ranges for the foundation soil

Constant head permeability tests were carried out in the laboratory on two samples of 'sand with some silt' from the coarser envelope shown in Figure 2, between 6m and 10m depth. These had D_{10} sizes of around 0.063mm, and the lab tests indicated permeabilities between $7x10^{-6}$ and $8.7x10^{-7}$ m/sec. Hazen's formula suggests a permeability of 4.5×10^{-5}m/sec.

3 SEISMIC CONDITIONS AND LIQUEFACTION EVALUATION

Static bearing or settlement was not an issue for the OOPS, as the structure was partially embedded into the ground. Structures of this type do not usually carry significant foundation loads due to load compensation from the excavation of soil, the prevention of buoyancy being a

more critical issue than bearing capacity. The main geotechnical challenge for the OOPS therefore arose from the issue of liquefaction.

3.1 Seismic Loading

A review of the earthquake records held by GNS in 2005, back analysed using the seismic attenuation relationship of Stirling et al. (2001) to give PGAs at the location of the oxidation ponds, is given in Figure 3. This indicates that the strongest ground shaking experienced in Christchurch since these records began in 1840 was from the 1901 Cheviot earthquake, which generated a peak ground acceleration of about 0.14 g at the site, representing an event with a return period between 25 and 150 years. The greatest level of earthquake shaking that the pond embankments would have experienced in the fifty years of their existence prior to the 2010 Canterbury Earthquake is likely to have been around 0.125g in 1978.

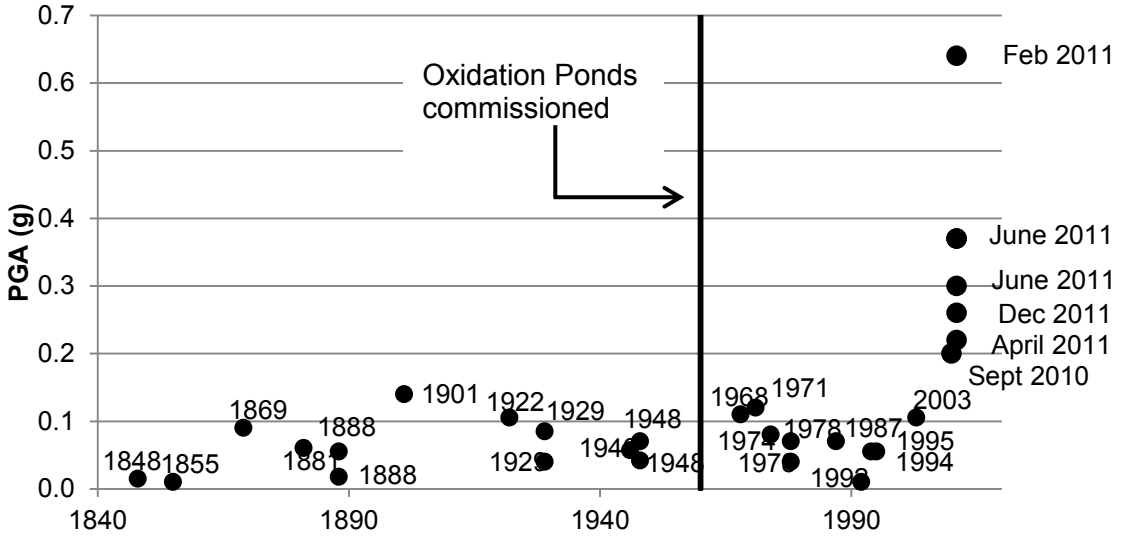


Figure 3. Backanalysed Historic PGAs (1848-2003), and 'conditional PGAs' from the 2010-2011 Canterbury seismic sequence as reported by the Canterbury Geotechnical Database (2013), at the Oxidation Ponds Pump Station.

3.2 Liquefaction Analysis

Fine to medium uniform sand, common across much of Christchurch and making up the bulk of the foundation soils at the OOPS, is highly liquefaction susceptible when loose or medium dense, and it was clear from the outset that some form of liquefaction mitigation would be required for the pump station. Liquefaction susceptibility was assessed using the CPT based method of Seed (2003), which is based on the NCEER simplified Cyclic Stress Ratio (CSR) liquefaction method (NCEER, 1997) with refinements to the normalisation of cone resistance, q_c, and sleeve friction, f_s, and to the shear stress reduction coefficient, r_d, which according to Seed provides an increased level of confidence in the results.

Liquefaction susceptibility was also checked with Davis and Berrill's Energy Method (Davis and Berrill, 1982) in order to provide a cross check with a fundamentally different method of analysis. This method is less conservative than the NCEER method and may understate liquefaction susceptibility, but where the two methods both indicate that liquefaction is likely this is taken as an indicator of high likelihood of susceptibility.

The analysis indicated liquefaction susceptibility down to levels below the proposed base level of the pump station at RL 6.35m. In some locations this was almost continuous from the surface down to a level of RL 4.8m (6.2m deep), with the Davis and Berrill method confirming susceptibility to that elevation. A further susceptible zone, generally thin but up to 1.5m thick

in one location, occurred at around RL 2m (9m below ground level), overlain by some non-liquefiable material. These analyses concentrated on the design PGA of 0.47g, but in most locations liquefaction susceptibility commenced at much lower PGA levels, below 0.14g, and the zones simply increased in thickness with increasing PGA.

Free field settlement from the full depth of liquefiable ground was calculated to be 200mm to 250mm, based on an average strain of 3.7%.

4 MITIGATION DESIGN

It was decided that ground treatment would be carried out to the base of the upper liquefiable zone, and keyed 1m into the underlying non-liquefiable ground at RL 3.8m (7.2m deep). This was based mainly on the fact that the free field settlement from the remaining deeper liquefiable ground was limited to 50mm, which was considered acceptable.

4.1 Ground Treatment Methods

It was recognised that the cleaner sand in the foundation would react positively to vibro-densification methods of ground treatment, however there was concern that the variable silt content and silt layers in the upper deposits may be sufficient to make the process unviable or unsuccessful. Vibro-replacement using stone columns, which would be expected to be more successful in these siltier conditions, was ruled out since the introduction of gravel would increase the permeability of the pump station foundations. This was undesirable as the pump station forms part of the water retaining structure around the ponds.

4.1.1 Deep Soil Mixing (DSM)

Deep soil mixing was then considered since this technique is effective in sands with high silt contents. A system of overlapping deep soil mixed columns was developed for the pump station foundation, forming a latticework of continuous walls dividing up the foundation into a number of discrete cells. In a liquefaction event the cells would retain any liquefied soils and prevent its movement from under the structure, which would then be effectively supported on the column-walls.

The deep soil mixing treatment was designed with an area ratio of 0.32 (the ratio of treated to total area), with treated sands attaining a 28 day shear strength of 0.5 MPa, and silts 0.25MPa (UCS 1 MPa and 0.5MPa respectively). These strengths are easily attainable for soil-cement mixes with low cement content installed by deep soil mixing (Taki and Yang, 1991). Columns were specified to overlap by 150mm. Conservatively assuming that a shear strength of only 250kPa was achieved in all soils, and allowing for a 0.8 seismic strength reduction factor, the average shear strength of the combined treated-untreated foundation during liquefied conditions was 64kPa, ignoring the uncertain very low liquefied shear strength of the untreated soil.

4.1.2 Soil Replacement

The contract went out to tender based on this deep soil mixing ground treatment design. However, following award the successful tenderer offered an alternative foundation treatment scheme, consisting of complete ground replacement to the same depth as the deep soil mixing design. Following negotiations this alternative was accepted, as it offered significantly lower risk to the client, particularly since deep soil mixing had not been carried out in the South Island of New Zealand at that time. A foundation consisting of entirely replaced soil, recompacted to a high standard in thin layers, was considered to provide a more secure foundation with lower risk of damage from a liquefaction event than the DSM solution.

The offer of the alternative scheme came about due to misinterpretation of the term ‘lattice’. The tender design had specified that the DSM columns were to form a lattice but had not shown

this diagrammatically, since the shape of the cells was immaterial and in an effort not to provide unnecessary restrictions on the contractor. The contractor offered the alternative soil replacement scheme to resolve this issue, and at no greater cost to the client than the original foundation treatment scheme.

The most significant issue to address with the soil replacement scheme was the fact that the only soil readily available in sufficient quantity suitable for use as fill, was fine to medium uniform sand, locally won or available as a by-product of screened river alluvium. Gravels were ruled out due to their high permeability, for the reason mentioned above. The sand fill was eventually obtained partially from the pump station excavation itself, partially as a by-product from aggregate production in existing commercial quarries and partially as spoil from the Ocean Outfall pipeline tunnel, which was being excavated at that time. These sources all provided a good consistent material.

A relative density (RD) of approximately 80% was required to achieve a liquefaction resistant fill. Maximum and minimum 'index' density tests on the processed quarry sand indicated index dry densities of 1.80 and 1.28 t/m^3 respectively, and a target dry density of 1.686 t/m^3 was therefore set. This amounted to 98% of MDD from the vibrating hammer compaction test.

The partially filled excavation is shown in Figure 4.

5 PERFORMANCE IN THE CANTERBURY EARTHQUAKE SEQUENCE

Substantial damage occurred to the old oxidation ponds embankments during the M7.1 Darfield earthquake on September 4th 2010 and the subsequent M6.3 Feb 2011 event. Damage to the new embankments constructed with the OOPS in 2007-2008 was insignificant, with only narrow cracks being apparent on the surface and no slumping of the embankments. It was clear from the emergence of sand boils that the soils in the estuary had liquefied on more than one occasion.



Figure 4. Partially filled excavation for the Pump Station soil replacement. Dewatering wellpoints can be seen within each pan of the sheetpile cofferdam, and a line of dewatering wellpoints can be seen running across the centre of the excavation in the right of the photograph.

Surveys carried out in May 2012 (CH2M Beca, 2012) indicated that the wet well of the pump station had remained at a level consistent with the surrounding ground following the earthquakes. The structures were not affected by tilting. However the surrounding ground, including the embankments, had dropped by some 200mm from pre earthquake levels, which is broadly consistent with the elevation changes from the seismic events in this part of Christchurch. Two deep chambers located on the pipeline immediately adjacent to the pump station apparently remained static at elevations consistent with their pre earthquake levels, 200mm above the surrounding ground following the earthquakes. This appears to be coincidental and in reality these structures are thought to have lifted relative to the surrounding ground. A pigging wye on the same pipeline appears to have lifted by 290mm, or 90mm in relation to the chambers.

6 CONCLUSIONS

An Ocean Outfall Pump Station was constructed within an area of liquefiable soils in Christchurch during the years leading up to the Canterbury seismic sequence.

New Zealand Geotechnical Society Inc. 19th Symposium, Queenstown 2013

Liquefaction analysis indicated that settlement of 200mm to 250mm should be expected at the pump station under a PGA of 0.47g, and ground treatment was therefore designed to mitigate liquefaction effects. Initial ground treatment design was based on the isolation of liquefied soils within confined cells created by forming walls with deep soil mixing.

An alternative foundation treatment solution of soil replacement was implemented at no greater cost than the deep soil mixing. This treatment utilised uniform fine to medium sand as the replacement soil, a particle size that is typically liquefiable unless in a dense state. The sand was compacted to 98% MDD, equivalent to a relative density of 80%.

During the Canterbury seismic sequence the area around the pump station, and the pump station itself, dropped by approximately 200mm. No damage or tilting occurred to the pump station. The existing embankments around the ponds, constructed during the 1960, suffered severe damage from slumping and required treatment, but the new embankments constructed around the pump station suffered only minor cracking and did not require any remedial measures.

7 ACKNOWLEDGEMENTS

The author wishes to thank Christchurch City Council and his former employer URS New Zealand Limited for permission to publish this paper.

REFERENCES

Canterbury Geotechnical Database (2013). Conditional PGA for Liquefaction Assessment. Map Layer CGD5110-11 Feb 2013, retrieved May 2013 from https://canterburygeotechnicaldatabase.projectorbit.com/

CH2M Beca (2012). Ocean Outfall Pump Station And Structures Level Survey.

Moore J, Fleming R, and Jones G. (2008). Microtunnelling the Ocean Outfall Pipeline, Christchurch, New Zealand. *Proc. 13th Australian Tunnelling Conference*.

NCEER (1997) I.M. Technical Report No NCEER-97-0022. *Proceedings of the NCEER Workshop on Evaluation of Liquefaction Resistance of Soils*. Edited by Youd, T.L., Idriss, December 1997.

Price, C.H. (2010) Christchurch Ocean Outfall microtunnel settlement back analysis. *Proceedings of the 11th Congress of the IAEG, Auckland*.

Seed, R. B., et al (2003) Recent Advances in Soil Liquefaction Engineering: A unified and consistent framework. *Keynote Presentation to the 26th Annual ASCE Los Angeles Geotechnical Spring Seminar*.

Stirling, M., Pettinga, J., Berryman, K.R. and Yetton, M. (2001). Probabilistic Seismic Hazard Assessment of the Canterbury Region, *New Zealand. Bulletin of the New Zealand Society of Earthquake Engineering* 34, pp 318-334.

Taki, O and Yang, D.S. (1991) Soil Cement Mixed Wall Technique. *ASCE Special Conference*, Denver, Colorado.

Sinclair, T.J.E. (2013)
Removable flood barriers: Geotechnical considerations
Proc. 19th NZGS Geotechnical Symposium. Ed. CY Chin, Queenstown

Removable flood barriers: Geotechnical considerations

T.J.E. Sinclair
Tonkin & Taylor Ltd

Keywords: removable flood barriers, seepage exit gradient, seepage cut-off

ABSTRACT

Removable barriers have been used for flood protection in many parts of the world, particularly in locations where rising levels can be predicted in time for installation. The use of these was considered for protection of Queenstown and Wanaka for times of extreme rising lake levels, following floods of 1999 that resulted in inundation of parts of both towns. This paper describes the geotechnical considerations for the design of the temporary barriers, particularly relating to seepage, the effects of sub-surface cut-offs on controlling exit gradients and seepage volumes under flood conditions, and the effects of such cut-offs on disturbing ambient groundwater flow. The effectiveness of temporary upstream aprons, both with and without cut-off barriers, was also analysed. Various different types of demountable barrier were considered. Brief descriptions of the types with the respective pros and cons are given and the paper concludes with discussion of some of the issues that needed to be addressed by Councils in working up their flood risk management strategy.

New Zealand Geotechnical Society Inc. 19th Symposium, Queenstown 2013

1 INTRODUCTION

In November 1999, sustained heavy rainfall in the headwaters of the southern lakes led to widespread flooding within the Clutha River catchment. Lake Wakatipu and Lake Wanaka reached their highest and second highest levels in over one hundred years of records, causing considerable flooding within parts of Queenstown, Wanaka and several other towns in the region (see Figure 1- from ORC/QLDC 2006).



Figure 1: Floods of November 1999: Queenstown and Wanaka

The Otago Regional Council (ORC) and Queenstown-Lakes District Council (QLDC) set out to develop a strategy for mitigating the effects of flooding on the affected communities. Temporary and demountable flood barriers were identified as options possibly well suited for use in the towns of Queenstown and Wanaka. However, the potential for seepage through the alluvial gravels on which the proposed defences would be founded posed a risk with regard to stability of the barrier and volumes of seepage water to be controlled.

2 FLOOD DETAILS

The main cause of high lake levels is the natural imbalance between the capacity of the lake outlet and the magnitude of inflows during heavy rainfall events. Figure 2 shows the behaviour of Lake Wakatipu during the November 1999 floods. The inflow to the lake is many times greater than the outflow which itself is impeded by the Shotover River flood. Hydrological solutions have been investigated but none have been considered suitable. Of interest in the hydrograph is the four-day duration of lake rise and the 36-hour lag between the peak inflow and the peak lake level. This suggests that a certain amount of time is available to erect some form of temporary barrier once the nature of the event becomes evident.

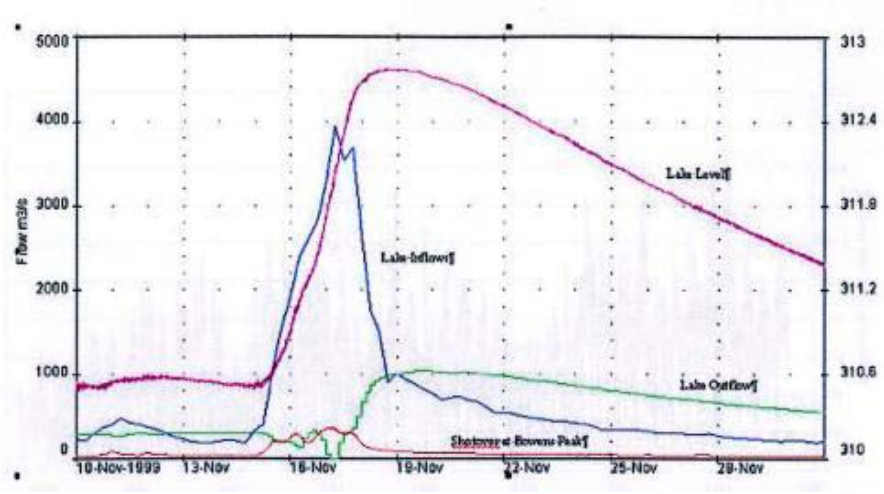


Figure 2: Lake Wakatipu flood of November 1999

Figure 3 shows the extent of 1999 flooding in Queenstown, together with proposed alignment of temporary flood barriers. The lengths of barrier would be about 700 m and 500 m for Queenstown and Wanaka respectively.

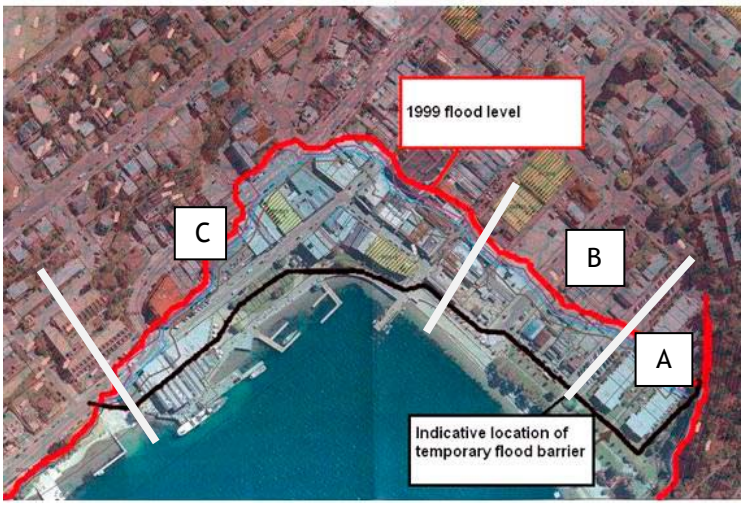


Figure 3: Extent of flooding in Queenstown

3 BARRIER TYPES

A literature review shows that temporary and removable flood defence barriers have been used successfully for river flood controls in other parts of the world, particularly in the United Kingdom and Europe. The review did not give any examples of use associated with lake environments nor mention of any geotechnical related failures. Whilst river protection works

New Zealand Geotechnical Society Inc. 19th Symposium, Queenstown 2013

must withstand high velocities, flood durations are likely much shorter than would apply for a lake, and wave actions not as severe. There is therefore little experience base by which to judge the effectiveness of these types of flood defence in conditions similar to Queenstown and Wanaka.

There are a number of proprietary barriers available (See Figure 4).



a) Steel A-frame and plastic sheeting.



b) A-frame and wooden pallets with plastic sheeting.



c) Post and panel.



d) Water-filled geo-membrane.

Figure 4: Examples of temporary barriers

4 GEOTECHNICAL CONSIDERATIONS

4.1 Issues

Because of the permeable nature of the ground on which the above-ground flood barriers will be placed, seepage under the barriers must be addressed. The principal issues to be considered are:

- Stability of the ground and barrier foundation
- Amount of seepage water to be controlled
- Effects of seepage on downstream features/surfaces.

The barriers alone may not be sufficient with regard to these issues and it is necessary to consider subsurface cut-off barriers to seepage flows. That then raises the question of how such subsurface cut-off's would affect the existing groundwater flow conditions.

4.2 Methodology

The above four issues can be addressed using conventional seepage analyses, usually with the help of purpose-made software. The output from these analyses is usually summarised with

some form of flow-net. A flow-net generally provides two sets of lines representing the seepage pattern:

- Flow lines: Indicates direction of flow and "intensity" of flow
- Equipotentials: Indicates drop in groundwater pressure from seepage entry point to exit point. The distance between equipotentials gives the "hydraulic gradient".

4.3 Ground and foundation stability

It is this latter set (equipotentials) that enables assessment of ground stability. Loss of soil strength and bearing capacities can occur if the hydraulic gradient at the seepage exit point exceeds a certain critical value. Such conditions are often termed "quick" or "boiling".

For vertical upward flow in granular materials, the critical hydraulic gradient (i_c) depends only on soil density and, would be about i_c=0.8 for these site materials. The parameter (i_c) can range from about 0.6 for very lightweight pumice soils to 1.0 for (say) iron sands but is very unlikely to be outside the range of 0.7 to 0.9 for these soils.

The analyses allow comparison of the computed "exit hydraulic gradients" with the critical hydraulic gradient. For the general situation, a factor of safety of 2 on the exit gradients was considered appropriate, giving target maximum exit gradients of 0.4, but reducing to about 0.25 close to buildings with greater factor of safety.

Whilst this policy means that "quick" conditions would not occur, any upward seepage would result in some reduction of bearing capacity. The upper 0.4 limit would reduce the bearing capacity of a surface footing to 50% of that with static ground water at ground surface. The barrier design should take this into account but would likely not be a problem as the bearing capacity of gravels is relatively high.

Care is needed where barriers are to be placed hard up against existing buildings with shallow footings. Such buildings would have a factor of safety of 3 on their normal bearing capacity and hence there would be a reduction to about 50% to 70% of this with the upward seepage. Failure would not occur but some additional settlement might result.

4.4 Seepage volume

The seepage analyses enable an estimate of the rate of seepage flow below the barriers. Results depend on permeability values which are difficult to determine within an order of magnitude. Therefore a factor of safety of ten is usually applied to seepage volumes.

The seepage volumes to be controlled depend on whether a subsurface collection trench is employed. If not, water will seep up through the ground surface over a wide area, with a gradually increasing free water depth. If a collection trench is constructed to sufficient depth to prevent seepage at the surface, then the water volume to be pumped away could be much greater. This is because the trench draws water from all directions and the hydraulic gradients are increased.

4.5 Effects of seepage on downstream features

Upward seepage will occur to some extent immediately downstream of the barriers. This assumes that the ground surface is a permeable boundary. If, instead, an impermeable rigid boundary is present, flow would be diverted further inland and upward pressures would be applied to the impermeable surface. The magnitude of the uplift pressures would depend on the overall geometry, including apron length and cut-off depth.

New Zealand Geotechnical Society Inc. 19th Symposium, Queenstown 2013

However, sealed road surfaces would generally not have sufficient weight to resist even small upward pressures (e.g. 60 mm head of water) and so would be lifted and cracked. The resulting cracked surface would then revert to a permeable boundary. Block paving surfaces would serve better due to slightly greater weight and because seepage could occur through joints. Grass surfaces would merely become wet and very soft as the topsoil lifts off the gravels.

The above statements assume that there is no sump or collection trench immediately downstream of the barrier. Provided exit gradients are less than given above, there would be no theoretical need for such a trench to maintain stability. However, it would serve as a practical measure to collect the seepage water, and would help maintain the ground surfaces from cracking or saturating.

4.6 Existing groundwater regime

The normal regional groundwater regimes at Queenstown and Wanaka involve general seepage from high ground towards the lakes. If a subsurface cut-off barrier is constructed, downslope flow will be inhibited and there is risk of seepage emerging at ground surface. Clearly the risk of rising groundwater is greatest when there is a thin surface layer of high permeability. Such conditions appear to exist at Wanaka and some zones for Queenstown. Typically a permanent cut-off that penetrates more than about 85%-95% through a top permeable layer would cause emergence of seepage at the surface or uplift pressures on impermeable surfaces.

5 SEEPAGE ANALYSES

5.1 Ground model and analysis cases

A number of models were analysed, representing different zones along the proposed barrier alignment (termed Zones A, B, C: - see Figure3). All models however, involved one or two permeable gravel layers of variable thickness overlying an impermeable fine-grained layer.

Numerous analyses were carried out using program SEEP/W for the various ground models, different cut-off depths, and the historical (flood of 1999: RL 312.78m) and extreme flood level (design ultimate: RL 314m). Figure 5 shows a typical SEEP/W model output.

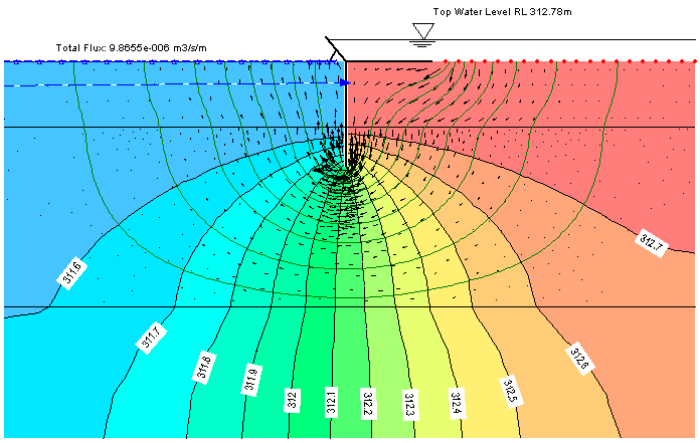


Figure 5: Typical seepage model output

5.2 Seepage rates below barriers

Figure 6 summarises the seepage rates (in ℓ/s per m of barrier), showing the effects of cut-off depths and whether there is a 5 m 'apron' or no apron.

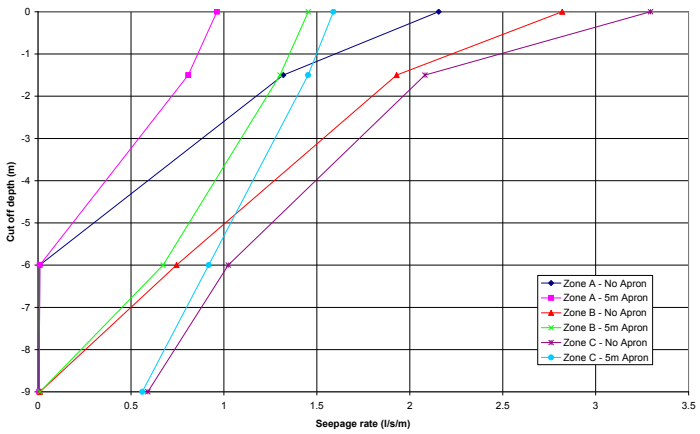


Figure 6: Unit seepage estimates beneath flood barriers for Queenstown

The total estimated seepage within each zone is as shown in Table 1.

Table 1: Total seepage estimates beneath barriers (ℓ/s) for lake level 312.78 m

Cut off depth (m)	Zone A - No Apron	Zone A - 5m Apron	Zone B - No Apron	Zone B - 5m Apron	Zone C - No Apron	Zone C - 5m Apron
0	345	154	451	233	428	207
-1.5	211	129	309	208	271	189
-6	2	2	119	108	133	119
-9	1	1	2	2	77	73

5.3 Exit hydraulic gradient

It the exit gradient exceeds a certain rate (approximately 0.7 to 0.8 m/m) then a loss of ground support may be experienced on the landward side of the barrier and result in failure of the defence. In addition, a high exit hydraulic gradient may damage paving, road surfaces and building foundations.

Due to the short term duration of the flooding it is usually acceptable to design to a slightly lower safety factor. Accordingly, an exit hydraulic gradient of 0.4 m/m should be considered as maximum.

Table 2 and Figure 7 summarise the maximum exit gradient for each of the design cases considered.

Table 2: Maximum exit hydraulic gradients (m/m) for lake level 312.78 m

Cut off depth (m)	Zone A - No Apron	Zone A - 5m Apron	Zone B - No Apron	Zone B - 5m Apron	Zone C - No Apron	Zone C - 5m Apron
0	0.82	0.31	0.88	0.32	0.98	0.32
-1.5	0.30	0.18	0.38	0.22	0.28	0.18
-6	< 0.01	< 0.01	0.06	0.05	0.07	0.06
-9	< 0.01	< 0.01	< 0.01	< 0.01	0.04	0.03

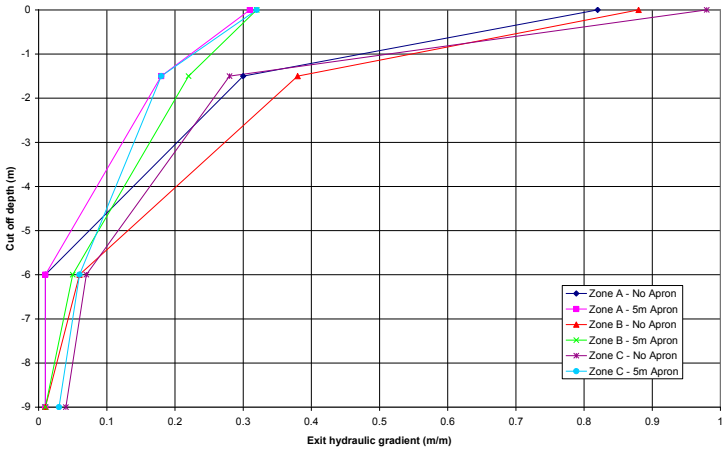


Figure 7: Exit hydraulic gradients for Queenstown

These results show that either a 1.5 m deep cut off wall or a 5 m long apron is required to reduce exit hydraulic gradients to an acceptable level at the very least, with a combination of both or deeper cut-offs in more critical situations.

6 SENSITIVITY TO ASSUMPTIONS

6.1 Permeability

The permeability of the soils along the defence alignment is probably the greatest uncertainty in the seepage analysis. The permeability is likely to vary along the length. This is to some extent covered by the various zones but there may be more localised buried channels or lenses of much higher permeability. Seepage volumes are directly related to permeability but exit gradients are independent of permeability.

6.2 Apron length

Figure 8 illustrates the effect of apron length on seepage rates and exit gradient. Clearly, as apron length increases, both factors improve but the benefits diminish beyond about 5m

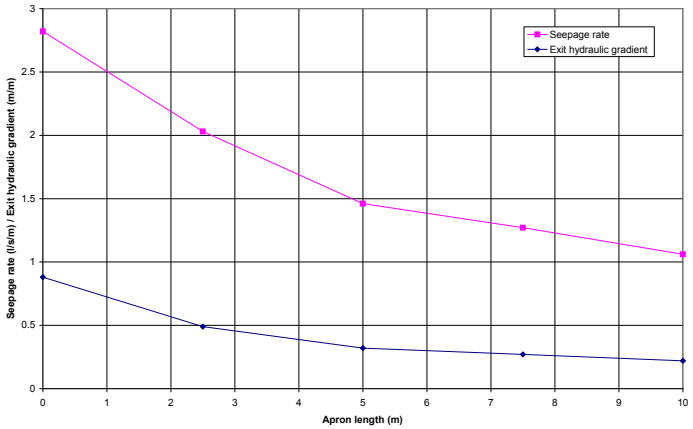


Figure 8: Sensitivity to different apron lengths

6.3 Increasing lake level

Increasing the lake level from the historic flood level (RL 312.78 m) to a possible extreme level (RL 314 m), approximately doubles both the seepage rates and the exist gradients, at least for 5 m aprons and shallow cut-offs.

7 CONCLUSIONS

Whilst all the barrier types are to be "temporary" above ground, they may need to operate in conjunction with a permanent in-ground component (e.g. subsurface cut-off or apron) to provide for the geotechnical issues.

- The principal geotechnical issues to be considered are: Stability of the ground and barrier foundation, amount of flood seepage water to be controlled, effects of flood seepage on downstream features/surfaces, effects of permanent in-ground components on natural groundwater regime.
- With respect to seepage quantities, a 5 m apron is more practical than a shallow cut-off. For example a 5 m apron is equivalent to 2.8 m cut-off (best areas)
- For stability, a 5 m apron alone would be equivalent to a 1.5 m deep cut-off (for all zones). For FoS=3 for all zones, a 5 m apron together with a 1.5 m deep cut-off would be necessary. With no aprons, cut-off depths of 3 m to 4 m would be required.
- There is little benefit in increasing the apron length to much more than 5 m, with respect to both stability and seepage rates.
- If cut-off depth is greater than about 1.5 m, there is a risk that groundwater could rise to ground surface landwards of the barrier under reasonably frequent rainfall events.
- With expected permeabilities and apron/cut-off combinations required to meet the stability requirements, the total seepage flow for the whole alignment would be about 600-700 ℓ/s, at lake levels similar to the 1999 flood.

The temporary barrier plan was not implemented (though may still be considered) for various reasons, some administrative and some technical. Amongst the latter was the need to manage significant volumes of water from both seepage and overland flow.

REFERENCES

ORC & QLDC (2006). *Learning to live with flooding: A flood risk management strategy for the communities of Lakes Wakatipu and Wanaka.*

ACKNOWLEDGEMENTS

This study drew on previous work by SKM and others. The authors acknowledge the help from Otago Regional Council and Queenstown Lakes District Council and their permission to publish this paper.

New Zealand Geotechnical Society Inc. 19th Symposium, Queenstown 2013

Tatarniuk, C.M. & Bowman, E.T. (2013)
A simplified numerical model of deep soil mixed columns used for road slip mitigation in 2D vs. 3D
Proc. 19th NZGS Geotechnical Symposium. Ed. CY Chin, Queenstown

A simplified numerical model of deep soil mixed columns used for road slip mitigation in 2D vs. 3D

C M Tatarniuk
Department of Civil and Natural Resources Engineering, University of Canterbury, NZ
ctatarniuk@hotmail.com (Corresponding author)

E T Bowman
Department of Civil and Structural Engineering, University of Sheffield, UK
(formerly Dept. Civil and Natural Resources Engineering, University of Canterbury, NZ)
e.bowman@sheffield.ac.uk

Keywords: deep soil mixing, finite element modelling, lateral loading

ABSTRACT

Slope failure is common in the Northland region of New Zealand due to the unique geology of the area and the heavy rainfall that can occur. Deep soil mixing (DSM) has successfully been used as a remedial solution for road slips in this area for several years. Numerical modelling is a common design tool, and often two dimensional models are used in place of more realistic three dimensional models in practice, due to budget and time constraints. The 'replacement ratio method' is often used to model DSM columns in two dimensions (2D). This method involves modelling the DSM columns together with the surrounding soil as a block of composite material. The column spacing is accounted for by allocating averaged properties to the 2D columns, based on the ratio by volume of the soil to column material.

A simplified model of laterally loaded DSM columns with a representative region of soil surrounding them has been developed based on an hybrid method for analysing slope stabilizing piles by Kourkoulis et al. (2012). The model is examined in both 2D and in three dimensions (3D) at different column spacings. Through the examination of the resultant force, displacements, and total stresses, the effectiveness of the replacement ratio method and how it varies from the 3D scenario is investigated. It is found that the resisting force and horizontal stresses are overestimated in the 2D model. Closer column spacing results in less deviation between 2D and 3D results.

New Zealand Geotechnical Society Inc. 19th Symposium, Queenstown 2013

1 INTRODUCTION

Road slips are a common occurrence in the Northland region of New Zealand. The Northland Allochthon geological unit is particularly problematic. Deep soil mixing (DSM) has been found to be an economical and effective option for addressing road slips in this area, and it has become a commonly implemented solution.

Numerical modelling is often used as a tool in DSM column design. Two dimensional (2D) analyses tend to be much more economical than three dimensional (3D). Several methods can be used to represent DSM columns in a 2D model. This study focuses on what is often called the replacement ratio method (RRM) (Finlan et al., 2004; Gani, 2004; Leung et al., 2006; Oliveira et al., 2011; Terzhagi et al., 2004) where the DSM columns are modelled in the out-of-plane direction together with the surrounding soil as a block of composite material. For the RRM, strength and stiffness properties of columns (Young's modulus, cohesion and the angle of friction) are derived from a weighted average of the volume of soil with the volume of DSM column material in the out-of-plane direction.

In this study, a simplified slope model stabilized with DSM columns was developed based on a hybrid method for analysing slope stabilizing piles proposed by Kourkoulis et al. (2012). This approach combines accurate 3D analysis with simple and accepted analytical techniques. It consists of two steps. The first step utilizes the results of conventional slope-stability analysis to

determine the lateral resisting force (RF) required for the desired factor of safety against slope failure. The second step consists of decoupling the slope geometry from the computation of pile lateral capacity. This allows numerical simulation of only a limited region of soil around the piles. Kourkoulis et al. (2012) validated the method against experimental, field and theoretical results.

This simplified decoupled approach assumes that the slope failure surface pre-exists, having been generated by a previous event that caused strength mobilization along a continuous surface. This pre-existing plane will not change due to the installation of piles or, in this case, columns. Since in most cases, DSM columns are installed to mitigate road slips that previously exist, this is a legitimate assumption. The resisting force mobilised during shearing along the pre-existing plane was determined in order to provide a direct measurement of how well the columns were resisting the lateral load. The 3D analyses were then compared to the corresponding RRM (2D) for three different column spacings.

2 FINITE ELEMENT MODEL

2.1 2D Model Geometry and Boundary Conditions

Plaxis 2D (V9) (Plaxis, 2008) was used for the 2D model. Three different column spacing scenarios are examined for 0.6 m diameter columns: 2s (where 's' is the spacing, from centre to centre), 3s, and 4s. The 2s scenario is shown in Figure 1. Points selected for load-displacement curves are shown (A, B and C). Points A and C were changed for each column spacing in order to be directly in front of the column.

This model simulates a representative slice of an infinitely long slope. Therefore, the boundary conditions applied on the left and right sides constrain out-of-plane displacement (z-direction) but allow vertical and horizontal displacements. The vertical displacement of the bottom nodes is restrained, as is the horizontal displacement of bottom far left and far right side nodes.

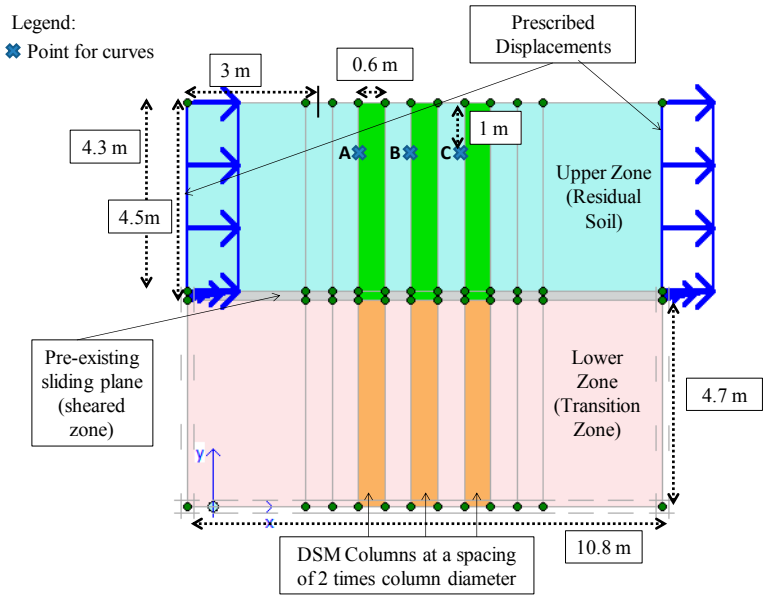


Figure 1: Model geometry in 2D with 2s spacing

2.2 Resisting Force

The resisting force (RF) represents the reaction against the prescribed displacements provided by the system (soil and columns). The RF is calculated as shown in Figure 2 from the vertical total stress, angle of friction, cohesion, and the area of the interface (sliding plane) where failure is occurring. This is based on the shearing resistance provided by material. The RF is depicted

in Figure 2, where RF_{FF} is the free field resisting force (with no columns installed), and RF_{column} is the resisting force of the columns. G is the shear modulus of the soil which can be determined from the Young's modulus (E) and Poisson's ratio (ν).

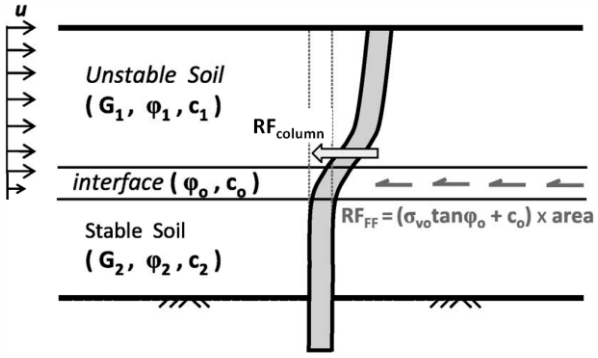


Figure 2: Calculation of the net resistance force of the columns (RF_{column}) against the applied displacement (u) (adapted from Kourkoulis et al., 2012)

2.3 DSM Column and Soil Properties

The soil properties used for the model are given in Table 1. The soil properties are derived from triaxial tests on Northland Allochthon residual clay soil (O'Sullivan, 2009).
Ye et al. (1994) reported that the cohesion of soil-cement mixtures is about 20%-30% of the unconfined compressive strengths (UCS). Based on laboratory results, DSM columns in Northland Allochthon residual clay soil have a UCS of approximately 2 MPa, and a cohesion of around 400-600 kPa (O'Sullivan, 2011; Opus, 2010). However, it was found that when the DSM column cohesion was 600 kPa (i.e. equivalent to a cohesion of 165 kPa for the 2s 2D composite column), the RF was no longer influenced by changes in the column properties, and failure no longer occurred in the sheared zone (i.e. through the columns), but rather in the soil around the columns, above the slip surface. Therefore, a sensitivity analysis was performed to identify the maximum column cohesion that could be used while still ensuring failure through the columns.

The cohesion of the columns was varied between 10 kPa to 200 kPa for the 2s and 4s cases. Figure 3 shows how the resisting force at failure varies with column cohesion in the 2D model for the 2s and 4s cases. In both cases, at cohesion values of greater than ~80 kPa, the resisting force changes little. As the slope remains linear until approximately 70 kPa, suggestive of a common mechanism to this point, 70kPa was selected as the cohesion for the 2s case in 2D.

Back calculating via the RRM with this value gave a value of 162 kPa for the cohesion of the full strength DSM columns. The column properties used are shown in Table 1. The parameter ψ is the angle of dilation. The Mohr-Coulomb constitutive model is used for this analysis, with drained conditions. The estimated unit weight of the soil and columns is 20 kN/m^3.

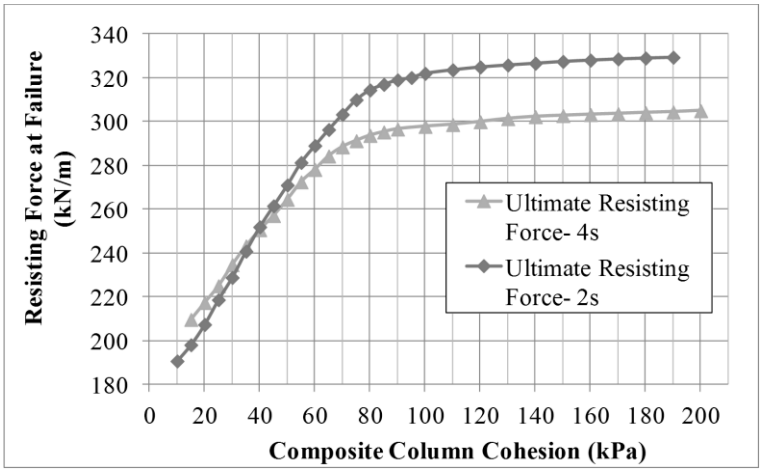


Figure 3: Change in RF vs. composite column cohesion at 2s and 4s column spacings

Table 1: Soil and DSM column properties

Parameter	Unit	Residual Soil	Transition Zone	Sheared Zone	DSM Columns (Transition Zone)	DSM Columns (Residual soil)
E	**kN/m^2**	5.00E+03	4.00E+04	5.00E+03	1.08E+06	1.08E+06
ν		0.25	0.25	0.25	0.2	0.2
c	**kN/m^2**	10	10	0.1	162	162
φ	°	24.6	26.6	8	32	30
ψ	°	2	1	0	1	2

2.4 3D Model Development

Plaxis 3D Tunnel (V2) (Plaxis, 2004) was utilized for the 3D model. Due to software limitations, the columns were modelled as rectangles with dimensions of 0.6 m by 0.47 m. These dimensions ensured the volume of the columns was identical to that of circular columns with a diameter of 0.6 m. The plan view geometry of the 3D model at 2s spacing is shown in Figure 4. Planes 1 and 2 are the planes where the points for load-displacement curves (A, B and C in Figure 1) have been selected.

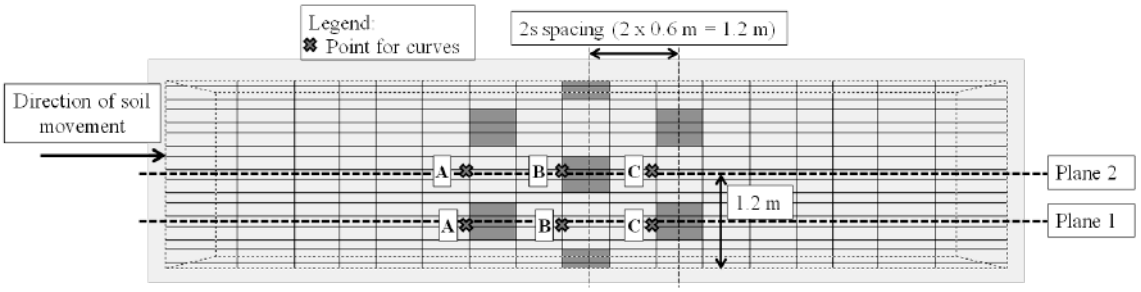


Figure 4: Plan view of 3D model at 2s spacing

Rao et al. (2000) found that the ultimate lateral capacity of square piles made of steel was approximately 5% to 20% more than that of circular piles with the same area, depending on the consistency index (I_c) and undrained sheared strength of the soil. This is because arching mechanisms are affected by the shape of the piles or columns to some degree. The difference in the ultimate pressure on rectangular and circular columns of the dimension stated above at 3s spacing was examined in a plan view model in the drained condition, based on Tatarniuk and Bowman (2012). The soil properties were the same as those shown for the residual soil in Table 1. Figure 5 shows that the ultimate pressure on rectangular columns 0.6 m by 0.47 m in size is approximately 10% more than that of circular columns of the same area. However, the RF in this study is expected to be much less affected by the shape of columns compared to the ultimate capacity in an ultimate state analysis where the columns are fixed, and failure is occurring in the soil around them. The RF is based on a failure mechanism occurring through the sheared zone (through the soil *and* columns) rather than in soil plastic flow around the columns. There is indeed much less arching (and therefore much less influence from column shape) occurring along the sheared zone where the reaction force is measured, which is discussed in further detail in section 3.4.

New Zealand Geotechnical Society Inc. 19th Symposium, Queenstown 2013

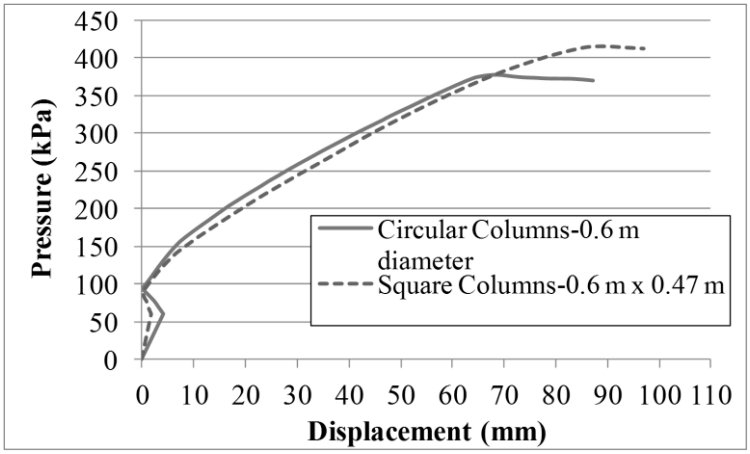


Figure 5: Horizontal pressure at column face versus displacement between columns for rectangular vs. circular laterally loaded column DSM columns in a 2D plan view analysis

3 COMPARISON BETWEEN 2D AND 3D RESULTS

New Zealand Geotechnical Society Inc. 19th Symposium, Queenstown 2013

3.1 Base Model

In order to ensure that the 2D and 3D models were behaving the same, horizontal stress versus displacement was compared for points A, B and C between the 2D model and 3D model without any DSM columns ("base models"). The resultant force for each of the models was also compared. The curves were identical for both models.

3.2 Horizontal Stress vs. Displacement

Horizontal stress versus displacement was examined at points A, B and C for all three column spacings in the 2D model, and plane 1 (points A and C) and plane 2 (point B) in the 3D model (i.e. points chosen to be in front of the respective staggered columns). The results are shown in Figure 6.

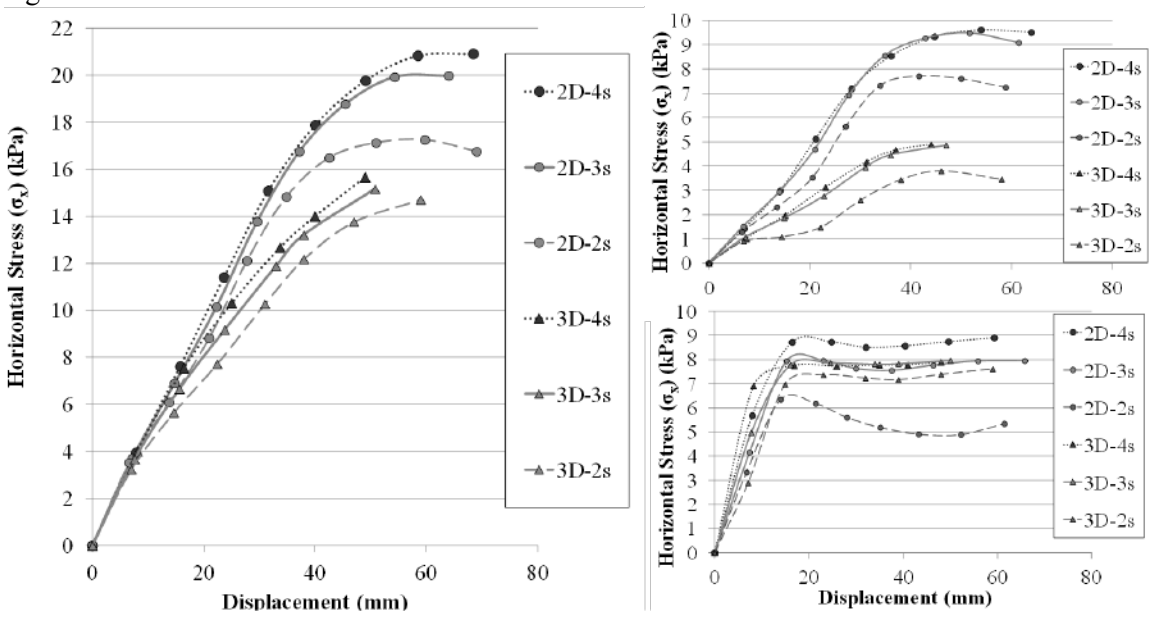


Figure 6: Horizontal stress vs. displacement at point A (left), point B (top right), and point C (bottom right)

The horizontal stress is highest at the face of the columns on leftmost side of the model (point A, top left figure) as these columns are carrying most of the load due to the "shadow effect".

Considering work on laterally loaded piles, the shadow effect is created from the front pile (or in this case, column) to the rear one (Reese et al., 1992) and it causes the action of soil against the rear pile to be minimal compared to that against the front one. Analytical results (Poulos et al., 1980) reveal that the rear pile in a laterally loaded system may develop only about 20% of the front pile's resistance, depending on the pile distance.

The horizontal stress is higher in the 2D model than the 3D model at all column spacings at points A and B. At Point C, it is the 2D-2s case that has the lowest stress. This may be due to a more significant shadow effect in this scenario. Increasing the column spacing results in a greater ultimate pressure on the column, which is in agreement with Tatarniuk and Bowman (2012) for drained conditions. At Point C, the 3D analyses show only a minor increase in the horizontal stress due to an increase in column spacing. This could also be due to an increased shadow effect at this location.

3.3 Resisting Force

The RF was computed for each of the three spacings. The free field RF (the RF computed in the base models) was subtracted from the results to give the RF for the columns alone. The results are shown in Figure 7.

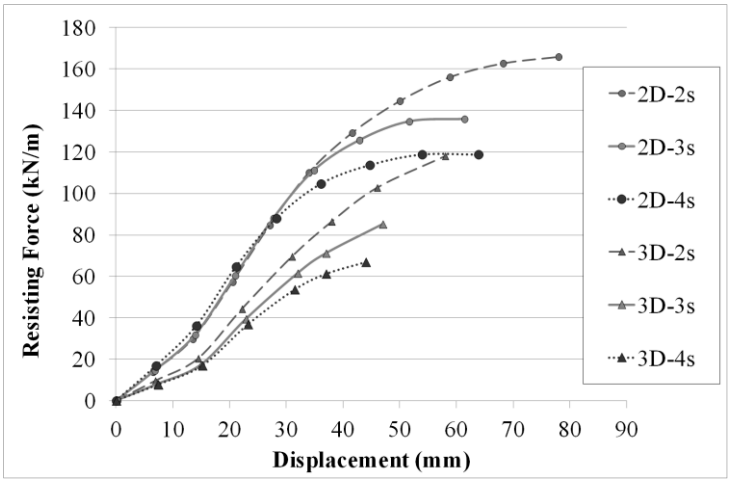


Figure 7: Resisting Force

The results indicate that the RF is overestimated in the 2D model. Closer spacing results in less deviation between the two models with the 2D model overestimating the RF of the 3D model by approximately 141% at 2s, 160% at 3s, 178% at 4s and 149% at 3s spacing with only the centre row of columns.

3.4 Soil Arching

The ratio of inter-pile ground displacement (u_{ip}) to the displacement of the pile (u_p) gives an indication of the amount of soil arching. If this ratio is maintained at close to 1, the pile and the inter-pile soil displace by nearly the same amount and the piles can be considered to be effective in terms of arching (Kourkoulis et al., 2011). The higher the u_{ip}/u_p ratio, the less the arching effect. Figure 8 shows the u_{ip}/u_p ratio with depth for 2s, 3s and 4s column spacings at the left and right columns at failure. Less arching (higher u_{ip}/u_p ratio) is observed at higher column spacings and more arching occurs at the leftmost column than the rightmost column. The u_{ip}/u_p ratio also increases significantly at the top of the sheared zone, where failure is occurring. Arching is effective in the top 3.5 m of the columns.

New Zealand Geotechnical Society Inc. 19th Symposium, Queenstown 2013

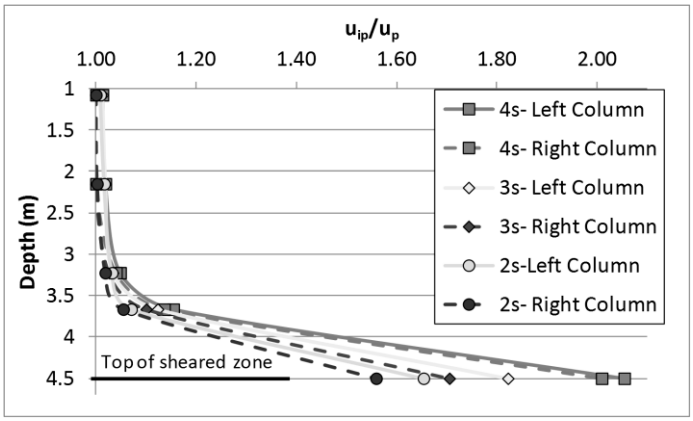


Figure 8: Ratio of inter-pile displacement to pile displacement with depth at different column spacings

4 CONCLUSIONS

New Zealand Geotechnical Society Inc. 19th Symposium, Queenstown 2013

It is evident that the resistance and horizontal pressure withstood by the DSM columns subjected to lateral loading is greater in 2D using the RRM than in 3D. Closer column spacing results in less deviation from the 3D results. Soil arching is evident at all three column spacings examined.

Future work includes a modification of the RRM to better match the resistance provided by the columns in 2D to the 3D results. Although the RRM overestimates the resistance provided by the columns and could therefore be improved upon, it is only one mechanism of failure. Failure of the columns in tension (due to bending) rather than in shear could change how well the 2D and 3D results correspond.

5 ACKNOWLEDGEMENTS

The authors are grateful for the support of Hiway Geotechnical Ltd. and the Commonwealth Scholarship Plan.

6 REFERENCES

Finlan, S., Quickfall, G., & Terzaghi, S. (2004). *Innovation in slip and settlement remedials: The soil mixing option*. Paper presented at the 9th Australia New Zealand Conference on Geomechanics, Auckland, New Zealand.

Gani, C. (2004). *Slope stabilisation- site investigation, design and application of deep soil mixing.* Paper presented at the 6th Australia-New Zealand Young Geotechnical Professional Conference, Auckland, New Zealand.

Kourkoulis, R., Gelagoti, F., Anastasopoulos, I., & Gazetas, G. (2011). Slope Stabilizing Piles and Pile-Groups: Parametric Study and Design Insights. *Journal of Geotechnical and Geoenvironmental Engineering, 137*(7), 663-677.

Leung, H., Gani, C., & Okada, W. (2006). Comparison of the effectiveness of deep soil mix columns using 2-D and 3-D Plaxis. *Plaxis Bulletin, 20,* 20-22.

O'Sullivan, A. S. (2009). *Suitability of advanced soil models for stability analysis of slopes in northland soils.* Masters of Engineering, University of Auckland, Auckland.

O'Sullivan, A. S. (2011, June). [Unconfined Compressive Strength of DSM Columns in Northland Allochthon Residual Clay Soil].

Oliveira, P. J. V., Pinheiro, J. L. P., & Correia, A. A. S. (2011). Numerical analysis of an embankment built on soft soil reinforced with deep mixing columns: Parametric study. *Computers and Geotechnics, 38*(4), 566-576.

Opus. (2010). Unconfined Compressive Stress with Young's Modulus, Kahoe Hill. Auckland, New Zealand: Hiways Stabilizers Ltd.

Plaxis. (2004). *Plaxis 3D Tunnel Manual, Version 2*. Delft: Plaxis.

Plaxis. (2008). *Plaxis 2D Manual, Version 9.0*. Delft: Plaxis.

Poulos, & Davis, E. H. (1980). Pile Foundation Analysis and Design (pp. 397). New York, NY: John Wiley & Sons.

Rao, K. M., Prasad, K. N., & Pullaiah, M. (1999). *Influence of shape of pile on lateral response of pile foundations*.

Reese, L. C., Wang, S.-T., & Fouse, J. L. (1992). Use of drilled shafts in stabilizing a slope. *ASCE Geotechnical Special Publication, No. 31, Stability and performance of slopes and embankments, 2*, 1318-1332.

Tatarniuk, C. M., & Bowman, E. T. (2012). *Two dimensional numerical modelling of landslide stabilizing deep soil mixed columns*. Paper presented at the 11th International & 2nd North American Symposium on Landslides, Banff, Alberta, Canada.

Terzhagi, S., Wataru, O., & Houghton, L. (2004). *Deep soil mixing In New Zealand- role in slope stabilisation.* Paper presented at the ASEP-GI International Symposium, Paris, France.

Ye, S. L., Han, J., & Ye, G. B. (1994). Soil Improvement and Underpinning Techniques. *China Architecture and Building Press*.

Wharmby, N., Clark, L. & Johnson, J. (2013)
The use of vibro-replacement on the Ngaruawahia Section of the Waikato Expressway to mitigate potential seismic liquefaction
*Proc. 19th NZGS Geotechnical Symposium.*Ed. CY Chin, Queenstown

The use of vibro-replacement on the Ngaruawahia Section of the Waikato Expressway to mitigate potential seismic liquefaction

N Wharmby & L Clark
Brian Perry Civil, Auckland, NZ.
nickw@fcc.co.nz (Corresponding author)

J Johnson
Beca Ltd, Auckland, NZ
james.johnson@beca.com

Keywords: Ground improvement, Vibro-replacement, Seismic mitigation, Liquefaction

ABSTRACT

The design and build of the 12.3km Waikato Expressway – Ngaruawahia Section was awarded to the Fletcher Construction Company by the NZTA. The project includes five local road overbridge structures and two state highway bridges; one over the Waikato River and the other an underpass to link into the future Hamilton section. The geology of the area is dominated by Piako Subgroup (Recent Alluvium and Hinuera Formation) overlying the Walton Subgroup. The Piako deposits comprise variable layers of sands, silts and clays and mixtures thereof.

For both the state highway structures the design requirement to adopt a 1 in 2500 year ULS seismic event necessitated some form of ground improvement due to the presence of layers of liquefiable loose to medium dense sands, silty sands and silts combined with a high ground water level. A number of options were considered, including predominantly structural options, but a vibro-replacement ground improvement methodology was ultimately adopted. This paper describes the:

- Ground improvement options and selection process
- Design methodology adopted for the vibro-replacement
- Construction methodology trials and evaluation
- Lessons learnt during construction
- Testing and design verification

The full scale trials performed using different installation methods provides a valuable insight with regard to the effect of the construction methodology adopted. The successful use of vibro-replacement on the project as liquefaction mitigation for the sand, silty sand and silt mixtures is an indication that this form of treatment can be more widely applied to provide a ductile ground improvement system.

New Zealand Geotechnical Society Inc. 19th Symposium, Queenstown 2013

1 INTRODUCTION

The $248 million Ngaruawahia Section of the Waikato Expressway is expected to be completed in late 2013. Fletcher Construction has been tasked with delivering this project, with design provided by Beca and Parsons Brinckerhoff.

The Ngaruawahia Section will connect the future Huntly Section to the north and to the Te Rapa and future Hamilton sections in the south. The project consists of approximately 12.3 km of four-lane expressway crossing potentially liquefiable soils and peat.

Five local road over bridges and two state highway bridges were designed as part of the project. Both state highway bridges were required to be designed for a 1 in 2500 year ULS seismic event. Ground displacements associated with these bridges were required to be limited to 20mm

due to their sensitive nature. This paper is focussed on the Hamilton Underpass structure and describes the options considered during tender design and the journey through detailed design to construction verification.

2 GROUND IMPROVEMENT OPTIONS

With the driving force of the approach embankments during seismic events, large displacements were predicted that could not be reasonably tolerated by the bridge structure. During development of the tender design consideration was given to a number of ground improvement methodologies ranging from those that improve the strength of the soil to those that are structural elements that reduce the load applied to the soil as a function of their strength and stiffness to prevent liquefaction during the design seismic event. Table 1 provides a summary of some of those considered.

Table 1: Available Ground Improvement Options for Hamilton Underpass

Type of Ground Improvement	Overall Improvement Mechanism		Overall System Ductility	Relative Cost	Reason Not Developed
	Soil	Structure			
Dynamic Compaction	✓✓✓✓✓		✓✓✓✓✓	$	Soil + Depth
Vibrocompaction	✓✓✓✓✓		✓✓✓✓✓	$$	Soil
Dynamic Replacement	✓✓✓	✓✓	✓✓✓	$$	Depth
Vibroreplacement	✓✓✓	✓✓	✓✓✓	$$$	Selected
Deep Mass Soil Mixing		✓✓✓✓✓	✓✓	$$$$	Depth + Cost
Deep Soil Mix Columns		✓✓✓✓✓	✓	$$$	Rejected
Deep Soil Mix Walls		✓✓✓✓✓	✓✓✓	$$$$$	Cost
CFA / DFA Piles	✓✓	✓✓✓	✓✓	$$$	Cost
Timber Piles	✓✓	✓✓✓	✓✓	$$$	Cost
Containment Walls		✓✓✓✓✓	✓✓✓	$$$$$	Cost

Improving the strength of the soil requires an appropriate methodology to treat the given soil types and depth. Whilst the sands are readily treatable by dynamic compaction or vibrocompaction the silty sands and silts mixtures are unlikely to be improved. The depth of treatment of up to 12m is beyond the 5m that can be achieved with dynamic replacement and mass mixing. Based upon the cost of the remaining practical solutions, deep soil mix columns were the priced option at tender stage.

One key aspect of the Principal's Requirements that was particularly applicable to the bridge structure seismic design was that the structures needed to be able to withstand a "significantly" greater event than ULS without failure. This would appear logical given the uncertainty surrounding seismic loading and analysis coupled with the use of displacement based geotechnical designs approaches.

The residual strength of individual unreinforced, 1MPa to 3MPa, 0.6m diameter soil mix columns is negligible once the ultimate capacity is exceeded. The capacity of a vibroreplacement solution is derived from the improvement of the surrounding ground and the strength of the 0.8m to 1.0m diameter gravel column. The capacity is only significantly reduced if there is a commensurate reduction in effective column area or soil strength following the seismic event. Trials of soil mix columns failed to achieve strength and ductility requirements at economic cement content and area replacement ratios; this lead to the adoption of a vibroreplacement solution.

3 GROUND IMPROVEMENT DESIGN

3.1 Geology

New Zealand Geotechnical Society Inc. 19th Symposium, Queenstown 2013

The geologic profile at Hamilton Underpass consists of Hinuera Formation overlying Walton Subgroup. The Hinuera formation comprises 11 to 14m of loose interbedded sands and silt, underlain by 2.5 to 3.5m of organic silt and clay. The underlying Walton Subgroup soils consist of interbedded loose to medium dense sands and silt, with lenses of firm to hard organic soils. The soils become gradually stronger with depth, becoming dense to very dense at 20m depth, consistent with the Karapiro Formation. The geologic profile is shown in Figure 1.

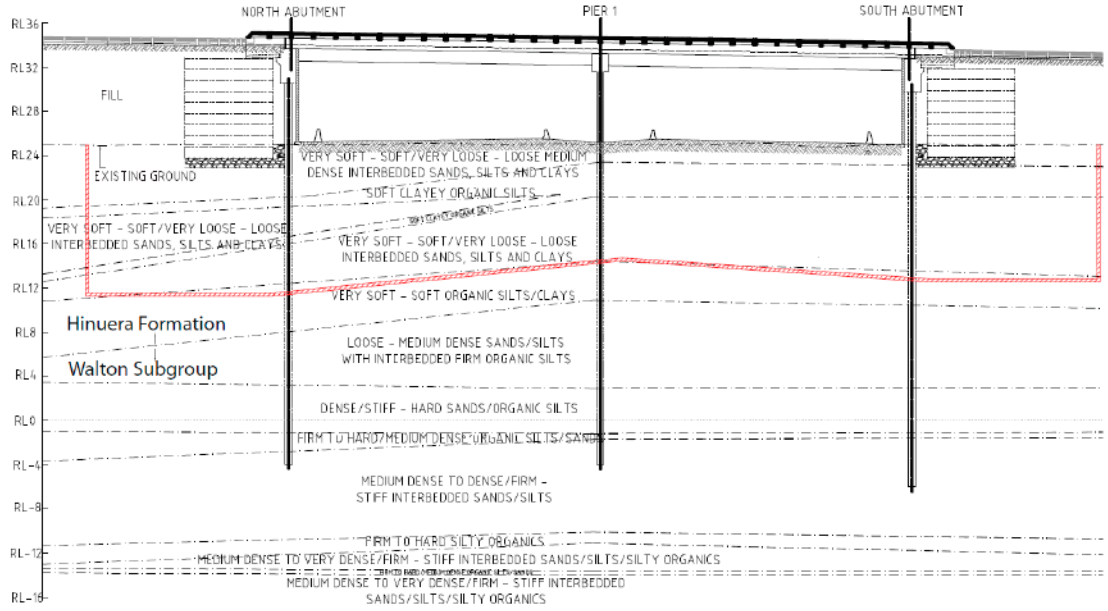


Figure 1: Geologic Profile

The ground water level is very high across the length of the project, typically being encountered between 1m and 2m depth. At the Hamilton Underpass ground water was encountered at 1m depth.

3.2 Liquefaction

Liquefaction analyses were carried out at the bridge location. The assessment was based on the NCEER proceedings, utilising both CPT and SPT data. Liquefaction was identified to be possible under the ULS seismic event between 1 and 11m depth and 15 and 18m depth.

3.3 Design Approach

The Hamilton Underpass Bridge crosses SH1 at an angle of 55 degrees on fill embankments approaching 10m in height. The severe skew of the bridge made the structure very sensitive to displacements in any direction.

The design of the vibroreplacement solution was carried out using the recommendations of Baez and Martin (1993). This method requires the shear stiffness ratio between the soil and included stiff element (Gsc/Gc) to be known. The stiff element is assumed to act only in shear which is reasonable when considering the granular column formed by the vibroreplacement. Whilst the stiffness of the ground can be determined by using well established relationships for CPTs, the stone column stiffness had to be estimated. The design strategy comprised the adoption of a Gsc/Gc ratio of 6.9 and full scale trials to refine the design and mitigate risk.

The use of vibroreplacement columns also allowed provision for densification of clean sands. This was included by allowing for a twofold improvement in the CPT tip resistance, qc, of clean sands.

The final solution allowed for a "Z" shaped area of vibroreplacement columns, with landscape fill toe weights at either side of the approach embankments. Basal geotextile was also included in the approach embankments to help limit displacements in the longitudinal direction. The solution is shown in Figure 2.

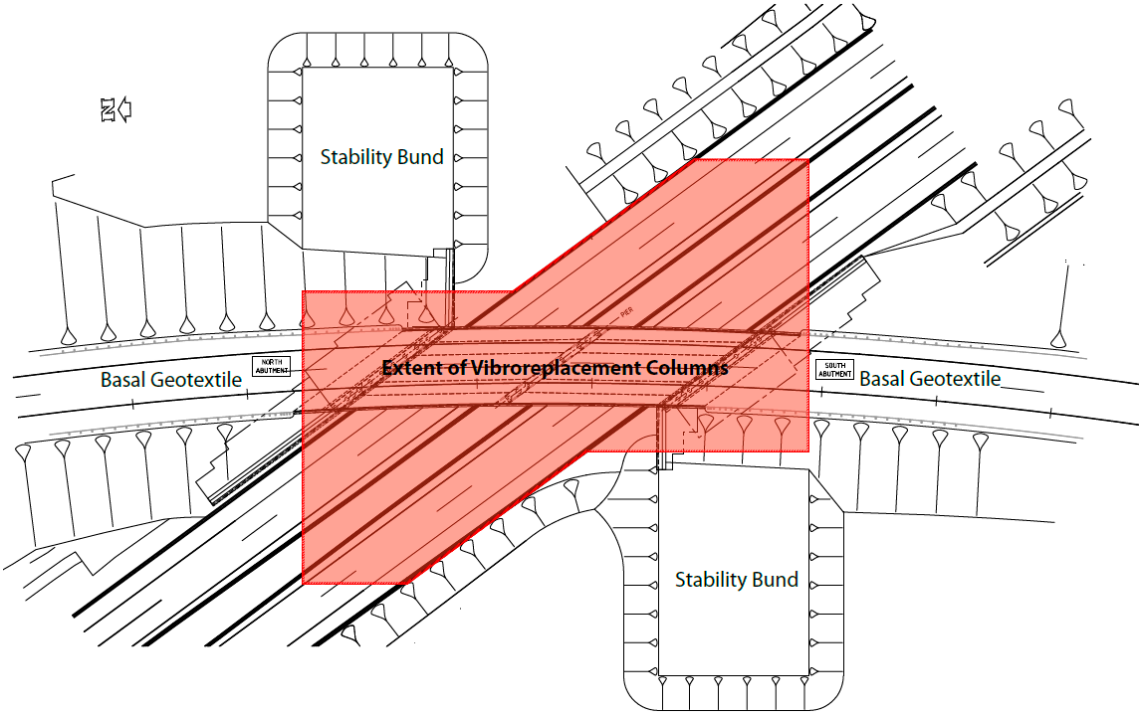


Figure 2: Plan of ground improvements at Hamilton Underpass

4 CONSTRUCTION TRIALS

Given the design requirements and the interaction of vibroreplacement process with the surrounding ground it was necessary to perform trials to confirm the level of soil densification and stone consumption given the energy applied and nature of the ground. Typically pre-treatment CPTs are used to define the soil profile and provide a benchmark with post-treatment CPTs used to measure the improvement. The vibroreplacement process results in the formation of a stone column; the use of coring down the stone column and SPTs is problematic but can provide an indication of their strength.

With significant zones of silty material (Fr > 1.0, Ic = 2.0 to 2.6) that will not be improved sufficiently by the vibroreplacement process the design relied on the strength and stiffness of the stone column. Construction methodology trials were performed using both a conventional vibro-probe and also a using a vibro-hammer and casing with a trap door.

The casings methodology uses a PTC50 piling vibro hammer with a 300kW power pack; a powerful unit is required to mobilise the casing mass and surrounding soil. This methodology has the ability to construct a column of consistent diameter.

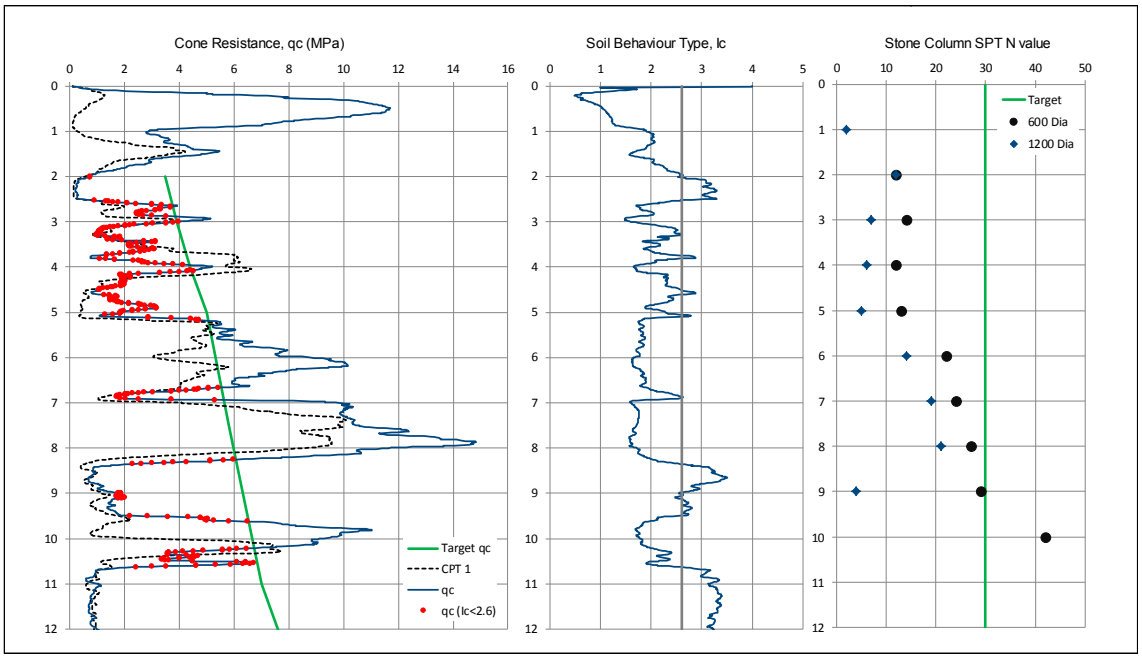


Figure 3: Test results from columns installed using casing methodology

CPT testing between the columns and coring down the stone column to facilitate SPT testing was performed. As can be seen in Figure 3 the cone resistance (qc) in some layers has increased due to the soil displacement as the casing is installed. However, the column SPT N-value is below the target average value of 30 required for both the 600mm and 1200mm diameter columns.

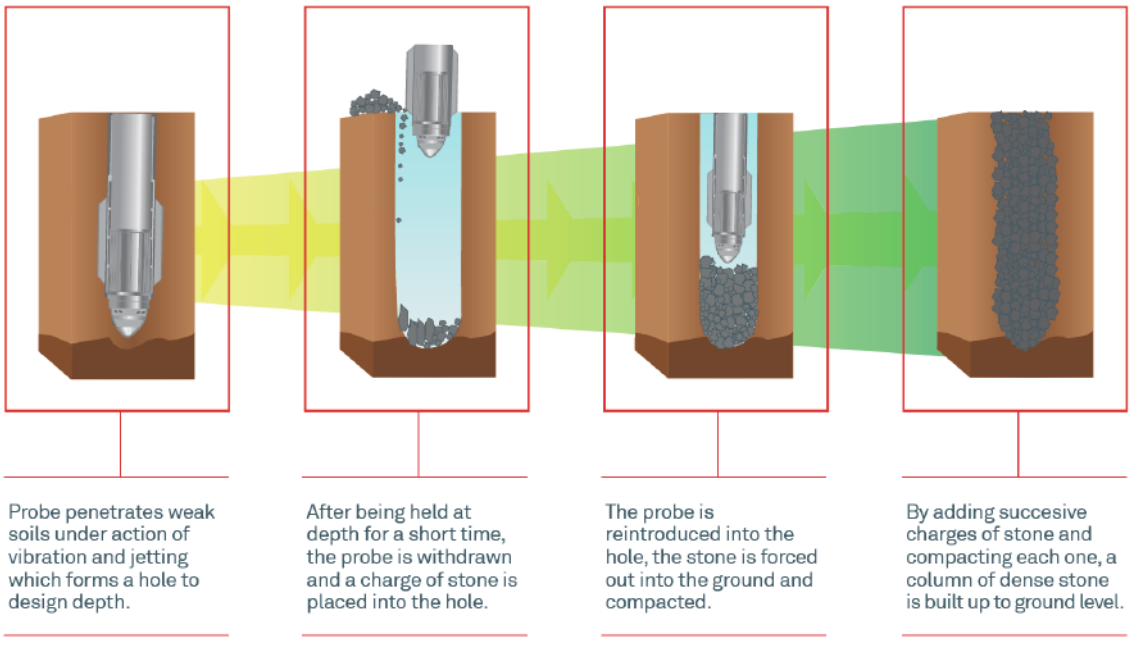


Figure 4: Vibroreplacement methodology

For the conventional vibrocompaction trials a 55kW electric probe with 7.6mm amplitude at 50Hz and centrifugal force of 146kN was used using the wet top feed methodology. Whilst the power, amplitude and centrifugal force are lower than that of the PTC50 vibro hammer the vibro probe is significantly more efficient at compacting the surrounding ground. This is because the energy is applied directly and locally to the soil and the stone introduced. The probe penetrates

the stone displacing it laterally and vertically resulting in larger diameter columns in weaker soils due to the level of confinement. The basic methodology is described in Figure 4.

To ensure the design criterion could be achieved and to optimise the construction methodology trial areas comprising a 4 by 4 grid of vibroreplacement points were installed with area replacement ratios (Ar) of 17%, 20% and 25%. CPTs were carried between the vibroreplacement points and SPT N-values down the centre of the column. Analysis of the results was predominantly based upon qc, Ic, and N. A target Ar = 20% was adopted based upon this and reasonable level of engineering judgement given the interpretation of CPT data in layered soils and the effect of drilling in to the columns.

5 TESTING AND VERIFICATION

The same equipment and installation procedures were adopted for the production vibroreplacement and the testing regime as set out in Table 2 was used to verify the design assumptions.

Table 2: Testing and Verification

Testing	Purpose of testing	Frequency
SPT down the centre of vibroreplacement columns	Confirmation of design stiffness	First 5, then next 10 out of 50 followed by 1 in 35 if adequate and consistent results were obtained or 1 in 25 if not.
CPTs between columns	Confirmation of stiffness of the soil and any densification achieved	1 per 200m^2
Particle size distributions and Plasticity Index	Confirmation of permeability of vibroreplacement columns and drainage blanket	Stockpile Size: 0 to 400m3 – 2 tests 400 to 1,500m3 – 3 tests 1,500 to 4,000m3 – 4 tests >4,000m3 – 1 test for each additional 1,000m3

A specific target qc or SPT N-values for the respective soil and column stiffness is not truly relevant for this type of ground improvement. The soil type needs to be assessed when considering qc and the soil stiffness when considering the SPT N-value. Figure 5 provides an example of the evaluation process adopted. The shear modulus of the soil (Gs) is calculated from CPT data and used to generate specific target SPT N-values in the column based upon the required design shear modulus ratio (Gsc/Gs).

Overall the testing confirmed that the construction had generally met the design requirements and assumptions. There were some thin isolated lenses of potentially liquefiable material following the installation of the columns. However, the suitably robust design could accommodate this and the resulting displacements calculated.

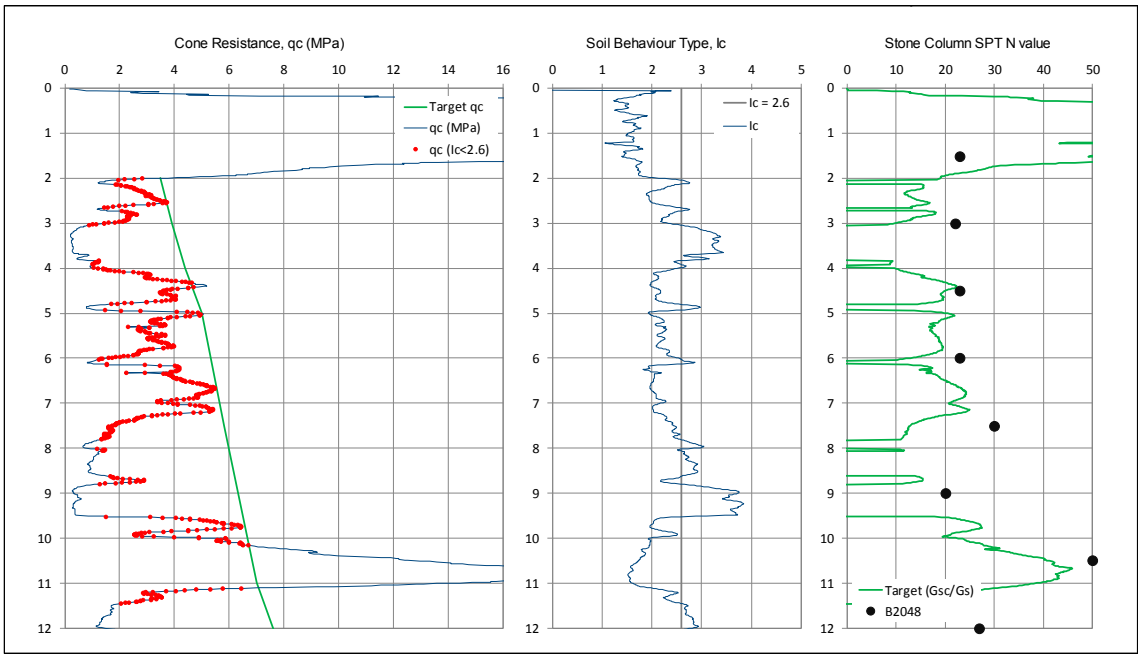


Figure 5: Vibroreplacement Verification

6 LESSONS LEARNT

There are many lessons learnt even on the design and installation of the ground improvement on the one bridge structure but the key elements are as follows:

1. The ductility and residual strength of a ground improvement solution needs to be considered particularly with ULS seismic load cases
2. The use of a piling vibro hammer and casing technique requires a high level of vibratory energy to displace and mobilise the soil; plant is required operate above normal duty cycle levels
3. The vibro probe applies the energy locally and directly to the soil and stone; a stronger / stiffer stone column formed when compared to that formed using the casing methodology.
4. Soils with an Ic > 2.0 or Fr > 0.8 cannot be reliably improved using vibratory techniques hence reliance on the column strength is required.
5. The stone column strength or stiffness achievable is limited by the confinement afforded by the surrounding ground (overburden pressure and strength).
6. Drilling and SPT testing down a column is problematic particularly when the column is of a small diameter and poorly confined.
7. Due to the interaction of vibrocompaction with the ground full scale trials are essential to verify design assumption and refine the construction methodology.
8. Detailed analysis of CPT test data combined with engineering judgement is required to evaluate the ground improvement achieved

7 CONCLUSIONS

There are a large number of options available to form a zone of improved the soil and mitigate seismic effects such as liquefaction; these range from improvement of the in-situ soils to structural elements that essentially attract the load. The most cost effective are those that improve the soils in-situ, however, soils with an Ic > 2.0 generally cannot be improved to a sufficient level, so the capacity of the "structural" elements needs to be considered.

The use of a design and construct contract allows the necessary construction experience to be incorporated into the design which is particularly advantageous when considering what can be achieved with ground improvement technologies. Even with this input, the value of full scale trials to confirm the methodology and the performance requirements can be achieved should not be underestimated. Vibroreplacement trials were performed to refine the construction methodology and finalise the target replacement ratio.

Layered sands, silty sand and silts present challenges when reviewing CPT and other test data as part of the ground improvement verification process. Detailed analysis of the data and clarity around the design philosophy are required to develop an effective review system to which engineering judgement can be applied. Assessment of shear modulus from CPT data and use of the shear modulus ratio to generate specific Target SPT N-value was successfully adopted to provide timely review for the vibrocompaction works.



Figure 5: Vibroreplacement installation

The risks pertaining to the ground improvement design and construction at the Hamilton Underpass structure were effectively managed and vibrocompaction ground improvement methodology successfully implemented.

ACKNOWLEDGEMENTS

The Authors would like to acknowledge the NZTA and their advisors for the opportunity to build the project and Keller Ground Engineering for their technical assistance.

REFERENCES

Baez, J. and Martin, G. (1993) Advances in the Design of Vibro System for the Improvement of Liquefaction Resistance, Proc. Symposium on Ground Improvement, Vancouver, Canada.

Wharmby, N. Gibb, N. Knapp, T & Koelling, M. (2013)
Low mobility grout (LMG) at the Southern Cross Hospital to re-level ground bearing floor slabs and improve seismic performance
Proc. 19th NZGS Geotechnical Symposium. Ed. CY Chin, Queenstown

Low mobility grout (LMG) at the Southern Cross Hospital to re-level ground bearing floor slabs and improve seismic performance

N Wharmby & N Gibb
Brian Perry Civil, Auckland, NZ.
nickw@fcc.co.nz (Corresponding author)

T Knapp
Hayward Baker, Denver, USA
tjknapp@haywardbaker.com

M Koelling
Keller Ground Engineering, Brisbane, Australia
m.koelling@kellerge.com.au

Keywords: Grout, Ground improvement, Seismic mitigation, Liquefaction

New Zealand Geotechnical Society Inc. 19th Symposium, Queenstown 2013

ABSTRACT

Following the seismic events of September 2010 and February 2011, the Southern Cross Hospital on Bealey Avenue, Christchurch experienced liquefaction in the car park and displacement of the ground bearing floor slabs. The piled super structure was in place and the hospital functional albeit with differential displacements of up to 150mm in the floor slabs. Options to re-level the slabs and improve seismic performance were limited by the fact that the work had to be carried out inside the existing building with access and headroom restriction together with live M&E plant. The fact that the hospital remained operational meant that the majority of work had to be done during the 2011Christmas shutdown period. The use of hand tools and low mobility grouting was selected as the only real option to meet these constraints. The paper will describe:

- The low mobility grout (LMG) process
- The design approach and peer review process
- The site trials performed and results
- Operational achievements
- Construction review and design verification

The re-levelling of the slabs was achieved in highly constrained conditions and improvement in the seismic performance was verified from site records and post CPT testing. The project highlighted in particular the response of different soils types to the injection of LMG.

1 INTRODUCTION

During the seismic events of September 2010 and February 2011 the REHS strong-motion monitoring station recorded horizontal PGA values of 0.26g and 0.72g respectively. This is located 330m from the Southern Cross Hospital at the intersection of Bealey Avenue and Durham Street. The piled main hospital structure remained operational following both events, however, significant displacement of the ground bearing floor slabs was observed. The Tonkin & Taylor geotechnical assessment revealed the following prevailing ground conditions:

0.0 – 2.5m	Loose to medium dense sand
2.5 – 4.0m	Soft to firm organic silt
4.0 – 8.5m	Interbedded medium dense sand and silt
8.5m -	Dense sandy gravels

With a groundwater level taken at a depth of 1.0m the potential for liquefaction during a seismic event to depths of 8.5m required evaluation. The report considered grout / resin injection to

directly lift the slab, low mobility grout (LMG) to 8.5m depth or replacement of the slabs. Given the operational constraints the replacement of the slabs was considered too disruptive and, unless piled, would not result in any improved seismic performance. Grout / resin injection to directly lift the slabs was a practical solution but was rejected in favour of LMG by the Client advisors because it would result in improved performance during future events. This paper focuses on the LMG process, design, application and verification of the process carried out by RElevel, a joint venture between Brian Perry Civil and Keller Ground Engineering.

2 LOW MOBILITY GROUT METHODOLOGY

The LMG process has its origins with Denver Grouting, now part of Hayward Baker Inc. and the Keller group who has used the method extensively in the USA and Japan, with partners Sanshin, to re-level commercial, residential and industrial structures. The method comprises the injection of a low slump cement based grout in to the ground to form durable "bulbs" as shown in Figure 1.

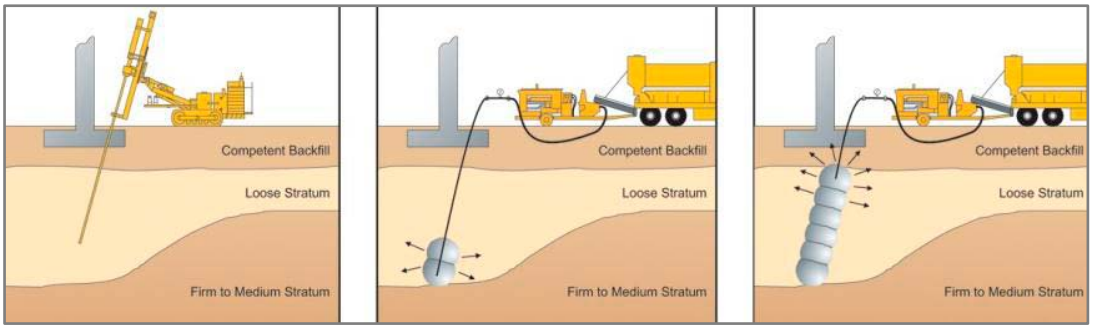


Figure 1: LMG Methodology

The grout is injected into the ground at high pressure below the existing foundation which results in displacement of the surrounding soil causing heave of the ground and, dependent upon the soil type, densification of the soil. Typically the grout has the following properties:
The following are highlighted:

- Target slump of the grout = 25 - 50mm
- Compressive strength of grout at 28 days = 2 - 4MPa
- Stable to pump at pressures of 500 to 4000KPa

The grouting sequence can be either bottom up as shown in Figure 1 or can include some top down injection where the foundation is on weak ground or to enhance confinement. Given the depth and soil types present at the site hand-held pneumatic drivers can be used to install the segmental casing to the required depth which minimises access requirements.

3 DESIGN OF THE LMG SOLUTION

Whilst the use of LMG had been used in seismically active areas around the world it was relatively new to New Zealand. The technical solution was developed in conjunction with experienced Hayward Baker Inc. engineers and it was considered appropriate to extend the design review process to include University of Auckland and Beca.

Given that the structure had already been subjected to estimated loads greater than the design ULS load case and the LMG was targeted at the ground bearing slabs the design was focussed on the SLS load case. This load case was specified as a magnitude 7.5 event with R = 0.33 and pga = 0.11g with a settlement limit of 25mm. The evaluation of the LMG treatment was based upon the CPT data outside the building foot print. Available software packages LiquefyPro and CLiq were used to evaluate liquefaction potential and estimate the resultant settlements. Cavity expansion theory was used to estimate grout injection volumes to achieve the necessary improvement and thus limit liquefaction potential. From this analysis a target injection volume

of 15% in the liquefiable deposits was adopted to define a 2.5m square primary grid spacing with offset secondary grid at the same spacing.

4 LMG TRIALS AND RESULTS

The design of LMG for ground improvement and response of the ground to the high pressure injection is challenging to define and further complicated by the variable and interbedded nature of the soils. The rate of pore pressure dissipation is a primary factor influencing the degree of improvement that can be achieved and the heave that may result. To improve understanding of the ground response to LMG injection and essentially verify the design trials were performed in the car park outside the building. The trial areas comprised 6 primary and 2 secondary injection points with volume and injection pressure monitoring. CPT testing was carried out between the grouting points and adjacent to the test area as a reference.

During the Trial 1 the target 15% injection volume was achieved in the liquefiable zones at 1.0 to 3.0m depth and 5.0 to 8.0m depth, however, the surface heave was greater than 100mm. The aim of the Trial 2 was to limit the surface heave to 25mm; the actual volume injected was 11%.

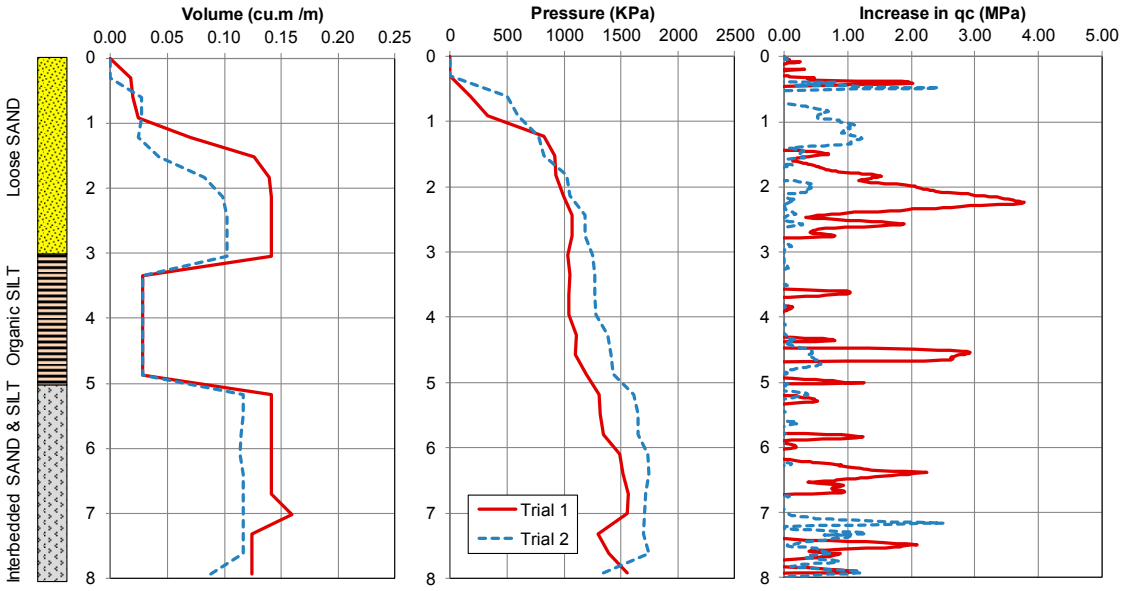


Figure 2: LMG Trial Results

The "increase" in cone resistance, qc is measured by way of a reference CPT close to the trial area but 5.0m from the nearest injection point. Whist the variability of the soils impacts on the results, Figure 2 indicates that a higher level of improvement is realised where the injection volume is greater. Furthermore, the increase in measured qc in the zone of the organic silts is very limited. The trial confirmed the optimum improvement possible could be achieved by targeting the upper and lower zones with up to 15% injection volume. However, the actual injection volume under the slabs would be restricted by the lift observed.

5 SLAB RE-LEVELLING WORKS

The slab re-levelling works were programmed within hospital during a Christmas shutdown period 2011. Some preparatory work was carried out prior to starting on 23/12/2011 but essentially 324 injection points and a total of 412 cu.m of grout was placed by 17/1/2012. On the 23/12/11 during the first day of grout placement the site was subject to a M6 seismic event; the REHS strong motion monitoring station recorded a horizontal pga = 0.35g. The site was evacuated and the structure formally assessed prior to re-entry and continuation of the works.

The same injection layout used in the trial was adopted for the main works with adjustment to suit the structure layout. The presence of walls and hospital M&E components required flexibility, careful planning and work in highly confined environment (Figure 3). A Primary and secondary injection regime was generally sufficient to re-level the slab in all but a small number of locations where tertiary injections were necessary to achieve the target lift.



(a) Installing Casing **(b) Grout Injection**

Figure 3: LMG application within the hospital confines

Given that the target slab lift required was in the range of 40mm to 150mm it was not envisaged that a uniform injection volume would be achievable across the slabs; the primary control mechanism was the lift achieved and not the volume injected. The slabs were successfully re-levelled but as shown in Table 1 the injection volumes are significantly less than the target value particularly when adjusted for the lift volume.

Table 1: LMG injection volume assessment

Area Ref.	LMG Ratio Injected (%)				Corrected LMG Volumes in Liquefiable zones			
	Primary		Secondary		Total LMG	Est. Lift	Nett	Ratio
	Upper	Lower	Upper	Lower	(m3)	(m3)	(m3)	(%)
A	9	12	3	7	198.1	30.8	171.5	6.9
B	5	10	2	6	166.9	33.4	139.7	4.8
C	5	9	1	2	47.1	2.8	41.6	5.4
D	3	9			35.8	6.1	29.7	6.7

6 REVIEW OF CONSTRUCTION DATA

The same approach to the injection of LMG used in Trial 2 was adopted for the main works. Injection was targeted at potentially liquefiable upper zone at 1.0m to 3.0m depth and a lower zone from 5.0m to 8.0m below ground floor level. As can be seen in Table 1 there are clear trends with greater volumes in the lower primary injection points and the lowest volumes in the upper secondary points. From this data it is reasonable to conclude that:

- The depth and associated confining pressure results in greater injection volumes and lower surface expression
- The primary injection serves to increase the density of the adjacent soil, increasing the lateral resistance to secondary injection and promoting lift

There are three primary factors that can affect the grout injection volume possible given a limited lift; for this structure these are highlighted and discussed:

1. Soil type and state
   The density of loose to medium dense sands can be increased by the injection of LMG because they drain allowing volume change and the capacity to take up a volume of grout without significant heave. Soils that behave in an undrained manner, given the rate of pressure application, will simply be displaced by the injection of grout.

   The relatively clean sands in the upper 2.5m will be improved given sufficient confinement. However, the improvement of the non-liquefiable organic silt layer would not be expected so injection of grout would result in heave. The Inter-bedded sands and silts that extend to 8.5m are unpredictable in that the layer thicknesses, permeability and structure will determine the rate of drainage and thus whether densification occurs.

2. Variation in soil profile with depth
   The thickness and depth of liquefiable / non-liquefiable deposits impacts the volume of grout needed and what can be injected prior to excessive lift occurring.

   The pre-construction CPT data was located outside the building footprint and indicates the organic silt is present between 2.5m and 3.0m below ground level extending to 4.0m to 4.5m depth. The post-construction CPT data from within the building indicate these clays extend from 2.5m to 6.0m

3. Confinement
   The presence of a capping layer, structural slab or structural loading serves to resist upward movement of the soil thereby increasing the densification possible.

   With the structure supported on piled foundations the load on the slabs is very limited therefore confinement is limited to that provided by the mass of the slabs themselves.

Initial analysis of the CPT testing performed immediately after completion of the LMG re-levelling using CLiq v.1.5.1.26 Liquefaction Assessment Software. The SLS vertical settlement was calculated to be between 32mm and 56mm respectively (Figure 4). However, given the observed displacements resulting from a greater than ULS event were of a similar order the analysis was considered unacceptably conservative.

The calculations revealed that more than 50% of the settlement would occur in the upper sand layer between 1.5 and 2.5m depth based upon a ground water level at 1.0m depth. Site observations indicated the static ground water level was between 2.2 to 2.5m below ground level i.e. this layer is unlikely to liquefy. With the ground water level at 2.0m depth the resulting liquefaction settlement predicted is less than the 25mm design limit.

Furthermore, the methodology does not consider the effect of either the piles or grout inclusions in the ground when evaluating the liquefaction potential. Revised analysis adopting a Baez & Martin (1993) approach with a replacement ratio, Ar = 5% and shear stress reduction factor, Kg = 0.78 indicates the settlement would be less than 25mm for the design SLS seismic event.

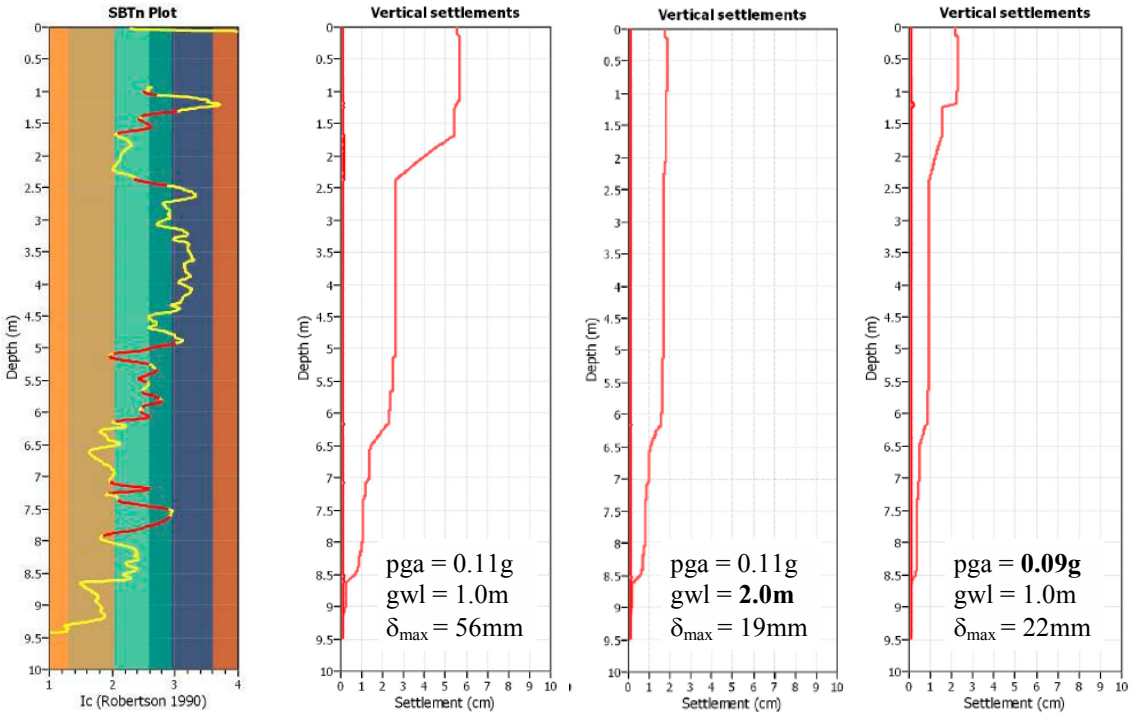


Figure 4: Post LMG settlement evaluation

Based upon the aforementioned the performance of the slabs under the M7.5, PGA = 0.11g seismic event is not expected to exceed the design settlement limit of 25mm.

7 CONCLUSIONS

Whilst the LMG process has now been more widely used in New Zealand, at the time this project was delivered experience was limited so considerable value was gained from the robust design and technical development process with input from experienced personnel based in the USA, Australia and New Zealand. It is imperative that a trial is performed if ground improvement is required because the response of the ground to LMG injection is affected by subtle changes in soil parameters and stratigraphy; the evaluation process is highly observational and experiential.

Given the soil type is a fundamental factor when considering potential improvement and lift during LMG injection Table 2 is presented as a simple guide based upon site observations. Essentially, the liquefiable Silts to Sands range can be improved with the silts likely to realise minimal improvement and the clean sands significant improvement.

Table 2: Effect of LMG injection on soil types

	Effect of Low Mobility Grout	
Soil Type	Densification	Pore pressure
Sands	**Yes**	**No change**
Silty Sands / Sandy Silt	**Limited**	**Limited increase**
Silts	**Minor**	**Minor increase**
Clayey Silts / Silty Clays	None	Increased
Clays	None	Increased
Organic Clay / Silt	None	Increased

Ground conditions at the site were variable and defined by data outside the building footprint. Typically this would be sufficient but it is clear that in this particular case the depth of potentially liquefiable material was less under the building and it is worth noting that the building loads could also affect the soil state. Given the additional CPT data within the building footprint the design grout injection volumes would have been re-assessed and targeted accordingly.

The surface expression and improvement achieved is also affected by the confinement afforded by the ground and, where present, the overlying structure. Further benefit can also be realised by adopting a primary and secondary injection point sequence.

The use of the LMG methodology to re-level and provide improvement was successfully applied in extremely constrained environment; it is difficult to imagine another methodology that could have achieved the same results given and timeframe and the limited functional disruption to the operation of hospital.

8 ACKNOWLEDGEMENTS

The authors would like to thank The Southern Cross Hospitals Ltd and Fletcher Building & Interiors for the opportunity to work on this interesting and challenging project and the site team that delivered an outstanding project under extremely difficult conditions.



Wyering, L.D., Villeneuve, M.C. & Wallis, I.C. (2013)
The effect of hydrothermal alteration on the mechanical and physical rock properties of lithologies from the Ngatamariki, Rotokawa and Kawerau geothermal fields, Taupo Volcanic Zone, NZ.
Proc. 19th NZGS Geotechnical Symposium. Ed. CY Chin, Queenstown

The effect of hydrothermal alteration on mechanical and physical rock properties of lithologies from the Ngatamariki, Rotokawa and Kawerau geothermal fields, Taupo Volcanic Zone, New Zealand

L D Wyering
Department of Geological Sciences, University of Canterbury, P O Box 4800, Christchurch 8041, New Zealand
latasha.wyering@pg.canterbury.ac.nz (Corresponding author)

M C Villeneuve
Department of Geological Sciences, University of Canterbury, P O Box 4800, Christchurch 8041, New Zealand
marlene.villeneuve@canterbury.ac.nz

I C Wallis
Mighty River Power, 283 Vaughan Road, P O Box 245, Rotorua 3040, New Zealand
Irene.Wallis@mightyriver.co.nz

Keywords: Hydrothermal alteration, Geothermal, Rock Properties.

ABSTRACT

This paper describes the results between hydrothermal alteration and the physical/mechanical rock properties of selected formations from three geothermal fields within the Taupo Volcanic Zone, New Zealand. Geomechanical characterisation of hydrothermally altered rocks will lead to an improved understanding of rock mechanics in a geothermal reservoirs and will support drilling optimization, wellbore stability studies and geomechanical modelling. To characterise the physical and mechanical rock properties of the selected Formations, subsamples were prepared from intact core for non-destructive and destructive laboratory testing. The hydrothermal alteration assemblages were characterised using optical mineralogy and existing petrography reports. We have developed an Alteration Strength Index (ASI) equation to address the effect that hydrothermal alteration has on mechanical rock properties. This equation involves analysing factors that affect rock strength and includes secondary mineralization, rock defects and effective porosity. Results were compared to measured uniaxial compressive strength (UCS) data to illustrate the effectiveness of the ASI in correlating with rock strength.

1 INTRODUCTION

Two types of alteration are observed in volcanic environments: weathering and hydrothermal. Alteration is an unavoidable process that produces significant changes in almost all the mineralogical, chemical and physical properties of rocks (Pola et al. 2012). The influence of secondary mineralization on the strength and durability of rock is of particular interest to the conventional geothermal industry because few rocks in a hot, dynamic, liquid and/or steam filled reservoir are fresh. Various petrographic and weathering indices have been proposed to identify alteration impacts on lithologies. These mainly relate to chemical, petrological and mechanical rock properties (Arel & Tugrul, 2001; Rigopoulos et al. 2010). In the Brady Hot Springs, Nevada, observations of rock strength found that siliceous lithologies had higher rock strengths (uniaxial compressive strength) than argillaceous lithologies because the high crystal content in the siliceous samples supports the rock against compression (Lutz et al. 2011). Tools that predict mechanical and physical rock properties are useful for reservoir development, management and prospect evaluation during exploration because there is usually very limited or no borehole-based rock property data (Ameen et al. 2009; Tamrakar et al. 2007). Relationships between strength and porosity, density or mineralogy for a specific rock formation are

developed based on laboratory tests on rock core from a given field or lithology. This is in order to develop empirical relationships that can be used to derive the mechanical properties. Although the most accurate method of developing these relationships utilises direct measurement on core samples, the small volume of material available from geothermal drilling is a drawback to this method. Furthermore, testing techniques are expensive, leading to only limited numbers of samples tested in a given field. Therefore, many researchers and industry practitioners commonly apply empirical strength relationships to geophysical wireline data or limited laboratory data (Cobanoglu & Celik, 2008; Dincer et al. 2004). Chang et al. (2006) reviewed thirty-two empirical relationships for sedimentary rocks where physical rock properties were derived from geophysical wireline tools. His review made clear that a few of the empirical correlations appeared to work fairly well for some subsets of the rocks studied, while most of the other relations do a poor job in fitting measured data. The downfall of these empirical relationships is that they are only applicable to the particular lithologies being studied, and do not necessarily correlate for all rock types, especially silicic volcanic rocks affected by secondary mineralisation. Whilst the equations presented in the Chang et al. (2006) review paper may be useful to a practitioner in the geothermal industry as a first order approximation, they are focused on sedimentary rocks with no high temperature secondary mineralisation.

This paper will address the hydrothermal alteration of selected Formations from Ngatamariki, Rotokawa and Kawerau geothermal fields. It will involve developing an empirical relationship that can be used to correlate alteration to the mechanical properties. This empirical relationship will be useful for exploration and development of geothermal reservoirs.

2 GEOLOGY OF TVZ AND GEOTHERMAL FIELDS

The Taupo Volcanic Zone (TVZ) is located in the central North Island of New Zealand in a 300 km long and 60 km wide belt, defined by caldera structural boundaries and vent positions (Wilson et al. 1995) It formed on a Mesozoic basement assemblage of metasedimentary rocks that have been reached by drillholes in Kawerau, Ohaaki, Rotokawa and Ngatamariki geothermal developments (Browne, 1989). Over the last 2 Ma the TVZ has erupted between 15,000 - 20,000 km^3 of volcanic rocks, with 80% being rhyolitic pyroclastic and subordinate lava flows from several caldera centres (Hochstein, 1995). At present, a few andesitic volcanoes are located in the northeast and southwest of a predominantly rhyolitic volcanism section, where very high rates of magma generation and eruptions are associated with high temperature geothermal activity (Bibby et al. 2008; Cole & Spinks, 2009).

3 METHODOLOGY

Samples were obtained from the selected Formations across three geothermal fields – Ngatamariki, Kawerau and Rotokawa, depending on core availability. Table 1 below lists the stratigraphic succession of these three fields and shows the location of sampled formations within this succession.

3.1 Porosity and Density

Effective porosity and density testing was carried out according to the saturation and caliper techniques (ISRM, 1978). Determining effective porosity of a hydrothermally altered rock sampled from below ~150°C is challenging as they commonly contain swelling clays, so instead dichloromethane was used as a saturation medium as it is a non-polar solvent.

Table 1: Generalised stratigraphy of the three geothermal fields and the known thicknesses; highlighted units tested in this study (adapted from Rae et al, 2007; Chambefort & Bignall, 2011; Milicich et al. 2012).

	Estimated Thickness	Ngatamariki	Estimated Thickness	Rotokawa	Kawerau
Shallow Formations	15-85 m	Surficial	>30 m	Surficial	Surficial
	>70-285 m	Huka Falls Formation	<150 m	Huka Falls Formation	Matahina Ignimbrite
	115-315 m	Rhyolite/Rhyolite Breccia	200 m	Pararíki Breccia	Caxton Formation (Upper)
	0–240 m	Waiora Formation	460 m	Waiora Formation	Tahuna Ash
	100-200 m	Wairakei Ignimbrite	550 m	Rhyolite Lava and Breccia	Caxton Formation (Middle)
	0–285 m	Rhyolite Breccia	190 m	Wairakei Ignimbrite	Tahuna Formation (Upper)
					Caxton Formation (Lower)
					Caxton Formation (intrusive)
					Tahuna Formation (Lower)
Deep Formations	0–2000 m	Tahorakuri Formation	230 m	Tahorakuri Formation	Karaponga Formation
	0–1000 m	Andesite lava and Breccia	>1300m	Rotokawa Andesite	Onerahi Formation
	0 - >300 m	Igneous intrusions			Kawerau Andesite
					Raepahu Formation
					Kawerau Andesite
					Tasman Formation
					Te-Teko Formation
					Rotoroa Formation
					Waikora Formation
Base	-	Greywacke Basement	-	Greywacke Basement	Greywacke Basement

3.2 Uniaxial Compressive Strength Testing

Uniaxial compressive strength tests were conducted using the ASTM (2010) and ISRM (1979) standards. Electrical resistance strain gauges were placed on each of the subsamples to measure sample deformation during uniaxial loading.

3.3 Petrological Analysis

Petrological analysis, using a polarized light microscope, was undertaken in order to characterise the primary and secondary mineral assemblage. This included identifying veining in the sample vein infill, microfractures, and natural planes of weaknesses on the core sample. The primary and secondary textures in the samples were noted when they could be identified.

4 ALTERATION STRENGTH INDEX

All the samples have experienced hydrothermal alteration and, as mentioned above, secondary mineralization has a significant impact on rock strength. We have, therefore, described the petrography of the samples using our own thin section examination and existing geological reports (Rae et al. 2007; Chambefort & Bignall; 2011). Petrographic analysis also included

identifying fractures and veining. Due to the difficulty of being able to give an exact percentage of different minerals in thin sections, mineral occurrence was classified as abundant when the sample was comprised of >50% of that mineral species, common when <50-20%, minor when <20-5%, and finally rare occurrence is <5%. We then ranked the minerals by decreasing order of abundance from i.e. 1, 2, 3.

We have developed a relationship, Alteration Strength Index (*ASI*), to facilitate comparison between observed alteration mineralogy and measured rock properties:

$$ASI = \left[\left(P_m \times \left[1 - \frac{AI}{100}\right]\right) + \left(S_m \times \frac{AI}{100}\right) - \eta_e + 50\right] \times S_{nf}$$

where P_m (primary mineralogy factor) and S_m (secondary mineralogy factor) are representative values based on the hardness of the minerals and the relative proportion of these minerals contained in each sample. This value is obtained by multiplying the representative percentage of the minerals with the hardness index of that mineral found in each sample. S_{nf} is a number between zero (significant large fracture), and one (intact sample), which is assigned to each sample and represents the presence of microfractures observed in the thin section and/or natural planes of weakness within the bulk rock. AI is the percentage of the sample that has been hydrothermally altered. The sum of P_m and S_m is multiplied by the percentages of the sample, out of 100, that are unaltered and altered, respectively, to weight its impact on the overall strength. The effective porosity (η_e) is then subtracted, based on the assumption that more void space results in lower compressive strength. Finally the S_{nf} value is multiplied to the whole equation to emphasise the impact of the natural fractures/weakness planes on the strength of the sample.

5 LABORATORY RESULTS

5.1 Porosity and Density

The Tahorakuri Formation, Matahina Ignimbrite, Tonalite and Rotokawa Andesite show strong relationships between porosity and density with the porosity increasing as the density decreases. The Te-Teko Formation and Andesite Breccia have lower variability for porosity and density, resulting in a weak formation-specific trend. However, they fall within the broader trend defined by all Formations (Figure 1). The plot has been divided into representative zones of smectite, illite and siliceous alteration based on observed alteration.

5.2 Petrological analysis of the strength tested samples

The Andesite Breccia from Ngatamariki is an intensely altered, pale green to dark green, clast-supported breccia. This breccia contains clasts of greywacke, granite, andesitic lava, rhyolite lava and siltstone. The matrix is altered to epidote, chlorite, quartz, illite, calcite, pyrite and titanium oxide. The alteration assemblage in the Andesite Breccia primarily consists of epidote, chlorite and quartz, with minor calcite, pyrite, albite, adularia, and titanium oxide. The breccia contains small veins and veinlets (<1-2 mm) with calcite, epidote, and quartz fills.

The Rotokawa Andesite is an intensely altered, dark green lava or breccia. The primary minerals, which consist of plagioclase and pyroxene, have been altered to calcite, quartz, chlorite, epidote, albite, titanium oxide and pyrite. No veins were seen in the thin sections.
The Te-Teko Formation is white to light green ignimbrite, and is moderately to strongly altered. The sample is primarily composed of quartz, plagioclase and ferromagnesian minerals that have been altered to quartz, clay, titanium oxide, calcite, albite, chlorite, pyrite and wairakite. The Te-Teko Formation contains a high concentration of veins that appear to be in-filled with clay or calcite.

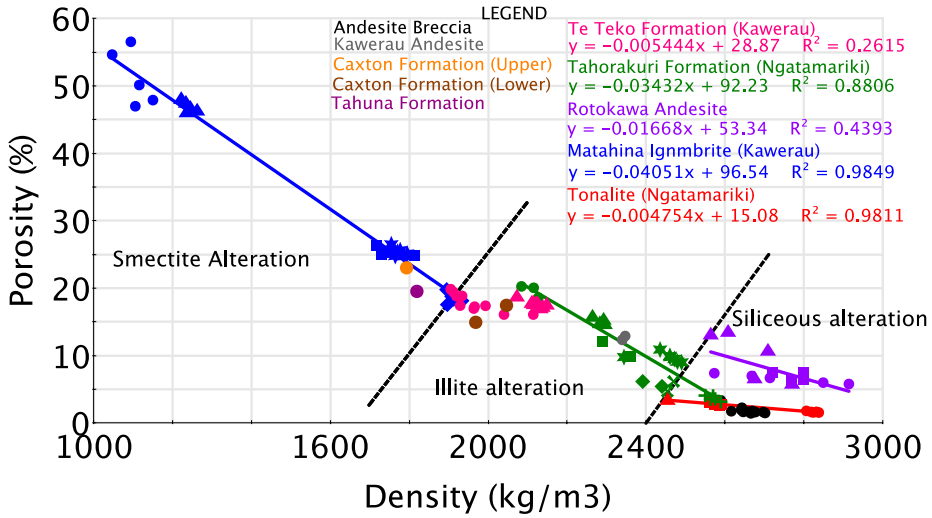


Figure 1: Porosity and density plot. Andesite Breccia, Tahorakuri Formation, Tonalite Matahina Ignimbrite, Te-Teko Formation, Rotokawa Andesite Kawerau Andesite. Symbology differentiates samples taken from different wells.

5.3 Strength Testing

Uniaxial compressive strength (UCS) testing was undertaken on 25 samples from three formations (Table 1). The UCS values for the ignimbrite are lower than those measured for the andesite samples. Although in the first instance this is likely due to the difference in primary rock type, it is likely the argillic alteration present in the Te-Teko Ignimbrite is further weakening this rock. One of the Ngatamariki Andesite Breccia samples had a comparatively low UCS value of 36.7 MPa that was caused by the sample failing through a pre-existing fracture.

Table 2: Samples and the corresponding UCS. In depth, mD refers to depth in meters measured along the well track from the drill floor and no well deviation exceeds 30°. Units in MPa.

Ngatamariki Andesite Breccia	Rotokawa Rotokawa Andesite			Kawerau Te Teko Formation
2179-2184 mD	2121.1-2123.2 mD	2310.6-2313.2 mD	2321.0-2322.4 mD	1102.25-1145.25 mD
188.08	69.53	92.07	126.53	41.22
[1]36.72	79.91	109.91	137.97	39.36
113.12	85.99	137.31	148.44	49.66
174.40	105.26	146.24	157.93	43.75
127.09	211.05	126.53	162.71	

[1] This sample failed on a fracture.

5.4 ASI vs. UCS

The results from the ASI and UCS testing show a clear trend – such that as the measured strength of the rock increases so does the ASI. This is shown in Figure 2, where the correlation between these two factors produced an R^2 value of >0.87, indicating a very strong relationship.

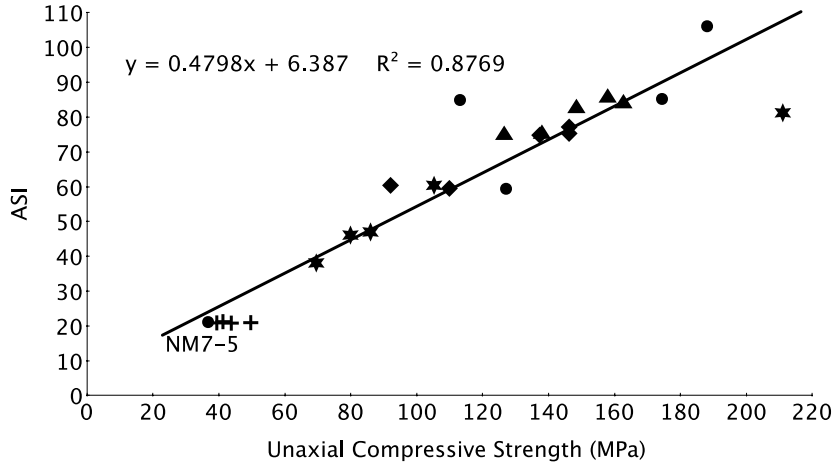


Figure 2: ASI vs. UCS plot, Ngatamariki Andesite Breccia (circle), Rotokawa Andesite (stars, triangles, diamonds) and Te-Teko Formation (cross).

6 DISCUSSION

A wide variety of hydrothermal minerals have been recognized in active and extinct geothermal systems. Establishment of a particular mineral species is highly dependent on temperature, and some minerals only occur over a specific temperature range that in a given system can be approximately correlated to specific depth ranges (Browne 1978). Smectite alteration typically occurs in the shallow Formations, illite alteration usually occurs in deeper Formations at higher temperatures, and finally siliceous alteration normally occurs at even higher temperatures and depth (Figure 1). Pressure is an important variable because it controls the distribution of two-phase (boiling) zones, which are often characterised by the occurrence of bladed calcite and vein minerals. Permeability, both by its extent and nature, determines which alteration minerals form by controlling the amount of contact between fluids and reservoir rocks (Cox & Browne 1998). Hydrothermal fluid-rock interaction results in the development of secondary minerals that fill pores, cracks, substitute matrix and replace primary minerals, and therefore can result in part or wholesale changes in the rock composition and, consequently, mechanical behaviour.

To determine the variation of physical and mechanical rock property data in the geology from the different geothermal fields, samples have been used from numerous wells that encounter the same Formation. The Tahorakuri Formation, Tonalite (Ngatamariki), Matahina Ignimbrite (Kawerau) and Rotokawa Andesite samples came from different parts of the geothermal system (i.e., deep, shallow, internal and marginal) and have therefore undergone different types and intensities of hydrothermal alteration. The impact of this is seen in the porosity and density plot (Figure 1) where the different units each have a large spread of data. When grouped as a unit the Tahorakuri Formation has an R^2=0.88 for the porosity and density plot. The data for this unit is from seven different wells located across the field. As individual wells the samples are more closely related, demonstrating that samples that come from the same section of well have closely related physical properties. The Andesite Breccia, Kawerau Andesite and Te-Teko Formation have less variable porosity and density data as the samples are from one area of the field. This produces porosity and density data that is similar to one another as the hydrothermal alteration and physical properties are comparable.

Volcanic rocks typically give a wide range of primary matrix porosity, which can be enhanced or reduced by alteration (Rejeki et al. 2005). As seen in Figure 1, the samples that contain smectite alteration have a higher porosity and lower density than those that contain illite and siliceous alteration. For example, in their study of porosity in the Darajat Geothermal Field, West Java, Indonesia, Rejeki et al. 2005 suggest porosity is mainly controlled by rock type and alteration processes.

The samples were prepared and tested for UCS to the standards (ISRM and/or ASTM). All strength results, including those that are considered "invalid" according to the standards, were taken into consideration for the ASI equation as it is being developed for the purpose of giving ranges of strength for different formations and lithologies based on different rock conditions/properties, including pre-existing fractures.
The ASI equation we have developed correlates well with the strength of the Andesite Breccia, Rotokawa Andesite and Te-Teko Formation. The systematic variation of ASI with alteration mineralogy fits well with our conceptual model and the experimental data, which show that mineralogy is a dominant control for rock strength. One sample of Andesite Breccia (as highlighted in Table 2 and Figure 2) of interest for the empirical relationship is NM7-5. It had a large fracture and a higher porosity (2.26%) than the other samples tested (~1.68%) from the same section of core. This sample had a UCS of 36.7 MPa because the sample failed along a pre-existing fracture, thus reducing the tested strength. The ASI value calculated for this sample predicted a lower strength than the other four samples tested because of the higher porosity and presence of fracturing. It follows that this sample allowed the equation to be fine-tuned with regards to the impact that pre-existing fractures have on the overall strength of a sample. The Rotokawa Andesite samples had no evidence from thin sections or core that veining or fractures were present, so the variation of the ASI was due to the variation in porosity and the amount of hydrothermal alteration of the sample. The Rotokawa Andesite therefore had a smaller range of ASI than the Andesite Breccia. However, tests in this Formation emphasised the effect porosity and alteration mineralogy had on the samples. As seen in Figure 2, samples from the Te-Teko Formation have a small range of UCS and ASI values due to similarity in mineralogy, veining and porosity, which explains the absence of variability in the ASI and UCS data. Further testing will be undertaken on samples from these and other Formations used for the porosity and density testing to expand the data set required to calibrate that ASI equation.

7 CONCLUSION

The sample set from Ngatamariki, Rotokawa and Kawerau geothermal fields show a wide variety of physical rock properties. Samples from the same Formation, but different parts of the geothermal system, have variable porosity, density and rock strength. They therefore produce better data sets to apply to the problem of understanding how mineralisation affects physical properties. The mechanical properties of a rock are significantly affected by the presence of fractures and high porosity; in this case causing two samples that are identical in mineralogy to have a UCS that differs by 151 MPa.

We developed an index (ASI) equation that provides a correlation of the strength of a rock sample based on the current mineralisation, fractures and porosity data. The ASI equation successfully correlated with rock strength within a small variability for all Formations tested in this study - the Andesite Breccia, Rotokawa Andesite and Te-Teko Formation - and has been statistically analysed as a strong relationship (R^2=0.88).

ACKNOWLEDGEMENTS

We would like to thank Mighty River Power for supporting this project, and to the Rotokawa Joint Venture Limited and Ngati Tuwharetoa Geothermal Assets Limited for allowing access to material.

REFERENCES

Ameen, M et al. (2009) Predicting rock mechanical properties of carbonate from wireline logs (A case study: Arab-D reservoir, Ghawar field, Saudi Arabia). *Marine and Petroleum Geology*. Vol. 26. pp. 430-444.

Arel, E & Tugrul, A. (2001) Weathering and its relation to geomechanical properties of Cavusbasi Granitic rocks in northwestern Turkey. *Bull Eng Geol Env.* pp. 123-133.

ATSM International. (2010) D 7012-10 Standard Test Method for Compressive Strength and Elastic Moduli of Intact Rock Core Specimens under Varying States of Stress and Temperatures. *Annual book of ATSM standards*. Vol. 04-09.

Bibby, H et al. (2008) Resistivity structure of western Taupo Volcanic Zone, New Zealand. *Journal of geology and geophysics.* vol. 68. pp. 231-244.

Browne, P. (1978) Hydrothermal alteration in active geothermal fields. *Ann. Rev. Earth Planet. Sci.* pp. 229-50

Browne, P. (1989) Contrasting alteration styles of andesitic and rhyolitic rocks in geothermal fields of the Taupo Volcanic Zone, New Zealand. *Proc. NZGW.*

Chambefort, I & Bignall, G. (2011) Petrographic review of stratigraphic units of the Ngatamariki geothermal field. *GNS Science consultancy report*.

Chang, C et al. (2006) Empirical relations between rock strength and physical properties in sedimentary rock. *Petroleum science and Engineering.* pp. 223-237.

Cobanoglu, I & Celik, S. (2008) Estimation of uniaxial compressive strength from point load strength, Schmidt hardness and P-Wave velocity. *Bull. Eng. Geol. Env.* pp. 491-498.

Cole, J & Spinks, K. (2009) Caldera volcanism and rift structure in the Taupo Volcanic Zone, New Zealand. *Geological Society.*

Cox, M & Browne, P. (1997) Hydrothermal alteration mineralogy as an indicator of hydrology at the Ngawha geothermal field, New Zealand. *Geothermics*. pp 259-270.

Dincer, I et al. (2004) Correlation between Schmidt hardness, uniaxial compressive strength and young's modulus for andesite, basalts and tuffs. *Bull. Eng. Geol. Env.* pp. 141-148.

Hochstein, M. (1995) Crustal heat transfer in the Taupo Volcanic Zone (New Zealand): comparison with other volcanic arcs and explanatory heat source models. *J. volc. and geoth. res.* pp. 117-151.

ISRM. (1978) The complete ISRM suggested methods for rock characterization, testing and monitoring: 1974-2006. *Turkish National group*. pp 85-92.

ISRM. (1979) The complete ISRM suggested methods for rock characterization, testing and monitoring: 1974-2006. *Turkish National group.* pp 121-132.

Lutz, S. et al. (2011) Lithologies, Hydrothermal Alteration, and Rock mechanical Properties in Wells 15-12 and BCH-3, Brady's Hot Springs Geothermal Field, Nevada. *GRC Transactions.*

Milicich et al. (2012) U-Pb dating of zircon in hydrothermally altered rocks as a correlation tool: A case study from the Kawerau Geothermal Field, New Zealand. *Proc. NZGW.*

Pola, A et al. (2012) Influence of alteration on physical properties of volcanic rocks. *Tectonophysics.* pp. 67-86.

Rae, A (2007) Rotokawa Geology and Geophysics. *GNS Science consultancy report.*

Rejeki et al. (2005) Porosity study for detail reservoir characterization in Darajat Geothermal Field, West Java, Indonesia. *Proc WGC 2005.*

Rigopoulos, I., et al (2010) The influence of alteration on the engineering properties of dolerites: The examples from the Pindos and Vourinos ophiolites. *Rock mechanics and mining sciences.* pp.69-80.

Tamrakar, N et al. (2007) Relationship among mechanical, physical and petrological properties of siwalik sandstones, Central Nepal Sub-Himalayas. *Engineering geology.* pp. 105-123.

Wilson et al. (1995) Volcanic and structural evolution of Taupo Volcanic Zone, New Zealand: a review. *J. volc. And geoth. Res.* pp. 1-28.

Bradley B. A. (2013)
Estimation of site-specific and spatially distributed ground motion in the Christchurch earthquakes: application to liquefaction evaluation and ground motion selection for post-event investigation
Proc. 19th NZGS Geotechnical Symposium. Ed. CY Chin, Queenstown

Estimation of site-specific and spatially distributed ground motion in the Christchurch earthquakes: application to liquefaction evaluation and ground motion selection for post-event investigation

B A Bradley
Department of Civil and Natural Resources Engineering, University of Canterbury, NZ
brendon.bradley@canterbury.ac.nz

Keywords: Ground motion, Liquefaction evaluation, Christchurch earthquakes

ABSTRACT

This paper presents a methodology by which both site-specific and spatially distributed ground motion intensity can be obtained immediately following an earthquake event. The methodology makes use of both prediction models for ground motion intensity and its correlation over spatial distances. A key benefit of the methodology is that the ground motion intensity at a given location is not a single value but a distribution of values. The distribution is comprised of both a mean and also standard deviation, with the standard deviation being a function of the distance to nearby strong motion stations**.**

The methodology is illustrated for two applications. Firstly, maps of conditional peak ground acceleration (PGA) have been developed for the major events in the Canterbury earthquake sequence. It is illustrated how these conditional maps can be used for post-event evaluation of liquefaction triggering criteria which have been adopted by the Department of Building and Housing (DBH). Secondly, the conditional distribution of response spectral ordinates is obtained at a specific location for the purposes of determining appropriate ground motion records for use in seismic response analyses of important structures at locations where direct recordings are absent.

New Zealand Geotechnical Society Inc. 19th Symposium, Queenstown 2013

1 CONDITIONAL GROUND MOTION DISTRIBUTIONS OVER A SPATIAL REGION

1.1 Theory

Because of the complexity of a ground motion time series, the engineering representation of ground motion severity typically comprises one or more ground motion intensity measures, IM. Below the general *IM* variable will be used, while subsequent applications will make use of a specific IM (e.g. peak ground acceleration, PGA, or pseudo-acceleration response spectral ordinates, SA(T)).

The representation of *IM* at a single location *i,* for the purposes of ground motion prediction, is generally given by:

$$lnIM_i = \overline{lnIM_i}(Site, Rup) + \eta + \epsilon_i \quad (1)$$

where $lnIM_i$ is the (natural) logarithm of the observed IM; $\overline{lnIM_i}(Site, Rup)$ is the median of the predicted logarithm of *IM* as given by an empirical ground motion prediction equation (GMPE), which is a function of the site and earthquake rupture considered; η is the inter-event residual; and ϵ_i is the intra-event residual. Based on equation (1), empirical ground motion prediction equations can provide the (unconditional) distribution of ground motion shaking as:

$$lnIM_i \sim N(\overline{lnIM_i}, \sigma_\eta^2 + \sigma_\epsilon^2) \tag{2}$$

where $X \sim N(\mu_X, \sigma_X^2)$ is short-hand notation for X having a normal distribution with mean μ_X and variance σ_X^2.

By definition, for a given ground motion intensity measure, (e.g. peak ground acceleration, *PGA*) all observations from a single earthquake event have the same inter-event residual, η. In this regard, the inter-event residual represents the correlation between all observations from a single event, which may occur as a result of a unique effect occurring during the earthquake rupture, which subsequently affects the ground motion at all locations in a systematic manner. On the other hand, the intra-event residual, ϵ_i varies from site to site. In this regard the intra-event residual represents all other randomness which leads to a difference between the observed ground motion intensity, the predicted median ground motion intensity, and the systematic inter-event residual. While the intra-event residual varies from site to site, it is correlated spatially as a result of similarities of path and site effects between various locations.

Based on the aforementioned properties of η and ϵ_i, use can be made of recorded *IM* values at strong motion stations to compute a conditional distribution of *IM* at an arbitrary site of interest as discussed further below.

Firstly, an empirical ground motion prediction equation (GMPE) is used to compute the unconditional distribution of ground motion intensity at the strong motion stations where ground motions were recorded. A mixed-effects regression (Abrahamson and Youngs 1992, Pinheiro et al. 2008) can then be used to determine the inter-event residual, η, and the intra-event residuals, ϵ_i's, for each strong motion station.

Secondly, the covariance matrix of intra-event residuals is computed by accounting for the spatial correlation between all of the strong motion stations and the site of interest. The joint distribution of intra-event residuals at the site of interest and the considered strong motion stations can be represented by:

$$\begin{bmatrix} \epsilon^{site} \\ \boldsymbol{\epsilon^{SMstation}} \end{bmatrix} = N\left(\begin{bmatrix} 0 \\ \mathbf{0} \end{bmatrix}, \begin{bmatrix} \sigma^2_{\epsilon_{site}} & \boldsymbol{\Sigma}_{12} \\ \boldsymbol{\Sigma}_{21} & \boldsymbol{\Sigma}_{22} \end{bmatrix} \right) \tag{3}$$

where $\boldsymbol{X} \sim N(\boldsymbol{\mu_X}, \boldsymbol{\Sigma})$ is short-hand notation for $\boldsymbol{X}$ having a multivariate normal distribution with mean $\boldsymbol{\mu_X}$ and covariance matrix $\boldsymbol{\Sigma}$ (i.e. as before, but in vector form); and $\sigma^2_{\epsilon_{SMstation}}$ is the variance in the intra-event residual. In Equation (3) the covariance matrix has been expressed in a partitioned fashion to elucidate the subsequent computation of the conditional distribution of ϵ^{site}. The individual elements of the covariance matrix can be computed from:

$$\boldsymbol{\Sigma}(i,j) = \rho_{i,j}\sigma_{\epsilon_i}\sigma_{\epsilon_j} \tag{4}$$

where $\rho_{i,j}$ is the spatial correlation of intra-event residuals between the two locations i and j; and σ_{ϵ_i} and σ_{ϵ_j} are the standard deviations of the intra-event residual at locations i and j. Based on the joint distribution of intra-event residuals given by Equation (3), the conditional distribution of ϵ^{site} can be computed from (Johnson and Wichern 2007):

$$\begin{aligned} \left[\epsilon^{site} \middle| \boldsymbol{\epsilon^{SMstation}}\right] &= N\left(\boldsymbol{\Sigma}_{12} \cdot \boldsymbol{\Sigma}_{22}^{-1} \cdot \boldsymbol{\epsilon^{SMstation}}, \sigma^2_{\epsilon_{site}} - \boldsymbol{\Sigma}_{12} \cdot \boldsymbol{\Sigma}_{22}^{-1} \cdot \boldsymbol{\Sigma}_{21}\right) \\ &= N\left(\mu_{\epsilon^{site}|\boldsymbol{\epsilon^{SMstation}}}, \sigma^2_{\epsilon^{site}|\boldsymbol{\epsilon^{SMstation}}}\right) \end{aligned} \tag{5}$$

Thirdly, using the conditional distribution of the intra-event residual at the site of interest given by Equation (5), and substituting into Equation (2), the conditional distribution of *IM* at the site of interest, IM_{site}, can be computed from:

$$[lnIM_{site}|ln\boldsymbol{IM_{SMstation}}] = N\left(\overline{lnIM_{site}} + \eta + \mu_{\epsilon^{site}|\boldsymbol{\epsilon^{SMstation}}}, \sigma^2_{\epsilon^{site}|\boldsymbol{\epsilon^{SMstation}}}\right) \quad (6)$$

That is, the conditional distribution of IM at a specific site is a lognormal random variable (i.e. the log of *IM* is a normal random variable) which is completely defined via the conditional median and conditional standard deviation.

It should be noted that in cases where the site of interest is located far from any strong motion stations the conditional distribution will be similar to the unconditional distribution, and for sites of interest located very close to a strong motion station the conditional distribution will approach the value observed at the strong motion station.

2 SPATIAL PGA MAPS IN THE CANTERBURY EARTHQUAKES

This section discusses the earthquake sources considered, as well as the ground motion prediction and spatial correlation equations which were adopted to compute the spatial PGA maps.

2.1 Earthquake sources

The spatial distribution of ground motion intensity was considered for major events in the Canterbury earthquake sequence. The finite fault models for the 4 September 2010, 22 February 2011, 13 June 2011 (2:20pm) and 23 December 2011 (2:18pm) events from Beavan et al. (2012) were adopted, while those for the 16 April 2011, 13 June 2011 (1:01pm), and 23 December 2011 (2:18pm) events were obtained in a first-order manner by using the CMT solutions from the GeoNet catalogue (Ristau 2008), and then fault dimensions based on magnitude scaling relationships (Stirling et al. 2007).

2.2 Ground motion prediction and spatial correlation equations

As illustrated from the theory in the previous section, ground motion prediction equations (GMPE's) and spatial correlation equations are required to compute the conditional ground motion at each location. The Bradley (2010, 2013) GMPE is adopted to provide the unconditional PGA distribution. Figure 1a provides a comparative example of the PGA amplitudes observed in the 4 September 2010 Darfield earthquake compared with the model prediction. Further scrutiny of this model against observations in the Canterbury earthquakes can be found in elsewhere (Bradley 2012b, Bradley 2013, Bradley and Hughes 2013). Figure 1b illustrates the adopted spatial correlation model of Goda and Hong (2008) for PGA as a function of the separation distance between two locations. As expected on physical grounds, the correlation is 1.0 for a separation distance of zero (i.e. two points at the same location), and tends toward zero as the separation distance increases. Thus, on the basis of Figure 1b and the previous theoretical discussions, it can be understood that if the recorded ground motion PGA is above the median prediction at a given strong motion station then it is more likely that the PGAs near this station will also be above average. The strength of this statement will decrease as the separation distance from the station and the site of interest increases.

New Zealand Geotechnical Society Inc. 19th Symposium, Queenstown 2013

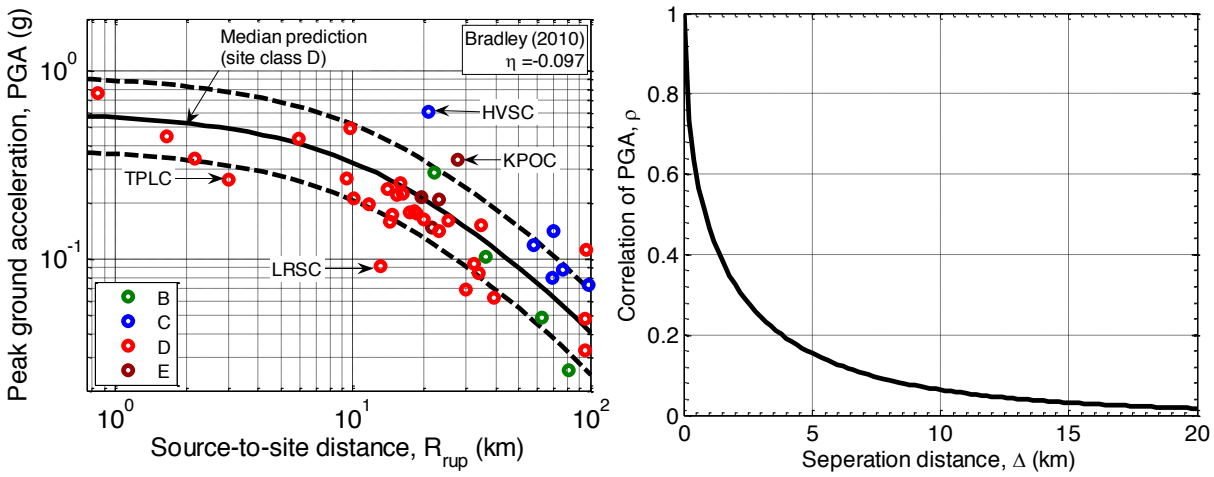


Figure 1: (a) Example comparison of observed PGA values with the empirical prediction of Bradley (2010) for the 4 September 2010 earthquake (M_w7.1); and (b) correlation of intra-event residuals for PGA as a function of separation distance (Goda and Hong 2008).

2.3 Computed spatial PGA maps for the Canterbury earthquakes

Figure 2 and Figure 3 provide examples of the spatial PGA maps produced for the 4 September 2010 and 22 February 2011 earthquakes, respectively. As illustrated in section 1.1, the distribution of PGA at any given location is lognormal, and therefore defined by a median and standard deviation. In Figure 2 and Figure 3 the median values are portrayed by contours, while the standard deviation is given according to the color map in the figure legend.
Several features are worthy of note in Figure 2 and Figure 3:

- Firstly, the median PGA amplitudes display a typical attenuation in amplitude as the distance from the earthquake source increases.
- In the proximity of strong ground motion stations, the contours can be observed to vary markedly as a result of differences between some observed PGA. This is consistently the case in Heathcote Valley for all events, due to strong basin-edge effects (Bradley 2012d); and also apparent at Kaiapoi High School during the 4 September 2010 earthquake as a result of wave-guide effects (Bradley 2012a). However, as shown by the median PGA contours, these effects are expected to be localised.
- The conditional standard deviations shown at the bottom panel of each of the figures provide an indication of the level of uncertainty in the conditional median PGA prediction. Near strong motion stations the conditional standard deviations decrease toward zero. This implies that the prediction of PGA is more accurate close to strong motion stations, and less accurate as the distance from strong motion stations increases.

3 CONDITIONAL PGA VALUES FOR LIQUEFACTION ASSESSMENT

There are several applications of the conditional ground motion distribution theory, and in particular, the maps of conditional PGA. Here, their application for liquefaction assessment is discussed.

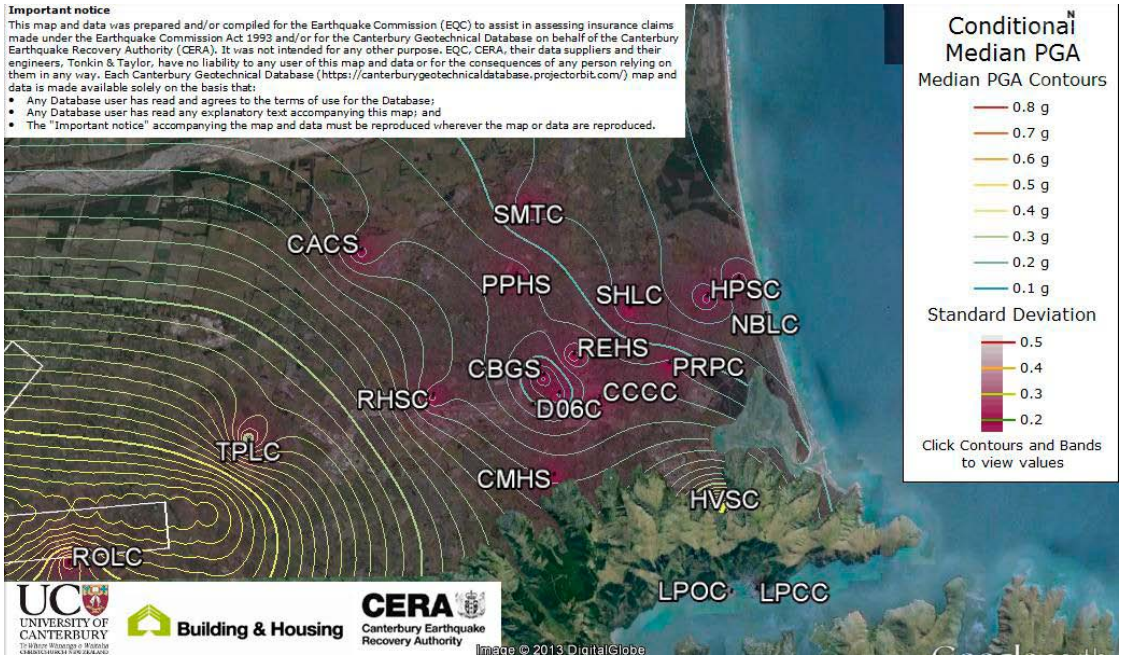


Figure 2: Conditional median (top) and conditional standard deviation (bottom) of PGA predicted in Canterbury from the 4 September 2010 earthquake.

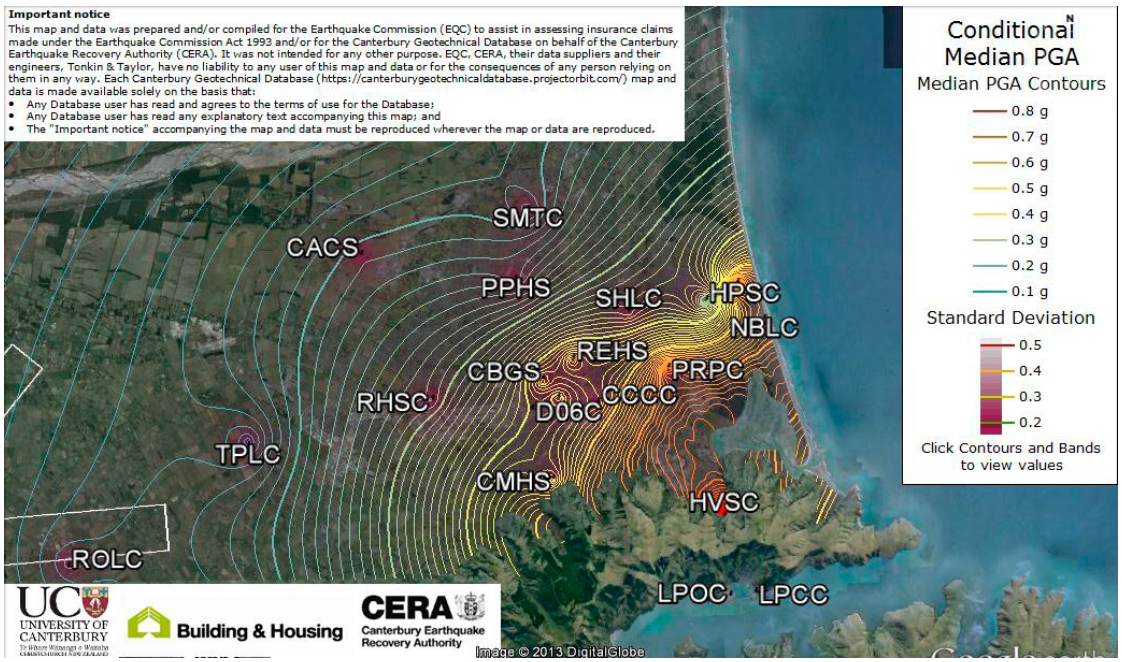


Figure 3: Conditional median (top) and conditional standard deviation (bottom) of PGA predicted in Canterbury from the 22 February 2011 earthquake.

3.1 Simplified method for liquefaction evaluation

Liquefaction assessments conventionally utilise a stress-based approach in which the factor of safety (FS) against liquefaction is obtained from the cyclic stress ratio (*CSR*) and the cyclic resistance ratio (*CRR*) (New Zealand Geotechnical Society 2010). Specifically,

$$FS = \frac{CRR_{7.5}}{CSR_{7.5}} \tag{7}$$

where the subscripts in both the denominator and numerator indicate that the ratios are representative of a M_w7.5 earthquake. The *CRR* can be obtained via various insitu testing methods (e.g. CPT, SPT, Vs) or laboratory data, but importantly is a property of the geotechnical conditions at the site of concern (New Zealand Geotechnical Society 2010). The *CSR*, which represents the ratio between the cyclic shear stress and vertical effective stress in the soil, can be estimated using the general equation:

$$CSR_{7.5} = 0.65 \frac{a_{max}}{g} \frac{\sigma_{vo}}{\sigma'_{vo}} r_d \frac{1}{MSF} \tag{8}$$

where a_{max} is the average horizontal (geometric mean) peak ground acceleration (PGA) at the ground surface; g is the acceleration of gravity; σ_{vo} is the vertical total stress at the depth of interest; σ'_{vo} is the vertical effective stress at the depth of interest; r_d is a reduction factor to account for the soil flexibility; and MSF is a magnitude scaling factor to account for the number of cycles of significant ground motion as a function of moment magnitude, M_w. The value of MSF can be obtained from several published equations, for example (Idriss and Boulanger 2008):

$$MSF = 6.9 * exp\left(-\frac{M_w}{4}\right) - 0.058 \leq 1.8 \tag{9}$$

It should be noted that the a_{max} in Equation (8) is that provided by the previously discussed spatial PGA maps. Hence, such maps enable a site-specific evaluation of the FS against liquefaction for all major events in the Canterbury earthquake sequence. Comparing field observations of ground deformation following each of these events, with the respective liquefaction FS computed, enables a first-hand assessment of the accuracy and precision of the simplified liquefaction evaluation procedure on a site-by-site basis. Such first-hand validation is critical, because it must be recalled that this methodology is highly simplified, and region-specific soil characteristics and in situ conditions may lead to systematic differences between prediction and reality.

3.2 Implementation by the Engineering Advisory Group (MBIE)

The previously discussed methodology and spatial PGA maps have been adopted by the Engineering Advisory Group to the Ministry of Business, Innovation and Employment (MBIE 2012) for liquefaction evaluation as outlined in the previous section. In order to make use of the spatial PGA contour plots (e.g. Figure 2 and Figure 3) for a site-specific liquefaction assessment, Google Earth files have been created and are publically available on the Canterbury Geotechnical Database (https://canterburygeotechnicaldatabase.projectorbit.com).

4 CONDITIONAL RESPONSE SPECTRA VALUES FOR SITE-SPECIFIC GEOTECHNICAL AND STRUCTURAL ASSESSMENT

The theory in section 1.1 can also be extended to examine the prediction of response spectral ordinates of different vibration periods, $SA(T)$. Such assessments can therefore provide a site-specific estimate of the response spectrum of the unknown ground motion which occurred during these past events.

This methodology has been applied to estimate the site-specific response spectrum at the location of the CTV building from the 22 February 2011 earthquake (Bradley 2012c). Figure 4 illustrates the median, 16th and 84th percentiles of the conditional response spectrum predicted at the site as well as the geometric mean response spectra of four ground motions recorded in the general vicinity of the CTV site. In this particular application the observed ground motions can

be seen to provide a good representation of the conditional response spectrum, and therefore there ground motions could be utilized as input in response history analyses of the CTV structure, in lieu of a direct ground motion record at that site.

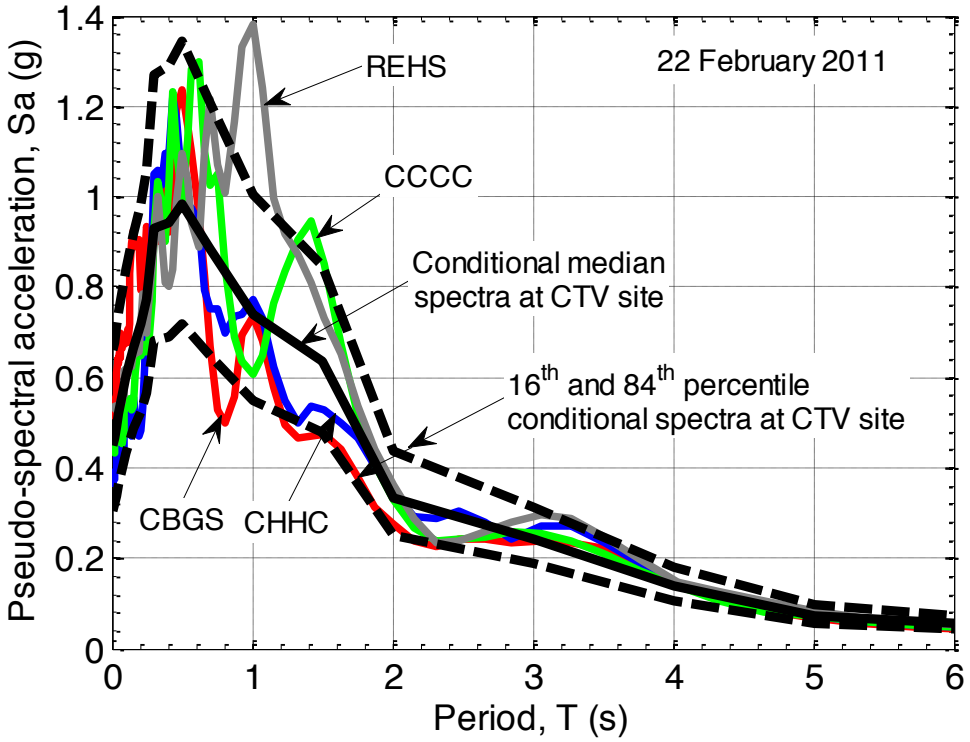


Figure 4: Comparison of the ground motions observed at the four 'CBD' strong motion stations (i.e. CCCC, CHHC, REHS, CBGS) with the conditional response spectrum distribution at the CTV site for the 22 February 2011 Christchurch earthquake.

In addition to using conditional response spectral ordinates for detailed post-event analyses of structures, it can also be used to obtain a rapid estimation of the seismic demand imposed on structures in an urban region for post-event triaging of buildings. While such information is certainly not a substitute for a rigorous field inspection, an understanding of the likely seismic demand (and consequent dynamic response) of the system will assist in identifying what forms of seismic distress may be apparent.

5 CONCLUSIONS

This paper presents a methodology by which a conditional distribution of ground motion intensity can be determined following an earthquake event. The predicted values are dependent on both the general manner in which ground motion intensities are observed to vary over a region from a given causative fault (as predicted by empirical ground motion models), combined with the actual recorded PGA values at various strong motion stations in the region. As such, the predicted intensity values are termed 'conditional', that is, the prediction is conditional on the observations at distinct locations.

The methodology was illustrated by first developing maps of the spatial distribution of PGA for the major events in the Canterbury earthquake sequence for the assessment liquefaction triggering. The methodology was also applied to the site-specific estimation of response spectra for use in determining appropriate ground motions for response history analyses.

6 REFERENCES

Abrahamson, N. A., R. R. Youngs, (1992). A stable algorithm for regression analyses using the random effects model, *Bulletin of the Seismological Society of America*, 82, 505-510.

Beavan, J., M. Motagh, E. J. Fielding, N. Donnelly, D. Collett, (2012). Fault slip models of the 2010–2011 Canterbury, New Zealand, earthquakes from geodetic data and observations of postseismic ground deformation, *New Zealand Journal of Geology and Geophysics*, 55, 207-221. 10.1080/00288306.2012.697472

Bradley, B. A., (2010). NZ-specific pseudo-spectral acceleration ground motion prediction equations based on foreign models, Department of Civil and Natural Resources Engineering, University of Canterbury, Christchurch, New Zealand. 324 pp. http://ir.canterbury.ac.nz/handle/10092/5126

Bradley, B. A., (2012a). A critical analysis of strong ground motions observed in the 4 September 2010 Darfield earthquake, *Soil Dynamics and Earthquake Engineering*.

Bradley, B. A., (2012b). Ground motion and seismicity aspects of the 4 September 2010 and 22 February 2011 Christchurch earthquakes, *Technical Report Prepared for the Canterbury Earthquakes Royal Commission* 62 pp.

Bradley, B. A., (2012c). Ground motion aspects of the 22 February 2011 Christchurch earthquake related to the Canterbury Television (CTV) building, *Technical Report Prepared for the Canterbury Earthquakes Royal Commission* 26 pp.

Bradley, B. A., (2012d). Strong ground motion characteristics observed in the 4 September 2010 Darfield, New Zealand earthquake, *Soil Dynamics and Earthquake Engineering*, 42, 32-46. 10.1016/j.soildyn.2012.06.004

Bradley, B. A., (2013). A New Zealand-specific pseudo-spectral acceleration ground-motion prediction equation for active shallow crustal earthquakes based on foreign models, *Bulletin of the Seismological Society of America*, 103. doi: 10.1785/0120120021

Bradley, B. A., M. Hughes, (2013). Conditional Peak Ground Accelerations in the Canterbury Earthquakes for Conventional Liquefaction Assessment: Part 2, *Technical Report Prepared for the Ministry of Business, Innovation and Enterprise* 19 pp.

Goda, K., H. P. Hong, (2008). Spatial correlation of peak ground motions and response spectra, *Bulletin of the Seismological Society of America*, 98, 354-465. 10.1785/0120070078

Idriss, I. M., R. W. Boulanger, (2008). Soil Liquefaction During Earthquakes. Earthquake Engineering Research Institute.

Johnson, R. A., D. W. Wichern, (2007). Applied Multivariate Statistical Analysis. Prentice Hall: Upper Saddle River, NJ.

MBIE, (2012). Guidelines for the investigation and assessment of subdivisions on the flat in Canterbury, Ministry of Business, Innovation and Employment, *Version 2* 15 pp.

New Zealand Geotechnical Society, (2010). Geotechnical earthquake engineering practice: Module 1 – Guideline for the identification, assessment and mitigation of liquefaction hazards, 34 pp.

Pinheiro, J., D. M. Bates, S. DebRoy, D. Sarkar, the R Core team, (2008). nlme: linear and nonlinear mixed effects models, *R package version 3.1-89.*

Ristau, J., (2008). Implementation of routine regional moment tensor analysis in New Zealand, *Seismological Research Letters*, 79, 400-415. doi: 10.1785/gssrl.79.3.400

Stirling, M. W., M. Gerstenberger, N. Litchfield, G. H. McVerry, W. D. Smith, J. R. Pettinga, P. Barnes, (2007). Updated probabilistic seismic hazard assessment for the Canterbury region, *GNS Science Consultancy Report 2007/232, ECan Report Number U06/6* 58 pp.

Use of geographical information systems to assist with management of the EQC Canterbury Geotechnical Investigation Project

J J Carter
Tonkin & Taylor Ltd, Christchurch, NZ.

A Fairclough
Tonkin & Taylor Ltd, Christchurch, NZ.

Keywords: GIS, fieldwork, management, planning, Christchurch, earthquake, disaster response, ESRI, SQL, iPAD, ArcGIS, TC3.

ABSTRACT

In 2012 the Earthquake Commission (EQC) commissioned the EQC Geotechnical Investigation Project (EQC GI Project) to collect "deep" post-earthquake geotechnical data to inform and expedite the Canterbury Earthquake recovery process. The investigation area primarily incorporated approximately 28,000 residential properties which were assessed to lie within the Department of Building and Housing (DBH) designated "Foundation Technical Category 3" zone. In total 1,441 machine drill holes and 4,722 cone penetrometer tests were completed as part of the EQC GI project over a 14 month period.

Geographical Information Systems (GIS) technology was implemented in the early stages of the EQC GI project to manage the large spatial databases which were being created and compiled. Multiple sources were linked to centralised databases to capture and manage the ever-changing data which included geotechnical investigation results and progress, claim details and status, land damage information and service plans. All of this information was used concurrently to manage, plan, optimise and track the project.

Both office planning and field work dimensions were captured, and the data management methods evolved from a system which relied upon Microsoft Excel, Google Earth and CAD, to a centralised, integrated ESRI ArcGIS Geodatabase with GIS mapping and an Online SQL based tracking system. This progression was further extended into the field operations, enabling staff to make use of iPads applications in the field. The GIS systems allowed reliable progress reports to be generated at any time by the management team, and, ongoing review and optimisation of the investigation locations to be undertaken in a rapid and highly efficient manner.

This paper describes how GIS proved vital to the planning and management of the project, outlines some of the issues GIS resolved, and, presents lessons learnt to assist with planning and implementation of similar projects in the future.

New Zealand Geotechnical Society Inc. 19th Symposium, Queenstown 2013

1 INTRODUCTION

Between March 2012 and June 2013 1,441 machine drill holes and 4,722 cone penetrometer tests were completed as part of the EQC Geotechnical Investigation Project (EQC GI project).

Geographical Information Systems (GIS) technology was implemented early in the EQC GI project to manage the large spatial databases which were being created and compiled. Due to the magnitude and speed of the project, systems had to be implemented in a short timeframe to enable both the rapid response to the natural disaster and longer term project planning to be completed effectively.

GIS is proven technology, which is concerned with the description, explanation and prediction of patterns and processes at geographical scales (Longley et al., 2005.) ESRI ArcGIS was the main GIS technology used on the EQC GI Project. This platform allowed the project to connect multiple database sources which contained information for a variety of topics such as land damage inspection results, claim data, property information, DBH Foundation Technical Category zone boundaries, CERA "Red" and "Green" zone boundaries, service plans, and the results of the ongoing geotechnical investigations.

GIS systems not only have an ability to join multiple types of data to a centralised database, but importantly GIS can keep track of location and display data to show trends not easily identified in tabular data. These benefits, along with various analyst tools, allow for information to be concurrently managed, updated, optimised and tracked throughout the project programme.

2 INTEGRATING DATA INTO GIS

After the M6.3 seismic event of 22 February 2011, the Department of Building and Housing (DBH) subdivided the Canterbury Earthquake Recovery Authority (CERA) "Green Zone" into three technical category zones for foundation systems. These zones, which are commonly referred to as TC1, TC2 or TC3, were established using information from observed land damage, observed property damage data, ground water information and known soil conditions (MBIE, 2013). In the TC3 Zone, most residential foundation repairs, and all foundation rebuilds, require geotechnical information to a target depth of between 10 and 20m to enable appropriately informed liquefaction susceptibility analysis and engineering design to be completed.

The first major application for GIS in the project involved solving the problem of reliably estimating the type and amount of geotechnical investigation that was likely to be needed, and, how the various types of borehole and Cone Penetrometer Test (CPT) investigations would be distributed throughout the city. To enable this, the project team needed to be able to identify individual properties within the investigation area and integrate the relevant claim, foundation damage data and existing geotechnical information which was available from multiple sources.

To solve the issue the property database and investigation pods were imported into ESRI ArcCatalog as GIS 'layers.' The pods were based on dividing suburb regions into manageable areas of approximately 150 dwellings. Once the layers were overlayed, then a spatial one to one join ran to connect the each property to the pod it was contained within using GIS. The spatial join identifies all property's point locations within the polygon and then we exported the selected points to create a list of the 28,000 properties, the claim information and their associated investigation pods within the TC3 Zone.

A benefit of the property database was the ability to link this layer using a unique property identifier 'QPID' to the EQC claim database and the observed land damage database from the

Land Damage Assessment Team (LDAT) using one-to-one and one-to-many table joins in GIS. Instantly, in the GIS system we now had the ability to provide breakdown of property info, by suburb, pod, claimant costing, foundation type and attributes from LDAT.

The integration of Google earth and Microsoft Excel into GIS allowed detailed analysis of the LDAT data in GIS. This enabled the identification of properties most likely to require geotechnical investigation, mapping the data uncovered spatial trends in the evolving database.

3 GEOTECHNICAL INVESTIGATION LOCATION PLANNING AND PROGRAMME

At the start of the project, to help ensure the overall program design and execution was completed in a logical manner, the project manager divided the entire investigation area into 227 sub-areas called "PODS". Each POD generally contained between 50 and 150 adjacent properties that were expected to be underlain by similar geotechnical conditions. POD boundary plans were generated in Google Earth format (kmz file), and these formed the base layer for the subsequent overlay of information which was required to manage and plan the upcoming fieldwork.

In the early stages of the project the Geotechnical Engineers and Engineering Geologists worked side-by-side with the GIS analyst to create investigation location plans using disconnected databases for the land damage records and claim information, and, manual comparisons to existing geotechnical investigation data. Details of the investigation type and location were added to the Google Earth kmz files, and location maps were produced for the fieldwork teams in CAD using the kmz locations. However, it was quickly realised that this was a very time consuming process and somewhat difficult to manage as investigation location plans had to be generated for two different program options, and, countless ongoing amendments to be made as the program was adjusted to incorporate the additional geotechnical data which was being generated by the project. GIS is a much more flexible and robust tool for this type of situation, and the project team promptly switched to planning and managing the investigation locations using GIS as it afforded the following benefits:

- Maps could be produced straight from the GIS database. This resulted in a significant time saving over the previous CAD based system.
- It created a geotechnical investigation database, which could be collated and converted into map overlays and expedite the planning and optimisation process.
- Live investigation data could be captured with relative ease and this significantly improved the reliability and speed at which the progress reports, including program and budget, could be completed.

Figure 1 shows an example Progress Summary Map which was presented by EQC at public information meetings. On Figure 1 the green areas indicate the areas where the geotechnical investigation fieldwork had been completed, the blue areas showed where investigations were currently in progress, and, the red colour showed those areas where the investigations had not yet commenced. These maps were updated and reprinted a few hours before each public meeting to ensure they were as accurate as possible.

GIS made "real-time" progress reports, planning, amendment and forecasting possible. Property statistics were interpolated in suburbs and PODS where investigations were in progress, or yet to commence, to give more accurate predictions of the project program and cost to completion. Engineers used this data to estimate the expected progress of drilling by Pod, which in turn was mapped using GIS over space and time.

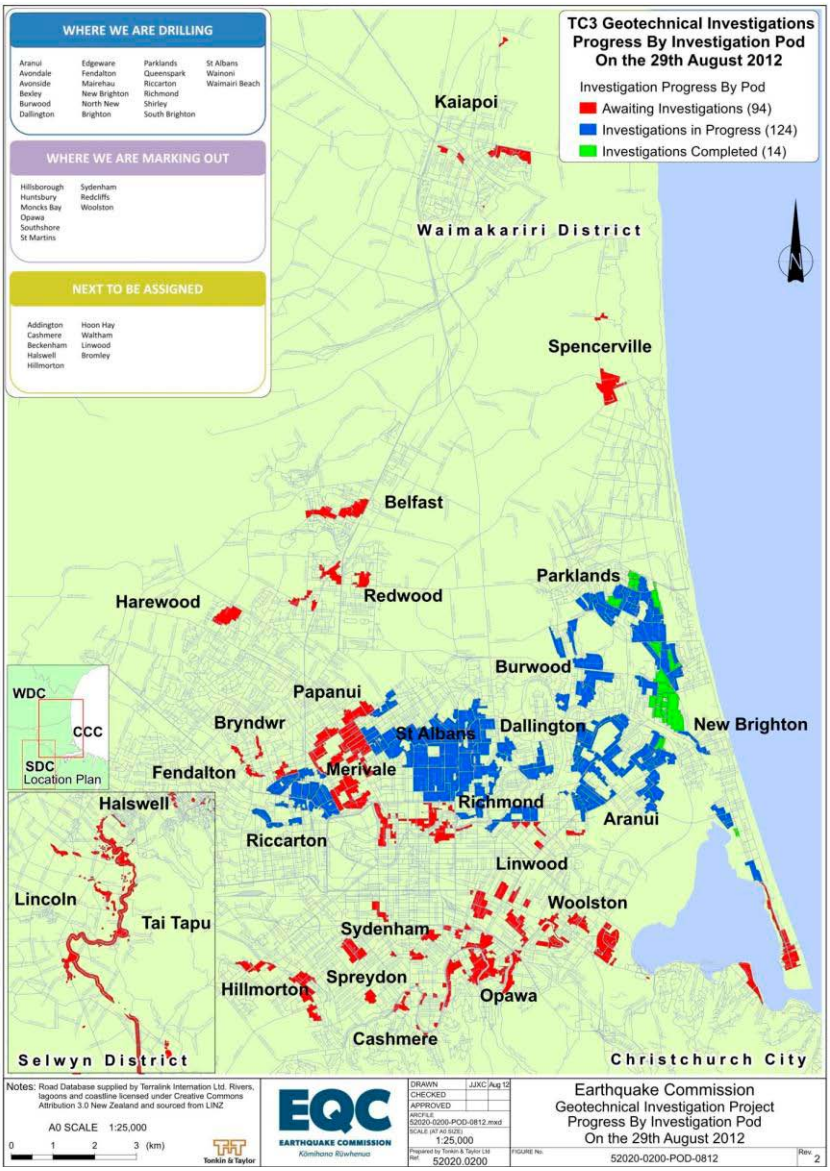


Figure 1: Example Progress Summary Map which was presented by EQC at public information meetings

4 MANAGING DATABASES, TRACKING CHANGES AND PROGRESS

Given the project scale and high level of public interest the EQC GI Project required accurate and reliable tracking and reporting systems. Two main GIS databases were used too manage and track the programme changes and progress. Firstly, the investigation database which included the investigation type, method, location and related property details, and secondly, the investigation area properties database which included information such as owner, physical address and legal description for all 28,000 properties that were located within the TC3 zone.

The two centralised databases described above were also connected to:

- The TC3 Zone boundary layer, which was updated on several occasions,
- The Property IQ property database which gave property location data within each land parcel,
- The Land Damage Assessment Team (LDAT) database, which was continually updated as land damage assessments progressed,
- Databases summarising the service line and manhole locations,

- The EQC claims database,
- The EQR database which contained repair details for the properties that EQC intended to repair or rebuild,
- The land owner access permissions database which tracked when permission had been given by the land owner to access the property and commence the physical investigation works, and,
- The geotechnical investigation database which contained information on the investigations and their current status such as the investigation type and target depth, and, any tasks completed to date such as finalisation of location, services clearance completed, physical works completed and laboratory testing completed.

Additional databases were also generated in the early stages of the project to:

- Collate any publically-available information regarding soil contamination.
- Collate any publically-available information regarding indigenous sacred sites.

The above information was plotted, reviewed and embedded into the design and planning process to ensure appropriate actions were taken prior to and during execution of the works and to ensure compliance with the project Resource Consent conditions. Areas of concern with respect to health and safety, such as the soil contamination database, were spatially joined so that all investigations within these areas were clearly identified to field staff during scheduling of the physical works.

The investigation and TC3 property databases which were created for this project had to adjust and reflect all the changes in the connected databases. The method for doing this was through two identifiers, a unique ID created for each investigation (which contained suburb, POD, investigation type and number components), and, the Property ID (QPID) taken from the PIQ Property database. The QPID was vital in joining the databases. The LDAT database is an online SQL database, so by using ESRI ArcGIS SQL database connections the link was live and ongoing amendments and updates were immediately visible in all maps showing the properties requiring geotechnical investigations. The claims database was an external source, so manual joins were used in GIS to update the TC3 property database if, for example, a property had been reassessed as “over cap” and no longer the responsibility of EQC to repair or rebuild. All of this information was used concurrently to manage, optimise and track the project progress, in particular when permission had been given by property owners to commence the physical work.

Continual improvement was encouraged by the project management team for the entire duration of the EQC GI project. An example of this was the development and deployment of applications to allow portable, digital data collection with iPads in the field. This improvement could only be achieved after the data management systems had been moved from an Excel based system to an online system that could cope with a high number of multiple users. The online system was also set-up to expedite the cleansing of data, the removal duplicate lists of the same investigations, and, allow live layers in GIS which was used for creating location and progress maps which could be accessed in the field via iPads. The iPads were also used to collect data in the field and automatically download this to the master database at the end of each day.

In summary, centralising the databases and migrating to an Online SQL based system greatly expedited the project design and planning process and allowed for simultaneous multiple-user access, instant progress reporting, and, accurate progress tracking. Having this robust and highly accessible system meant any issues were quickly identified and rectified and this had a very positive effect on the overall management of the project.

5 OPTIMISATION

From a geo-practitioner's perspective, a key benefit of the EQC GI project GIS was the ability to quickly collate, sort, analyse and visually present key geotechnical data. In addition, any geotechnical maps which were developed using GIS could be easily updated and reanalysed as additional data became available. This greatly assisted the investigation planning and design team to accurately evaluate issues such as the likely CPT refusal depth as the project advanced into a new POD. This meant that a more appropriate investigation type could be scheduled if unsatisfactory CPT penetration depth was likely to occur. This ultimately resulted in considerable time and cost savings, and, led to the collection of better quality data. Figure 2 presents the final version of the map "Inferred Typical CPT Refusal Depth" which was developed by the project design and planning team. For the purposes of Figure 2 CPT refusal generally corresponded to an ultimate cone tip resistance of between 20 and 40 MPa depending on the type of rig and equipment being used. In general, the CPT intensity which has been used to generate Figure 2 comprises an irregular 100 to 150m grid.

The geotechnical investigation database tracked basic as-built test information and results, including depth of test and reason for ending the test. Using this information, as well as the surveyed location, engineers directed GIS to display the depth and locations of selected tests to analyse geotechnical trends across the city. Using ESRI's ArcMap graduated colour quantitative symbology, maps of the CPT refusal depths were produced, revealing overall spatial patterns.

Further analysis in GIS using both Kriging and Inverse Distance Weighted (IDW) methods, created a solid (raster) layer which summarised the expected CPT refusal depth throughout the entire investigation area. Both techniques were experimented and trialled to identify which method returned the best prediction. IDW uses Tobler Law and relatively simple coding to denote values on nearby points, giving the greatest weight to neighbouring points. Kriging also interpolates surrounding surfaces, using solid theoretical foundations and distance from known points is more important, which usually results in a smoother surface raster (Longley et al, 2005).

To refine the predictions of CPT refusal depth in a natural ground profile the data had to be examined and modified to allow for artificial shallow CPT refusal, such as refusal due to the presence of large tree roots, service lines and/or land fill material. By mapping the CPT depths any unusual outliers were easily identified, and CPT results examined to eliminate CPTs that met with "early refusal" for reasons other than refusal on dense natural soils. The predictions of CPT refusal depth that are described above were cross-checked against the machine borehole results. This enabled the dense sand and gravel layers to be positively identified in the soil profile and verification of the predictions of CPT refusal depth which are summarised on Figure 2. Interestingly, the spatial patterns in the initial "draft" version of Figure 2 did not vary greatly from the final version which incorporated the results of three or four times the number of investigation results. This indicates the analysis techniques described above may provide a good indication of CPT refusal depth with a relatively low intensity of investigation data.

A key trend which is apparent on Figure 2 is CPT refusal occurring at a greater depth in the eastern suburbs of Christchurch City than in the western suburbs. Another key benefit of the centralised GIS database was the ability to constantly track and review the investigation coverage and progress, and, the predictions of program and cost.

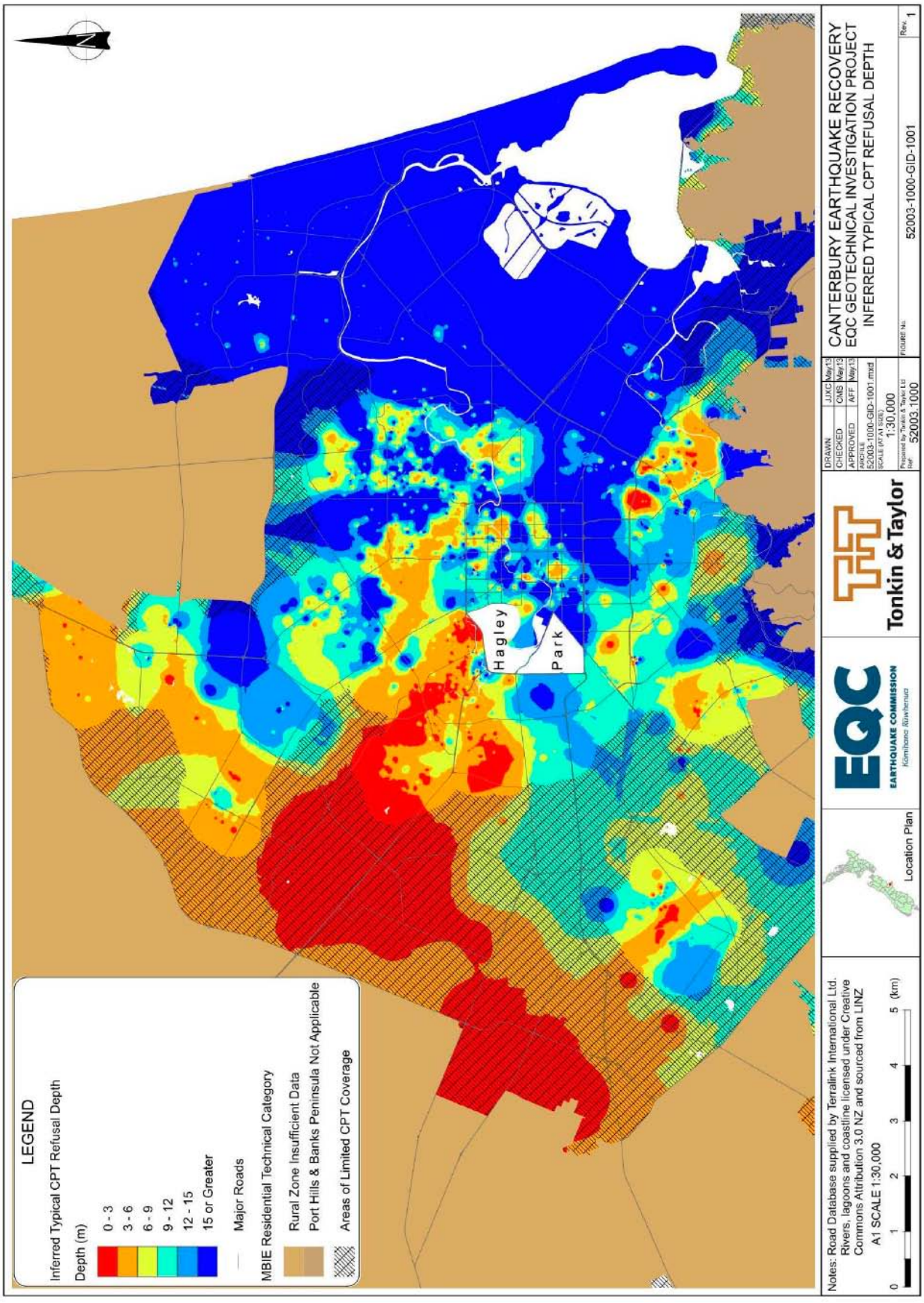


Figure 2: Inferred Typical CPT Refusal Depth

GIS was used to verify the investigation coverage by making use of the proximity analysis buffer tool. The tool extends the influence of any given point, to a set radius, and a map was generated to show a circle with a 50m radius around each CPT location. The circles were then shaded to highlight any unshaded areas where additional tests were required to achieve satisfactory investigation coverage. Conversely, the number of investigation locations was often reduced in those areas where it was identified that the investigation intensity was unjustifiably high. Use of the basic buffer tool also allowed predictions of the overall investigation program and cost to be easily reviewed and updated as appropriate.

6 CONCLUSIONS

In total 1,441 machine drill holes and 4,722 cone penetrometer tests were completed as part of the EQC Geotechnical Investigation project over a 14 month period. This project was commissioned by the Earthquake Commission as part of their recovery response to the Canterbury Earthquake sequence. GIS was an essential part of the success of the EQC Geotechnical Investigation project. It resulted in many positive outcomes, primarily in the areas of investigation planning and design, and, project management. Combining and centralising the numerous large datasets which were used on this project, and the adoption of ESRI's Arc GIS platform, proved to be vital to enable robust and reliable design, tracking, amendment, data collection, management and overview of an ever-changing programme. The ESRI ArcGIS system also provided flexibility and allowed continual improvements to be made such as the development of applications for the collection of field data using iPads and the automatic transfer of this data back into the master databases.

The primary recommendation for future projects of this nature would be to implement a smart flexible database system that can collate data from several different sources and enable the project progress to be tracked in detail. ESRI's Arc GIS is an attractive operating platform for this type of project as it can connect to multiple and a variety of sources such as Microsoft Excel, Google Earth, SQL Databases and CAD systems. The primary benefits include the ability to track changes and quickly generate updated tables and maps summarising the data collected to date. Displaying data spatially is also of significant advantage when reviewing geotechnical information, and, attempting to identify trends and/or patterns.

7 ACKNOWLEDGEMENTS

The authors would like to acknowledge and thank EQC and all members of the EQC Geotechnical Investigation project team for the high levels of professionalism, effort, foresight, collaboration and trust that they brought to the project. These core project principles ensured the output from the EQC Geotechnical Investigation project was of unparalleled value to the Canterbury earthquake recovery process. The authors also wish to acknowledge project team members Chris Soutar and Dan Ashfield who provided the geotechnical input during development and refinement of the map "Inferred Typical CPT Refusal Depth" which is reproduced as Figure 2 in this paper.

REFERENCES

Canterbury Earthquake Recovery Act (CERA) (2012) Canterbury Geotechnical Database website. https://canterburygeotechnicaldatabase.projectorbit.com

Longley, P. A., Goodchild, M. F., Maguire, D. J., Rhind, D. W. (2005) *Geographic Information Systems and Science*. 2nd Edition John Wiley & Sons, Ltd, England.

Ministry of Business, Innovation and Employment (MBIE), (2013) Canterbury Qa Technical Categories, https://dbh.govt.nz/UserFiles/File/Publications/Building/Guidance-information.

Recognition of geotechnical considerations in planning documents

B A Curley
GHD Limited, Wellington, NZ.
beverley.curley@ghd.com (Corresponding author)

R D Beetham
GHD Limited, Wellington, NZ (Previously GNS Science, Lower Hutt, NZ)
dick.beetham@ghd.com

B Simms
GHD Limited, Wellington, NZ
bruce.simms@ghd.com

Keywords: Natural hazards, Petone, Hutt City, policy, planning, geotechnical, earthquake, tsunami, shaking, fault rupture, tsunami, sea-level rise, flooding, Wellington Fault, District Plan.

New Zealand Geotechnical Society Inc. 19th Symposium, Queenstown 2013

ABSTRACT

In light of the Canterbury earthquakes, natural hazards, geology, and geotechnics have been thrust into the forefront of people's consciousness. More specifically the general public are becoming more aware of the hazards, risks, and consequences of naturally occurring events. As such those developing guidelines, providing input to local and regional councils, and making government decisions and polices, are also becoming more aware and are now more likely to seek technical advice.

Hutt City Council (HCC) is currently proposing a District Plan change (Plan Change 29) for the Petone West area of Hutt City. The Plan Change seeks to increase the intensity of development and land use. Petone West is susceptible to a wide range of natural hazards including, fault rupture (Wellington Fault), ground shaking, global uplift and subsidence, liquefaction, settlement from subsoil densification, tsunami, storm flooding and sea level rise. It could be argued that Petone West is one of the most hazard prone areas of Hutt City.

In preparation for the proposed plan change, and prior to requesting public submissions, HCC commissioned a review of the natural hazards for Petone West along with geotechnical considerations for mitigating or reducing the impact of those natural hazards. How the identified natural hazards and associated remedial solutions are adopted into the final plan change document remains to be seen, but in this post-Canterbury Earthquakes era, specialists in natural hazards, geology, and geotechnics have an increased opportunity to influence and educate policy and decisions makers.

1 INTRODUCTION

Natural hazards (events) are killers. Or rather they can be. They don't always have to be. There are plenty of disasters around the world and in New Zealand that demonstrate the lethality, and potential lethality of natural hazards. Some hazards trigger other hazards, some hazards impact upon the built environment and the built environment accentuates the damage. There is the old adage; the earthquakes don't kill people, buildings do. Of course, if no-one is around to be impacted upon by the hazard (event) then is it a problem? If people and infrastructure etc. are vulnerable to the hazard and its consequences then you can (and frequently do) have a disaster. However, if you can reduce the vulnerability of the people and infrastructure to the hazard then

the consequence of the event are reduced. Proper planning is one way to do this, be it in the form of civil defence or in the form of planning policy and documentation.

2 PROPOSED PLAN CHANGE 29

2.1 Proposed Plan Change 29 – Introduction

Hutt City Council developed Proposed Plan Change 29, which is a proposed zoning change to the Western End of Petone, Lower Hutt, to create a Mixed Used Area. The purpose being to promote more diverse activities in the proposed plan change area (Petone West). This proposed change would also likely result in intensification of the area.



Figure 1: Location of Proposed Plan Change 29

As part of the development of the proposed plan change, GHD (GHD) (with sub-consultants GNS Science) were engaged to carry out a desktop review about the nature, likelihood and significance of risks from natural hazards, and, based on the nature, likelihood and significance of risks from natural hazards, advise on measures to avoid, remedy or mitigate these risks. This study was commissioned as HCC were aware that a large amount of work has been carried out since the implementation of the current district plan, increasing the amount of understanding and information available on the natural hazards that have the potential to damage and harm to Petone West.

2.2 Natural Hazards of Petone West

Petone West is susceptible to a wide range of natural hazards including: fault rupture from the Wellington Fault which runs through Petone West, ground shaking (from any number of faults that can affect Greater Wellington), global uplift, global subsidence (from a Wellington Fault event and slow-slip seismic events), liquefaction, settlement from subsoil densification,

tsunami, storm flooding, and sea level rise. It could justifiably be argued that Petone West is one of the most hazard prone areas of Hutt City.

2.3 The Natural Hazards Review

As part of the review findings GHD divided Petone West into three (3) sections:

- West of the Fault Rupture Section,
- Fault Rupture Section (Wellington Fault); and,
- East of the Fault Rupture Section.

This geographic division was largely based around the Wellington Fault alignment and probable associated post-earthquake design criteria. The hazards that affect or have the potential to affect the different sections were detailed.

GHD also highlighted to HCC what it considered were the critical geotechnical issues in the proposed plan change area. They were:

- Ground level changes east of the Wellington Fault (global subsidence),
- Ground level changes of Petone West (global uplift); and,
- Fault Rupture.

The hazards relating to these critical issues and the possible consequence of them were detailed. The critical geotechnical issues were identified as such as they were considered to be hazards that could not be directly engineered against (i.e. stopping the fault from displacing).

Additional geotechnical considerations and consequences, and potential mitigation measures of those hazards were also detailed.

There were nine (9) review recommendations, covering required increased ground investigations, better constraining the Wellington Fault, additional restrictions of building within the Wellington Fault Special Study Area (HCC District Plan Chapter 14H), implementation of a ground engineering register, monitoring and implementation of the Canterbury Earthquakes Royal Commission recommendations, and a review of the local building consent processing requirements.

2.4 Notified Proposed Plan Change 29

HCC further developed Proposed Plan Change 29 after receiving all the technical/specialist reviews it had requested. Proposed Plan Change 29 analysis of the natural hazards concluded that "for the risks from other natural hazards, standards outside the District Plan are considered the most efficient and effective approaches in achieving the natural hazard objectives".
Essentially it appears that the natural hazards review, whilst documenting the hazards and risks of those hazards to the Petone West area, did not influence the Council to amend the plan change prior to notification and to grasp the opportunity to reduce the vulnerability of the (proposed) intensified area but to maintain the existing approach that was put in place when the current district plan became active in 2004.

2.5 Public Submissions

A record number of public submissions were received on all aspects of the Proposed Plan Change 29, 277 submissions. Of these submissions, 137 raised concerns regarding the treatment of natural hazards within the notified plan change.

New Zealand Geotechnical Society Inc. 19th Symposium, Queenstown 2013

2.6 Technical Review of Public Submissions

As a result of the public submissions technical reviews were sought by HCC. GHD was engaged to establish whether any changes were required to the Natural Hazards Review Report in light of the submissions particularly if the submissions contained technical data that needed to be considered. Also to provide HCC with recommendations of actions it could take outside District Plan in response to matters raised within the technical review.

GHD considered all submissions apart from those of GNS Science (GNS) and Greater Wellington Regional Council (GWRC), were considered not to contain any additional data for inclusion in the review. GNS reported that studies have shown that as a result of slow-slip seismic events Wellington City (approx. 10km from Petone West) has been subsiding on average 1.7mm/yr since 2000. Studies are also reported to show that Wellington has the highest sea level rise of all the main centres (independent of slow-slip seismic events). GWRC shared concerns regarding sea level rise and effects on drainage gradients and elevated groundwater tables, along with an increased reach of high and storm tides that may also lead to increased erosion and inundation.

The technical review resulted in revised and edited recommendations in light of some of the information contained in the submission, the contents of the proposed plan change (to make clearer the recommendations), and in light of the recommendations contained in the Canterbury Earthquakes Royal Commission. The recommendations (summarised) included:

- That HCC closely react to and incorporate the findings of the Canterbury Earthquake's Royal Commission, especially considering the geological and geotechnical similarities of Petone West and Christchurch.
- That HCC carry out a review of the HCC adopted standards and guidelines for infrastructure and building construction etc.
- All new structures and buildings, and those that are being retrofitted to an increased standard must have comprehensive and appropriate intrusive ground investigation data. It is generally accepted that intrusive investigations for liquefaction analysis should extend to 20-25m below ground level. The investigations must be scoped by qualified and experienced geotechnical professionals.
- That a specialist should be engaged to better constrain the location of the Wellington Fault to allow refinement of the Wellington Fault Section / Wellington Fault Special Study Area (WFSSA).
- That the restricted discretionary activity status continue to be applied with all structures and buildings where the whole site or a portion of the site falls within the WFSSA, and that no construction within Fault Rupture Zone to be buildings of BIC 2b-5 (inclusive). It is noted that in future when the Wellington Fault is better constrained the Fault Rupture Zone will be reduced in width.
- The implementation of a ground engineering register, so that technical or peer review of geotechnical investigations, assessments, analysis, and design inputs are carried out by pre-approved companies with geotechnical professionals who are recognised by Hutt City Council to be qualified to review geotechnical works.
- Above and beyond the ground engineering register, a register of Chartered Professional Engineers (CPEng) or Professional Engineering Geologists who are recognised by their peers as experts in the geotechnical / engineering geology field should be established, as a register of "Geotechnical Gurus", who can review the most complex or geotechnically

challenging of situations / designs – such as large heavy buildings or structures and multistorey buildings.

- All new buildings and structures should have a completed geotechnical and hazard desk study that consider natural hazards on a more global sense (i.e. greater than Lot specific) and site specific geotechnical intrusive investigation. Such investigations may be intrusive investigations to a minimum of 10m, and should be carried out for all small lightweight (residential) timber structures with a minimum or 2 tests per structure (i.e. per 200m^2 area) to allow for appropriate assessment of the ground conditions for the site specific foundation design process.
- That Section 14H Natural Hazards of the District Plan be revised to reflect the current level of knowledge natural hazards that have the potential to affect Hutt City, and with regards to Chapter 14H – Natural Hazards, of the District Plan, the part sentence "or that necessary engineering precautions have been taken" be removed from clause 14H 2.1.1 (i). This part of the clause creates a loophole or that the "necessary engineering precautions" are better defined.

2.7 Independent Commissioners' Hearing

For the independent commissioner's hearing, the (HCC) Officer's Report was prepared, discussing the submissions and technical reviews, along with issues with the existing plan provisions, evaluation of issues raised, and recommendations in light of those items. The officer's report contained a number of recommended amendments to the Proposed Plan Change 29. Of these were many relating to natural hazards, and how better to incorporated them in to the proposed plan change where possible. A point to note is that Council Officers can only respond to matters raised in submissions and not on matters that the public didn't raise (via the official process) comments on.

As part of the hearing submitters who wished to be heard were invited to talk about their submissions including the more technical submissions from GNS and GWRC. GHD provided professional geotechnical support for HCC. The commissioners requested clarity on issues or further information on technical matters, and sought to understand the hazards that could affect Petone West, and the consequences of those hazards.

The recommendations of the independent commissioners were not published at the time of writing this paper.

3 THE PUBLIC'S UNDERSTANDING

In the last few years extended media coverage, and natural hazard events within New Zealand, particularly the Canterbury earthquake, have exposed the general public to natural hazards. Not just the number and type but also "scientific" explanations of the hazards and the consequences of them. If a survey was taken of the number of people in New Zealand who knew the term "liquefaction" prior to the Canterbury earthquakes of 2010 and 2011, we would imagine the term to be known to relatively few outside our profession and those who had experienced it. Take a survey today or anytime in the last 2 years, and it is probable that the number of people who have not only heard the term but also have some level of understanding of it has increased exponentially. However, of course, with this increased awareness and "knowledge" there is the likely potential for misunderstandings and "a little information is sometimes too much".

It seems that the heightened awareness of natural hazards has contributed to the high number of public submissions for this plan change (along with people's passion for the historical area of Petone West).

4 POLITICS

Prior to the notification of plan changes at HCC, a draft copy of the plan change provisions needs to be endorsed at a number of meetings; District Plan Sub-committee and full Council Meeting, and hence this involves obtaining a level of support from the Elected Councillors. A number of the public submissions indicate that the submitters do not believe the Council to have given the natural hazards (and natural hazards review) appropriate weighting and importance in notified Proposed Plan Change 29 (the authors share this view). There are always parties who put a high value on providing short to medium term economic growth and development, rather than long term economic and social costs and benefits, a view that does not create resilient communities.

The role of politics and politicians on plan changes is probably a hazy one, and one which the authors do not have extensive experience. However, it has been known throughout time that some politicians (even local government) have greater vested interests in some issues and others wise to leave their mark prior to their exit from the "arena". Has the role of those politicians driving the plan change been able to influence the process?

However, since the hearing had been proposed, and independent commissioners charged with reviewing the technical information provided for the proposed plan change, and the public submissions, there appears to be an increased acknowledgement of the technical data (as presented in the HCC Officer's report). Are politics and politicians having a negative (or positive) influence on planner's ability to incorporate technical data and understandings in to planning policy and documents? Or, more specifically to implement the recommendations of technical expertise.

5 NATURAL HAZARDS PLANNING TOOLS

There are a variety of tools available for planners or engineering geologists and geotechnical engineers etc. to help assist with understanding, planning, and policy making including but not limited to the following:

- Planning for the development of land on or close to active faults, Ministry for the Environment (2003);
- Guidelines for assessing planning policy and consent requirements for landslide prone land, GNS Science (2008);
- New Zealand's Next Top Model: Integrating tsunami inundation modelling into land use planning;
- Putting R(isk) in the RMA: Technical Advisory Group recommendations on the Resource Management Act 1991 and implications for natural hazards planning, GNS Science (2012); and,
- RiskScape – a joint venture between GNS and NIWA.

Of course the implementation of the Resource Management Act (1991) has sections that regard the effects of climate change, and the development or protection of land for the purpose of the avoidance or mitigation of natural hazards. Portions of the RMA state that any proposed district plans must give effect to the regional policy statement or regional plan. In this case is the Wellington Regional Policy Statement (WRPS). The WRPS was in a proposed status at the time of notification of Proposed Plan Change 29.

Part of the natural hazards planning tools must be the greater understanding of the hazards themselves, along with the opportunity and necessity of our professions to train and learn from the research and experience of others.

6 ABILITY TO IMPLEMENT

Within New Zealand no one agency is responsible for natural hazard management (Saunders and Beban, 2012). Within national and local legislation / documents some policies have sections/clauses that account for natural hazards, although some of them lack definitiveness about them, but have highlighted the "cause".

The Wellington Regional Policy Statement operative from 24 April 2013 contains policies (Policy 29) that state that the regional and district plans shall:

- Identify areas at high risk from natural hazards; and,
- Include policies and rules to avoid inappropriate subdivision and development in those areas.

Along with policies (Policy 51) that aim to minimise the risk and consequences of natural hazards.

New Zealand Geotechnical Society Inc. 19th Symposium, Queenstown 2013

What has come to light for the authors, is that plan changes to existing District Plans are limited in the scope of matters that can be considered as part of a plan change. For example a large number of the natural hazards that affect Petone West also affect a large portion of the Hutt Valley (and beyond) and as such were not able to be considered in the Proposed Plan Change. Therefor a number of the recommendations by GHD and others fit within a document serving the wider Hutt City. Such as Chapter 14H - Natural Hazards of the HCC District Plan. This Chapter, as part of the district plan over arches proposed plan changes such as that for Petone West, and a reference can simply be made to Chapter 14H in the proposed plan change, unless there are specific hazards to that plan change area then they can be detailed within the proposed plan change. The risk is run that if certain policies/clauses are included within proposed plan changes with regards to natural hazards, then the neighbouring area just outside the proposed plan change area has a much lower standard of policy that may mean more people and infrastructure are in harm's way should an event occur. One would imagine that for those conscious of the differences and of natural hazards the differing levels of policy will have effects on those areas. Those who are conscientious may prefer the high level policy whilst those who may be less conscientious may seek to take advantage of the lower level of policy, possibly to the detriment of the building's or structure's users at a later date.

As HCC seeks to be consistent in its approach to natural hazards, and stay abreast of requirements and developments within natural hazards. HCC is committed to undertaking a full review of the District Plan, and Chapter 14H Natural Hazards of the District plan is expected to be reviewed in the next Council triennium. Hopefully this review will incorporate recommendations and allow additional policy to arch over Petone West and Hutt City. However, it should be noted that some of the recommendations go beyond the remit of the District Plan, such as procedural changes to the processing of building and resource consenting applications.

7 CONCLUSIONS

The HCC Proposed Plan Change 29 prompted a deeper understanding of the planning process for the authors and highlighted gaps in the understanding of planning processes and documentation by geotechnical professionals; along with the gap between planners and

geotechnical professionals regarding natural hazards; and the difficulties in the ability to implement planning for natural hazard events.

GHD's review of the natural hazards that do and can impact upon such a small area of Hutt City has highlighted and cemented the risks that our population and infrastructure face and the challenge of councils and planning officers to stay abreast of the issues in their towns/cities/regions.

The next Council triennium is committed to reviewing the full District Plan. This review will hopefully incorporate the technical recommendations and allow additional policy to arch over Petone West and Hutt City. HCC is being proactive and is seeking to stay informed and up to date about natural hazards that can and do affect there city, but this is not seen across the board of our councils.

A large portion of the planning legislation is influenced by past events (i.e. new flooding policies being introduced after significant flood events). Recent large earthquake events have provided a focus and opportunity to improve on local and central government conditions around natural hazard planning. This opportunity need to be capitalised on as an industry if we are to avoid several of the inadequacies exposed during recent events. It seems without effective land use planning it will be very difficult to create communities that are hazard resilient.

Perhaps we need more "translators" between the planners, policy makers and the geology / engineering world to get better recognition of geotechnical considerations in planning documents.

ACKNOWLEDGMENTS

Thanks to Bronwyn Little (HCC), and Allison Tindale (HCC), for imparting increased planning knowledge into the corresponding author. HCC as an organisation for approving the publication of the paper and having the planning foresight both pre and post the recent earthquakes around the consideration of natural hazards.

REFERENCES & BIBLIOGRAPHY

Curley, B.A., Beetham, R.D., & Simms, B. (2012) Report for Petone West District Plan Change – Natural Hazards Review & Geotechnical Considerations. February 2012. GHD Limited, Wellington.

Curley, B.A., Beetham, R.D., & Simms, B. (2013) *Proposed Plan Change 29: Petone Mixed Use Area – Technical Review.* 27 February 2013. GHD Limited, Wellington.

Hutt City Council (2012) *Proposed District Plan Change 29: Proposed Zoning Change to the Western End of Petone (Petone Mixed Use).* (Publically notified 26 June 2012) Hutt City Council.

Saunders, W.S.A., & Bedan, J.S. (2012) *Putting R(isk) in the RMA: Technical Advisory Group recommendations on the Resource Management Act 1991 and implications for natural hazards planning, GNS Science Miscellaneous Series 48 (August 2012).*

Tindale, A., Wesney, H., & Baily, M. (2013) *Officers Report for Independent Hearings Commissioners, for the Proposed District Plan Change29: Proposed Zoning Change to the Western End of Petone (Petone Mixed Use).* Hutt City Council.

Whiteley, R.J, Kelly, R.B & Stewart, S.B (2013)
Geophysical testing of soft soils and embankments for road construction and risk assessment
Proc. 19th NZGS Geotechnical Symposium. Ed. CY Chin, Queenstown

Geophysical testing of soft soils and embankments for road construction and risk assessment

R J Whiteley
Coffey Geotechnics, Sydney, Australia
bob.whiteley@coffey.com (Corresponding author)

R B Kelly
Coffey Geotechnics, Sydney, Australia
richard.kelly@coffey.com

S B Stewart
Coffey Geotechnics, Sydney, Australia
simon.stewart@coffey.com

ABSTRACT

Roads constructed on soft soils risk ongoing maintenance due to excessive ground settlement that causes poor road conditions and pavement damage. Risk assessment of potentially unstable embankments using conventional geotechnical practice is often difficult and costly. In both situations geophysical testing with appropriate combinations of seismic, electrical resistivity and electromagnetic geophysical technologies can provide detailed information on the extent of soft soils and weakened ground together with bulk in situ properties that provide initial geotechnical parameters such as G_0, void ratio and pre-consolidation pressure. Case studies from roads projects in eastern Australia demonstrate the application of these geophysical technologies. Surface wave seismic and electrical resistivity imaging are used to characterise soft estuarine clays along a section of a proposed coastal road link between Sydney and Brisbane. Ground Penetrating Radar (GPR) and a modified version of land seismic refraction provided enhanced subsurface information over potentially unstable embankments covering buried drains and culverts as part of a stability risk assessment process.

Overall, combined geophysical and geotechnical testing is a cost-effective enhancement for site characterisation in soft soils and risk assessment of potentially unstable embankments. This approach overcomes many of the limitations of conventional methods of site investigation that provide point location data only. The incorporation of geophysics in a well-crafted site investigation also allows concentration of fewer but higher quality soil probings and boreholes.

New Zealand Geotechnical Society Inc. 19th Symposium, Queenstown 2013

1 INTRODUCTION

Rapid population growth along the coast of eastern Australia is increasing demand for new and upgraded transport infrastructure within floodplain areas that are underlain by considerable thicknesses of recent soft alluvial and marine clay sediments. These deposits are often highly variable over short distances with very low bearing capacities and excessive settlement characteristics. If characterisation of these deposits is inadequate these factors can increase road construction risks and costs and affect long-term road stability and serviceability. Case studies of a major coastal highway upgrade demonstrate how combining seismic and electrical geophysical testing with conventional geotechnical testing enhances characterisation of these very soft soils. A further issue related to increased road use in both floodplain and hinterland areas is embankment instability. This can manifest during road construction or, for existing embankments, as a result of aging of buried culverts and drains, adverse weather events or

seismic activity. Assessing causes of instability of existing embankments and risks with conventional geotechnical methods is often difficult and costly due to access and safety problems. In these situations the combination of electrical, ground penetrating radar and seismic technologies can rapidly provide information on the conditions below both the roadway and embankment. A case study shows the application of these technologies on an unstable embankment in Australia.

2 CASE STUDIES

2.1 Road Upgrades

Upgrades to the Pacific Highway, in northern New South Wales required a new crossing of the Richmond River valley that is infilled with thick deposits of very soft estuarine clay and a complex history containing distinct Pleistocene and Holocene elements. The Holocene sediments typically overlie Pleistocene estuarine and lacustrine sediments (mottled clays and muds) and basal fluvial gravels. Extensive geotechnical investigations were undertaken along this section (Kelly and Whiteley, 2013). These incorporated borehole drilling and piezocone penetrometer testing (CPTu) with adjacent downhole shear vane testing. Typically, 100MPa capacity piezocones were specified for stratigraphic profiling, but as cone resistance in the soft to very soft soils could not be measured to sufficient accuracy, these were unable to provide engineering parameters for detailed design. The field vane test also provided data of insufficient quality for this purpose. Consequently, an alternative approach was adopted to assess stratigraphic changes along the section. This involved further borehole drilling and U75 sampling together with Multi-channel Analysis of Surface Waves (MASW) geophysics. A seismic dilatometer (SMDT), a 10 MPa capacity piezocone, a 75 mm wide by 150 mm long downhole vane shear and a 160 mm wide by 40 mm thick T-bar were also used for this investigation.

New Zealand Geotechnical Society Inc. 19th Symposium, Queenstown 2013

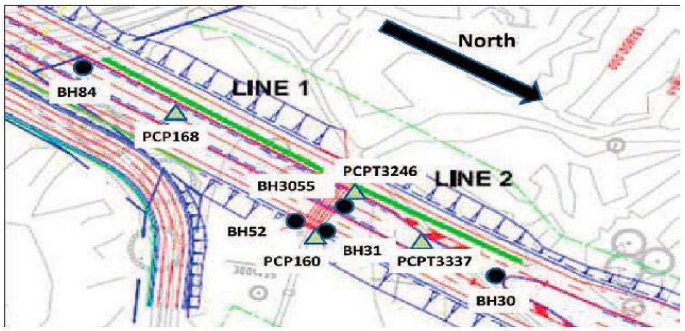


Figure 1: Site Plan, MASW lines (1&2) and geotechnical test locations

(Figure 1) shows the site plan from one location with the MASW lines (Line 1 and 2, green lines in Figure 1), boreholes and in situ test sites. The CPTu, Tbar, shear vane and SDMT were performed at PCPT3246 near the start of Line 2 in Figure 1. The MASW lines were either side of a creek culvert between BH52 and BH31 and the northern end of Line 2 approached a weathered rock ridge.

The S-wave velocity sections (V_s) from the MASW testing are shown in Figures 2 and 3. These show velocities ranging from 40 m/s to 300 m/s with the highest velocities occurring at depth on Line 2 where relatively steep velocity gradients suggest the presence of weathered rock. This interpretation is supported by offset BH 52 that was drilled between the MASW lines (Figure 1) and encountered weathered rock at about 10 m depth. Also S-wave velocities increase rapidly on the eastern side of Line 2 as the rock ridge is approached and the interpreted soil-rock interface is relatively steep in this region. The lowest velocities occur in a relatively thin layer near the road surface. Excavation during subsequent construction showed that the region

delineated by the 40 m/s S-wave velocities had high organic content. On both MASW lines beneath this low velocity region velocities increase relatively slowly with depth to about 70 m/s and then more rapidly below this depth where rock is expected. Piezocone PCP168 (Figure 1) showed a rapid increase in tip resistance at about 10 m depth where S-wave velocities are about 75 m/s. This indicates that the base of the very soft soils is indicated by velocities near this level. On Line 1 the known paleochannel appears to extend to about 11 m depth from about Ch. 25 to 40 m. On Line 2 a further paleochannel extending to about 8 m depth is indicated.

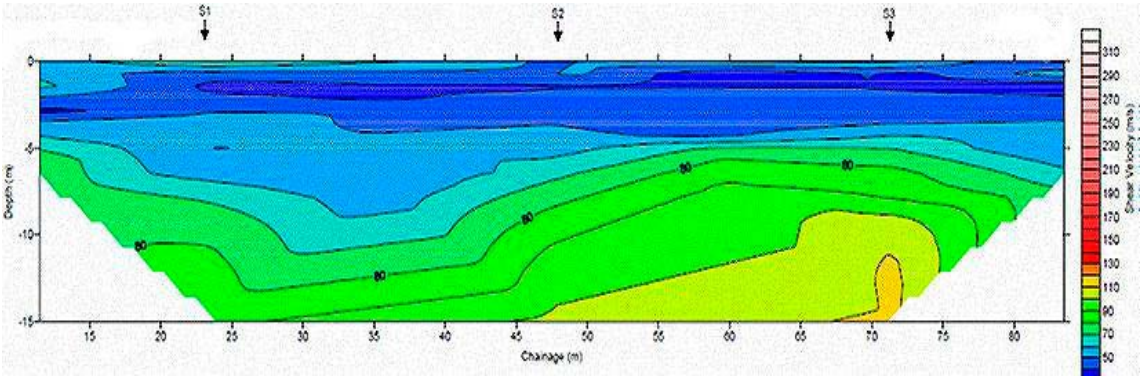


Figure 2: S-wave velocity section Line 1

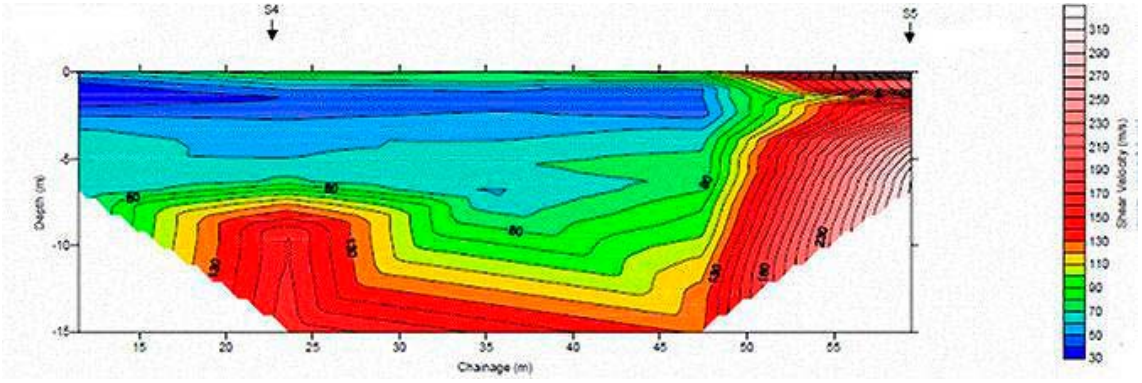


Figure 3: S-wave velocity section Line 2

MASW and SDMT S-wave velocities are compared in (Figure 4). MASW S3 lies closest to the SDMT test location. The velocities compare well to the base of soft clay at about 9 m depth. The velocities from MASW are lower than the SDMT velocities below about 9 m depth that is near the limit of the depth of investigation of the MASW set up that was used. Empirical factors for assessment of undrained shear strength and yield pressure for T-bar and CPTu tests appear to lie at the extremes of published values. In contrast, correlations between VST and DMT lie within published ranges (Kelly & Whiteley, 2013). It is suggested that these soils are sensitive to the applied shear strain rate.

S-wave velocity (Vs) obtained with MASW or other methods may also be used to provide first-order estimates of useful geotechnical parameters (Mayne, 2005) for road design and construction, for example, initial void ratio and pre-consolidation pressure. Initial void ratios estimated from the averaged MASW results over the paleochannel using Mayne (2005) are compared in (Figure 5) with values back-calculated from laboratory moisture content tests and using a specific gravity of 2.6. There is very good agreement between the two data sets. From this data the unit weight of the soil can be estimated along with the in-situ effective stress.

Pre-consolidation pressures estimated from the MASW results are compared with data from laboratory and other forms of in-situ testing in Figure 6. The values from the MASW data lie below those from other forms of in-situ testing and are comparable with the laboratory test data.

The MASW values probably underestimate the pre-consolidation pressure of the soil in this instance but provide a credible first-order estimate. The over-consolidation ratio and undrained shear strength of the soil can be estimated from the pre-consolidation pressure and in-situ effective stress using conventional critical state soil mechanics relationships.

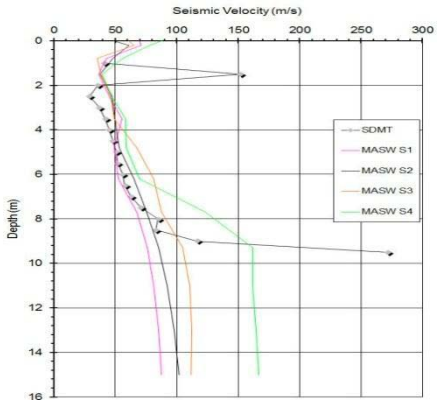


Figure 4: Comparison of MASW and SDMT S-wave velocities

New Zealand Geotechnical Society Inc. 19th Symposium, Queenstown 2013

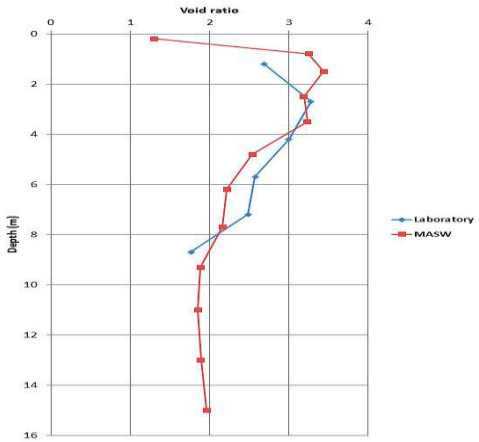


Figure 5: Comparison of void ratios computed from Lab. and MASW results

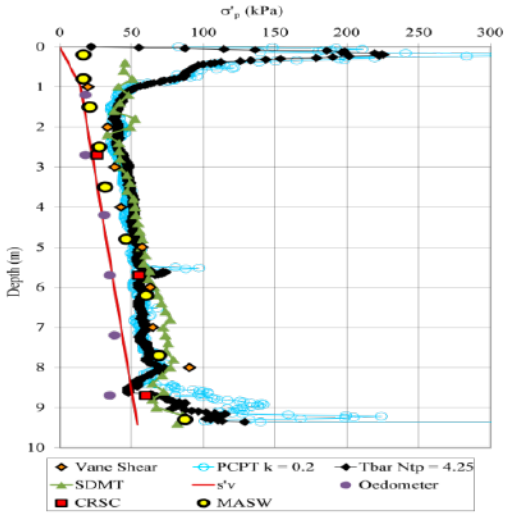


Figure 6: Comparison of pre-consolidation pressures estimated from MASW Line 3 with data from laboratory and other forms of in-situ testing

A further section of this highway upgrade required construction of a major interchange in similar conditions. In this area a single borehole encountered about 20m generally soft estuarine soils (N =1 to 5) infilling a Pleistocene palaeochannel and incising a weathered sandstone bedrock. Electrical Resistivity Imaging (ERI) was used to rapidly assess the extent of the

palaeochannel and to assist with siting CPT. Typically, soils have a much lower resistivity than rocks and geotechnical properties such as saturation, void ratio and hydraulic conductivity can be estimated from resistivity (Bryson, 2005). In saltwater conditions soil resistivities are mainly controlled by the groundwater resistivity and Archie's (1942) law can be used to predict the soil resistivity (ρ_s) from the saline groundwater resistivity (ρ_w) and porosity (Φ or void ratio $e = \Phi/(1-\Phi)$, Kim et al. 2011) i.e.

$$\rho_s = \alpha\, \rho_w \Phi^{-m} \qquad (2)\ \alpha \text{ and } m \text{ are empirical constants.}$$

(Figure 7) shows one of the interpreted ERI sections near the proposed interchange and the targeted CPT. This section essentially shows three geoelectric layers from the ground surface: an upper thin resistive layer corresponds to the dry and partially saturated clayey soils above a thick very low resistivity layer of very soft saturated Holocene clays and silts within the palaeochannel then a resistive layer corresponding to the weathered sandstone bedrock. The rapid increase in resistivity at the base of the palaeochannel can be clearly seen in Figure 7. This interface was interpreted at the 2.5 ohm m resistivity contour. These results agree well with the subsequent CPT results at CPT 2, 4 and 6 that show both low tip resistance (Qc) and Sleeve Friction (Fs) within the low resistivity silts/clays and higher values to refusal generally close to or just below the 2.5 ohm m resistivity contour near -20 m RL. The situation is somewhat more complicated in the region of CPT 3. The ERI section in this region shows higher and more variable resistivities in the low resistivity layer indicating the presence of resistive sand/gravel layers within the Holocene silts and clays. The 2.5 ohm m resistivity contour is probably mapping the top of gravel lenses in this region. The presence sand/gravel layers are also indicated from the higher and more variable Qc and Fs values observed within the Holocene sediments in CPT 3. Eqn. (2) can provide initial estimates void ratios within the very soft soils encountered in most of the CPT. For example, the average ρ_s is ~ 1.2 ohm m from the ERI section and the saline pore water resistivity, ρ_w is ~ 0.3 ohm m from independent information. α is ~ 1 is for normally consolidated clays and unconsolidated soils and m is ~ 3 for very soft clays (Campanella and Weemees 1990). With these values $\Phi = 0.63$ and $e = 1.7$. These values are within 15% of those estimated from direct test results.

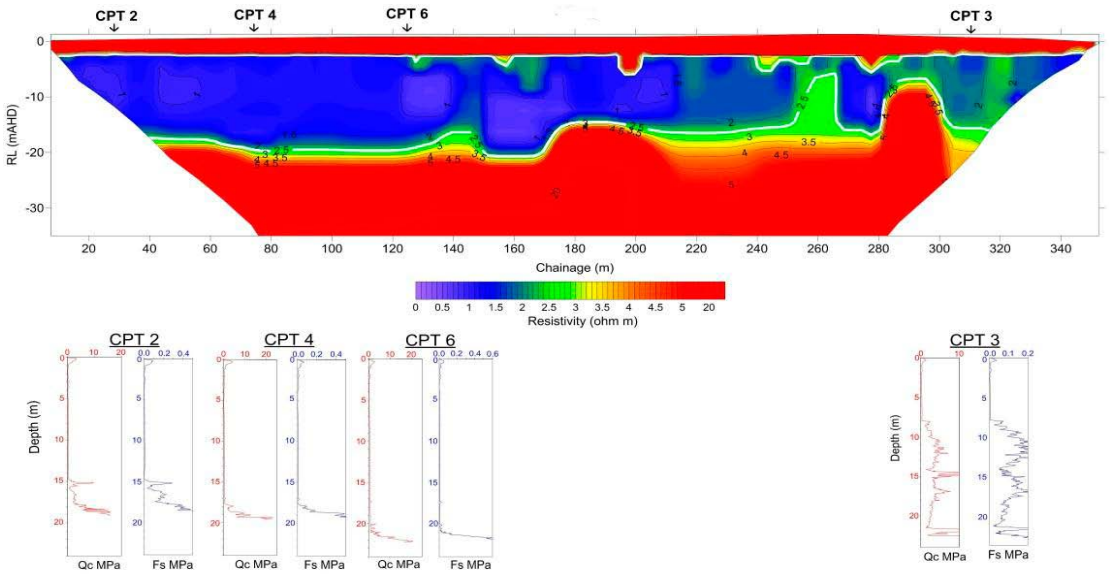


Figure 7: Comparison of ERI section near the proposed interchange with CPT results

2.2 Embankment Assessments

In the NSW road network it is estimated that some 77,000 road embankments, many within coastal and hinterland areas, are crossed by buried culverts and drains. Sadly, when these fail,

unexpected loss of life can result (Shackell & Retsos, 2012). Inspection and geotechnical testing of these embankments for the many roads that have been in service for years is often difficult and costly as they are frequently bounded by relatively steep-sided and overgrown embankments. Fortunately, and with minimal traffic disturbance, these embankments and the condition of the pavement layers beneath the road can be rapidly assessed non-destructively using a modified P-wave land seismic refraction (LSR) method deployed across the roadway and on both sides of the embankment together with Ground Penetrating Radar (GPR) testing on the road surface. The GPR system typically only provides information on the pavement layers to about 3-5 m depth while the LSR method provides information to the full depth of the embankment. Road closures for a short duration, typically a one day-night operation, are required for deployment both technologies and it is normal to complete the GPR first as this may identify features in the fill or pavement layers indicative of potential problems. The LSR system uses geophone deployed at close intervals using rock plates on the road and base-spikes on the embankments for seismic coupling.

Figure 8 shows an example of the P-wave seismic image produced across a road embankment containing mainly crushed sandstone fill. This image was obtained above the culvert where pavement cracking was observed and initial GPR testing had indicated disturbances and separation of the pavement layers with some moisture accumulations. Based on previous experience, Table 1 provides a general relationship between P-wave velocity and geotechnical classification in dry or partially saturated granular soils and fills.

Table 1: P-wave seismic velocity and inferred geotechnical conditions for granular soils

P-wave seismic velocity (m/s)	Inferred SPT N-value	Geotechnical classification
< 350	0 to 4	Very loose
350 to 500	4 to 10	Loose
500 to 750	10 to 30	Medium dense to dense
750 to 1700	30 to 50	Dense to very dense
> 1700	>50	Very dense

This seismic image clearly shows the bulk of the material beneath the roadway has P-wave velocities > 600m/s and falls in the medium dense to dense range (Table 1) including the region near and immediately below the culvert. This suggests that culvert is not causing the pavement disturbances. This figure also shows that loose material (< 500m/s) occurs beneath the embankments and shoulders as expected but this may not be a significant concern as the velocities do not enter the very loose range. However, this loose material also extends beneath part of the roadway at shallow depth from Ch. 35 to 30 m and may be of concern from the viewpoint of long-term road stability.

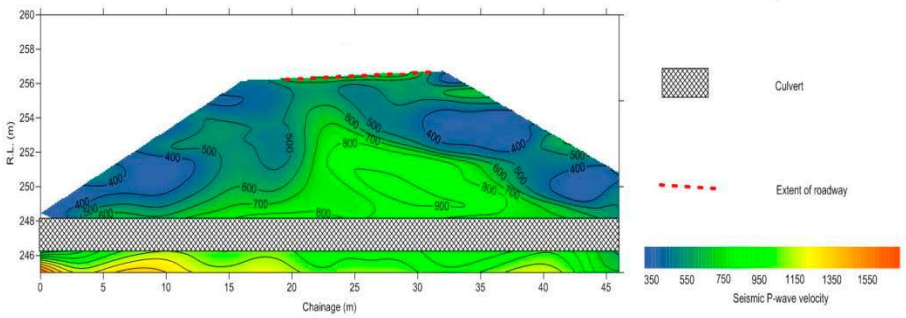


Figure 8: P-wave seismic image produced across the embankment above the culverts

(Figure 9) shows an enlargement of the seismic image (Figure 8) beneath the upper section of roadway with the GPR section to its full depth of investigation. GPR reflections can be observed from the various pavement layers, however, these are not laterally consistent beneath the roadway suggesting disturbance has occurred as also indicated on the seismic image. From Ch. 20 to Ch. 27 m strong dipping, negative GPR reflectors suggest possible separation of the pavement layers with the accumulation of moisture along the interfaces. This is a region where the higher velocity (denser) materials are indicated and the dip direction of the GPR reflectors is similar to that of the velocity contours. From Ch. 29 to Ch. 31 m the GPR reflectors near RL. 255m are depressed and the GPR image is more "transparent" indicating an overall reduction in dielectric constant within these materials. This typically occurs where the materials are drier and more freely draining. As this region is also located where lower P-wave velocities persist to greater depth its identification as a region of concern for follow-up geotechnical investigation is substantiated. The disturbed character of the GPR section beyond Ch. 31m is indicative of the embankment fill and vegetation roots. The results of this geophysical testing suggest that parts of the sub-base and embankment are potentially unstable but that the culvert is not the likely cause of the potential instability and further geotechnical testing of the embankment is warranted.

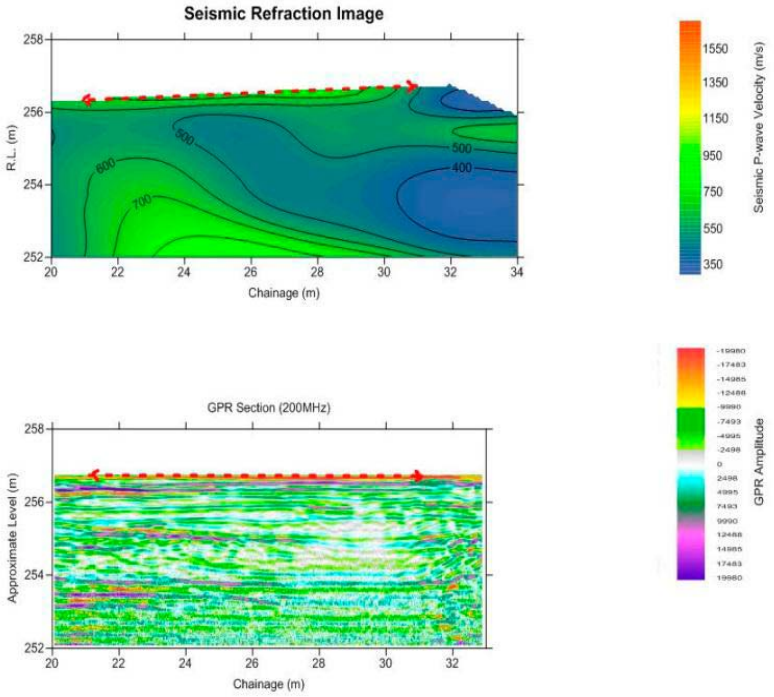


Figure 9: Comparison of the upper section of the P-wave seismic image beneath the roadway with the GPR section to its full depth of investigation

3 CONCLUSIONS

Conventional methods of site investigation provide point location data only whereas geophysics provides 2D and 3D information on stratigraphy. The use of geophysics in a well-crafted site investigation also allows concentration of fewer but higher quality soil probings and boreholes.
The case studies from various roads projects have demonstrated that combining appropriate geophysics with conventional in situ and laboratory geotechnical investigations is an effective means for characterising very soft and soft estuarine clays and for locating material property changes related to palaeodrainage processes in these environments. Geophysics also has a use in forensic engineering to assess potential embankment instability and risk of culvert failure prior to catastrophic events occurring. Using appropriate combinations of seismic, electrical resistivity and electromagnetic geophysical technologies can provide detailed information on the extent of soft soils and weakened ground together with bulk in situ properties that provide initial estimates of geotechnical parameters such as G_0, void ratio and pre-consolidation pressure.

Overall, combined geophysical and geotechnical testing is a cost-effective enhancement for site characterisation in soft soils and risk assessment of potentially unstable embankments.

REFERENCES

Archie, G. E. (1942) The electrical resistance log as an aid in determining some reservoir characteristics, Trans. Am. Inst. Min., Metall. Pet. Eng. 146, 54-62

Bryson, L. S. (2005) Evaluation of geotechnical parameters using electrical resistivity measurements. Earthquake Engineering and Soil Dynamics, Am. Soc. Civil Eng. 1-12.

Campanella, R. G. & Weemees. I. (1990) Development and use of an electrical resistivity cone for groundwater contamination studies. Can. Geotech. Jour., 27, 557-567.

Kelly, R. B. & Whiteley, R. J. (2013) Geotechnical model development for a very soft estuarine clay with MASW geophysics, in-situ and laboratory testing. Geotechnical and Geophysical Site Characterization 4, Coutinho & Mayne (eds), Taylor & Francis, London,1579 – 1584.

Kim. J. H. et al (2011) Void ratio estimation of soft soils using electrical resistivity cone probe. Jour. of Geotechnical & Environmental Engineering, Jan. 2011, 86 – 93.

Mayne, P. W. (2005) Integrated ground behaviour: in-situ and lab. tests. Proc. 3rd. Int. Symp. on Deformation Characteristics of Geomaterials, Lyon, 2003, Di Benedetto et al. (eds.) Taylor and Francis, London, 155 -176.

Shackell, C & Restos, P. (2012) Pile Creek Embankment Collapse – the investigations, the expert findings and subsequent improvements in asset management of culvert structures on major roads in NSW. Proc. 2012 Aust. Geomech. Symposium: Advances in Geotechnics of Roads and Railways, Wed. 12 Oct, 2012, 89-96.

Bearing capacity of foundation on slope

A Balachandra
Sinclair Knight Mertz Pty Ltd., Auckland, NZ (formerly University of Auckland)
abalachandra@globalskm.com

Z Yang
Structex Ltd, Christchurch, NZ (formerly University of Auckland)
JYang@structex.co.nz

R P Orense
Department of Civil Engineering, University of Auckland, NZ
r.orense@auckland.ac.nz (Corresponding author)

Keywords: bearing capacity, slope, discrete layout optimization

ABSTRACT

The problem of a footing on slope is encountered regularly in engineering practice, with some noteworthy examples being bridge abutments and basement excavations. This paper discusses the use of Discontinuity Layout Optimisation (DLO) technique in analysing the behaviour of shallow, strip footings near sloping ground problem through the LimitState:GEO software. Modification factors for N_γ, N_q and N_c were proposed for a number of different combinations of variables, such as slope angle, edge distance, embedment depth, friction angle, slope length and cohesion. The results were then summarised in the form of design charts. Furthermore, the bearing capacity of embedded footings was also investigated and modification factors in terms of total bearing capacity were also recommended. It was found that sloping ground had significant effect on the bearing capacity, with the greatest reduction observed when footings were located at the edge of the slope. The validity of the results was confirmed by performing a thorough comparison with results using limit equilibrium method, upper bound solutions and FEM-based techniques. The design charts developed may be of significant interest to the profession, considering Auckland's topography, with many houses built along sloping grounds.

1 INTRODUCTION

The natural topography of much of New Zealand can be described as either hilly or rolling terrain. Therefore, often in engineering projects, such those involving bridge abutments, building foundations and road pavements, foundations requiring to be constructed near sloping ground are encountered. The bearing capacity on sloping grounds has often been assessed using limit equilibrium method (Castelli and Motta, 2010; Hansen, 1970; Saran et al., 1989), upper bound method (Kumar and Rao, 2003) and finite element analysis (Loukidis and Salgado, 2009; Georgiadis, 2010). Of these methods, the Limit Equilibrium method (LEM) has been commonly used due to its simplicity; however, it is limited by the need to assume a failure mechanism.

In this paper, the computer program LimitState:GEO, which is based on discontinuity layout optimisation, is used to model and analyse the problem of a footing located near sloping ground. Based on the results of analysis, the effects of different factors that contribute to the bearing capacity are analysed. The results of the analyses are compared to those available in the literature. Finally, the results obtained are presented in the form of design charts, which could be used in engineering practice for foundation design.

2 DISCONTINUITY LAYOUT OPTIMISATION

LimitState:GEO, a computer program developed at Sheffield University, was used in this study. It uses the discontinuity layout optimisation (DLO) method for analysis and can be used to analyse a number of other geotechnical problems including slope failure, retaining walls, pipelines, tunnels and anchors (LimitState, 2010). The DLO procedure refers to an optimisation technique which is able to determine the critical layout of discontinuities, thereby producing the critical failure mechanism and the lowest collapse load. This is done by considering all connections between a node and all other nodes in the soil model. Therefore, far more connections are considered using the DLO method as opposed to say the finite element analysis. The connections themselves refer to the boundaries between the rigid blocks. Therefore, by performing a systematic search through all the connections available, a critical slip line could be determined (LimitState, 2009).

The LimitState:GEO software uses the above DLO theory but modified slightly to reduce both memory usage and time required to perform the computations. The modification considers only connection between a node and neighbouring nodes, and performing a search through the available connections to find an upper bound solution. Using this upper bound solution an input, a search through all the discontinuities connecting each node with every other node is performed. In the process, the previously obtained solution is optimised, eliminating non-critical discontinuities until the correct solution is found (LimitState, 2009). An arrangement of nodal connections considered by LimitState:GEO is shown in Figure 1.

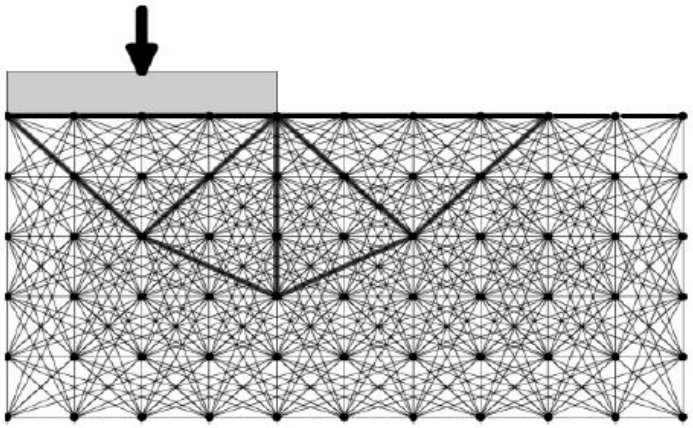


Figure 1. Example of nodal connections (LimitState, 2009).

3 METHODOLOGY

3.1 Soil model

The bearing capacity of footings is a function of the slope angle (β), distance between the footing and slope (d), embedment depth (D_f) and slope length (L). These are illustrated in Figure 2. The soil parameters include the friction angle (φ) and cohesion (c), as well as the unit weight of the soil (γ). For the parametric analysis, all the length parameters were normalised by the width of the footing, B. It was verified that that such normalisation did not have an effect on the bearing capacity as long as the nodal density was kept constant. The range of parameters considered in the study is presented in Table 1. The vertical and horizontal boundaries were specified a sufficient distance away from the footing so that they had no impact on the results. In this study, footings were analysed with a scale factor of 3 (i.e. 3 nodes for every 0.5m distance). This was determined considering both computational time and accuracy of the solution (less than 1% change in value).

Table 1: Range of parameters considered

Parameters	Range of values
φ	25, 30, 35 and 40^0
c	10, 50, 100 and 150 kPa
β	$0 - 40^0$ *
d/B	0 – 8 *
D_f/B	0, 0.5 and 1.0
L/B	2, 4, 5 and 7

Note:* - or until the threshold value is reached.

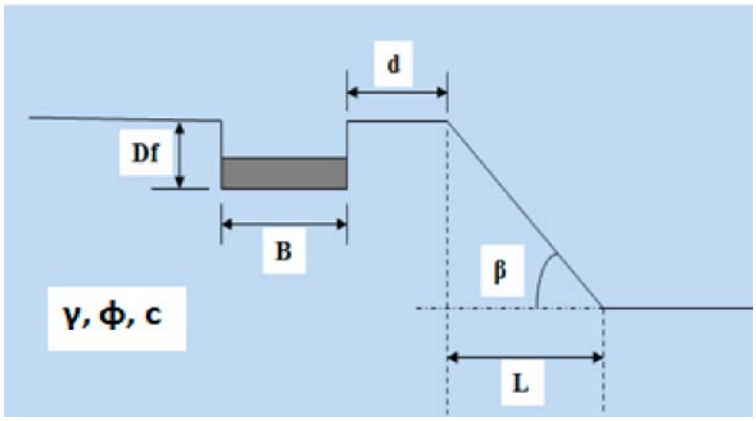


Figure 2. Soil Parameters investigated

3.2 Determination of modification factor for N_γ

The output from the software LimitState:GEO was in the form of an adequacy factor. This can be multiplied by the applied load to determine the failure load. Therefore, knowing the area on which the ultimate load was applied, the bearing capacity of the soil at failure can be determined. However, as the adequacy factor does not differentiate the ultimate bearing capacity into three components as proposed by Terzaghi (1943), a purely cohesionless soil with no surcharge was considered so that the entire ultimate bearing capacity was solely due to the self-weight of the soil.

Based on the parametric analysis, the modification factors were determined by computing the ratio between the reduced bearing capacity due to the presence of the sloping ground and the bearing capacity for level ground. Thus, the modification factor applies to N_γ, where it modifies the N_γ factor to take into account the effect of the sloping ground.

3.3 Determination of modification factor for N_q

As the software was unable to analyse bearing capacity problems involving weightless soils, a cohesionless soil with a known surcharge was used to determine the modification factors for N_q. Following the same process as above, the total bearing capacity and the bearing capacity due to the self-weight of the soil were determined. Though simple subtraction it was possible to find the bearing capacity due to the surcharge component. As before, the modification factors for N_q were calculated as the ratio of the bearing capacity for sloping ground and that of level ground. Note that in the software, only normal or shear loads are permitted to be applied and therefore, the surcharge load was applied normal to the slope surface. Likewise, a constant surcharge was applied on the surface boundary for the entire soil profile.

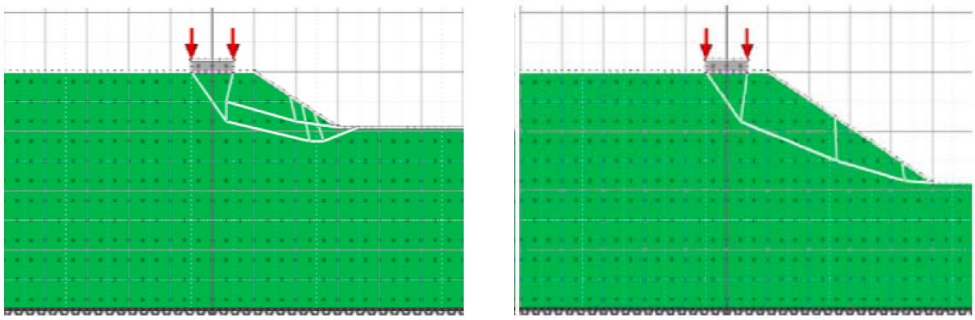
3.4 Determination of modification factor for N_c

Similar procedure as outline above was followed with the only difference being a purely cohesive soil under short-term conditions was considered. Again no surcharge was applied and as only short term undrained conditions were investigated, the friction angle of the soil was equal to zero. The modification factors for N_c was determined by calculating the ratio of bearing capacity of soil when sloping ground is present over the level ground bearing capacity.

3.5 Effect of slope length

For any slope angle there is a direct relationship between the slope height and slope length. Therefore, as opposed to slope height, the slope length was the parameter investigated. The effect on bearing capacity of different slope lengths was due to significant differences in the failure mechanism. Figure 3 shows the failure mechanism observed for slope lengths, L/B of 2 and 4, where for the former, the failure mechanism does not end at the toe of the slope but instead ending some distance to the right of the toe.

New Zealand Geotechnical Society Inc. 19th Symposium, Queenstown 2013



(a) (b)

Figure 3. Failure mechanism for (a) $L/B = 2$; and (b) $L/B = 4$.

3.6 Effect due to embedment

The footings were modelled as simple footing with a uniform load applied to the top face. This was done so that it was valid for comparison with footings located above ground. However, in practice, embedded footings will be generally loaded with a column and therefore checks were performed to determine if the solutions obtained from the simple model were similar to the solutions obtained from the column model. It was found that the difference in the results obtained was very small; therefore, the simple model was deemed to be suitable.

The effect of embedment depth on N_γ and N_q was difficult to determine as the final output was in terms of total bearing capacity. In this study, the modification factors for embedded footings were given in terms of factors that modify the total bearing capacity as opposed to modifying the individual bearing capacity factors. The factors were calculated as a ratio of the total bearing capacity for an embedded footing near a sloping ground over the bearing capacity of an embedded footing on level ground.

4 RESULTS AND DISCUSSION

In the preliminary analysis, the N_γ values obtained in the present study were compared with well-established solutions in the literature to gauge the validity of the model. Figure 4 shows the results where it is seen that the present solutions are in general agreement with those in the literature.

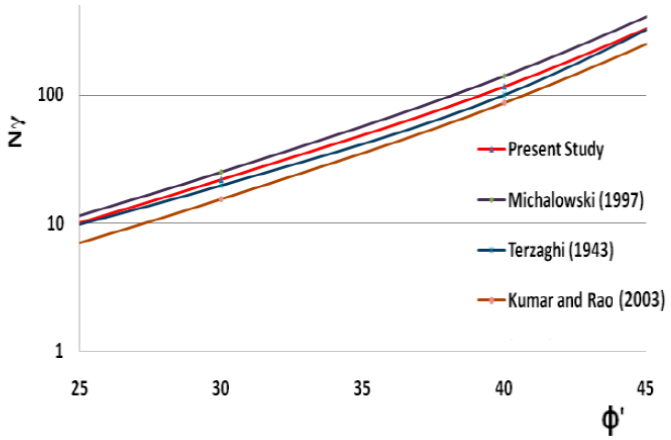


Figure 4. Comparison of N_γ for level ground with existing solutions.

Modification factors for N_γ for friction angles of 30 and 35 degrees are presented in Figures 5. As explained earlier, the modification factors are the multipliers applied to level ground values due to the presence of the slope. It can be observed that both figures show very similar trend. For cohesionless soils, the threshold slope angle was found to be the same as the friction angle, with even a slight increase above the limit resulting in an unstable slope. This is indicative of a change in mode of failure, from bearing capacity to slope failure. Moreover, for high slope angles and when the footing was located at the very edge of the slope, a dramatic reduction in bearing capacity occurred. At high slope angles, the modification factor followed more or less a linear behaviour. Furthermore, the threshold distance at which sloping ground had no effect on the bearing capacity also increased with increasing sloping angle.

In addition, the effect due to different slope lengths was pronounced for large slope angles and small d/B values. However, it could be seen that the effect due to slope length decreases as d/B value is increased. Likewise, the effect of slope length or the difference in bearing capacity observed for $L/B = 2$ and $L/B \geq 5$ was greater when higher friction angles were considered.

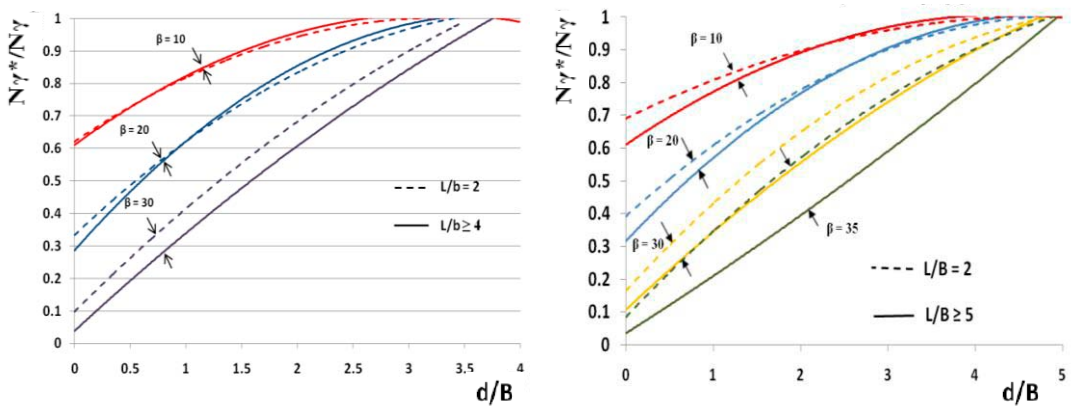


Figure 5. Modification factor for N_γ for D_f/B=0 and: (a) φ = 30°; and (b) φ = 35°.

The calculated modification factors for N_q are shown in Figure 6 for φ = 30° and 35°. At higher friction angles and slope lengths, there was approximately a linear relationship between N_q^*/N_q and d/B, with a very slight decrease in gradient at lower d/B values. However, the decrease in gradient, when moving from higher d/B values to zero, was much more pronounced for shorter slope length and lower friction angles. Like N_γ modification factors, there was a significant loss

in bearing strength for footings located near the slope. However, unlike N_γ, recovery of much of the bearing strength does not occur until about three d/B units away from the slope.

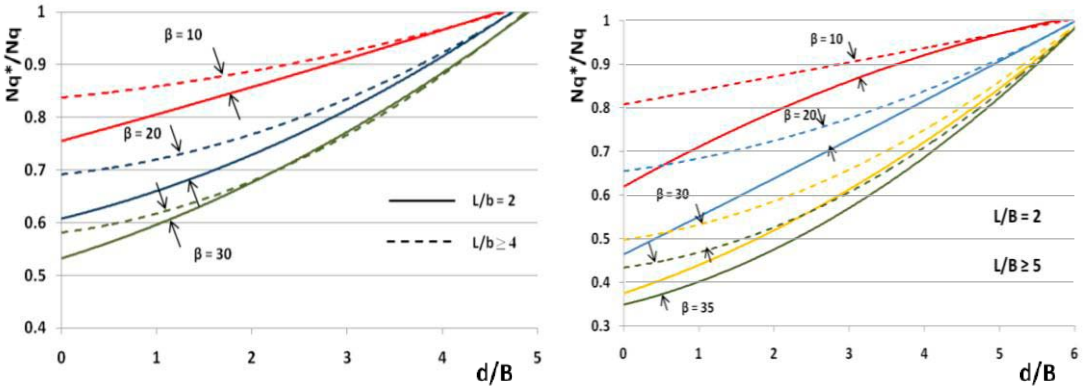


Figure 6. Modification factor for N_q for D_f/B=0 and: (a) φ = 30°; and (b) φ = 35°.

In determining the modification factors for N_c, only the short term bearing capacity behaviour of cohesive soil and undrained conditions were assumed (friction angle was assumed as zero). Modification factors for representative undrained shear strength are presented in Figure 7 for L/B=4. The sloping ground did not have the same drastic effect in reducing the N_c component as it had in reducing the N_γ and N_q terms, even for footings located very near the sloping ground. Much of the cohesive component of the bearing capacity was recovered when the slope was a few d/B units away from the footing. In addition, threshold distances for cohesive soils were far smaller than that observed for cohesionless soils. Therefore, it could be concluded that for soils that are predominantly clayey, a sloping ground will have very little effect on the bearing capacity if it was built even a fairly small distance away from the sloping ground.

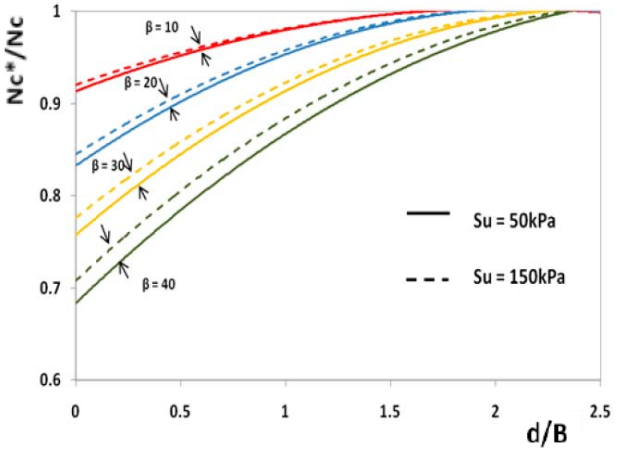
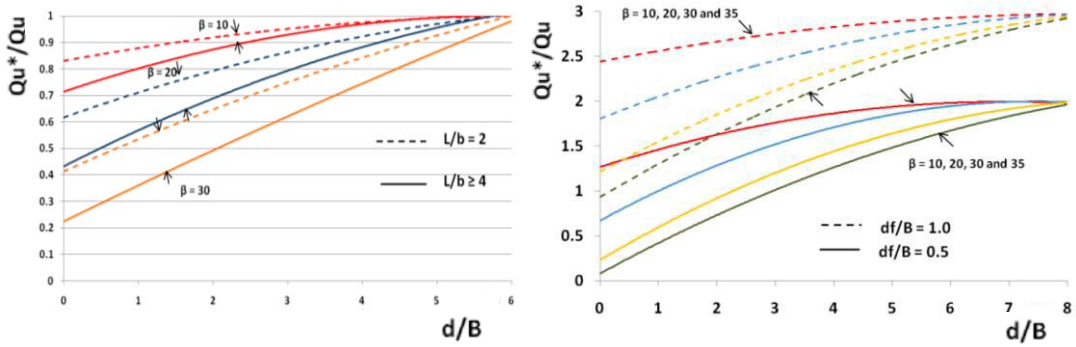


Figure 7. Modification factor for N_c with D_f/B=0.

As mentioned earlier, the modification factors for embedded footings were given in the form of factors that modified the total bearing capacity. In Figure 8(a), modification factors for embedded footings near sloping ground relative to footings with the same embedment ratio on level ground are provided. Figure 8(b) on the other hand shows modification factors for embedded footing near sloping ground relative to footings located above surface on level ground. Therefore, Figure 8(b) is useful in determining the amount of bearing strength that was gained through embedment and the percentage of which that was lost as a result of sloping ground. From Figure 8(a), it could be seen that there was a similar trend to N_γ for lower slope

angles while an increasingly linear trend was observed as slope angles were increased. In comparing the modification factors obtained for embedded footings, with factors found for N_γ and N_q, it could be seen that for the same friction angle, the modification factors for embedded footing were generally greater than the respective N_γ modification factor while being significantly lower than the respective N_q modification factors.
From Figures 8(a) and other calculations made, it was also noted that slope length had



(a) (b)

Figure 8. Modification factor for ultimate bearing capacity considering embedment depth: (a) φ = 35° and D_f/B=0.5; and (b) cohesionless soil with φ = 35°.

significant effect on the modification factors, with the effect increasing with increasing embedment depth. For very small slope lengths, the toe of the slope was almost level or only a small distance beneath the bottom of the footing. Therefore, if a line joining the bottom corner of the footing with the toe of the slope could be drawn, the relative slope angle of that to the footing was significantly less than the actual slope angle. Thus, a considerably greater bearing capacity was calculated for smaller slope lengths as opposed to larger slope lengths.

On the other hand, Figure 8(b) shows the extent of increased bearing capacity that was obtained through embedment. This could be seen by examining the case of a footing with the relevant parameters being D_f/B of 1, β = 35 and d/B of 0. For this footing the modification factor is almost equal to one. This indicates that it has the same bearing strength as a footing placed above ground that is not affected by sloping ground.

Finally, as modification factors provided in Figure 8(a) were relative to footing embedded on level ground and therefore the effect due to depth was already accounted for, the modification factors only account for the presence of the sloping ground and should be used together with depth correction factor for the general bearing capacity equation.

5 CONCLUSIONS

LimitState:GEO software was used to analyse the bearing capacity of footing near a slope for a number of different combination of parameters. It was found that the presence of the slope had significant effect on the bearing capacity and played an important role in foundation design. The major conclusions observed are as follows.

- The greatest reduction in bearing capacity was seen when footings were located at the edge of the slope.
- The reduction, however, decreased with increasing edge distance until the sloping ground had no effect.
- The threshold distance also increased with increasing slope angles and friction angles.
- For cohesionless soils the threshold slope angle was equal to the soil friction angle.
- Shorter slope lengths had significant effect on N_γ and N_q. This effect, however, diminished at larger slope lengths.

New Zealand Geotechnical Society Inc. 19th Symposium, Queenstown 2013

- Slope length, $L/B = 2$ generally produced a less conservative solution than when higher slope lengths was used.
- Due to difficulty in separating the bearing capacity components for embedded footings, modification factors for total bearing capacity were proposed.

ACKNOWLEDGEMENTS

The authors would like to thank Dr Colin Smith of Sheffield University for allowing them to use the software with academic license. This study was the Part 4 research project of the first two authors in 2010, and they would like to thank all people involved in the research.

REFERENCES

Castelli, F. & Motta, E. (2010) Bearing capacity of strip footings near slopes. *Geotechnical and Geological Engineering*, Vol. 28, 187-198.

Georgiadis, K. (2010) Undrained bearing capacity of strip footings on slopes. *Journal of Geotechnical and Geoenvironmental Engineering*, 136(5), 677–68.

Hansen, J. (1970) A revised and extended formula for bearing capacity. *Bulletin No. 28*, Danish Geotechnical Institute, Copenhagen, 5-11.

Kumar, J. & Rao, V. (2003) Seismic bearing capacity of foundations on slopes. *Geotechnique*, 53, 347-360.

Limitstate (2009) *LimitState:GEO Manual*, Version 2.0.

Limitstate (2010) *Analysis & Design Software for Engineers*, http://www.limitstate.com/

Loukidis, D. & Salgado, R. (2009) Bearing capacity of strip and circular footings in sand using finite elements. *Computers and Geotechnics*, 36, 871-879.

Michalowski, R. (1997). An estimate of the influence of soil weight on bearing capacity using limit analysis. *Soils and Foundations,* 37**,** 57-64.

Saran, S., Sud, V. & Handa, S. (1989) Bearing capacity of footings adjacent to slopes. *Journal of Geotechnical Engineering*, 115, 553.

Terzaghi, K. (1943) *Theoretical Soil Mechanics*, Wiley New York.

Clendon, N.K., Ho, K. & Poulos, H.G. (2013)
Engineering properties of pumice material and the design of piled foundations
Proc. 19th NZGS Geotechnical Symposium. Ed. CY Chin, Queenstown

Engineering properties of pumice material and the design of piled foundations

N K Clendon
Coffey Geotechnics, Wellington, NZ
nick.clendon@coffey.com (Corresponding author)

K Ho, H G Poulos, Coffey Geotechnics

Keywords: Pumice, Pile Foundations, Cyclic Loading, Strength, Uplift.

ABSTRACT

Pumice material is located extensively around the central part of the North Island, New Zealand, as a result of numerous eruptions from volcanoes in the Taupo and Rotorua regions. The pumice materials possess several characteristics which distinguish them from quartz based soil deposits. These include highly vesicular structure, low density but high friction angle, easily crushable particles, and highly dispersive. Despite these generally unfavourable characteristics, the material can often exceed expectations. For example, fine to coarse sand with a bulk density of 12.9kN/m^3, and an SPT N value of 13, has given an effective friction angle Φ' of 42° and an apparent effective cohesion of 17kPa. These values are well in excess of those recommended for traditional sandy soils where Φ' of 30-34°, cohesion of 0kPa and a bulk density of 19kN/m^3, would be more typical. The following paper collates and summarises existing data on pumice-based silts and sands and provides recommendations for geotechnical parameters for foundation design. Specific experience relating to the design of piled foundations for transmission structures, and their performance, is discussed.

1 INTRODUCTION

In 2011 a new transmission line was commissioned to upgrade the existing capacity between Wairakei (just north of Taupo, central North Island, New Zealand) and Whakamaru (WRK-WKM Line C) and allow for the removal of a smaller existing line. As part of the transmission line works was the design and construction of the foundations for the proposed 104 tower sites. Loads for the towers ranged from 850kN to 2300kN for uplift loads. Compression loads were in the range of 1050kN to 2500kN.

Design of the foundations utilised an effective stress approach, with pile design for skin friction based on Equation 1:

Ultimate Shaft Friction (f_s) = $K_s \sigma_v'$ tan(δ) (1)
K_s = lateral stress coefficient
σ_v' = effective vertical stress
δ = effective interface friction angle between soil and shaft (δ = M.Φ)
M =ratio of interface friction angle to soil friction angle

The suitability of the above equation for design of piled foundations in pumice material and the selection of an appropriate K_s value are discussed below.

2 GEOLOGY

The local geology consists of Taupo Pumice Formation, eruptives and alluvium deposited during the last major eruption of the Taupo Caldera ~ 1800 years ago. Underneath the Taupo Pumice Formation is the Whakamaru & Oruanui Ignimbrites & Haparangi Rhyolites. At both the eastern and western ends of the transmission line (Wairakei & Whakamaru townships) the geology is the Hinuera Formation (Pleistocene Alluvium). The Hinuera formation contains a range of material from silt to very large boulders (several metres across). (New Zealand Geological Survey, 1978).

New Zealand Geotechnical Society Inc. 19th Symposium, Queenstown 2013

3 PUMICE MATERIAL

The pumiceous deposits located throughout central North Island have often been referred to as "*Crushable Soils*" (Hind, 2008). "*Pumice sand particles have a vesicular nature, making them light and crushable*" Kikkawa et al (2010). Comments by Wesley et al. sum up the nature of pumice material. "*The result of the vesicular nature is that light weight particles have rough surfaces and are easily crushed*". Figure 1 below taken from Pranjoto et al. (1996) shows the difference between quartz grains and pumice grains. The work of Pender et al. (2006) details Puni (Pumice) Sand (sieved to medium to coarse sand) as having a loose friction angle of 41° and a dense angle in the range 41-48°. The maximum dry density ranged from 0.766 to 0.955t/m^3 (7.5-9.36kN/m^3).

A paper by Hind (2008), compares the testing details from Wharmby et al. (2008), with the Stella Bridge Passage. Hind (2008) notes actual shaft capacity vs. design for the Stella Bridge Piles ranged from 5-100%. The use of oversized cutting shoes during construction has been identified as a cause of gapping around the pile. The Tauranga Harbour Link constructed with bentonite support fluid achieved shaft friction capacities of 40-150kPa, compared to the estimated shaft friction in the range of 2-67kPa (Hind, 2008).

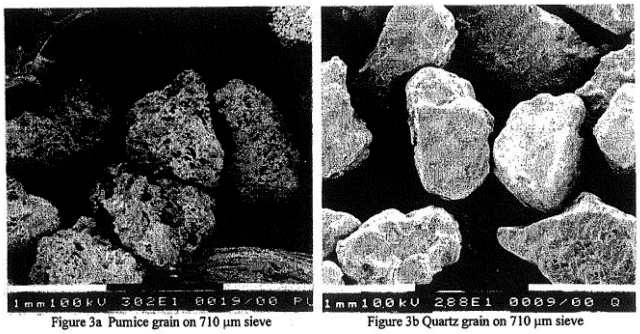


Figure 3a Pumice grain on 710 µm sieve Figure 3b Quartz grain on 710 µm sieve

Figure 1 - Image taken from Pranjoto et al (1996)

4 SOIL PROPERTIES

4.1 Soil density

Soil density of pumice soils is significantly lower than traditional soil counterparts. Typically values used in CPT interpretations range from 18 to 20 kN/m^3, with empirical tables having a range of 16-22 kN/m^3 for sand and gravel. A total of 6 triaxial test results were carried out with bulk density ranging from 12.9 to 17.8 kN/m^3, while a bulk density range of 12.9 to 14.8 kN/m^3 was identified for medium dense sand. Pumice material has a soil unit weight 20-30% less than its equivalent traditional quartz counterparts. Dry density results from the triaxial tests were 5.7 to 14.2 kN/m^3 with medium dense sand in the range of 8.0 to 8.8 kN/m^3 and moisture content ranging between 62-67%.

4.2 Internal friction angle & cohesion

The internal friction angle of pumice material has significantly higher values than the soil density or SPT N values would indicate. A pumice soil with a bulk density value of 12.9 kN/m^3, and SPT N value of 13, has an effective friction angle Φ' of 42° and an effective cohesion of 17 kPa based on a triaxial test (effective consolidation pressure ranged 25-100 kPa). The testing was carried out using single sample multi-stage tests, due to difficulties with obtaining multiple coherent samples. These values are well in excess of those recommended for traditional sandy soils where Φ' of 30-34°, cohesion of 0kPa and a bulk density of 19kN/m^3 would typically be recommended. Figure 2 compares the relationship of traditional soils to pumice material for internal friction angle against SPT N values.

From Figure 2, the use of the CPeT-IT software provides the best correlation with the lab test data. A small increase in friction angle of 1-2° is seen where the correct soil density is used. Care needs to be taken in the selection of a friction angle, notably where the soils contain a reasonable amount of silt material, as recorded friction angles drop quickly to values of between

20° and 31°. Apparent effective cohesion is a significant parameter in the triaxial testing, with gravelly sand showing cohesion as high as 17kPa.

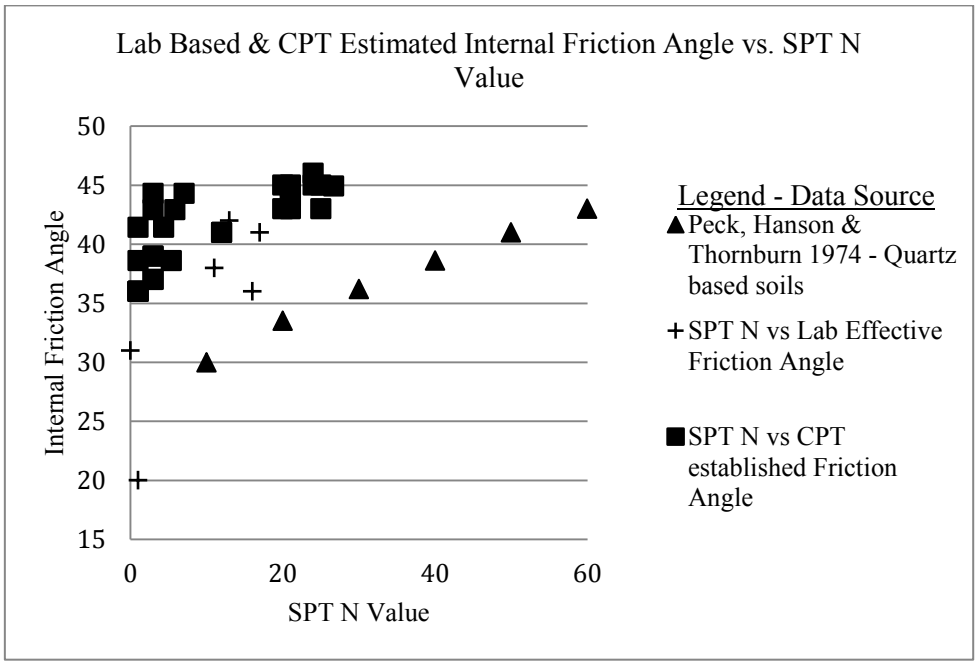


Figure 2 – Friction Angle vs. SPT N for Pumice Material

4.3 Construction parameters

Two construction based parameters were used, M (Ratio of Interface Friction Angle to Soil Friction Angle), was considered to be 1.0, as the piles were to be cast insitu, and casing not to be used during construction. K_s/K_o value of 1.0 was selected as minimal disruption to the insitu stresses was expected from cast insitu piles, with piles typically bored and constructed within a single day.

5 PILE TESTING

5.1 Pile construction

The test piles were 750mm bored cast in situ piles. A section of temporary casing was utilised at the top of both tests piles during construction to prevent collapse. The casing was withdrawn during pouring. The two test locations were:

T66 – Poihipi Road, Whakamaru,
T75 – Kaahu Road, Whakamaru

Location T66 was constructed utilising polymer support fluid to test the construction and tremie methodology for construction purposes. Polymer was not required. T75 was constructed dry and the concrete placed under free fall conditions. The concrete was placed down the pile centre and prevented from contacting the reinforcing cage via a short chute and vibrated over the upper 6.0 m. Both piles were finished level with the existing ground surface. Both test piles had the same steel reinforcing:

- 16D500E32-S-544PCD, D300E12-SP-200P-588PCD (PCD = Pitch Circle Diameter)

Reaction load was provided via four compression piles via a 640 t (5800kN max load) calibrated jack with two pressure gauges. The four compression piles were 750 mm diameter, bored and cast insitu to 17.0 m depth. The vertical pile steel was connected to the jack via a 50PL Flange Plate and eight 40 mm Macalloy 1030 Bars at 521PCD. The test pile load was transferred via two Piletech 1564 Custom Welded Beams 9.0m reaction beams. The reaction beam was surveyed throughout the test with no displacements measured. Shorter Piletech cross beams linked the two reaction piles at either end together (not shown in Figure 3 below).

New Zealand Geotechnical Society Inc. 19th Symposium, Queenstown 2013

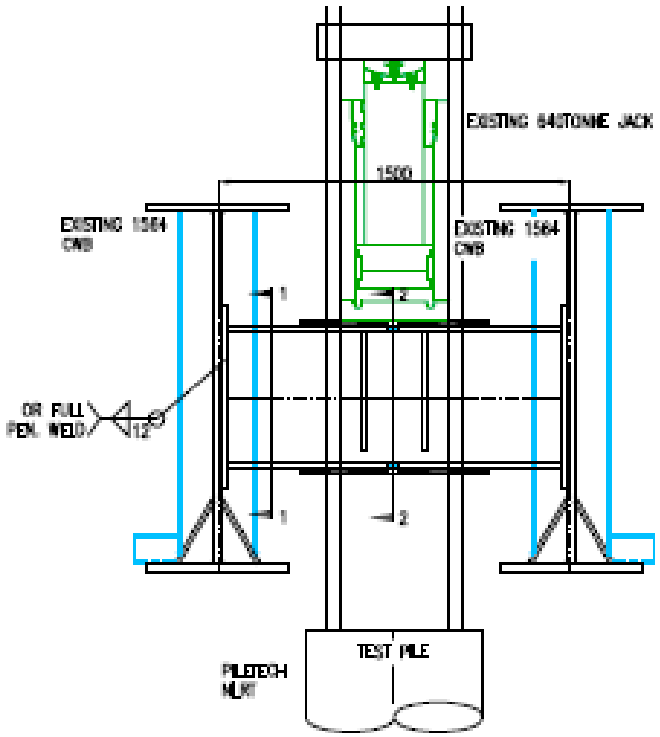


Figure 3 – Pile Test Setup

5.2 Pile testing instrumentation

The instrumentation for the test pile is listed in Table 1.

Table 1 – Pile Testing Instrumentation

Manufacturer	Model No.	Quantity		Type of Instrument
		T66	T75	
CDI	BG2720 50mm	4	4	Digital Dial Gauges
GEOKON	4911-4	12	8	Sister Bar Strain Gauges
GEOKON	1300-2-50mm	2	2	A9-Vibrating Wire Displacement Transducers
GEOKON	1300-1-25mm	2	1	A9-Vibrating Wire Displacement Transducers
GEOKON	1300-2	1	1	Bottom Anchor

Table 2 & 3 detail the set out location for the testing equipment listed in Table 1.

Table 2 – Pile Testing Instrumentation for T66

Instrument	Depth to centre of test point (m)					
Extensometers	0.07	5.3	9.5	14.8	17.0	-
Sister Bars	1.5	3.9	7.5	10.8	13.4	15.9

Table 3 – Pile Testing Instrumentation for T75

Instrument	Depth to centre of test point (m)			
Extensometers	1.5	3.8	7.0	9.95
Sister Bars	1.5	3.8	7.0	9.95

Note two sister bars located at each level on opposing sides of the pile.

5.3 Pile testing investigation & profiles

A borehole, CPT and sDMT were carried out at each site to a depth of refusal or 22.0m below ground level. The results of the investigation are presented in Tables 4 & 5.

It should be noted that the values presented in Tables 4 & 5 are more representative of quartz based soils and not reflecting the values of soil parameters discussed in Section 4. The two reasons are the triaxial test data was received late and was not incorporated into the original

design, and the performance of the soils under cyclic loading was not understood and therefore a low value was taken for design as shown in the tables. K_s/K_o values have also been taken as 1.0. This suggests that OCR ranges from 1.1 to 8.0 for the soils listed below and are considered representative of soil with their associated densities and histories. OCR and K_s is discussed further in Section 5.6. For pumice soils the parameters may not directly represent consolidation history as much as depositional environment. Pumice material is typically deposited at elevated temperatures and as such has an apparent (longer than expected) history as well as a strong apparent cohesion from interlocking grains and welding of particles. Further research is required on OCR.

The soft silt layers have also been assessed with an effective stress approach. This is considered reasonable as pore pressures dissipate rapidly during loading, and typically, drained conditions would be expected. This is also consistent with assessing the pile for long-term cyclic loading.

Table 4 – Soil/Rock Profile – T75

Top Depth	Description	Insitu Test Values			Soil Properties			Design Values		
		SPT N	Q_c	F_s	γ	φ'	c'	M	K_s/K_o	K_s
m			kPa	kPa	kN/m^3	^{0}	kPa			
0	Very loose SAND	1	500	20	15	32	0	1.0	1.0	0.6
3.1	Soft SILT	0	500	100	13	25	0	1.0	1.0	0.6
4.5	Medium dense SAND	20	10,000	200	16	34 (36)	0	1.0	1.0	0.6 (1.0)
9.6	Dense SAND	40	20,000	400	17	36 (38)	0	1.0	1.0	0.6 (1.0)
10.5	Very dense SAND	70	n/a	n/a	17.5	38 (40)	0	1.0	1.0	0.6 (1.0)

Values in brackets ( ) were used for construction post-testing following initial analysis.

Table 5 – Soil/Rock Profile – T66

Top Depth	Description	Insitu Test Values			Soil/Rock Properties			Design Values		
		SPT N	Q_c	F_s	γ	φ'	c'	M	K_s/K_o	K_s
m			kPa	kPa	kN/m^3	^{0}	kPa	1.0	1.0	0.6
0	very loose SAND	1	2000	25	15	32	0	1.0	1.0	0.6
3.3	very soft SILT	0	500	15	13	25	0	1.0	1.0	0.6
4.4	loose SAND	3	1000	100	15.5	34	0	1.0	1.0	0.6
4.7	soft SILT	0	1000	100	13	25	0	1.0	1.0	0.6
5.3	medium dense SAND	25	12000	300	16	34 (36)	0	1.0	1.0	0.6 (1.0)
9.5	dense SAND	40	20000	400	17	36 (38)	0	1.0	1.0	0.6 (1.0)
12	very dense SAND	70	20000		17.5	38 (40)	0	1.0	1.0	0.6 (1.0)
14.8	very weak RHYOLITE	200	20000		19	45	0	1.0	1.0	0.6 (1.0)

5.4 Pile test results

The displacement curves on Figure 4 are based on the dial gauges located at the pile top. The extensometer data from the toe of the pile for T66 does not show any appreciable movement. It is considered that the toe of the pile socketed into the Rhyolite did not experience any

significant strain. Exhuming test pile T75 post testing allowed for measurements of the pile circumference, and the additional soil weight due to the cone was estimated at 600kN, reducing to 95kN at pile failure. It is thought this was as large as 1200kN during the early loading stages, prior to 1700kN ~2.5mm displacement, following which the cone appears to have reduced in size from around 4.3m at the top to 2.8m across. From the circumference measurements the cone forms from 3.3m below ground level. It is considered likely that a cone would have developed at T66, and to support this contention, some minor ground cracking was identified during testing.

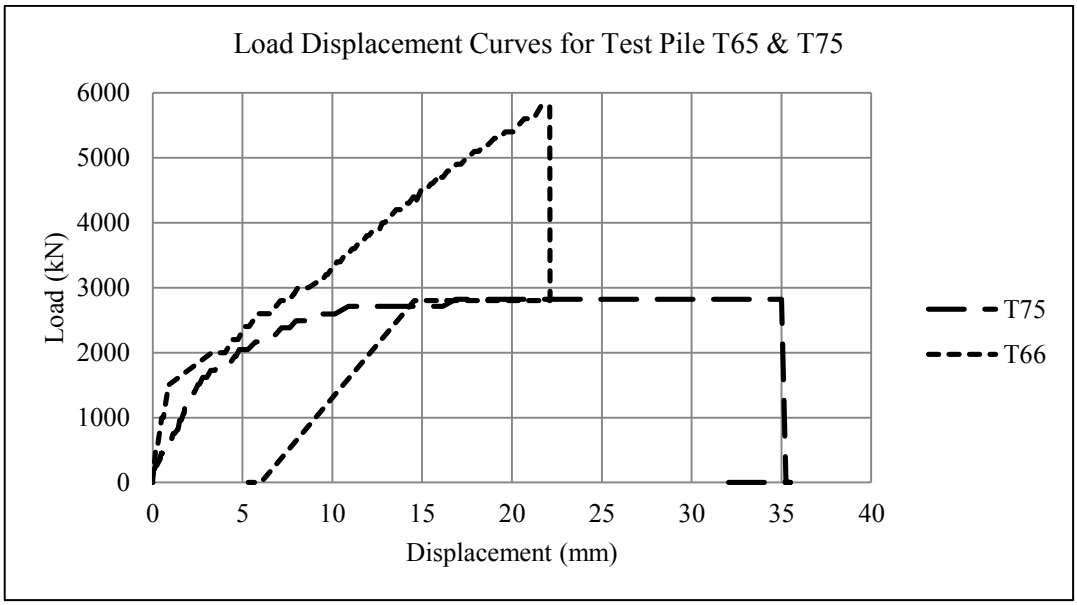


Figure 4 – Load Displacement Curves for T66 and T75

In Table 6, Design Strength = Factored Load Capacity (Design Load), and Design Capacity = Un-Factored Geotechnical Capacity (Ultimate Load)

Table 6 – Results of Uplift Pile Testing

Location	Pile Depth	Calculated		Test Results
		Design Strength	Design Capacity	Test Capacity (failure taken as 13mm displacement)
Tower 66	17.0m	1,418 (2,099)kN	2,461 (3,159)kN	4,000kN. Pile was loaded up to 5,800kN with 22mm of movement)
Tower 75	10.6m	515 (812)kN	861 (1204)kN	2,711kN (pile failure at 10.9mm upward displacement)

Note: the values in brackets are those used during the construction of the tower foundations following testing and as outlined above.

5.5 Pile test interpretation

In order to calculate the skin friction and K_s values discussed in section 5.6, the secant (tensile) modulus of the composite pile was calculated based on the tangent modulus ($\Delta_\sigma/\Delta_\varepsilon$ against micro strain). Then the stress equals the measured strain time's the secant modulus. However the strain experienced by the pile over the length varies significantly, resulting in the elastic modulus of the pile decreasing down its length as the test progresses. The method is based on Fellenius, 2001, but modified as the pile is tested in tension and the relationship between tangent modulus and micro strain is non-linear. At 2.5mm displacement, the strain in the test piles (T66 & T75) significantly reduces the tangent modulus of the pile from around 50GPa to 5-7GPa (tension value). This displacement relates to a load of 2,200kN for T66 and 1,500kN for T75 (around 80-200 micro strain). Exceeding 2.5mm of displacement would likely result in

fatigue of the skin friction as the capacity of the upper shaft (and beneficial cone) starts to decrease. Repeated cycling of the upper shaft would likely reduce the size/weight capacity of the cone. For the skin friction and Ks calculations in Tables 7 & 8, the data from the upper set of instruments has not been published as they produce very high skin friction capacities due to the additional cone weight.

Using the above procedure, skin friction (f_s) values have been estimated from the test data. For soft silt to medium dense sand at T75, the skin friction was estimated to be 55kPa at geotechnical failure and could be considered a low bound for medium dense sand. Loose-medium dense, dense and very dense sand at T66 produced skin friction values of 102, 151 and 248kPa respectively at the maximum test load of 5800kN. The above should be used with caution and are indicative only, as a reasonable amount of interpretation was required to assess the pile modulus E_p of the pile in tension. As the strain increases the sensitivity of the test interpretation to the E_p values likewise increases. However, the test results do indicate skin friction capacities well in excess of what is traditionally used. The average skin friction capacities are also provided in Table 7.

Table 7 – Estimated Skin Friction from Pile Uplift Tests

Test Site	Medium dense sand (some soft silt at top)	Loose-medium dense sand	Dense sand	Very dense sand	Average Ultimate Skin Friction Along Shaft Length
		kPa	kPa	kPa	kPa
T66	-	102	151	248	139 (95kPa at 13mm)
T75	55	-	81+	-	102

The dense sand in T75 is unlikely to be the maximum skin friction achieved. It is likely that the peak result occurred directly after loading and prior to failure, and was not captured.

5.6 OCR & K_s

Back calculation of K_s from the skin friction calculated in Table 7, and utilising Equation 1, produced a value of 0.81 for soft silt to medium dense sand at geotechnical failure. Values of 1.62 (possibly affected by a cone failure), 1.18 and 1.24 for loose to medium dense, dense and very dense sand respectively, were deduced for test pile T66 without geotechnical failure occurring, however, the acceptable displacement of 13mm had been exceeded. Testing carried out by Tucker (1987), identified K_s values ranging from 1.2 to 4.0 for drilled shafts in granular soil, and values as high as 10 in rock. However, for design it was recommended limiting K_s to K_p as a maximum. This also correlates well with existing Transpower test data (Transpower, 2007) where granular material ranges from 0.81 to 1.68 in bored piles, 3-4m in depth.

Table 8 below compares the original Design OCR (based on K_s=0.6 or 1.0) values with the back calculated OCR values from the pile test using Equation 2. The calculations utilise the effective friction angle as taken from Figure 4 for pumice material.

$$K_s = (1-\sin \phi') (OCR)^{0.5} \qquad (2)$$

Table 8 – Back Calculated OCR's from Pile Test

Soil Strength	K_s	Assumed φ'	Test OCR	Design OCR
Loose – Medium Dense	0.81-1.62	41	5.6-22.2	1.6-6.2
Dense	1.18	41	11.8	6.8
Very Dense	1.24	42	14.1	7.9

It should be noted that the K_s value of 1.62 for loose-medium dense material may have been affected by the presence of a cone failure at T66 and should be considered with caution.

OCR from seismic dilatometer (sDMT) tests varies from <0.8 to 6.3 within the space of 1.5m, with no consistent pattern identified. This can produce a difference of a factor of 4 for values of K_s. Further work is required to assess the accuracy of OCR data derived from sDMT.

For design purposes a K_s value of 0.6 was taken for loose material or weaker and 1.0 was used for medium dense or stronger. The K_s value adopted for the project is lower than the values identified above in Table 8. A lower bound value has been adopted as the performance of the soils in the long term is not well understood, due to cyclic loading, and hasn't been fully investigated.

6 CYCLIC LOADING

Only a limited amount of information regarding cyclic loading can be taken from the test data due to the limited number and locations of the test sites. However, the following can be noted. T75 was jacked post-failure and a residual capacity of 1532kN was recorded. This relates to an average skin friction of 75kPa and compares to an average skin friction of 98-143kPa depending on the size of cone present post-failure. This indicates a soil fatigue factor (or degradation factor) of 0.5 to 0.77. The value of 0.5 should be considered an upper limit of cyclic fatigue. In the case of calcareous soils after cyclic loading (No.=100 cycles), Poulos (1988) indicates that the load capacity may be reduced to 40% of the static value, and additional displacement is required to mobilise the capacity.

7 CONCLUSIONS

Traditional investigation methods are suitable for the investigation of pumice soils, however, new or modified methods of interpretation are required in order to adequately assess the material, and to develop foundation design parameters. The use of traditional design methods for pumice material will produce satisfactory design results; however, significant risks occur where construction methodology is not addressed at the design stage. Typically bored cast insitu piles perform better than cased piles. The use of K_s=1-sin ϕ' as a design value will produce a conservative pile design for cast insitu piles. Although pumice sands have a low density, and are easily crushable, they can perform very well as founding soils where their high friction angles are utilised and the material is suitably confined to prevent the formation of erosion features or gaps around foundations.

REFERENCES

Fellenius, B. H. (2001). From Strain Measurements to Load in an Instrumented Pile. *Geotechnical News Magazine, 19*(1), 35-38.

Hind, K. J. (2008). Predicting axial performance of piles in pumiceous material. In C. Y. Chin (Ed.), *Proc. 18th Geotechnical Symposium on Soil-Structure Interaction* (pp. 28-33). Auckland: Tonkin & Taylor Ltd.

Kikkawa, N., Pender, M. J., Orense, R. P., St George, J. D., & Matsushita, E. (2010, July 7). Ko compression and stress relaxation of pumice sand. *Journal of Geotechnical and Geoenvironmental Engineering*.

New Zealand Geological Survey. (1978). *The Geology of New Zealand.* Wellington: E. C. Keating Government Printer.

Pender, M. J., Wesley, L. D., Larkin, T. J., & Pranjoto, S. (2006, February). Geotechnical Properties of a Pumice Sand. *Soils and Foundations, 46*(1), 69-81.

Poulos, H. G. (1988). *The Mechanics of Calcareous Sediments, John Jaeger Memorial Address.*

Pranjoto, S., Larkin, T. J., Wesley, L. D., & Pender, M. J. (1996). Some Engineering Properties of a Volcanic Sand. *New Zealand Geomechanics News*(51), 53-58.

Transpower. (2007). *Transmission Line Foundation Design Guide TP.DL 01.01 Draft 9*.

Tucker, K. D. (1987). Foundations for Transmission Lines. *American Society for Civil Engineers* (pp. 142-159). Atlantic City: ASCE.

Wesley, L. D., Meyer, V., & Pender, M. J. (n.d.). *Cone Penetrometer Tests in Pumice Sand.* Auckland: Department of Civil Engineering, University of Auckland.

Wharmby, N., Zame, M., Hillier, R., & Burton, P. (2008). Tauranga Harbour Link foundation pile constructing and testing. In C. Y. Chin (Ed.). (pp. 22-27). Proc. 18th NZGS

Gibson, M.F.L., Green, D.P., Holmes, S.F., & Newby, G. (2013)
Designing earthquake resilience into pump station foundations
Proc. 19th NZGS Geotechnical Symposium. Ed. CY Chin, Queenstown

Designing earthquake resilience into pump station foundations

M F L Gibson
SCIRT, Christchurch, NZ
Marcus.Gibson@scirt.co.nz (Corresponding author)

D P Green
SCIRT, Christchurch, NZ
David.Green@scirt.co.nz

S F Holmes
SCIRT, Christchurch, NZ
Simon.Holmes@scirt.co.nz

G Newby
Beca Ltd, Christchurch, NZ
Grant.Newby@beca.com

Keywords: Pump Station, Seismic Performance, Liquefaction, Ground Improvement, Resilience

New Zealand Geotechnical Society Inc. 19th Symposium, Queenstown 2013

ABSTRACT

Christchurch city's terminal wastewater pump stations have suffered extreme differential seismic settlement resulting from the Christchurch Earthquake Sequence. Lessons learnt from observation of pump station earthquake damage have been used to develop understanding of criticality of failure mechanisms. Providing an indispensable resource to aid the development of 'resilient' designs of pump station foundations and associated infrastructure connections, to control the key failure mechanisms. A prioritisation method for the selection and incorporation of additional resilience in foundation design was developed. This considered; the specific topography and ground conditions, seismic vulnerability of the complete pump station design, the importance of the pump station in the network and the consequence of functional failure.

This paper presents one example of application of the resilience prioritisation method, with design of terminal Pump Station 136 (PS136), to replace a severely damaged existing wastewater terminal pump station in Aranui.

1 INTRODUCTION

Christchurch's terminal wastewater pump stations suffered significant damage in the recent Canterbury earthquake sequence (CES), many experiencing extreme differential seismic settlement and damage to connecting infrastructure resulting from earthquakes of 4 September 2010 (Mw 7.1), 22 February 2011 (Mw 6.2) and 13 June 2011 (Mw 6.0). Most significant damage was sustained as a result of the February 2011 event, characterised by extensive liquefaction and high ground accelerations.

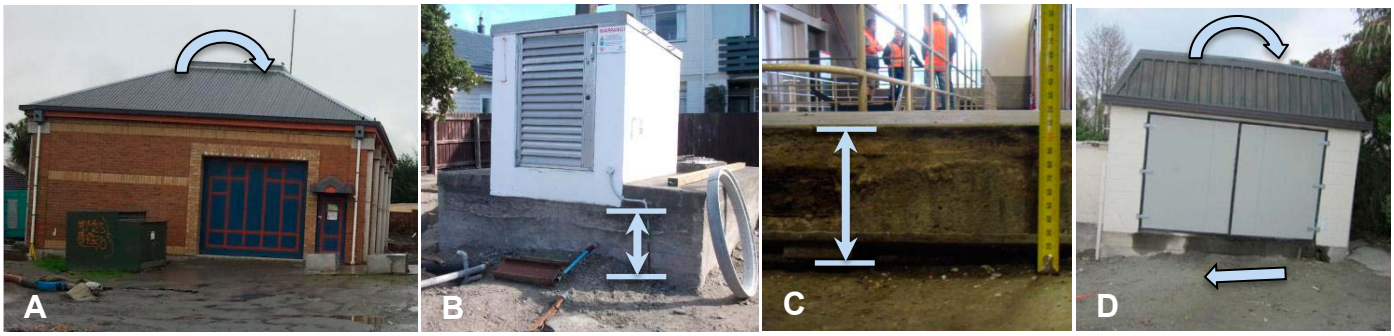
The Stronger Christchurch Infrastructure Rebuild Team (SCIRT) was established in response to the extensive damage sustained during the 22 February 2011 earthquake. This alliance comprises the New Zealand Government (CERA and NZTA), Christchurch City Council (CCC), and civil contractors, with support from an integrated design office of engineers from number of local engineering consultants. SCIRT was tasked with the assessment of infrastructure earthquake damage, and the design and construction of necessary repairs or replacement. The mantra of SCIRT was to provide resilient infrastructure, whilst also providing value for the client organisations.

The design of replacement wastewater pump stations in Christchurch has required a focus on providing seismic resilience, in order to satisfy CCC's legal requirements, such as continued post-disaster operation. Pump station failure mechanisms observed during the CES have identified critical and vulnerable components of the pump stations, allowing designers to target particular pump station components for seismic resilience measures. The performance of the foundations and the interface with connecting infrastructure has the greatest influence on the extent of earthquake damage. Foundation and ground improvement systems, as well as appropriate detailing of pipe connections, provide an opportunity to add significant seismic resilience for future earthquake events, providing security for Christchurch's wastewater network.

2 OBSERVED PERFORMANCE OF WASTEWATER PUMP STATION FOUNDATIONS

Inspections of damaged wastewater pump stations, and associated infrastructure, throughout Christchurch provided a valuable insight into the key mechanisms leading to pump station failure. The severity of damage observed was related to the following factors:

- Robustness of the foundation design;
- Layout of pipework, and construction materials;
- Extent of liquefaction, seismic settlement and lateral spreading;
- Ground accelerations experienced at the site.



A: Rotation of Pump Station 36, resulting from differential seismic settlement across the pump station and differences in founding depth for the pump station wet well and building.

B: Uplift of Pump Station 30 and seismic settlement of the surrounding ground, resulting in differential movement shearing pipe and service connections.

C: Differential settlement and shearing between sections of the Pump Station 1 building, associated with differential seismic settlement between one half of the building founded on shallow foundations and the other half at depth.

D: Rotation of Pump Station 63 resulting from buoyancy uplift, lateral spreading and slope instability, total and differential seismic settlement across the site, and differences in founding depths of the pump station elements.

Figure 1: Photographs showing common pump station foundation failure mechanisms

The key geotechnical mechanisms that were observed to have greatest influence on the extent of damage to pump station structures, and associated infrastructure, during the CES are summarised in Table 1. Understanding of these mechanisms, along with lessons learnt during the emergency response to reinstate service of the wastewater network, have provided an indispensable resource to aid the development of 'resilient' designs and verifying their appropriateness.

Table 1: Typical foundation failure mechanisms and effects on pump station functionality

Earthquake Ground Response	Description	Typical Consequences for Pump Station
Lateral Spread	Pump stations located within a zone of lateral spread are subject to translation, and the shallow non-liquefied 'crust' soil can exert passive pressures on the structure. These effects are most commonly observed where pump stations are located close to the free face.	• Total and differential settlement of structure. • Rotation of the structure. • Translation of structure towards the free face. • Damage to connecting pipe infrastructure. • Damage to the pump station structure.
Seismic Settlement	Variation in ground conditions beneath the pump station can result in differential seismic settlement.	• Differential settlement and rotation of structures. • Damage to connecting pipe infrastructure.
	Pump station elements and connected infrastructure founded at different depths can experience differing magnitudes of seismic settlement.	• Differential settlement between sections of the pump station structure founded at different depths causing rotation and/or structural damage. • Settlement of surrounding ground and infrastructure relative to the pump station structure, leading to damage to pipe connections.
	Gravity pipes within the catchment are laid shallower than the pump station wet well, which can lead to differential seismic settlement between the gravity catchment and the pump station.	• Reduced or reverse pipe grades on connecting gravity pipes, possibly resulting in flooding upstream.
Buoyancy	Elevated pore water pressures within liquefied soils exert uplift pressures (approximately equivalent to total stress).	• Uplift of the structure. Magnitude dependent on the factor of safety resisting uplift, the thickness of the surface crust, and the duration of ground shaking. • Rotation of the structure. • Damage to connecting pipe infrastructure. • Damage to the pump station structure.
Bearing Failure	Reduced bearing capacity of liquefied soils beneath the foundations, and associated reduction in soil stiffness, leading to bearing failure.	• Total and differential settlement of the structure. • Rotation of the structure. • Damage to connecting pipe infrastructure. • Damage to connecting structures.
Dynamic Structural Damage	Differences in seismic response between pump station structural elements and pipes.	• Damage to connecting pipe infrastructure and adjacent structures.

3 FOUNDATION DESIGN PHILOSOPHY

The overarching philosophy within SCIRT for the design of pump station foundations and associated infrastructure connections was to include appropriate measures to control the key failure mechanisms identified for the specific project. This would then limit future earthquake damage, reduce the risk to post-disaster functionality, and allow timely and cost-effective temporary repairs. The design solution also had to provide maximum 'value', considering potential future earthquake risk and damage.

Earthquake resilience for pump stations was typically provided by design though:

1. Considering the potential seismic performance and resilience of the pump station when selecting the pump station site;
2. Considering potential differential settlements and anticipated seismic behaviour when designing the spatial arrangement of pump station elements;
3. Providing ease of access to vulnerable elements of the pump station to aid post-earthquake repair;
4. Providing consistency in founding depth and performance between pump station elements;
5. Considering potential relative settlement of the catchment and pump station wet well, including an assessment of the effect of multiple earthquakes;
6. Attempting to control the location of failure of the pump station and associated infrastructure, to assist with the rapid location of damage and ease of repair;
7. Including allowance for potential future re-levelling of structures where appropriate and feasible.

4 DEVELOPMENT OF THE RESILIENCE PRIORITISATION METHOD

The generic prioritisation method for the selection and incorporation of additional resilience measures for pump station foundation designs within SCIRT projects is provided in Table 2. This was developed by considering observations from existing pump stations during the CES. Specific prioritisation for the design of each new pump station foundation system should consider the specific topography and ground conditions at the site, seismic vulnerability of the complete pump station design, the importance of the pump station in the network and the consequence of functional failure.

When incorporating additional resilience into pump station foundation design that incurred a capital cost, to maximise 'value', the designers also considered:

- The likelihood of an earthquake event severely damaging the pump station;
- The quantitative improvement in pump station seismic performance and post disaster functionality;
- The initial capital cost of the improved resilience measures and potential cost savings during future repairs.

Such an assessment would often be based on engineering judgement, supported by appropriate analysis and consideration of the whole of life cost. This informed the assessment of prioritisation of individual pump stations and helped assess the appropriate level of resilience.

Table 2: Generic resilience prioritisation for pump station foundation design

Prioritisation	Description	Typical mitigation incorporated into foundation design
1	**Improve slope stability and mitigate lateral spreading** to limit the translation and rotation of the structures**.**	• **Consider alternative sites** for pump station; increase distance from the free face. • **Install ground improvement or large diameter piles** to limit lateral displacements or resist lateral loads exerted on the structure.
2	**Limit differential settlement** of the wet well structure and associated rotation, to reduce damage to connecting infrastructure and reduce the cost of post-earthquake repair or replacement.	• **Install ground improvement or piles** beneath the pump station, to limit differential settlement across pump station. • **Install ground improvement** surrounding the pump station to support the sides and resist the potential for differential settlement. • **Provide consistency in foundation depth and performance** for structures and connecting infrastructure to reduce the potential for structure rotation, differential settlement and damage to pipe connections.
3	**Limit buoyancy uplift** of the pump station structure under both hydrostatic and seismic conditions.	• **Relieve excess pore water pressures** through the use of permeable backfill or base drains. • **Install tension piles or anchors** to resist uplift forces. • **Add weight to the structure or utilise an extended base** to resist the uplift force.
4	**Provide compatibility between total settlement of the wet well structure and connecting infrastructure** to limit damage, and reduce potential differential settlement across the structure.	• **Appropriate ground improvement design** beneath and surrounding the pump station, to limit differential settlement across the wet well. • **Piling of the pump station** to limit differential settlement across wet well, with flexible connections to accommodate differential settlement between the pump station and connecting infrastructure. • **Design slightly deeper wet wells and over steepen inlet gravity pipes** to accommodate potential differential seismic settlement between the catchment and wet well, considering multiple future earthquakes. • **Extend and transition ground improvement depth beneath critical pipe connections** to control in the rate of differential settlement and reduce the risk of damage from shearing. • **Use flexible PE pipes, flexible pipe connections, and provide slack in service connections** to accommodate anticipated future differential settlement.
5	**Design of pump station layout for straightforward post-earthquake repairs.**	• **Layout components of the pump station within the site to ensure that access is available,** to allow repair of earthquake damage without temporary relocation of components or complicated and costly temporary works.
6	**Design of pump station structure to accommodate post-earthquake re-levelling**	• **Consider future re-levelling in the structural design of foundations**, especially where shallow foundations are utilised for ancillary buildings.

5 APPLICATION OF THE RESILIENCE PRIORITISATION METHOD DURING THE CHRISTCHURCH REBUILD – EXAMPLE PUMP STATION 136

5.1 New Pump Station 136

CCC elected to construct a new Pump Station 136 (PS136) within Bexley Park in Aranui, across Pages Road from an existing Pump Station 36 that was extensively damaged by the 22 February

2011 earthquake requiring replacement. PS136 services the 254 hectare PS36 catchment located in Aranui in eastern Christchurch, as well as receiving wastewater from pump stations located in the north eastern quadrant of the city. The pump station transfers around 16% of Christchurch's wastewater direct to the Christchurch Wastewater Treatment Plant.

The pump station is underlain by liquefiable sand and silty sand of the Christchurch Formation, typically to depths exceeding 20m. The local topography limits risk of lateral spreading under liquefied conditions. The depth to groundwater is approximately 3m, with seasonal fluctuation.

The new pump station comprised a combined wet well, approximately 9.4m x 8m in plan and founded at approximately 9m below ground level (bgl). An adjoined valve chamber, approximately 9.4m x 3.3m in plan and founded 3.8m bgl, and separate Pressure Main 36 (PM36) valve chamber founded 3.4m bgl were also included. Wastewater enters the pump station via twin 1200mm diameter PE gravity pipes and exit via composite 500mm diameter ductile iron and 710mm diameter PE pressure mains. A 7m high building is sited above the wet well, adjoined to a control room on separate foundations, and a separate generator room is sited nearby.

New Zealand Geotechnical Society Inc. 19th Symposium, Queenstown 2013

5.2 Seismic Design Criteria and Assessment

Seismic design criteria for the new pump station was selected in accordance with NZS 1170, adopting an Importance Level of 3 and a 100 year design working life. The ultimate limit state (ULS) event of 0.61g peak ground acceleration and a moment magnitude, Mw, of 7.5 was assessed to result in similar liquefaction effects to the 22 February 2011 earthquake.

The design was focussed on seismic performance and the interaction of key elements within the pump station system. Sensitivity analyses were performed during design to assess the performance of the foundation system during future large magnitude earthquakes in the Canterbury region, including consideration of a characteristic Alpine Fault earthquake. Site observations of seismic performance of the ground at the site during the CES were invaluable, providing the designers the ability to calibrate analyses for three significant earthquake events (4 September 2010, 22 February 2011 and 13 June 2011). Liquefaction analyses compared to site observation suggested that liquefaction potential appears to be slightly underestimated when utilising SPT data, and overestimated by assessment based on CPT data.

5.3 Design Philosophy

Priorities were given to pump station elements in order of the consequence of failure, with consideration of the cost of effective treatment. The resilience prioritisation for the foundation design of PS136 is provided Table 3. As previously described, lateral spreading was not considered a significant risk at this site, making the mitigation of differential settlement the top priority.

5.4 Foundation Design Options

Foundation solutions considered during design included piled foundations, excavate and replace, vibro-replacement, stone columns and high modulus ground improvement (both discrete columns and lattice shear walls). A ground improvement solution was chosen over a piled foundation, as piles would leave the pump station raised above the catchment, which may settle around the structure (~350mm ULS), and due to the high costs associated with founding below 30m depth. A high modulus ground improvement solution was adopted for PS136, as it provided the best value technically feasible ground improvement solution. Continuous flight auger (CFA) columns provided a lower capital cost high modulus ground improvement option, and had the lowest construction risk and highest productivity advantage of the options reviewed. CFA piling rigs were readily available in Canterbury facilitating timely completion. The 600mm diameter 20MPa concrete columns do not provide densification of surrounding soils;

liquefaction mitigation is provided by stress concentration, with shear deformation of the stiffer elements reducing the cyclic shearing of the surrounding soil.

Table 3: Resilience prioritisation for PS136

Prioritisation	Description	Mitigation Considered
1	Protect the wet well from adverse differential settlement and rotation	• Incorporate ground improvement • Install piled foundation system • Provide consistency in foundation depth where feasible and economic
2	Limit the potential for seismic buoyancy uplift of the wet well	• Include extended base with granular backfill • Install tension piles
3	Limit the risk of damage to the gravity inlet pipes	• Use flexible pipe materials, detail resilient pipe connections to accommodate anticipated differential settlement • Transition depth of ground improvement to control the rate of differential settlement
4	Limit differential settlement between the wastewater catchment and wet well	• Increase depth of wet well to accommodate differential seismic settlement resulting from two to three ULS-level earthquakes
5	Provide support to the sides of the wet well to limit rotation of the structure	• Include granular backfill surrounding wet well • Install ground improvement surrounding pump station
6	Allow for future re-levelling (generator building)	• Where appropriate, detail shallow raft foundations to allow for future re-levelling

5.5 Resilience in Foundation Design

The ground improvement system was designed to limit the anticipated total and differential seismic settlement of the structure. Beneath the top priority pump station elements, the wet well and valve chamber, the ground improvement comprised rectangular lattice structures constructed of contiguous CFA columns to a depth of 6m below the founding level the wet well. The lattice shear walls limit shear strains within the contained soils, providing the highest level of resilience and technical confidence for mitigating liquefaction. Columnar ground improvement, comprising individual CFA columns installed in a triangular grid at nominal 1.5m centres, was provided below the control building and valve chambers to provide compatibility in the reduction of seismic settlement to that of the wet well. The pump station components are also surrounded by columnar ground improvement and granular hardfill providing side support and the width to height aspect ratio limiting adverse differential settlements. Gravity inlet and pressure main outlet pipe connections are underlain by depth-transitioned columnar ground improvement to control the rate of differential seismic settlement beneath pipes connecting to the pump station, reducing the risk of breakages at pipe connection points. Figure 2 provides a schematic of the ground improvement arrangement.

In anticipation of global catchment settlements, the inlet pipe sections at all pump stations (terminal and satellite structures included) have been designed over steepened by approximately 1m to accommodate for seismic settlement of the wastewater catchments relative to the pump stations following multiple earthquakes.

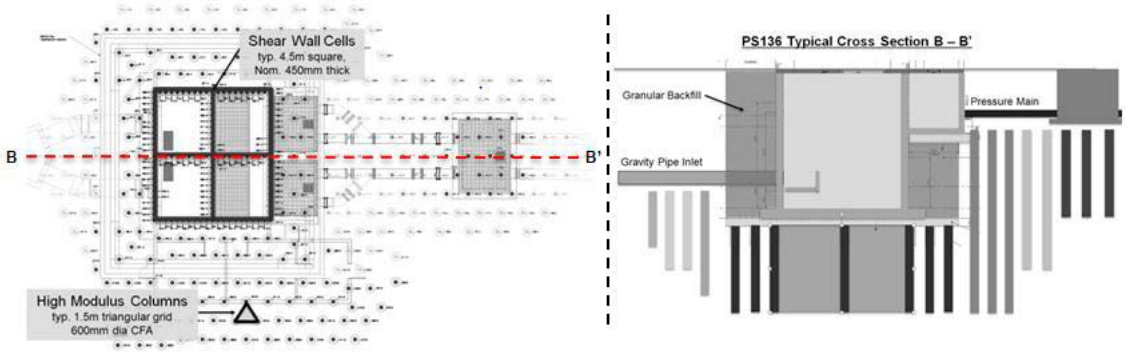


Figure 2: Schematic of PS136 ground improvement and foundation arrangement

6 CONCLUSIONS

New Zealand Geotechnical Society Inc. 19th Symposium, Queenstown 2013

Christchurch's terminal wastewater pump stations suffered significant damage in the recent earthquakes in Canterbury. The design of replacement terminal pump stations has required a focus on providing seismic resilience. This focus has made it necessary to consider observed failure mechanisms in the recent CES to provide an understanding of the key pump station elements susceptible to seismic effects.

Based on the observed seismic performance of pump stations, a resilience prioritisation method was developed that allows geotechnical designers to focus on mitigating the key failure mechanisms and apply resilient measures where they are of most benefit. This approach provides value by considering the consequences of failure and whole of life costs, allowing for multiple future earthquakes.

The resilience prioritisation method was used to design a resilient and cost-effective foundation system for the new Pump Station 136, including high modulus lattice structure and columnar ground improvements constructed with CFA columns. The design of the ground improvements considered prioritisation of pump station elements and consideration of vulnerable elements such as pipe connections. Transitioning of ground improvement has been used to control seismic settlement. These details provide seismic resilience for Christchurch's wastewater network during future earthquakes.

ACKNOWLEGEMENTS

The authors would like to thank Christchurch City Council and SCIRT for supporting the sharing of details contained in this paper.

REFERENCES

NZS 1170.0: 2002 Structural Design Actions – General Principles

NZS 1170.5: 2004 Structural Design Actions – Earthquake Actions

Nguyen, T. V. Rayamajhi, D. Boulanger, R. W. Ashford, S. A. Lu, J. Elgamal, A. Shao, L. (2012) "Effect of DSM Grids on Shear Stress Distribution in Liquefiable Soil", GeoCongress 2012, ASCE.

Rauamajhi, D. Nguyen, S. A. Ashford, R. W. Boulanger, R. W. Lu, J. Elgamal, A. Shao, L. (2012) "Effect of Discrete Columns on Shear Stress Distribution in Liquefiable Soil", GeoCongress 2012, ASCE.

Hillier, R.P. & Langbein, A.C. (2013)
Grouting of basalt to improve seismic resilience for bridge foundations
Proc. 19th NZGS Geotechnical Symposium. Ed. CY Chin, Queenstown

Grouting of basalt to improve seismic resilience for bridge foundations

R P Hillier
Tonkin & Taylor, NZ
rhillier@tonkin.co.nz

A C Langbein
Tonkin & Taylor, NZ
alangbein@tonkin.co.nz

Keywords: shallow foundations, bearing capacity, basalt, grouting, settlement

ABSTRACT

The 700 m long Newmarket Viaduct, Auckland, is a safety critical lifeline structure and carries motorway traffic flows of up to 160,000 vpd. The structure is supported on 12 pairs of piers, towering up to 20 m over Broadway in central Newmarket, Auckland.

Twelve of the individual bridge piers are founded on shallow pads bearing on the Mt Eden and Mt Hobson basalt flows. These shallow pad foundations have been designed for loads typically of the order of 25 MN. Peak design bearing pressures (seismic overturning) beneath the edges of the pads have been calculated to be of the order of 5 MPa. The structural and material consistency characteristics of the basalt provide a high risk to the static and seismic performance (settlement and bearing capacity) of the foundations under relatively onerous load conditions.

This paper presents the results and some observations of the characteristics of the basalt as identified from an extensive drill and grout programme undertaken to provide resilience for the foundations, particularly under the high seismic overturning load case scenarios.

New Zealand Geotechnical Society Inc. 19th Symposium, Queenstown 2013

1 INTRODUCTION

The Newmarket Connection was a four year project involving the replacement of the original Newmarket Viaduct with a modern structure capable of supporting this life line link whilst providing for additional lane capacity and upgraded barrier safety. The Viaduct supported by12 pairs of piers is a double curvature structure spanning a total distance of approximately 700 m, towering up to 20 m over Broadway in central Newmarket and carries motorway traffic flows of up to 160,000 vpd.

Twelve of the individual bridge piers are founded on shallow pads, 6 m or 7 m square in plan, bearing on the Mt Eden and Mt Hobson basalt flows. The remaining 12 bridge piers are founded on piles that are either socketed into the East Coast Bays Formation weak sandstone or into basalt where the basalt surface is too deep for a shallow foundation option.

The variability in the quality and consistency of the basalt lava flows provided many of the design and construction challenges. Locally, the basalt was found to be thinner and/or of poorer quality than originally anticipated. Conversely, where deep excavations have been required to accommodate future and adjacent basement developments the basalt has proven both obstinately thick and massive, but also variably and locally loose and rubbly.

The shallow pad foundations were designed for loads typically of the order of 25 MN, equating to average bearing pressures beneath the 6 m or 7 m square pads of approximately 500 kPa. Under seismic load conditions, peak bearing pressures (overturning) beneath the edges of the pads have been calculated to be of the order of 5 MPa. The performance of the founding basalt

layers, particularly under the seismic design load cases, is therefore critical to the performance of the viaduct structure.

To ensure resilience of the structure, all the pad foundations for the new structure founded on the basalt flows were subject to extensive grid drilling and grouting works. These works have been undertaken to confirm adequacy of the basalt and to cement these materials where the basalt is found to be excessively fractured and/or voided. This paper presents some observations and findings relating to the grout treatment of the basalt.

2 GEOLOGICAL SETTING

The viaduct generally runs along an east-west alignment, starting from the south-western foot of the Mt Hobson Volcano cone to the north-eastern side and foot of the Mt Eden volcano cone.

The site is underlain at depth by early Miocene aged East Coast Bays Formation weak rock (sandstone and mudstone), with younger deposits and volcanic-derived soils above. Pleistocene aged Tauranga Group alluvial deposits fill a paleo-valley above the rock surface. The Pleistocene aged soils are in turn locally capped by basalt lava flows, one from Mt Eden and one from Mt Hobson. These flows ran towards each other and towards the centre of the viaduct but don't physically converge. The combined basalt flows are typically in excess of 10 m thick, and thin to nominal thickness at their edges. The basalt is generally overlain, and also underlain in some areas, by volcanic ash deposits.

Further alluvial deposits were also encountered above the basalt in some areas and also overlain with uncontrolled fill from previous land development including the original viaduct construction, which this present project replaced.

3 GROUND INVESTIGATIONS

For the construction of the existing viaduct during the 1960's, a total of 23 boreholes were drilled at the original viaduct pier locations. A further series of geotechnical investigations were undertaken for the present project, including a total of 87 machine drilled boreholes, with associated in-situ strength testing, laboratory testing on representative samples, and some pressuremeter tests and geophysical surveying.

The original site construction records (see also Ref. 1) and ground investigation data were reasonably comprehensive and all the data and investigations highlighted the variability in the consistency, quality and spatial distribution of the basalt.

4 BASALT CHARACTERISTICS

Basalt lava flows can prove a notoriously variable and difficult founding medium, particularly where individual flows are relatively thin. At locations where the flow is thick enough the basalt can be found to be relatively massive with columnar cooling joints whilst elsewhere the lava can be highly broken, rubbly and irregular shaped with fissures infilled with ash and soft alluvial soils. Generally individual thin rubbly flows are separated by scoria and infill materials, giving rise to a material more akin to a matrix of gravels within a loose/soft ash matrix, but also containing open structured rubble basalt. In addition voids and cavernous lava tubes exist within the flows. The transition between the above range of soil/rock conditions found within the lava flows can occur over a very short distance both horizontally and vertically, making the accurate definition of conditions encountered by borehole investigations difficult to interpret.

5 DESIGN METHODOLOGIES FOR FOUNDING ON BASALT

Foundation design solutions to dealing with such conditions include wide foundation pads, that can span over areas of poor quality materials and potential subterranean voids, and grouting works to cement the loose rubble and fill open voids. Where wide pad foundations are adopted it is also common practice to drill a rotary percussive hole to confirm the absence of major voiding. However, even with the large pad sizes adopted the critical design case remains the overturning load case where foundation pressures can be concentrated towards a corner or edge of a foundation. Without saturation of ground investigation points such weaknesses might normally only be exposed during a seismic event.

Grouting works can be undertaken on the basis of gravity grouting or pressure grouting approaches, but both have limitations. For gravity grouting there is the risk that lateral grout penetration beyond the original drill hole will be limited and that more intensive secondary grid drilling may be required. For pressure grouting there is the risk that very open structured rock mass will absorb very significant quantities of grout beyond the area that requires treatment and if back pressures can't be established then the grouting programme can extend significantly. Grout penetration can be limited in both methods where the cavities are tightly packed with low permeability materials, including cohesive alluvial and ash deposits.

New Zealand Geotechnical Society Inc. 19th Symposium, Queenstown 2013

Where drilling and grouting is undertaken it is normally over a limited depth beneath the pad foundations, such that sufficient confidence can be gained that any voiding/poor quality pockets that may be present beneath the treated area are effectively spanned by both the large foundation size and grout cemented cap.

6 GROUT TREATMENT BENEATH THE ORIGINAL VIADUCT PIER FOUNDATIONS

Foundation pads on the basalt, as constructed for the original viaduct, had been subject to pressure grouting treatment. The methodology involved drilling grout holes at each corner of a pad and grouting at depths of 1.5 m, 3 m and 4.5 m (albeit some pads do not appear to have been treated). Beneath the taller piers additional inclined drilling and grouting was also undertaken. The volumes of grout injected varied considerably between piers with final volumes ranging between nominal and up to 152 tonnes of cement with 248 m^3 of sand at one pier. This variability in grout take is consistent with the variability of the basalt characteristics as described above and the higher volumes also signalled potential cost and programme control issues for the grouting works for the new replacement viaduct.

7 GROUT TREATMENT FOR REPLACEMENT VIADUCT

Given the variability of the basalt and potential for voids to affect the performance of the structure, particularly under the high seismic loading scenarios, an extensive programme of drilling and grouting was undertaken under each and every pad foundation. To provide some greater confidence in the costs and programme a gravity grouting methodology with saturation drilling was adopted, with the option to step to a pressure grouting process. The methodology established provided for clear step changes in drill density and grouting techniques to accommodate variable ground conditions as they were encountered.

Gravity grouting of the basalt was principally targeted at testing and treating the 4 m depth of basalt immediately below the proposed founding level. However, due to the variable nature of the basalt it was also necessary to check the characteristics of the basalt to greater depths (8 m below formation level beneath the corners of each pad) to check for any larger potential voids.

Drilling followed an initial primary grid layout, with secondary infill holes where both drill and grout records indicated larger voids or grout acceptance. Locally tertiary and quaternary infill

drilling would also be required. Perimeter drilling was undertaken first to try to stem any potential excessive lateral grout flow beyond the immediate foundation footprint (NB these would not prevent grout loss through unfavourably orientated fractures). These grout holes were drilled using a percussive drilling rig. Rotary cored proof drilling was undertaken post-grouting to check on the efficiency of the grouting process.

The basic gravity grouting process is outlined briefly below:

- 16 primary perimeter holes drilled (4 on each side of the pad at 2 m centres). For any primary holes that took more than 0.3 m3 of grout, 2 secondary perimeter holes were drilled either side. This process was repeated for tertiary and quaternary holes.
- 25 primary internal holes within the foundation footprint at 1 m centres. For any primary internal holes that took more than 0.3m3 of grout, 4 secondary holes were drilled around the primary hole. This process was repeated for tertiary and quaternary holes.

8 DRILLING AND GROUTING OBSERVATIONS

The basalt encountered during the drilling process was, as expected, extremely variable in thickness and competency. Large voids were encountered within the basalt at some locations, as well as zones of fractured/scoriaceous basalt at various depths.

New Zealand Geotechnical Society Inc. 19th Symposium, Queenstown 2013

Figure 1 shows the protruding temporary PVC plastic casing, marking the drill hole layout in an area where a large void was encountered which interconnected with several of the drill holes.



Figure 1: Typical grid drilling layout



Figure 2: Lava tube feature as observed from a drill-hole. Note the adjacent drill-holes (temporarily cased) in the background (CCTV camera image) (approximately 1.5 m between drill casings).

8.1 Foundation Pads with Nominal Grout Takes

Six pads took nominal volumes of grout, and only required localised secondary and tertiary drilling and grouting. These pads took a total of between 6.5 m^3 and 10 m^3 of grout (an average grout volume of approximately 0.2 m^3/hole). These grout volumes equate to approximately 3% - 7% of the total basalt volume enclosed by the drill holes beneath the pads.

8.2 Foundation Pads with High Grout Takes

Four pads took larger volumes of grout, and required secondary, tertiary, and quaternary drilling and grouting. These pads took a total of between 30 m^3 and 60m^3 of grout each. The average

grout volume per hole reduced from 0.7 m^3/hole for the primary holes, to 0.4 m^3/hole for the secondary holes, and down to 0.15 m^3/hole for the tertiary and quaternary holes. These total grout volumes equate to approximately 12% - 27% of the volume of the basalt enclosed by the drill holes beneath the pad.

Of particular note was a lava tube feature within the basalt that was identified at one of these piers. This feature was picked up in several adjacent drill-holes by a drop of the drill rod during drilling, and CCTV inspections of the drill holes were undertaken to identify the size and continuity of the void (Fig. 2). The inspections indicated that void was between approximately 8.5 m to 10.5 m below ground level and had an approximate surface area of 15 m^2. Rather than using grout, a 6 mm aggregate concrete fill was used to pack this particular void. This feature alone took 30 m^3 of concrete to fill.

During the CCTV inspections of this feature, the camera was put down both percussion drill holes and fully cored rotary diamond holes. The differences between the bore profiles created by percussive and rotary drilling are illustrated (Figs. 3 and 4). These images highlight one of the potential difficulties of grouting through a percussion hole in basalt, where open fissures and void linkages have the potential to be blocked by the drill debris evident in the uncleaned percussive hole but absent in the cored hole. This effect could be sometimes observed in subsequent excavations through the grouted basalt where fine drill chippings could be observed obstructing potential grout flow paths.

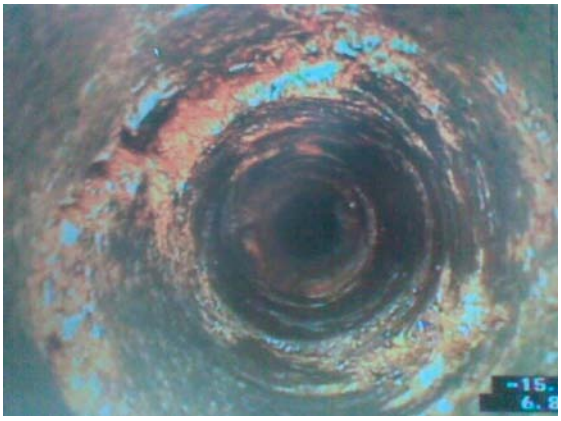


Figure 3: Corehole CCTV clean bore

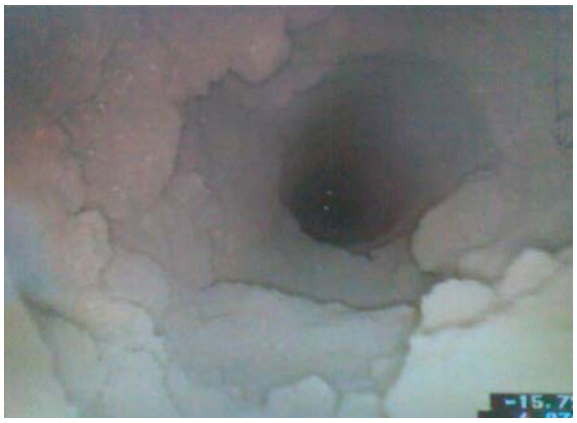


Figure 4: Percussive hole (dirty and clogged)

During the excavation (down to the design founding level) on one of the piers, the results of the grouting process were observed first-hand. The original foundation level was identified as comprising rubbly, scoriaceous basalt within an ash matrix. Excavation below the original design formation level could be undertaken relatively easily and it could be readily identified that the grout penetration into the soils and rock matrix was limited by the presence of the finer materials. The foundation excavation was therefore extended to a level at which consistently competent consolidated basalt was encountered. The walls of the excavation exposed grout columns where grout migration was clearly visible within the fractured basalt layer (Fig. 5).

New Zealand Geotechnical Society Inc. 19th Symposium, Queenstown 2013



Figure 5: Confined grout column (at top centre) with a bulbous migration of grout into the soil/rock matrix lower half of photo (grout clearly distinguishable as light grey)

8.3 Foundation Pads requiring pressure grouting

For two of the foundation pads the initial gravity grouting procedures had been completed to the process outlined above. However from observations of proof coring holes, which identified limited lateral grout migration and poor core recovery, and during initial excavations to formation level, the pier foundations were identified as requiring further grouting (deeper excavation to a more consistently competent formation level not being a practical option). A pressure grouting procedure was therefore trialled and developed as follows.

For the first pier, a highly fractured/scoriaceous layer existed between a depth of 3 m and 7 m. A pressure grouting regime was established through a trial series of rotary cored drill-holes. One of the objectives of the trial was to identify the potential distance for lateral migration of the grout. Coreholes were drilled 0.5 m, 1 m and 3 m away from a series of initial pressure grouted coreholes. During the trials, different coloured grout mixes were used to distinguish between various grouting stages. Significant grout migration was identified in the coreholes up to 1m away, but with grout (minor volumes) also identified up to 3 m distant from the injection point. For pressure grouting a drill hole density of 1.5 m spacing was therefore adopted.

Pressure grout holes were drilled to approximately 6 m depth (into the centre of the fractured/scoriaceous layer). A total of 17 holes were drilled in a grid pattern across the pad. Grout was pumped into each hole at a maximum pressure of 700 kPa. A total of 41 m^3 of grout was pumped into these holes during the pressure grouting process. This grout volume equates to approximately 23% of the total basalt volume enclosed by the drill holes beneath the pad.

A reduction of the grout takes/hole (almost to a nominal amount of approximately 0.15 m^3/hole) was observed for the last few holes drilled across the pad. A core photo of one of the later holes drilled is shown in Figure 6.



Figure 6: Core photo on completion of pressure Grouting



Figure 7: Large in-filled fissure within the competent basalt (minimal grout penetration)

Upon excavation of this pad down to founding level it was also observed that, even with both gravity and pressure grouting operations, grout penetration into a fissure feature within the basalt surface, infilled with fine ash materials, was limited. This feature, see Figure 7, was over-excavated and backfilled with mass concrete.

For the second pressure grouted pier, the founding level had been set at 5 m below existing ground level to allow for future development of the adjacent site for car park basements. During the course of excavation for this pier foundation a 4 m thick layer of competent basalt was removed leaving only 1 m of competent basalt below the pad formation level, below which it deteriorated into a highly fractured and scoriaceous zone.

The total grout volume taken by this pad (at the completion of the gravity grouting process) was 68 m^3. Proof coreholes showed that the fractured layer (6 m to 9 m depth) had not been adequately consolidated by the gravity grouting process. Also, an inspection at the foundation formation showed voids had remained open in close proximity to grouted holes. One of these voids accepted approximately 5m^3 of 6mm aggregate concrete. Due to these observations, a secondary pressure grouting regime was also adopted at this pier.

As this pier construction was on the critical path of the project, the pad base had to be excavated and poured. A grid of PVC pipes were therefore fixed to the reinforcing cage to enable drilling and pressure grouting below the pad base to occur following the pier construction. A total of 32 holes were drilled and grouted and a total of 26 m^3 of grout was pumped into these holes during this pressure grouting process. The average grout take/hole reduced considerably from 1.5 m^3/hole for the first few holes to 0.44 m^3/hole for the last few holes. This grout volume (when including the 68 m^3 from gravity grouting as mentioned earlier) equates to approximately 37% of the total basalt volume enclosed by the drill holes beneath the pad.

8.4 Observations of Grout Takes

Approximately 70% of all of the holes that were gravity grouted took nominal grout volumes of less than 0.3 m^3. The grout volume distribution per hole is shown in Figure 8 below. This graph also illustrates the sequential reduction in grout volumes through the primary, secondary, tertiary, and quaternary grouting stages.

New Zealand Geotechnical Society Inc. 19th Symposium, Queenstown 2013

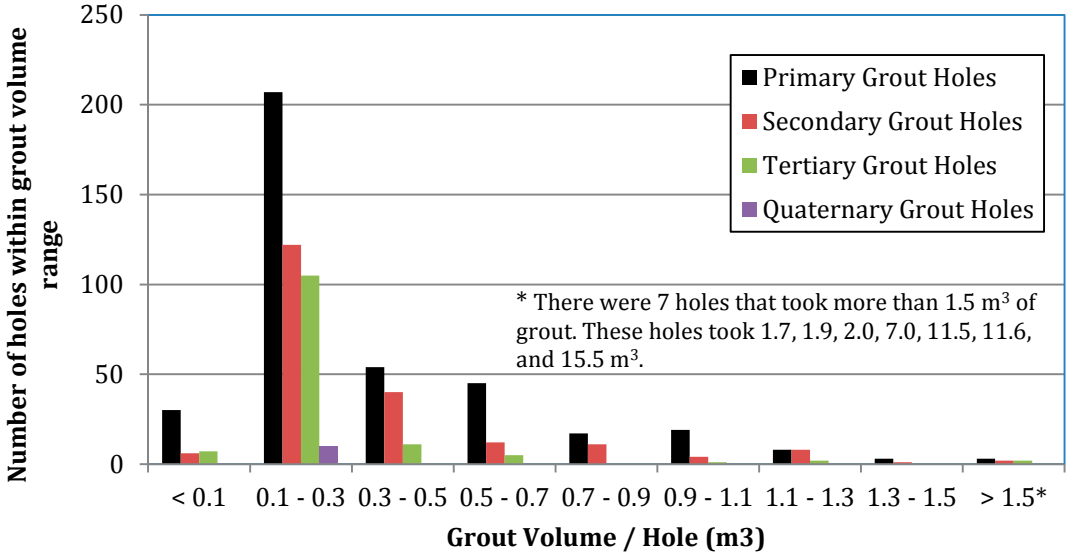


Figure 8: Distribution of grout volumes

9 CONCLUSIONS

The basalt encountered beneath the route of the viaduct has proven a difficult foundation medium to deal with, having highly variable, non-predictable spatial changes in composition and structure. Grout (and concrete) takes between drill holes have been highly variable, ranging between nominal drill hole volumes and up to 30 m^3, with grout acceptance characteristics changing over very short distances.

It is evident, from the progressive decay in grout take volumes between primary and subsequent drill holes, that gravity grouting was effective where the condition of the basalt was of good to moderate quality and consistency. Where gravity grouting has not been effective, especially where the rock is more rubbly, this was identified by post-grouting coring and formation inspection. The rapid decay in grout volumes between stages is also indicative of successful pressure grouting operations, also confirmed by post-grouting cores.

Even with saturation drilling it is evident that features within the basalt rock mass, particularly where inflilled with compact fine grained materials, can remain undetected and untreated, by pressure and gravity grouting techniques, and only become evident on exposure of the formation. Construction operations, including the drill, grout and verification processes therefore need to be flexible and adaptable, and construction programme float should be considered for construction on basalt.

REFERENCES

Built, J. W. (1965). The Newmarket Viaduct, Part 1 – *Site Investigation and Supervision*. NZ Engineering, pp491-498.

Snap-back response of piles in stiff clay

R J M Millin, L M Wotherspoon (Corresponding author), M J Pender
Civil and Environmental Engineering, The University of Auckland, NZ
l.wotherspoon@auckland.ac.nz

Keywords: Pile foundations, dynamic response, computational modelling

ABSTRACT

This paper details the results of a series of snap-back field tests of tubular steel piles embedded in well characterised stiff clay deposits. The effect of pile head mass and the magnitude of the pull-back force on the response of the system was investigated, with low magnitude impact hammer testing used to quantify the changes in elastic stiffness and damping of the system as a result of yielding of the soil and gap development adjacent to the pile after each snap-back. The static and dynamic response of the pile-soil system was modelled using Ruaumoko, with the pile-soil interaction represented using a range of discrete spring, dashpot and contact elements down the length of the pile. Good agreement between model and field test results was achieved for static pull-back tests and for the low load dynamic response throughout the test duration. For the high load dynamic response, the significant damping due to impact between the pile and soil was captured in the early parts of the dynamic response using contact elements, however these results diverged from the test data in the subsequent response cycles. The response of these later cycles of the tests could be captured separately using a model without contact elements. Modifications to the model capabilities are therefore needed to be able to capture the overall response of these tests with significant impact effects.

1 INTRODUCTION

The dynamic response of a pile subject to lateral loading is a complex phenomenon, resulting in interactions between the pile and surrounding soil. This type of loading represents real life scenarios of earthquake, wind, wave and machine vibration forces on a foundation. Extensive research (Matlock, 1970; Reese and Welch, 1975; Matlock et al., 1978; Gazetas and Dobry, 1984; Wotherspoon, 2009; M.Sa'don, 2012) has been carried out in this area, in particular, small scale model testing and the development of analytical and numerical models to simulate pile-soil interaction on the response of a laterally loaded pile. Most full-scale testing has used forced vibrations to investigate the dynamic response from the pile. However, recently snap-back testing has been shown to be a more economical alternative, whilst still providing similar results to forced vibration tests (M.Sa'don, 2012). From the available data it is still unclear what level of damping and stiffness should be used when considering non-linear soil behaviour.

This paper details the results of a series of snap-back field tests of tubular steel piles embedded in well characterised stiff clay deposits. Details of the set-up and results of snap-back field testing of tubular steel piles embedded in stiff clay are first presented. The test response is then numerically modelled in Ruaumoko using discrete spring, dashpot and contact elements to represent the pile-soil interaction.

2 TEST SET-UP

Testing was carried out on two 273 mm diameter steel tube piles from an existing 2x2 pile group (centre spacing of 11 pile diameters) driven closed ended to an embedment depth of approximately 24 pile diameters. The site in Albany, Auckland had a stiff residual clay soil profile, with extensive site characterisation using seismic CPT, spectral analysis of surface

New Zealand Geotechnical Society Inc. 19th Symposium, Queenstown 2013

waves (SASW) and lab testing indicating a variation in small strain shear modulus from 36 MPa at ground surface to 86 MPa at the pile embedment depth. Two of the piles in this group were used as test specimens for this research, with the remaining piles used as reaction piles. Lead masses were added to a steel bracket attached to the pile head to vary the inertial forces during the snap-back response, with four different levels of pile head mass tested during the study. A double acting jack and hydraulic ram were used to provide the static pull-back force, which was measured using a load cell. Linear Variable Displacement Transducers (LVDTs) and strain gauges were used to measure pile head displacement and force respectively.

2.1 Snap-back test procedure

Snap-back tests were carried out by jacking the test pile towards a reaction pile to a target force, and then releasing the test pile to produce the snap-back free-vibration response. The pull-back phase of the snap-back tests defines the static pile lateral response. The key components of snap-back test set-up are provided in Figure 1, with the dynamic response initiated using a quick-release coupling. Free vibration hammer tests were carried out before and after each snap back, where a low input force from a blow of a cushioned sledgehammer was applied to the top of the pile to excite the elastic natural period of the pile-soil system. The testing program is outlined in Table 1.

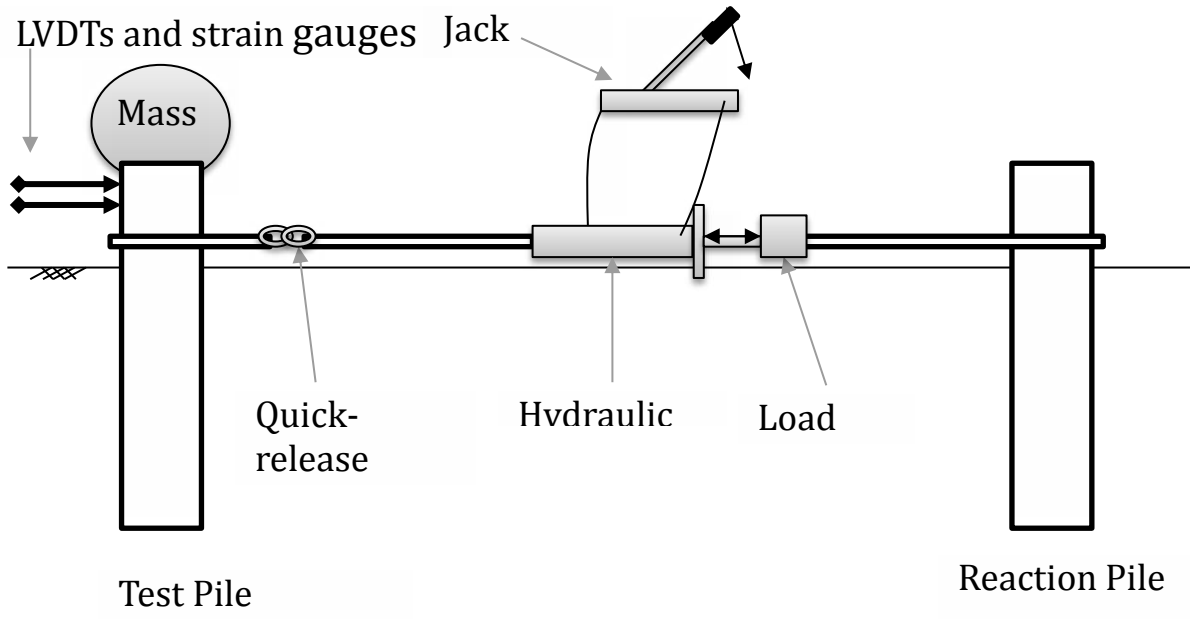


Figure 1. Schematic of snap-back test procedure

Table 1. Snap-back test program including hammer test details

Snap-back test details Pile 1	Hammer test number before/after snap-back
10 kN 324 kg pile head snap-back 1	1-2
10 kN 609 kg snap-back 1	3-4
10 kN 1275 kg snap-back 1	5-6
120 kN 324 kg snap-back 1	7-8
120 kN 609 kg snap-back 1	9-10
120 kN 1275 kg snap-back 1	11-12
120 kN 1275 kg snap-back 2	13-14
120 kN 609 kg snap-back 2	15-16

Snap-back test details Pile 1	Hammer test number before/after snap-back
120 kN 324 kg snap-back 2	17-18

3 STATIC PILE RESPONSE FROM FULL-SCALE FIELD TESTS

Force displacement plots for 120 kN pull-back tests on the test pile are presented in Figure 2. The separation between curves for successive tests has been attributed to an observed increase in the pile-soil gap depth during testing (measurements not shown). An increased gap depth results in less pile-soil contact and hence a softer response for subsequent tests. The greatest change in stiffness for an individual test occurs during the first 120 kN pull-back test. No residual gapping was observed around the pile at the start of the test, therefore a greater change in pile-soil contact and hence stiffness was possible. Non-linearity in the static stiffness is generally more evident during the early loading stages. Non-linear response occurs as a result of soil yielding and/or pile-soil gap formation, due to soils inability to support tensile stresses. A relatively linear stiffness is present at later loading stages because the linear cantilever pile deformation governs the response when large gap depths have developed.

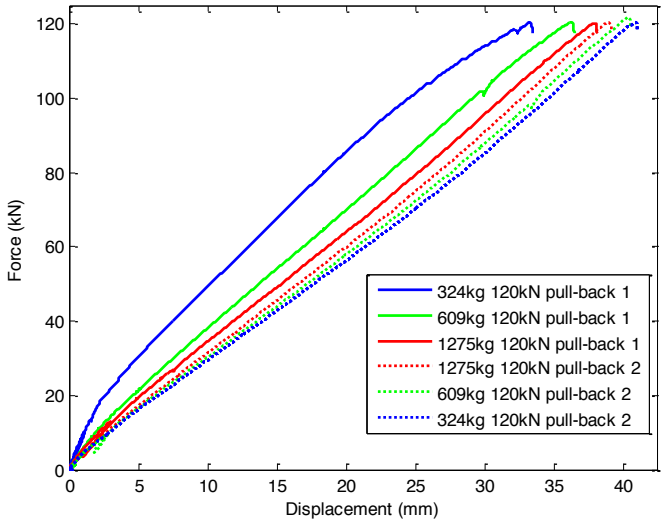


Figure 2. Pull-back force displacement plots for 120 kN snap-backs on test pile.

4 DYNAMIC PILE RESPONSE FROM FULL-SCALE FIELD TESTS

4.1 Change in natural frequency

The variation in the natural frequency of the test pile is presented in Figure 3, with the three different levels of pile head mass used during testing highlighted. Frequency is plotted against the hammer test number, with hammer tests carried out before and after each of the snap-back tests listed in Table 1. There is a negligible change in natural frequency before and after each of the 10 kN snap-back tests, supporting the visual observations indicating no gap development between the pile and surrounding soil during these tests. The variation in the natural frequency between these first three snapback tests (hammer tests 1-6) results from the addition of mass to the pile head. The soil gapping that developed during the 120 kN tests is evident through a reduction in natural frequency for each pile head mass, where a reduction has occurred between bars of the same colour, or mass. A maximum gap depth of approximately four pile diameters was measured during testing.

4.2 Damping

4.2.1 Damping ratio collection techniques

Two techniques are used to calculate the level of damping associated with the test response. The logarithmic decrement method (Thompson, 1988) utilises the relative magnitude of two adjacent peaks of the free vibration response to determine a value of damping for the pile-soil system response. The second damping collection technique is defined by exponential envelopes corresponding to the displacement solution for an equivalent viscously damped SDOF system (Chopra, 2006), where these envelopes are fitted to give the 'system' damping of the response.

Significant energy dissipation effects due to impact between the pile and surrounding soil led to two distinctly different portions of the response. Impact energy dissipation occurs during the early cycles of the test, resulting in a heavily damped response ('impact response'). In the absence of this impact, a response with a lower level of damping is present during later cycles ('cyclic response'). Thus two separate pairs of exponential envelopes are fitted to each portion of the response to provide a measure of the system damping during the 'impact' and 'cyclic' response of the system.

New Zealand Geotechnical Society Inc. 19th Symposium, Queenstown 2013

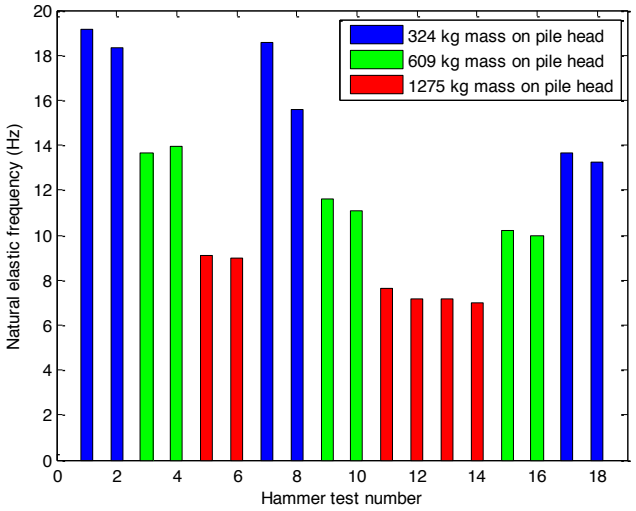


Figure 3. Natural elastic frequencies of the test pile

4.2.2 Damping ratio data

Using the approaches explained above, one value of system damping is obtained for each test, while multiple values of the logarithmic damping are obtained as a value is calculated for each cycle of oscillation in the test. Damping ratio data from all the low input force hammer tests is presented in Figure 4. Exponential system damping appears to account for the varied nature of the response. Higher damping is expected for lower mass levels and for later tests where a reduction in stiffness has occurred due to pile-soil gap depth growth. There is a general agreement with this trend in Figure 4; however, some inconsistencies are evident for lower mass levels, particularly the 324 kg pile head mass. At lower pile head mass levels the greater contribution of distributed pile mass to the overall pile response may move the response away from the SDOF assumption.

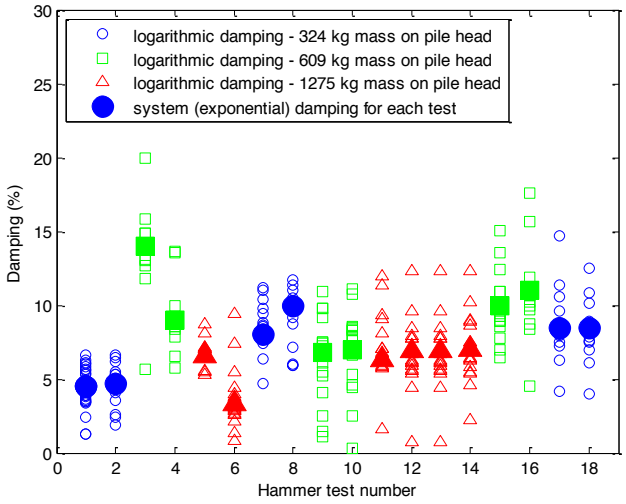


Figure 4. Damping ratios computed from hammer tests using the logarithmic decrement method and exponential system damping envelopes.

Impact and cyclic response exponential system damping for all snap-back tests is shown in Figure 5. Impact response system damping is shown to increase as pile head mass increases, a consequence of larger masses increasing the impact energy dissipation effects as the pile impacts with the surrounding soil following the initial pull-back peak release. The maximum impact response system damping computed is 50% from the 1275 kg pile head.

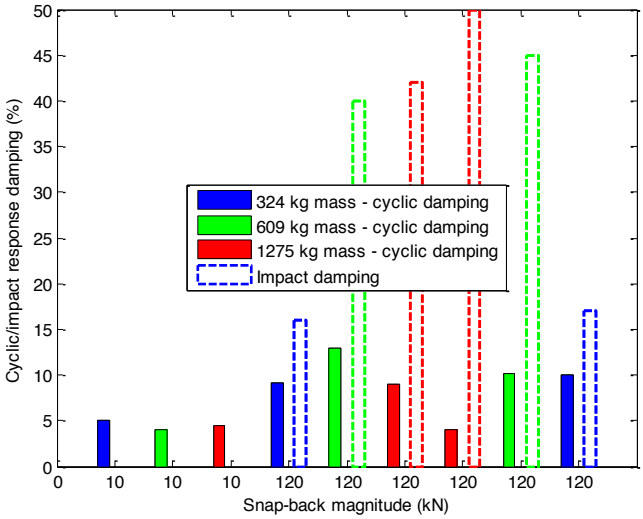


Figure 5. Exponential system damping for all snap-back tests, illustrating snap-back order.

5 NUMERICAL MODELLING OF LATERAL PILE RESPONSE

The dynamic test response is compared with those predicted by the numerical Winkler spring model (Vesic, 1961; Matlock, 1970; Reese and Welch, 1975; Matlock et al., 1978; Gazetas and Dobry, 1984; Wotherspoon, 2009) developed in Ruaumoko 3D (Carr, 2004). An overview of the Winkler spring model developed for this research is provided in Figure 6. Discrete horizontal spring and dashpot elements were used to represent soil pile-soil interaction, connected to pile nodes at a spacing of 0.05m on both sides of the pile, with pile mass lumped at these nodes. At each depth these elements were arranged with a non-linear spring attached to the pile node, in series with an elastic spring and dashpot in parallel. The key components of the model are as follows, with the latter two points used for modelling the dynamic response:

- Spring members were used to represent soil stiffness.

New Zealand Geotechnical Society Inc. 19th Symposium, Queenstown 2013

- Bi-linear hysteresis rule with slackness utilised to model the inability of soil to support tensile stresses and the development of residual gapping around the pile. A bi-linear response was used to account for compressive soil yield and soil hysteretic damping.
- *P-y* curves for static loading were developed from CPT data, utilising procedures from Reese and Welch (1975) for stiff clays with no free water to model the non-linear load deformation response of the springs. The bi-linear hysteresis model was fitted to the p-y curves at representative depths by defining a yield point and a post-yield stiffness factor of the initial stiffness.
- Soil radiation damping was represented using dashpot members.
- Contact members were introduced into the model to account for effects of pile-soil impact energy dissipation during the initial stages of the snap-back.

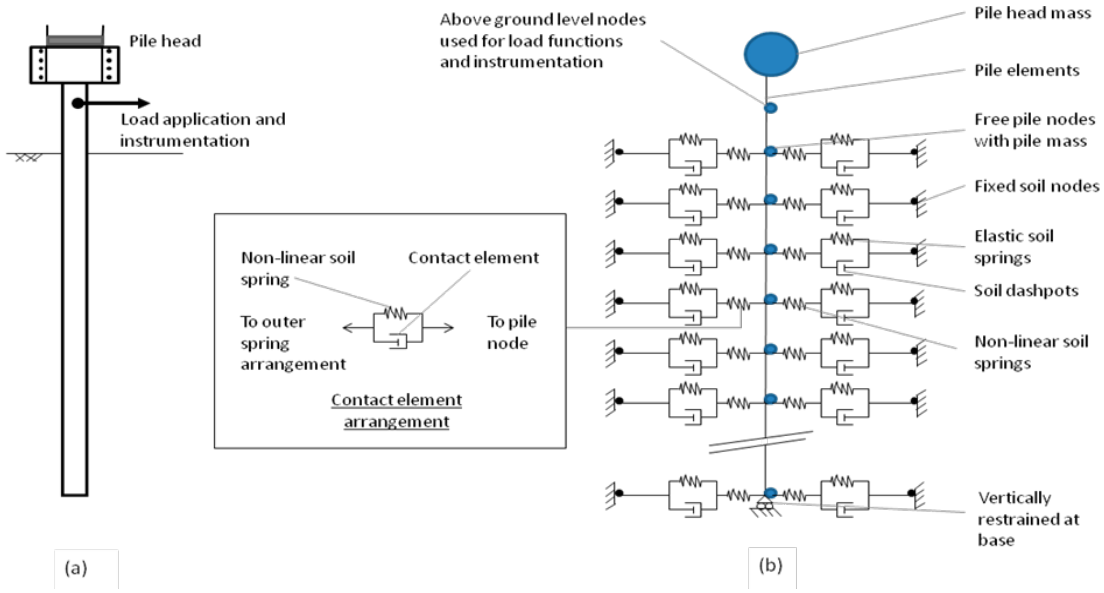


Figure 6. (a) Field testing set-up; (b) Numerical Winkler Spring model representation.

5.1 Pushover response comparison with field data

The comparison between pushover model and Pile 2 test data for three pull-back tests is shown in Figure 7. Lower force tests are presented as a greater range of non-linearity is experienced during these earlier tests, where a relatively shallow residual gap is present compared with large residual gap depths implemented for higher force tests. The residual gap depth is altered between models to follow a similar response to the corresponding field test. Both the initial and non-linear stiffness are represented reasonably well by the numerical model. There is some small deviation at later loading stages as soil deformation is at a maximum.

5.2 Dynamic response comparison with field data

The series spring model developed to predict the dynamic response is only capable of capturing the test response at later cycles where the inelasticity evident in the response is not dominated by impact effects. Contact members were incorporated to account for impact energy dissipation developed in the initial stages of the snap-back. Figure 8 compares the model and test results for the 120 and 7.5 kN snap-back test on Pile 2. The series spring model (Fig. 8 (c)) is released from the third peak of the 7.5 kN snap-back response where impact effects are not significant and produces a good comparison with the snap-back test beyond this point. Although damping is well represented there is a slight stiffness shift which is attributed to the reduced pull-back peak of the model compared with the original pull-back peak during testing. This results in a stiffer model response due to a reduction in gap growth.

The models with contact elements (Figs 8 (a), (b)) achieve the necessary energy dissipation developed during testing over the first few peaks, however it diverges with the test data during later cycles where there are no impact effects. The arrangement of the contact member means that a high level of energy dissipation is provided throughout the response and cannot be removed from the response after several cycles, where pile-soil impact effects become negligible during testing. The 120 kN snap-back contact model (Fig. 8 (a)) contains a greater level of forces than the corresponding 7.5 kN snap-back (Fig. 8 (b)), so divergence with test data is more prominent. The only difference between the contact model and series spring model is the addition of the contact elements. Further research with some modification of the contact element model is required to account for the overall test response.

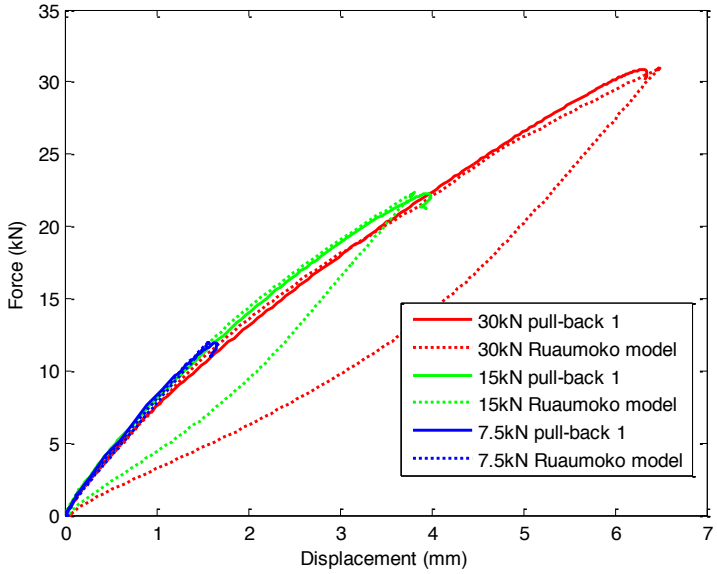


Figure 7. Ruaumoko pushover modelling for 7.5, 15 and 30 kN series one pull-back tests Pile 2.

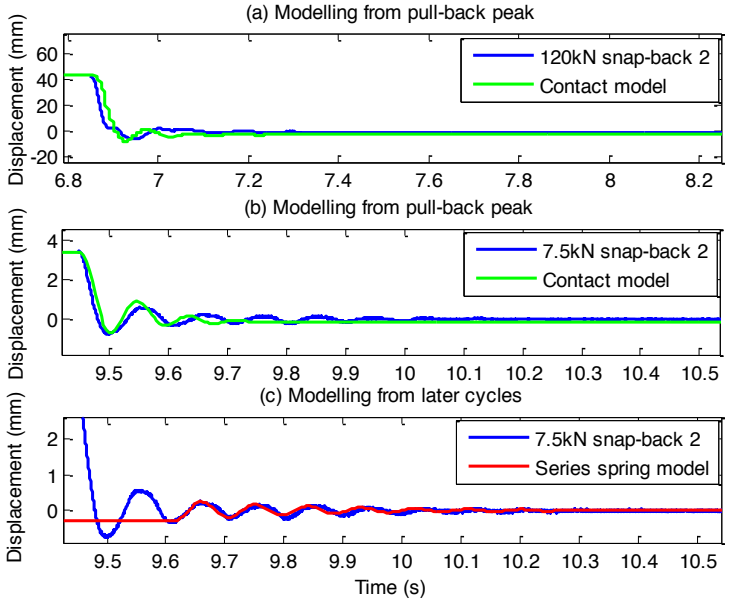


Figure 8. Ruaumoko contact and series spring model comparison on Pile 2 with (a) 120 kN snap-back from start of test; (b) 7.5 kN snap-back from start of test; (c) 7.5 kN snap-back from third peak.

6 CONCLUSIONS

A series of full-scale snap-back field tests on a 273 mm diameter tubular steel pile was performed at a stiff residual clay site in Albany with varying pile head masses. This paper presented the computation of changes in the natural frequency and damping throughout the test series. The test response has been captured with reasonable accuracy using a discrete spring model in Ruaumoko. The following key points are summarised from this paper:

- A reduction in pile natural frequency determined from free-vibration hammer tests has been observed during testing due to increased gap growth around the pile. A maximum gap depth of four pile diameters was measured during testing.
- Damping determined from hammer tests is typically in the order of 5 – 10%.
- Impact energy dissipation developed near the pull-back peak for snap-back tests has resulted in two distinctly different portions of the response at the start and for the later cycles. Separate envelopes were fitted to give an ‘‘impact’ and ‘‘cyclic’ response system damping for the respective portions. Unsurprisingly, impact response system damping increased as the pile head mass increased. A maximum impact response system damping of 50% was computed for the largest mass level.
- Modal, pushover and dynamic responses were represented reasonably well in Ruaumoko using a Winkler spring model (Millin, 2012). Contact members were introduced into the dynamic model to account for contact damping developed near the pull-back peak of snap-back tests. A limitation identified in the modelling approach is that the contact model is unable to account for the later cycles of the test response where contact damping is no longer present during field testing.

REFERENCES:

Carr, A. (2004). *"RUAUMOKO 3D inelastic three-dimensional dynamic analysis program: User manual."* University of Canterbury – Department of Civil Engineering, Christchurch, NZ.

Chopra, A. K. (2006). *"Dynamics of structures: theory and applications to earthquake engineering."* Third edition, Prentice Hall, Englewood Cliffs, New Jersey, 2006.

Gazetas, G. and Dobry, R. (1984). “Horizontal response of piles in layered soils”, *Jnl. Geotechnical Engineering* 110 (1), 20-40.

M.Sa’don, N. (2012). Full scale static and dynamic loading of a single pile. *PhD thesis*, Civil and Environmental Engineering Department, University of Auckland.

Matlock, H. (1970). "Correlations for design of laterally loaded piles in soft clay". *2nd Offshore Technology Conference*, Houston, 1, 577-594.

Matlock, H., Foo, S. H., and Bryant, L. L. (1978). "Simulation of lateral pile behaviour." *Earthquake Engineering and Soil Dynamic*, ASCE, Pasadena, California, 600-619.

Millin, R. J. M. (2012). Characterising the snap-back response of single piles in stiff clays, *Masters Thesis*, Civil and Environmental Engineering Department, The University of Auckland.

Reece, L. C. and Welch, R. C. (1975). “Lateral loading of deep foundations in stiff clay”, *Jnl. Geotechnical Engineering* 101, 633-649.

Thompson, W. T. (1988). *“Theory of vibration with applications”*, 3rd edition. Prentice-Hall.

Vesic, A. (1961). "Beams on elastic foundations." *5th Int. Conference on Soil Mechanics and Foundation Engineering*, Paris, 1, 845-850.

Wotherspoon, L. M. (2009). Integrated modelling of structure-foundation systems, *PhD Thesis*, Civil and Environmental Engineering Department, The University of Auckland.

A pragmatic and non-intrusive procedure for assessing the post-earthquake structural integrity of piled foundations

S R Moniz
Coffey Geotechnics, Christchurch, New Zealand
Safia_Moniz@coffey.com (Corresponding author)

N K Harwood
Coffey Geotechnics, Christchurch, New Zealand
Nick_Harwood@coffey.com

H G Poulos
Coffey Geotechnics, Chatswood, Australia
Harry_Poulos@coffey.com

Keywords: piles, liquefaction, lateral pile capacity, non-destructive, bridges

New Zealand Geotechnical Society Inc. 19th Symposium, Queenstown 2013

ABSTRACT

Following the Canterbury Earthquake Sequence, several piled structures were damaged, but not beyond repair. This resulted in a situation where the structural integrity of existing, in-service piles needed to be evaluated without extracting the piles. Structural engineers needed this evaluation for future load carrying capacity and, conversely, property owners needed a useful evaluation of the likelihood and extent of damage that occurred to the foundations to determine the current integrity of the structure.

Following natural disasters, when communities are hanging by a thread, there is a dire need for easily executable, high-quality, yet practical, seismic geotechnical engineering solutions for input into evaluating the safety of structures for use.

Attempting to bridge the gap between theory and practice, this paper describes a pragmatic, non-intrusive means of evaluating the likely damage to, and a structural integrity assessment of, existing piled foundations following an earthquake. This approach involves carrying out a pseudostatic lateral pile analysis where account is taken of (1) inertial loads from the superstructure, (2) kinematic loads due to cyclic ground displacements and (3) degraded soil parameters of liquefiable soil. The resulting bending moments and shear forces generated from the lateral pile analysis are then compared to the design moment and shear capacity of the piles. The method developed is practical, requires comparatively little computation effort, allows the user to "get a feel" for what may have occurred regarding the likelihood of damage and provides an indication of how the existing piles are likely to perform under future design events.

1 INTRODUCTION: EVOLUTION OF THE METHOD

During the Canterbury Earthquake Sequence, several piled structures (including bridges) were damaged, but not beyond repair. A need arose where the structural integrity of existing piled foundations needed to be evaluated without extracting the piles. Structural engineers needed this evaluation for future load carrying capacity and, conversely, insurers and property owners needed a practical evaluation of the likelihood and extent of damage that occurred to the foundations.

The objective of this study was to develop a simple, practical method of addressing this specific problem: to determine the structural integrity of in-service piled foundations. This method was first developed for a piled building. However, the same principles can be applied to a piled bridge.

To evaluate existing piled foundations, the authors first explored the notion of using a physical method to test the piles. The first method considered was the PIT (Pile Integrity Test). This test is a routine method used to assess the integrity of piles at the time of construction. The PIT involves striking the top of the installed pile with a small hammer. The impact of the hammer generates a compressive stress wave in the pile, and an accelerometer placed on top of the pile monitors the accelerations associated with this wave. The stress wave propagates down the pile shaft, and is reflected when it encounters either the pile toe or a non-uniformity of the shaft (e.g. a crack or necking). These reflections cause a change in the acceleration signal measured on the pile top, which is picked up and processed by the equipment and interpreted by an experienced engineer[1].

After discussions with the manufacturers of the PIT equipment, it became apparent that it would not be possible to assess the structural integrity of piles under existing structures, especially in situations where access to the pile top is precluded, there are no reliable 'as-built' records and the lengths of the piles are not accurately known. Data acquisition and analysis of test records of existing, in-service piles can be particularly challenging as the data is often complex and does not always allow for confident interpretation.

The authors concluded that an alternative method had to be considered that relied upon non-intrusive methods and analysis. A literature review of the methods used to assess the structural integrity of in-service piles was carried out. Given the 'real-world' time and cost restraints and considering the frenzied post-earthquake environment, not only would the selected method have to be technically robust, but it would also have to be relatively quick to perform, not depend on expensive lab and field testing, be easy to repeat and be able to use existing commercially available software.

The method must also be able to be adaptable to the soil conditions in Christchurch. The soils in Christchurch consists of geologically-young, deep alluvial soils. These ground conditions are complex, highly variable over short distances and generally provides numerous challenges for geotechnical engineers. The city of Christchurch is low lying and as a result the groundwater table is generally high all year round. These ground conditions provide the perfect conditions for liquefiable soils. It is therefore not surprising that one of the main geo-hazards in the region is the severe ground deformations associated with liquefiable soils.

Liyanapathirana and Poulos (2005) state that liquefaction of saturated soils subjected to earthquake loading is one of the major factors affecting the behaviour of pile foundations and subsequent building failure in seismically active areas. They discuss a number of methods for the seismic analysis of piles based on the one-dimensional Winkler model. However, these methods cannot predict pile behaviour in liquefiable soil and are therefore inappropriate for instances where deep liquefiable deposits will govern the pile response during seismic events. Since then other Winkler-type models have been developed but these methods require complex dynamic finite element analyses be carried out to determine the pile response in liquefiable soils. These methods are technically challenging and time consuming and are difficult to apply in routine practice. It would be difficult to employ these methods under time and delivery constraints for a large volume of projects.

[1] http://www.grlengineers.com/services/pit/

More recently, pseudostatic methods have been developed to evaluate the response of single piles under earthquake loading. Although simplified methods to carry out pseudostatic analyses on piles have been proposed (e.g. Tabesh and Poulos 2001, Liyanapathirana and Poulos 2005, Castelli and Maugeri 2009), they still require relatively advanced analyses, such as seismic free-field analysis to obtain time histories and soil displacements.

The authors have found that the pseudostatic lateral analysis presented by Cubrinovski, Ishihara and Poulos (2009), provides the user with a simple, practical and user-friendly means of calculating the bending moments and shear forces generated in a pile subject to earthquake loading. The crux of the method presented in our paper to assess the post-earthquake structural integrity of piles foundation is based on this method. This paper also discusses how the results of the developed analysis method were interpreted and their practical significance.

2 THE PROCEDURE

A flow chart has been developed to describe the procedure used for assessing the structural integrity of in-service piled foundations, Figure 1.

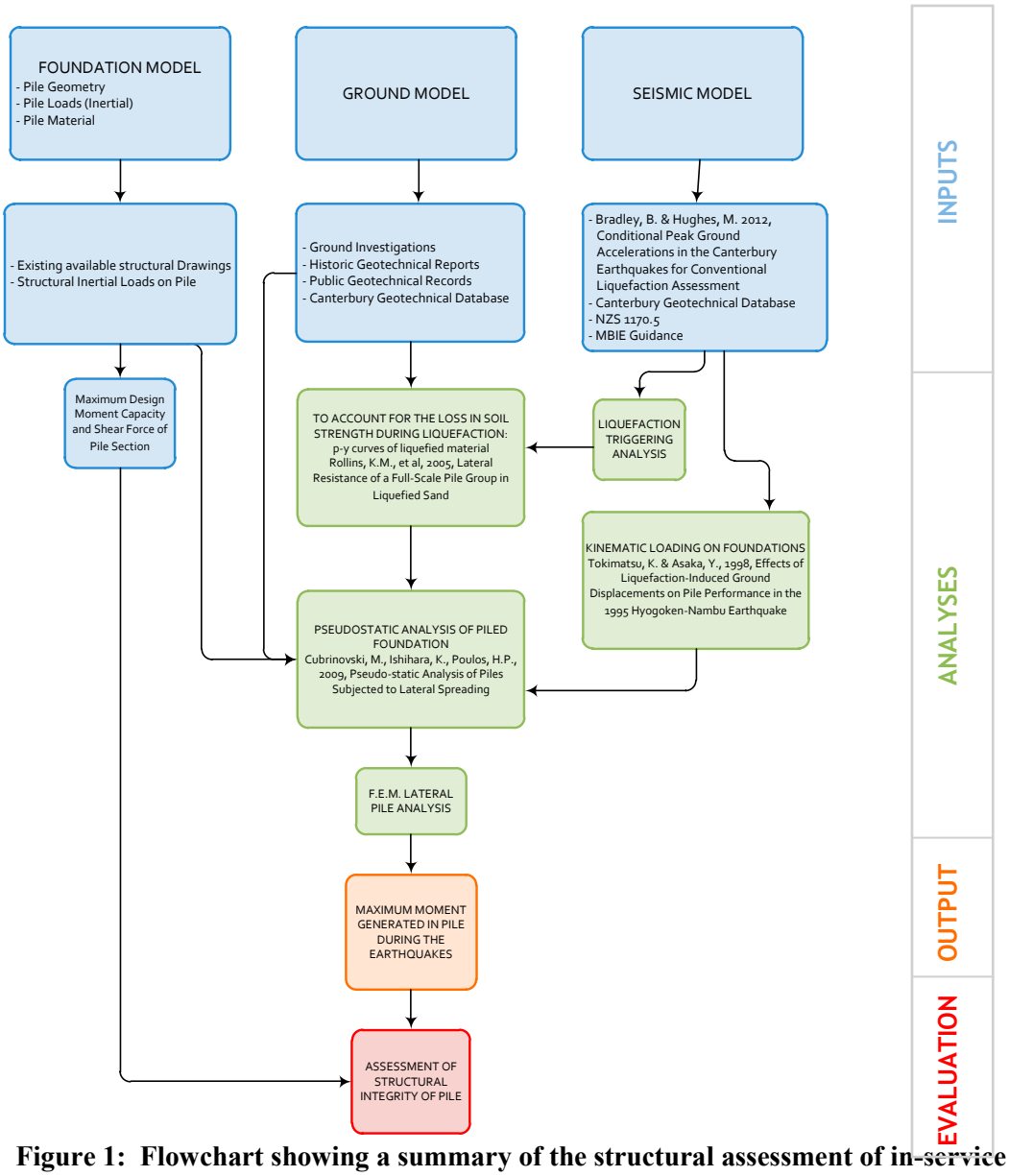


Figure 1: Flowchart showing a summary of the structural assessment of in-service piled foundations

2.1 Inputs

Inputs of the procedure are the foundation model of the existing piled foundation, the ground model under the existing structure, and the seismic demand that the structure has been or will be subjected to.

Modelling existing in-service foundations can be a real challenge, depending on the quality and availability of as-built drawings and the age of the structure. The user should be aware that they are essentially modelling an idealized version of the foundations that were actually installed. Examination of construction quality control documents can provide an appreciation of the as-built condition of the existing foundations, which can differ significantly from the design drawings. This, of course, is one of the limitations of modelling an existing foundation.

The ground model can be determined from conventional geotechnical investigation methods. Bradley and Hughes (2012) developed a methodology for prediction of experienced conditional peak ground acceleration (PGA) values which provides distributions with both median and standard deviations for the major events of the Canterbury Earthquake Sequence. These values are represented through contours and are available on the Canterbury Geotechnical Database. These contours were used to estimate the ground demand experienced at a particular site in the Canterbury region for individual events. The demand from each event, in the form of the cyclic stress ratio profile was then compared to the ground demand from various proportions of design events (e.g. 50% ULS, 75% ULS, 100% ULS). This is useful because it allows the user to evaluate the actual damage that occurred to the site using the design event as an index. Additionally, it is easier to estimate inertial loads for some proportion of a design event than it is for an actual event where time-history data is not available.

A liquefaction analysis was carried out using the standard proprietary software. From analysis the soil layers which are susceptible to liquefaction triggering are deduced and the ground model for the analysis is developed.

2.2 Using the simplified pseudostatic analysis

The method of pseudostatic lateral pile analysis is a lateral pile analysis where account is taken of (1) inertial loads from the superstructure, (2) kinematic loads due to cyclic ground displacements and (3) degraded soil parameters of liquefiable soil layers.
The pseudostatic method, as presented by Cubrinovski et al. (2009) is based on the model presented in Figure 2. The model is based on a three-layer soil system where the pile is represented by a continuous beam. The upper layer is a non-liquefiable 'crust' layer. Its contribution to the ground response is accounted for in the form of a lateral earth pressure.

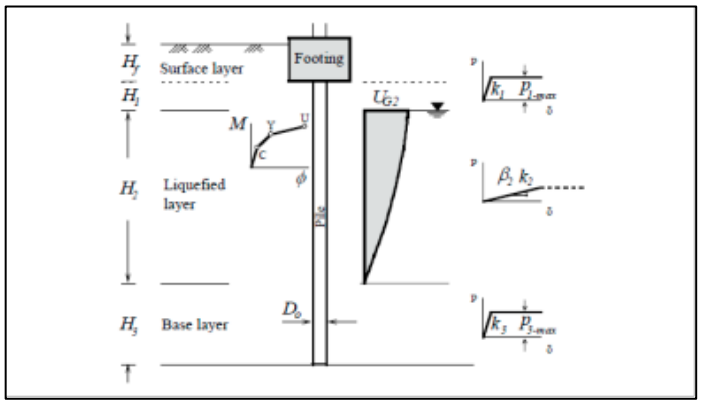


Figure 2: Characterization of non-linear behaviour and input parameters of the pseudo-static model

The interaction between the soil and the pile in the liquefied layer is represented by an equivalent spring (b_2k_2). The subgrade reaction is represented by k_2. b_2 is a scaling factor representing the degradation of stiffness due to liquefaction and nonlinear behaviour.

To estimate b_2 a relationship between stiffness degradation and ground displacement was provided in the paper by Cubrinovski, Ishihara and Poulos (2009). However, the uncertainty in the range of values provided for b_2 was the greatest for ground displacements less than 10 cm. This made it difficult to incorporate stiffness degradation into the analyses for cases where lateral spread had not occurred, and the cyclic ground displacements and pile deflections were not large. As a result, other methods for accounting for the stiffness degradation were explored.

Rollins et al. (2005) developed an empirically derived equation which describes the load-displacement relationship for fully liquefied sand. Subsequently, *p-y* curves were developed using this equation and has since been integrated into the commercially available software LPILE. Users are cautioned that the use of the equation be limited to deflections of less than 150mm. Rollins et al (2005) state that these *p-y* curves provide reasonable estimates of the measured response of full-scale piles in liquefied sand. Another benefit of using LPILE was that it allows the user to analyse a more detailed soil system.

The kinematic loads due to cyclic ground displacements were derived using a method presented by Tokimatsu and Asaka (1998). In their paper, a chart is presented giving the maximum cyclic shear strain developed during an earthquake as a function of SPT *N-value* and the Cyclic Stress Ratio. When the strain is multiplied by the thickness of the liquefied layer, the result is the cyclic ground displacement.

3 CASE STUDY

The following case study is a simplified example of the procedure. When we have run an analysis for a project we have conducted sensitivity checks and run a series of load cases. The entire process can be carried out parametrically, proportionately varying the ground demand and the inertial loads; however, in this case, the process will be demonstrated once. The resulting bending moment and shear force profiles are examined and an evaluation of the structural integrity of the piles can be made.

3.1 Case Study - Inputs

FOUNDATION MODEL
275mm Square Reinforced Concrete Pile
Pile Length: 20m
Concrete Compressive Strength: 82.5 MPa (Note: This is the estimated long-term in-ground strength from a real site)
Max. Coarse Aggregate Size: 19mm
Rebar Yield Strength: 460 MPa
Elastic Modulus: 200,000 MPa
Bar Size: US Std. #8
No. of Bars: 12
Concrete Cover to Edge of Bar: 76.2mm
Pile Loads (Inertial): Axial Load = 500kN and Shear Force = 20kN, 40 kN and 60 kN (Provided by the structural engineer).

New Zealand Geotechnical Society Inc. 19th Symposium, Queenstown 2013

SEISMIC MODEL

Seismic Demand: Design ULS IL2 Event, M: 7.5 and PGA: 0.35g

Note: This earthquake demand was just for the purpose of the case study. If a back analysis were actually being carried out then the demand from the actual event would be used in the analysis.

If the demand from an actual event is not readily available then the author suggests that a sensitivity analysis be carried out to ascertain the possibility of damage based on the range of likely demand experienced. Or if no data at all is available then this method would not be applicable.

GROUND MODEL

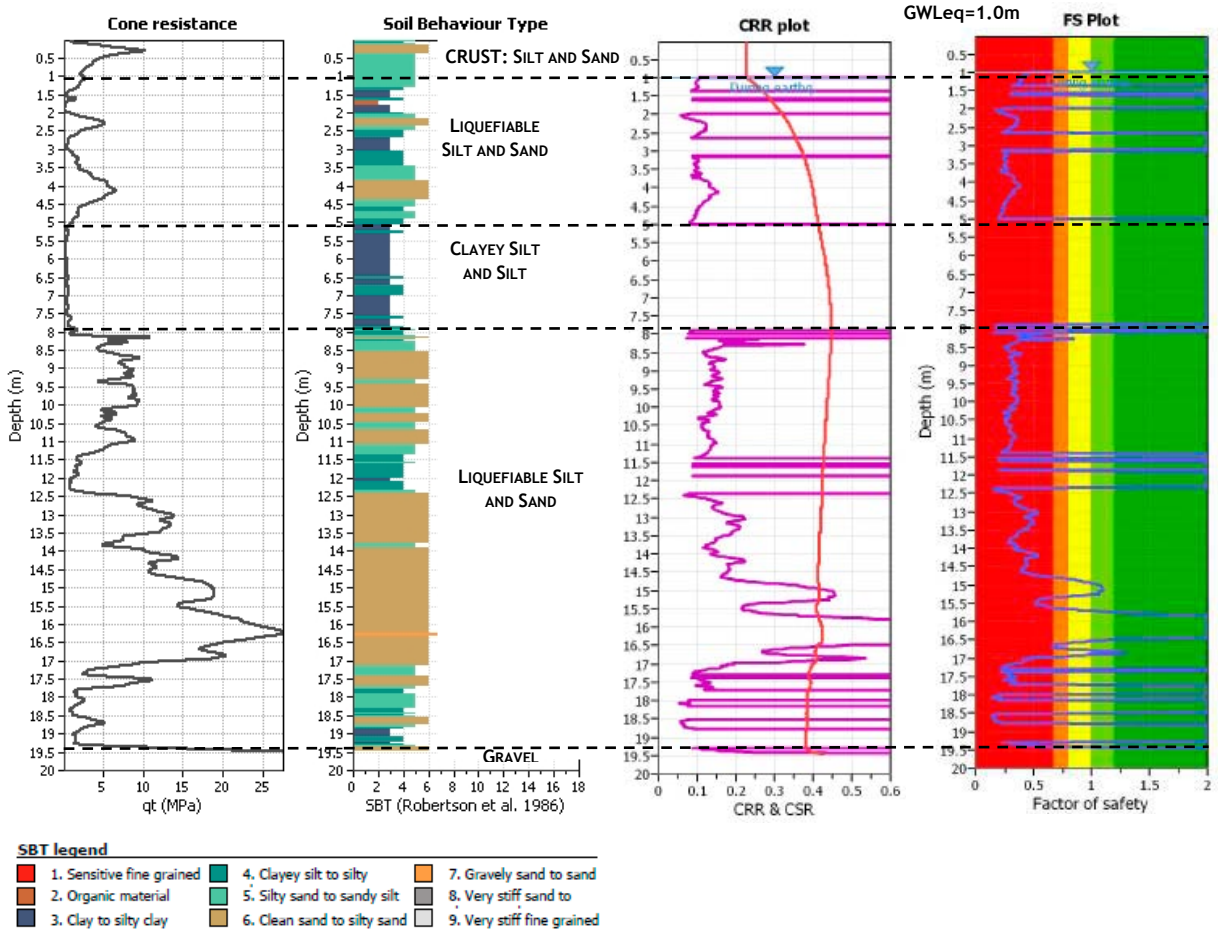


Figure 3: Ground model identifying liquefiable soil layers

3.2 Case Study - Analyses

The ground displacement profile was carried out using the method presented in Figure 9 of Tokimatsu and Asaka (1998). This ground displacement profile and the inertial pile loads were entered into LPILE. The following charts (see Figure 4) show how the soil profile was modelled and the soil parameters that were assigned to each layer.

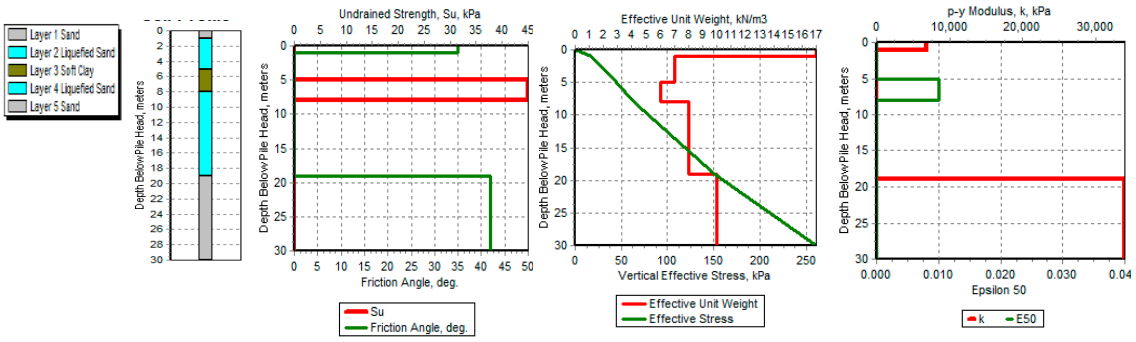


Figure 4: Idealised soil profile and soil parameters used in case study

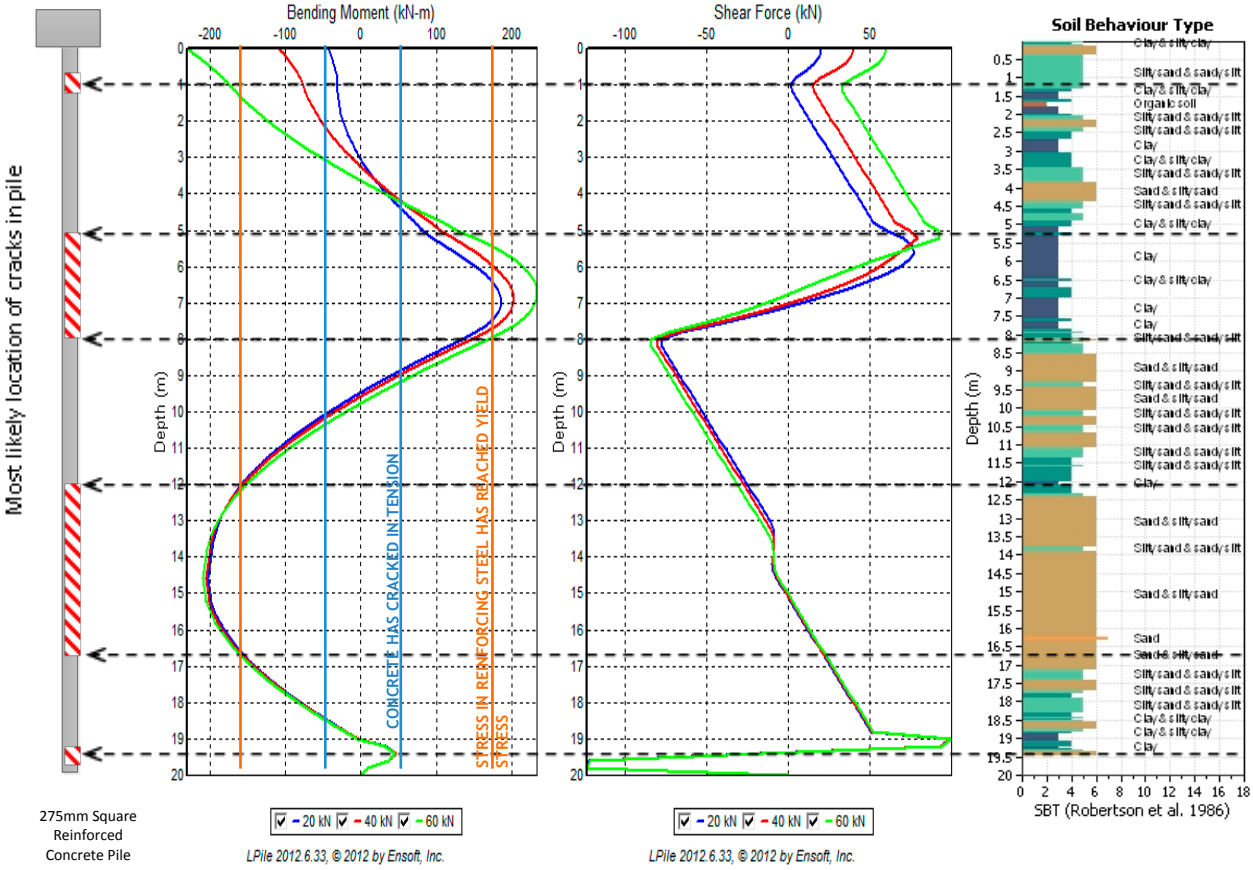


Figure 5: Pseudostatic lateral pile analysis results: bending moment and shear force diagrams

The results of the analysis are presented in Figure 5. During physical inspection of piles damaged during the 1995 Kobe earthquake it was found that most of the piles suffered the most damage at the pile top and in the zone of the interface between the liquefied layer and the underlying non-liquefied layer. (Cubrinovski et al. 2009). The results of the analyses in this case study show that the maximum shear forces are developed at these interfaces. We infer that it is most likely that damage may occur at these locations.

A more refined analysis can be carried out by splitting the soil profile into more layers but the complexity of the soil model needs to be consistent with the quality and quantity of the given input data and also consistent with the inherent limitations the analysis method presents. This

case study is presented for illustrative purposes only. An actual project will require a more in depth examination of the output.

4 CONCLUSIONS

The authors considered that this simplified method should be published and made readily available to practicing engineers, to assist in closing the gap between theory and practice. This paper is a demonstration of how a complex theoretical procedure can be adapted for use in everyday practice. The authors recognize the limitations of this method. This method is meant to be a 'first-cut' determination in forming an opinion as to the likely damage to the pile. Additional work clearly needs to be done to refine and define the applicability of the method.
Physical examinations of in-service piles subjected to earthquakes in liquefiable soils need to be done to verify the accuracy of the predictions of this method. Although similar methods have been verified in other parts of the world, such as Japan, and have had favourable correlations with predicting damage, minimal work has been carried out to date in Christchurch to the authors' knowledge.

REFERENCES

Bradley, B.A. and Hughes, M. (2012) *Conditional Peak Ground Accelerations in the Canterbury Earthquakes for Conventional Liquefaction Assessment*. Technical Report prepared for the Department of Building and Housing.

Castelli, F. and Maugeri, M. (2009) *Simplified Approach for the Seismic Response of a Pile Foundation*. Journal of Geotechnical and Geoenvironmental Engineering, ASCE. 1440-1451.

Cubrinovski, M. and McCahon, (2011) *Foundations on Deep Alluvial Soils*. Technical Report Prepared for the Canterbury Earthquake Royal Commission.

Cubrinovski, M., Ishihara, K. and Poulos, H.G. (2009) *Pseudo-static Analysis of Piles Subjected to Lateral Spreading*. Bull. New Zealand Soc. for Earthquake Eng., 42(1): 28-38.

Liyanapathirana, D.S. and Poulos, H.G. (2005) *Pseudostatic Approach for Seismic Analysis of Single Piles*. Jounal of Geotechnical Engineering.1480-1487.

Rollins, K. M., Gerber, T. M; Lane J. D., Ashford, S. A. (2005) *Lateral resistance of a Full-Scale Pile Group in Liquefied Sand.* Journal of Geotechnical and Geoenvironmental Engineering: ASCE. Vol 131.115-125.

Tabesh, A. and Poulos, H.G. (2001) *Pseudostatic Approach for Seismic Analysis of Single Piles*. Journal of Gotechnical Engineering.757- 765.

Tokimatsu, K. and Asaka, Y. (1998) *Effects of Liquefaction-Induced Ground Displacements on Pile Performance in the 1995 Hyogoken-nambu Earthquake*. Special Issue of Soils and Foundations, Japanese Geotechnical Society.163 – 177.

Bruggers, D.; Skinner, R., & Rudolph, W.R. (2013)
Mitigation of a landslide impacting a rural road in Alameda County, California
Proc.19th NZGS Geotechnical Symposium. Ed. CY Chin, Queenstown

Mitigation of a landslide impacting a rural road in Alameda County, California

D Bruggers
ENGEO Incorporated
San Francisco, CA
dbruggers@engeo.com (Corresponding author)

R Skinner
ENGEO Incorporated
San Ramon, CA
rskinner@engeo.com

R William Rudolph
ENGEO Incorporated
brudolph@engeo.com

ABSTRACT

The Eden Canyon Road landslide is a deep-seated, 150-m (500-ft) long, 50-m (160-ft) wide landslide that affected approximately 50 m (160 ft) of roadway. The slide, activated by heavy rainfall during winter 2006, was evaluated through field exploration, including drilling and sampling of test borings, downhole logging of 60-cm (24-in) diameter borings, and installing an inclinometer. The slide plane was estimated to be at a depth of 12 m (40 ft) below the roadway. Upslope, numerous areas of seepage were observed within the landslide area and slow seepage was observed from the sidewalls of the borings. Groundwater was observed in the exploratory borings at depths of about 6 m (20 ft). The active landslide was associated with the reactivation of a portion of an older, dormant landslide. Complete repair of the active landslide was ruled out for several reasons.

Mitigation included horizontal drains up to 185 m (600 ft) long and a gravity buttress. The gravity buttress was an innovative system of counterfort subsurface walls of overlapping drilled shafts that were filled with cast-in-place concrete. The drilled shafts were approximately 1 m (3 ft) in diameter and extended from about 1.5 m (5 ft) below the roadway surface to a depth of at least 3 m (10 ft) below the base of the landslide.

1 INTRODUCTION

A deep-seated landslide affected Eden Canyon Road near Mile Marker 1.85 in Alameda County, California. Figure 1 depicts the landslide geometry and geologic units.

County staff first observed significant distress to the roadway in this area during the first week of April 2006. After performing an initial reconnaissance of the landslide, a detailed geotechnical exploration was initiated to characterize subsurface conditions in the landslide area and to develop conclusions and recommendations for remedial measures. The exploration included:

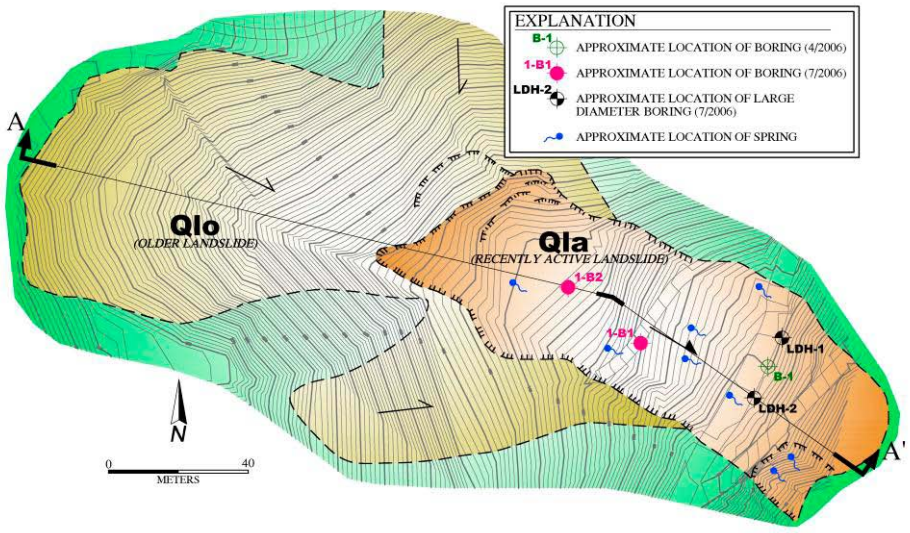


Figure 1: Landslide Geometry

- Geologic reconnaissance mapping of the landslide area.
- Examination of aerial photographs of the area.
- Drilling of four exploratory borings to depths of about 18 m (60 ft).
- Laboratory testing of selected samples.
- Analysis of the field and laboratory data.
- Development of mitigation recommendations.

EXISTING SITE CONDITIONS AND OBSERVATIONS

Eden Canyon Road is located on an east-facing slope, inclined at approximately 2H:1V to 3H:1V above and below the roadway. There is a creek located approximately 18 to 21 m (60 to 70 ft) downhill (southeast) of the roadway. The landslide impacted a portion of Eden Canyon Road approximately 50 m (160 ft) in length extending southwestward from a point approximately 60 m (200 ft) southwest of Mile Marker 1.85. This entire section of roadway had moved downslope roughly 1.5 to 1.8 m (5 to 6 ft).

The toe of the landslide is located in the Eden Canyon Creek bed and a clearly visible scarp was observed along the head scarp and lateral margins of the slide area. The scarp was up to about 1 m (3 ft) high at the authors' last site visit in October 2006.

The recently active landslide is a portion of an older, dormant landslide shown on published landslide mapping by Nilsen (1975), whose mapping is based on interpretation of aerial photographs.

Based on information from the Alameda County Public Works Agency, the authors understand that the County's maintenance records revealed no indications of any landslide problem at Eden Canyon Mile 1.85 prior to 2006.

INITIAL EXPLORATION

The initial exploration of the slide was conducted in April 2006 immediately after the slide occurred. One boring was drilled on the east shoulder of Eden Canyon Road in the central portion of the landslide area at the location shown in Figure 1. The boring was drilled to a depth of about 17 m (55 ft) using hollow-stem augers equipped with a dry coring sampling system.

An inclinometer was installed in the borehole and initial readings were taken on the morning of April 18, 2006. Subsequent readings were taken in the afternoon of April 18, 2006, and over 1.3 cm (½ in) of downslope deflection was observed at a depth of about 12 m (40 ft) as depicted in Figure 2.

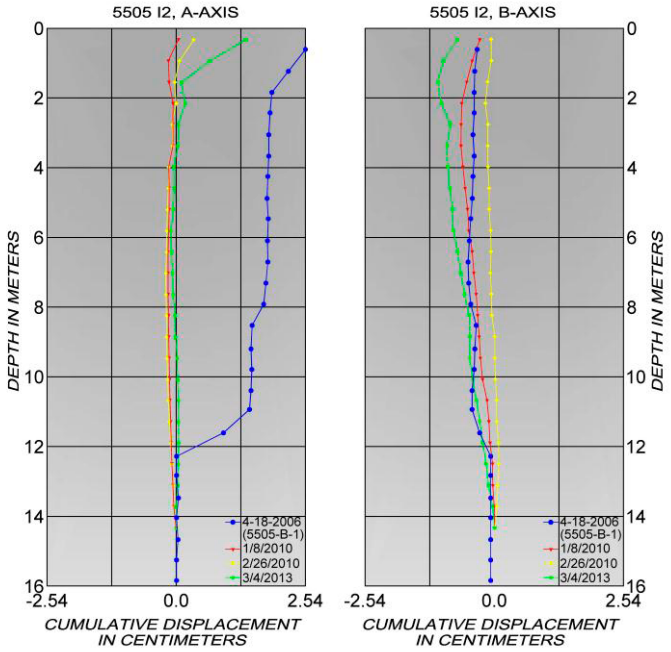


Figure 2: Inclinometer Profile

Reading of the inclinometer was attempted on April 19, 2006; however, the inclinometer probe could not pass the 12-m (40-ft) depth due to deformation of casing. This boring and inclinometer data indicated that the landslide was 12-m (40-ft) thick where it crossed Eden Canyon Road.

ADDITIONAL EXPLORATION AND LABORATORY TESTING

An additional two borings were drilled on private property upslope of Eden Canyon Road, as shown in Figure 1. These boring were used to define the depth and orientation of the slide plane upslope of the affected roadway. The borings were drilled using a track-mounted drilling rig and hollow-stem augers.

Two 60-cm (24-in) diameter borings were drilled in the road right-of-way using a Casagrande drilling rig. These borings were used to evaluate subsurface condition, as well as to investigate the feasibility of installing uncased, overlapping drilled shafts without excessive caving through the slide debris below groundwater. Cuttings produced from the drilling were logged and bulk samples of the cuttings were collected at 1.5-m (5-ft) deep intervals.
Laboratory testing was performed on selected samples recovered during drilling and included natural unit weight and moisture content, plasticity index, compaction, and remolded direct shear.

FINDINGS

Based on the findings of the reconnaissance mapping and exploratory borings, the authors' interpretation of the landslide configuration is depicted on the attached Geologic Cross Section, Figure 3.

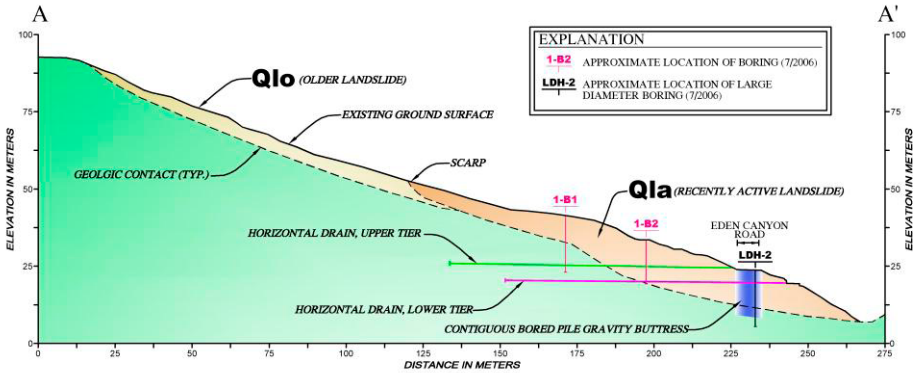


Figure 3: Cross Section

The landslide appears to range up to about 12 m (40 ft) thick. At the time the drilling was performed, the landslide mass was found to consist of stiff fissured clay with trace amounts of sand and gravel. Laboratory test results indicate that the slide debris appears to have moderate to high plasticity (liquid limit 44 and plasticity index 30). The intact slide mass consists of heavily over-consolidated fissured clays that have moderate undrained shear strength, but are subject to swelling and softening over long periods of time and to experience significant strength loss to low residual values upon remolding. Underlying the landslide mass, siltstone bedrock was encountered that is moderately strong and moderately fractured. The current slide surface appeared to be controlled by reactivation of an historic, well-defined slide plane located at the base of the slide debris.

Upslope of the roadway, numerous areas of seepage were observed within the landslide area as indicated in Figure 1. Seepage and indications of shallow groundwater were observed in the landslide area throughout the summer season and during a site reconnaissance in October 2006. Downslope of the roadway, a portion of the landslide had degraded into a mud flow that undermined the private driveway and caused mud and debris to flow into Eden Canyon Creek.

Slow seepage was observed from the side walls of the large-diameter borings within several zones below a depth of about 3m (10 ft) in the summer/fall of 2006. Groundwater levels during the winter when the slide occurred were postulated to be at or within a few meters of the ground surface.

CONCLUSIONS AND DISCUSSION

Based on the exploration, the authors' concluded that the 2006 landslide was the result of the reactivation of a portion of an older, dormant landslide. The reactivation of the landslide was likely triggered by pore water pressure associated with elevated winter water levels combined with fully softened shear strengths due to swelling and creep of the fissured clays along the slide plane. Once the movement occurred, friction angles along the slide plane likely reduced further to residual values. As a result, the potential for additional landslide movement during the forthcoming winter season was considered high. Additional landslide movement would likely have led to increased damage to Eden Canyon Road. Depending on the severity of the winter weather, and the magnitude of slide movement that occurred, it was possible that Eden Canyon Road would need to be temporarily closed to traffic while repairs were conducted. Additionally,

if left unmitigated, the additional impact to the downslope residence driveway was anticipated. Several remedial alternatives were considered and discussed with County staff including remedial grading, such as a shear keyway and valley buttress fill, and retaining wall systems, such as drilled piers with tie-backs and a contiguous pier wall.

Complete repair of the active landslide does not appear to be a viable remedial alternative for several reasons. The findings of our exploration indicate that the recent active landslide involves about 76,450 cubic m (100,000 cubic yd) of material. Moving this large quantity of material would be costly. Construction issues are significant and include: (1) the difficulty of stockpiling material and constructing haul roads in the steep terrain adjacent to the landslide area; (2) the high potential for triggering movement of the upslope dormant landslide; and (3) the closure of Eden Canyon Road for a prolonged period may be necessary. The environmental impacts of such an extensive grading operation are also a consideration.

Following analysis of access constraints, construction and traffic considerations, and comparative costs, the following horizontal drain and gravity buttress system was deemed to be the preferred remedial alternative.

1.1 Horizontal Drains

Following the winter months, movement of the slide mass had been arrested by the natural drainage of the hillside, which reduced piezometric levels. A key factor in mitigating future instability was to further reduce and maintain lower groundwater levels within the landslide. As a result, a system of horizontal drains was installed to drain the hillside as depicted in Figure 4.

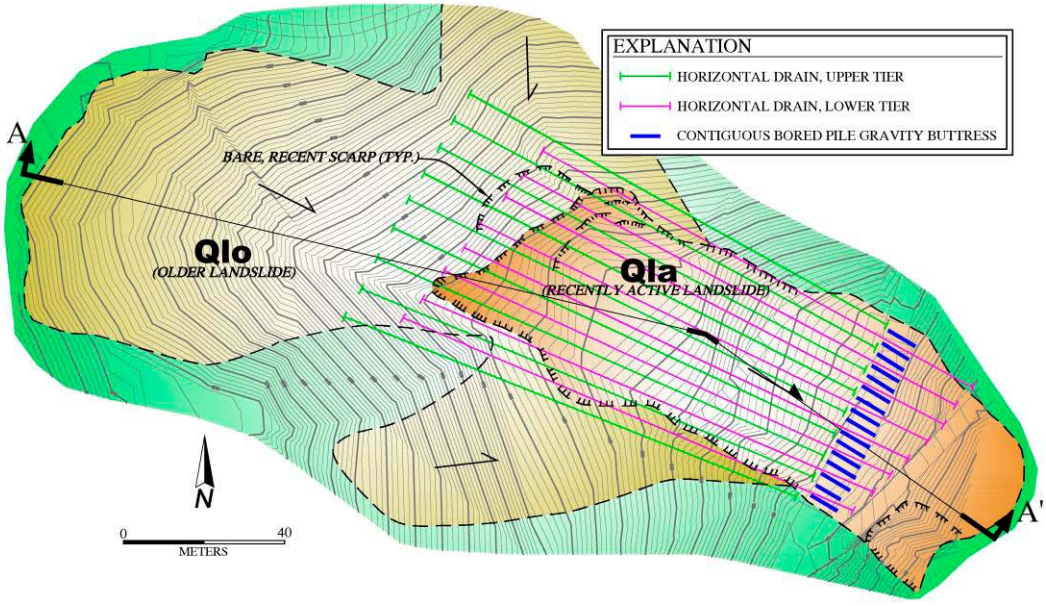


Figure 4: Repair Plan

An upper tier of horizontal drains was installed along the upslope side of Eden Canyon Road as an interim measure to increase stability before installing the gravity buttress. A lower tier of drains was proposed along the upslope side of the private driveway, and it was installed after the gravity buttress.
Drain pipes that consisted of 5.8-cm (2-in) diameter Schedule 80 PVC, factory manufactured as screen pipe with a slot size of 50.8 microns (0.002 in), inclined 3 to 5 degrees upward from horizontal, drilled to an average length of 120 m (400 ft) were recommended. All of the

New Zealand Geotechnical Society Inc. 19th Symposium, Queenstown 2013

horizontal drains were connected to a system of pipes designed to conduct the collected water outside the landslide area.

1.2 Gravity Buttress

While lowering of water levels through both natural drainage and the installation of the horizontal drain system was sufficient to arrest slide movement, this measure alone was not considered an acceptable degree of long-term reliability as the sole mitigation measure. It is common for horizontal drains to fowl over time and reduce in efficiency. Periodic observation, maintenance and replacement of the drains will be required to maintain effectiveness. In addition, while the drainage improvements increased the global stability of the reactivated slide mass, there were remaining concerns with the local stability of the downslope roadway embankment that may not be fully mitigated by the drainage improvements. As a result, the authors recommended the construction of a gravity buttress within the road right-of-way as depicted in Figure 4. The gravity buttress was a system of counterfort subsurface walls of overlapping drilled shafts that were filled with cast-in-place concrete having an unconfined compressive strength of at least 17,235 kPa (2500 psi). The drilled shafts are 0.9 m (3 ft) in diameter and extend from about 1.5 m (5 ft) below the roadway surface to a depth of at least 3 m (10 ft) below the base of the landslide. The shafts were planned to be drilled using a large-diameter auger similar to the one used during our exploration. The exploratory drill holes were completed without drilling problems such as caving, rapid inflow of groundwater, or slow drill advancement. Alternating shafts were constructed as an initial phase and then subsequent phases of shafts were installed between the initial ones. Following concrete placement in the initial shafts, the adjacent shafts were carefully bored to maintain overlap of 5.1 to 7.6 cm (2 to 3 in) between them such that each row of contiguous concrete-filled shafts acts as a single continuous concrete "shear wall" structure.

The drilled shafts were not designed to act as structural elements in bending or diagonal shear, but were designed as soil improvement elements to increase the composite horizontal shear strength, thereby disrupting and strengthening potential slide surfaces. Since the slide was essentially stabilized by the drainage improvements, the buttress is not expected to be subjected to high lateral working loads. Essentially, the buttress raises the factor of safety for the roadway embankment to acceptable levels and mitigates local instability.

1.3 Stability Analysis

Stability analysis was performed to evaluate the effectiveness of the recommended remedial measures. The analysis was performed on the cross section depicted in Figure 3 through the central portion of the slide mass. The analysis was performed using the computer program, "Slide 5."

Initially, a back-calculation was performed to estimate the strength parameters along the slip surface at the time of failure. Given the seepage conditions observed in the slide area, various shallow groundwater surfaces were modeled for the back-calculation. The authors initially considered that the slide was triggered due to high water levels and strengths represented by a fully softened friction angle. Subsequent to the failure, strengths were likely reduced further to residual friction angle values due to remolding; however, water levels dropped and, ultimately, arrested slide movement. Based on the results of the back-calculation and laboratory testing, the authors estimated the shear strength parameters summarized in Figure 5. These values were compared to published values for fully softened and residual friction angles for stiff fissured

clays published by Stark and Eid (1994 and 1997) as a function of liquid limit. The values that the authors determined from back-calculation are consistent with the published relationships. The lower residual friction angle was used in all subsequent forward-looking analyses.

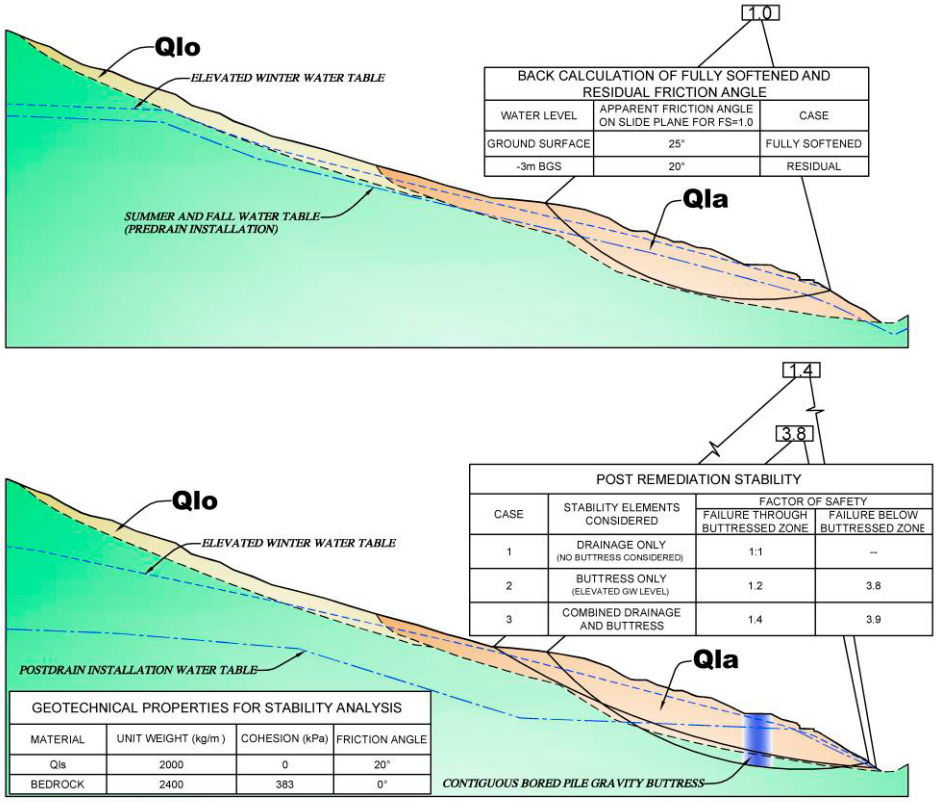


Figure 5: Slope Stability Analyses

The Case 1 analysis was performed to evaluate the effect of a lower groundwater level through the use of only the horizontal drain system on the safety factor. The safety factor for this case must be greater than 1.0 since the slide was stable prior to installing the buttress. However, judgments suggest that the slide was marginally stable in this condition and the safety factor should be only slightly greater than 1.0. The results are generally consistent with this assumption.

For Case 2, where a gravity buttress is modeled without lowering of the groundwater level, the calculated static factors of safety are 1.2 for a failure surface that passes through the gravity buttress and 3.8 for a failure surface that passes under the gravity buttress. The buttress was modeled using a unit weight of 2,400 kg/m^3 (150 pcf) and an undrained shear strength of 431 kPa (9,000 pcf). The composite soil strength was determined consistent with standard practice for soil improvement. The average shear strength was estimated based on the assumption of a 20 percent replacement ratio and of drilled shafts filled with concrete having an unconfined compressive strength of 17,236 kPa (2500 psi). In this case, the buttress provides resistance to the driving force of the slide mass. The limit equilibrium slope stability analysis provides an evaluation of the global safety factor for slope stability following the construction of the buttress, but is not referenced to potential slope deformations. In order to evaluate the future range of possible slope and roadway performance, we estimated the working load applied to the buttress associated with Case 2. Our slope stability analyses indicates this applied slope force is about 19,300 kN per cm (132,000 kips per linear ft) of buttress width. We then calculated the available passive resistance downslope of the buttress. We estimate that about 80 percent of the passive resistance will be mobilized by the applied slope force. Using the passive pressure mobilization curve shown in Figure 4-6 of FEMA 365, we estimate a total horizontal buttress deformation of approximately 30 cm (12 in).
The Case 3 analysis was performed to evaluate the increase in factor of safety when the buttress is added to the effects of deep drainage provided by the system of horizontal drains. When both

system components are considered together, the factor of safety increases to 1.4 for a failure surface that passes through the buttress, and to 3.9 for a failure surface that passes under the buttress. In this case, the slope is stabilized by the dewatering, and the working slope force on the buttress is nil. The buttress provides the additional safety factor and reduces the risk of future movement in the event of future groundwater rise.

The results of the authors' analysis indicated that the proposed remedial measures are expected to significantly improve the stability of the slide and control roadway deformation to tolerable limits.

CONSTRUCTION DURING THE WINTER OF 2006

1.4 Construction Sequence

Construction was performed during February and March 2006 by Condon Johnson & Associates. The construction sequence was as follows:

- Installation of upper tier of horizontal drains (8 drains).
- Installation of additional inclinometers.
- Construction of contiguous piers within southbound lane (northbound lane used for traffic).
- Construction of contiguous piers within northbound lane (southbound lane used for traffic).
- Installation of lower tier of horizontal drains (6 drains).
- Construction of horizontal drain water collection system and other storm drainage elements.
- Re-grading of roadway within repair area, placement of base rock and asphaltic concrete pavement.

The project was completed within 30 working days. There were neither changed conditions nor unanticipated conditions claimed by the contractor.

Flows produced from the horizontal drains were measured by the contractor immediately after completing the drilling of each drain and periodically thereafter. Most of the horizontal drains produced less than 3.8 L (1 gal) per minute immediately after drilling; however, two drains in the upper tier experienced flows greater than 38 L (10 gal) per minute. Within a period of several hours, the high flow rates tapered off to less than 4 liters per minute. Three years after the construction, the flow rate from the entire horizontal drain system (14 drains total) was about 1.9 L (½ gal) per minute. Six years latter the flow rate declined to less than 0.5L (1/8 gal) per minute.

Subsequent to construction, the authors were retained by the County to monitor the inclinometers on an irregular basis. As indicated in Figure 2, no indications of deep seated movement have been observed.

REFERENCES

Nilsen, T.H. (1975) Preliminary Photointerpretation Map of Landslide and other Surficial Deposits of the Hayward 7 ½ ' Quadrangle, Alameda County, California, U. S. Geological Survey, Open File Map 75-277-19.

Stark, T.D., and Eid, H.T. (1994) "*Drained residual strength of cohesive soils.*" ASCE, *J. Geotech. Engrg.* 120: 856–871.

Stark, T.D., and Eid, H.T. (1997) "Slope stability analyses in stiff fissured clay." ASCE, *J. Geotech. Engrg.* 123(4): 335–343.

Lochhead, S.E. (2013)
The impact of new springs affecting residential properties in Christchurch following the Canterbury 2010/2011 earthquake sequence
Proc. 19th NZGS Geotechnical Symposium. Ed. CY Chin, Queenstown

The impact of new springs affecting residential properties in Christchurch following the Canterbury 2010/2011 earthquake sequence

S E Lochhead
Tonkin & Taylor Ltd, Christchurch, NZ
slochhead@tonkin.co.nz

Keywords: springs, groundwater, land damage, aquifer, wells, earthquake, Christchurch

ABSTRACT

Seismic activity during the 2010/2011 Canterbury Earthquake Sequence (CES) caused widespread damage to land in Christchurch. During assessment of land damage on residential properties, undertaken for the Earthquake Commission (EQC), it became apparent that a number of areas within the city experienced ponding and flooding by new springs as a result of the CES.

This paper documents some of the effects and changes to land from the earthquake-induced springs that have occurred within Christchurch. It considers whether many of these springs are new phenomena or whether, given the hydrogeological setting of Christchurch and the surrounding area, such consequences following extensive ground shaking could have been expected. The paper provides a general overview of the adopted solutions used to control groundwater flows allowing land to be returned to its original pre-earthquake utility. The paper concludes with learning outcomes from the effects of the CES to assist other regions which may be prone to spring formation following seismic activity.

New Zealand Geotechnical Society Inc. 19th Symposium, Queenstown 2013

1 BACKGROUND

1.1 Effects of earthquakes on the groundwater regime

Changes in groundwater regimes in response to earthquakes are well documented around the world (Wang & Manga, 2010). These are typically identified by groundwater level changes in wells, emergence of springs and/or increased spring discharges amongst other groundwater features. Understanding the groundwater regime of Canterbury, and more particularly Christchurch, is key to understanding the process of spring formation which has impacted on many residential properties as a result of the Canterbury Earthquake Sequence (CES).

Earthquake-induced groundwater changes in Christchurch, observed through monitoring wells, were first noticed in 1989 as a result of an M8.2 earthquake which occurred more than 1500 km south of Christchurch (Van Ballegooy et al. 2013). Since the 2010/2011 CES, the impacts on Christchurch's hydrogeological regime have become hot topics for future research.

Following the 4 September 2010 earthquake, a systematic review of earthquake-induced hydrological responses associated to this earthquake event was first carried out by Cox et al. (2012) where observations in persistent groundwater level changes and short-term groundwater oscillations were noted in wells. Groundwater level responses to the CES have been recorded throughout New Zealand as far as Northland (Gulley et al., 2013), therefore it should be no surprise that the localised effects on groundwater has been significant within areas of Christchurch.

Investigations into the causes of spring formations are ongoing. However, it is considered the response in groundwater level changes in aquifers associated with spring formation as a result of longer term groundwater level change in the aquifer system rather than a short term oscillatory response to seismic shaking (Gulley et al., 2013). Although detail of the groundwater movement between the aquifers and through the aquitards is still being researched,

it is apparent with the formation of new springs and re-emergence of historic springs that there has been a material change in the aquitards as a result of the CES either through enhanced permeability or fracturing to promote artesian flow at the surface (Gulley, 2013). The occurrence of these springs has had a localised, but significant effect on land and in some cases, on dwellings on individual properties. In some instances entire streets have also been impacted by spring occurrence.

2 HYDROGEOLOGY OF CHRISTCHURCH

The geology of the Canterbury Plains and Christchurch area comprises interbedded alluvial gravels and finer sediments deposited during the glacial and inter-glacial periods of the last 500,000 years. The Canterbury Plains have typically been deposited by fluvial environments (Brown, 2001). Closer to the coastal margins in Christchurch, the influence of marine depositional environments is evident with finer sediments interfingered with the coarser sediments (Van Ballegooy et al. 2013). These interfingered deposits form the vast layered aquifer system of the Canterbury Plains and Christchurch area, in which the upper five aquifers are named to correlate with the main named gravel units (Brown & Wilson, 1988). Recharge to the aquifers originates from leakage of the Waimakariri River (White, 2012) and infiltration of rainfall on the Canterbury Plains.

New Zealand Geotechnical Society Inc. 19th Symposium, Queenstown 2013

To the south of the city lie the Port Hills, a volcanic outcrop of predominantly basaltic to trachytic lavas (Forsyth, Barrell & Jongens, 2008). This geology yields very little groundwater resource compared to the gravel aquifers and is a completely different aquifer system known as the Banks Peninsula volcanic rock aquifers.

2.1 Historical control of groundwater in Christchurch

Groundwater levels beneath Christchurch are high and close to the ground surface, which is reflected in the surface of the upper most (unconfined) aquifer. This varies in depth from near surface in the east (which contributes to many of the wetland areas within and around the eastern part of the city) to greater than 10 metres deep in the western parts of the city.

Historically, to control these high groundwater levels and to allow development of the city on drier ground, a network of drainage ditches were installed. These ditches were installed by the Christchurch Drainage Board as early as 1875 with a dual task of land drainage and wastewater management (Watts, 2011). The drainage ditches remain a major infrastructure asset across the city with new drainage installed as Christchurch expands onto new sites. In addition, in areas more prone to high groundwater levels, an extensive network of field drains were and continue to be installed in local areas eg the suburb of Woolston and at the foot of the Port Hills.

Groundwater resources are important to Christchurch. A vast array of groundwater wells exist in Christchurch which exploit this resource for potable water supply. Originally private wells were installed on many properties at the time of site development, then following the introduction of the potable reticulation system, the Council installed wells and pumping stations to serve this purpose.

2.2 Spring types

There are many different types of springs which can be generally categorised relating to the groundwater source and the geological setting. Investigation into the spring types goes well beyond the scope of this paper and the remit of the work undertaken for the Earthquake Commission (EQC). However, recognising different spring types assists in understanding the conceptual hydrogeological model and provides an insight into the potential longevity of the springs.

Many of the springs in Christchurch, particularly on the flat land, are understood to be ‘water table’ springs where depressions in the geographical terrain associated with high groundwater levels result in groundwater seepages and flows.

The 'traditional' artesian springs can be identified by a different groundwater chemistry to surface waters and a change in hydraulic head. The traditional type of springs are more likely along the margins of or within the Port Hills. Whilst spring occurrence along the flanks of the Port Hills is not well documented, the occurrence of (thermal) springs along the boundary of the Banks Peninsula volcanic rock aquifers and the gravel aquifers of the Canterbury Plains is recognised (Brown & Weeber, 1994). Work reported by Earl (1998) also identifies the occurrence of many springs on the Banks Peninsula which typically form at the interface between the volcanic bedrock and colluvium at the margins of the hills.

2.3 Spring Occurrence pre-Canterbury Earthquake Sequence

Prior to the CES, the existence of springs within Christchurch was typically unnoticed by the population and relatively few springs were noted to emerge through the confined aquifers to the east and south of the city (Van Ballegooy et al. March 2013). Combined records from various sources identified 425 springs within the city prior to the CES (White, 2007), as shown in Figure 1. It is well known that springs provide baseflows to the main rivers of Christchurch eg Styx, Heathcote, Avon. This appears to be reflected in the majority of known springs being observed in the western half of the city. However, this could be merely due to the fact that the more in depth studies of springs were associated with river flows rather than due to the complete absence of springs in other areas.

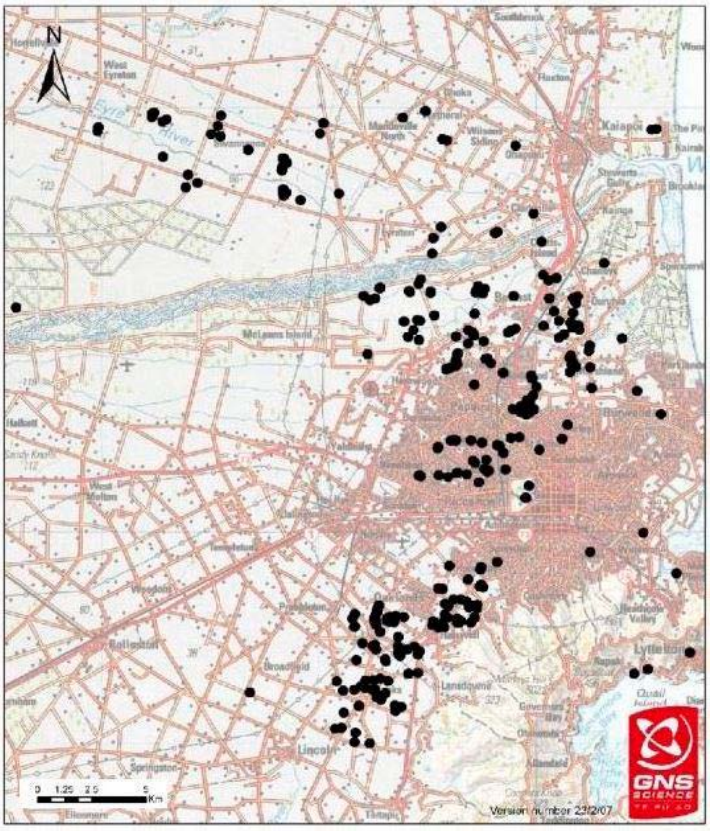


Figure 1: Springs mapped by Environment Canterbury, Christchurch City Council and the Sibly 1856 map by Wilson 1989 (White et al 2007)

3 LAND DAMAGE ASSESSMENT WORK

Over the last two years, geotechnical engineers and geologists from many engineering consultancies across NZ have been working in the Land Damage Assessment Team (LDAT) for the EQC in response to the CES. The role of the LDAT staff has been to undertake land damage assessments on residential land to document and categorise the land damage (an EQC term) across Christchurch and the surrounding Canterbury region which has resulted from the CES. One of these types of land damage relates to new groundwater springs.

3.1 Spring occurrence post Canterbury Earthquake Sequence

Following the CES, many new springs were noted as a result of the extensive ground shaking formed in combination with other damage. Figure 2 shows that many new springs have occurred to the east and south of the city since the CES, although the author considers that not all spring occurrences both pre- and post-CES are mapped. There are a number of reasons behind the new spring formations across certain parts of the city, but the main consensus for the spring development, as described earlier, is due to a weakening and thinning (in many cases) of the confining layers of the aquifer in combination with a fracturing of the layers, associated with ground oscillation liquefaction processes.

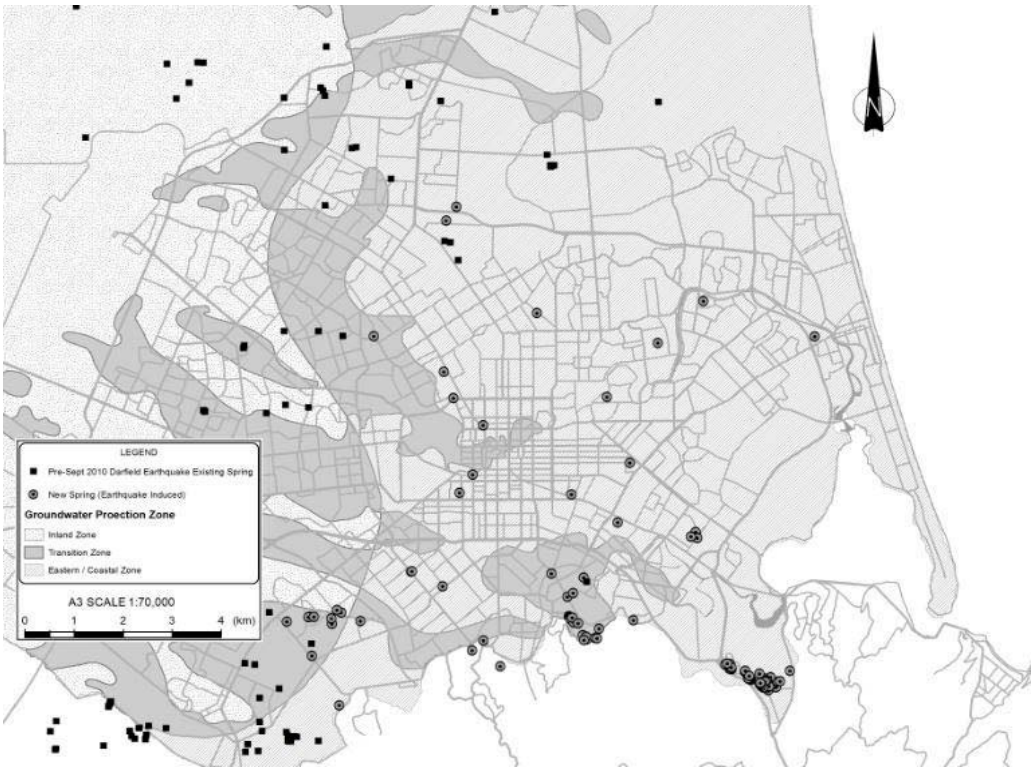


Figure 2: Known spring locations pre and post September 2010 Darfield Earthquake (Van Ballegooy et al, March 2013)

3.2 Typical effects of new springs observed on land

The effects of new springs on land has resulted in localised ponding and flooding, as well as softening of ground on many properties. In some cases, this ponding has been short-lived either naturally drying up over several months or has abruptly stopped following an aftershock or another earthquake event. However, many springs have been persistent; discharging volumes in excess of 1 litre/minute continuously regardless of seasonal changes or weather conditions, clearly flowing under artesian conditions. Many spring occurrences have been isolated cases with land affected by the groundwater limited to a small area (eg less than $5m^2$) on a single property. In some areas within the city much larger areas have been affected, particularly in the suburbs of Woolston and Heathcote, as shown in Figure 3.

The appearance of ground affected by springs is variable with some springs observed to occur at a discrete source, clearly upwelling in specific locations such as a fracture or small depression. New springs have also appeared as seepages/diffuse flows over larger areas (eg more than $50m^2$) making the identification of a spring source difficult. The evidence of this type of spring flow suggests a general increase in permeability of the confining layer combined with near surface groundwater levels, indicating a 'water table' type spring.

During the land damage assessments for the EQC, identification of springs has been complicated by other earthquake-related damage such as burst water mains, broken stormwater and field drains, as well as general ponding, particularly during the wetter months.



Figures 3: Spring land damage in Woolston



Figure 4: Old artesian well

Another groundwater-related issue has been the extensive damage to private artesian wells. Old well casings of previously sealed wells have ruptured causing wells to flow (uncontrollably) in many situations. Typically, the well casing has been pushed up after the covering layer has ruptured. Figure 4 shows typical well land damage.

3.3 Case Study - Hillsborough

An example of extensive, localised effects of spring formation impacting on the land is seen in the suburb of Hillsborough. This residential area lies in a valley between Rapaki and Huntsbury at the foot of the Port Hills. The setting for this suburb is a low lying, narrow valley floor with the profile being flat to gentle, underlain by alluvial deposits whilst the sides of the valley become moderately inclined as the geology changes to volcanic bedrock overlain by colluvium.

Figure 5 shows the mapped springs and other observed wet areas on Vernon Terrace, a street in the suburb, where spring formations appear to have emerged at a similar elevation, slightly upslope, but parallel to the valley floor. As with other areas, the distinction between discrete spring locations and seepages/high groundwater levels is not clear. However, the large number of seepages indicates that many of these new springs may be 'water table' springs associated with a high groundwater level. The presence of two open drainage channels extending through the valley and a network of field drains in the area suggests that groundwater levels have been at near-surface levels historically and have required control by way of drainage.

At some locations where flows are more distinctive, sampling of spring water has indicated a groundwater chemistry associated with volcanic rocks, suggesting a possible deeper artesian spring source. Such spring source could be represented by that identified by Earl (1998) where springs have formed at the interface between the volcanic bedrock and colluvium at the margins of the hills, particularly where reactivation of old springs has occurred due to the earthquakes. The observed damage to land from these persistent higher flowing springs has been extensive with water flowing into basements of several dwellings whilst the surrounding land has become saturated and softened. In some instances, the effects of springs on this land has resulted in dwellings requiring removal to repair the underlying land.

Anecdotal evidence reveals the presence of springs in the valley prior to the earthquakes with the owners of two properties visited indicating they have had a spring at their property for more than 50 years. Flows from these springs have been successfully controlled by discharging the groundwater into the stormwater drain system via field drains in such a manner that it has gone unnoticed and has made little impact on these properties. Although, at one property, a new drain had to be installed following the CES before the land could return to its pre-earthquake condition.

It should be noted that similar spring occurrences have been identified on the other side of the valley to Vernon Terrace, along Albert Terrace.

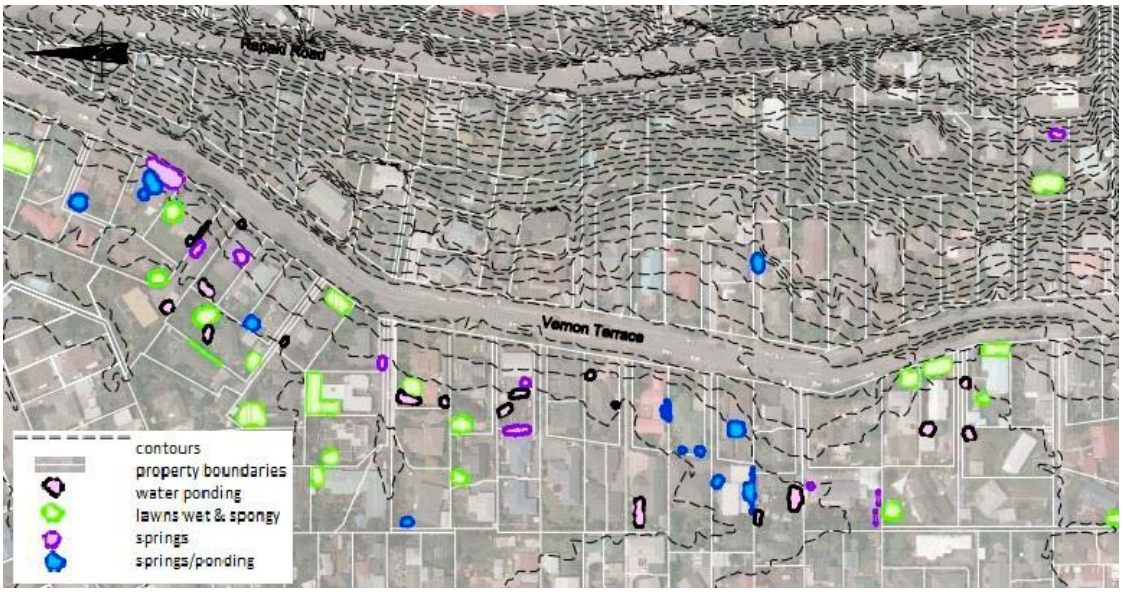


Figure 5: Locations of springs and other groundwater features on Vernon Terrace

4 REMEDIAL SOLUTIONS

Proposed solutions to repair the spring related land damage have been provided to the EQC for settlement claiming purposes. Varying ground conditions and the nature of a spring source can make repair of spring-related land damage difficult. Sealing a spring by grouting alone in unconsolidated sediments may not guarantee cessation of the spring flows and it could potentially force the groundwater to flow at another weak point within the aquitard. Therefore, the remedial solutions considered focused on controlling spring flows to allow the (residential) land to return to its pre-earthquake condition and restoring its utility, which is the objective of EQC land repair.

A non-site specific drainage solution comprising subsoil drains installed at various depths has been designed to help mitigate the effects of saturation of surface soils. The collected groundwater is discharged to the most appropriate existing stormwater drain. Some situations require installation of a pump and sump where the fall of the land prohibits gravitational flow of the discharge. In areas where extensive spring damage has prevailed, drainage blankets are recommended to allow a greater area of groundwater interception to be achieved. In some cases, to achieve the repairs, dwellings need to be removed to repair the underlying land. Since only a non-site specific solution is provided, specific tailoring to each affected property is required depending on the circumstances and extent of the spring-related damage. Figure 6 shows a non-site specific remedial design.

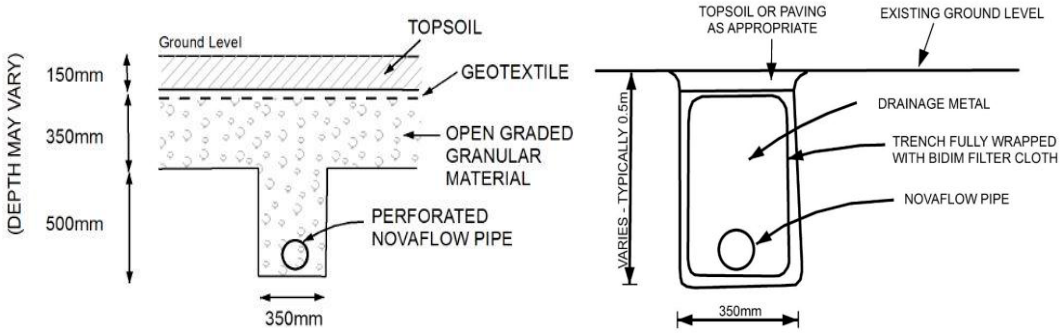


Figure 6: Typical section of non-site specific drainage blanket and subsoil drain design

5 DISCUSSION

Through the work undertaken for the EQC, it has become apparent that there are many instances across Christchurch where springs have formed in areas where historical springs have occurred or in areas of very high groundwater levels. In addition, this report suggests that not all springs have been documented prior to and after the CES. Since Christchurch is a low lying city with generally very high groundwater levels and an extensive aquifer system, the realisation of spring emergence in many areas should not come as a surprise.

The origins of the groundwater sources creating the spring formations have not been investigated, so it can only be speculated that there are different processes behind the spring formation in different areas. Since the emergence of new springs, predominantly as a result of the 4 September 2010 and 22 February 2011 earthquakes, some spring flows have reduced or completely disappeared. It is not known whether this is a result of lower groundwater levels associated with the dry summer of 2013 or whether this is a permanent groundwater change. There is huge research potential and interest for investigating the spring occurrences and sources in the future.

We need to consider how learning from the emergence of springs resulting from the CES can assist in other regions should a similar natural disaster occur. Areas of land potentially prone to new spring formation could be identified and mapped in other regions. This information could be used to inform Territorial Authorities, the insurers (including EQC) and land owners of the potential risks should significant earthquakes occur.

6 CONCLUSION

Localised areas of Christchurch have been impacted by the formation of new springs as a result of the CES. Prior to the CES, the existence of springs within Christchurch was reported to be relatively few. Whilst in depth research into the origins of the springs has yet to be completed and published, work has been undertaken for the EQC to address the spring-related land damage and repair solutions have been provided. Through this work, it is apparent that spring formation has generally been in areas of high groundwater levels and in areas where springs have historically occurred. There is therefore potential to assess these instances and to develop a model of occurrences which could be used to assist other regions prone to spring occurrences should a similar earthquakes occur in those regions.

ACKNOWLEDGEMENTS

The author would like to thank the EQC and Tonkin & Taylor Ltd for the support in preparation of this paper.

REFERENCES

Brown, L. J. (2001) 'Chapter 23 Canterbury' in: Rosen M. R., White P. A. eds *Groundwater of New Zealand*. Wellington, NZ, Hydrological Society Inc., pp 441-459.

Brown, L. J. & Weeber, J. H. (1994) Hydrogeological implications of geology at the boundary of Banks Peninsula volcanic rock aquifers and Canterbury Plains fluvial gravel aquifers. NZ Journal of Geology & Geophysics. Vol 37: 181-193.

Brown, L. J. & Wilson, D. D. (1988) Stratigraphy of late Quaternary deposits of the northern Canterbury Plains. New Zealand Journal of Geology and Geophysics 31(3): 305-335.

Cox, S. C. et al (2012) Hydrological effects of the Mw 7.1 Darfield (Canterbury) earthquake, 4 September 2010, New Zealand. NZ Journal of Geology and Geophysics 55(3): 231-247.

Earl, P. (1998) Groundwater Springs: A literature review of existing classification schemes and studies, and proposal for a Canterbury spring classification system. Environment Canterbury Report U98/7.

Forsyth, P. J., Barrell, D. J. A., Jongens, R. (compilers) (2008) Geology of Christchurch area. 1:250 000 geological map 16. 1 sheet + 67 p. GNS, Lower Hutt, New Zealand.

Gulley, A. K. et al (2013) Groundwater responses to the recent Canterbury earthquakes: a comparison. Manuscript submitted to Journal of Hydrology, reviewed and under revision.

Van Ballegooy, S et al (2013) Median water table elevation in Christchurch and surrounding area after the 4 September 2010 Darfield Earthquake. Version 1 Draft. GNS Science Report 2013/01.

Wang, C-Y & Manga, M. (2010) Earthquakes and water: Lecture Notes in Earth Science, Springer, New York.

Watts, R. H. (2011) The Christchurch waterways story. Landcare research science series No 38

White, P. A. et al (May 2007) Waterways, swamps and vegetation of Christchurch in 1856 and baseflow discharge in Christchurch city streams. GNS Science Consultancy Report 2007/103.

White, P. A. et al (2012) Groundwater-surface water interaction in the Waimakariri River, New Zealand and groundwater outflow from the river bed. Journal of Hydrology (NZ) 51 (1): 1-24

Effect of specimen size on the laboratory measurements of electrical resistivity of soils

M N Neishabouri
Faculty of Engineering, The University of Auckland, NZ.
mnag216@aucklanduni.ac.nz (Corresponding author)

H M Abuel-Naga
Faculty of Engineering, The University of Auckland, NZ.
h.naga@auckland.ac.nz

Keywords: electrical resistivity, numerical, laboratory testing, specimen size, Wenner array

ABSTRACT

Experimental and theoretical relationships suggest that some geotechnical parameters can be predicted using the results of electrical resistivity surveying. Wenner array which involves four evenly spaced electrodes is the most common experimental method to measure the electrical resistivity of soils. In fact, the measured electrical resistivity by Wenner approach is controlled by the geometry of the equipotential lines induced by subjecting the soil to electrical potential at the outer electrode points. In the lab scale, the soil specimen size could disturb the geometry of the equipotential lines leading to a remarkable change in the measured electrical resistivity. In this study, the effect of the soil specimen size on the laboratory measured electrical resistivity was assessed experimentally and numerically. Furthermore, a correction factor is proposed to consider the effect of the specimen size on the laboratory measured electrical resistivity.

1 INTRODUCTION

Direct two and four electrodes methods are usually utilized for measuring the electrical resistivity of soils (McCarter 1984;McCarter and Desmazes 1997;Rinaldi and Cuestas 2002). Some other electrode-based probes and devices are also common (Campanella and Weemees 1990; Zha et al. 2007; Kim et al. 2010; Ekwue and Bartholomew 2011). Among all methods, direct Wenner array is the most common arrangement of electrodes for measuring the electrical resistivity (Kalinski and Kelly 1994; Abu-Hassanein, Benson et al. 1996; ASTM 2010; ASTM 2012) where four electrodes are evenly spaced in a line, the outer electrodes are operating as point sources of current and the two inner electrodes are to observe potential difference as shown in Figure 1.

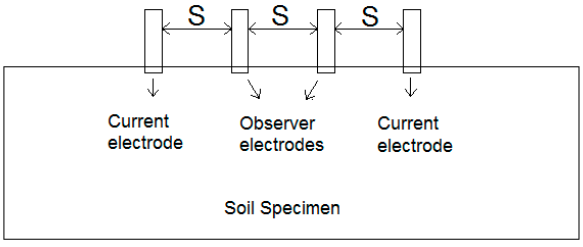


Figure 1: Schematic Electrode Location in Wenner Array Configuration

In general, the output potential drop and electrical resistivity are functions of some soil properties such as porosity, water content, compaction effort, Atterberg limits, and ion composition effect (Archie 1942; Atkins Jr and Smith 1961; Mualem and Friedman 1991; Pozdnyakov et al. 2006; Kibria and Hossain 2012). However, in the laboratory scale where the size of the testing specimen is limited, the measured electrical resistivity by Wenner approach can also be affected by the size of the testing specimen that could disturb the geometrical pattern

of the equipotentials that induced by the current flows through the outer electrodes in the soil (Samouëlian et al. 2005). In fact, this effect was not considered in the previous laboratory scale electrical resistivity studies that used Wenner approach. In this study, the effect of the testing specimen length on the Wenner array electrical resistivity measurements will be investigated experimentally and numerically. Results of the conducted experimental and numerical research program will be presented and discussed and conclusions will be drawn.

2 EXPERIMENTAL TESTS

Reconstituted specimen of New Zealand Kaolin clay was used in this study. The characteristics of New Zealand clay are listed in Table1. The experimental program in this study involves measuring the electrical resistivity of identical reconstituted clay specimens having different heights. For this purpose, a reconstituted specimen was moulded in a multi-split PVC pipe having a diameter of 100 mm and comprises six PVC rings with different heights as shown in Figure 2. Therefore, several specimen lengths can be obtained by cutting the specimen through the predefined split planes as listed in Table 2. An electrode holder comprises a rectangular PVC beam (20×150mm) with equally spaced hole (S = 7mm) was located at the centre of the top ring. Four brass electrodes with diameter of 3mm were utilized to complete the circuit. The electrical resistivity was measured by the standard calibrated electrical resistivity meter (Tinker & Rasor - model SR-2). The device is manufactured based on ASTM standard for electrical resistivity measurements by direct Wenner array.
Figure 3 shows the experimental electrical resistivity results as the ratio L/S changes where L is the specimen height, and S is Wenner array spacing as shown in Figure 2. In general, the experimental results show that the specimen height could affect the measured electrical resistivity where the electrical resistivity values decrease as L/S increases. However, inevitable laboratory experimental scatter is observed at higher L / S values.

New Zealand Geotechnical Society Inc. 19th Symposium, Queenstown 2013

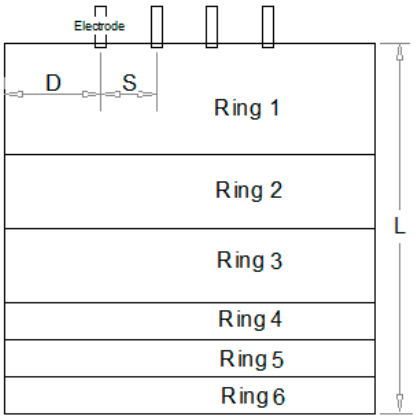


Figure 2: Electrode and PVC Ring Locations in experimental test.

Table 1: Characteristics of New Zealand Kaolin

New Zealand Kaolin	
Specific Gravity	2.55
Surface Area	20 m^2/gr
Cation Exchange Capacity	10 meq./100grs of clay
PH of Aqueous Slurry at 20 percent Solid	4.8-5

Table 2: Specimen Dimensions in Electrical Resistivity Measurements

Electrode spacing, S (mm)	Specimen width beside electrodes, D (mm)	Specimen length, L (mm)
7	39.5	100
7	39.5	70
7	39.5	50
7	39.5	30
7	39.5	20
7	39.5	10

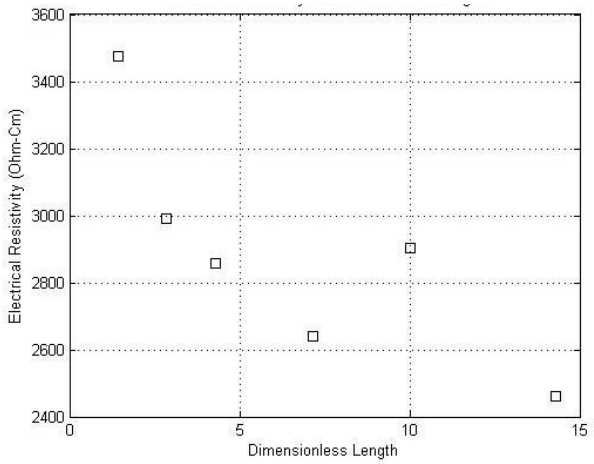


Figure 3: Experimental Electrical Resistivity vs. Dimensionless Length (L/S)

3 NUMERICAL MODEL DEVELOPMENT

3.1 Coupled Flow Theory

Each type of gradient through soil can drive different currents (Mitchell and Soga 2005). In general form, the current, Γ_E, can be induced by different gradient field, Φ_j, and is quantified by the coupled flow theory as follows:

$$\Gamma_E = \sum_j L_{ij}.\nabla\Phi_j \tag{1}$$

where L_{ij} is conductivity coefficient and Φ_j is different gradient fields. Thus, the electrical current in the soil may be induced by hydraulic, temperature, chemical ion concentration and electrical potential gradient (Mitchell and Soga 2005).

$$\Gamma_E = L_{Eh}\nabla(-\Phi_h) + L_{EC}\nabla(-\Phi_C) + L_E\nabla(-\Phi_E) + L_{ET}\nabla(-\Phi_T) \tag{2}$$

where Φ_h, Φ_C, Φ_E, Φ_T denote hydraulic, chemical, electrical and thermal gradients, respectively. L_{Eh}, L_{EC}, L_E, L_{ET} denote conductivity coefficients for hydraulic, chemical, electrical and thermal flows, respectively. In the case of Wenner test, the soil specimen is subjected to electrical gradient in absence of other gradients. Therefore, the coupled flow equation is simplified to the ohm's law.

$$\Gamma_E = L_E\nabla(-\Phi_E) \tag{3}$$

The numerical model was developed based on fundamental current continuity equation.

$$\nabla \Gamma_E = I \tag{4}$$

where I is external current pass through the specimen. Current continuity equation was modified by substitution of ohm's law (simplified coupled flow equation) assuming isotropic electrical conductivity over control volume.

$$\nabla(L_E \nabla(\Phi_E) = -I \tag{5}$$

In the absence of external current,

$$\nabla(L_E \nabla(\Phi_E) = 0 \tag{6}$$

The governing equation for current continuity is solved by the finite element solver FlexPDE with an automatic adaptive mesh method. The numerical model was conducted with L, S and D similar to the experimental test listed in Table 1 where D is the radial distance between the outer electrode and the specimen ring. Figure 4 shows the numerical electrical resistivity results for different (L/S) values. In general, the numerical results show a similar trend as the experimental results shown in Figure 3.

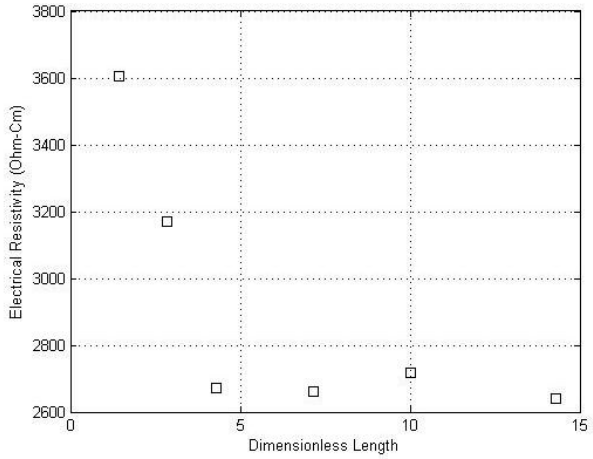


Figure 4: Numerical Electrical Resistivity vs. Dimensionless Length (L/S)

4 VALIDATION AND ERROR ANALYSIS

For validation purpose, the numerical results were compared with the experimental results where ± 10% error for the individual laboratory measurement was considered as shown in Figure 5. The Mean Absolute Standard Error (MASE) is employed for examining the numerical model accuracy as follows:

$$MASE = \frac{\sum_{i=1}^{n} \rho_r}{n} \tag{7}$$

$$\rho_r = \begin{cases} \dfrac{\rho_{num}}{\rho_{\exp}} & \text{if } \rho_{num} \geq \rho_{\exp} \\ \dfrac{\rho_{\exp}}{\rho_{num}} & \text{if } \rho_{num} \leq \rho_{\exp} \end{cases} \quad (8)$$

where ρ_{num} and ρ_{exp} are the electrical resistivity obtained from the numerical and the experimental study, respectively. The value of MASE equal or closer to 1.0 should give the most accurate results. Numerical results in this study show that MASE = 1.05.

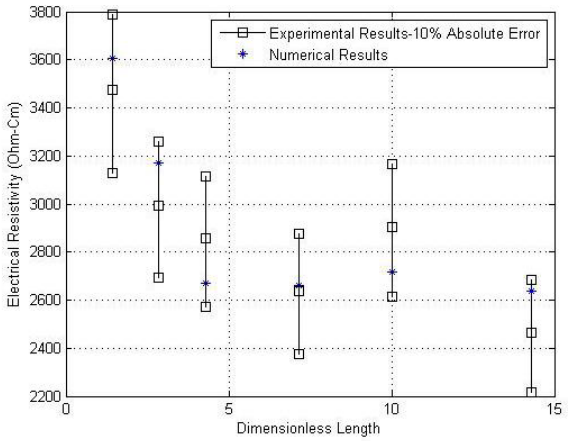


Figure 5: Comparison between Numerical and Experimental Results

5 DISCUSSION

In Wenner array, the equipotential geometric configuration controls the output voltage at the inner electrodes. To obtain most accurate electrical resistivity result, the equipotential curves need to be undisturbed, as shown in Figure 6, for L / S = 15.

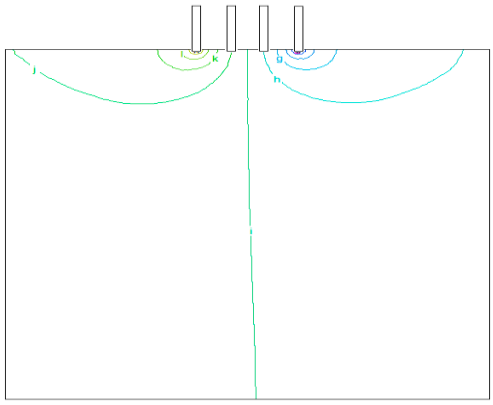


Figure 6: Undisturbed Equipotential Curves at L / S = 15

In fact, reducing L leads to equipotential disturbance and changes in the measured electrical resistivity value. The electrical resistivity results in this study show that from L / S = 15 to L / S = 5, the disturbances in equipotential curves have insignificant effect on the measured electrical resistivity (less than 5 %). However, for L / S < 5, the equipotential curves are highly affected by the soil specimen height as shown in Figure 7. Therefore, the electrical resistivity values show more than 50% error in some points compared to the electrical resistivity value at L/S =15.

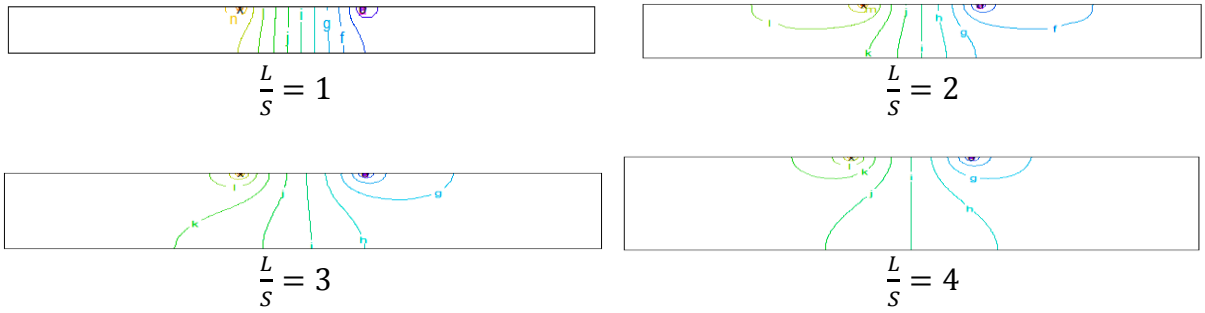


Figure 7: Disturbed Equipotential Curves for L/S<5

For L / S < 5, to exclude the effect of L/S on the electrical resistivity results, a correction factor, CF, is proposed in this study as follows:

$$\rho_{corr} = CF\ \rho_{\exp} \tag{9}$$

New Zealand Geotechnical Society Inc. 19th Symposium, Queenstown 2013

where ρ_{corr} and ρ_{exp} are the corrected and the laboratory measured electrical resistivity, respectively. The proposed CF corrects the measured electrical resistivity value to be equal to the value of electrical resistivity is at L / S ≥ 5 where the effect of L/S is insignificant. Using the nonlinear regression method, the electrical resistivity results in this study were used to determine CF as function of L / S, as shown in Figure 8, where:

$$\text{For } L/S \geq 5: \quad CF = 1$$

$$\text{For } L/S < 5: \quad CF = 0.625\left(\frac{L}{s}\right)^{0.323} \tag{10}$$

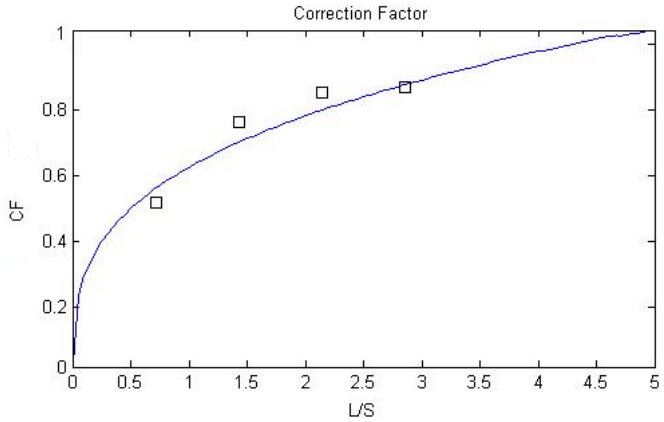


Figure 8: Electrical Resistivity Correction Factor

6 CONCLUSIONS

Experimental and numerical studies were conducted to investigate the effect of the soil testing specimen size, in terms of the specimen height, on the measured electrical resistivity values using Wenner approach. The results indicate that for the testing specimens having L/S <5, Wenner approach overestimates the electrical resistivity value of the soil. Based on the experimental and the numerical results in this study, a correction factor was introduced to

consider the effect of the testing specimen height on the measured electrical resistivity values using Wenner approach.

REFERENCES

Abu-Hassanein, Z. S., C. H. Benson, et al. (1996). "Electrical resistivity of compacted clays." Journal of geotechnical engineering 122(5): 397-406.

Archie, G. E. (1942). "The electrical resistivity log as an aid in determining some reservoir characteristics." Trans. AIMe 146(99): 54-62.

ASTM (2010). " Using the Direct Current Resistivity Method for Subsurface Investigation." ASTM International, West Conshohocken, PA, 2010, DOI: 10.1520/D6431-99R10,www.astm.org.

ASTM (2012). "Standard Test Method for Field Measurement of Soil Resistivity Using the Wenner Four-Electrode Method." ASTM International, West Conshohocken, PA, 2012 , DOI: 10.1520/G0057-06R12, www.astm.org

Atkins Jr, E. and G. Smith (1961). "1560-G-The Significance of Particle Shape in Formation Resistivity Factor-Porosity Relationships." Journal of Petroleum Technology 13(3): 285-291.

Campanella, R. and I. Weemees (1990). "Development and use of an electrical resistivity cone for groundwater contamination studies." Canadian geotechnical journal 27(5): 557-567.

Ekwue, E. and J. Bartholomew (2011). "Electrical conductivity of some soils in Trinidad as affected by density, water and peat content." Biosystems Engineering 108(2): 95-103.

Kalinski, R. and W. Kelly (1994). "Electrical-resistivity measurements for evaluating compacted-soil liners." Journal of geotechnical engineering 120(2): 451-457.

Kibria, G. and M. Hossain (2012). "Investigation of Geotechnical Parameters Affecting Electrical Resistivity of Compacted Clays." Journal of Geotechnical and Geoenvironmental Engineering1: 452.

Kim, J. H., H. K. Yoon, et al. (2010). "Void Ratio Estimation of Soft Soils Using Electrical Resistivity Cone Probe." Journal of Geotechnical and Geoenvironmental Engineering 137(1): 86-93.

McCarter, W. (1984). "The electrical resistivity characteristics of compacted clays." Geotechnique 34(2): 263-267.

McCarter, W. and P. Desmazes (1997). "Soil characterization using electrical measurements." Geotechnique 47(1).

Mitchell, J. K. and K. Soga (2005). "Fundamentals of soil behavior." Wiley, New York.

Mualem, Y. and S. Friedman (1991). "Theoretical prediction of electrical conductivity in saturated and unsaturated soil." Water Resources Research 27(10): 2771-2777.

Pozdnyakov, A., L. Pozdnyakova, et al. (2006). "Relationship between water tension and electrical resistivity in soils." Eurasian Soil Science39: 78-83.

Rinaldi, V. A. and G. A. Cuestas (2002). "Ohmic conductivity of compacted silty clay." Journal of Geotechnical and Geoenvironmental Engineering 128(10): 824-835.

Samouëlian, A., I. Cousin, et al. (2005). "Electrical resistivity survey in soil science: a review." Soil and Tillage Research83(2): 173-193.

Zha, F., S. Liu, et al. (2007). Evaluation of Change in Structure of Expansive Soils upon Swelling Using Electrical Resistivity Measurements. Advances in Measurement and Modeling of Soil Behavior, ASCE.

Neeson, F.C. (2013)
Developments in geotechnical site investigations in Christchurch following the Canterbury earthquake sequence
Proc. 19th NZGS Geotechnical Symposium. Ed. CY Chin, Queenstown

Developments in geotechnical site investigations in Christchurch following the Canterbury earthquake sequence

F C Neeson
Opus International Consultants, Christchurch, NZ
Frances.Neeson@opus.co.nz

Keywords: Site Investigations, Sonic Drilling, Standard Penetration Tests (SPT), Cone Penetration Tests (CPT)

ABSTRACT

Following the Canterbury earthquake sequence beginning 4th September 2010, site investigation techniques and practices have rapidly developed. Contractors locally and nationally have been quick to respond to the demand in Christchurch resulting in innovative applications of existing techniques sometimes not previously available in the New Zealand market.

Updated design codes and better informed clients have led to more comprehensive site investigations and geotechnical assessments post 4th September 2010. Guidelines have been revised and the Ministry of Business, Innovation and Employment (MBIE) (formerly the Department of Building and Housing) stresses the need to use calibrated Standard Penetration Test (SPT) hammers.. In the past liquefaction potential was assessed using SPT testing in boreholes often drilled by air flush rotary or direct push methods mainly due to uncertain ground conditions and limited budgets. At present liquefaction potential analysis commonly uses Cone Penetrometer Test (CPT) test results. However, Christchurch's interbedded alluvial geology often prevents CPT tests reaching sufficient depths and therefore boreholes with SPTs are still utilised below these depths.

The availability and selection of a range of site investigation techniques, accuracy of the factual data gathered during site investigations and resulting geological model are critical to the accuracy of the resulting analysis and applicability of geotechnical models.

This paper explores the development of site investigation techniques used in Christchurch since September 2010 and will compare the use of CPT and SPT N results for ground assessment.

New Zealand Geotechnical Society Inc. 19th Symposium, Queenstown 2013

1 INTRODUCTION

Christchurch is New Zealand's second largest city and is located on the east coast of New Zealand's South Island. The city is situated near the coast, on alluvial outwash plains and on the western flanks of the Lyttleton volcano of the Banks Peninsula volcanic complex. The South Island of New Zealand accommodates the Pacific and Australian tectonic plate boundary by a system of faults, most notably, the Alpine Fault.

At 4:35am 4th September 2010, the previously unknown Greendale Fault and at least two neighbouring blind faults ruptured inducing strong ground shaking felt across the South Island. This fault rupture has become known as the 'Darfield Earthquake' Ms7.1. The epicentre was located 45km south of Christchurch's CBD. The earthquake caused severe effects including widespread land damage due to liquefaction in addition to shaking induced damage of buildings which in some cases resulted mainly in the collapse of unreinforced masonry buildings. Following this initial fault rupture there has been a well recorded aftershock sequence (Geonet,

2013) including large aftershocks now referred to as the Boxing Day quake (26th December 2010), the Ms6.3 22nd February 2011 (Christchurch quake) where the epicentre was located just 8km from the CBD, June 13th quakes and December 23rd aftershock.

Surface expression of liquefaction has been clearly evident following several large seismic events of the Canterbury Earthquake sequence. Flooding and ejected sand and silt were wide spread following the September and February events but also occurred during smaller seismic events in more localised areas, for example the suburb of Parklands was particularly hard hit following the December 23rd aftershock. Liquefaction had dramatic effects and led to bearing failures beneath buildings, floating of buried structures, differential settlement damage to infrastructure and buildings, sinkholes or voids, lateral spreading and surface deposits of silt and sand with associated flooding.

2 GEOLOGICAL SETTING

2.1 General Setting

Christchurch is situated on Holocene sedimentary deposits and on the slopes of Miocene aged volcanic rock (Brown & Weeber, 1992). Christchurch is located near the east coast of the South Island on the Pacific Ocean, where large alluvial fans have been deposited from rivers and glaciers in the Southern Alps. The Waimakariri River, a large braided river has been the dominant source of alluvial materials.

The geological setting of Christchurch is comprised of swamp deposits formed behind beach dune sand; estuaries and lagoons; gravel, sand and silt derived from river channel and overbank flood deposits of the Waimakariri River floodplain. Marine sand deposited with the last marine transgression incurs beneath the CBD and underlies the eastern half of the city. The Avon and Heathcote rivers originate from springs west of Christchurch and meander through the city to form the main drainage system.

2.2 Stratigraphy

Typical stratigraphy in the Christchurch area consists of river channel and overbank silt, sand and gravel of the Springston Formation in the central and west of the city, much of the CBD is underlain by 3-6m of shallow gravel. Underlying the Springston Formation are marine and estuarine deposits of the Christchurch Formation which predominantly consist of silt and sand. Below this lies the Riccarton Gravel Formation, this is typically brown or blue gravel with some sand or silt. It is also the top most aquifer, and can demonstrate artesian pressures in wells and boreholes, historically this formation has been targeted as a water resource and the gravel is now often targeted for piled foundations.

3 GEOTECHNICAL INVESTIGATIONS PRE-QUAKE

3.1 General Practice

Prior to the seismic activity beginning in September 2010, Geotechnical practitioners faced a ‘hard sell’ in order to ensure clients spent money on geotechnical site investigations in Christchurch. Although widely known as a drained swamp, Christchurch had been relatively seismically quiet this century. As such, when clients commissioned geotechnical assessments and site investigations, budgets were kept tight restricting the scope of investigations and designers had to make do with minimal investigations. Cone penetration tests (CPTs) were only used occasionally, as they risked being limited by potential shallow refusal on gravel lenses. Boreholes with Standard Penetration Testing (SPTs) were favoured, as whatever the local ground conditions were, information in the form of material samples and SPT results would be

obtained. However, these compromises tended to lead to a 'one size fits all' approach when designing site investigations and alternative investigation techniques were often not used, if at all considered.

3.2 Available Site Investigation Methods

Prior to the Canterbury Earthquake sequence, site investigations in Christchurch predominantly consisted of hand auger, Scala Penetrometer testing and test pitting for shallow investigations and boreholes for deeper investigations.

Boreholes were generally conducted by air flush rotary/ concentrix or cable tool drilling (downhole hammer) or direct push (top of hole hammer) drilling. Airflush/concentrix techniques produced a disturbed sample which was flushed from the borehole usually using compressed air. Samples are bagged for each run and coarse materials such as coarse gravel or cobbles are broken into smaller sized pieces. This technique is quick in coarse alluvial materials such as sand and gravel, but slower in cohesive soils. SPTs allowed samples with fewer disturbances to be collected and allow for a more accurate soil description. However, the energy efficiency of different hammers were not often calibrated.

Direct Push drilling methods were more recently introduced which produce a disturbed sample by jacking the core barrel with an internal plastic liner. The core barrel is retrieved from each run and the plastic liner containing the soil samples removed and the soil samples are found in their relative positions but does not maintain their relatively density (see Figure 1 below). This method generally produces a consistent core sample, although gravel sampling is limited to the core barrel/ plastic liner size. This method is however, limited to shallower depths than downhole hammer techniques and until recently was not able to penetrate sufficiently into dense gravels found in the Springstons and Riccarton Formations.

Conventional triple tube coring was also undertaken in Christchurch with varying success (Figure 1). However, it can tend to wash fines from the core samples and drilling in the Riccarton gravel formation proves tough on drill bits.



Figure 1a: Example of Direct Push Core from Christchurch (Springston Formation)



Figure 1b: HQ Rotary Core from Sydenham, (Christchurch Formation and Riccarton Gravel)

CPTs were used relatively infrequently in Christchurch prior to the earthquake sequence as their success was not guaranteed across a site nor between sites. Concern for the CPT tests pulling up short due to shallow gravel led to the testing being considered costly to both time and budget (i.e. mobilisation costs) and with no guaranteed result. Where client's budgets for site investigations were restricted, a borehole with SPTs was favoured over a CPT which may or

may not reach the target depth. Predrilling was rarely used to enable CPTs to be advanced below shallow gravels.

Hand augers, Scalas and test pits have and continue to provide valuable information on surficial soils up to 3.0 metres for a small expense. However, in the past hand auger and Scala results in some cases tended to have been heavily relied upon, sometimes without additional deeper site investigations.

3.3 Liquefaction Hazard

Liquefaction was a well-known hazard prior to the Canterbury earthquake sequence. The Canterbury Region Council, Environment Canterbury (ECan) have the role of monitoring natural hazards in the region. ECan produced a Liquefaction Hazard Map for Christchurch in 2006 which used information gained from ground investigations to predict where damaging liquefaction may occur in a future seismic event. Prior to this the University of Canterbury had conducted many research programmes and produced a series of papers on liquefaction and developed a CPT rig in the 1990's.

4 GEOTECHNICAL INVESTIGATIONS POST-QUAKE

4.1 Post-Quake Developments

Following the Canterbury Earthquake sequence, there has been a rapid increase in Site Investigation methods available in Christchurch. CPTs have become common place with numerous rigs now available from both local and national contractors and consultants. Significant investments have been made by local and national contractors to adapt, and purchase new testing equipment in response to the demand for site investigations following the earthquakes. New methods now available in Christchurch include Sonic drilling, seismic CPTs, Dilatometer testing (DMT), Geophysical techniques including Multi-Channel Analysis Surface Waves (MASW), Gel-Push sampling, and SPT calibration. Two of these new methods are discussed in further detail below.

4.2 Sonic Drilling

Drilling using Sonic methods is a new technique in the Christchurch market and is relatively new to New Zealand. Numerous drilling companies now offer variations of sonic drilling. Advantages of sonic drilling include the timeliness of the investigation, a 25m sonic drilled borehole can be achieved in one to one and a half days; a disturbed but well recovered core sample is collected (see Figure 2), recoveries of near 90 to 100% are usual; sampling appears representative, with both fine and coarse material recovered (ie fines within the Riccarton Gravel are recovered, as opposed to rotary coring where they can be washed away); and sonic drilling is capable of reaching significant depths, similar to rotary and much greater than direct push methods.



Figure 2: Example of Sonic Core from Christchurch CBD (Riccarton Gravel Formation)

Some limitations of sonic drilling have been and continue to be discussed amongst the industry including concern regarding sonic disturbance of the insitu soil sediments and its effect on SPT results. Two main types of sonic drilling techniques are available in Christchurch these are dual sonic and bottom out sonic. The dual sonic method consists of the casing and sampler advanced together using sonic methods with little need for water. Bottom out methods advance the sampler to the bottom of the run first then the casing is advanced to the same depth. If this method is used, water may need to be used to flush the hole to prevent material jamming between the sampler and the casing. There are concerns that this flushing may disturb the in-situ materials below the toe of the sampler. These effects have yet to be quantified. This possible disturbance however, is only one variable of many that may affect SPT results. Idriss and Boulanger (2008) assert that the most important variable of the SPT test is the amount of energy delivered by each drop of the hammer to the drill rods which can vary by 30-90%. In addition the seating drive or first 150mm of the SPT test is designed to accommodate some drilling induced disturbance.

4.3 Cone Penetration Tests (CPT)

Following the Canterbury earthquakes CPTu's have become the prevalent site investigation testing method for liquefaction analysis in Christchurch. This is mostly likely due to the results being continuous, testing being relatively quick and affordable (compared to boreholes), and comprehensive geotechnical investigations becoming more prevalent. CPT testing has developed over time from mechanical CPTs to electric piezocones (CPTu) and more recently to seismic CPTs where cones have a built in geophone. Rigs vary from truck to track mounted, some have drilling equipment integrated so that testing is not limited by course fill or shallow gravel and now it is also possible to use rigs with sampling capacity.

5 CPT AND SPT COMPARISONS IN CHRISTCHURCH

CPTs are now the preferred site investigation method for liquefaction analysis in preference to SPT test results that were widely used in the past. SPT testing must be conducted with a drill rig and tests are most commonly conducted at 1 to 1.5m intervals. SPT tests are undertaken over 450mm rather than continuous results gained as the CPT probe is advanced. However, there are still situations where SPT testing is required either in addition to or without CPTs. The presence of gravel horizons or lenses within Christchurch's alluvial sediments can lead to shallow refusal of CPTs and therefore SPTs are still used to provide soil parameters for liquefaction at depths below CPT termination.

A comparison of SPT results and adjacent (within 2-3m) CPT tests has been conducted at three different sites across Christchurch. Drilling has been undertaken by Sonic, Direct Push and Conventional rotary coring methods. SPT testing was conducted at each site as per NZS4402 Test 6.5.1 where a standard 63.5kg hammer with automatic release was dropped on the anvil to drive the split spoon 450mm or to a refusal value of N= 60+. All hammers however have different energy efficiencies which refer to the amount of energy delivered through the SPT rods. Robertson et al. (1983) suggest this is the most significant factor affecting the measured N value and Idriss and Boulanger (2008) assert that the actual delivered energy can vary by 30-90% of the theoretical maximum. This variance becomes important when measured (N_M) raw SPT N values are near the boundary of liquefiable or non-liquefiable conditions. Measured SPTs for all three sites have been corrected using Idriss and Boulanger's (2008) following equation:

$$N60 = C_E\, C_B\, C_R\, C_S\, N_M$$

Where C_E is the measured or empirical energy ratio correction factor, C_B is the borehole diameter correction factor, C_R corrects for SPT rod length, C_S provides correction for the spoon

New Zealand Geotechnical Society Inc. 19th Symposium, Queenstown 2013

sampler and N_M is the measured SPT N value. Where measured energy efficiencies are not available empirical estimates have been suggested by Idriss and Boulanger (2008). The empirical estimates contain considerable uncertainties and Idriss and Bolanger (2008) have suggested ranges to allow for the underlying uncertainties as shown in Table 1 below. Also shown is the measured C_E for the Automatic trip hammer as provided by the contractor for one of our case study sites.

Table 1: C_E estimated ranges (from Idriss and Boulanger 2008) and measured values

Site	Hammer type	C_E Empirical estimate	Measured C_E
Heathcote	Doughnut hammer	0.5 – 1.0	-
Estuary	Safety hammer	0.7 – 1.2	-
CBD - Avon	Automatic trip hammer	0.8 – 1.3	1.424

For each site, a CPT derived ($N_1$60) plot has had measured SPT N values (N_M) overlain for comparison. Three different types of SPT hammers namely a Safety Automatic, Doughnut and Safety Hammer were used for the investigations conducted. The N_M SPT results are plotted against the CPT derived $N_1$60 continuous plot and in addition the upper and lower C_E values suggested by Idriss and Boulanger (2008) have also been shown in Figure 3.

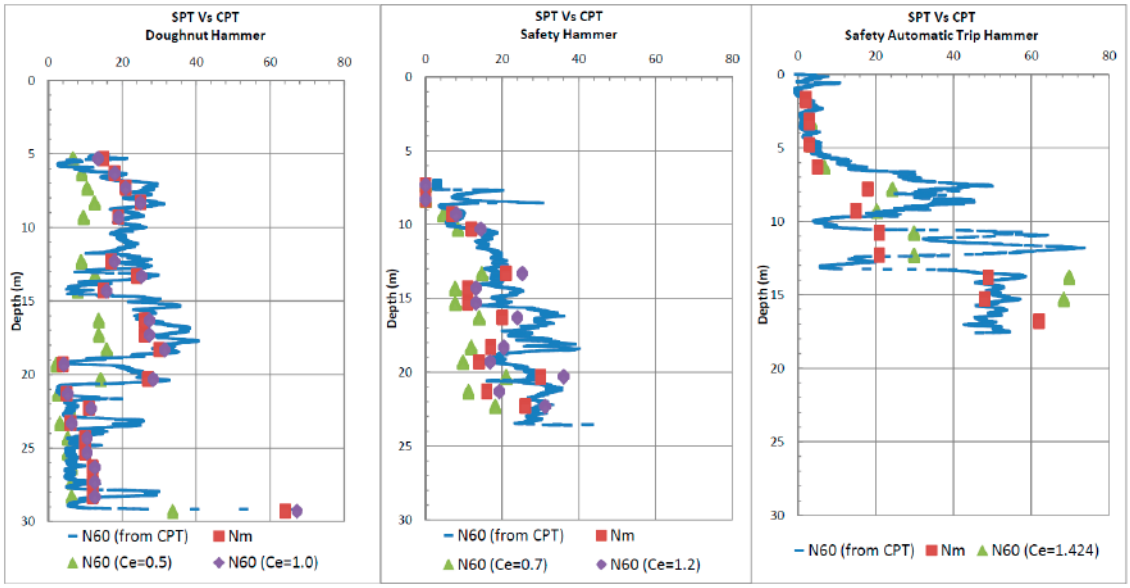


Figure 3: SPT N values and CPT derived $N_1$60 for three different SPT hammers.

As illustrated each hammer has variable energy efficiency (C_E) and the ranges suggested by Idriss and Boulanger (2008) result in significant possible variables. Energy corrected N60 (C_E1.0) for the Doughnut Hammer shows a good correlation with the CPT results up to 20m depth, however below this point an N60 (C_E0.5) appears to have a better correlation with the CPT results. The Safety Hammer and Safety Automatic Trip Hammer also show a poor correlation at depth. The Safety Automatic Trip Hammer has been calibrated for energy efficiency and it compares well to the CPT plot at this location to approximately 15m depth, where it appears a smaller C_E value would provide a better correlation with the CPT plot. The poor correlation at depths greater than 15-20m could be due to several possibilities not accounted for in this analysis, such as overburden effects or fines content adjustments. Furthermore, it could be due to a poor correlation between CPT outputs and the derived N60 at depths greater than 15m.

The discrepancies between corrected SPT N values (N60) and CPT derived N_160 values should be considered when undertaking liquefaction and lateral spreading analyses. By conducting at least one CPT next to a borehole during site investigations, comparisons between the two in-situ testing methods and results can be made. SPTs allow for samples to be collected which can then be used for soils description and laboratory analysis methods such as particle size and behaviour tests. CPT tests produce cone resistance (qc), sleeve friction (fs) and dynamic pore pressure (u2) outputs from which numerous other empirical results are derived, such as equivalent N60 values and soil types. The comparisons of SPTs allow checks to be conducted on empirical CPT outputs.

In-situ test repeatability is another aspect to consider, while SPTs are conducted to a standard (NZS4402) there may be inherit differences when conducted by different operators. Robertson et al (1983) highlighted this issue before automatic trip SPT hammers were common place. This suggests there is value in comparing calibrated SPT hammers to adjacent CPT results, as there may be slight operator induced differences and it is a quick verification method.

6 CONCLUSIONS

Site Investigation methods and budgets have developed following the Canterbury Earthquake sequence. Prior to the seismic activity, Geotechnical practitioners often faced a somewhat 'hard sell' to ensure clients invested in geotechnical site investigations. As such, investigations were tailored to provide maximum information gained at minimal expense. This lead to CPTs being underutilised as Christchurch's highly variable ground conditions could not guarantee their success due to the presence of gravel lenses at shallow depths across the city.

Drilling contractors have been quick to respond to the demand for site investigations in Christchurch and this had led to the emergence of Sonic drilling capability in Christchurch and subsequently the New Zealand market. Sonic drilling provides various advantages in Christchurch's variable ground conditions including arguably the best core recovery of any drilling method currently present in Canterbury, quick sampling and sufficient depth and penetration into the dense Riccarton Gravels, which are a significant formation often targeted for piled foundations. Various opinions exist regarding sonic disturbance of the in-situ soils and its effect on SPT results however, this is just one of the many possible variables that can affect SPT results and Robertson et al (1983) and Idriss and Boulanger (2008) assert that the most important varible affecting SPT results is the amount of engery delivered to the drill rods, known as the energy efficiency of the hammer.

CPT tests have become the most favoured method for deriving site specific soil characteristics and conducting liquefaction potential analysis. CPTs are relatively quick and affordable in comparison to traditional drilling methods which used SPTs to determine liquefaction analysis parameters. Value can be added to both boreholes and CPT test results when they are conducted side by side and the results are compared. CPT results measure a continuous output of cone resistance, sleeve friction and dynamic pore pressure, however boreholes and SPT results allow for description of the soil sample by an engineering geologist, provide samples for laboratory testing and allow groundwater conditions to be monitored or further analysed. By comparing both methods empirical results derived from CPT measurements can be compared to retrieved samples and laboratory analysis.

Measured SPTs need to be corrected for energy efficiency which can vary from 30-90% of the theoretical energy (Idriss and Boulanger, 2008). The MBIE now advocates for the use of calibrated SPT hammers and contractors are responding to this requirement. Other variables that need to be included when deriving a SPT N60 value include rod length, borehole diameter and SPT sampler. Comparisons to CPTs show that other considerations may also need to be incorporated at depth, due to the poor correlation between corrected SPTs and CPT derived N60

New Zealand Geotechnical Society Inc. 19th Symposium, Queenstown 2013

plot at depth. Further work needs to be conducted to determine if fines content corrections, overburden affects or drilling method have an effect on this poor correlation at depth. In addition the reliability of the CPT derived $N_1$60 correction needs to be looked at as this could also be a contributor to the poor correlation from 15m or deeper.

The comparison of CPT and SPT data would suggest that neither CPT nor SPT data should be used in isolation when considering liquefaction potential at depth. By comparing CPT and SPT results, the designer is able to build a better geological model of the sub-surface soil characteristics and properties at each site. If the differences between CPT and SPT results are considered, the designer has more understanding of the site characteristics and limitations of both in-situ test methods when opting to use CPT or SPT or both methods for liquefaction and lateral spreading analysis.

ACKNOWLEGEMENTS

I wish to thank Opus International Consultants and my colleagues, in particular Greg Saul, Christine Parkes and Kelly Walker, who have reviewed my abstract and paper.

REFERENCES

Brown, L & Weeber, J (1992) Geology of the Christchurch urban area. Scale 1:25,000. Institute of Geological & Nuclear Sciences geological map 1. 1 sheet + 104p Institute of Geological and Nuclear Sciences Limited, Lower Hutt, New Zealand.

Environment Canterbury (2006) The Solid Facts on Christchurch Liquefaction http://ecan.govt.nz/publications/General/solid-facts-christchurch-liquefaction.pdf

Geonet (2013) Canterbury Quakes http://info.geonet.org.nz/display/home/Canterbury+Quakes

Idriss I.M and Boulanger R.W (2008) Soil Liquefaction During Earthquakes, Earthquake Engineering Research Institute Monograph pp70-83

Robertson, P.K; Campanella, R.G; M ASCE; Wightman, A (1983) SPT-CPT Correlations, Journal of Geotechnical Engineering, Vol. 109, No. 11, pp1449 - 1459

O'Sullivan, A., Soric, D. & Terzaghi, S. (2013)
Stress path approach to settlement analysis of soft ground
Proc. 19th NZGS Geotechnical Symposium. Ed. CY Chin, Queenstown

Stress path approach to settlement analysis of soft ground

A. O'Sullivan
Hiway GeoTechnical Ltd, Silverdale, NZ
andy@hiways.co.nz (Corresponding author)

D. Soric
Soil & Rock Consultants
damir@soilandrock.co.nz

S. Terzaghi
Arup, Sydney
sterzaghi@arup.com.au

Keywords: Stress history, Seismic dilatometer testing, Oedometer testing, Secondary consolidation, settlement analysis, deep jet mixing (DJM), ground improvement

New Zealand Geotechnical Society Inc. 19th Symposium, Queenstown 2013

1.0 ABSTRACT

The paper will describe the site investigation, laboratory testing and detailed design analysis carried out to determine the settlement profile for a large commercial structure (approx. 2,500m^2) constructed on a 25m thick layer of recent to Holocene aged, soft alluvial deposits (typical su = 10-20kPa). The initial settlement prediction for the site indicated that without any ground improvement, the construction of the building would result in settlements in the order of 300mm which was unacceptable from a structural point of view. As a result, it was deemed necessary to install some form of ground improvement.

During the site investigation phase, three difference investigation methods were used, namely boreholes (BHs) with standard penetration tests (SPT), cone penetration tests (CPTs) and seismic dilatometers (sDMT). All three gave very different interpretations of the soil properties, particularly in terms of soil stiffness. In addition to the in-situ tests, a series of oedometer tests were carried out.

Both the sDMT and the laboratory testing indicated the material had an overconsolidation ratio (OCR) between 1.3 and 1.7, despite the upper layers being recently deposited and in a manner associated with normally consolidated behaviour.

The detailed design concentrated on obtaining reliable values for both the primary and secondary consolidation of the soft alluvium. As part of the detailed design analysis, finite element modelling was carried out using a constitutive model which incorporates the effects of secondary consolidation through the input of a value for c_α. The paper will describe the importance which stress path (depositional history) played in determining both reliable values for the primary and secondary consolidation and how the differences in stiffness between the sDMT and oedometer tests were reconciled.

2.0 BACKGROUND

The proposed structure is intended to replace an existing, 50 year old, structure on an adjacent site which has undergone very significant total and differential settlements, the latter being in the order of 250mm. By back analysing the settlement profile for the existing structure, the

designer was able to use this information to calibrate the soil parameters used in the detailed design analysis of the proposed structure. This is discussed in further detail below.

From the outset, it was deemed uneconomic to install foundations to the base of the 25m thick alluvial layer. Rather, the client accepted an option to carry out ground improvement to a sufficient depth such that the overall settlement could be kept to an acceptable level. This was set at 120mm over the lifetime of the building with limited differential settlements being tolerated. The challenge for the designer was therefore to determine at what depth this could be achieved and what the potential risks to the project were. Figure 1 below shows the site location in Dargaville.



Figure 1: Geological Map of the site location (Edbrooke SW, 2012)

3.0 SITE INVESTIGATION AND LABORATORY TEST RESULTS

In order to characterise the soil properly, a number of different test methods were utilised, both in-situ and ex-situ. These included 7no. CPTu, 2no. sDMTs, as well as one fully cored BH with two samples taken at 3.5m and 11m depth. Hand shear vane readings and SPTs were taken at uniform intervals during the BH drilling. Oedometer tests were carried out on the two sample tubes recovered. Figure 2 below shows the site investigation layout plan for the site.

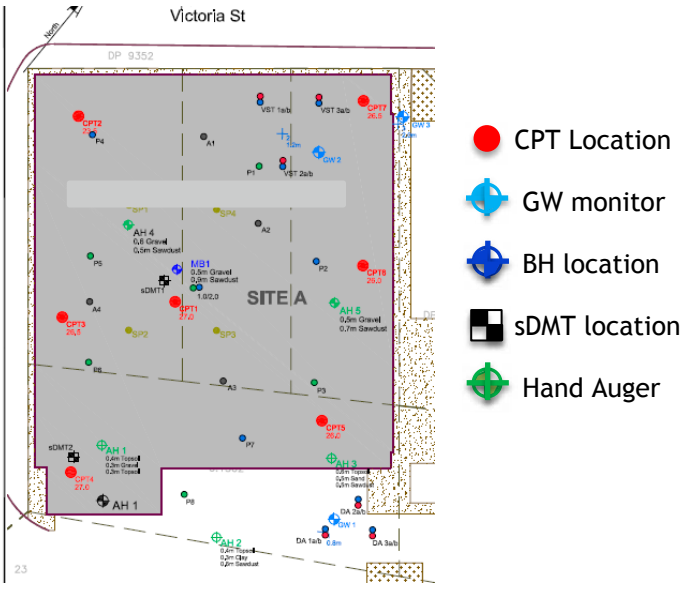


Figure 2: Site Investigation Layout Plan

As expected, the SPTs provided the most conservative assessment of the ground conditions. The values obtained were typically 0-1. Surprisingly, the CPTs also indicated extremely low

strength and soil stiffness. By comparison, the oedometer tests and particularly the sDMTs indicated significantly better ground conditions. A comparison between the CPT profile and the sDMT profile is shown in Figure 3 below.

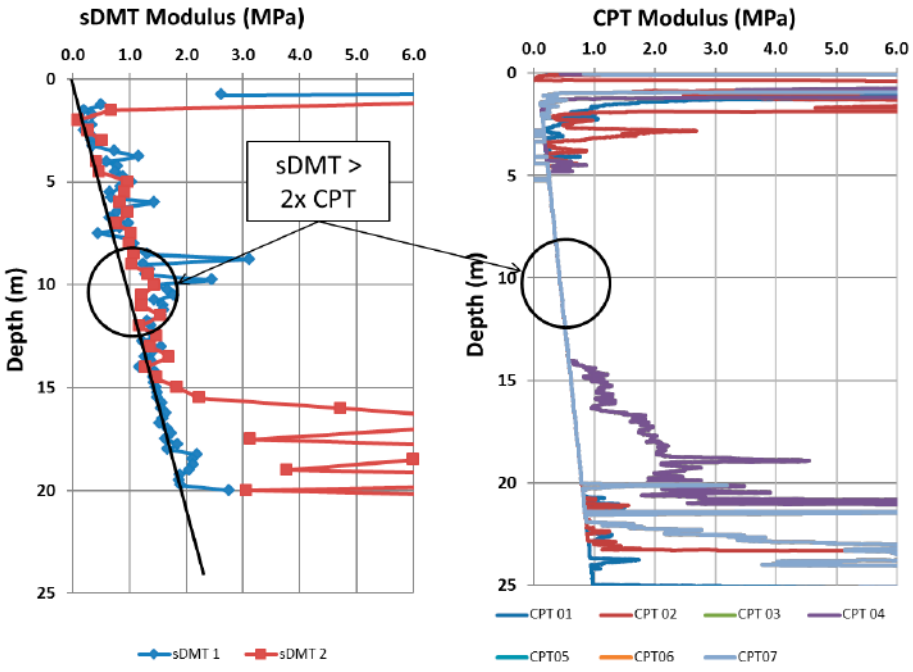


Figure 3: Comparison in Constrained Modulus Interpretation between sDMT and CPT

The site investigation also allowed a number of other observations to be made on other soil characteristics such as the relationship between engineering strain and small strain modulus. Figure 4 below illustrates this relationship, which implies that the $E_0/E \approx 10$ for the soft alluvium. This is within the normal range for soft, normally consolidated clays given in the literature. (Brinkgrieve R, 2013) (Marchetti, 2013). E_0 was obtained from the shear wave velocity profile, whereas E (E50) was obtained from the dilatometer modulus E_D (Marchetti, 2013).

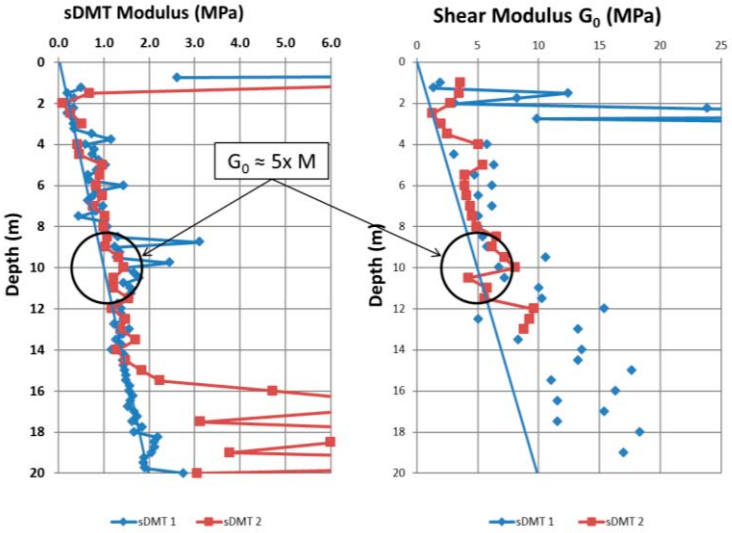


Figure 4: Comparison in Constrained Modulus (M) and small strain Shear Modulus (G_0) from the sDMTs

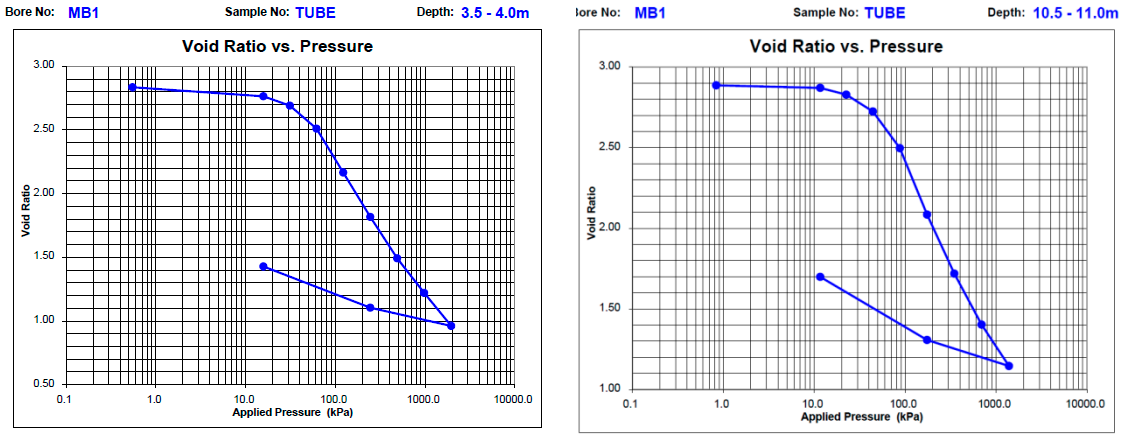


Figure 5: oedometer test results for sample taken at 3.5m and 10.5m. (Mv = 1.2-1.3m^2/MN for both tests at confining pressure)

Sample	Depth (m)	Liquid Limit (%)	Plastic Limit (%)	Plasticity Index
1	3.8 – 5.0	129	37	92
2	6.0 – 6.8	117	34	83

Figure 6: Atterberg Limits (all plot above A-line)

As previously noted, the site investigation indicated that the soils exhibited an overconsolidation ratio (OCR) in excess of 1, despite the upper layers being recently deposited and in a manner associated with normally consolidated behaviour. The OCR profile for the in-situ shear vane results (based on a relationship of OCR = $s_v/(0.3*\sigma'_v)$), the sDMT tests and the oedometer test is shown in Figure 7 below.

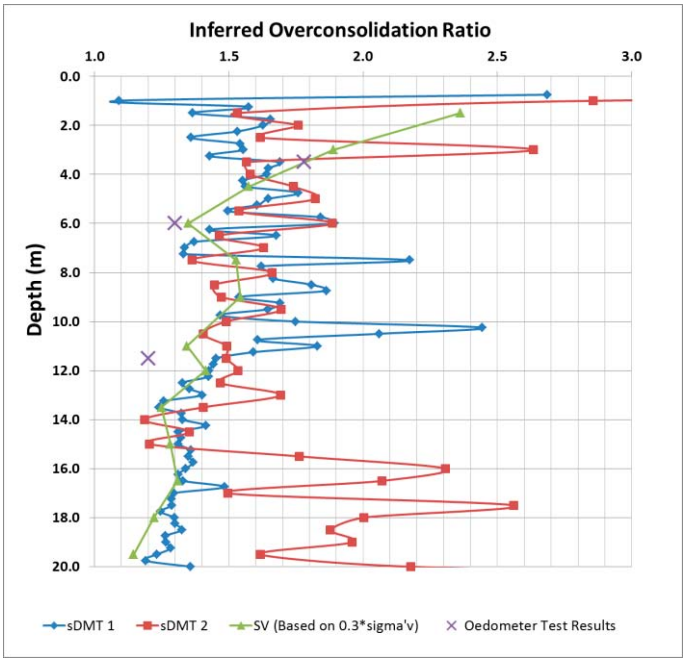


Figure 7: Inferred Overconsolidation Ratio profile against depth

4.0 CALIBRATION OF MODEL AND DETERMINATION OF DESIGN PARAMETERS

Given the main design challenge was reliably determining the rates for primary and secondary consolidation, the four main soil parameters required for the analysis were deemed to be:

(a) Constrained Modulus (M or E_{oed})
(b) Unload stiffness (E_{ur})
(c) OCR
(d) Permeability (k_x and k_y)

The initial model calibration concentrated on obtaining a reliable constrained modulus value (M). In order to derive this, a simulation of the oedometer tests was carried out in the FE programme Plaxis. The exact test cell dimensions, load increments and time steps were used in the simulation. The results of the simulation for both oedometer tests are shown in Figure 8 below. (3)

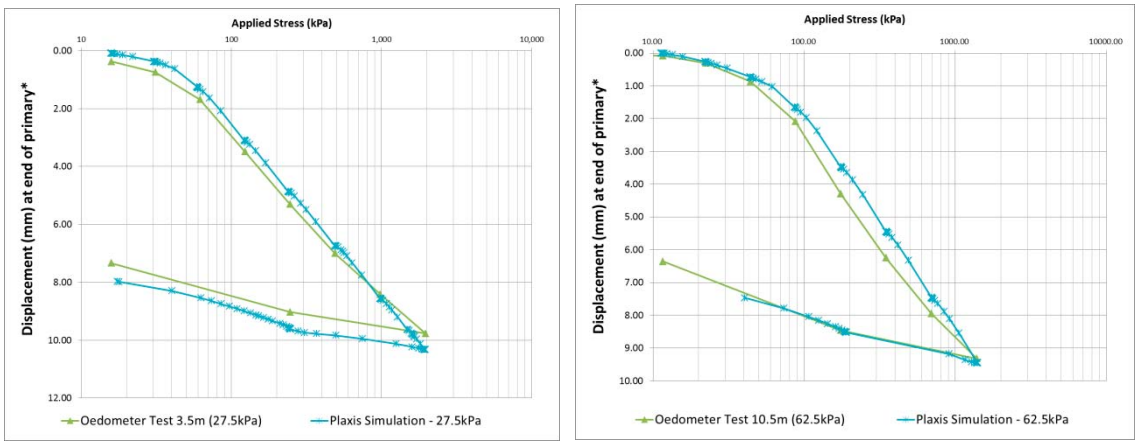


Figure 8: Comparion between Oedometer Test results and simulation of test using FE model for oedometer tests at 3.5m and 11m depth respectively.

Following this simulation exercise, the same soil parameters were entered into a full scale model of the overall site in the FE programme and the settlement of the existing building modelled. This showed that the predicted differential and total settlements over the lifetime of the building (50 years) exceeded that observed on site by an order of magnitude (predicted total settlement in model was approx. 900mm and predicted differential settlement in model was approx. 470mm). Hence, the constrained modulus value was doubled and the analysis re-run. This revised modulus value was more in line with the modulus value for the soil predicted by the sDMT tests. The results of this second calibration were much closer to the actual observed settlements for the existing adjacent building. Hence this constrained modulus value was used in the final analysis.

The unload stiffness was assumed to be five times the primary loading stiffness. This was based on the ratio of c_s to c_c obtained from the oedometer tests (0.15 to 0.86 resp.) and also information obtained from the literature. (Brinkgrieve R, 2013) (Bjerrum, 1967)

Permeability values (k_x and k_y) for the soils were estimated from the oedometer and CPT tests. k_x was assumed to be an order of magnitude higher than k_y based on the depositional history of the site.

4.0 DETERMINATION OF CREEP RATE AND OVERCONSOLIDATION RATIO (OCR)

Figure 9 below shows the results of the oedometer test taken at 3.5m depth, which is equivalent to an effective confining pressure of 27.5kPa. The NC line is shown along with three points A, B & C. In addition, the vertical insitu confining pressure line is shown. Given that the material is normally consolidated, the theoretical void ratio at deposition is at point A assuming no additional loading has been applied since deposition. The difference in void ratio between point A and B is therefore as a result of creep. By estimating the age of the material (10,000 years) from the geological information provided, the creep rate for the soil can therefore be estimated. The value obtained for c_α (plaxis) on this basis was 0.02. This is within the normal range of secondary consolidation rates for normally consolidated clays given in the literature. (Buisman, 1936), (Lambe TW, 1979) (Terzaghi K, 1996)

However, as the void ratio decreases from point A to point B, the yield surface remains on the NC line and hence the ratio of confining pressure between point C and point B is the OCR generated through creep as the soil moves from point A to point B. This explains how a normally consolidated soil can display an OCR in excess of 1.

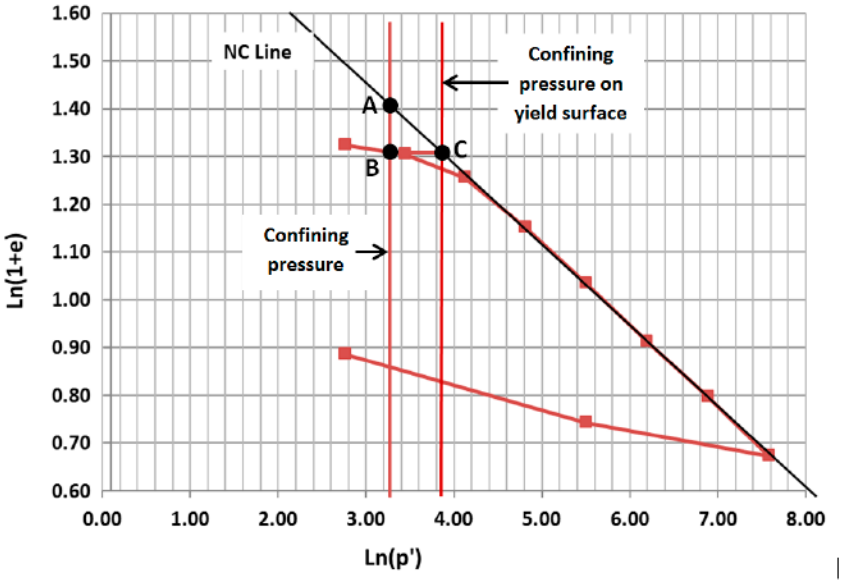


Figure 9: oedometer test ln v (1+e) against ln p´

The FE model was then re-run with the full stress history for the site. The following stages were modelled:

(1) Gravity
(2) Deposition and Aging of material (10,000 years)
(3) Recent construction of existing adjacent building (50 years)
(4) Construction of proposed structure (1 year)
(5) Long-term settlement of proposed building (50 years)

For stage 1, the initial void ratio at deposition was entered. An OCR value of 1.0 and a c_α value of 0.02 were entered into the model. Stages 1, 2 & 3 were then run. Note that Stage 3 ends at the current time. This stress path equates to the path from Point A to Point B in Figure 9 above.

By carrying out the analysis using the stress history of the site, this allowed the model to generate the current OCR through creep (difference between point B and C above) and thus

adjust the void ratio to the present day value (point B). The predicted OCR profile in the model was then compared to that measured on site. The results of this are shown in Figure 10 below.

The importance of using the OCR for the analysis was deemed to be high as the OCR will provide the confining stress at which the soil stiffness reverts from a much higher unload stiffness (within the yield surface) to the normal primary loading stiffness (on the NC line).

Using the parameters obtained from this analysis, the proposed structure was then modelled (Stages 4 & 5 above). The results indicated that the proposed settlement criteria could be achieved by installing a series of Deep Soil Mixed (DSM) columns, 800mm diameter at 2.4m centres to depths ranging from 8m to 13m depending on the location underneath the building and the local structural load influences. Three 2-D models were generated which represented typical cross-sections through the building. As expected, the influence of the existing adjacent structure (which is to be demolished once the new structure is completed) proved to be very significant. The results of the settlement outputs are shown in Figure 11. The final adopted design parameters are provided in Table 1 below.

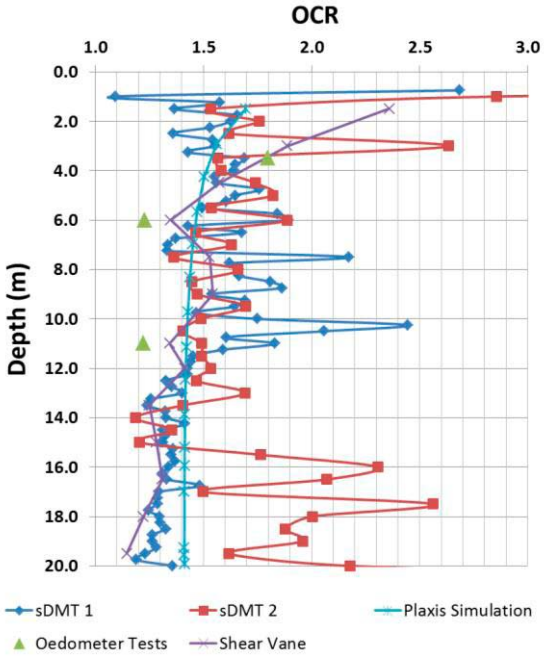


Figure 10: OCR Profile with depth showing FE simulation against values obtained on site

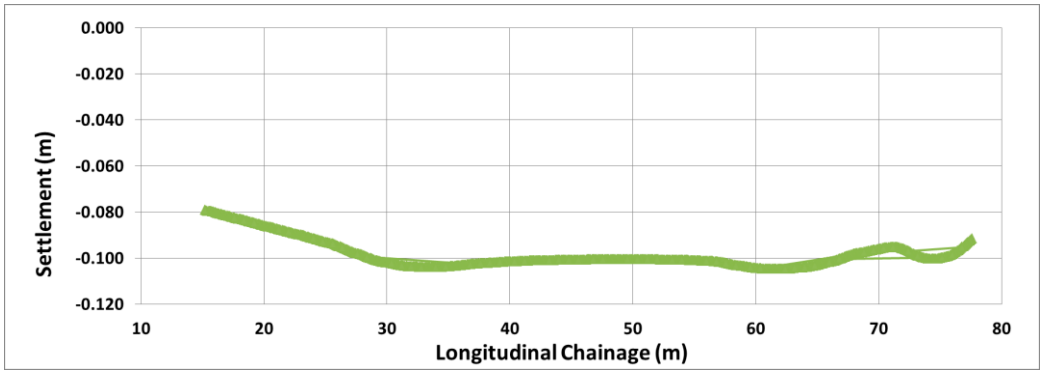


Figure 11: Predicted long-term settlement profile under proposed structure (max. = 128mm; differential under building = 25mm)

New Zealand Geotechnical Society Inc. 19th Symposium, Queenstown 2013

Table 1: Final adopted soil parameters

Soil Unit	Effective friction angle ø´ (°)	Apparent cohesion (c´) kPa	Cc	Cs	Cα
Recent Alluvium	24	4	0.65	0.12	0.02

5.0 CONCLUSIONS AND DISCUSSION ON RESULTS

The analysis highlighted a number of key areas of importance when assessing settlement of structures on soft soils. These can be summarised as follows:

(1) Soils exhibiting an OCR in excess of 1.0 will have a much higher constrained modulus to up the point at which the confining stress intersects the NC line. Beyond this point, the constrained modulus will revert to the normally consolidated primary loading value.
(2) The creep value of a soil can be estimated if the age of the soil and a reliable current OCR value are known.
(3) The influence of adjacent structures on the settlement prediction of a new structure is very significant. This zone of influence can extend to half the width of the existing structure beyond that structure.
(4) The CPT, SPT and oedometer tests significantly under-predicted the soil stiffness, whereas the sDMT tests provided a considerably more reliable assessment based on the back analysis carried out on the existing 50 year old adjacent building.
(5) The oedometer test however provided a reliable estimate of OCR and an indication of the relationship between unload and primary loading stiffnesses.

The low stiffness values obtained from the oedometer tests were attributed to sampling disturbance. In addition, it is important to note that the level of strain in oedometer tests is very high (2-5% volumetric strain at overburden stress) compared to that which the soils on site as they undergo settlement beneath the proposed structure (typically 0.25-0.5% vol. strain). By contrast the sDMT provides the stiffness at a far lower level of strain (0.1% volumetric strain). When corrected for strain level, the two provided much close predictions of overall stiffness.

6.0 ACKNOWLEDGEMENTS

The authors would like to thank the client for allowing the use of the site investigation information and analysis to be included in this paper.

7.0 BIBLIOGRAPHY

Bjerrum, L. (1967). Seventh Rankine Lecture: Engineering geology of Norwegian normally consolidated marine clays as related to settlements of buildings. *Geotechnique*, 17:81-118.

Brinkgrieve R, W. D. (2013). *Plaxis 2-D, 2012 Manual*. Delft: Plaxis.

Buisman, K. (1936). Results of long duraction settlement tests. *1st Internation Conference on Soil Mechanics and Foundation Engineering* (pp. Vol 1:103-107). Cambridge Mass.: ASCE.

Edbrooke SW, B. F. (2012). *QMAP Whangarei Area*. Wellington: GNS.

Lambe TW, W. R. (1979). *Soil Mechanics SI Version*. John Wiley & Sons.

Marchetti, P. L. (2013). *The Marchetti Dilatometer*. Retrieved from The Marchetti Dilatometer: www.marchetti-dmt.it

Terzaghi K, P. R. (1996). *Soil Mechanics in Engineering Practice, 3rd Ed*. J Wiley & Sons.

A new multiple-step loading triaxial test method for brittle rocks

A Taheri, E Chanda
Deep Exploration Technologies Cooperative Research Centre, University of Adelaide, Australia
abbas.taheri@adelaide.edu.au (Corresponding author)

Keywords: Triaxial compression test, multiple-step loading, brittle rocks

ABSTRACT

To evaluate mechanical properties of rocks by triaxial compression (TC) testing, several identical samples are required. Multiple-step loading (ML) TC testing permits determination of a failure envelope for different confinement stress levels using a single sample. The test consists of a series of consolidation and shearing steps, and in each step the axial loading is stopped or reversed before a complete failure. In the method suggested by the International Society of Rock Mechanics (ISRM), axial load should be increased until the axial stress-strain curve shows a horizontal tangent. However, in most brittle rocks, at peak stress failure occurs almost instantaneously and without any precursory signs. In this situation, attempting the ML test is very difficult. A new ML loading test method is proposed for the determination of the triaxial compression strength envelope in brittle rocks. A series of uniaxial compressive strength (UCS), single-step loading (SL) and ML TC tests were conducted on pyritic schist rock samples. It was observed that, during axial loading, the point at which the value of secant Young's modulus is maximum (E_{sec}=max), is the most suitable criterion for estimating the imminent rock failure. Using the proposed method, the peak and residual strengths at different confining pressures, as obtained by a set of SL TC tests, can be determined rather accurately from the results of a ML test using a single specimen. Finally, it was concluded that, in brittle rocks, ML test increasing σ_3 produces more reliable results as compare to ML test decreasing σ_3.

1 INTRODUCTION

To evaluate the shear strength parameters using a single sample of rock, multiple-step loading (ML) triaxial compressive (TC) tests, consisting of a series of consolidation and triaxial compressive (TC) loading steps, are often employed. The ML TC test is now one of the standardized tests for rock recommended by ISRM (Kovari et al., 1983). By performing a series of ML TC tests on multiple core samples from a given site, it becomes possible to accurately evaluate the spatial variability of the strength of rock represented by a failure criterion.

However, results of previous research works reveal that the differences in the peak strength between the ML tests and the Single-step Loading (SL) TC tests can be variable (Taheri and Tani, 2008a, Kim and Ko, 1979). This can be explained by the fact that, during an ML test, the operator cannot confidently recognize the peak strength and likely halts the test prematurely. The results depend critically on the ability of the experimenter to recognize imminent failure of the test specimens and can therefore be inconsistent between different laboratory operators.

In an effort to optimize the ML test procedure, various criteria for determining the load reversal point have been evaluated. The point most widely used by researchers is that of "a sample exhibiting failure". Kovari and Tisa (1975) showed that the peak strength obtained in ML tests using this point is negligibly different from that obtained by SL tests. These results justified the use of this criterion in a number of studies. However, there is no doubt that this point is not easily identifiable during the test. Additionally, a large amount of plastic deformation takes place in the samples experiencing these stress magnitudes. Moreover, Kim and Ko (1979) described the dependency of the effectiveness of this method on the type of stress-strain curve. They used a ML loading method to test three different types of rock; Pierre shale, Raton shale

New Zealand Geotechnical Society Inc. 19th Symposium, Queenstown 2013

and Lyons sandstone. The stress path they used involved applying an initial confining pressure followed by axial loading until the sample showed signs of failure. At that point, the test was halted and the confining pressure was increased to the next level without removing the deviator stress. This procedure was repeated for as many confining pressures as required. "Sign of failure" was defined as the plateau of the stress-strain plot after leaving the elastic region. Similarly, the ISRM (1989) have suggested to increase axial load until the axial stress-strain curve shows a horizontal tangent (E_{tan}=0). Taheri and Tani (2008b) examined this method on a sedimentary soft rock. They experienced that due to large plastic deformations in the specimen immediately before arriving to this critical point (E_{tan}=0), the shear strengths obtained by this method show poor correlation with those measured using several identical intact specimens.

Subsequently, Cain et al. (1986) developed a modified test procedure and a different criterion for the detection of imminent failure in ML tests. Examination of the stress/strain relationships from uniaxial and triaxial tests on Amherst sandstone identified that for constant confining pressure, the point at which the volumetric strain returned to zero on a volumetric strain versus axial strain plot appeared to be a suitable criterion for prediction of the imminent failure of the rock sample. Similarly, Crawford and Wylie (1987) used the volumetric strain as a criterion to determine load reversal point. In the study performed by Pagoulatos (2004), the load reversal point is defined as the point where the volumetric strains start decreasing from contraction to dilation after recording the maximum contraction and the derivative of the curve at that point is equal to zero. However, the test has to be performed under low confining pressure to allow brittle failure of the dilative specimen. Another approach proposed by Youn and Tonon (2010) suggests that ML test should be stopped when deviator stress/radial strain relationship displays a yielding point.

Using lateral or volumetric strain as a criterion to recognize failure needs precise measurement of the axial and lateral deformations of the specimen. However, it is usually difficult to measure local deformations of the specimen during shearing due to possible malfunctioning of local measurement devices and/or some abnormal local displacements due to non-uniform deformations of the specimen. In a study performed recently by Taheri and Chanda (2013), strain gauges were used to measure axial and lateral deformations of the specimen inside a Hoek cell. To prevent the strain gauges from being damaged, different strain gauge protection methods were practiced. However, strain gauges were damaged in some of the tests before peak axial stress point and in most of the ML tests after a few loading steps. Consequently, it is extremely difficult to use strain gauge results to recognize a premature failure during a ML test. Indeed, when using local measurement result to recognize load reversal point, it is necessary to re-set the strain values for the next step of the test on a reference value of zero permanent strain, which may result in having more difficulty during testing and analysing the data.

Regardless of the approach, ML triaxial test has proven to be difficult in brittle rocks because of sudden failure of the material while loading. Indeed, using lateral or volumetric strain as a criterion to recognize failure turned out to be unsuccessful due to difficulties in measuring local deformation during five or more cyclic loadings in a ML test. Therefore, there is a need to design a test method for brittle rocks that could be followed smoothly and easily to yield a failure envelope from a single specimen by a ML test, comparable to the one obtained using several identical intact samples.

Taheri and Tani (2008b) proposed a new method for determining the axial load reversal point in ML test in a mudstone. They suggested that the axial loading should be ceased and reversed when the secant Young's modulus (E_{sec}) reaches its maximum value. They found that using the proposed method, the specimen can avoid experiencing large plastic deformations and therefore the consistency between original results of SL test and ML test was greatly improved.

Although, using the proposed method in a soft rock yielded good results, the applicability of this method (E_{sec}=max) on brittle rocks has not been studied yet. As a result, it is aimed in this study to further develop this method to cover the case of brittle rocks.

2 MULTIPLE-STEP LOADING TEST METHOD

In this study, the axial load reversal point was evaluated at each confining pressure based on the secant Young's modulus, E_{sec}, and the axial strain curve measured by the external measurement device (LVDT). This method is proposed to avoid partial or total failure of the specimen. During ML test, the secant stiffness keeps increasing; the "Sigh of failure" is defined as the plateau of the secant Young's modulus-axial strain plot after leaving the elastic region before E_{sec} starts decreasing.

In Figure 1, the suggested method and the ISRM suggested method (Kovari and Tisa, 1983) are compared by plotting deviator stress –axial strain and secant stiffness – axial strain curves. As it is shown, the point where stress increments become smaller marks the beginning of the stress state where the specimen has unstable fracture propagation. This point is recognized as the point where secant stiffness becomes a peak (E_{sec}=max). Author's previous study (Taheri and Tani, 2008b) confirmed that; using this criterion to define the axial load reversal point, the specimen never experiences much beyond the elastic region and its integrity until end of the test will be guaranteed. In contrast, the specimen may experience a large amount of plastic deformations and even premature failure, if E_{tan} =0 (Kovari and Tisa, 1983) method is chosen to recognize the axial load reversal point.

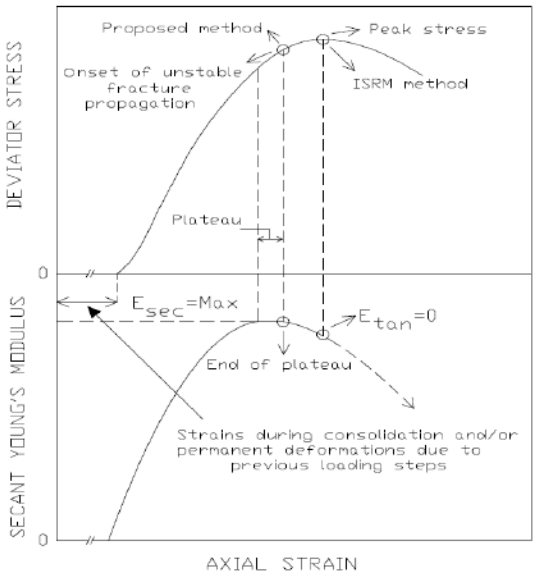


Figure 1: Suggested method to stop axial loading during ML test

Figures 2a & b, show axial stress-strain relations together with secant Young's modulus-axial strain relations in two SL tests performed at σ_3= 5 & 15 MPa. As can be seen in these figures, the secant stiffness evaluated by external LVDT keeps increasing until the axial stress become close to the failure point. It is fairly easy to identify a plateau after which the secant stiffness starts decreasing. In this method (E_{sec}=max) the end of this plateau is the point where axial loading is reversed. However, the operator has the ability to even pass the point without risking failure.

3 EXPERIMENTAL STUDY

A number of pyritic schist rock samples, were collected from Brukunga abandoned mine in South Australia. Cylindrical specimens measuring 42 mm in diameter and 100mm in length were prepared from the cored pieces according to ISRM standards. A total of 17 specimens were made to conduct uniaxial and triaxial tests.

A closed-loop servo-controlled testing machine with a loading capacity of 1000 kN and a loading rate capability in the range 0.001–10mm/s were used. A high-pressure Hoek cell and a hydraulic pressure system were used to apply confining pressure. Using the system the confining pressure is applied by pumping hydraulic oil to the triaxial cell and pressure is

maintained uniform using a pressure control system. The triaxial cell is equipped with a linear variable differential transformer (LVDT) to measure axial displacement and control axial loading. The load and strain data are acquired automatically by a data acquisition system.

The axial and lateral strains were measured with pairs of axial and lateral strain gauges pasted on the centre of the specimens in axial and lateral directions. To prevent the strain gauges from being damaged different strain gauge protection methods were practiced. However, strain gauges were damaged in some of the tests before peak strength and in most of the tests after the peak strength or after few cyclic loadings in ML tests. As a result, performing ML test using lateral or volumetric strain as a criterion to recognize failure based on results of local strain measurement turned out to be very difficult and unsuccessful. Consequently, effort has been made in this study to propose a ML test method using axial displacement values measured by external LVDT.

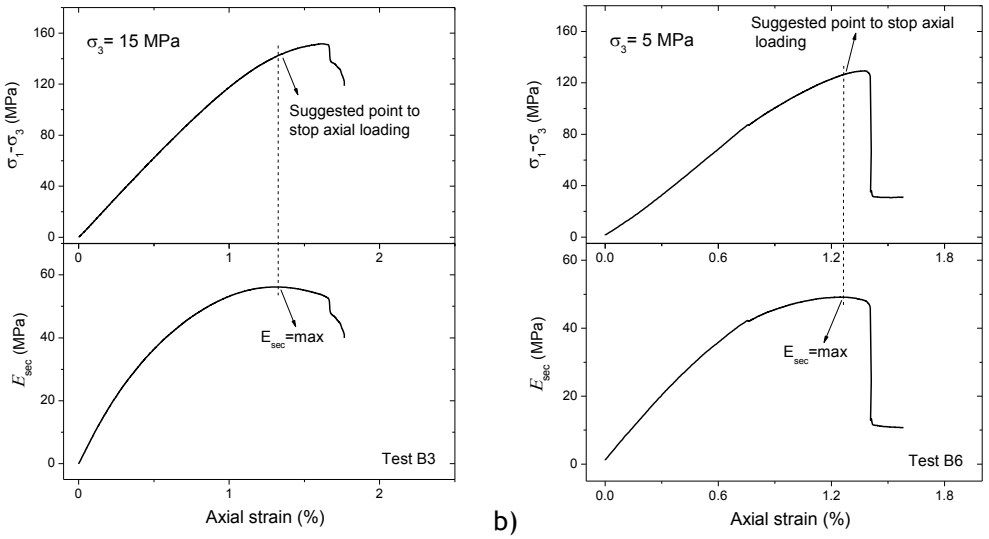


Figure 2: Deviator stress – axial strain and secant stiffness –axial strain relations measured in SL TC tests: a) σ_3= 15 MPa; b) σ_3= 5 MPa

The following series of TC tests were performed on specimens. The axial strain rate during TC loading was equal to 0.02 mm/min in all the tests:

Series 1 (SL TC tests at different constant confining pressures, σ_3 (Figure 3a): The specimen was isotropically consolidated inside Hoek cell at σ_3= 5 (2 tests) or 10 (2 tests) or 15 (2 tests) or 20 or 30 or 40 MPa and then subjected to continuous TC loading toward post-peak regime to determine the original peak strength and stress-strain properties at constant σ_3 that are free from any effects of previous TC loading history at the same σ_3 or other σ_3s. Residual strength was also measured in most of the TC tests. Using the similar loading method, one uniaxial compression strength (UCS) test was also performed which its results will be presented together with series 1 TC tests results.

Series 2: Seven ML tests were performed by different methods:
a) A ML test with full unloading of the deviator stress q= σ_1-σ_3 followed by an increase in σ_3 to measure peak strengths (Figure 3b): At the first step at σ_3= 5 MPa, during axial loading, when the secant Young's modulus (E_{sec}) appeared to reach its maximum value (refer to section 2), TC loading was terminated. Then, q was reduced to zero and σ_3 was increased to 10 MPa under isotropic stress conditions to perform the next step of TC loading. This procedure was repeated to perform TC loading at σ_3= 5, 10, 15 and 20 MPa. In the last loading step, axial loading continued until post-peak state to measure residual strength at σ_3= 20 MPa. Following this test method, 3 more ML tests were performed at σ_3= 2, 4, 6, 8 and 10 MPa.

b) A ML test with full unloading of q followed by an increase in σ_3 to measure peak strengths and a decrease in σ_3 to measure residual strengths (Figure 3c): First, the test procedure described in a), was followed until post-peak regime at σ_3= 20 MPa. In the last loading step at σ_3= 20 MPa, after some post-peak plastic deformation happened, q was reduced to zero and σ_3 was decreased to 15 MPa under isotropic stress conditions to perform the next step of TC loading. This procedure was repeated to measure residual strengths at σ_3= 20, 15, 10 and 5 MPa.

c) Two ML tests with full unloading of q followed by a decrease in σ_3 to measure peak strengths and an increase in σ_3 to measure residual strengths (Figure 3d): At the first step at σ_3= 20 MPa, when the secant Young's modulus (E_{sec}) appeared to reach its maximum value during axial loading, TC loading was terminated. Then q was reduced to zero and σ_3 was decreased under isotropic stress conditions to 15 MPa to perform the next step of TC loading. This procedure was repeated to perform TC loading at σ_3= 20, 15, 10 and 5 MPa. In the last loading step, axial loading continued until post-peak state to measure residual strength at σ_3= 5 MPa. Then q was reduced to zero and σ_3 was increased under isotropic stress conditions to 10 MPa to perform the next step of TC loading. This procedure was repeated to measure residual strengths at σ_3= 5, 10, 15 and 20 MPa.

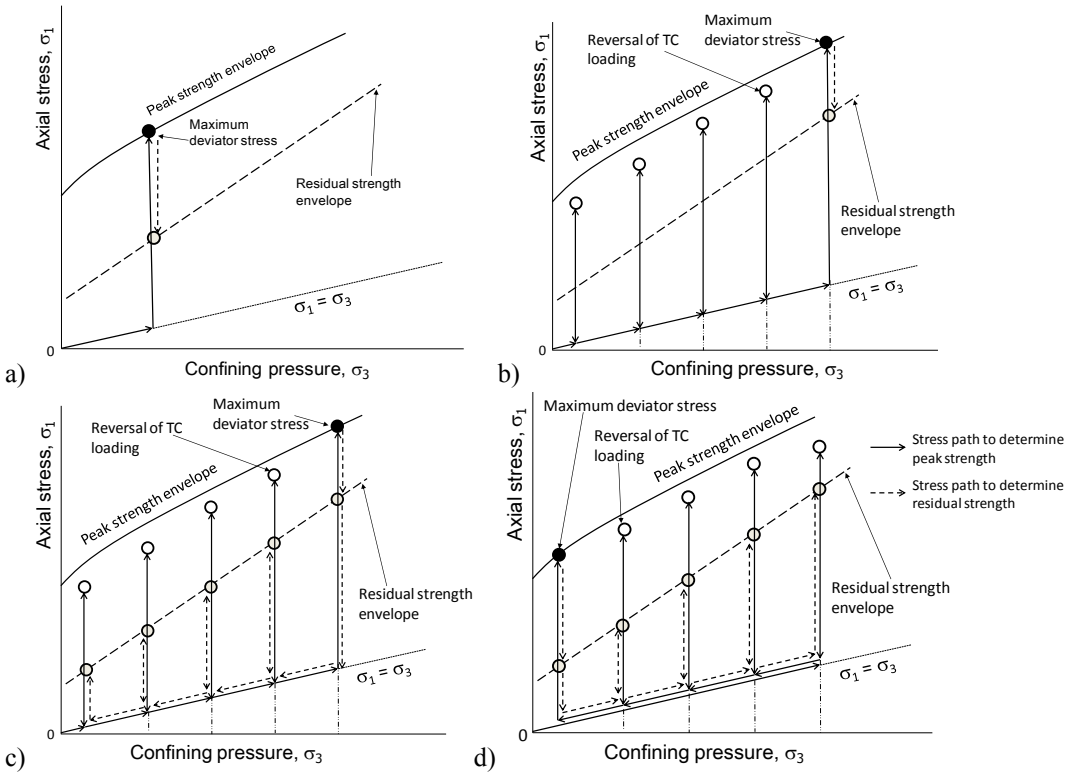


Figure 3: Stress paths of: a) SL tests, b) ML tests - increasing σ_3; c) & d) ML tests with measuring residual strength increasing and decreasing σ_3.

4 STRESS-STRAIN RELATIONS

Figure 4a shows the relations between deviator stress q and the axial strain from ten SL TC tests at different σ_3 and one UCS test (Series 1). With an increase in σ_3, the axial strain at the peak stress state and residual strength increase and failure mechanism becomes less brittle. These results are used below as the reference for the ML TC tests (Series 2).

One of the major issues of the present study is whether or not the proposed ML test method is applicable to measure peak and residual strength at different confining pressures using a single specimen comparable to those measured by SL tests using several intact specimens. Figures 4b–d demonstrate examples of the results from ML TC tests (Series 2).

Figure 4b shows the results from a ML test increasing σ_3 (series 2a). The stress–strain behaviour during the first primary loading, as well as before the last loading step at the later steps at higher σ_3s, all exhibit strain-hardening until the end of the TC loading. That is, at all the steps, the TC loading was terminated before reaching the respective peak stress states. No marked damaged observed during cyclic loading until the last loading step where the specimen were sheared until post-peak regime. Correspondingly, the maximum deviator stress, q_{max}, at each step increased with an increase in σ_3. In the post-peak regime, residual strength values recorded in the last loading step after a rapid stress drop, are seemingly constant.

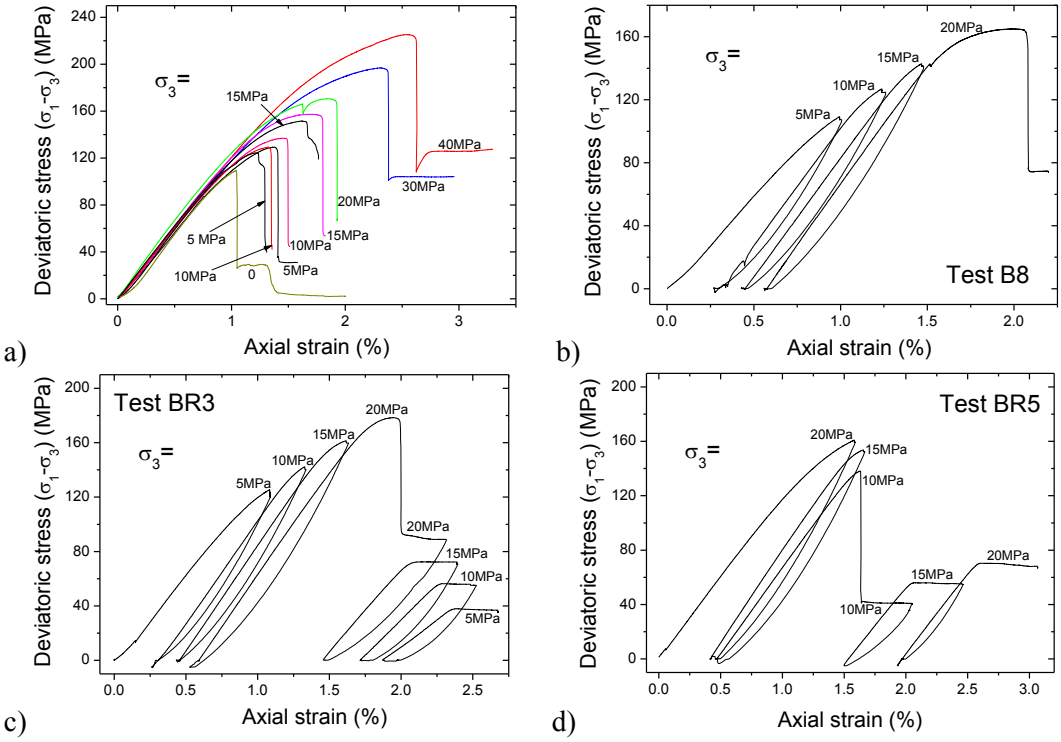


Figure 4: Deviatoric stress-axial strain relations from a) SL TC tests, and ML TC tests: b) increasing σ_3, c) increasing σ_3 W/RSM, d) decreasing σ_3 W/RSM, w/RSM: with residual strength measurement)

Figures 4c-d show examples of the results from the ML test increasing or decreasing σ_3 with residual strength measurement (w/RSM) (series 2b&c). Similar to the discussion above, the maximum deviator stress, q_{max}, at each step increased with an increase in σ_3 and decreases with a decrease in σ_3. Residual strength values measured at different σ_3s follow a similar trend.

As a result, it is obvious that using the proposed method (E_{sec}=max) the specimen can avoid experiencing unstable damage and its integrity until end of the test will be maintained. Only in one of ML tests decreasing σ_3 at σ_3= 10 MPa, sudden brittle failure happened before the secant Young's modulus (E_{sec}) reach its maximum value (Figure 4d). Consequently, a sudden failure happened without unloading and reloading at σ_3= 5 MPa. This trend of behaviour is due likely to following two factors: (1) in ML decreasing σ_3 tests, due to compression of the sample in the first and the second loading steps, at σ_3= 20 & 15 MPa, in the third loading step, at σ_3= 10 MPa, pre-peak non-linear hardening region after yield point became very small; (2) An increase in the

stiffness and brittleness at the same stress state by cyclic loading due to the elasto-viscoplastic properties. Consequently, in ML decreasing σ_3 after several loading steps, failure becomes very brittle and abrupt without clear non-linear strain-hardening behaviour. Practising ML test in this situation is very difficult. To avoid this situation, therefore, it is recommendable to follow ML test increasing σ_3 in brittle rocks.

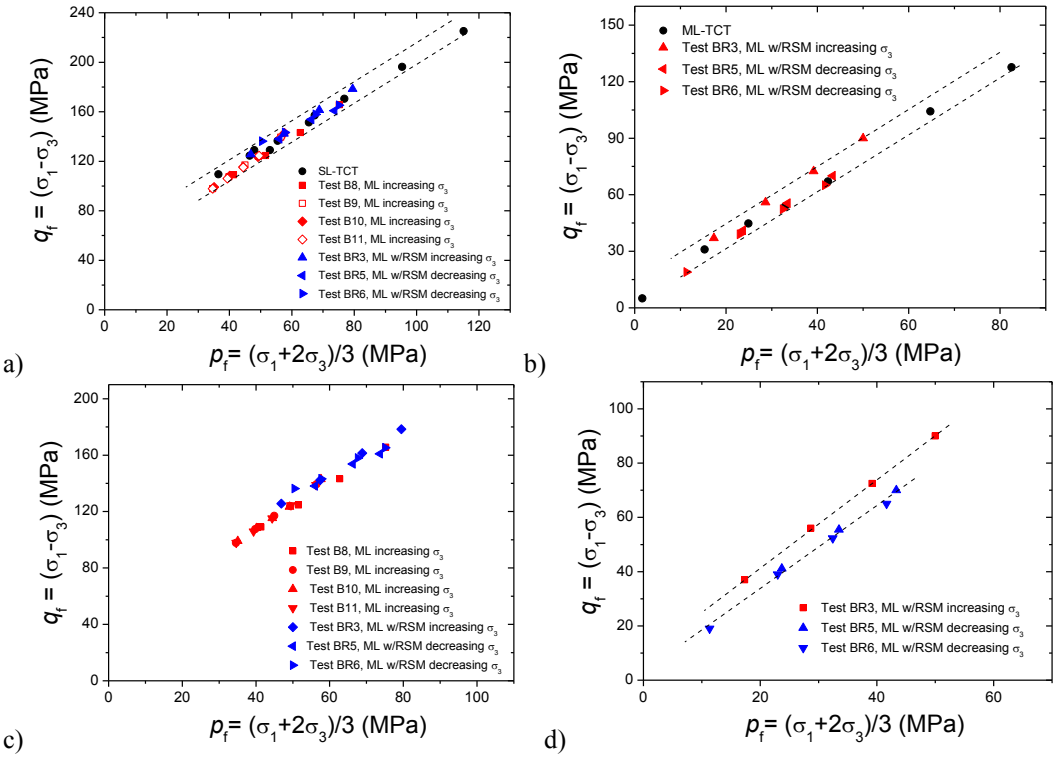


Figure 5: comparison of a) peak strength values obtained from SL and ML tests, and b) residual strength values obtained from SL and ML tests, c) peak strength values obtained from ML tests, d) residual strength values obtained from ML tests, (w/RSM: with residual strength measurement).

5 SINGLE-STEP TRIAXIAL TEST VS. MULTIPLE-STEP TRIAXIAL TEST

To examine whether the failure envelope obtained by such ML tests as performed in the present study is comparable to the one obtained from the conventional SL tests, the maximum shear stresses and residual strengths at all the TC loading steps in the ML tests, together with the peak and residual strengths from the SL tests, are summarized in Figures 5a & b. In each figure, it may be seen that all the data from the ML and SL tests are located in a narrow zone between two broken curves. This result indicates that, the peak and residual strengths at different σ_3s as obtained by a set of SL TC tests can be determined rather accurately from the results of a proposed ML test using a single specimen.

To study whether ML tests increasing σ_3 and ML test decreasing σ_3 produce similar results, the maximum shear stresses and residual strengths at all the TC loading steps in the ML tests are presented in Figures 5c & d. It may be seen in Figure 5c that peak strength values obtained in two different ML test method are very similar to each other. In the other hand, higher residual strength values were resulted from ML test increasing σ_3 with residual strength measurement (w/RSM) as compare to ML tests increasing σ_3 w/RSM. This trend is likely due to the fact that in ML test decreasing σ_3, which the specimen is first compressed at the highest confining pressure level (σ_3= 20 MPa), with step-wise decrease of σ_3, the failure mechanism at the last

loading step (σ_3= 5 MPa) is very brittle (i.e. significant amount of rapid stress drop; discussed earlier for Figure 4d). This behaviour also influences the residual strength values measured in the subsequent loading steps in ML decreasing σ_3. Due to the above trend, the residual strength values observed in ML tests decreasing σ_3 may be under-estimated. This re-stresses the conclusion made earlier which recommends practising ML increasing σ_3 in brittle rocks.

6 CONCLUSIONS

A new approach for defining the axial load reversal point to perform ML test in brittle rocks is proposed. The axial load reversal point is defined as the end of plateau of the secant stiffness – axial strain plot after leaving the elastic region before starts decreasing (E_{sec} =max, method). Using the proposed method, peak and residual strengths at different confining pressures (σ_3s) of a brittle rock can be determined by a multiple-step loading (ML) test using a single specimen. In ML test decreasing σ_3, after a few cyclic loading, pre-peak non-linear hardening region after yield point became very small; failure becomes very brittle and abrupt without clear non-linear strain-hardening behaviour. Practising ML test in this situation is very difficult. Indeed, residual strength values measured in stepwise manner may be under-estimated. As a result, in brittle rocks, ML test increasing σ_3 is preferable to ML test decreasing σ_3.

ACKNOWLEDGEMENTS

The work has been supported by the Deep Exploration Technologies Cooperative Research Centre whose activities are funded by the Australian Government's Cooperative Research Centre Programme. This is DET CRC Document 2013/205.

REFERENCES

Cain, P., Yuen, G., Crawford, A. and Lau, D. (1986) Triaxial testing of brittle sandstone using a multiple failure state method. Energy, Mines and Resources, *Canada – CANMET, Energy Research Progrom, Coal Research Laboratories, Division Report ERP/CRL 86-104*.

Crawford, A. and Wylie, D. (1987) A modified multiple failure state triaxial testing method, *Proc. of 28th US Sym. on Rock Mechanics*, 133-140.

Kim, M.M. and Ko, H.Y. (1979) Multistage triaxial testing of rocks, *Geotechnical Testing Journal*, 2, 98-105.

Kovari, K. and Tisa, A. (1975) Multiple failure state and strain controlled triaxial tests, *Rock Mechanics*, 7, 17-33.

Kovari, K., Tisa, A., Einstein, H.H. and Franklin, J.A. (1983) Suggested methods for determining the strength of rock material in triaxial compression: revised version. *Int. J. Rock Mech. & Min. Sci.*, 20 (6), 283-290.

Pagoulatos, A. (2004) Evaluation of multistage triaxial testing on Berea sandstone. *MSc dissertation, The University of Oklahoma*.

Taheri, A. and Tani, K. (2008a) Use of down-hole triaxial testing apparatus to estimate the mechanical properties of heterogeneous mudstone. *Int. J. Rock Mech. & Min. Sci.*, 45(8), 1390-1402.

Taheri, A. and Tani, K. (2008b) Proposal of a new multiple-step loading triaxial compression testing method. *Proc. of 5th Asian Rock Mechanics Symposium*, 517-524.

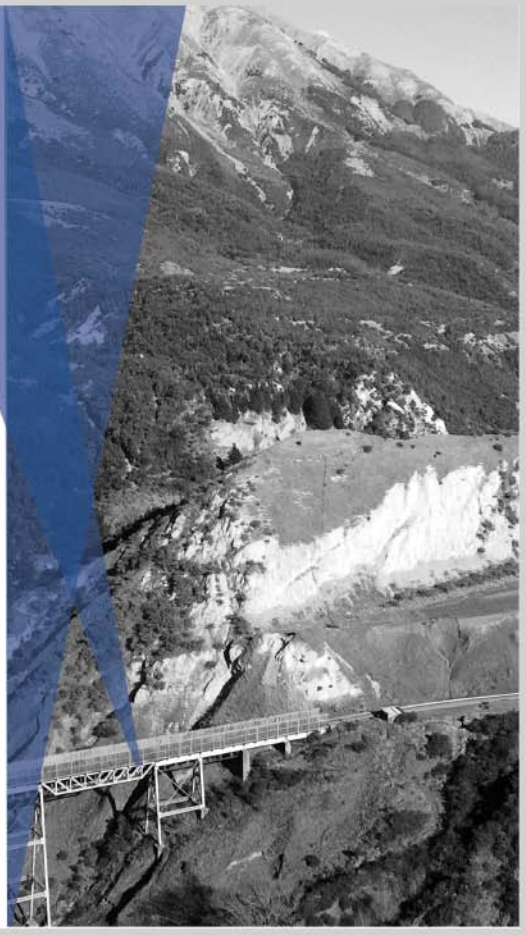
Youn, H. and Tonon, F. (2010) Multi-stage triaxial test on brittle rock. *Int. J. Rock Mech. & Min. Sci.*, 47, 678-684.

GEOSCIENCE
A proud partner of ENGEO

Engineering Geology
Environmental Engineering
Geotechnical Engineering
Geological Hazard Mitigation
Materials Testing and Inspection
Stormwater Management

www.nzgeoscience.co.nz
033289012

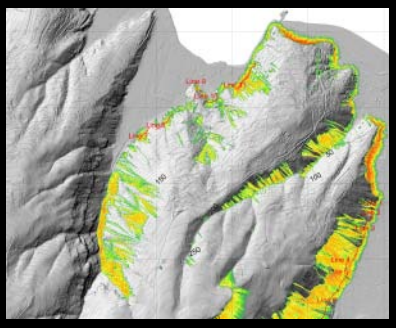
Christchurch | Wellington | Auckland | California



GEOVERT







- ground improvements
- compensation grouting
- foundation grouting
- micro piling
- tunnel remediation & strengthening
- retaining walls
- confined space & low overhead drilling
- slope stabilisation & rockfall protection
- debris flow systems

Providing innovative & economic solutions, Geovert will add value to geotechnical construction works requiring ground engineering, slope stabilisation or rockfall protection work throughout Asia Pacific in any environment.

www.geovert.com

AUCKLAND
P +64 9 837 7808
F +64 9 837 7809
15 Kaimahi Rd
Wairau Valley
North Shore 0627

CHRISTCHURCH
P +64 3 962 5840
F +64 3 962 5841
5/18 Taurus Place
Bromley
Christchurch 8062

New Zealand || Australia || Indonesia || Singapore

National coverage with offices in Auckland and Christchurch



Hiway GeoTechnical

GEOTECHNICAL SOLUTION PROVIDERS

Design and Construction

specialists in liquefaction control, in-situ & ex-situ stabilization for commerical, residential & infrastructure

Ground Improvements

Auckland +64 9 426 3419
E: info@hiways.co.nz

Christchurch +64 3 3417 603
W: www.hiways.co.nz



MACCAFERRI 25 years 1988-2013

COME CELEBRATE OUR 25 YEARS IN GEOTECHNICAL SOLUTIONS

JUST BY VISITING OUR STAND YOU CAN GO INTO THE DRAW TO WIN A CENTRAL OTAGO FOOD & WINE HAMPER

DESIGN AND TECHNICAL ASSISTANCE

BETTER SERVICE

Maccaferri is NZ's leading Geosynthetic supplier and the partner of choice for most of NZ's leading contracting companies.

We lead the market with regionally focussed logistical support and look to continually develop service levels beyond what's considered to be the norm in the Civil Construction market in NZ.

THE MACCAFERRI ADVANTAGE

We offer the complete Quality Assurance approach which includes independent batch testing of the materials we supply in NZ so you can be sure you are getting what you pay for

- Onsite assistance and training
- Stock held at convenient regional locations including major stock holdings in Auckland and Christchurch
- We represent the world's foremost geosynthetic manufacturers including Geofabrics, Tensar, Ten Cate, Presto and of course Maccaferri



0800 60 60 20
sales@maccaferri.co.nz
www.maccaferri.co.nz

ABSEIL ACCESS
ROPE ACCESS ENGINEERING

- ROCK ANCHORS
- SLOPE STABILISATION
- ROCKFALL NETTING & CATCHFENCES
- OFFICES IN WELLINGTON & CHRISTCHURCH

CALL 04 801 5336
abseilaccess.co.nz

We've got it covered





GEOTECHNICAL
Rope Access

AVALON
// ROPE ACCESS SERVICES
We minimise your risks!
P +64 7 846 1686 E admin@avalonltd.co.nz
www.avalonltd.co.nz

OPUS

GEOTECHNICAL ANALYSIS AND DESIGN CONSULTANCY
HAZARDS ASSESSMENT AND INFRASTRUCTURE RESILIENCE STUDIES
DYNAMIC TESTING OF DEEP FOUNDATIONS
GEOTECHNICAL LABORATORY TESTING



www.opus.co.nz

www.griffithsdrilling.co.nz

RESULT DRIVEN GEOTECHNICAL SPECIALISTS SINCE 1970.

GRIFFITHS DRILLING
RESULT DRIVEN GEOTECHNICAL SPECIALISTS

McMILLAN Drilling GROUP



NZDF NEW ZEALAND DRILLERS FEDERATION INC

www.drilling.co.nz

120 High St, Southbridge Ph 03 324 2571

PERRY GEOTECH

SPECIALISTS IN GEOTECHNICAL TESTING AND INVESTIGATIONS

Phone: (07) 578 0072, TAURANGA
Mobile: 0274 304 554

WWW.PERRYGEOTECH.CO.NZ

PERRY GEOTECH

PRO-DRILL
SPECIALIST DRILLING ENGINEERS

- Roto Sonic Drilling 150Hz
- CPT Investigation
- Mud Rotary Coring

www.prodrill.co.nz

0800 477 637

Index

	Author	Paper
H.M	Abuel-Naga	858
G.C	Archibald	513
G	Ashby	29
D.J	Ashfield	29, 346, 354
P.C	Augustinus	447
M.B	Avery	521, 608
A	Balachandra	794
R	Ballagh	125
N	Barounis	251
D.J.A	Barrell	290, 455
G	Basheer	423
K	Bassett	314
S.H	Bastin	314
R.D	Beetham	778
J.G	Begg	290, 298
K	Berryman	
S.J	Bourke	521
H.J	Bowen	45
E.T	Bowman	731
P	Brabhaharan	407, 439, 655
B.A	Bradley	148, 211, 762
J.D	Bradshaw	691
M.A	Brideau	447
D	Bruggers	841
J.M	Bryant	545
L.R	Buhagiar	53
J	Callosa-Tarr	415
J.M	Carey	513
J.J	Carter	770
G.A	Cassidy	552
E	Chanda	882
H.E	Cherrill	699
G	Chiaro	61
C.Y	Chin	101
L	Clark	739
P.J	Clayton	69, 691
R	Clements	85
N.K	Clendon	802
J	Codd	623
S	Cooke	631
S.C	Cox	322
B	Croucher	423
M	Cubrinovski	148, 211
M.J	Cunningham	537
B.A	Curley	778
S.E	Dickenson	117
J.N	Dismuke	77
G.R.W	East	275, 676
M	Easton	529
M.J	Eggers	306
S.F	Eldridge	699
R.M	Ellis	338
J	Elvy	243
J.M	Engel	560
A	Fairclough	346, 354, 770
G.B	Farquhar	463
P	Faulkner	85
D.L	Fellows	423
D	Fink	447
N	Fitch	29
A.J.A	Fon	338
P.D	Forrest	568
M	Gadsby	290
L.C	Gerrard	362
N	Gibb	747
M.F.L	Gibson	810
M	Goldsmith	545
R.B	Graafhuis	576
R.A	Green	314
D.P	Green	810
A.K	Griffin	370
JR	Grindley	377
P.G	Guerra	584
G	Halliday	85
B.M	Harvey	385
N.K.	Harwood	834
S.L	Haydon	338
G	Hayes	439
M.-C	Hébert	93
J.A	Herbert	362
R.P	Hillier	818
K	Ho	802
E.J	Hodgkinson	592
J.K	Holliday	683
S.F	Holmes	810
K	Horikoshi	211
S	Hornblow	455
M.E	Howard	600
C.G.C	Hughes	391, 631
R.P	Hunter	109
A.G	Irvine	306
H	Jack	290
M.E	Jacka	45, 140, 163
M	Jackson	470
I.R	Jenkins	423
I	Jennings	399, 616
J.T	Johnson	69, 739
K.E	Jones	298
M.E	Jorat	537
D.J	Kain	385
P	Kathigamanathan	415, 529
C	Kayser	101
C	Keepa	282
R.B	Kelly	786
D.K	Kirkcaldie	282
M	Koelling	747
J	Koseki	61
V	Lacrosse	163
E	Ladley	29
D	Lally	251
C	Lambert	219
A.C	Langbein	818
T	Le	584
J	Lees	125
N.J	Litchfield	290, 455
J.N	Lloyd	282
S.E	Lochhead	850
D.J	Lowe	537
B	Lukovic	513

D.F Macfarlane 494
A.G Mahoney 552
P Malan 163
D Mason 407, 439
C.I Massey 513
B McDowell 470
N McHugh 662
R McLachlan 415
T.J McMorran 600
L Mejia 478
R.J.M Millin 826
Y Mirjafari 36
A Mokhtari 391
J.W.H Molloy 568
S.R Moniz 834
V.G Moon 537
J Morris 415
T Morz 537
K.M Murahidy 195
A.K Murashev 282, 529
F.C Neeson 866
M.N Neishabouri 858
G Newby 810
K Newton 455
B Ni 275
A Nicol 455
N Norris 171
B O'Loughlin 243
A O'Sullivan 874
R.P Orense 36, 125, 179, 203, 267 794
S.J Palmer 195, 235
E Pearse-Danker 133
M.J Pender 179, 259, 826
J Pettinga
G.M Pinches 707
Z.J Pletz 623
A.D Pomfret 647
H Poulos 802
H.G Poulos 1, 834
P Power 29
P.M Power 140
C.H de G Price 715
G.P Quickfall 423
M Quigley 314, 455
R Ramilo 298
M.S Rattenbury 298
K.J Read 616, 631
P Retsos, 431
T.A.J Revell 362
T Reynolds 322
R.C Roberts 243
P.N Robins 385
K Robinson 148
W.R Rudolph 841
G Salt 85
H Salzmann 608
P Sasnett 455
G Saul 251, 377
E.S Savage 219
C Shackell 431
B.S Simms 778
T.J.E Sinclair 723
R Skinner 841
T Smith 29
D Soric 874
C.M Soutar 354
S.R Soysa 647
D.L Stewart 655
S.B Stewart 786
L.B Storie 259
D.T Strong 290
N Suemasa 36
S.W Sutherland 195
L Swatton 623
C.G Sweeney 447
M.R Taha 227
O.M Taha 227
A Taheri 882
C.M Tatarniuk 731
M.L Taylor 211
A Teen 608
S Terzaghi 874
C Thurlow 322
E.P Torvelainen 699
D.B Townsend 290
H Udell 156
J.P Underhill 463, 576
S van Ballegooy 163, 322
R.J Van Dissen 290, 455
P Villamor 455
N Villard 662
M Villeneuve 219, 306, 639, 754
S Wallace 670
I Wallis 754
I Walsh 377
S Wang 267
J Watson 330
F.J Wentz 117, 354
B West 391
N Wharmby 739, 747
R.J Whiteley 786
A Wightman 171
T Wilson 423, 639
L.M Wotherspoon 179, 826
J.B Wyatt 537
L.D Wyering 754
Z Yang 794
K Yates 639
M.D Yetton 494